# BINDING OF EXTERNAL CHLORIDES BY CEMENT PASTES

by

Hassan Zibara

A thesis submitted in conformity with the requirements

for the degree of Doctor of Philosophy

Graduate Department of Civil Engineering

University of Toronto

# ABSTRACT


**BINDING OF EXTERNAL CHLORIDES**
**BY CEMENT PASTES**

Doctor of Philosophy, 2001

Hassan Zibara

Graduate Department of Civil Engineering

University of Toronto

Chloride-induced reinforcement corrosion is the dominant cause of premature deterioration of reinforced concrete structures worldwide. The need to quantify the durability of new and existing structures led to the development of service life prediction models. This requires a clear understanding of the mechanisms of chloride penetration into concrete cover. This research looks into chloride binding when chlorides are introduced after the hydration of cement.

Highlights of this research include the X-ray diffraction (XRD) results which provide insight into some mechanisms of chloride binding. They show that several calcium aluminate hydrates (C-A-H), including monosulphate, convert to Friedel's salt. The monosulphate converts to Kuzel's salt at low concentrations before transforming into Friedel's salt at higher concentrations. Evidence suggests that ettringite starts converting to Friedel's salt at high chloride concentration. Friedel's salt peaks kept increasing at chloride exposures above 1.0 M, indicating that chemical binding is not exhausted at low chloride concentrations.

The results indicate the chloride binding capacity of cement paste results from the contribution of hydrates of different cement phases. The $C_3A$ has a strong effect on chloride binding, especially at high chloride concentrations (1.0 - 3.0 M). Evidence from synthetic compound pastes and cement pastes indicate that $C_4AF$, $C_3S$, and $C_2S$ bind chlorides and significantly contribute to the binding capacity. The binding isotherms of cement pastes can be predicted from the chemical composition of cements.

The results show that chloride binding isotherms are non-linear, and the Freundlich isotherm

is the best fit in the chloride concentration range 0.1 M- 3.0 M. In general, the partial replacement of cement with fly ash, ground granulated blast furnace slag (GGBFS), or metakaolin, increased chloride binding. Partial replacement with silica fume reduced chloride binding. An increase in the pH (13-14) of the storage solution reduced chloride binding. The presence of sulphate ions in the storage solution at 0.1 M concentration reduced chloride binding. Pre-carbonation of cement pastes greatly reduced chloride binding. An increase in temperature between 7°C and 38°C reduced chloride binding at 0.1 M chloride exposure, but increased it at 3 M exposure.

# ACKNOWLEDGEMENTS

I want to thank my two supervisors, Professor M.D.A Thomas and Professor R.D.Hooton, for their excellent guidance and for sharing their knowledge. I greatly appreciate their continuous support and encouragement. I also like to thank Ursula Nytko for being very helpful in the lab. I was fortunate to work with a group of graduate and undergraduate students that created a pleasant and stimulating work atmosphere at the concrete materials lab. Special thanks to Materials and Manufacturing Ontario (MMO) for their financial support, and to Lafarge (France and Canada) for providing "pure" cement phases and for their technical support. Dr. S. Petrov of the department of chemistry for his help with the X-ray diffraction tests. Finally, I want to thank my family for their unlimited support.

# TABLE OF CONTENTS

# LIST OF TABLES

# LIST OF FIGURES

# LIST OF APPENDICES

# LIST OF NOTATIONS

| | |
|---|---|
| a | Coefficient of Langmuir chloride binding isotherm. |
| $\alpha$ | Coefficient of Freundlich chloride binding isotherm. |
| b | Coefficient of Langmuir chloride binding isotherm. |
| $\beta$ | Coefficient of Freundlich chloride binding isotherm. |
| C | Chloride concentration at a given depth (%of cement mass). |
| $C_1$ | chloride concentration at equilibrium excluding the effect of evaporation (mole/Litre). |
| $C_o$ | Surface chloride concentration (% of cement mass). |
| $C_b$ | Binding capacity or amount of bound chloride in sample (mg Cl/g sample). |
| $C_e$ | Chloride concentration at equilibrium in the host solution (mole/Litre). |
| $C_{e2}$ | Chloride concentration after second equilibrium (mole/Litre). |
| $C_{ee}$ | Chloride concentration at equilibrium including the effect of evaporation (mole/Litre). |
| $C_f$ | Free chloride concentration in sample (mole/Litre). |
| $C_i$ | Initial chloride concentration in the host solution (mole/Litre). |
| $C_t$ | Total chloride content at a given depth (mg Cl/g sample). |
| $d_s$ | Density of chloride solution (g/ml). |
| $D_a$ | Apparent diffusion coefficient ($m^2/s$). |
| erf | Error function. |
| $\xi_{11}$ | Evaporable water content at 11% RH (g water/g sample). |
| k | Coefficient of Linear chloride binding isotherm. |
| RH | Relative humidity (%). |
| T | Temperature (°C). |
| t | Time of exposure (s). |
| $V_1$ | Volume of solution taken out, including first titration (ml). |
| $V_2$ | Volume of distilled water added (ml). |
| $V_{ee}$ | Solution volume including the effect of evaporation (ml). |
| $V_{sol}$ | Volume of the host solution (ml). |
| $W_{11}$ | Weight of the sample at 11% RH (g). |
| $W_d$ | Weight of the dry sample (g). |
| $w_e$ | Evaporable water content (g water/g sample) or ($m^3$ water/$m^3$ concrete). |
| $W_{ee}$ | Weight of the host solution at equilibrium after evaporation occured (g). |

$W_{sol}$ Weight of the host solution. (g).

$W_s$ Weight of the saturated sample (g).

x Depth from concrete surface (m).

$\zeta$ Zeta potential (mV).

$1/\kappa$ Thickness of the electrical double layer (m).

$[Cl^-]$ Concentration of sulphate ion in the solution (mole/L).

$[OH^-]$ Concentration of sulphate ion in the solution (mole/L).

$[SO_4^{2-}]$Concentration of sulphate ion in the solution (mole/L).

# CHAPTER 1

# INTRODUCTION

## 1.1 Introduction

The corrosion of steel reinforcement due to penetration of chlorides from marine and de-icing salts is the dominant cause of premature deterioration of reinforced concrete stuctures in Canada and many other countries around the world (*Racheeduzzafar et al., 1991; Maage et al., 1995; Thomas et al., 1995; Wood & Crerar, 1995*). This enormous problem has mobilized huge efforts by government agencies and the construction industry to find preventive or remedial measures. Numerous advances have been made in concrete technology (*Hooton & McGrath, 1995*). The use of high performance concrete (HPC) has been on the rise in an effort to extend the service life of new reinforced concrete structures exposed to severe chloride environments *(Thomas et al., 1995; Bickley, 2000)*. HPC mixtures, characterized by binary or ternary cement systems (with the addition of supplementary cementing materials), low water-to-cementitious materials ratio (W/CM), a combination of chemical admixtures, have a high resistance to the penetration of chlorides, and will supposedly lead to improved durability *(Thomas et al., 1995; Bickley, 2000)*.

The need to quantify the durability of new and existing structures has become very important. In recent practices emerging both internationally and in Canada, clients for new reinforced concrete structures are specifying service lives of 100 years or more (*Hooton & McGrath, 1995; Wood & Crerar, 1995; Bickley, 2000)*. Owners want to be assured that the new stucture will achieve the required service life. They also want to evaluate the different constuction alternatives through the use of life-cycle costing *(Gerwick, 1994)*. With such requirements, reliable service life prediction models would be extremely valuable. For new structures, these models would enable the design of concrete mixtures to ensure the designed life. For existing stuctures, these models would permit the prediction of the remaining service life, and help in the planning of timely and effective maintenance and repair *(Maage et al., 1995; Thomas et al., 1995; Wood & Crerar, 1995)*.

Many of the models currently being used are overly simplistic and assume that chloride ingress takes place by diffusion alone *(Hooton & McGrath, 1995, Thomas et al., 1995)*. These models are based on the assumptions that chlorides penetrate the cover layer by diffusion (a process described using Fick's second law of diffusion *(Crank, 1975))*, and that once a threshold chloride concentration is reached at the level of reinforcement (time determined using Crank's solution to Fick's second law), corrosion starts and proceeds rapidly, marking the end of the structure's service life *(Hooton &*

*McGrath, 1995)*. Therefore, for a new structure, a knowledge of the diffusion coefficient, $D_a$, and the chloride concentration at the surface, $C_s$, would permit the calculation of an estimated service life. In addition to ignoring the corrosion propagation time, which would be significant in the case of HPC, this approach overlooks several other mechanisms which significantly influence the chloride penetration process, including capillary sorption, permeation, wicking, and chloride binding. This shows the need to improve these models through the studying of the processes leading to the deterioration of reinforced concrete structures exposed to severe chloride environments.

This work is part of the ongoing research at the University of Toronto to understand the physical and chemical processes governing the chloride penetration and corrosion, and leading to the deterioration of concrete. It is hoped that this knowledge would serve the efforts to develop and improve service life prediction models *(Boddy et al., 1999)* that describe the chloride ingress and the corrosion process in a more accurate way, so that they would be of use to civil engineers. This work focuses on chloride binding in hydrated cement pastes exposed to external chlorides.

Chloride binding has an important effect on chloride penetration, and hence, on the time to corrosion initiation, since only free chlorides are likely to move further to the rebars level and initiate corrosion. The chloride binding process removes part of the chloride ions from the diffusion path (chlorides are chemically and physically bound to the cement hydrates), and consequently reduces the concentration gradient that drives the ionic diffusion. As a result, the rate of chloride ion penetration is decreased and the time for a threshold level to reach the steel surface is increased. Hence, it is important to take into account chloride binding as a part of the chloride penetration process in service life prediction models. To do so, it is important to study the chloride binding mechanisms and the factors that affect the chloride binding process, in order to model it accurately, which justifies the present research.

It is known that chloride ions react with tricalcium aluminate ($C_3A$) to form calcium monochloroaluminate, known as Friedel's salt (*Roberts, 1962; Mehta, 1977; Diamond, 1986; Taylor, 1990*). There is also increasing evidence to suggest that the calcium silicate hydrates (C-S-H) bind chlorides *(Ramachandran, 1971; Ramachandran et al., 1984; Blunk et al (1986); Wowra and Setzer, 1997, 2000)*. The relative importance of the $C_3A$ and C-S-H roles in chloride binding is not well understood. Several other parameters are also known to affect the binding capacity, including chloride concentration *(Tuutti, 1982; Blunk et al., 1986; Byfors)*, pH *(Tritthart, 1989)*, temperature *(Arya et al., 1990; Maslehuddin et al. 1996, 1997)*, carbonation *(Suryavanshi and*

*Swamy, 1996)*, sulphate *(Hussain & Rasheeduzzafar, 1994; Hussain et al., 1994; Xu, 1997)*, cation associated with chlorides *(Al Hussaini et al., 1990; Arya et al., 1990; Wowra & Setzer, 1997, 2000; Xu, 1997)*, *(Tritthart, 1989; Al Hussaini et al., 1990; Arya et al., 1990)* and supplementary cementing materials (SCM) *(Arya & Xu, 1995)*. There is, however, a clear lack of information, both quantitative and qualitative, in many aspects of the chloride binding process (especially in the case of chlorides penetrating hardened concrete from external sources). The experimental program in this work was specifically designed to address some of these issues.

## 1.2 Objectives

This work has focussed on studying chloride binding in the case of external chloride exposure. The objectives of this research were the following:

1. To examine the influence of some factors affecting chloride binding including:
   a. Environmental factors: study the influence of temperature, carbonation, pH, $[SO_4^{2-}]$ on the chloride binding capacity of cement paste.
   b. Cement composition: investigate the effect of $C_3A$ content, $C_4AF$ content, $SO_3$ content, fineness, alkali, W/CM, partial substitution with SCMs, and age.

2. To understand the roles of cement's mineral phases in chloride binding by:
   a. Studying the importance of $C_3A$, $C_4AF$, $(C_3S+C_2S)$ in chloride binding, and aiming to explain the different trends reported in the literature.
   b. Attempting to quantify the contributions of the mineral phases to the chloride binding capacity of cement.

3. To explore the possibility of modelling chloride binding through:
   a. Examining the nature of the relationship between free and bound chloride (chloride binding isotherms).
   b. Investigating the existence of relationships between the binding capacity and the various parameters affecting chloride binding.

## 1.3 Scope of Work

This research focuses on the chloride binding properties of hydrated cement pastes exposed to an external source of chlorides (i.e. where chlorides are introduced to the system after the cement has hydrated) since this case is more relevant to the chloride related deterioration process than admixed chlorides. An examination of the literature reveals a lack of information about chloride binding in this case. Most of the research on chloride binding has focused on admixed chlorides (chlorides present at the time of mixing), and this was partly due to the fact that $CaCl_2$ was used an accelerating agent in the 1960's and 1970's, and partly to the fact that, in some countries, the mixing water and aggregates contain chlorides. This underlines the need for more research on this subject and justifies the present work.

This thesis is divided into six chapters. Chapter 2 is a literature review of chloride binding. It includes a definition of chloride binding (chemical and physical binding), methods used to determine the distribution of chlorides between the hydrates and the pore solution, and an examination of various factors that influence chloride binding. A table summarizing the effects of the different factors is also included at the end of this chapter.

Chapter 3 describes the experimental program and the experimental procedures used in this research. It includes a description of the test methods used to determine chloride binding, mixture design, chemical compositions, and sample preparations.

Chapter 4 presents the results of the different studies done in this research. Each section presents the results of a different test and a limited analysis and discussion of these results.

Chapter 5 is a series of discussions regarding the main issues addressed in this thesis, and based on the results of the different studies done in this research. The synthesis of the results of the different studies, related to these issues, gives more insight and a better understanding of the phenomena involved. Chapter 6 is a summary of the main conclusions of this work and their implications. It also contains recommendations for future research.

# CHAPTER 2

# LITERATURE REVIEW

## 2.1 Chloride Binding

### 2.1.1 Definition

Chloride binding involves the processes through which chloride ions in the pore solution of concrete are fixed to different extent on certain cement hydrates. The term "bound chlorides" applies to any chloride ions that are not able to move freely in the pore solution of concrete. Chloride binding processes are generally classified in two categories:

- chemical binding
- physical binding

This classification is based on the mechanisms that are believed to be involved in the binding of chloride ions. These mechanisms are not well understood, and the partition between chemically and physically bound chlorides is not completely known and is a controversial subject.

### 2.1.2 Chemical Binding

Chemical binding as the name implies, is the result of chemical reactions between chlorides and certain cement phases, leading to the binding of chloride ions. There is no complete understanding, however, of the nature or the mechanisms of these chemical reactions. It is known that the $C_3A$ phase in cement reacts with chloride ions to form calcium chloroaluminate hydrate, $C_3A.CaCl_2.10H_2O$, commonly known as Friedel's salt (*Roberts, 1962; Mehta, 1977; Diamond, 1986; Taylor, 1990; Rasheeduzzafar, 1992; Neville, 1995; Suryavanshi & al., 1996).* It is also believed that a similar reaction between $C_4AF$ and chlorides results in the formation of an equivalent product to Friedel's salt, known as calcium chloroferrite, $C_3F.CaCl_2.10H_2O$ (*Roberts, 1962; Taylor, 1990; Rasheeduzzafar, 1992; Neville, 1995; Suryavanshi et al., 1995*). However, the importance of this reaction in chloride binding is not known yet. Some studies showed evidence of the formation of Friedel's salt in the case of admixed or external chlorides *(Diamond, 1986; Saito & Kawamura, 1992; Kouloumbi & Batis, 1994; Suryavanshi et al., 1995; Suryavanshi & Swamy, 1996).* In the case of admixed chlorides, it is commonly believed that the $C_3A$ phase of Portland cement chemically reacts with chloride ions during the hydration process to form Friedel's salt (*Roberts, 1962; Diamond, 1986; Taylor, 1990; Suryavanshi et al., 1995).* However, the presence of sulphates in

cement creates a competition for the available $C_3A$ between the chloride and the sulphate ions. In fact, it is believed that $C_3A$ reacts preferentially with sulphates *(Richartz, 1969; Schwiete et al., 1969; Mehta, 1977; Enevoldsen et al., 1994)*. *Richartz (1969)* reported that during the hydration of Portland cement in the presence of chlorides, ettringite formed first until all the sulphate was consumed, then Friedel's salt was formed. *Schwiete et al. (1969)* reported a similar trend. They found that ettringite formed first until the sulphate was consumed, followed by the formation of Friedel's salt until the chloride was consumed, followed by the formation of monosulphate from the ettringite and the rest of the $C_3A$ or $C_4AF$. *Glasser (1999)* referred to Taylor who quoted Tenoutasse as finding that during the hydration of mixtures of $C_3S$ and $C_3A$, in the presence of gypsum and $CaCl_2$, Friedel's salt formed only after all the sulphate was consumed.

In the case of external chlorides that penetrate the hardened cement paste, the situation is different since most of the $C_3A$ phase has already hydrated in the absence of chlorides. *Mehta (1977)* referred to a study by Lerch et al. in which they found that in a hydrated cement paste, in the presence of chloride solutions (external chlorides), the ettringite and monosulphate phases remained unchanged. *Migdley & Illston (1984)* found that only unhydrated $C_3A$ reacts with penetrating chloride ions, but others suggested that certain hydrated $C_3A$ phases will also react with chloride ions to form Friedel's salt *(Nagataki et al., 1993; Glasser, 1999)*.

*Ben-Yair (1974)* explained chloride binding as the result of a direct chemical reaction between the $C_3A$ phase in the cement and the $CaCl_2$, which was initially added to the mix water, leading to the formation of Friedel's salt. In the case of admixed NaCl, he explained the chloride binding by the following reactions:

$$Ca(OH)_2 + 2NaCl \rightleftharpoons CaCl_2 + 2Na^+ + 2OH^- \qquad (1)$$

$$C_3A + CaCl_2 + 10H_2O \rightarrow C_3A.CaCl_2.10H_2O \qquad (2)$$

More recent studies suggest the ion exchange mechanism to explain the formation of Friedel's salt *(Yonezawa, 1989; Suryavanshi et al., 1996; Glasser, 1999)*. The ion exchange mechanism suggested, explains chloride binding as a replacement of hydroxyl ions present in the interlayers of the hydroxy AFm ($Al_2O_3$-$Fe_2O_3$-mono) phase by chloride ions present in the pore solution or chloride penetrating from external sources as shown in Figure 2-1. This ion exchange mechanism leads to the formation of Friedel's salt as expressed in the following reaction given by Suryavanshi et al. (1996):

$$R\text{-}OH^- + Na^+ + Cl^- \rightarrow R\text{-}Cl^- + Na^+ + OH^-$$

where R is the principal layer of the hydroxy-AFm, $[Ca_2Al(OH^-)_6.nH2O]^+$, and the value of n is related to the type of hydoxy-AFm. While *Yonezawa (1989)* explained the formation of Friedel's salt, as a result of chloride addition to the mix, solely by the ion exchange mechanism. *Suryavanshi et al. (1996)* who also studied chloride binding in the case of admixed chlorides, suggested that the ion exchange mechanism is responsible for only a minor fraction of the bound chlorides. They explained that the AFm phases (Friedel's salt being one type of AFm) have layered structures derived from the structure of portlandite by the ordered replacement of one $Ca^{2+}$ out of three in a $Ca(OH)_2$ layer by a $Al^{3+}$ which results in a charge imbalance in each principal layer; the formation of Friedel's salt results from the adsorption of a $Cl^-$ in the interlayer space between the principal layers to balance the charge. Thus, it can be concluded from their analysis that Friedel's salt is mainly formed directly as an AFm product during the hydration of cement in the presence of admixed chloride, and only a minor part of Friedel's salt is formed by the conversion of hydroxy Afm through ion exchange between chloride and hydroxyl ions.

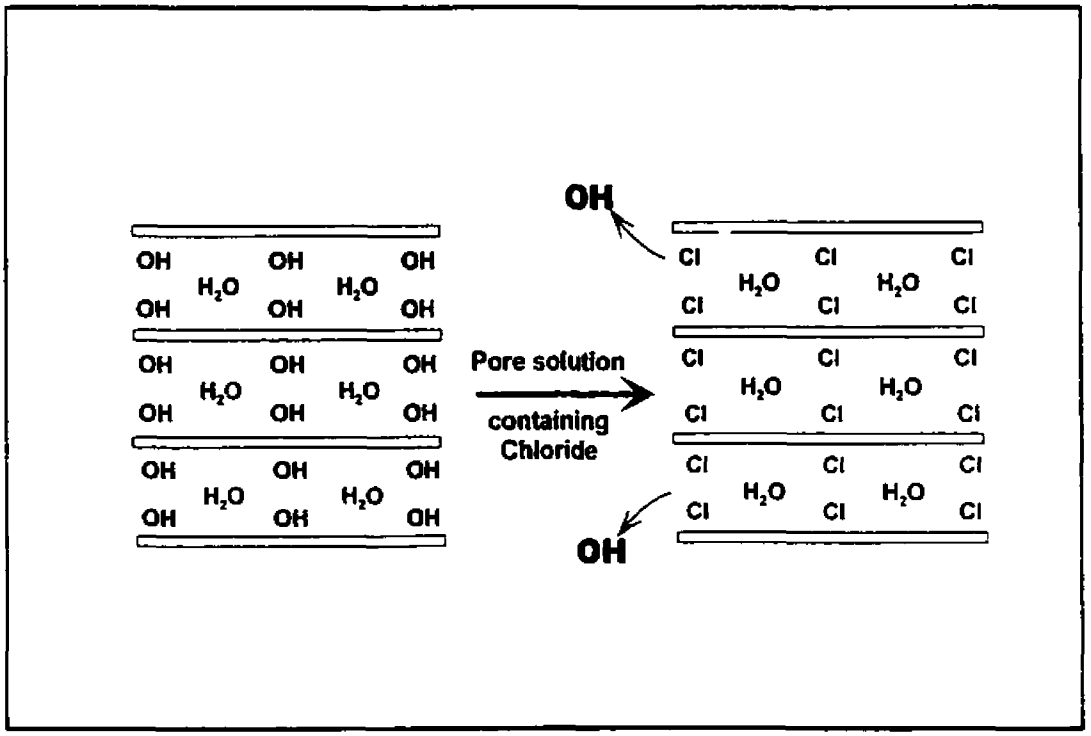


Figure 2-1: Schematic showing the ion exchange between the chloride ion and the hydroxyl ion residing in the interlayer spaces of a hydroxyl Afm phase. From *Glasser (1999)*.

### 2.1.3 Physical Binding

Physical binding is believed to be the result of physical adsorption of chlorides on the surface of the C-S-H hydrates *(Diamond, 1986; Blunk et al., 1986; Tang & Nilsson, 1993; Wowra & Setzer, 1997; Larsen, 1998)*. Physical adsorption is due to electrostatic or Van der waals forces between charged particles. In this case it is between the chloride ions and the surface of the C-S-H. The mechanism of physical binding, or adsorption, is not well understood. This also includes the extent of physical binding .

Recent studies are pointing to the electrical double layer theory, known in the field of physical chemistry *(Laidler & Meiser, 1982)*, to explain the mechanism of chloride adsorption on the surface of C-S-H *(Nagataki et al., 1993; Wowra & Setzer, 1997; Larsen, 1998)*. *Larsen (1998)* explains that the surfaces of the hydrated cement are negatively charged *(Jawed et al., 1983; Taylor, 1992; Chatterji & Kawamura, 1992)*, but due to the adsorption of cations ($Ca^{2+}$, $Na^{+}$) in the alkaline pore solution and the formation of the so-called Stern-layer *(Laidler & Meiser, 1982)*, the surfaces appear to be positively charged. This leads to the formation of an electrical, diffuse double layer (known as the Gouy-Chapman layer), and the adsorption of the negatively charged chloride ions takes place in the diffuse double layer to satisfy the electro-neutrality as shown in Figure 2-2. The adsorption capacity in the double layer depends on the surface area of the C-S-H, and on the potential (zeta potential) on the plane between the adsorbed cations and the diffuse double layer. This potential is a function of the valence of the adsorbed cations, temperature, and the concentration of ions in the pore solution. According to *Larsen (1998)*, the presence of $Ca^{2+}$ in the pore solution is decisive for the value and sign of the zeta potential . He referred to *Diamond et al. (1964)* who found that the zeta potential of tobermorite gel was initially positive, but became negative at a pH around 10, following the gradual removal of $Ca(OH)_2$ by washing the gel with distilled water.

In addition to physical adsorption, it was suggested that chlorides can be bound in other forms to the C-S-H according to some studies *(Ramachandran, 1971; Diamond, 1986)*. *Diamond (1986)*, reported to have noticed many times the presence of chlorides within local regions of C-S-H when examining concretes exposed to chlorides by energy dispersive X-ray analysis in a scanning electron microscope. He suggested that some of the bound chlorides are most likely resident within the C-S-H (when they are present at the time of mixing). *Ramachandran (1971)*, who studied the hydration of a $C_3S$ paste in the presence of $CaCl_2$, also suggested that chloride ions may also exist

in the interlayer space of the C-S-H. In addition, he concluded that a major part of chloride ions is also chemisorbed by the C-S-H, and some are incorporated in the C-S-H lattice. Chemisorption involves the formation of chemical bonds between the adsorbate (chloride) and the adsorbent (surface of the hydrates) at some chemically active sites. It should be mentioned that throughout this thesis, chemical binding will refer to the binding capacity of aluminate and ferrite hydrates, and physical binding will refer to the binding capacity of the C-S-H.

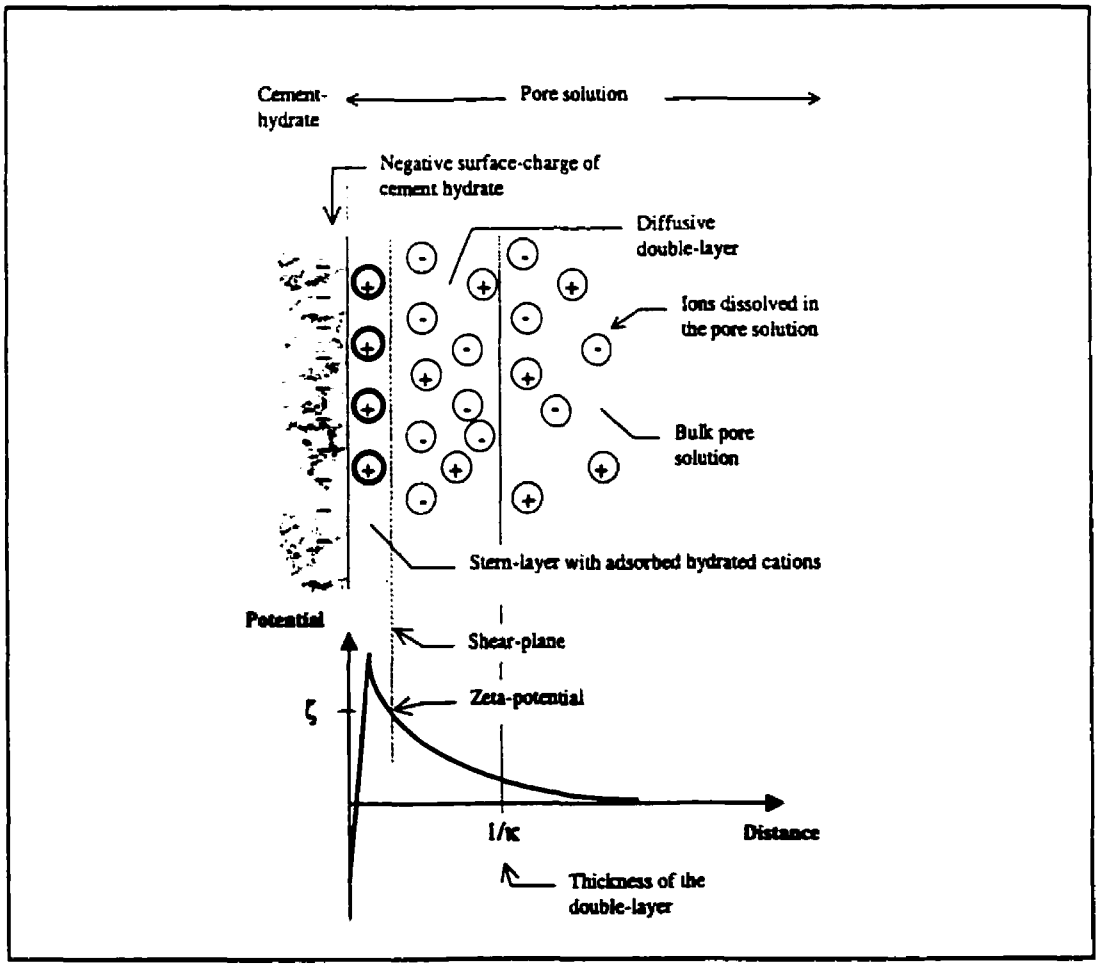


Figure 2-2 Illustration of the Stern model for the electrical double layer. *From Larsen (1998)*

## 2.2 Experimental Methods for Determining Chloride Distribution

Several methods have been used for the determination of chloride distribution between free and bound chlorides. However, none of them are standardized and very few of them are commonly used *(Nilsson et al., 1996)*. The differences between these methods are in general, the way the chlorides are introduced (internal or external), the unkown chloride variable to be determined (free chlorides or total chlorides), and the technique used to determine the unkown chloride quantity. This section present a review of some of these methods. The methods are classified based on whether the chlorides are admixed or external.

### 2.2.1 Methods Dealing with Admixed Chlorides

#### 2.2.1.1 Pore Solution Expression

This method is the most commonly used for the determination of chloride distribution inside paste or mortar. In this method, a known quantity of chloride (total chloride) is introduced during mixing and a sample from the paste or mortar is squeezed under high pressure in a pore solution expression device (*Barneyback & Diamond, 1981*) after being cured for a certain period of time. The pore solution is then analysed for its chloride concentration which is assumed to be the free chloride concentration in the pore solution. From the knowledge of the quantity of free pore water, the bound chloride can be determined as well. It has been reported that pore solution expression significantly overestimates the free chloride concentration in the pore solution (*Glass & Buenfeld, 1995; 1996*). It was suggested that the high pressure applied tends to release loosely bound chloride in the solution resulting in the increase of free chloride concentration (*Glass & Buenfeld, 1995; 1996*).

#### 2.2.1.2 Leaching Methods

The leaching methods are similar to the pore expression method described above, except that the free chloride content is determined using leaching instead of pore squeezing. Leaching is based on mixing samples, ground to powder, with a solvent and measuring the chloride concentration in the solution. Several published studies used different leaching techniques to determine the free chloride content in paste or mortar (*Monfore & Verbeck, 1960; Richartz, 1969; Ramachandran, 1971*). These techniques differ in the type of solvents (water or alcohol) and the mixing regimes. However, some studies have shown that ethyl alcohol, when used as a solvent, is ineffective in leaching

chloride and therefore underestimates the free chloride content (*Tritthart, 1989; Arya & Beunfeld, 1987*). *Arya and Newman (1990)* assessed several leaching techniques using water as solvent, and compared these techniques with pore expression; the results showed that no single technique was sufficiently accurate over the range of the total chloride studied, and that the choice of an appropriate leaching technique depends on the total chloride content and the cement type.

### 2.2.2 Methods Dealing with External Chloride

#### 2.2.2.1 Equilibrium Methods

Equilibrium methods are based on storing samples of paste or mortar in chloride solutions until equilibrium is reached between the external solution and the pore solutions of the samples. Two methods based on this concept are used; in the first one, the concentration of the chloride is kept constant until equilibrium is reached. At equilibrium, the free chloride concentration in the pore solution is equal to the chloride concentration in the external solution, and the total chloride of the submerged sample can be measured to determine one chloride binding point. The bound chloride content can also be determined if the capillary porosity is measured. This method has been used by *Sandberg & Larsson (1993)*. In the second method, the sample is stored in the chloride solution and the decrease in chloride concentration is measured after equilibrium is reached. The bound chloride content is then determined from the decrease in chloride concentration, and the free chloride concentration is equal to the chloride concentration in the external solution at equilibrium. Figure 2-3 show results obtained using this method. This method has been used by *Blunk et al. (1986)*, and *Byfors (1986)* before *Tang and Nilsson (1993)* developed its current form, which is being used more frequently by researchers *(Dhir et al., 1996; Dhir et al., 1997; Wiens & Schiessl, 1997)*. *Glass and Beunfeld (1995)* suggested that the use of a crushed sample in this test leads to the overestimation of bound chloride since the crushing exposes new binding sites which are otherwise unreachabale. *Nilsson et al. (1996)* suggested that the volume of the solution should be chosen in a way to keep the reduction in concentration small, because of hysteresis in chloride binding which will cause innacuracies if there is a large reduction in the chloride concentration. On the other hand, the reduction in concentration should be high enough to get accurate binding results.

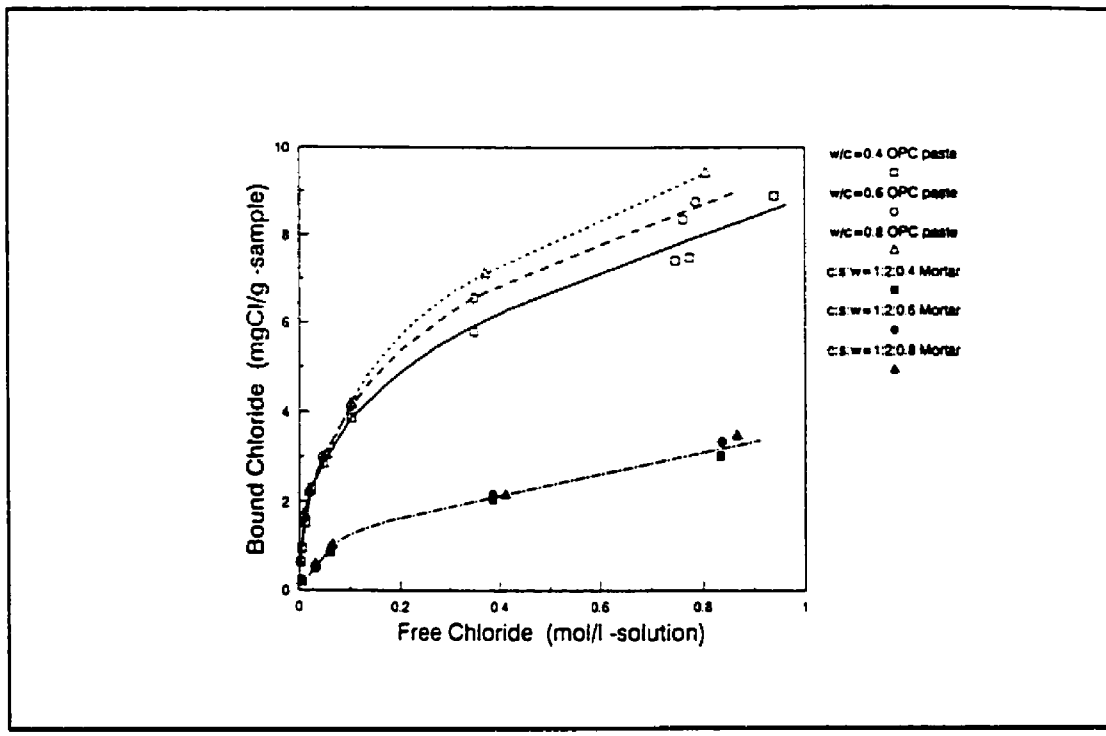


Figure 2-3: Chloride binding isotherms of OPC pastes and mortars, obtained by using the equilibrium method. From *Tang & Nilsson (1993)*.

### 2.2.2.2 Methods Using Pore Expression

These methods are based on immersing samples in chloride solutions for a certain period of time and then pore squeezing the samples to determine the free chloride content. One method which was used by *Sergi et al. (1992)* and *Yu et al. (1993)* is worth mentioning. It consists of immersing cylinders of paste in known chloride solution for a period of time and then determining the free and total chloride contents at different depths inside the cylinders. The free chloride content is measured by pore squeezing groups of slices taken from several cylinders at the same depth, to obtain enough pore solution. The total chloride content is measured as well by dissolving powdered samples in nitric acid and measuring the chloride concentration in the solution. The bound chloride content is then determined after measuring the evaporable water content. The advantage of this method is that it tries to simulate the chloride diffusion process and gives data about the apparent diffusion coefficient, the total chloride profile, the free chloride profile, and the chloride binding isotherm. The disadvantage of this method is the long time it takes to get these data, especially when testing mixes containing SCMs.

Recently, some studies suggested the use of diffusion cells *(Bigas et al., 1995, Glass et al., 1998)* and migration cells *(Arsenault et al., 1995)* tests to determine the chloride binding properties of concretes as additional information after the completion of these tests. The proposed methods are mostly based on the determination of the total and free chloride contents in the test specimen after the diffusion or migration test is finished. *Glass et al. (1998)* determined the chloride binding isotherms from diffusion cell tests used to determine the steady state diffusion coefficients. This was done by determining the total chloride profile across the depth of the specimens, and estimating the free chloride concentrations by assuming the concentration gradient to be linear under steady state conditions. Their chloride binding data were close to data obtained by other methods. The advantages of this method are the ability to produce a binding isotherm form a single specimen, and the ability to produce results on concrete specimens with low W/CM ratio. The biggest drawback is the long testing time in the case of the diffusion cell tests. *Arsenault et al. (1995)* suggested the use of steady state migration cell tests to determine the chloride binding isotherms. They argued that since the free chloride concentration is almost constant across the thickness of the specimen (for potentials > 2 volts), the bound chloride can be determined by measuring the total chloride content and the open porosity. By performing the test for different chloride concentrations in the upstream cell, a full binding isotherm can be determined. The advantage of this method is the short testing time. However, the application of an electrical field might affect the binding processes. *Castellote et al. (1999)* suggested that the electrical field could alter the electrical double layer potential and affect the interaction between the chloride ions and the surface of the hydrates. Moreover, *Glass and Beunfeld (1995)* found a lower chloride concentration inside the specimen than in the solutions in the upstream and downstream cells in migration tests. Obviously, more comparative work should be done in the case of the migration cell test before adopting such an approach for determining chloride binding, although it would be an advantage to be able to get binding data from the migration cell test.

## 2.3 Chloride Binding Isotherms

Chloride binding isotherms describe the relationships between free and bound (or total) chlorides in concrete at a given temperature. They are unique to each cementitious system since they are influenced by the components making up that system, such as $C_3A$ content, supplementary cementing materials, $SO_3$ content, and pH of the pore solution. Several mathematical models have been used in the published literature to describe chloride binding isotherms, and the following sections present a review of these models.

### 2.3.1 Linear Chloride Binding Isotherm

The linear isotherm is of the following form:

$$C_b = k\, C_f$$

where k is a constant. This relationship was proposed by *Tuutti (1982)*, and was a good fit for his reported data. But, he only reported free chloride concentrations lower than 20 g/l (0.56 M). This relationship is an oversimplification at high concentration, where it will overestimate chloride binding. It also underestimates chloride binding at low concentrations *(Nilsson et al., 1996)*. The linear relationship seems to be applicable within a limited range of free chloride concentrations *(Tang, 1996)*.

### 2.3.2 Langmuir Isotherm

The Langmuir isotherm is of the following form:

$$C_b = a\, C_f / (1 + b\, C_f)$$

where a and b are constants which vary with the binder composition. The Langmuir isotherm is borrowed from physical chemistry, and describes the adsorption of gas on a solid surface *(Physical Chemistry)*. It assumes monolayer adsorption, which explains the shape of the Langmuir curve at high concentration where the slope of the curve approaches zero and the curve becomes almost horizontal as the adsorption capacity is exhausted. In the case of chloride binding, this means that the binding capacity is exhausted at high free chloride concentrations. *Pereira and Hegedus (1984)* suggested the use of Langmuir isotherm to describe chloride binding. *Sergi et al. (1992)* used a langmuir isotherm to account for the non-linearity in the relationship between the free and bound

chloride in their experimental data. *Tang and Nilsson (1993)* found that the Langmuir isotherm was an excellent fit of their binding data at concentrations lower than 0.05 M.

### 2.3.3 Freundlich Isotherm

The Freundlich isotherm is described by the following equation:

$$C_b = \alpha C_f^{\beta}$$

where $\alpha$ and $\beta$ are binding constants with values related to the binder composition. The main difference between the Freundlich and the Langmuir isotherms is their behaviour at high concentrations; while the slope of the Langmuir isotherm approaches zero, allowing only minor changes in the binding capacity, the slope of the Freundlich isotherm is always higher than that of the Langmuir isotherm allowing an increase in the binding capacity at high concentration as shown in Figure 2-4. *Tang and Nilsson (1993)*, found that the Freundlich equation fits their data very well for free chloride concentrations between 0.01 M and 1 M. They suggested a Freundlich isotherm at concentrations higher than 0.01 M, and a Langmuir isotherm at concentrations lower than 0.05

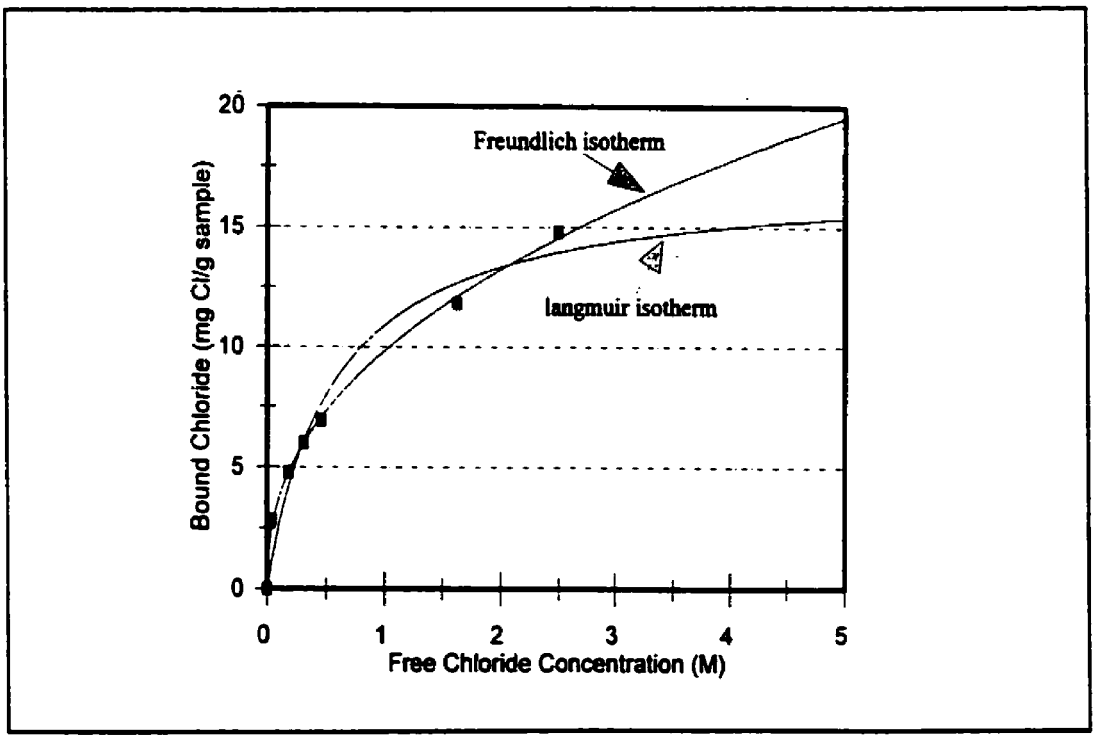


Figure 2-4: Plots of the Langmuir and Freundlich isotherms showing the difference between the slopes of these isotherms at high chloride concentrations.

M. They argued that their results indicate that a monolayer adsorption occurs at very low concentrations (which is better described by a Langmuir isotherm), but that adsorption becomes more complex at concentrations higher than 0.05 M and is described better by the Freundlich isotherm.

*Tang and Nilsson (1995)* recently attempted to use the modified BET theory (multilayer adsorption theory) to fit binding data to the BET equations. They found a good correlation between the theory and the experimental data up to a free chloride concentration of 1 mol/l. It is not known how good the correlation would be for concentrations higher than 1 mol/l since the authors did not have experimental data above this concentration.

## 2.4 Factors Affecting Chloride Binding

### 2.4.1 Cement Composition

#### 2.4.1.1 $C_3A$:

It is known and established that the $C_3A$ phase in Portland cements plays a significant role in chloride binding. The $C_3A$ phase in cement reacts with chlorides to form calcium chloroaluminate *(Roberts, 1962; Mehta, 1977; Taylor, 1990; Rasheeduzzafar, 1992)*. It was earlier believed that this was the only mechanism for chloride binding, according to *Nilsson et al. (1996)*. Later investigations on the hydration of tricalcium silicate in the presence of $CaCl_2$ found that the $C_3S$ phase binds a significant amount of chloride as well *(Ramachandran, 1971)*. More recently, a renewed interest in studying chloride binding was triggered owing to the possible role of chloride binding in retarding the onset of steel corrosion as mentioned earlier. This has created controversy on the importance of the role of $C_3A$ in chloride binding. While some studies show that the amount of $C_3A$ in cement is of decisive significance on the chloride binding capacity of cements *(Roberts, 1962; Holden et al., 1983; Rasheeduzzafar et al., 1992; Sandberg & Larsson, 1995)*, particularly in the case of internal chlorides, other studies show a less significant or minor role for $C_3A$ *(Byfors et al., 1986; Byfors, 1986 & 1990; Wowra & Setzer, 1997)*. Opinions range from suggesting that the $C_3A$ role or chemical binding by the formation of Friedel's salt is minor (especially in the case of external chloride) *(Wowra & Setzer, 1997)*, to suggesting that chemical binding, through the formation of Friedel's salt, is mostly responsible for chloride binding *(Nagataki et al., 1993)*.

In the case of admixed or internal chorides, some studies indicate the beneficial effect of $C_3A$ on chloride binding (*Roberts, 1962; Holden et al., 1983; Arya et al., 1990; Rasheeduzzafar et al., 1991, 1992; Suryavanshi et al., 1995*). *Roberts (1962)* studied an OPC and an SRPC with admixed chloride in varying amount, and found that chloride concentrations in the pore solution of the SRPC were significantly higher that those in the OPC for all levels of $CaCl_2$ addition. *Holden et al. (1983)* showed that the concentration of chloride in the pore solution of cement paste with admixed chloride (0.4% $Cl^-$ by mass of cement) decreased with the increase in the $C_3A$ content of cement. A similar trend was found by *Rasheeduzzafar et al. (1991, 1992)* when they tested four Portland cements with $C_3A$ content ranging from 2% to 14% and with different levels of chloride addition ( 0.3, 0.6, 1.2, and 2.4% $Cl^-$ by mass of cement). However, they also found that the beneficial effect of higher $C_3A$ content diminished as the level of chloride addition increased (Figure 2-5). They attributed this to the fact that $C_3A$ or other cement hydrates have a limited capacity to bind chlorides and as it gets

progressively exhausted, more chlorides would remain in the pore solution. *Suryavanshi et al.(1995)* found that an OPC bound more chlorides than an SRPC at all levels of chloride addition. Two studies *(Blunk et al., 1986; Ramachandran et al.,1984)* compared the binding capacities of $C_3A$ (mixture of $C_3A$ and gypsum), $C_3S$, and OPC pastes, and both showed that the $C_3A$-gypsum mixture bound much more chlorides than $C_3S$ and OPC pastes.

In the case of external chlorides the importance of $C_3A$ content in cement is less obvious. Published results suggest different trends. *Verbeck (1968)* investigated the corrosion resistance of reinforced concrete piles made with 22 Portland cements and exposed to sea water for a long period of time. The results showed that the average linear cracking due to steel corrosion decreased with the increase in $C_3A$ content of the cement. The cracking was three times less for concrete with $C_3A$ contents of 8 to 11 % in the cement than for those with $C_3A$ contents between 2 to 5 %.

Results by *Blunk et al. (1986)* showed that a pure $C_3A$-gypsum mixture bound the most chloride compared to an OPC and $C_3S$ paste when they were treated with chloride solutions of varying concentrations. *Sandberg & Larsson (1995)* found that an OPC bound more chlorides than

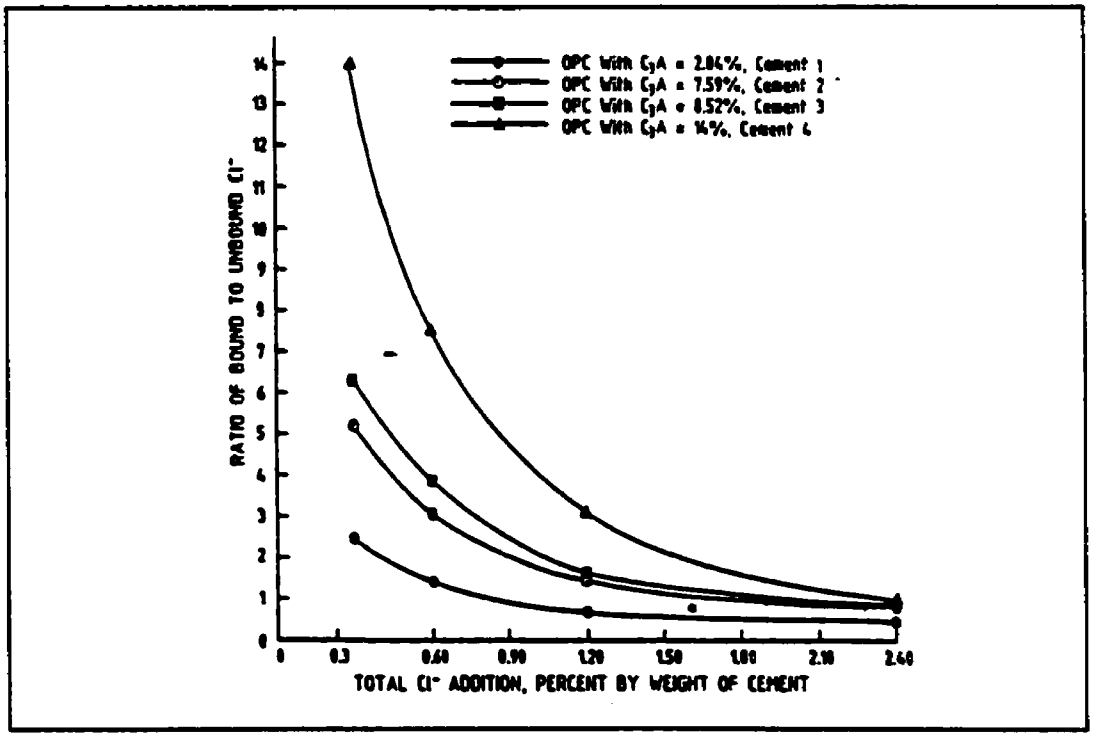


Figure 2-5: Effect of total chloride content on the ratio of bound to unbound chloride in OPC pastes with admixed chloride. From *Rasheeduzzafar et al. (1991).*

an SRPC paste upon treatment with chloride solutions of different concentrations. On the other hand, an opposite trend was found by *Byfors (1986, 1990)* as shown in Figure 2-6, and little effect of $C_3A$ content was detected by *Arya et al. (1990)* and *Wowra and Setzer (1997)*.

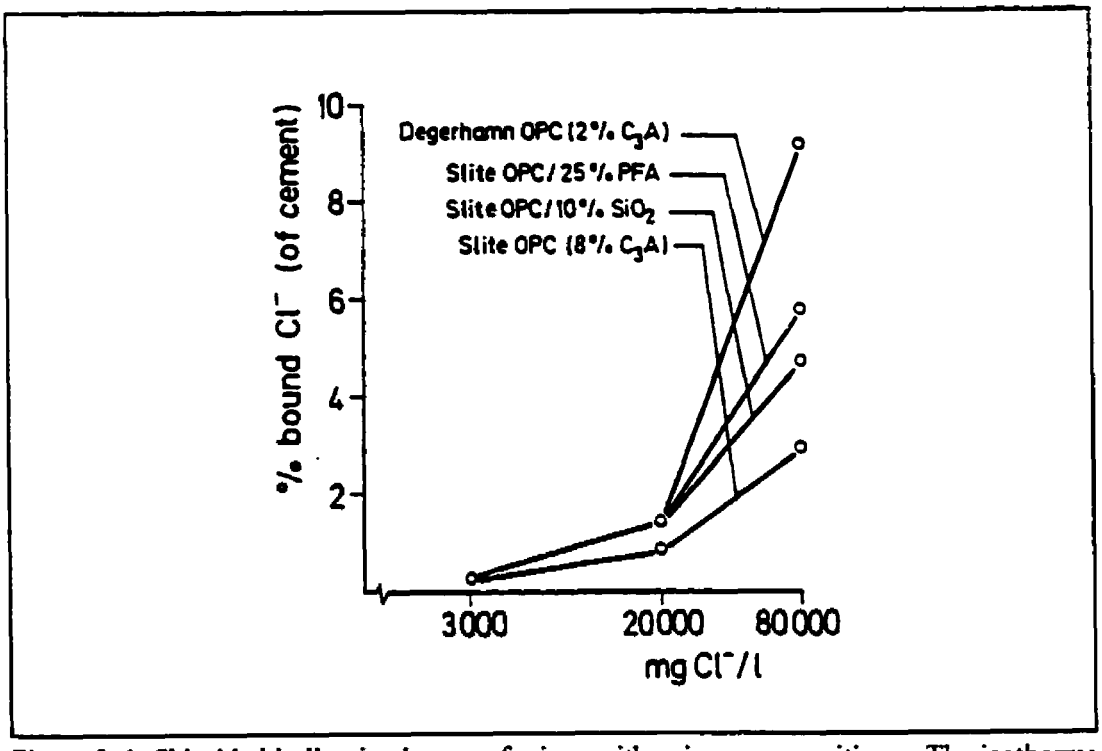


Figure 2-6: Chloride binding isotherms of mixes with vaious compositions. The isotherms were obtained using the equilibrium method. Note that the cement with lower $C_3A$ content had a higher binding capacity than the cement with higher $C_3A$. From *Byfors (1986)*.

### 2.4.1.2 Role of Calcium Silicates

Unlike the role of $C_3A$, the $C_3S$ (and $C_2S$) role in binding cannot be assessed directly in cement paste since the total content of calcium silicates ($C_3S$+$C_2S$) does not vary significantly from one cement to another as in the case of $C_3A$. Therefore, most of the studies on the role of $C_3S$ in chloride binding used pure $C_3S$. Despite the conflicting trends, more results show that $C_3S$ has a significant chloride binding capacity *(Ramachandran, 1971; Ramachandran et al., 1984; Blunk et al., 1986)* than a negligible chloride binding capacity.

*Ramachandran (1971)* studied the role of $CaCl_2$ in accelerating the hydration of $C_3S$ and suggested that a major portion of the chloride ions are rapidly removed from the pore solution and are chemisorbed by the C-S-H gel. In addition, he suggested that chloride ions may reside in the interlayer space of C-S-H and for larger hydration periods may be incorporated in the C-S-H lattice. It should be mentioned that he used ethyl alcohol in his leaching technique to estimate the chloride distribution. *Arya & Newman (1990)*, and *Tritthart (1989)* have shown the ineffectiveness of ethyl alcohol in leaching chlorides, and their results show that it grossly underestimates the free chloride content. In latter studies *(Ramachandran et al., 1984; Beaudoin et al., 1990)* it was found that a $C_3S$ paste binds a significant amount of chlorides (Figure 2-7), although, not as much as previously reported *(Ramachandran, 1971)*. *Blunk et al (1986)* found that $C_3S$ paste bound considerable amounts of chloride from both $CaCl_2$ and NaCl in the case of admixed chloride. It was suggested that physical adsorption is mostly responsible for binding in this case

On the other hand, *Lambert et al (1985)* did not detect any significant binding capacity for a $C_3S$ paste ($C_{54}S_{16}AM$) which according to them is representative of the $C_3S$ phase found in most commercial Portland cement.

In the case of external chloride, two studies indicate that $C_3S$ has a considerable binding capacity. *Blunk et al (1986)* found that $C_3S$ paste bound considerable amounts of chloride from both $CaCl_2$ and NaCl. It was suggested that physical adsorption is mostly responsible for binding in this case. *Wowra and Setzer (1997)* obtained similar trends.

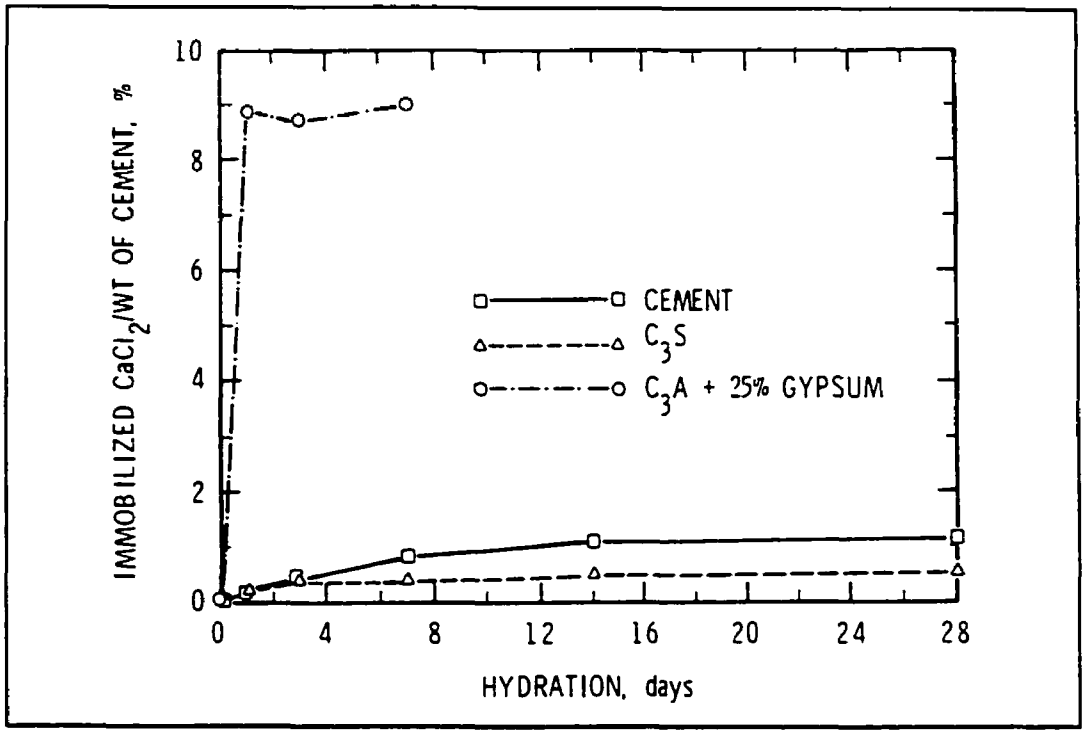


Figure 2-7: Bound calcium chloride ($CaCl_2$) (expressed as a % of the original amount of $CaCl_2$ added to the cementitious pastes) in various pastes. The admixed $CaCl_2$ was 1.5% of the solids. From *Ramachandran et al. (1984).*

### 2.4.1.3 Role of $C_4AF$

The reaction between $C_4AF$ and $CaCl_2$ leading to the formation of $C_3F.CaCl_2.10H_2O$ is known to occur *(Roberts, 1962).* Yet, there is hardly any study related to the role of $C_4AF$ in chloride binding. However, an examination of most studies that addressed the role of $C_4AF$ indicate that their role is secondary to $C_3A$ if not minor. These studies indicate that $C_3A$ content in cement is the major factor that determines which cement has a higher binding capacity regardless of the content of $C_4AF$ in the different portland cements. On the other hand, *Byfors (1986, 1990)* found that a portland cement with low $C_3A$ content (2%) bound higher amounts of chlorides than one with higher $C_3A$ content (8%) as shown in Figure 6. She noticed that in the low $C_3A$ cement, the sum of $C_4AF$ and $C_3A$ was higher than in the high $C_3A$ cement and suggested that this might be the cause for the higher binding capacity. *Suryavanshi et al. (1995)* concluded from an investigation into the binding capacity of an SRPC ($C_3A$ content of 1.4%) that chlorides were primarily bound through the formation of $C_3F{\cdot}CaCl_2{\cdot}10H_2O$ since the low $C_3A$ content could not explain the Friedel's salt peaks found in the

XRD patterns of the paste. This indirectly meant that the $C_4AF$ phase was mainly responsible for chloride binding in that case.

The published results, presented in the previous three subsections, show that the roles of cement phases in chloride binding are not well understood. Nevertheless, some facts can be learned from those results which further the understanding of the roles of cement phases. Despite the different opinions regarding the role of $C_3A$, the published results indicate that $C_3A$ is more likely to significantly influence the chloride binding capacity of cement. After all, two studies (*Ramachandran et al., 1984; Blunk et al., 1986*) showed the high binding capacities of pure $C_3A$ pastes. Furthermore, most studies, (especially in the case of admixed chloride) indicated that cements with higher $C_3A$ contents had higher binding capacities. However, those studies that showed little influence of the $C_3A$ content on the binding capacity (all of them in the case of external chloride) cannot be disregarded, and indicate that the source of chlorides (internal or external) might have a significant influence on the binding capacity of $C_3A$, and hence, on the effect of $C_3A$ content on the binding capacity. They might also indicate the possibility that other factors play significant roles in the binding process. The $C_3S$ seems to be one of those factors as more than one study show that pure $C_3S$ pastes bind significant amounts of chloride in comparison with cement pastes. As for $C_4AF$ it is possible that its role is not minor, but more studies are needed to show this role.

### 2.4.2 Supplementary Cementing Materials

#### 2.4.2.1 Fly Ash:

Most published results in the literature indicate a beneficial effect of fly ash replacement on chloride binding *(Byfors et al., 1986; Byfors, 1986, Arya et al., 1990; Arya & Newman, 1990; Hussain & Rasheeduzzafar, 1994; Arya & Xu, 1995; Dhir et al., 1997; Maslehuddin et al., 1997; Wiens & Schiessl, 1997)* as shown in Table 2-1. The reasons for this effect are attributed mainly *(Jones et al., 1993)* or partly *(Glass et al., 1997)* to the high alumina content, increase in chloride adsorption *(Arya et al., 1990; Dhir et al., 1994)*, or both *(Wiens & Schiessl, 1997)*.

*Dhir et al. (1994)* found fly ash concrete (with admixed chloride at 0.1%, and 2% by mass of cement) had reduced free chloride concentration compared to OPC concrete from as early as 7

Table 2-1: Summary of studies on the effect of cement substitution with fly ash on chloride binding

| **Admixed Chloride** | | | | | |
|---|---|---|---|---|---|
| Author | type of mix W/CM | $Cl^-$ content (% wt cement) | Replacement level (%) | Age (days) | Effect on $Cl^-$ binding |
| Arya et al. (1990) | Paste 0.5 | 1.0 (NaCl ) | 30 (Class F) | 28 | Increase |
| Arya & Newman (1990) | Paste 0.5 | 0.5, 1.0, 2.0 (NaCl, $CaCl_2$) | 30 | 28 | Increase |
| Arya & Xu (1995) | Paste 0.5 | 1.0 (NaCl) | 35 | 4, 7, 28, 90, 180 | Increase |
| Byfors et al. (1986) | Paste, 3 Type I 0.6 | 1.0 (NaCl ) | 25 | 90 | Increase |
| Holden et al. (1983) | Paste 0.5 | 0.4 (NaCl) | 30 (Class F) | 84 | Little Effect |
| Hussain & Rasheeduzzafar (1994) | Paste (Types I,V) 0.6 | 0.3, 0.6, 1.2 (NaCl) | 30 (Class F) | 180 | Increase |
| Kayyali & Quasrawi (1992) | Paste 0.4 | 1.0, 2.0, 2.5 (NaCl) | 30 (Class F) | 28, 84 | Increase* |
| Maslehuddin et al. (1997) | Mortar 0.5 | 0.8 (NaCl) | 20 (ClassF, Class C) | 90 | Increase |
| **External Chloride** | | | | | |
| Author | type of mix W/CM | [ $Cl^-$ ] (mole/L) | Replacement level (%) | Age, Exposure (days) | Effect on $Cl^-$ binding |
| Arya et al. (1990) | Paste 0.5 | 0.56 (NaCl) | 30 (Class F) | 28, 28 | Increase |
| Byfors (1986) | Paste 0.4 | 0.085, 0.56, 2.26 (NaCl) | 25 | 240, 7 | Increase |
| Dhir et al. (1997) | Paste 0.55 | 0.1, 0.5, 1.0, 5.0 (NaCl) | 17, 33, 50, 67 | 42, 14 | Increase |
| Nagataki et al. (1993) | Paste 0.5 | 0.54 (NaCl) | 30 | 28, 91 | Decrease |
| Wiens & Schiessl (1997) | Paste 0.5 | 0.05, 0.1, 0.5 (NaCl) | 20, 40 (Class F) | 365, 14 | Increase |

days of hydration and suggested that chemisorption was an important effect since fly ash concretes were not expected to bind chloride at an early age due to their slow pozzolanic reactivity. The results of *Arya & Xu (1995)* also show significantly lower chloride concentrations in the pore solution of cement-fly ash paste (35% fly ash, admixed chloride at 1% by mass of cement) compared to plain cement paste, from as early as 4 days of hydration.

*Hussain & Rasheeduzzafar (1994)* found an increase in the chloride binding capacities of an ASTM Type I and Type V cements (admixed chlorides; 0.3%, 0.6%, 1.2% by mass of cementitious materials) with the addition of a Class C and Class F fly ash (30% replacement level). Their DTA results showed that Friedel's salt peak was slightly shallower in the fly ash cement than in the plain cement indicating a reduction in Friedel's salt in the fly ash cement paste. They attributed this to the dilution of $C_3A$ in the fly ash cement, and attributed the increased binding capacity to the higher binding capacity of the fly ash itself without explaining the mechanism. *Kouloumbi & Batis, (1994)* and *Wiens and Schiessl (1997)*, on the other hand, reported an increase in Friedel's salt (XRD results) as a result of cement substitution with fly ash.

The results that were obtained by *Kayyali and Qasrawi (1992)* showed that the beneficial effect of fly ash replacement on chloride binding is dependant on the initial curing period and will be enhanced with longer initial curing. This was attributed to increased pozzolanic reaction. However, they found that the presence of fly ash was harmful to chloride binding when the fly ash cement pastes were subjected to carbonation. The effect was more pronounced with longer initial curing period. In another study *Kayyali and Haque (1995)* found that the presence of fly ash in concretes, containing a superplasticiser, did not have a beneficial effect on chloride binding. *Arya et al. (1990)* noticed that the beneficial effect of fly ash was considerably less pronounced in pastes subjected to external chlorides than in those containing internal chloride.

*Wiens and Schiessl (1997)*, using the Tang and Nilsson equilibrium method, found that the binding capacities of fly ash pastes were dependant on the grain size of the immersed samples. After a 14 days immersion period, the fly ash pastes had higher binding capacities than the cement paste at a grain size distribution of 0.063-0.125 mm, and slightly lower binding capacities at a grain size distribution of 0.5-1.0 mm. They attributed the lower binding capacities in the case of the 0.5-1 grain size distribution to the fact that some pore spaces and pore walls are not reached during the 14 days

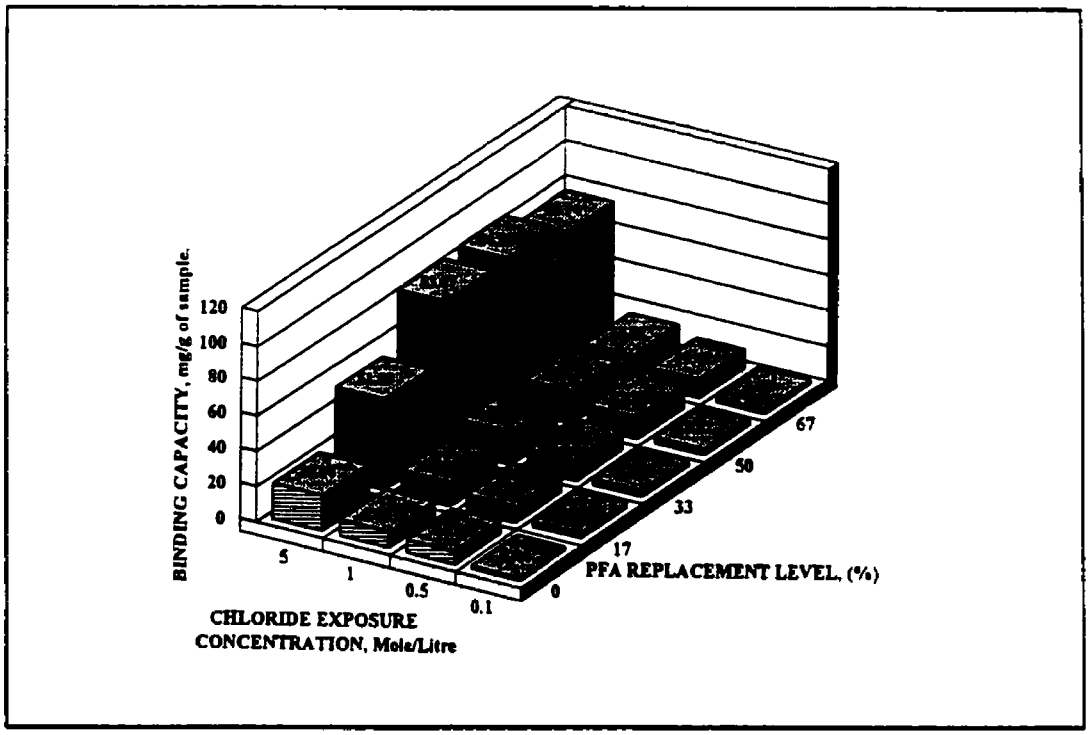


Figure 2-8: Chloride binding capacity of cementitious pastes, as a function of chloride exposure concentration and fly ash replacement levels (equilibrium method). From *Dhir et al. (1997)*.

immersion period due to the microstructural densification in the fly ash pastes. *Dhir et al (1997)*, also using the Tang and Nilsson equilibrium method found the chloride binding capacity to increase with the increase in the fly ash replacement level up to an optimum level of 50% and then decline at 67%, although still higher than that of the plain cement paste, as shown in Figure 2-8. *Nagataki et al. (1993)*, however, found that the addition of fly ash (30%) reduced the chloride binding capacity of cementitious paste in the case of external chlorides.

### 2.4.2.2 Slag:

The published data on the effect of slag on chloride binding show that cement substitution with ground granulated blast furnace slag (GGBFS) enhanced the chloride binding capacity in most cases *(Holden et al., 1983; Arya et al., 1990; Arya & Newman, 1990; Nagataki et al., 1993; Arya & Xu, 1995; Dhir et al., 1996; Maslehuddin et al., 1997; Xu, 1997)* as shown in Table 2-2.

Table 2-2: Summary of studies on the effect of cement substitution with GGBFS on chloride binding

| **Admixed Chloride** | | | | | |
|---|---|---|---|---|---|
| Author | type of mix W/CM | $Cl^-$ content (% wt cement) | Replacement level (%) | Age (days) | Effect on $Cl^-$ binding |
| Arya et al. (1990) | Paste 0.5 | 1.0 (NaCl ) | 70 | 28 | Increase |
| Arya & Newman (1990) | Paste 0.5 | 0.5, 1.0, 2.0 ($NaCl$, $CaCl_2$) | 70 | 28 | Increase |
| Arya & Xu (1995) | Paste 0.5 | 1.0 (NaCl) | 65 | 4, 7, 28, 90, 180 | Increase |
| Holden et al. (1983) | Paste 0.5 | 0.4 (NaCl) | 65 | 84 | Increase |
| Maslehuddin et al. (1997) | Mortar 0.5 | 0.8 (NaCl) | 70 | 90 | Increase |
| Xu (1997) | Paste 0.5 | 1.0 ($NaCl$, $CaCl_2$) | 65 | 180 | Increase[1] |
| **External Chloride** | | | | | |
| Author | type of mix W/CM | [ $Cl^-$ ] (mole/L) | Replacement level (%) | Age, Exposure (days) | Effect on $Cl^-$ binding |
| Arya et al. (1990) | Paste 0.5 | 0.56 (NaCl) | 70 | 28, 28 | Increase |
| Dhir et al. (1997) | Paste 0.55 | 0.1, 0.5, 1.0, 5.0 (NaCl) | 33.3, 50.0, 66.7 | 42, 14 | Increase |
| Nagataki et al. (1993) | Paste 0.5 | 0.54 (NaCl) | 30 | 28, 91 | Increase |

Some workers suggested that the relatively high aluminate content in GGBFS is one possible reason for the higher binding capacity *(Kouloumbi & Batis, 1994; Dhir et al., 1996; Glass et al., 1997)*. But, others have indicated that the increase in the amount of adsorbed chloride is responsible for the higher binding capacity *(Arya et al., 1990; Geiseler et al., 1995; Tang, 1996)*.

*Dhir et al. (1996)* found an increase in chloride binding with increasing GGBFS replacement levels in the case of pastes exposed to external chloride solutions of variuos concentrations, as shown in Figure 2-9. The increase was 5 times for the 66.7% replacement level and for an exposure solution of 5 mole/litre. The effect of GGBFS was attributed to the increase of the aluminate content

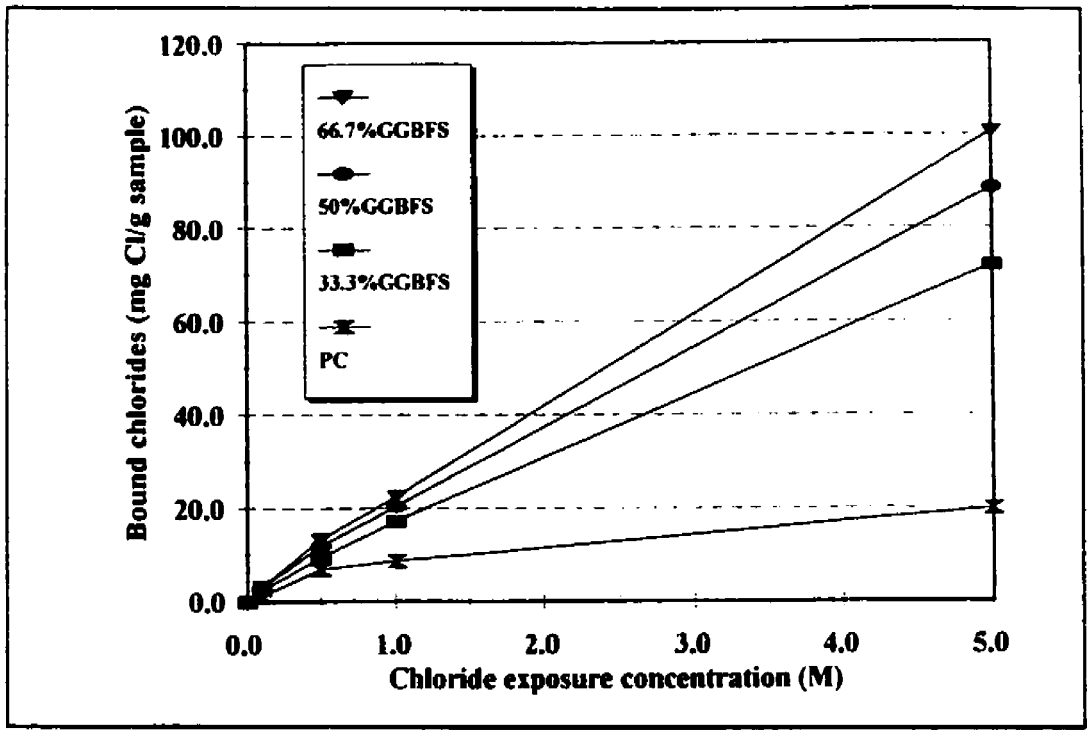


Figure 2-9: Chloride binding capacity of cementitious pastes, as a function of chloride exposure concentration and GGBFS replacement levels (equilibrium method). From *Dhir et al. (1996)*

of the cement-GGBFS pastes, leading to an increase in the production of Friedel's salt. Thermal analysis of some samples (PC & 50%GGBFS) showed an increase in Friedel's salt in the samples containing GGBFS. Results by *Kouloumbi & Batis (1994)* also showed an increase in Friedel's salt in mortars containing 50% GGBFS.

*Arya and Xu (1995)* studied the chloride binding capacity of cement pastes with admixed chlorides (1% $Cl^-$ by mass of cement). They found the highest chloride binding in a mix with 65% GGBFS replacement level compared to three other mixes with plain OPC, OPC with 30% FA, and OPC with 10% SF. The higher binding capacity of the GGBFS paste was obvious from as early as 4 days of hydration, and the chloride concentration seem to stabilize around 28 days.

*Arya et al. (1990)* found that the OPC with 70% replacement level GGBFS has a higher binding capacity both for admixed and external chlorides. However, they noticed that the binding capacity is lower in the case of exposure to external chloride than in the case of admixed chlorides.

*Andrade and Page (1986)* found that GGBFS cements had a higher chloride binding than plain cement both in the case of NaCl addition and $CaCl_2$ addition. *Xu (1997)* concluded that the main reason for the higher binding capacity of the GGBFS cement he tested is because of its lower

sulphate content. In other words, the beneficial effect of the GGBFS is caused by the dilution of sulphates in the GGBFS cement mixture. *Xu (1997)* came to this conclusion after finding that the higher binding capacity of the GGBFS cement dissapears when its sulphate content is raised to the same level as the one in the plain cement. It is interesting to note that results by *Holden et al.(1983)* indicate that the addition of sulphates to plain and blended cements had a significantly more negative effect on GGBFS cement paste than on plain cement paste, and the free chloride concentrations in both pastes were much closer to each other after the addition of sulphate. This evidence shows the significance of sulphate dilution, as a result of the GGBFS addition, in improving the chloride binding capacity of GGBFS cement. However, it does not exclude the possibility of other important reasons behind the increase in chloride binding, such as the higher aluminate content in GGBFS, which might lead
to higher levels of formation of Friedel's salt.

**2.4.2.3 Silica Fume:**

Except for a few studies *(Byfors, 1986; Byfors et al., 1986; Talib et al., 1994)*, most studies *(Page & Vennesland, 1983; Arya et al., 1990; Arya & Newman, 1990; Rasheeduzzafar et al., 1991; Sandberg & Larsson, 1993; Arya & Xu, 1995)* indicate that chloride binding decreases with an increase in the level of cement replacement with silica fume as shown in Table 2-3.

*Page and Vennesland (1983)* found that the replacement of Portland cement by increasing percentages of silica fume results in a progressive decrease in chloride binding of the cement pastes with admixed chloride ( 0.4 and 1 % by mass of cement) as shown in Figure 2-10. The authors reported that DTA and DTG analysis indicated a regular decrease in the quantity of Friedel's salts with the increase in silica fume content. They attributed the reduction in chloride binding to the increase in the solubility of Friedel's salts due to the reduction of the pH of the pore solution as a result of silica fume addition. However, several studies showed that an increase in the pH of the pore solution has an inhibiting effect on chloride binding *(Tritthart, 1989; Sandberg and Larsson, 1993)*. *Rasheeduzzafar et al. (1991)* found a decrease in the binding capacities of pastes with 10% and 20% silica fume respectively (admixed chloride at 0.6% and 1.2% by mass of cement) compared to that of the plain cement paste. The DTA results showed a reduction in Friedel's salt in the pastes with silica fume.

Table 2-3: Summary of studies on the effect of cement substitution with silica fume on chloride binding.

| Admixed Chloride | | | | | |
|---|---|---|---|---|---|
| Author | type of mix W/CM | $Cl^-$ content (% wt cement) | Replacement level (%) | Age (days) | Effect on $Cl^-$ binding |
| Arya et al. (1990) | Paste 0.5 | 1.0 (NaCl ) | 10 | 28 | Decrease |
| Arya & Newman (1990) | Paste 0.5 | 0.5, 1.0, 2.0 (NaCl, $CaCl_2$) | 10 | 28 | Decrease |
| Arya & Xu (1995) | Paste 0.5 | 1.0 (NaCl) | 10 | 28, 180 | Decrease |
| Byfors et al. (1986) | Paste 0.6 | 1.0 (NaCl ) | 10 | 90 | Increase |
| Maslehuddin et al. (1997) | Mortar 0.5 | 0.8 (NaCl) | 10 | 90 | Little Effect |
| Page & Vennesland (1983) | Paste 0.5 | 0.4, 1.0 (NaCl) | 10, 20, 30 | 35, 70 | Decrease |
| Rasheeduzzafar et al. (1991) | Paste 0.6 | 0.6, 1.2 (NaCl) | 10, 20 | 180 | Decrease |
| Talib et al. (1994) | Paste 0.6 | 0.6, 1.2 (NaCl) | 5, 10, 15, 20, 25 | 90 | Increase |
| **External Chloride** | | | | | |
| Author | type of mix W/CM | [ $Cl^-$ ] (mole/L) | Replacement level (%) | Age, Exposure (days) | Effect on $Cl^-$ binding |
| Arya et al. (1990) | Paste 0.5 | 0.56 (NaCl) | 10 | 28, 28 | Decrease |
| Byfors (1986) | Paste 0.4 | 0.085, 0.56, 2.26 (NaCl) | 10 | 240, 7 | Increase |
| Sandberg & Larsson (1993) | Paste 0.4, 0.5, 0.6, 0.75 | 0.1, 0.2, 0.4, 0.8 (NaCl) | 5 | 90, 90 | Decrease |

*Arya et al. (1990)* found that the partial replacement of Portland cement with 15% silica fume caused a decrease in chloride binding of cement paste both in the case of admixed chlorides and external chlorides. However, the results in the case of external chlorides are not conclusive sincethe samples with silica fume were not in equilibrium with the external chloride solution at the time of the test. *Sandberg & Larsson (1993)* found a decrease in the chloride binding capacity of a cement

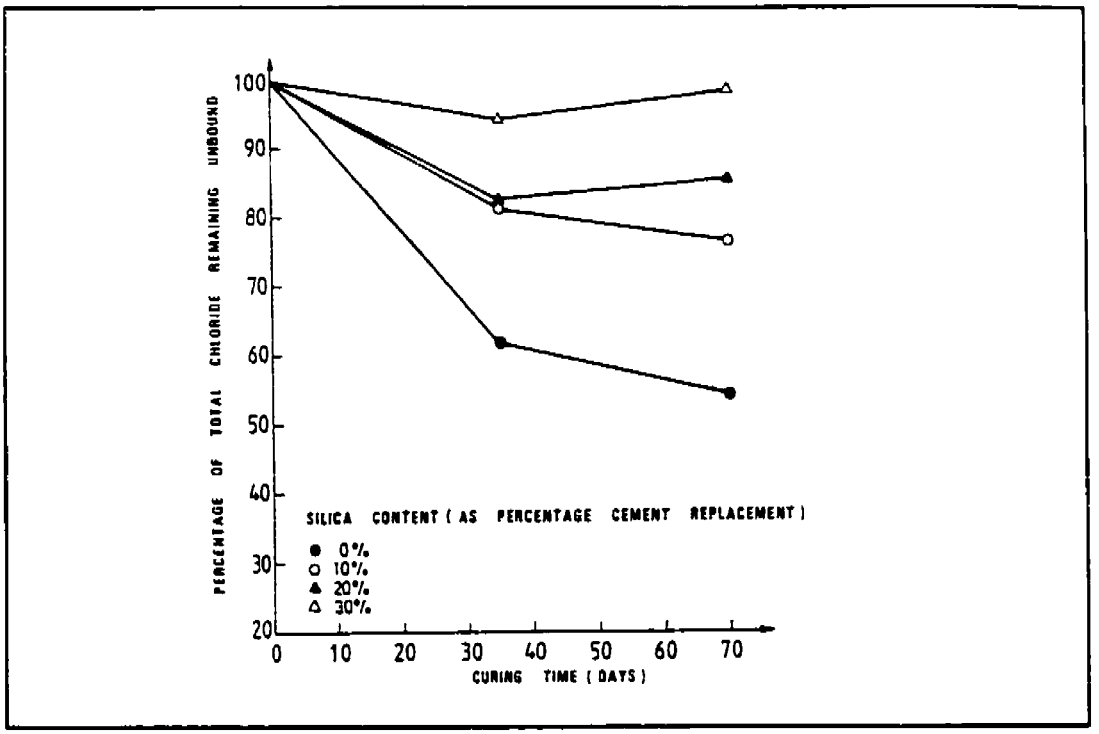


Figure 2-10: Free chloride in the pore solution expressed from plain and silica fume blended cement pastes with 1% (by mass of solids) chloride addition. From *Page & Vennesland (1983)*.

paste, exposed to external chloride solution, when cement was partially substituted with 5% silica fume. Few studies showed that partial replacement of cement with silica fume increase the binding capacity. The results by *Byfors (1986, 1990)* showed that the addition of 10% silica fume to an OPC increased its chloride binding capacity when exposed to external chloride solution as shown in Figure 2-6. *Byfors et al. (1986)* found similar results in the case of silica fume blended cement with admixed chloride. They attributed this increase to the higher specific surface area of the gel in the silica fume cement paste. *Talib et al.(1994)* found a steady increase in chloride binding with addition of silica fume up to an optimum of 15%, followed by a decrease for 20 and 25% addition. But even at 25% replacement the chloride binding was higher than for the mix with plain cement. They attributed this behaviour to the interactive effect of increased chloride binding and increased solubility of Friedel's salt due to the lower pH of the pore solution.

*Nilsson et al.(1996)* indicated that silica fume addition to cement influences binding in at least three ways: 1) the C-S-H content increases which they assume would increase binding, 2) the pH is reduced which should increase binding, 3) the $C_3A$ content will be lower which should

decrease binding. They reported results obtained by Sandberg that show the binding to decrease with the addition of 5% silica fume to cement, while keeping the $OH^-$ concentration constant.

The review of the literature on the effect of SCM on chloride binding showed that cement partial substitution with fly ash and GGBFS generally results in an increase in the binding capacity while cement substitution with silica fume generally results in a reduction in the binding capacity. The mechanisms behind these changes are not well understood, as reflected by the different interpretations of the observed changes. One of the reasons often used to explain the increase in binding is the increase in C-S-H leading to an increase in chloride adsorption. However, the C-S-H also increase in the case of silica fume cements. Yet, most results indicate that cement partial substitution with silica fume reduces the binding capacity. Dilution of the $C_3A$ is not likely to fully account for the observed reductions, especially at 10% replacement levels. Therefore, it is possible that the C-S-H binding properties depend on factors other than the surface area alone. *Larsen (1998)* and *Wowra & Setzer (2000)* suggested that the binding capacity of the C-S-H is dependent, among other factors, on the presence of $Ca^{2+}$ in the pore solution and the pore solution composition. Also, it has been suggested that the adsorptional binding capacity of the C-S-H depends on the C/S ratio, with a lower ratio resulting in a lower binding capacity *(Beaudoin et al., 1990)*. This might explain why, despite the increase in C-S-H as a result of partial substitution with silica fume, the binding capacity was reduced in most cases. This argument might also apply in the cases of cement substitution with fly ash or GGBFS, and the assumption that physical binding (adsorption) increases as a result of these substitution might not nessecarily be true in all cases. The positive effect of the high aluminate content in fly ash and GGBFS has been reported in some studies *(Kouloumbi & Batis, 1994; Wiens & Schiessl, 1997; Dhir et al., 1997)*. Results by *Wiens & Schiessl (1997)* (external chloride) suggest that the high aluminate and ferrite content of the fly ash was responsible for an important part of the improvement in binding capacity of the cement-fly ash paste. However, DTA results by *Hussain & Rasheeduzzafar (1994)* (admixed chloride) showed a slightly lower Friedel's salt content in the cement-fly ash paste than in the plain cement paste despite the higher binding capacity of the former paste. These results suggest that more than one mechanism are responsible for the observed changes in binding capacities, and these mechanisms might be dependent on many factors including the fly ash used (since they vary significantly in composition), the cement type, the source of chloride (admixed or external), pore solution composition, and testing conditions.

### 2.4.3 Chloride Concentration

It is obvious from the literature that the chloride concentration in the pore solution is one of the most decisive factors in chloride binding. This was shown in numerous studies on chloride binding *(Tuutti, 1982; Blunk et al., 1986; Byfors, 1986; Arya et al., 1990; Byfors, 1990; Sergi et al., 1992; Tang & Nilsson, 1993; Rasheeduzzafar et al., 1992; Suryavanshi et al., 1995; Dhir et al., 1996, 1997; Wiens & Shiessl, 1997; Wowra & Setzer, 1997)*. Most reported results indicated that the amount of bound chlorides increases with an increase in the chloride concentration in the pore solution. This was true in the case of admixed chlorides *(Tuutti, 1982; Blunk et al., 1986; Arya et al., 1990; Rasheeduzzafar et al., 1992; Suryavanshi et al., 1995)* and in the case of external chlorides *( Blunk et al., 1986; Byfors, 1986; Byfors, 1990; Sergi et al., 1992; Tang & Nilsson, 1993; Dhir et al., 1996, Wiens & Shiessl, 1997; Wowra & Setzer, 1997)*. However, there is no overall agreement on the form of the relationship between bound and free chlorides (binding isotherms). Some studies show a nonlinear relationship (*Byfors, 1986; Sergi et al., 1992; Tang & Nilsson, 1993; Wowra & Setzer, 1997*), while other studies show a linear relationship *(Tuutti, 1982; Arya & Newman, 1990; Dhir et al., 1996)*.

*Tang and Nilsson (1993)* described the relationship between free and bound chloride, to follow the Langmuir isotherms at low chloride concentrations (< 0.05 mol/l) and the Freundlich isotherm at concentrations higher than 0.01 mol/l. *Sergi et al. (1992)* found a non-linear relationship between free and bound chlorides. They used a Langmuir isotherm to represent this relationship. The solution to the modified Fick's second law, taking account of nonlinearity in binding, gave a better fit to the experimental free chloride profile than the one obtained with a linear approximation of the relationship between free and bound chlorides. *Byfors (1990)* obtained a unique relationship between free and bound chlorides which, despite being non-linear, was different in shape than the Langmuirian isotherm. In fact, this relashionship seems to follow a langmuirian shape until a certain concentration, then the chloride binding increases markedly at higher concentrations. *Byfors (1990)* attributed this to an increase in chloride adsorption on the pore walls at higher conctration, after the exhaustion of the chemical binding capacity.

On the other hand, *Tuutti (1982)* found a linear relationship and defined a factor $K_d$ which is the ratio between free and bound chlorides per unit weight of cement. *Arya and Newman (1990)* also found a linear relationship between free and total (or bound) chlorides with an intercept on the

total chloride axis. *Dhir et al. (1996)* found that the best fit for their chloride binding data (for a PC with different levels of GGBFS replacement) was a linear relationship.

While it is not possible to explain with certainty the reasons for the difference in the reported relationships, it is beneficial to mention some factors that might have contributed to the observed relationship. Among these factors is the range of chloride concentration (or total chloride contents) used in the tests, the number of chloride concentrations (or total chloride contents) tested, the accuracy of the fit, and experimental error.

**2.4.4 Cation Associated with Chloride:**

Several studies in the published literature indicate that the cation associated with chloride plays a significant role in chloride binding *(Tuutti, 1982; Blunk et al., 1986; Tritthart, 1989; Al Hussaini et al., 1990; Arya et al., 1990; Arya & Newman, 1990; Byfors, 1990; Wowra & Setzer, 1997, 2000; Xu, 1997)*. Most of these studies compare between NaCl and $CaCl_2$ since they are the most likely cations associated with chloride ions that will affect concrete structures. The results show that more chlorides are bound in the case of $CaCl_2$ than in the case of NaCl.

*Ben Yair (1974)* attributed the reduced chloride binding in the case of NaCl to the fact that NaCl has to react first with $Ca(OH)_2$ to form $CaCl_2$ before reacting with the aluminate phases to form Friedel's salt. *Arya et al. (1990)* who found increased chloride binding in the case of $CaCl_2$ compared to NaCl for both internal and external chlorides, explained that Friedel's salt is more readily formed in the presence of $CaCl_2$ than NaCl

*Tritthart (1989b)* concluded that the associated cations affect chloride binding through their influence on the hydroxide concentration in the pore solution. He compared the pore solutions compositions of OPC pastes with various admixed chloride salts and chloride salts combinations (1% by mass of cement). He found that chloride concentrations in the pore solutions of samples with otherwise identical composition, but with different chloride salts, were different only when their hydroxide concentrations were different. The results showed that the higher the hydroxide concentration, the higher the chloride concentration., and the addition of NaCl resulted in the highest chloride concentration, as shown in Figure 2-11. It is of interest to notice that while the addition of NaCl resulted in an increase in the hydroxide concentration, the addition of $CaCl_2$, $MgCl_2$, or HCl, resulted in a decrease in the hydroxide concentration, and the chloride and the hydroxide

concentrations in the pore solutions of pastes containing these salts were more or less the same. *Tritthart (1989b)* attributed the decrease in hydroxide concentration in the case of HCl to the reaction between the $H^+$ ions of the HCl and the $OH^-$ ions of the pore solution to form $H_2O$. The decrease in $OH^-$ ions in the cases of $CaCl_2$ and $MgCl_2$ was attributed to the precipitation of the $Ca^{2+}$ and $Mg^{2+}$ ions as $Ca(OH)_2$ and $Mg(OH)_2$ respectively in stongly alkaline solutions (such as that of cement paste). The increase in $OH^-$ ions concentration in the case of NaCl was attributed to the competition between $Cl^-$ and $OH^-$ ions for adsorption sites on the surface of cement hydrates, resulting in the replacement of some $OH^-$ ions by $Cl^-$ ions that are adsorbed instead.

*Blunk et al. (1986)* found more chlorides are bound from $CaCl_2$ than from NaCl. This was true for both admixed and external chlorides. The trend was more obvious at higher concentrations than at lower concentrations ( < 0.5% $Cl^-$ by mass of cement). It is interesting to notice that among the mixtures studied was a $C_3S$ and $C_3A$+gypsum pastes, and that the trend was noticeable for both mixtures. The significance of this is that the associated cation influences both chemical and physical binding. *Wowra & Setzer (1997, 2000)* also found, in the case of external chloride, that $C_3S$ paste bound more chloride derived from $CaCl_2$ than that derived from NaCl. They attributed the higher chloride binding in the case of $CaCl_2$ to the increase in anions adsorption ($Cl^-$ in this case) in the

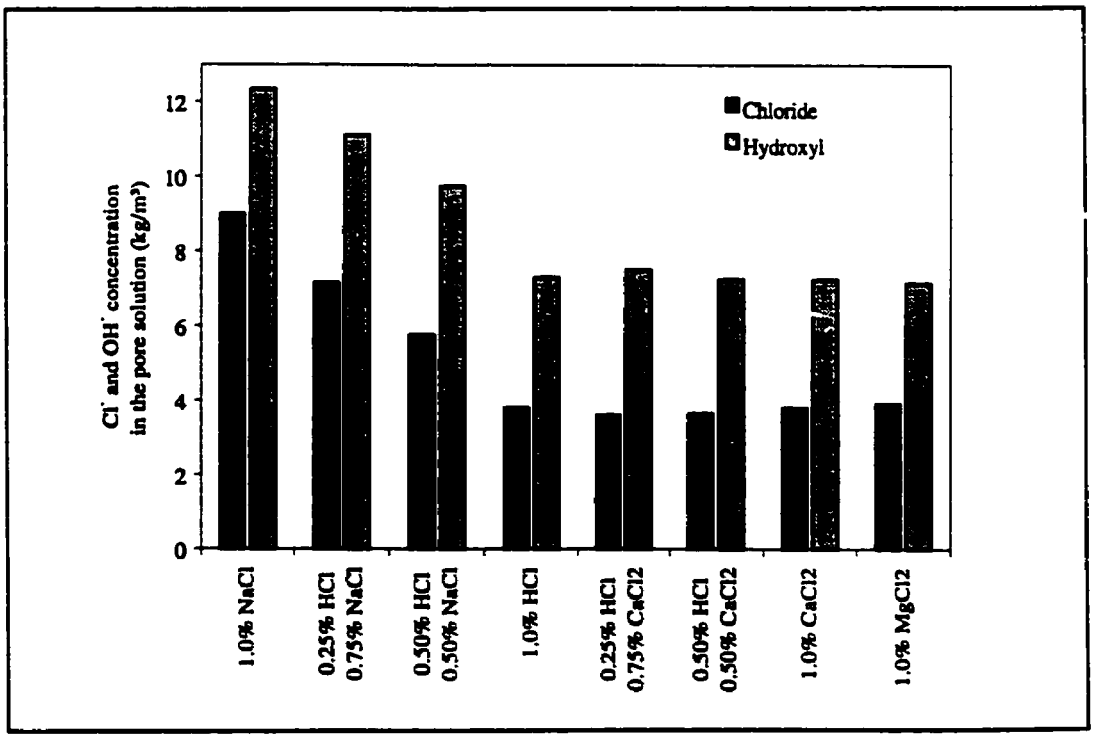


Figure 2-11: Influence of various chloride salts on the composition of the pore solution of OPC pastes with 1% (by mass of cement) chloride addition. From *Tritthart (1989b)*.

presence of calcium ions. They explained that the interaction between the calcium ions and the surface of the cement hydrates increased the number of adsorption sites and led to a more positive surface charge. This led to a possible enrichment of chloride ions (to balance the charge) in the electrical double layer.

*Arya and Newman (1990)* investigated pastes of W/CM = 0.5 that included SRPC, OPC and OPC with FA, GGBFS, and SF respectively. They found that greater proportions of chloride ions were bound from $CaCl_2$ than from NaCl for all mixes. *Xu (1997)* found a similar trend with OPC and OPC + GGBFS (70%) pastes (W/C=0.5) and with various levels of chloride treatement . *Tuutti (1982)* found that the amount of bound chlorides derived from $CaCl_2$ was higher than that derived from KCl. *Diamond (1986)* found that for a cement paste with admixed chlorides (added as $CaCl_2$ and NaCl), NaCl addtion resulted in a moderate reduction in chloride concentration compared to $CaCl_2$ for chloride treatment level of 0.2% and 0.5% (by mass of cement). NaCl addition resulted in a moderate increase when the treatment level was 1%. It should be mentioned that most of the other studies used chlorides levels equal or higher than 0.5.

It is obvious from the published results that more chloride is bound from $CaCl_2$ than from NaCl. This fact seems to apply in the case of physical binding (*Blunk et al., 1986; Wowra & Setzer ,1997, 2000)* as well as in the case of chemical binding *(Blunk et al., 1986)*. Two different reasons were given to explain the higher binding from $CaCl_2$ in the case of physical binding *(Tritthart, 1989b; Wowra & Setzer, 1997, 2000)* as mentioned before, and both might hold some truth. *Tritthart (1989b)* attributed the higher chloride binding from $CaCl_2$ to the decrease in pH, causing a decrease in the competition of $OH^-$ ions (with $Cl^-$ ions) for adsorption sites. *Wowra & Setzer (1997)* said that the increase in binding was induced by the adsorption of the $Ca^{2+}$ ions on the solid surface of the C-S-H, causing a reverse of surface charge (form positive to negative) or an increase in the positive charge of the surface and a consequent enrichement of $Cl^-$ (and other anions) in the electrical double layer. *Wowra & Setzer (1997)* considered the decrease in pH in the presence of $CaCl_2$ a direct result of the adsorption reactions, resulting in the adsorption of $Ca^{2+}$ ions and the release of $H^+$ ions as follow:

$$SiOH + Ca^{2+} \leftrightarrows SiOCa^+ + H^+$$

In the case of chemical binding, there is no proposed mechanism that explains the higher binding from $CaCl_2$ except the explanation by *Ben Yair (1974)*, as mentioned earlier. Nevertheless,

since the use of $CaCl_2$ results in a lower pH than NaCl, it would be expected that more Friedel's salt is formed in the case of $CaCl_2$ than in the case of NaCl, since the results by *Roberts (1962)* showed an increased solubility of Friedel's salt (solubility was assessed by measuring the chloride concentration in the host solution) with an increased pH of the host solution.

### 2.4.5 Influence of Sulphate:

The presence of sulphate is another factor that has a significant influence on chloride binding. Sulphate, as a cement component or as an outside agent that permeates into the hardened cement paste, has an inhibiting effect on chloride binding as the results in the literature suggest *(Holden et al., 1983; Blunk et al., 1986; Byfors, 1986, 1990; Sandberg & Larsson, 1993; Maslehuddin et al., 1997; Wowra & Setzer, 1997; Hussain & Rasheeduzzafar, 1994; Hussain et al., 1994; Xu, 1997).*

*Holden et al. (1983)* found a significant decrease in chloride binding as a result of sodium sulphate addition (1.5% $SO_3$ by mass of cement) to a series of Portland cement and blended cement paste (W/C=0.5) with admixed chlorides (0.4% Cl by mass of cement added as NaCl). The hydroxyl ion concentration increased significantly as well. The authors attributed the decreased chloride binding to the tendency of sulphate ions to react preferentially with $C_3A$ therefore preventing the formation of Friedel's salt. *Roberts (1962)* found an increased solubility of calcium chloroaluminates or Friedel's salts in calcium sulphate solutions, with saturated lime or without lime, compared to water or saturated lime solutions.

*Blunk et al. (1986)* examined the influence of equivalent addition (0.1 mole/kg cement) of sulphates (added as $CaSO_4$ and $Na_2SO_4$) and alkali hydroxide (added as $Na_2O$) on the chloride concentration in the pore solution of a Portland cement paste (W/C=0.5, 0.4% admixed $Cl^-$ by mass of cement). The $CaSO_4$ addition caused a slight increase in $Cl^-$ concentration while the $Na_2SO_4$ doubled the concentration. The addition of $Na_2O$ caused a significant increase in the chloride concentration. The authors argued that since $Na_2SO_4$ and $Na_2O$ increased the $OH^-$ concentration in the same range, the effect of $Na_2SO_4$ on chloride binding was the result of the action of both $OH^-$ and $SO_4^-$ anions.

*Hussain & Rasheeduzzafar (1994)* also observed the negative effect of sulphate addition to cements on chloride binding as shown in Figure 2-12. They attributed the increase in the $OH^-$ concentration in the pore solution following the addition of $Na_2SO_4$, to the reaction between $Na_2SO_4$ and $Ca(OH)_2$ which results in the formation of NaOH. The results of differential thermal analysis (DTA) and thermo-gravimetric analysis (TGA) showed a decrease in $Ca(OH)_2$ and Friedel's salt in the sample containing $SO_3$ compared to the one without sulphates. They suggested that the increase in chlorides in the pore solution due to $Na_2SO_4$ addition might be caused by either an increase in the alkalinity of the pore solution or the preferential combination of $C_3A$ with sulphate ions.

*Xu (1997)* studied the influence of $Na_2SO_4$ and $CaSO_4$ addition (2 to 9% by mass of cement) on the binding capacities of OPC and OPC with GGBFS (65% replacement) cement pastes (W/CM=0.5) with admixed chlorides (1% $Cl^-$ by mass of cement added as NaCl or $CaCl_2$). The results showed a very significant decrease in chloride binding as a result of the sulphate addition as shown in Figure 2-13 . The $Na_2SO_4$ addition had a more negative effect on chloride binding than

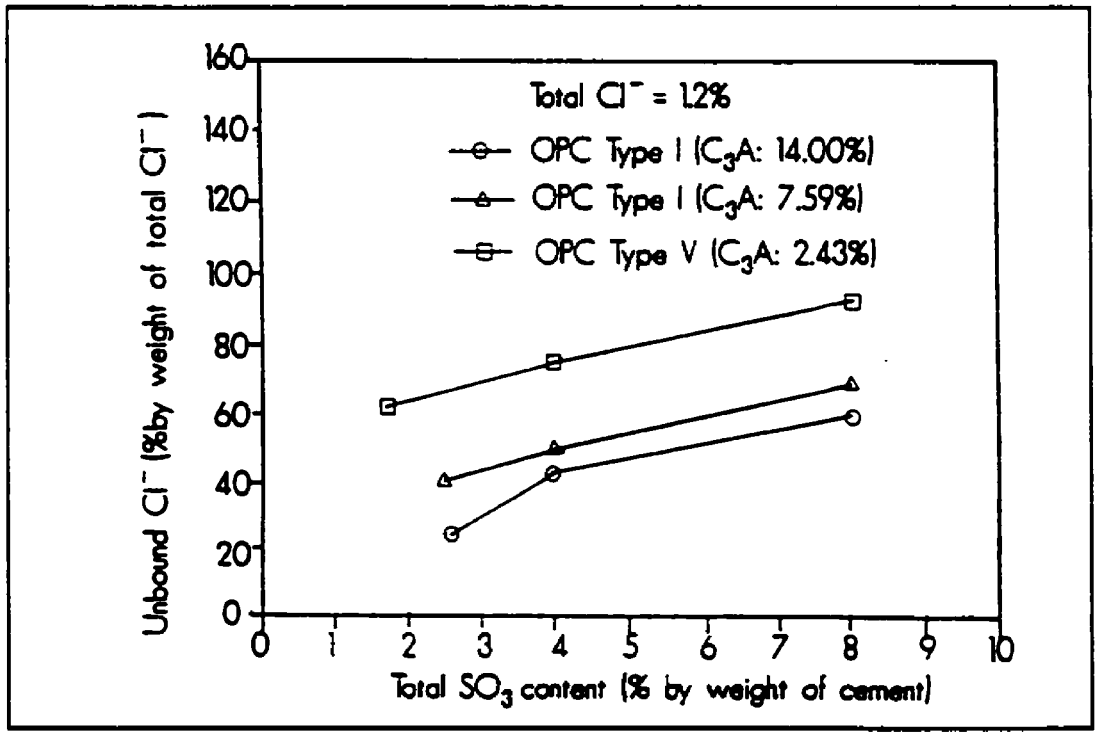


Figure 2-12: Effect of sulphates on the free chloride in the pore solution of cement pastes with 1.2% (by mass of cement) admixed chloride. From *Hussain & Rasheeduzzafar (1994)*.

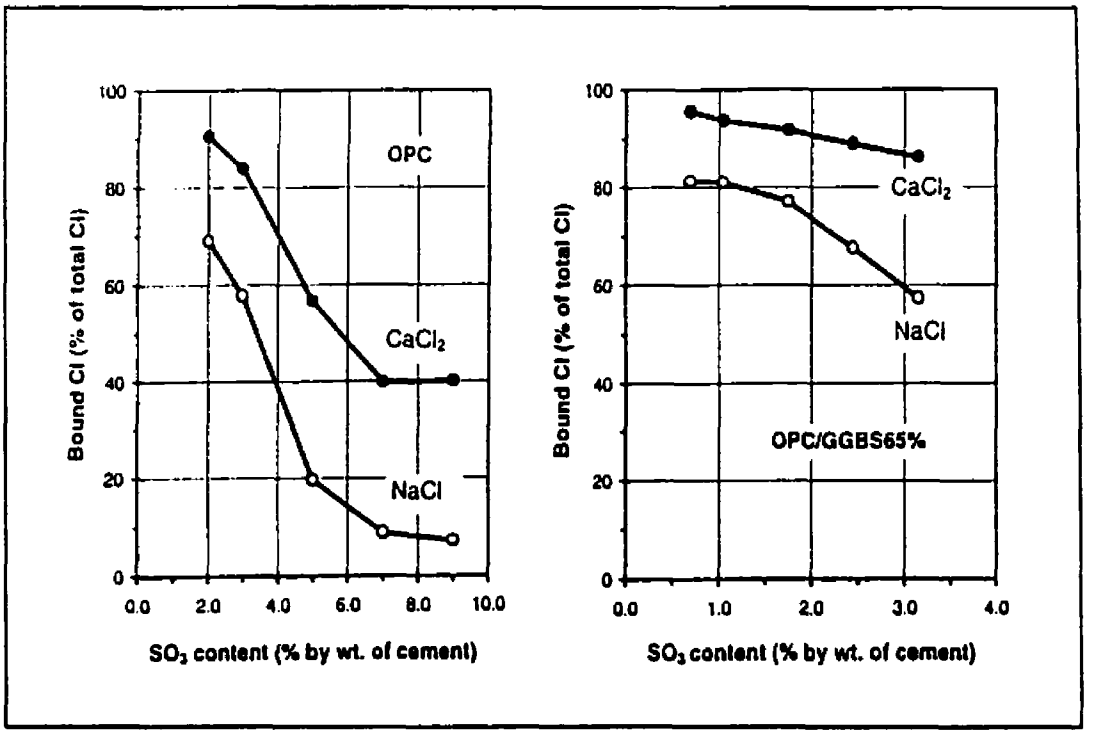


Figure 2-13: Effect of sulphate on the chloride binding capacity of an OPCpaste with 1% (by mass of cement) chloride derived from NaCl and $CaCl_2$. From *Xu (1997)*.

the $CaSO_4$. The $Na_2SO_4$ and $CaSO_4$ had opposite effects on the pore solution alkalinity. $Na_2SO_4$ increased the alkalinity while $CaSO_4$ reduced it. *Xu (1997)* suggested that the negative effect of $Na_2SO_4$ on chloride binding might be partly due to the increased alkalinity of the pore solution as a result of the $Na_2SO_4$ addition.

Few studies were done on the effect of sulphates on chloride binding in the case of external chlorides *(Byfors, 1986, 1990; Sandberg & Larsson, 1993; Wowra & Setzer, 1997)*. *Byfors (1986, 1990)* found a decreased chloride binding with increasing sulphate concentration (0 - 0.06 M $SO_4^{2-}$) in the host solutions. However, there was a relatively large scatter in her data. *Sandberg & Larsson (1993)* found the effect of sulphates in reducing chloride binding to be small relative to the significant effect of the hydroxyl ions. *Wowra and Setzer (1997)* investigated the influence of sulphate on the chloride binding capacity of a $C_3S$ paste (W/C=3). Their results showed that the chloride binding of $C_3S$ paste was reduced in the presence of sulphate ($CaSO_4$, 0.0074 M) in the host solutions.

The published results clearly indicate the negative effect of sulphates on the chloride binding capacity. Few results show that sulphates negatively affect the chemical *(Roberts, 1962)* and the physical *(Wowra & Setzer, 1997)* chloride binding capacties, as mentioned earlier. In the case of

chemical binding, and in the presence of chloride and sulphate, many suggest that $C_3A$ combines preferentially with sulphate and less Friedel's salt is formed *(Roberts, 1962; Holden et al., 1983; Hussain & Rasheeduzzafar, 1994)*. Even when the ion exchange mechanism is suggested as the mechanism by which chloride ions are bound, according to *Yonezawa et al. (1989)*, they reported that sulphate ions are more preferred in terms of the affinity between the negative ion exchanger and $Cl^-$, $OH^-$, and $SO_4^{2-}$ ions according to the following equation:

$$SO_4^{2-} > Cl^- >> OH^-.$$

In the case of physical binding, the presence of $SO_4^{2-}$ ions with $Cl^-$ ions in the pore solution would increase the competition for adsorption in the electrical double layer, resulting in higher amount of free chloride in the pore solution.

**2.4.6 Hydroxyl Ion Concentration:**

*Tritthart (1989)* obtained interesting results regarding the influence of hydroxyl ion concentration in the pore solution on the chloride binding. He investigated the influence of several chloride salts with different associated cations (NaCl, $CaCl_2$, HCl, $MgCl_2$), on the chloride binding of cement pastes with the same composition except for the type of admixed chloride salt. The results showed that the chloride concentrations in samples with otherwise identical composition, but with different chloride compounds, were different only when their hydroxide concentrations were different too as shown in Figure 2-11. *Tritthart (1989)* regarded the increase in hydroxide concentration upon the addition of NaCl as indicative of an adsorptive binding of $Cl^-$ and $OH^-$ apart from a chemical, and that $Cl^-$ and $OH^-$ compete for available adsorption sites. So, for a given total chloride content, the more chloride is bound the less hydroxyl ions compete for the adsorption site, which means the lower the hydroxide concentration in the pore solution.

*Roberts (1962)* showed the negative effect of a higher pH on the solubility of Friedel's salt. His results indicate that calcium chloroaluminate and chloroferrite are more soluble in an alkali solution saturated with lime than in a saturated lime solution and the solubility increases with an increase in the concentration of the alkali solutions (1 g of Friedel's salt or its ferrite equivalent in 150 ml solution). *Roberts (1962)* indicated that the dissolution of Friedel's salt was incongruent (solubility was measured through the equilibrium chloride concentration in the host solution) and

chloride was released into the solution. These results are important since they show the direct effect of hydroxide concentration on chemical binding (Friedel's salt).

*Blunk et al. (1986)* obtained a strong effect on chloride binding as a result of $Na_2O$ (0.62% by mass of cement) addition to a cement paste (W/C=0.5). Their data showed a significant increase in both $Cl^-$ and $OH^-$ concentration, indicating a decreased chloride binding with increased hydroxide concentration. *Hussain et al. (1995)* obtained a similar trend when they added NaOH to an OPC paste (W/C=0.6), that was treated with three levels of NaCl addition, to increase its original $Na_2O_e$ content from 0.65 % to 1.2%, indicating a decreased chloride binding with increased hydroxide concentration.

Few studies were done on the effect of pH on chloride binding in the case of external chloride. *Tritthart (1989)* found a negative effect of an increased pH value on chloride binding , when he conducted tests on cement pastes immersed in chloride solution with different pH. The results clearly showed the chloride binding increase with the decrease in pH of the host chloride solution as shown in Figure 2-14.

*Sandberg and Larsson (1993)* found a reduction in the chloride binding with increasing $OH^-$ concentration in the case of cement pastes immersed in synthetic pore solutions. The trend was clear

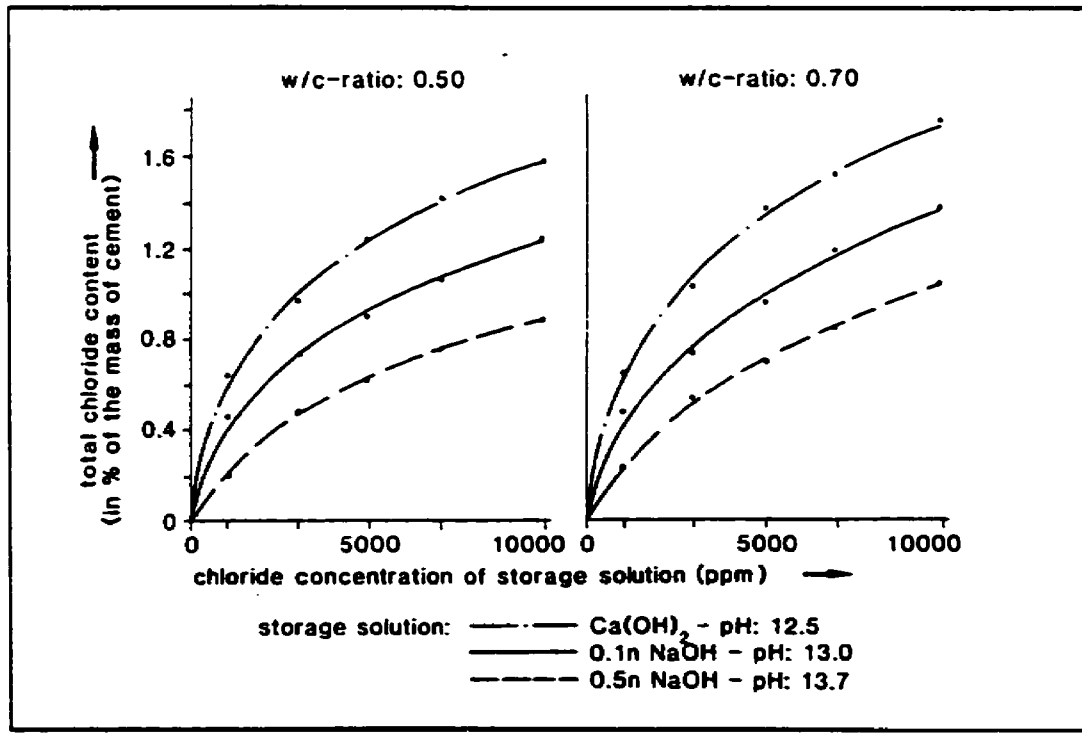


Figure 2-14: Chloride binding isotherms of cement pastes exposed to chloride solutions of different concentrations, and with different pH. From *Tritthart (1989b)*.

for all the cements studied (OPC, SRPC, and SRPC + 5% SF). *Byfors (1986, 1990)* obtained a similar trend in the case of cement pastes in equilibrium with external solutions. However, the trend was clear only up to 0.5 M hydroxide concentration and little effect was noticed above that concentration. It should be mentioned that the concentrations studied by *Sandberg & Larsson (1993)* and *Tritthart (1989)* were up to 0.64 M and 1 M respectively.

It is quite possible, as in the case of $SO_4^{2-}$ ion, the $OH^-$ ion concentration in the pore solution affects both the chemical and the physical binding capacities. The results by *Roberts (1962)* showed that the concentration of the $OH^-$ ions affected the solubility of Friedel's salt, and more chloride passed into the solution at higher $OH^-$ concentrations. *Roberts (1962)* indicated that in all the tests involving the treatement of Friedel's salt with various solutions (water, calcium Sulfate with and without saturated lime, saturated lime, sodium hydroxide and potassium hydroxide with crystalline calcium hydroxide) the equilibrium solution was incongruent, and that the final solid (at 25°C) was mostly a probable $C_3A.CaCl_2.aq.$-$C_4A.aq.$ solid solution, sometimes with aluminum hydroxide. It is therefore possible that the increase in $OH^-$ ion concentration led to the replacement of some $Cl^-$ ion by $OH^-$ ion (possibly by ion exchange) and the formation of the solid solution.

In the case of physical binding, if anions adsorption takes place in the electrical double layer as discussed earlier, then it would be expected that all anions in the pore solution (including $OH^-$) to compete for the adsorption sites. An increase in $OH^-$ ion concentration would probably result in less $Cl^-$ ions being bound.

### 2.4.7 Influence of Temperature:

The influence of temperature on chloride binding has been addressed by some workers, but the majority of the investigations were made on samples with admixed chloride. Most of the results indicate a decrease in binding capacity with an increase in temperature.

*Roberts (1962)* studied the influence of temperature on both an OPC and SRPC. The tests involved shaking mixes of cements and $CaCl_2$ (W/C = 1.5, 1.4% $Cl^-$ by mass of cement) at 25, 50, and 90°C, then filtering at specific periods and analysing the filtrates for chloride. He found an increase in chloride concentrations in the solutions as the temperature increased in the case of OPC. But the effect of temperature was very small in the case of SRPC. *Roberts (1962)* also found that the solubilities of Friedel's salt and its iron equivalent increase with an increase in temperature. It

is interesting to notice that the solubility of Friedel's salt did not increase significantly between 25°C and 50°C, but almost all the chloride passed into the solution at 90°C. The small effect of temperature on the binding capacity of the OPC and SRPC might be explained by the possibility that high temperature has a significant influence on the chemical binding capacity (Friedel's salt) and little influence on the physical binding capacity. Of course, it should also be assumed that the binding capacity of SRPC is mostly physical.

*Hussain & Rasheeduzzafar (1993)* examined the effect of temperature on the chloride concentrations in the pore solutions of 3 different Portland cements with $C_3A$ contents of 2.4, 7.6, and 14%. Three levels of admixed chlorides (from NaCl) were studied (0.3, 0.6, and 1.2% by mass of cement). The curing temperatures were 20 and 70°C. They found a strong increase in free chlorides in pore solutions for all three cements as the curing temperature was raised from 20 °C to 70 °C as shown in Figure 2-15. This effect was more pronounced for the higher $C_3A$ cements, which was in agreement with *Roberts (1962)* results. They attributed this to the fact that Type I cements bind significantly more chlorides as Friedel's salt than Type V cement, and that Friedel's salt decomposes at higher temperatures (similar to the interpretation given earlier).

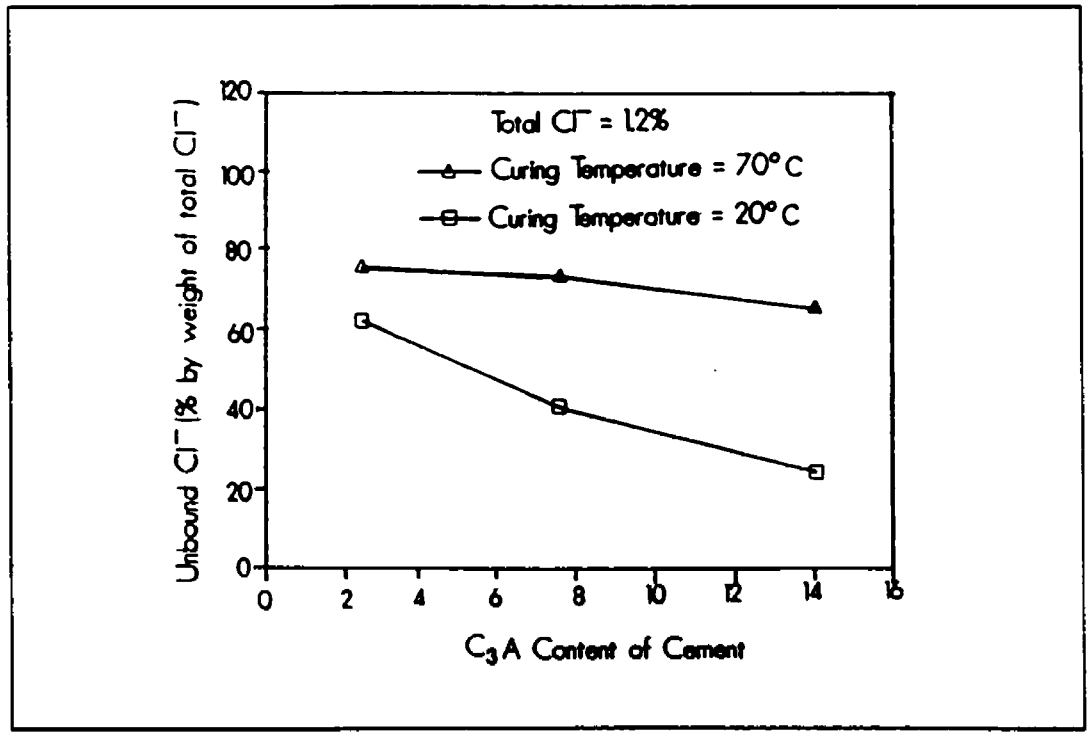


Figure 2-15: Effect of temperature on the free chloride in the pore solution of cement pastes with 1.2% (by mass of cement) admixed chloride. From *Hussain & Rasheeduzzafar (1993)*.

*Maslehuddin et al. (1996, 1997)* found a significant decrease in the chloride binding of mortars made with 2 OPCs (8.5% and 14.5% $C_3A$), an SRPC (3.5% $C_3A$), and several blended cements, when the curing temperature increased from 20°C to 40°C, 55°C, and 70°C. The chlorides were added at the time of mixing at a level of 0.8% $Cl^-$ by mass of cement.

*Larsen (1995)* found that an increase in temperature from 20 to 80 °C increased the chloride concentration in pore solution four times in both paste and mortar. It was not clear whether the chlorides were admixed or external.

Very few studies found an increase in binding with increasing temperature. *Arya et al. (1990)* examined the effect of temperature on OPC paste (28 days of age) with admixed chloride, and cured at temperatures of 8, 20, and 38°C. The results showed an increase in bound chlorides as the curing temperature increased. The increase between 20 to 38 °C was relatively small compared to that between 8 to 20 °C. The increase in binding was attributed to the faster reaction rates at higher temperatures.

*Wowra & Setzer (1997)* examined the effect of temperature (0°C and 20°C) on the chloride binding capacities of cement (2 types) and $C_3S$ pastes, using the equilibrium method (NaCl and $CaCl_2$ were used in the host solutions). They found an increased chloride binding with increased temperature in the case of $CaCl_2$ for both cements and the $C_3S$ paste. No significant effect of the temperature was observed in the case of NaCl.

### 2.4.8 Carbonation:

Very few studies have been done on the effect of carbonation on chloride binding. They show that carbonation reduces chloride binding. *Kayyali and Haque (1988)* studied the influence of accelerated carbonation on the chloride binding of mortar mixes made with Portland cement, with and without fly ash (30% replacement level), and with admixed chloride (1% $Cl^-$ by mass of cementitious material). The results showed a significant increase in chloride concentration in the pore solution of all carbonated mortars compared to the samples that were not carbonated. Longer curing periods were significantly beneficial in reducing the negative effects of carbonation on binding in the case of fly ash free mortars. But in the case of fly ash cement mortars longer curing accentuated the carbonation effect. This result was attributed to the depletion of $Ca(OH)_2$ due to the pozzolanic reaction before the start of carbonation leaving the $CO_2$ to react with the more complex

hydration products and resulting in the possible release of $Cl^-$ which are bound to these products. *Kayyali and Qasrawi (1992)* found similar trends in the case of pastes with and without fly ash (30% replacement level) with admixed chlorides (0.4%,1.0%, 1.2%, 1.6%, 2.0%, 2.5%). The decrease in the chloride binding capacity was attributed to the increased solubility of Friedel's salt in low pH environment caused by carbonation. *Suryavanshi and Swamy (1996)* studied the role of atmospheric carbonation on the stability of Friedel's salt in chloride contaminated reinforced concrete slabs. The slabs were subjected to 70 cycles of ponding (4% NaCl solution) and drying for a two and a half year period and they were left to carbonate in the laboratory environment for the same period. The results from XRD and DTA analysis showed that the existence and quantity of Friedel's salt was dependant on the existence and severity of carbonation. The higher the degree of carbonation, the lower the amount of Friedel's salt. The authors suggested that the stability of Friedel's salt is pH dependant, and the drop in alkalinity due to carbonation would cause the release of chlorides from the Friedel's salt. This explanation, however, is in contradiction with the findings of *Roberts (1962)*, where Friedel's salt was more soluble in solutions with higher alkalinity.

### 2.4.9 W/CM:

Since the water to cementing materials ratio (W/CM) affects the porosity and the amount of hydrated products, it would be expected that the W/CM would influence the chloride binding capacity.

While most reported results in the literature show an increase in chloride binding at higher W/CM *(Tuutti, 1982; Tritthart, 1989; Arya et al., 1990; Byfors, 1990; Nagataki et al., 1993; Sandberg & Larsson, 1993; Tang & Nilsson, 1993)*, the significance of this effect depends on the authors interpretation of the results. Some workers report a significant increase *(Arya et al., 1990; Nagataki et al., 1993)* while others report little or insignificant effect *(Tritthart, 1989; Byfors, 1990; Sandberg & Larsson, 1993)*. It is interesting to notice a trend shown in three different studies *(Arya et al., 1990; Byfors, 1990; Sandberg & Larsson, 1993)* where the difference in chloride binding was significant between 0.4 to 0.5 but insignificant between 0.5 and 0.6. *Sandberg and Larsson (1993)* attributed the lower binding capacity of the 0.4 W/CM paste to the fact that the mix with W/CM of 0.4 had a lower degree of hydration and concluded that the W/CM had little effect on chloride binding.

*Tang and Nilsson (1993)* found trends that were similar to those obtained by *Tuutti (1982)*. The W/CM had some influence on the chloride binding isotherms of cement pastes, but little influence on those of mortars (Figure 2-4). When they expressed the bound chlorides per mass of C-S-H gel, the W/CM had no influence on the chloride binding isotherms of the pastes, suggesting that the observed difference in the binding capacities among the pastes with different W/CM was due to the difference in their degrees of hydration (Figure 2-16).

*Midgley and Illston (1984)* and *Delagrave et al.(1994, 1996)* found that the formation of Friedel's salt (chemical binding) was dependent on the W/CM. *Midgley and Illston (1984)* tested cylindrical specimens of cement pastes exposed to chloride penetration through their top surface (30 g/l NaCl, and 150 g/l NaCl). They found that at the same depths, significantly lower Friedel's salt formed in the 0.23 W/CM paste than in the 0.47 and 0.71 W/CM pastes. It is important to mention, however, that the observed effect is mostly likely due to the lower chloride contents in the 0.23 W/CM paste at a given depth due to its lower porosity. *Delagrave et al. (1994, 1996)* found Friedel's salt in cement paste with 0.38 W/CM stored in NaCl solutions (3% NaCl, pH=8.5) for up to 3 years, but did not detect Friedel's salt in cement pastes with 0.25 W/CM even after 3 years of

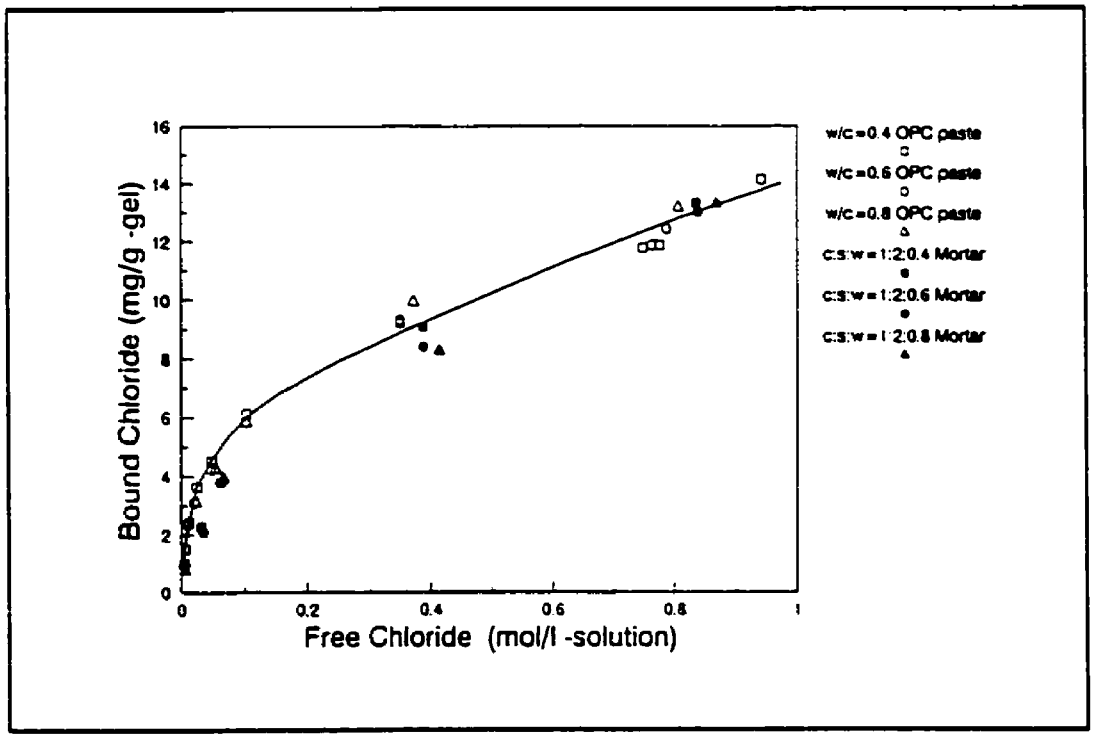


Figure 2-16: Chloride binding isotherms of OPC pastes and mortars. The bound chloride was expressed in unit mass of C-S-H gel. From *Tang & Nilsson (1993)*.

storage in the chloride solutions. They attributed this to the lower porosity of the 0.25 W/CM paste, and that the chloride content was not enough to promote the formation of Friedel's salt.

In addition to the degree of hydration, another reason to explain the higher chloride binding at higher W/CM, is the higher porosity at higher W/CM which probably makes potential binding sites more exposed and more accessible to chloride ions.

### 2.4.10 Desorption Isotherms:

There are very few studies in the literature on the desorption of chlorides when the free chloride concentration in the pore solution decreases. Both studies by *Tang and Nilsson (1993)* and *Wiens and Schiessl (1997)* showed that the chloride binding is not a reversible process with respect to chloride concentration, since a significant part of the bound chloride is not released into the pore solution when the chloride concentration drops as shown in Figure 2-17. *Tang and Nilsson (1993)* argued that this portion of chloride is chemically bound and that it is irreversible. It should be noticed that the desorption isotherms in both studies were constructed by joining the desorption results from every point on the adsorption curve. A more appropriate and accurate way to do that is to start from the same initial concentration and get the different desorption points by diluting to the different final concentrations.

### 2.4.11 Chemical Admixtures:

Little research has been done on the effect of chemical admixtures on chloride binding. The reported results on the influence of superplasticisers on chloride binding show conflicting trends.

*Byfors (1986, 1990)* found an increase in the chloride binding of cement pastes made with three different types of superplasticisers (melamine, lignosuphonate, and naphthalene) and exposed to external chlorides. She attributed the increase in binding to the good dispersion and high surface area caused by the superplasticisers. *Glasser (1991)* reported the results of a study on the influence of commercial superplasticisers on chloride binding. All three superplasticisers tested, increased chloride binding in the mortar specimens with admixed chloride. It was suggested that organic

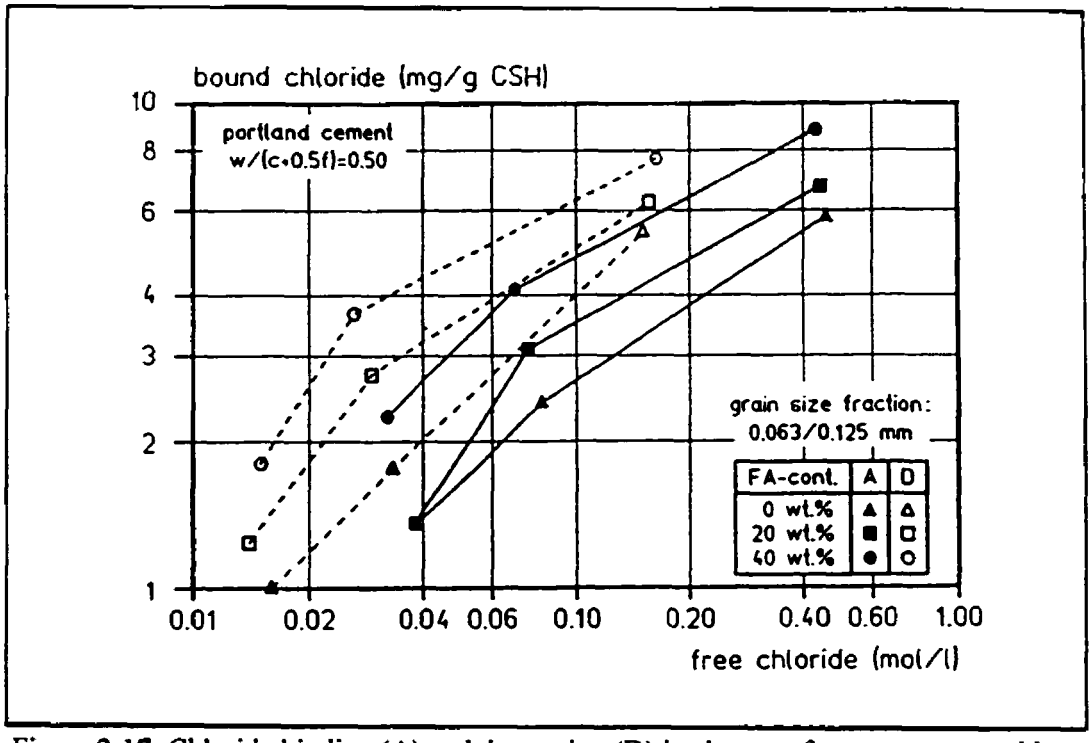


Figure 2-17: Chloride binding (A) and desorption (D) isotherms of cement pastes with or without fly ash. From *Wiens & Schiessl (1997)*.

groups on the superplasticisers were chlorinated, leading to the decrease in free chloride concentration in the pore solution.

*Haque and Kayyali (1995a, 1995b)* found that a concrete with a superplasticiser had a lower chloride binding than the one without a superplasticizer. However, it should be noted that the two concretes had different W/CM ratios which might have affected the chloride binding capacity too.

### 2.4.12 Source of Chloride

Very few studies in the literature attempt to make a direct and relevant comparison of the effect of the source of chlorides (internal or external) on the chloride binding capacity. The results of these studies show conflicting trends.

Results by *Rasheeduzzafar et al. (1992)* showed that for cement pastes having the same composition, and at a given level of total chloride content, the unbound chlorides in the specimens subjected to external chlorides were significantly higher than in those with admixed chloride. It should be mentioned that water extraction was used to determine the unbound chlorides in the

specimen with external chlorides, whereas pore squeezing was used in the case of specimen with admixed chlorides.

The results obtained by *Arya et al. (1990)* show that the bound chlorides, expressed as a percentage of total chlorides, were higher in most pastes exposed to external chlorides than in similar pastes with admixed chlorides, despite the fact that the total chloride contents in pastes with external chlorides were higher than the total chloride contents in the pastes with admixed chlorides. Therefore, it can be concluded that the chloride binding was higher in the case of external chloride than in the case of internal chlorides.

*Tuutti (1982)* concluded that the amount of bound chlorides, for lengthy exposure periods (allowing chemical equilibrium to stabilize), is independent of whether the chlorides are internal or external.

The results of *Blunk et al. (1986)* are not conclusive and show inconsistent trends. For chlorides that were derived from NaCl, chloride binding is higher in the case of external chlorides than in the case of internal chlorides. For chlorides that were derived from $CaCl_2$, most tested pastes showed slightly higher binding capacities in the case of internal chlorides than in the case of external chlorides.

It should be mentioned that in all these reported results, the methods used to determine the free or bound chlorides probably had significant effects on these results, especially when different methods for determining the free chloride content are used in the cases of external chlorides and internal chlorides.

## 2.5 Summary

This chapter included a review of published studies related to chloride binding in cement and concrete. The previous sections dealt with relevant topics related to chloride binding such as the definition of the chloride binding process, including chemical and physical binding, the current methods being used to determine the distribution of chloride between free and bound, and the important factors affecting chloride binding, including the binder compostion, the pore solution composition, and environmental factors. The effects of several important factors on the chloride binding capacity, as suggested by the published results, are summarized in Table 2-4. The examination of the published studies revealed the following things:

1. Most of the published studies examined chloride binding in the case of admixed chlorides. There was a clear lack of available studies on chloride binding in the case of external chloride.
2. Several methods are being used for determining the distribution of chloride between free and bound. None of those methods is standardized. Each method is based on different assumptions which might or might not be true. This in turn influences the results obtained using those methods, and makes the comparison between the results of the different studies difficult.
3. More research should be done to address the roles of cement phases in chloride binding. This includes the roles of $C_3A$, $C_4AF$, and $C_3S$ (and $C_2S$). The $C_3A$ plays a role in chloride binding (evidence of existence of Friedel's salt in chloride contaminated paste), however the importance and extent of this role is not fully understood. The role of the $C_3S$ is controversial, although more studies indicate that $C_3S$ play a significant (if not important) role. There are little evidence of a significant role of $C_4AF$ in chloride binding.
4. The mechanisms of SCM influence on the binding capacity of blended cement should be further investigated. Particularly, the role of the alumina content in GGBFS and fly ash, and the role of the C-S-H formed as a result of the pozzolanic reactions.
5. There are almost no studies that have examined the effects of carbonation and temperature on the chloride binding capacity in the case of external chloride, indicating the need to address the roles of these two important environmental factors.

Table 2-4 summarizes the effect of the different factors on the chloride binding capacity of cement

Table 2-4: Effect of different factors on the chloride binding capacity

| **Factor** (increase⇑,decrease ⇓) | **Effect on chloride binding capacity** | | **Comments** |
|---|---|---|---|
| | **Trend** | **Exception** | |
| **$C_3A$ content** (⇑) | ⇑ | yes | the importance of the role of $C_3A$ content is controversial |
| **$C_4AF$ content** (⇑) | no trend | | little evidence of $C_4AF$ binding, less effective than $C_3A$ |
| **$C_3S$+$C_2S$** | significant role | yes | role of $C_3S$ is controversial |
| **Fly ash** (⇑) | ⇑ | | effect attributed to higher aluminate . Others attributed it to higher surface area. |
| **Slag** (⇑) | ⇑ | | |
| **Silica fume** (⇑) | ⇓ | yes | the assumed effect of SF on C-S-H might not be true |
| **W/CM** (⇑) | ⇑ | | significant effect between W/CM≤0.3 and W/CM≥0.5 Insignificant between W/CMs≥0.5 |
| **Superplasticiser** | ⇑ | yes | |
| **Temperature** (⇑) | ⇓ | yes | |
| **Carbonation** (⇑) | ⇓ | | severe effect (very few studies) |
| **pH** (⇑) | ⇓ | | |
| **$[SO4^{2-}]$** (⇑) | ⇓ | | |
| **$[Cl^-]$** (⇑) | ⇑ | | one of the most important |
| **Cation** | more $Cl^-$ are bound from $CaCl_2$ than NaCl | | similar effect on chemical and physical binding |
| **Desorption** | binding not reversible | | some chlorides are irreversibly bound |

# CHAPTER 3

# EXPERIMENTAL PROGRAM

## 3.1 Overview of Experimental Program

As stated in the objectives, the aim of this work was to investigate chloride binding in cementitious materials (for the case of external chlorides) to provide insight into the distribution of chloride between free and bound, and the distribution of bound chloride among the different cement hydrates. The influences of cement type and composition as well as internal and external factors such as pH, sulphate, carbonation, temperature, and desorption were studied.

Two methods were used to investigate chloride binding in this program. The main method is similar to the one developed by *Tang and Nilsson (1993)* where cement paste samples are submerged in chloride solutions until equilibrium is achieved between the host solutions and the pore solutions of the submerged samples. The second method is similar to the one used by *Sergi et al.(1992)* where cylindrical cement pastes are submerged in NaCl solutions and only unidirectional chloride diffusion is allowed. After a specific period of time, the samples are analyzed for free and total chloride content along their depth, and bound chloride is determined from the difference between total and free chloride.

Phase 1 of the program had three parts. Part 1A focused on testing a variety of cementitious mixtures with a water to cementitious materials ratio (W/CM) of either 0.3 or 0.5. The mixtures with W/CM=0.3 represent typical proportions used in high-performance concrete. The purpose of this phase was to study the influence of supplementary cementing materials (type and replacement level) on chloride binding and examine the nature of the chloride binding isotherms. The influence of temperature and age was also studied. In Part 1B, four mixes from Part 1A were tested using Sergi's "ponding" method *(Sergi et al., 1992)* to compare the results from the two testing methods. In Part 1C, the reproducibility of results from the equilibrium method was examined, and the sensitivities of the results to sample size and solution volume were investigated.

Phase 2 of the program consisted of two parts. Part 2A consisted of studying the influence of the pH of the pore solution, sulphate ion concentration, carbonation, and desorption on chloride binding. The effect of temperature was re-examined since the results from the first phase were inconclusive as far as temperature influences were concerned. Part 2B focused on the influence of cement composition and type. Nine different Portland cements were tested. The aim was to check whether it is possible to predict chloride binding performance from the chemical and mineral

composition, and to examine the role of cement mineral phases and other cement components in binding.

Phase 3 of the program had two parts; Part 3A focused on the behaviour of the cement mineral phases by studying individual binding relationships for "pure" phases ($C_3A$, $C_3S$, $C_4AF$, $C_2S$). The chloride binding isotherms of the four phases were determined, and the influence of pH, sulphate ion concentration, temperature, carbonation, and desorption on the chloride binding of $C_3A$ and $C_3S$ was also examined. It was hoped that this study would give some insight not only into the role of cement phases in binding, but also into the mechanisms through which the internal and external environmental factors affect the chloride binding properties of cements. Finally, pure $C_3A$ and $C_4AF$ were added to low $C_3A$ and low $C_4AF$ cements respectively to check their influence on the binding properties of these cements, and whether their influence would be consistent with their behaviour when tested alone. In Part 3B, the influence of SCM's was further studied by testing SCM-lime blends including silica fume-lime and metakaolin-lime mixtures with varying proportions. A 100%GGBFS paste was also tested. The purpose of these tests was to examine the chloride binding properties of the hydration products of SCM and the factors influencing them. Table 3-1 summarizes the experimental program.

Table 3-1: Summary of the experimental program

| | | |
|---|---|---|
| **Phase 1** | **Part 1A** | Testing various blended cements with W/CM = 0.3 & 0.5:<br>Effect of SCM type and replacement level.<br>Effect of chloride concentration, temperature, W/CM, age. |
| | **Part 1B** | Equlibrium Method Vs Ponding Method:<br>Testing some of the above mixtures using Sergi's method. |
| | **Part 1C** | Equilibrium method:<br>Reproducibility of the results (4 replicas of the control mix).<br>Sensitivity of the results to sample size and solution volume. |
| **Phase 2** | **Part 2A** | Effect of environmental factors:<br>Influence of pH, $SO_4^{2-}$, Temperature, $CO_2$, desorption. |
| | **Part 2B** | Effect of Cement composition & type (9 cements).<br>Influence of $SO_3$ content, cement fineness |
| **Phase 3** | **Part 3A** | Testing Pure Phases ($C_3A$, $C_4AF$, $C_3S$, $C_2S$):<br>Roles of cement mineral phases in chloride binding. |
| | **Part 3B** | Testing of SCM-lime blends (SF-lime, MK-lime), 100%GGBFS.<br>Binding capacities of hydrates produced by metakolin, silica fume, and GGBFS. |

## 3.2 Materials and Mix Preparation

### 3.2.1 Raw Materials

The control cement was a CSA Type 20 Portland cement and the SCMs used were silica fume, metakaolin, blast furnace slag, and three fly ashes, one each of CSA A23.5 Types F, CI, and CH, covering a range of CaO contents. The mixtures included the CSA Type 20 PC with various levels of replacement with SCMs including ternary blends. Nine different Portland cements were used. They included three CSA Type 10, three Type 20, one type 30, and two type 50 cements. Four of these cements were actually obtained as ground clinkers. They were part of another research project on the optimum sulphate content in Portland cement. Two of these clinkers (C4, C8) were used as is, and the two others (C5, C6) were already interground with gypsum to obtain a target of 1.5% $SO_3$ content as part of the aforementioned research project. It was hoped that the use of these clinkers would clearly show the impact of sulphate on the chloride binding capacity of Portland cement, because of the large variations in their sulphate content. The Type 50 PCs (C1, C7) were of particular interest since one had a very low $C_3A$ and the other had a very low $C_4AF$. The pure cement phases were supplied by Lafarge's Central Research Laboratory in France and were "99% pure". Tables 3-2 to 3-4 show the chemical compositions of the different cementitious materials used in this research program. Chemical analyses were performed by Lafarge Cement's CTS laboratory in Montreal. The major elements were measured by X-ray fluoresence (XRF). The total sulfur content was determined by Leco SC-432.

Table 3-2: Chemical Composition of the Supplementary Cementing Materials

| Amount (%) by weight | Silica Fume SKW | Metakaolin | GGBFS Lafarge Slag | Fly Ash Ft. Martin Alegheney Type F (FA) | Fly Ash Coloumbia Type CI (FA1) | Fly Ash Coal Creek Type CH (FA2) |
|---|---|---|---|---|---|---|
| $SiO_2$ | 94.48 | 52.01 | 36.18 | 53.89 | 43.07 | 40.82 |
| $Al_2O_3$ | 0.24 | 44.72 | 10.02 | 24.65 | 20.78 | 11.09 |
| $TiO_2$ | 0.01 | 1.6 | 0.67 | 1.14 | 1.10 | 0.47 |
| $P_2O_5$ | 0.14 | 0.09 | 0.01 | 0.71 | 0.67 | 0.10 |
| $Fe_2O_3$ | 0.63 | 0.58 | 0.50 | 8.63 | 5.41 | 6.21 |
| CaO | 0.44 | 0.00 | 35.49 | 4.37 | 17.72 | 29.89 |
| SrO | 0.02 | 0.02 | 0.04 | 0.16 | 0.54 | 0.30 |
| MgO | 0.38 | 0.00 | 0.66 | 0.83 | 4.18 | 4.41 |
| $Mn_2O_3$ | 0.03 | 0.01 | 13.58 | 0.05 | 0.17 | 0.06 |
| $Na_2O_3$ | 0.16 | 0.32 | 0.43 | 0.6 | 1.46 | 1.14 |
| $K_2O$ | 1.01 | 0.19 | 0.50 | 2.14 | 0.75 | 1.71 |
| $Na_2O_e$ | 0.82 | 0.45 | 0.77 | 2.07 | 1.95 | 2.26 |
| $SO_3$* | 0.36 | 0.12 | 1.51 | 0.61 | 2.17 | 2.17 |
| LOI@1000 °C | 2.87 | 0.9 | 1.72 | 1.53 | 2.57 | 1.30 |

* $SO_3$ based on sulphur determined by LECO

Table 3-3: Chemical Composition of Portland Cements

| CSA Type / (% by weight) | C1 T50 | C2 T10 | C3 T30 | C4 T10 | C5 T20 | C6 T10 | C7 T20 | C8 T20 | OPC Control T20 |
|---|---|---|---|---|---|---|---|---|---|
| $SiO_2$ | 21.41 | 18.89 | 18.42 | 21.25 | 21.59 | 20.61 | 24.49 | 21.54 | 21.26 |
| $Al_2O_3$ | 2.81 | 5.51 | 5.36 | 5.61 | 4.25 | 5.25 | 1.83 | 4.22 | 4.09 |
| $TiO_2$ | 0.14 | 0.25 | 0.24 | 0.34 | 0.28 | 0.27 | 0.09 | 0.27 | 0.2 |
| $P_2O_5$ | 0.27 | 0.30 | 0.28 | 0.18 | 0.07 | 0.13 | 0.13 | 0.07 | 0.07 |
| $Fe_2O_3$ | 4.48 | 2.55 | 2.64 | 2.24 | 3.08 | 2.06 | 0.27 | 3.22 | 2.89 |
| CaO | 65.27 | 62.38 | 61.33 | 67.56 | 62.71 | 63.87 | 68.84 | 62.62 | 63.58 |
| SrO | 0.11 | 0.30 | 0.28 | 0.15 | 0.08 | 0.09 | 0.12 | 0.08 | 0.12 |
| MgO | 0.98 | 2.75 | 2.61 | 1.26 | 3.27 | 2.73 | 0.60 | 3.52 | 2.47 |
| $Mn_2O_3$ | 0.12 | 0.11 | 0.10 | 0.07 | 0.08 | 0.06 | 0.03 | 0.08 | 0.06 |
| $Na_2O_3$ | 0.12 | 0.51 | 0.49 | 0.28 | 0.21 | 0.31 | 0.24 | 0.21 | 0.17 |
| $K_2O$ | 0.24 | 1.04 | 1.06 | 0.30 | 0.66 | 1.09 | 0.07 | 0.53 | 0.62 |
| $Na_2O_e$ | 0.28 | 1.19 | 1.19 | 0.48 | 0.64 | 1.03 | 0.29 | 0.56 | 0.58 |
| $SO_3$* | 2.65 | 4.12 | 4.43 | 0.32 | 1.44 | 1.35 | 2.14 | 1.00 | 2.79 |
| LOI@1000 °C | 1.46 | 1.02 | 2.44 | 0.24 | 1.50 | 1.94 | 1.20 | 2.58 | 0.99 |
| (%) | BOGUE COMPOSITION | | | | | | | | |
| $C_3S$ | 70.0 | 57.9 | 57.2 | 71.6 | 54.1 | 61.2 | 75.3 | 55.35 | 57.6 |
| $C_2S$ | 8.6 | 10.5 | 9.7 | 7.0 | 21.2 | 13.0 | 13.5 | 20.09 | 17.6 |
| $C_3A$ | 0.0 | 10.3 | 9.7 | 11.1 | 6.1 | 10.4 | 4.4 | 5.74 | 5.9 |
| $C_4AF$ | 13.6 | 7.7 | 8.0 | 6.8 | 9.4 | 6.3 | 0.8 | 9.79 | 8.8 |
| Blaine ($m^2/Kg$) | 365 | 407 | 523 | 320 | 320 | 311 | 350 | 320 | 326 |

*$SO_3$ based on sulphur determined by LECO

Table 3-4: Chemical Composition of the Pure Phases

| Amount (% by weight) | Pure $C_2S$ | Pure $C_3S$ | Pure $C_3A$ | Pure $C_4AF$ |
|---|---|---|---|---|
| $SiO_2$ | 33.79 | 24.05 | 0.04 | 0.33 |
| $Al_2O_3$ | 0.07 | 0.22 | 36.37 | 18.76 |
| $TiO_2$ | 0.02 | 0.02 | 0.02 | 0.01 |
| $P_2O_5$ | 0.05 | 0.00 | 0.00 | 0.00 |
| $Fe_2O_3$ | 0.08 | 0.03 | 0.01 | 30.82 |
| CaO | 63.48 | 69.48 | 62.48 | 47.67 |
| SrO | 0.02 | 0.01 | 0.01 | 0.01 |
| MgO | 0.30 | 0.26 | 0.12 | 0.20 |
| $Mn_2O_3$ | 0.02 | 0.01 | 0.01 | 0.04 |
| $Na_2O_3$ | 0.06 | 0.07 | 0.08 | 0.05 |
| $K_2O$ | 0.00 | 0.00 | 0.00 | 0.00 |
| $SO_3$* | 0.07 | 0.08 | 0.08 | 0.19 |
| LOI@1000 °C | 1.39 | 5.45 | 0.46 | 0.54 |

*$SO_3$ based on sulphur determined by LECO

### 3.2.2 Mix Design, Casting, and Curing

All mixtures used in this research program were pastes containing cementitious materials and distilled water. The water to cementitious materials ratios, W/CM, used were 0.3 and 0.5. A superplasticiser was used for the 0.3 W/CM mixtures. This superplasticiser was supplied by Masters Builders, and is known under the brand name SPN. It was used at a dosage of 6 ml/kg of cementitious material. A typical mix design is presented in Appendix A.

The mixing was carried out in a high speed blender (Waring heavy duty blender, 3.8 L capacity, stainless steel) under vacuum to minimize air bubbles in the mix. Prior to mixing with water, the SCM and cement powder were mixed thoroughly with a spoon until the SCM was uniformly distributed in the cement. The mixing regime used was as follows:

step 1- one third of the mix water was added followed by one half of the cementitious materials, then one third of mix water, then the other half of the cementitious materials, and finally the last one third of mix water was added.

Step 2- blender was closed and put under vaccuum, and mixing was started at low speed (10000 rpm) for one minute.

Step 3- sides and top of the blender container were scraped and the vacuum re-applied and mixing was continued for another minute. 15 seconds at low speed and 45 seconds at medium speed (15000 rpm).

Step 4- Step 3 was repeated except that in the last 45 seconds, mixing was done at high speed (25000 rpm).

At the end of the mixing cycle, a check was made to ensure there were no lumps of dry powder in the mix. If lumps were present, they were crushed and remixed manually, and steps 3 and 4 repeated. Particular attention was paid to clumping with mixtures containing silica fume (or sometimes metakaolin) due to increased water demand in these mixtures which make them very difficult to mix. Manual pre-mixing was used in this case to ensure that no big clumps of dry cementitious materials were left, and that the mixture was in a plastic state. Only then was the mixing action of the blender effective.

After mixing, the paste was cast in 50-mm diameter x 100 mm cylindrical plastic molds. The casting was done in two layers, and each layer was tapped sixty times at a rate of 2 tap/second. The top of the molds was covered with a large plastic sheet and a lid was placed on top. Adhesive tape was applied around the lid to further prevent leaking or evaporation. The molds were then placed on a rotating wheel (12 rpm) for 24 hours to prevent segregation. After that, they were cured at room temperature ( 22°C +/-1 ) in sealed containers with small amount of water in each container to maintain a high humidity. The curing periods were 2 and 9 months.

### 3.2.3 Preparation of Synthetic Cement Phases (Pure Phases)

The synthetic cement phases ($C_3A$, $C_4AF$, $C_3S$, $C_2S$) were supplied by Lafarge's Central Research Laboratory in France. They were obtained from Lafarge as granular material and had to be ground. A steel ball mill (1 kg capacity) was used for this purporse. It was originally decided to grind the clinkers to a target surface area of 350 to 400 $m^2/kg$. Unfortunately, the $C_3S$ was overground to a 550 $m^2/kg$. So, it was then decided to grind the other three phases to around 450 $m^2/kg$ to lower any effect that might arise from a large difference between the surface area of the phases, while keeping the surface area close to the normal range found in Portland cement.

The $C_3A$ pastes were mixtures of $C_3A$, gypsum, and $Ca(OH)_2$. They were proportioned in terms of the molar ratios of $C_3A$, $SO_3$, and $Ca(OH)_2$. Molar ratios of $1.0C_3A/0.8SO_3/0.3Ca(OH)_2$ and $1.0C_3A/0.4SO_3/0.3Ca(OH)_2$ were used respectively. A mixture of $1.0C_4AF/0.8SO_3/0.3Ca(OH)_2$ was used to study the binding properties of the $C_4AF$ phase. The $C_3S$ and $C_2S$ pastes were 100% $C_3S$ and 100% $C_2S$ respectively. All pastes had W/CM = 0.5, and the mix water used for all mixtures had NaOH and KOH to simulate the pore solution of cement pastes. The NaOH and KOH concentrations were equal to those found in the pore solution of the OPC control paste. Details of the mix design and of tests performed on the pure pastes are provided in section 3.4.3.

## 3.3 Test Methods

### 3.3.1 Equilibrium Method for Determining Chloride Binding

#### 3.3.1.1 Sample Preparation

At the end of the curing period, the pastes were de-molded and the central portion was saw- cut into approximately 3-mm thick discs using a wet diamond blade lubricated with distilled water. The sliced samples were vacuum dried for three days in a desiccator containing silica gel and soda lime. They were then stored for a month in a glove box kept at 11% RH (using saturated lithium chloride solution). Soda lime was used to remove the carbon dioxide from the air inside the glove box. It is assumed that only a monolayer of water remains on the surface of cement hydrates at 11% RH *(Ramachandran et al, 1981)*. After storage, 25-g samples were stored in 125-ml plastic bottles and placed under vacuum for about two hours. The bottles were filled with a specific volume of NaCl solutions of varying concentrations (0.1, 0.3, 0.5, 0.7, 1.0, 2.0, 3.0 M Cl). The bottles were sealed and stored in the open laboratory atmosphere (22°C), in a fridge (7°C), or in an oven (38°C) for various periods of time (6 months for paste with W/CM = 0.3, 5-6 weeks for pastes with W/CM = 0.5 or 2) until test.

#### 3.3.1.2 NaCl Solutions

Reagent type sodium chloride (99% pure) was used to prepare the host solutions. Seven concentrations were used throughout this program: 0.1, 0.3, 0.5, 0.7, 1.0, 2.0, and 3.0 molar NaCl. The chloride concentrations were chosen to reflect different realistic exposures. Chloride concentrations lower than 1 M would exist in cases of reinforced concrete structures submerged in sea water. Higher chloride concentrations (between 1 M and 3 M and even higher) could exist in the splash zone or in bridge decks exposed to de-icing salts. In general, the chloride solutions were also saturated with calcium hydroxide (3g/l, pH = 12.5) unless mentioned otherwise. This was done to prevent the leaching of calcium hydroxide from the samples.

a) Effect of pH

Four levels of pH were selected to study the influence of pH on binding: 13.0, 13.4, 13.7, and 14.0. Reagent grade NaOH and KOH were used to obtain the desired pH level. The NaOH to KOH ratio was about 1/4 which was similar to that of the pore solution of the control mix. $Ca(OH)_2$ was not

used in these chloride solutions.

b) Effect of $[SO_4^{2-}]$

Three sulphate ion concentrations were selected to examine the influence of $[SO_4^{2-}]$ on binding: 0, 0.01, and 0.1 molar. Reagent grade $Na_2SO_4$ was used to obtain the desired concentration. NaOH was used to achieve a pH level of 12.5 equivalent to that of a saturated $Ca(OH)_2$ solution. No $Ca(OH)_2$ was used in these solutions.

c) Effect of carbonation

The sodium chloride solutions used for testing the carbonated samples were prepared without the addition of $Ca(OH)_2$ since it was assumed that there would be no $Ca(OH)_2$ left in the carbonated samples.

### 3.3.1.3 Titration

After equilibrium between the pore solution of the samples and the host solutions was reached, the host solutions were analysed for chloride concentration by means of potentiometric titration using 0.01 molar $AgNO_3$ titrant and a silver electrode. A Metrohm DMS 760 automatic titrator was used for this purpose.

Of the seven chloride concentrations used in this research, only the 0.1 molar was titrated directly without the need to dilute the solution. The rest of the solutions were diluted 20 to 100 times before being titrated. In the case of the 0.3, 0.5, 0.7 molar NaCl solutions, a 1 ml sample from the solution was diluted 50 times in a 50 ml flask, then a 2.5 ml sample of the diluted solution was titrated. In the case of the 1.0, 2.0, and 3.0 molar NaCl solutions, a 1 ml sample from the solution was diluted 100 times in a 100 ml flask, then a 1 ml sample of the diluted solution was titrated.

### 3.3.1.4 Determination of Binding Isotherms

In the equilibrium method, it is assumed that after equilibrium is reached between the external solution and the pore solution of the sample, the reduction in the concentration of the host solution is attributed to chloride being bound by the cement. Then, knowing the initial and final

concentration, the volume of the external solution and the dry mass of the sample, the amount of bound chloride can be calculated according to the following formula:

$$C_b = 35.453 * V * (C_i - C_e)/W_d$$

where $C_b$ : amount of bound chloride in mg Cl/g of sample,

$V$ : volume of the external solution in ml.

$C_i$ : initial chloride concentration of the external solution in mol/l,

$C_e$ : free chloride concentation at equilibrium of the external solution in mol/l.

$W_d$ : dry mass of the sample in g, and

35.453 is the molar mass of the chloride ion.

The $W_d$ mass is calculated using the following formula:

$$W_d = W_{11} \bullet (1 - \xi_{11})$$

where $W_{11}$: mass of the sample at 11% rh in g,

$\xi_{11}$: evaporable water content at 11% rh

Each tested chloride concentration represents a point in the binding isotherm. In this case the binding isotherms were obtained by plotting, for every concentration studied, the free chloride concentration at equilibrium ($C_e$) against the bound chlorides ( $C_b$).

### 3.3.1.5 Desorption Tests

Desorption isotherms were determined for selected cases. After equilibrium was reached, and one point of the chloride binding isotherm was determined, the remaining chloride solution was mostly removed (using a pipette). The sample was then moved to another bottle, and either 200 ml or 1000 ml of distilled water saturated with $Ca(OH)_2$ (pH = 12.5) was added to the sample. After a storage of 4 months to ensure that a second equilibrium was established, the free chloride concentration of the solution was measured. The amount of bound chloride remaining in the sample, after the second equilibrium, was determined from the following equation:

$$C_b = 35.453 * (V * C_i - V_1 * C_e - C_2 * (V + V_2 - V_1))/W_d$$

where $C_2$ : chloride concentration after second equilibrium, mole/litre,

$V_1$ : volume of solution taken out, including first titration, ml, and

$V_2$ : volume of distilled water added, ml.

$C_2$ and $C_b$ (determined from equation (2)) represent one point of the chloride desorption isotherm.

### 3.3.2 Ponding Method for Determining Chloride Binding

#### 3.3.2.1 Sample Preparation

The specimens were demoulded at the end of the curing period and about 1 cm from the cast end was removed by saw-cutting with a diamond blade lubricated with distilled water; these end pieces were discarded. All surfaces were epoxy coated except for the cut one (Figure 3-1). The specimens were left for 24 hours exposed to the laboratory air to allow the epoxy to harden. They were then stored in plastic containers filled with 1 molar NaCl solutions saturated with calcium hydroxide (Figure 3-2). The cylinders were vertically positioned with the uncoated surface facing the top and covered with about 4 to 5 cm of solution. The NaCl solutions were changed every six weeks during the storage period.

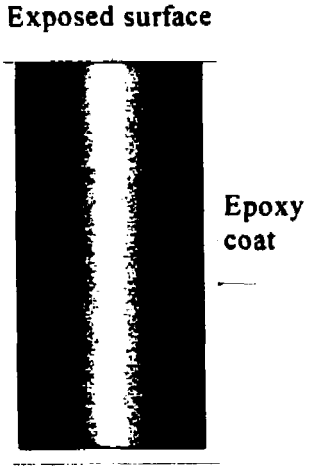


Figure 3-1: Cylinders are coated with epoxy on all sides except the exposed surface.

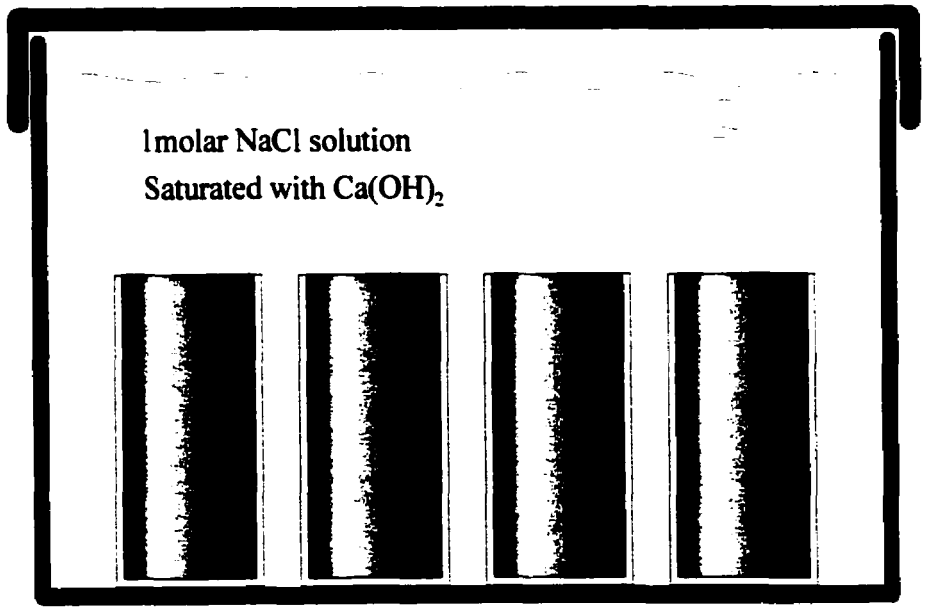


Figure 3-2: The paste cylinders are stored in 1 M chloride solution saturated with $Ca(OH)_2$, with the exposed surface facing upward.

### 3.3.2.2 Free Chloride

A) Slicing

At the end of the ponding period, one cylinder was taken out and was split open before being sprayed with $AgNO_3$ solution. The change in colour due to the reaction between the $Cl^-$ and $AgNO_3$ indicated the approximate depth of chloride penetration. Based on this information, a set of specimens was taken out and sliced with a dry diamond blade. The thickness of the sliced discs was 1/6th of the penetration depth so that discs were obtained from every specimen at six different depths. Each group of discs from the same depth were stored together in double plastic bags sealed tightly until pore squeezing. Another set of specimens were sliced at the same thickness except that a top layer, half the thickness of the discs, was cut off before slicing the discs. This way an overlapping effect is created between the two sets of discs and up to twelve free chloride measurements were determined along the axis of the specimen. Figures 3-3 to 3-6 summarise the procedure.

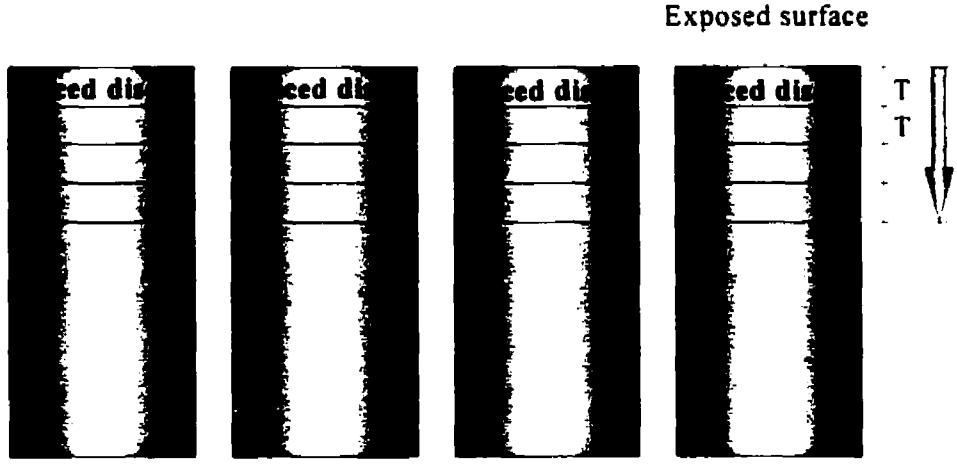


Figure 3-3: At the end of the exposure period, discs of specified thickness "T" are cut from the exposed surface inward to the depth of chloride penetration. This depth is approximately determined by spraying freshly broken cylinders with a silver nitrate solution.

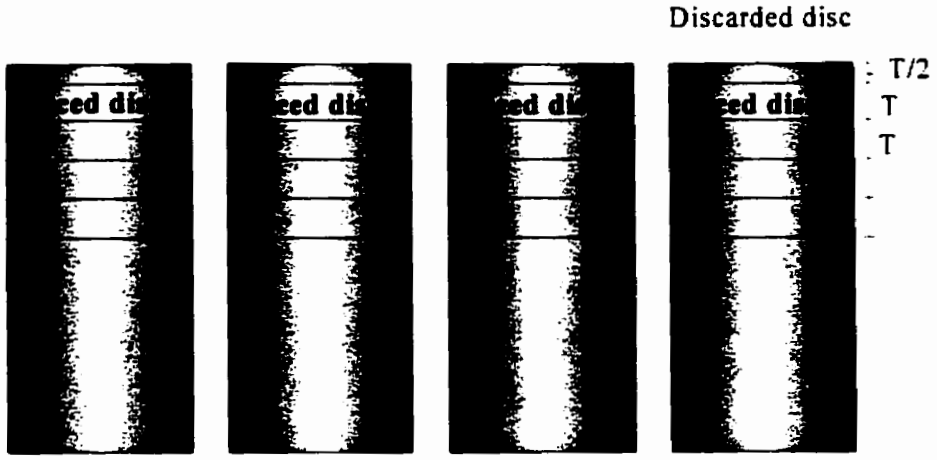


Figure 3-4: Another group of cylinders is sliced, but a top layer of "T/2" thickness is discarded before collecting the rest of the discs. This creates an overlapping effect, and more data points are determined in the chloride distribution profile.

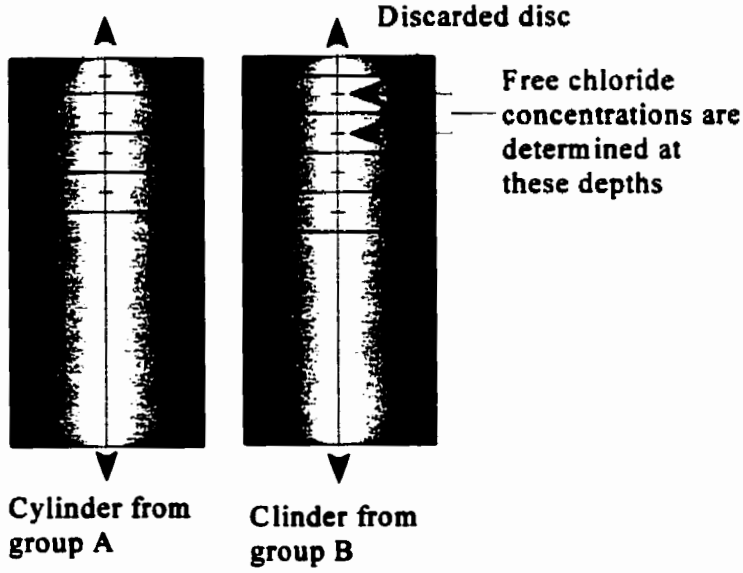


Figure 3-5: This figure illustrates how the overlapping effect, created by discarding the top part of cylinders from group B, results in more data points along the depth of chloride penetration.

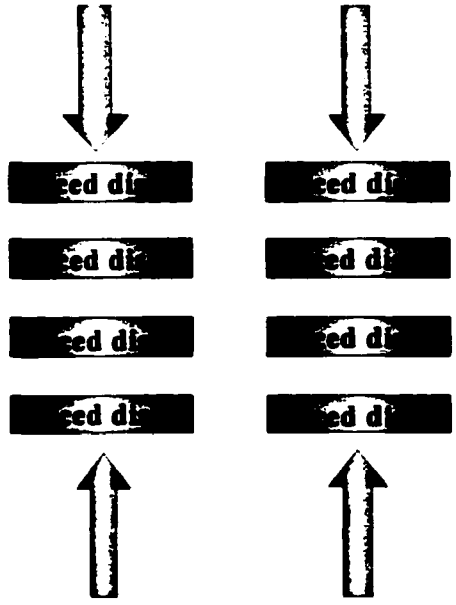

Figure 3-6: sliced discs from the same depth are pore pressed, and the $Cl^-$ and $OH^-$ concentrations are determined by titration.

B) Pore Squeezing

Pore solution expression was done using a device similar to that described by *Barneyback & Diamond (1981)*. The specimens were subjected to increasing pressure at a rate of 2 MPa per second up to 160 MPa, where the pressure was sustained for about 1 minute while the pore solution is collected under vacuum. The pressure was then released and was allowed to decrease until it reached zero. The loading cycle was repeated 2 more times were the maximum pressures attained were 320 MPa and 480 MPa respectively. The pore solutions were stored in tightly sealed plastic vials, until testing for chloride and hydroxyl ion concentrations.

C) Titration

About 1.5 to 3.0 ml sample of pore solution was obtained from pore squeezing. A 1 ml sample was used to determine the chloride concentration using the titrator mentioned earlier. The samples of chloride solutions obtained from depths close to the surface of the specimens had to be diluted 10 times before being titrated. This included the first 6 to 7 points. The remaining samples obtained at

depth were titrated directly without dilution.

0.5 ml or 1ml samples were used to determine the hydroxyl ion concentration in the pore solution. by automatic titration using a 0.05 N $H_2SO_4$ titrant and a electrode.

### 3.3.2.3 Total Chloride

a) Profile Grinding

At the end of the ponding period, one cylinder was removed from the NaCl solution. and powder samples 1.5 to 3.0 mm thick were ground from the exposed surface inwards to depths of 33 to 55 mm. A milling machine was used for this purpose. Before being mounted on the milling machine. the epoxy coated sides of the sample, along the grinding path were chiselled off so that the epoxy layer would not contaminate the ground sample. The specimen was then carefully levelled on the bed of the milling machine. Individual layers were ground using a 50-mm diameter diamond impregnated core bit. Not all layers were collected. as only 6 to 10 points are needed to generate a reliable profile. Each layer which was to be analysed was collected on wax paper sheets placed on either side of the sample. A small brush was used to brush the powder layer from the sample on to the paper. The powder sample was then transferred from the weighing paper to a glass storage container. The depth from which this layer was gound was recorded on the glass container.

In order to prevent cross-contamination between layers, the sample and the surrounding area were cleaned first with a vacuum. and then with compressed air. The ground powder samples which were collected were then dried in an oven at 105 °C for 24 hours.

b) Nitric Acid Digestion

After the ground samples, from the different layers. are dried in an oven (105°C), they are sieved (315 μm) and around 2g samples are taken for filtering and digestion. Water (35 ml) and nitric acid (7 ml) are added to the powder sample and stirred. and the mixture is boiled. The mixture is double filtered using filter papers (coarse porosity) placed in a funnel connected to a flask under vaccuum. The filtered solution is collected in a beaker. and a sample of this solution is weighed (5-60 g) before being transferred for titration.

c) Titration

The chloride content in parts per million (ppm) of each layer was determined using a Metrohm DMS 760 potentiometric titrator which uses a 0.01 mol/L silver nitrate titrant.

The apparent diffusion coefficient was determined from the results of the chloride analysis. Total chloride content versus depth was plotted to obtain a chloride distribution profile. The chloride penetration is assumed to follow Fick's Second Law of Diffusion:

$$\frac{dC}{dt} = D_a \frac{d^2C}{dx^2} \tag{2-1}$$

The following numerical solution of Equation (2-1) was fitted to the chloride profile:

$$C = C_s[1 - erf(\frac{x}{2\sqrt{D_a t}})] \tag{2-2}$$

Where:

| | | |
|---|---|---|
| C | = | the chloride concentration at a given depth [%of cement mass] |
| $C_s$ | = | the surface chloride concentration [% of cement mass] |
| x | = | depth from concrete surface [m] |
| t | = | time exposed [s] |
| $D_a$ | = | the apparent diffusion coefficient [$m^2/s$] |
| erf | = | error function |

The unknowns in this equation are $D_a$ and $C_s$. Using a curve fit software package (Jandell-Table Curve). The best fit values of these variables are found by iterations using least squares.

### 3.3.2.4 Bound Chloride

The bound chlorides are calculated from the difference between the total and free chlorides at every depth. However, since the total chlorides and free chlorides are obtained in different units, values need to be converted before a calculation of the bound chlorides can be done. In order to do the conversion, a knowledge of the evaporable water content is necessary (assuming that the content of the pore solution containing the free chlorides is equal to the evaporable water content):

$$w_e = (W_s - W_d)/ W_d$$

where : $w_e$ : evaporable water content, g water/g sample

$W_s$ : mass of the saturated sample, g

$W_d$ : mass of the dry sample , g

The bound chlorides are calculated using the following formula:

$$C_b = C_t - 35.453 * w_e * C_f$$

where: $C_b$ : bound chloride, mg Cl/g sample

$C_t$ : total chloride, mg Cl/g sample

$C_f$ : free chloride, mmol/ml

the binding isotherms can be presented either as free versus bound chlorides, or free versus total chlorides.

### 3.3.3 Evaporable Water Content

The evaporable water content was determined using the following formula:

$$w_e = (W_s - W_d) / W_d$$

where : $w_e$ : evaporable water content, g water/g sample

$W_s$ : weight of the saturated sample, g

$W_d$ : weight of the dried sample (in an oven at 105°C), g.

The evaporable water content was used in the ponding method to determine the free chloride content. It was assumed that the pore solution containing free chlorides is equal to the evaporable water content. For each of the tested pastes, a cylinder was taken out of the chloride solution at the end of the exposure period, and was sliced across the depth with a dry diamond blade. Four samples (15 to 30 g) were immediately weighed ($W_s$), and then dried to constant weight in an oven at 105°C ($W_d$). The $w_e$ was the average of the four determination from the four samples.

The evaporable water content at 11% RH was determined on 20 g to 25 g sample using the following formula:

$$\xi_{11} = (W_{11} - W_d) / W_d$$

where $\xi_{11}$: evaporable water content at 11% rh

$W_{11}$: weight of the sample at 11% rh, g

$W_d$ : weight of the dried sample (in an oven at 105°C), g.

The $W_{11}$ was measured at the end of the sample's conditioning period at 11% RH. $W_d$ was measured after drying the sample to a constant weight in an oven at 105°C.

### 3.3.4 X-Ray Diffraction

The samples to be tested were taken out of the chloride solutions. The surfaces of the fragmented samples were wiped with a dry cloth to take off the excess solution. The samples were then vacuum-dried for three days in a dessicator containing silica gel and soda lime. After drying, the samples were removed to a glove box kept at low RH (11%) and containing soda lime (to absorb the $CO_2$ in the air). They were ground to powder inside the glove box and sealed in vials. The vials were stored inside the dessicator until the time of testing.

The X-ray diffraction patterns were obtained on a Siemens D5000 X-ray diffractometer using Ni-filtered CuKα radiation with a wavelength $\lambda = 15.418$ nm.

## 3.4 Program Details

### 3.4.1 Phase One

Part 1A involved the testing of various OPC-SCM blends with different types and replacements levels of SCM. and with W/CM ratios of 0.3 and 0.5. The SCM included silica fume, GGBFS, 3 types of fly ash (Type F, Type CH, Type CI), and metakaolin. The Type F fly ash and the GGBFS were used at 25% and 40% replacement levels, while the two other fly ash were tested at 25% replacement level. The silica fume and the metakaolin were tested at 8% replacement level. Ternary blends with silica fume-slag, and silica fume-fly ash were also used at two different replacement levels. Table 3-5 shows the compositions and designs of mixtures used in Phase 1. The effect of temperature was examined; four mixtures (W/CM = 0.3) were tested at 7°C and 38°C in addition to the standard test temperature of 23°C. replicates of these mixtures were tested to check the reproducibility of the results. The influence of age (curing period) was examined by testing 5 mixtures (W/CM = 0.5) at 2 months and 9 months. Table 3-6 and 3-7 summarize the experimental details of Part 1A

Part 1B focused on comparing the results from the equilibrium method and the ponding method. Four mixtures with W/CM of 0.5 (OPC, 8SF, 8MK, 25FA) were tested using the ponding method, and the resulting binding isotherms were compared with those obtained from the equilibrium method. Table 3-5 shows the mix compositions, and Table 3-7 summarizes the experimental details of Part 1B.

In Part 1C, more tests were done to evaluate the reproducibility of the results as well as the sensitivity of the results to the sample size and host solution volume at W/CM ratio of 0.5. OPC was chosen to study the reproducibility. Four replicate mixtures were prepared and tested at seven chloride concentrations. OPC, 8SF, and 8MK were selected to check the sensitivity of the results to sample size and host solution volume. Three sample sizes were tested at a 3.0 M chloride concentration. Three solution volumes were tested at a 3.0 M chloride concentration. Table 3-8 summarizes the tests.

Table 3-5: Proportioning of Mixtures Used in Phase 1

| Mix | W/CM | OPC (%) | SF (%) | MK (%) | FA (%) | BFS (%) |
|---|---|---|---|---|---|---|
| **OPC** | 0.3, 0.5, 0.7 | 100 | | | | |
| **8SF** | 0.3, 0.5 | 92 | 8 | | | |
| **8MK** | 0.3, 0.5 | 92 | | 8 | | |
| **25FA** | 0.3, 0.5 | 75 | | | 25 | |
| **25FA1** | 0.5 | 75 | | | 25 | |
| **25FA2** | 0.5 | 75 | | | 25 | |
| **40FA** | 0.3 | 60 | | | 40 | |
| **25SL** | 0.3, 0.5 | 75 | | | | 25 |
| **40SL** | 0.3 | 60 | | | | 40 |
| **25FA6SF** | 0.3, 0.5 | 69 | 6 | | 25 | |
| **40FA5SF** | 0.3 | 55.2 | 4.8 | | 40 | |
| **25SL6SF** | 0.3, 0.5 | 69 | 6 | | | 25 |
| **40SL5SF** | 0.3 | 55.2 | 4.8 | | | 40 |

Table 3-6: Summary of Experimental Program in Part 1A (mixtures with W/CM=0.3)

| Mix | Curing period: 2 mos<br>NaCl concentrations: 0.1, 0.3, 0.5, 0.7, 1, 2, 3 M | | |
|---|---|---|---|
| | T= 7 °C | T= 23 °C | T= 38 °C |
| OPC | X | X X | X |
| 8SF | X | X X | X |
| 8MK | | X | |
| 25FA | X | X X | X |
| 40FA | | X | |
| 25SL | X | X X | X |
| 40SL | | X | |
| 25FA6SF | | X | |
| 40FA5SF | | X | |
| 25SL6SF | | X | |
| 40SL5SF | | X | |

Table 3-7: Summary of Experimental Program in Part 1A and Part1B (mixtures with W/CM=0.5)

| Mix | Part 1A | | Part 1B |
|---|---|---|---|
| | Equilibrium method<br>Curing : 2 months<br>NaCl concentration :<br>0.1, 1.0, 3.0 M | Equilibrium method<br>Curing : 9 months<br>NaCl concentration :<br>0.1, 0.3, 0.5, 0.7, 1.0,<br>2.0, 3.0 M | Ponding method<br>Curing : 2 months<br>Ponding:18 mos<br>NaCl concentration : 1M |
| OPC | X | X | X |
| 8MK | X | X | X |
| 8SF | X | X | X |
| 25FA | X | X | X |
| 25FA1 | X | | |
| 25FA2 | X | | |
| 25SL | X | X | |
| 25FA6SF | | X | |
| 25SL6SF | | X | |

Table 3-8: Summary of Experiments on the Repeatability and Sensitivity of the Equilibrium Method in Part 1C.

| | Reproducibility of Results | Effect of Sample size | Effect of Host solution volume |
|---|---|---|---|
| Mix studied | OPC | OPC, 8SF, 8MK | OPC, 8SF, 8MK |
| Chloride Concentrations (M) | 0.1, 0.3, 0.5, 0.7, 1.0, 2.0, 3.0 | 3.0 | 3.0 |
| Number of replicas | 4 | | |
| Sizes tested (g) | | 12.5, 25, 50 | 25 |
| Volumes tested (ml) | | | 30, 40, 60 |

### 3.4.2 Phase Two

Table 3-5 shows the mix designs and compositions of the mixtures used in Part 2A. Three mixes were chosen for this study: the OPC control mix, the 8SF, and the 8MK. The W/CM ratio was 0.5. It was decided that three chloride concentrations were enough to study the effect of the different variables since the shape of the binding isotherms was already established from Phase One. NaCl concentrations of 0.1, 1.0, and 3.0 molar were selected. It was also decided to re-examine the effect of temperature after evaporation occured in the samples from Phase 1. The bottles were sealed with wax this time to prevent evaporation.

The carbonation study consisted of testing samples carbonated before being tested for chloride binding, and samples carbonated after being tested for binding to check the influence of carbonation on the release of bound chloride. The samples to be carbonated were cut up into 3mm thick discs. They were laid out on perforated plastic boards and stored in glass containers kept at 65% RH by using saturated sodium nitrate; this RH is almost optimum for carbonation *(Neville, 1990)*. The containers were continuously flooded, at a low rate, with a gas mixture of nitrogen and 5% carbon dioxide. The method used to check for carbonation consisted of spraying freshly exposed surfaces with an ethanol solution with 1% phenolphthalein indicator. The carbonated areas remain colourless while the uncarbonated areas turn violet.

The control sample was carbonated in about three weeks to a month, but the 8SF and 8MK samples were not totally carbonated after two and a half months. The samples were then stored in a special chamber where vacuum was applied before the chamber was flooded with the gas mixture. The RH was also kept at 65% and the vacuuming and gas purging was applied daily. The samples were totally carbonated in about a week.

To study the influence of sulphate ion, three sulphate concentrations were used: 0, 0.01, and 0.1 molar. $Na_2SO_4$ was used to obtain the desired sulphate concentration, while NaOH was used instead of saturated $Ca(OH)_2$ to obtain a pH of 12.5. The use of $Ca(OH)_2$ would have reacted with $Na_2SO_3$ to form NaOH and $CaSO_4$. The calcium sulphate would have precipitated due to its low solubility thus preventing the sulphate ions from interacting with the cement hydrates and affecting the binding process.

Four pH levels were chosen to examine the influence of pH on chloride binding. They were 13.0, 13.4, 13.7, and 14.0. NaOH and KOH were used to obtain the desired pH level. The NaOH/KOH ratio was 1/4, which was similar to that of the pore solution of the control mix. A

sample of the pore solution of the control mix was obtained using a pore pressing machine. The $K^+$ and $Na^+$ concentrations in the pore solution of the control mix were determined by analysing the pore solution using flame photometry Tables 3-9 to 3-12 summarize the experimental details of Part 2A.

Table 3-9: Summary of Experiments on the Effect of pH in Part 2A

| **Factor studied** | Effect of pH of host solution |
|---|---|
| **Mixtures** | OPC, 8SF, 8MK |
| **W/CM; Age; Temperature** | 0.5; 2 months; 23°C |
| **NaCl concentrations tested** | 0.1, 1.0, 3.0 molar |
| **Chloride solution composition** | NaCl, KOH, NaOH |
| **pH tested** | pH = 13.0, 13.4, 13.7, 14.0 |

Table 3-10: Summary of Experiments on the Effect of Sulphate in Part 2A

| **Factor studied** | Effect of sulphate ions in solution |
|---|---|
| **Mixtures** | OPC, 8SF, 8MK |
| **W/CM; Age; Temperature** | 0.5; 2 months; 23°C |
| **NaCl concentrations tested** | 0.1, 1.0, 3.0 molar |
| **Chloride solution composition** | NaCl, $Na_2SO_4$, NaOH |
| **Sulphate concentrations tested** | $[SO_4^{2-}]$ = 0.00, 0.01, 0.10 molar |

Table 3-11: Summary of Experiments on the Effect of Temperature in Part 2A

| **Factor studied** | Effect of temperature |
|---|---|
| **Mixtures** | OPC, 8SF, 8MK |
| **W/CM; Age** | 0.5; 2 months |
| **NaCl concentrations tested** | 0.1, 1.0, 3.0 molar |
| **Chloride solution composition** | NaCl, $Ca(OH)_2$ |
| **Temperatures tested** | T= 7°C, 23°C, 38°C |

Table 3-12: Summary of Experiments on the Effect of Carbonation in Part 2A

| **Factor studied** | Effect of carbonation |
|---|---|
| **Mixtures** | OPC, 8SF, 8MK |
| **W/CM; Age; Temperature** | 0.5; 2 months; 23°C |
| **NaCl concentrations tested** | 0.1, 1.0, 3.0 molar |
| **Chloride solution composition** | NaCl |
| **Conditions tested** | Non-carbonated Vs carbonated samples |

In Part 2B, nine different Portland cements (Table 3-3) were tested for their chloride binding capacity. This study was conducted to check the influence of cement composition ($C_3A$, $C_4AF$, $C_3S$, $SO_3$, $Na_2O_e$) on the binding capacity. The effect of the $C_3A$ content was of particular interest in this study, since the published results in the literature do not show a consistent trend regarding the influence of the $C_3A$ content, or it is likely that the published results indicate that the $C_3A$ content of cement is not the only important factor that influence the binding capacity. The $C_3A$ content of the cements varied between 0% and 11%. Two of these cements were of particular interest since they had 0% $C_3A$ and close to 0% $C_4AF$, respectively. It was hoped that the behaviour of these two cements with respect to the other cements would help in better understanding the roles of $C_3A$ and $C_4AF$ in chloride binding. In addition to $C_3A$ and $C_4AF$, the $SO_3$ and $Na_2O_e$ contents varied over relatively large ranges. Experimental details are summarized in Table 3-13.

Table 3-13: Summary of experimental details of the influence of cement type in Part 2B

| **Factor studied** | Effect of cement composition and type |
|---|---|
| **Mixtures** | OPC, C1, C2, C3, C4, C5, C6, C7, C8 |
| **W/CM; Age; Temperature** | 0.5; 2 months; 23°C |
| **NaCl concentrations tested** | 0.1, 1.0, 3.0 molar |
| **Chloride solution composition** | NaCl, $Ca(OH)_2$ |

Two cements, C1 and C4, were used to study the influence of sulphate content on the binding capacity. The test involved adding gypsum to the two cements in specified quantities, and comparing the binding capacities of the resulting cements with the original cements. The addition

of gypsum resulted in about 4% $SO_3$ and 7% $SO_3$ contents (in addition to the $SO_3$ content of the original cements) in the resulting cements C1-4$SO_3$ and C4-7$SO_3$ respectively. The specific amounts of added gypsum were chosen so that the sulphate content of the resulting cements would be more than enough to transform all the $C_4AF$ content into ettringite in the C1 cement, and enough to transform the $C_3A$ and $C_4AF$ contents into ettringite and monosulphate. It was hoped that by comparing the binding capacities and XRD results of C1 and C1-4$SO_3$, and C4 and C4-7$SO_3$ would provide some insight into the influence of sulphates, and the roles of the chemical and physical binding capacities in cements. Table 3-14 shows the details of the test.

The influence of cement fineness was also studied. Cements C2 and C3 were produced at the same plant, and had similar chemical composition except that C2 (CSA Type 10) had a surface area of 334 $m^2/kg$ and cement C3 (CSA Type 30) had a surface area of 523 $m^2/kg$. Also, cement C4 was ground for an extra two hours to give cement C4', and the binding capacities of the two cements were compared. Table 3-15 shows the details of the test.

Table 3-14: Summary of Experiments on the Effect of Sulphate content of Cement in Phase 2B

| **Factor studied** | Effect of sulphate content |
|---|---|
| **Mixtures** | C1, C1-4$SO_3$, C4, C4-7$SO_3$ |
| **W/CM; Age; Temperature** | 0.5; 2 months; 23 °C |
| **NaCl concentrations tested** | 0.1, 1.0, 3.0 molar |
| **Chloride solution composition** | NaCl, $Ca(OH)_2$ |
| **Conditions tested** | C1 vs C1-4$SO_3$, and C4 vs C4-7$SO_3$ |

Table 3-15: Summary of Experiments on the Effect of Cement Fineness in Phase 2B

| **Factor studied** | Effect of cement fineness |
|---|---|
| **Mixtures** | C2, C3, C4, C4' |
| **W/CM; Age; Temperature** | 0.5; 2 months; 23 °C |
| **NaCl concentrations tested** | 0.1, 1.0, 3.0 molar |
| **Chloride solution composition** | NaCl, $Ca(OH)_2$ |
| **Conditions tested** | C2 vs C3, and C4 vs C4' |

### 3.4.3 Phase Three

Part 3A focused on the behaviour of the cement mineral phases by studying the individual chloride binding properties of pure phases, $C_3A$, $C_3S$, $C_4AF$, and $C_2S$. The pure cement phases were obtained from Lafarge as granular material and had to be ground. A steel ball mill (1 kg capacity) was used for this purporse. It was originally decided to grind the clinkers to a target surface area of 350 to 400 $m^2/kg$. Unfortunately, the $C_3S$ was overground to a 550 $m^2/kg$. So, it was then decided to grind the other three phases to around 450 $m^2/kg$ to lower any effect that might arise from a large difference between the surface area of the phases, while keeping the surface area close to the normal range found in Portland cement.

The $C_3A$ mix prepared was not 100% pure $C_3A$, but a mixture of $C_3A$, gypsum, and $Ca(OH)_2$. The reason for this was to include the important role sulphates play in chloride binding, and particularly in the case of the $C_3A$ phase. Two different mixtures were used to study the effect of sulphate content on the binding properties of the $C_3A$ phase.. They were proportioned in terms of the molar ratios of $C_3A$, $SO_3$, and $Ca(OH)_2$. Ratios of $1.0C_3A/0.8SO_3/0.3Ca(OH)_2$ and $1.0C_3A/0.4SO_3/0.3Ca(OH)_2$ were used for the two mixtures respectively. Similar to $C_3A$, a mixture of $1.0C_4AF/0.8SO_3/0.3Ca(OH)_2$ was used to study the binding properties of the $C_4AF$ phase. The $C_3S$ and $C_2S$ mixes were 100% $C_3S$ and 100% $C_2S$ respectively. A W/CM = 0.5 was chosen, and the mix water used for all mixes had NaOH and KOH in concentrations equal to those of the control mix (0.085 M, and 0.345 M respectively). Table 3-16 shows the compositions of all mixtures.

Table 3-16: Proportioning of Mixtures Used in Part 3A

| Mix | W/CM | Composition ( % ) | | | | | |
|---|---|---|---|---|---|---|---|
| | | $C_3S$ | $C_2S$ | $C_3A$ | $C_4AF$ | Gypsum | $Ca(OH)_2$ |
| $C_3S$ | 0.5 | 100 | | | | | |
| $C_2S$ | 0.5 | | 100 | | | | |
| $C_3A8$ | 0.5 | | | 63.23 | | 31.57 | 5.2 |
| $C_3A4$ | 0.5 | | | 75.08 | | 18.74 | 6.18 |
| $C_4AF$ | 0.5 | | | | 75.57 | 20.98 | 3.46 |

All mixtures were tested for their chloride binding capacity at different chloride concentrations. Four NaCl concentrations were used: 0.1, 0.5, 1.0, and 3.0 molar. The $C_3A8$ and $C_3S$

mixtures were further tested for the influence of pH, sulphate ion concentration, temperature and carbonation on their chloride binding capacity. In these tests, pH = 14, $[SO_4^{2-}]$ = 0.1 M, and T = 7° C and 38° C were used. Three NaCl concentrations were used in these tests: 0.1, 1.0, and 3.0 molar. The $C_3A$ mix was only tested at T= 38° C (in addition to 23°C) since there were not enough samples to test at 7° C and 38° C. Tables 3-17 to 3-21 summarize the tests details of Part 3A.

Table 3-17: Summary of Experiments on the Effect of Chloride Concentration in Part 3A

| **Factor studied** | Effect of chloride concentration |
|---|---|
| **Mixtures** | $C_3S$, $C_2S$, $C_3A8$, $C_3A4$, $C_4AF$ |
| **Chloride solution composition** | NaCl, $Ca(OH)_2$ |
| **NaCl concentrations tested** | 0.1, 0.5, 1.0, 3.0 molar |

Table 3-18: Summary of Experiments on the Effect of pH in Part 3A

| **Factor studied** | Effect of pH of solution |
|---|---|
| **Mixtures** | $C_3S$, $C_3A8$ |
| **NaCl concentrations tested** | 0.1, 1.0, 3.0 molar |
| **Chloride solution composition** | NaCl, KOH, NaOH (pH=14.0)<br>NaCl, $Ca(OH)_2$ (pH=12.5) |
| **pH tested** | pH = 12.5, 14 |

Table 3-19: Summary of Experiments on the Effect of Sulphate in Part 3A

| **Factor studied** | Effect of sulphate ions in solution |
|---|---|
| **Mixtures** | $C_3S$, $C_3A8$ |
| **NaCl concentrations tested** | 0.1, 1.0, 3.0 molar |
| **Chloride solution composition** | NaCl, $Na_2SO_4$, NaOH ($[SO_4^{2-}]$=0.1 molar)<br>NaCl, $Ca(OH)_2$ ($[SO_4^{2-}]$=0.0 molar) |
| **Sulphate concentrations tested** | $[SO_4^{2-}]$ = 0.0, 0.1 molar |

Table 3-20: Summary of Experiments on the Effect of Temperature in Part 3A

| Factor studied | Effect of temperature |
|---|---|
| Mixtures | $C_3S$, $C_3A8$ |
| NaCl concentrations tested | 0.1, 1.0, 3.0 molar |
| Chloride solution composition | NaCl, $Ca(OH)_2$ |
| Temperatures tested | T = (7°C)*, 23°C, 38°C |

* The C3A paste was not tested at T = 7°C

Table 3-21: Summary of Experiments on the Effect of Carbonation in Part 3A

| Factor studied | Effect of carbonation |
|---|---|
| Mixtures | $C_3S$, $C_3A8$ |
| NaCl concentrations tested | 0.1, 1.0, 3.0 molar |
| Chloride solution composition | NaCl |
| Conditions tested | pre-carbonated Vs non-carbonated samples |

In Part 3B, mixtures of SF-lime and MK-lime were tested for their chloride binding capacity. Three different proportions were used for each mixture. They were 1/2, 2/1, and 1/1 by mass (SCM/lime). These proportions were chosen on the basis that up to 30% SF replacement is needed to react with all the $Ca(OH)_2$ produced as a result of hydration. Hence, a 2/1 ratio of SF to lime was used as an upper limit and the other two ratios were spread out in the hope that the resulting C-S-H hydrates would have different C/S ratios. This would enable us to examine the influence of the C/S ratio on the binding properties of C-S-H.

A W/CM ratio of 2.0 was chosen after several trials to obtain workable mixes without the addition of a superplasticiser. This high W/CM was due to the high water absorption of SF and MK especially at 2/1 proportions. The mix water contained NaOH and KOH in concentrations similar to those found in the control mix. The mixes were cured for 2 months at 38° C to accelerate the pozzolanic reactions. In addition to the SCM-lime mixtures, a 100% GGBFS mixture (100SL) and a 50%OPC-50%GGBFS (50SL) mixture were tested for their chloride binding capacities. Tables 3-22 and 3-23 show the mixture compositions and the experimental details, respectively. A summary of the experimental program is presented in Table 3-24.

Table 3-22: Proportioning of Mixtures Used in Phase 3B

| Mix | W/CM | Composition (% mass) | | | | |
|---|---|---|---|---|---|---|
| | | OPC | SF | MK | GGBFS | $Ca(OH)_2$ |
| SF12† | 2 | | 33.33 | | | 66.66 |
| SF11† | 2 | | 50 | | | 50 |
| SF21† | 2 | | 66.66 | | | 33.33 |
| MK12† | 2 | | | 33.33 | | 66.66 |
| MK11† | 2 | | | 50 | | 50 |
| MK21† | 2 | | | 66.66 | | 33.33 |
| 50SL | 0.5 | 50 | | | 50 | |
| 100SL | 0.5 | | | | 100 | |

† The mixing water in the SCM-lime mixtures contained NaOH and KOH in concentrations similar to those of the OPC paste.

Table 3-23 Summary of Experimental Details of Part 3B

| | SCM-lime Mixtures | OPC-GGBFS Mixtures |
|---|---|---|
| **Mixtures** | SF12, SF21, SF11, MK12, MK11, MK21 | 50SL, 100SL |
| **Curing** | 2 months, 38°C | 2 months, 23°C |
| **NaCl concentrations tested** | 0.1, 1.0, 3.0 molar | 0.1, 1.0, 3.0 molar |
| **Chloride solution composition** | NaCl, $Ca(OH)_2$ | NaCl, $Ca(OH)_2$ |

Table 3-24: Summary of the experimental program

| | | |
|---|---|---|
| **Phase1** | **Part 1A** | **Testing various blended cements with W/CM = 0.3 & 0.5:**<br>● Influence of SCM type and replacement level (OPC, 8SF, 8KM, 25FA, 40FA, 25SL, 40SL, 25FA6SF, 40FA4.8SF, 25SL6SF, 40SL4.8SF, 25FA1, 25FA2)<br>● Reproducability of results (replicas of OPC, 8SF, 25FA, 25SL)<br>● Influence of temperature (7°C, 23°C, 38°C) (OPC, 8SF, 25FA, 25SL)<br>● Influence of age (2mos, 9mos) (OPC, 8SF, 8MK, 25FA, 25SL) |
| | **Part 1B** | **Equilibrium method Vs Ponding method:**<br>● Testing some of the above blends using the Ponding method (OPC, 8SF, 8MK, 25FA) |
| | **Part 1C** | **Reproducibility and sensitivity of the equilibrium method:**<br>● Reproducibility of the results (4 replicas of the control paste)<br>● Sensitivity of the results:<br>Influence of sample size (OPC, 8SF, 8SF)<br>Influence of solution volume (OPC, 8SF, 8SF) |
| **Phase2** | **Part 2A** | **Influence of environmental factors:**<br>● Effect of pH (pH=13, 13.4, 13.7, 14) (OPC, 8SF, 8MK)<br>● Effect of $SO_4^{2-}$ ( $[SO_3^{2-}]$=0 M, 0.01 M, 0.1 M) (OPC, 8SF, 8MK)<br>● Effect of Temperature (7°C, 23°C, 38°C) (OPC, 8SF, 8MK)<br>● Effect of Carbonation (OPC, 8SF, 8MK)<br>● Desorption isotherms (OPC, 8SF, 8MK, C4) |
| | **Part 2B** | **Influence of cement composition and type:**<br>● Binding isotherms (C1, C2, C3, C4, C5, C6, C7, C8, OPC)<br>● Effect of $SO_3$ content (C1 Vs C1-4$SO_3$ and C4 Vs C4-7$SO_3$)<br>● Effect of cement fineness (C2 Vs C3 and C4 Vs C4 (2hr) ) |
| **Phase3** | **Part 3A** | **Testing Pure Phases ($C_3A$, $C_4AF$, $C_3S$, $C_2S$):**<br>● Chloride binding isotherms ($C_3A8$, $C_3A4$, $C_4AF$, $C_3S$, $C_2S$)<br>● Effect of pH (pH=14) ($C_3A8$, $C_3S$)<br>● Effect of $SO_3^{2-}$ ( $[SO_3^{2-}]$=0.1 M) ($C_3A8$, $C_3S$)<br>● Effect of Temperature (7°C, 23°C, 38°C) ($C_3A8$, $C_3S$)<br>● Effect of carbonation ($C_3A8$, $C_3S$)<br>● Desorption ($C_3A8$, $C_3S$)<br>● Cement substitution with $C_3A$ (C1 Vs C1-6$C_3A$ and C1-10$C_3A$)<br>● Cement substitution with $C_4AF$ (C7 Vs C7-7$C_4AF$) |
| | **Part 3B** | **Testing SCM-lime mixtures:**<br>● SF-lime (SF21, SF11, SF12)<br>● MK-lime (MK21, MK11, MK12)<br>● Testing OPC-GGBFS blends (50SL, 100SL) |

# CHAPTER 4

# RESULTS AND ANALYSIS

## 4.1 PHASE ONE

### 4.1.1 Equilibrium Method

#### 4.1.1.1 Analysis of Data

In the equilibrium method, it is assumed that after equilibrium is reached between the external solution and the pore solution of the sample, the reduction in the concentration of the host solution is attributed to chloride being bound by the cement. Then, knowing the initial and final concentration, the volume of the external solution and the dry mass of the sample, the amount of bound chloride can be calculated according to the following formula:

$$C_b = 35.453 * V * (C_i - C_e)/W_d$$

where $C_b$ : amount of bound chloride in mg Cl/g of sample,

$V$ : volume of the external solution in ml,

$C_i$ : initial chloride concentration of the external solution in mol/l,

$C_e$ : free chloride concentation at equilibrium of the external solution in mol/l, and

$W_d$ : dry mass of the sample in g.

The $W_d$ mass is calculated using the following formula:

$$W_d = W_{11} * (1 - \xi_{11})$$

where $W_{11}$: mass of the sample at 11% rh in g,

$\xi_{11}$: evaporable water content at 11% rh

Each tested chloride concentration represents a point in the binding isotherm. In this case the binding isotherms were obtained by plotting, for every concentration studied, the free chloride concentration at equilibrium ($C_e$) against the bound chlorides ( $C_b$). An example of a typical chloride binding isotherm is shown in Figure 4-1.

Desorption isotherms were determined for selected cases. After equilibrium was reached, and one point of the chloride binding isotherm was determined, the remaining chloride solution was mostly removed (using a pipette). The sample was then moved to another bottle and either 200 ml or 1000 ml of distilled water saturated with $Ca(OH)_2$ was added to the sample. After a second equilibrium was established, the free chloride concentration of the solution was measured. The

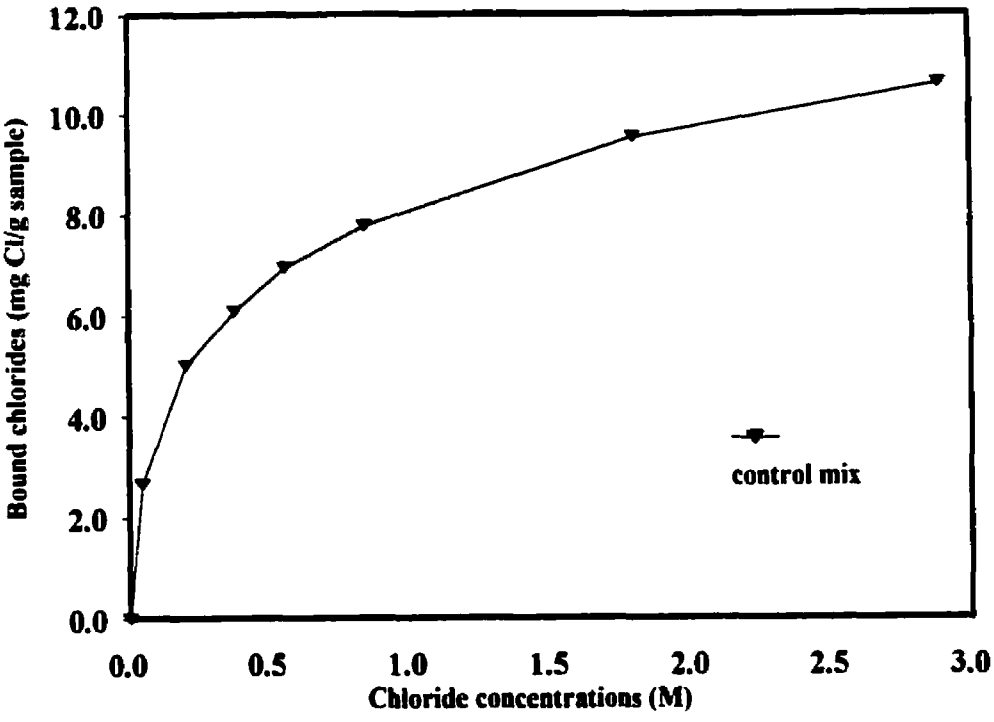


Figure 4-1: Chloride binding isotherm of the control mix (CSA Type 20 PC) at T=23°C, and W/CM=0.5.

amount of bound chloride remaining in the sample, after the second equilibrium, was determined from the following equation:

$$C_b = 35.453 * (V * C_1 - V_1 * C_e - C_2 * (V + V_2 - V_1))/W_d \quad (2)$$

where $C_2$ : chloride concentration after second equilibrium, mole/litre,

$V_1$ : volume of solution taken out, including first titration, ml, and

$V_2$ : volume of distilled water added, ml.

$C_2$ and $C_b$ (determined from equation (2)) represent one point of the chloride desorption isotherm. The desorption isotherms obtained in this research consisted of three points as described in Chapter 3.

#### 4.1.1.2 Reproducibility of the Equilibrium Method

To test the reproducibility of the results of the equilibrium method, used throughout this reseach, several mixtures were replicated. The comparisons included mixtures that were cast and tested at different times, and mixtures that were cast and tested during the same period of time and under the same conditions (same chloride solutions, same titrant). The results indicated that the reproducibility of the results was better when the replicas were cast and tested at the same time, than when they were cast and tested at different times. The reason for this is likely to do with the errors associated with titrator, the titrant, and the pipette. Figures 4-2 shows the chloride binding isotherms of four replicas of the control paste, tested at the same time, and Table 4-1 summarizes the relevant statistics for each chloride exposure. The coefficients of variations indicate a very good reproducibility. Note that the coefficient of variation of the data obtained at 0.1 M exposure is lower than the other coefficients of variation. This is possibly due to the fact that no dilution was needed to determine the equilibrium chloride concentrations at 0.1 M chloride exposure. Figure 4-3 shows another example.

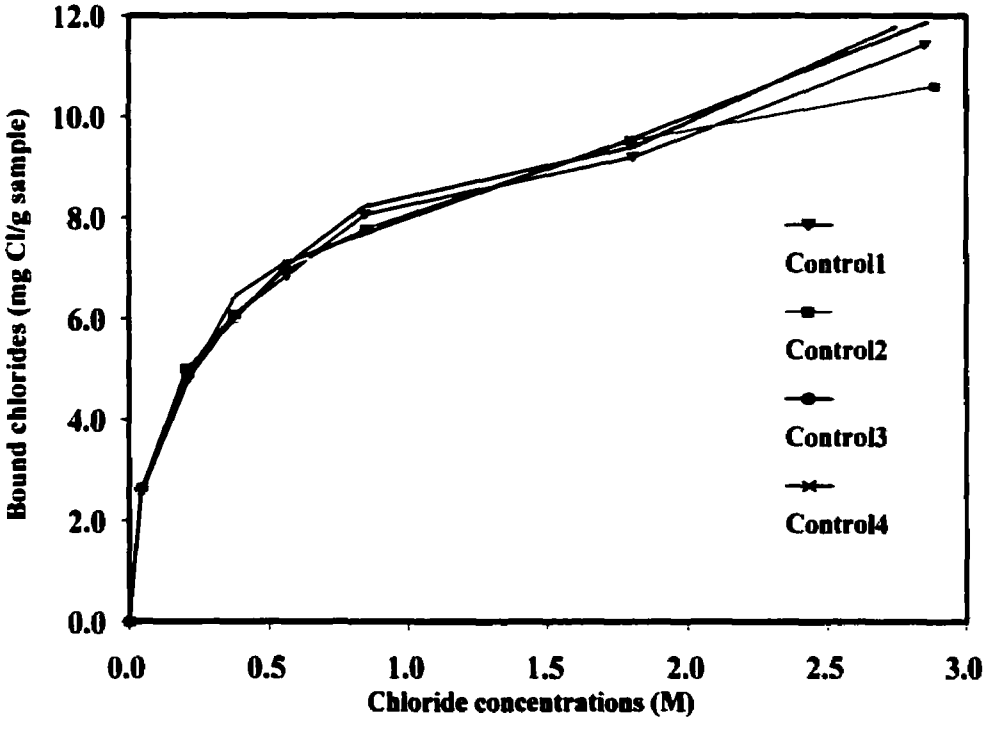


Figure 4-2: Chloride binding isotherms of 4 replicas of the control mix. T=23 °C, and W/CM=0.5.

Table 4-1: Statistics for the chloride binding data of 4 replicas of the control paste (shown in Figure 4-2).

| | Chloride exposure (mole/litre) | | | | | | |
|---|---|---|---|---|---|---|---|
| | 0.1 M | 0.3 M | 0.5 M | 0.7 M | 1.0 M | 2.0 M | 3.0 M |
| Minimum | 2.58 | 4.79 | 6.01 | 6.85 | 7.70 | 9.21 | 10.60 |
| Maximum | 2.66 | 5.02 | 6.23 | 7.11 | 8.22 | 9.55 | 11.88 |
| Range | 0.08 | 0.23 | 0.22 | 0.25 | 0.52 | 0.35 | 1.28 |
| Mean | 2.62 | 4.88 | 6.10 | 7.00 | 7.94 | 9.43 | 11.42 |
| Standard Deviation | 0.03 | 0.11 | 0.09 | 0.12 | 0.24 | 0.16 | 0.58 |
| Confidence Level (95%) | 0.03 | 0.11 | 0.09 | 0.12 | 0.24 | 0.16 | 0.57 |
| Coefficient of variation | 0.01 | 0.02 | 0.02 | 0.02 | 0.03 | 0.02 | 0.05 |

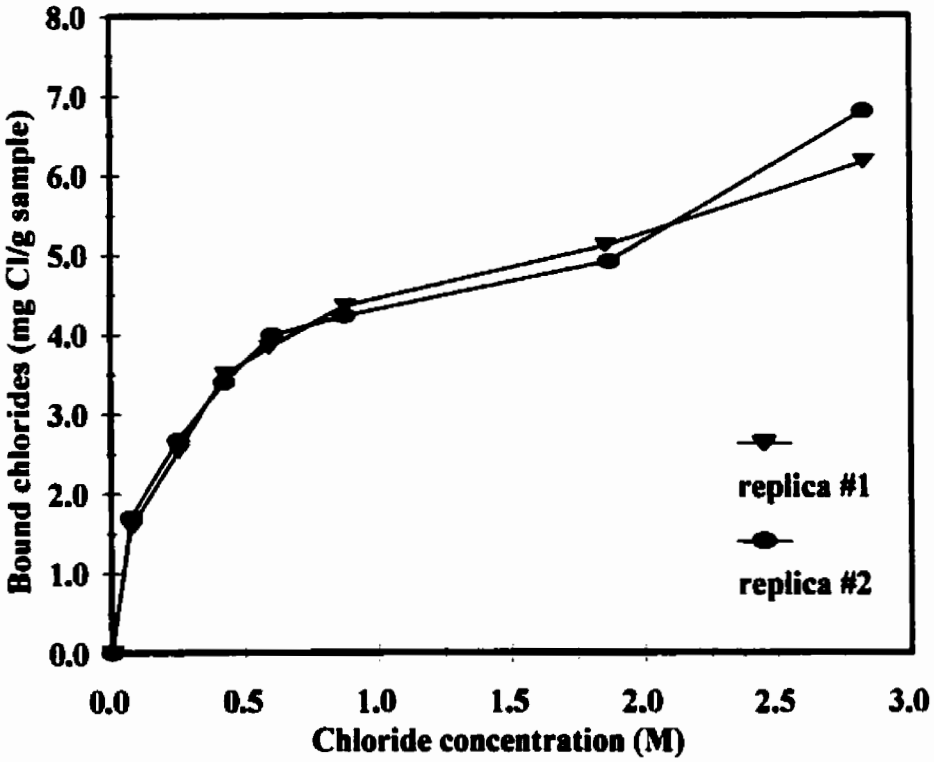


Figure 4-3: Chloride binding isotherms of 2 replicas of the 8SF(8% silica fume) paste. W/CM = 0.3

#### 4.1.1.3 Influence of Sample Size

Three different sample masses were tested: 12.5 g, 25 g, and 50 g. The liquid to solid ratio was the same for all three sizes. The initial chloride concentration of the host solutions was 3 M. The results in Figure 4-4 show no clear trend indicating that the sample size has an influence of on chloride binding. The differences between the binding capacities of samples of the same paste were small.

#### 4.1.1.4 Influence of Solution Volume

Figure 4-5 shows the results of the study on the influence of the host solution volume on the chloride binding capacity of cement pastes. Three different volumes of NaCl solutions were tested: 30 ml, 40 ml, and 60 ml, while keeping the mass of samples at 25 g (different liquid to solid ratios). The initial chloride concentration in the host solutions was 3 M. No clear trend was detectable in these results.

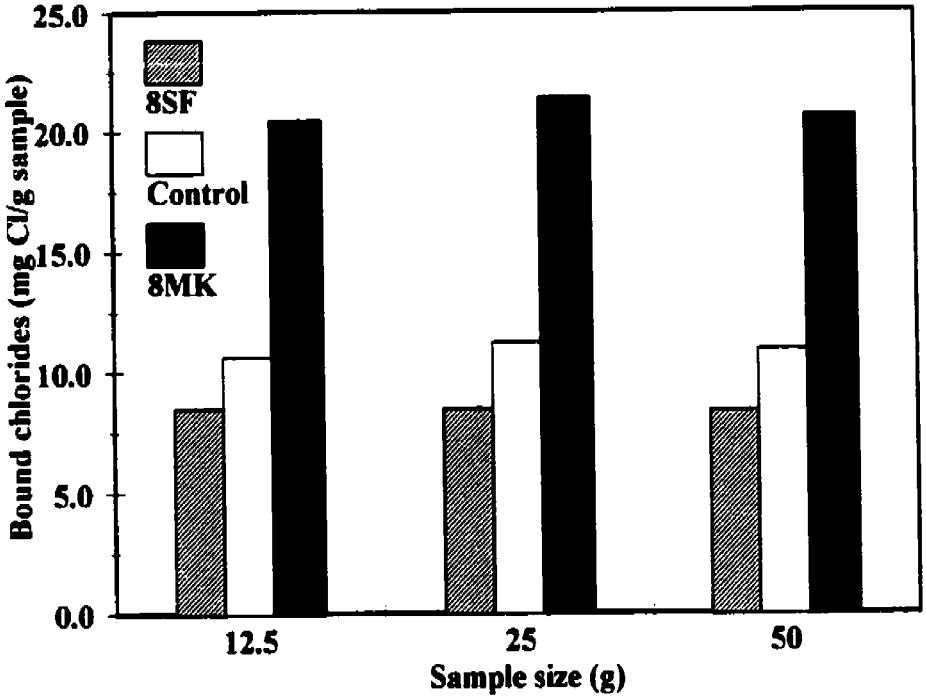


Figure 4-4 Influence of the sample size on the chloride binding capacity of paste. The W/CM ratio is 0.5 and the chloride concentration of the solutions is 3 M.

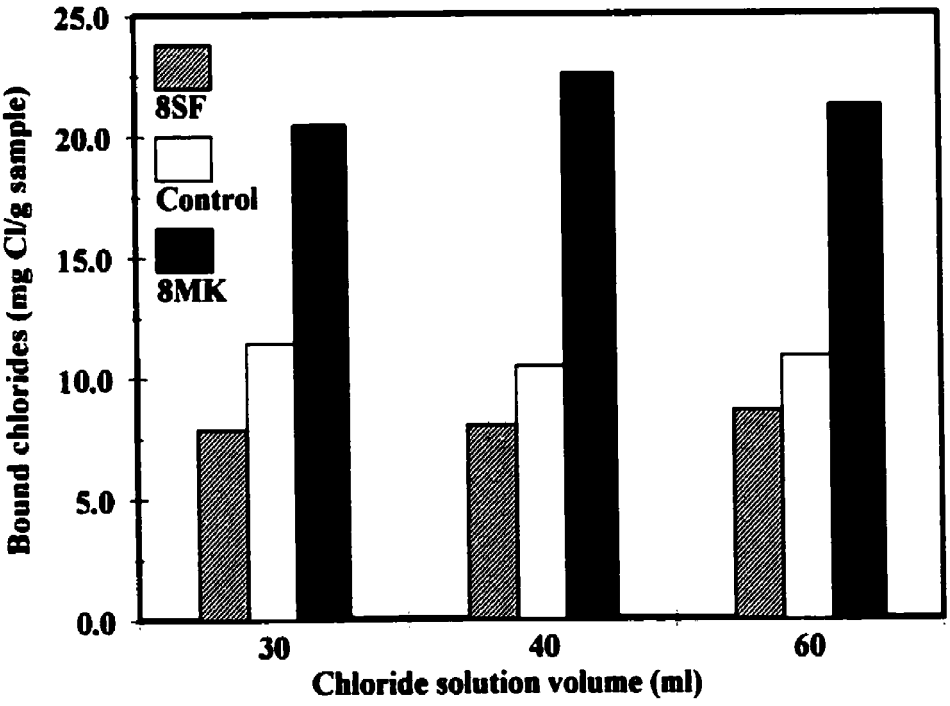


Figure 4-5: Influence of the chloride solution volume on the binding capacity of paste. The W/CM is 0.5, and the initial chloride concentration of the solutions is 3 M.

#### 4.1.1.5 Time to Equilibrium

The time to reach equilibrium between the external solution and the pore solution of the paste samples was determined by checking the chloride concentration of additional samples prepared specifically for this purpose. The initial chloride concentration of these samples was 3 M since it was assumed that the samples with the highest initial chloride concentration would take the longest time to reach equilibrium. The results show that the time to reach equilibrium was a function of the W/CM and mix composition as shown in Figures 4-6 and 4-7. In the case of samples with 0.5 W/CM, the chloride concentration starts to stabilize after about one to two weeks and becomes nearly constant after about three weeks. This was the case for all cements used. The mixture with silica fume took a longer time to reach equilibrium. The chloride concentration stabilized after about three weeks and became constant after around one month period. Specimens from pastes with 0.5 W/CM ratio were titrated after six to eight weeks of being submerged in chloride solutions. For the samples with 0.3 W/CM ratio, the chloride concentration started to level off after approximately one month and became constant at around two months in the case of the control mixture. The chloride concentration in the mixture with silica fume was still decreasing at a very small rate after three months. These samples were titrated after six months of exposure to the chloride solutions.

#### 4.1.1.6 Chloride Binding Isotherms

Figure 4-8 shows a typical set of experimental data for one of the studied mixtures. The X - axis represents the free chloride concentration at equilibrium in (mole/litre), and the Y- axis represents the amount of bound chloride in (mg of chloride/g of sample). As mentioned before, this relationship is a chloride binding isotherm. It is clear from this figure that chloride binding isotherms are non-linear. Other researchers also found non-linear binding isotherms *(Sergi et al., 1992: Tang & Nilsson, 1993)*. To illustrate this, both linear and non-linear isotherms were fitted to the experimental data. An example is shown in Figure 4-9 which indicates that the Freundlich isotherm best describes the binding relationship. This was the case for all 11 mixtures. The Langmuir isotherm also fitted the data well (Table 4-2), but had a lower coefficient of determination, $r^2$.

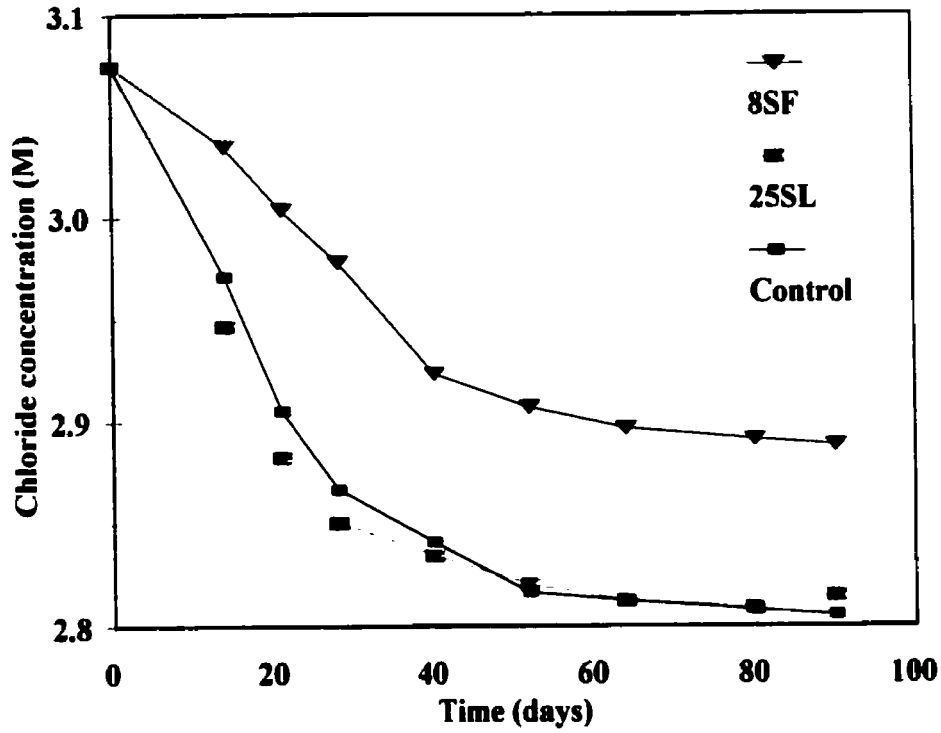


Figure 4-6: Time required for the chloride concentration to reach equilibrium between the host solution and the pore solution of pastes with W/CM of 0.3.

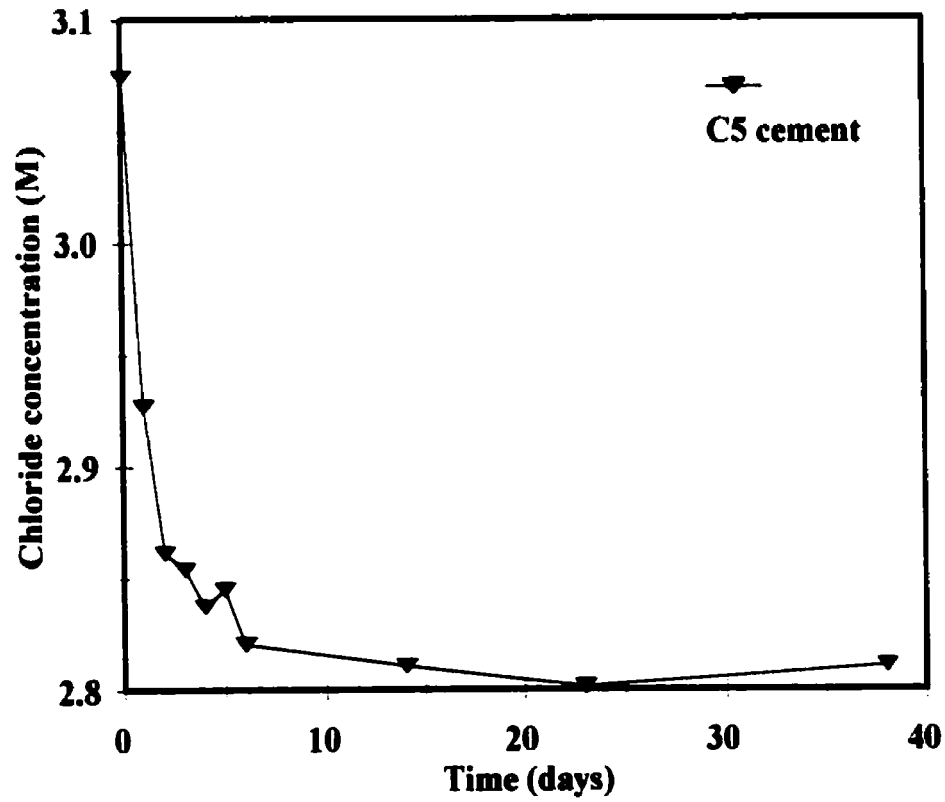


Figure 4-7: Time required to reach the equilibrium chloride concentration between the host solution and the pore solution of the C5 cement paste with W/CM of 0.5.

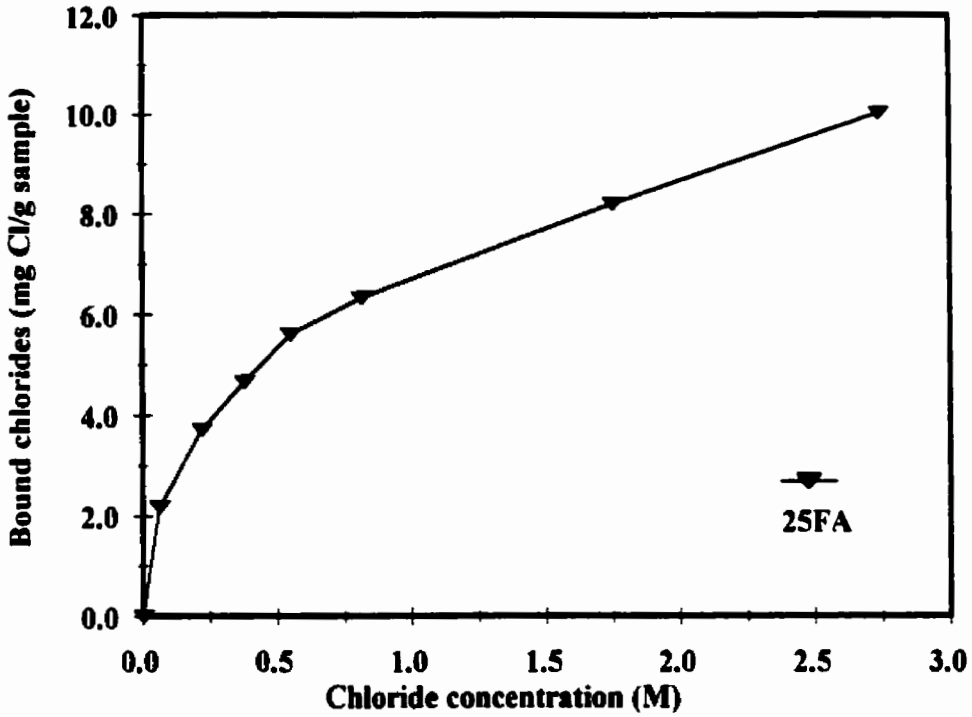


Figure 4-8: Chloride binding isotherm of the 25FA mix. W/CM = 0.3 and T= 23°C.

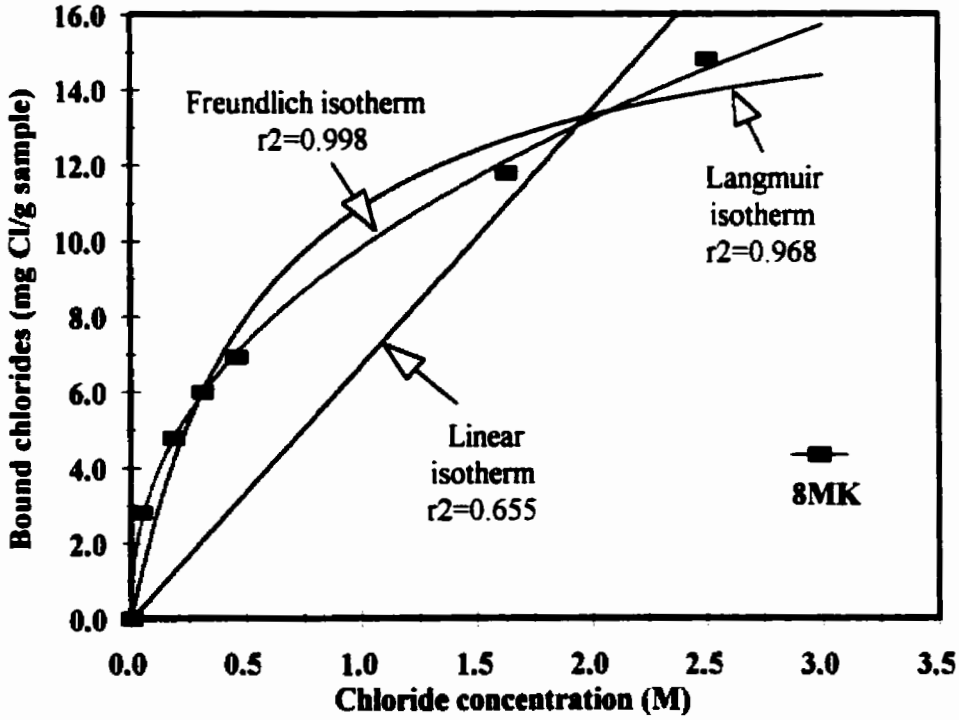


Figure 4-9: Curve fitting of the experimental chloride binding data of the 8MK paste (W/CM = 0.3), using the Freundlich, Langmuir, and linear isotherm.

Table 4-2: Coefficients of the Freundlich and Langmuir isotherms (and the corresponding coefficients of determination, $r^2$) which were fitted to the chloride binding data of the mixtures. The coefficients correspond to units of the binding capacity: mg Cl/g of sample. W/CM=0.3, T=23°C.

| | Freundlich | | | Langmuir | | |
|---|---|---|---|---|---|---|
| **Mixture** | **α** | **β** | **$r^2$** | **a** | **b** | **$r^2$** |
| **Control** | 7.60 | 0.31 | 0.999 | 35.23 | 3.30 | 0.918 |
| **25FA** | 6.78 | 0.38 | 0.998 | 21.92 | 1.97 | 0.972 |
| **40FA** | 7.55 | 0.45 | 0.998 | 19.24 | 1.35 | 0.978 |
| **25SL** | 7.93 | 0.30 | 0.993 | 41.85 | 3.91 | 0.947 |
| **40SL** | 8.62 | 0.33 | 0.979 | 37.76 | 3.05 | 0.931 |
| **8SF** | 4.38 | 0.33 | 0.990 | 17.78 | 2.74 | 0.978 |
| **8MK** | 9.84 | 0.43 | 0.998 | 29.95 | 1.75 | 0.968 |
| **25FA6SF** | 4.56 | 0.59 | 0.993 | 7.66 | 0.58 | 0.982 |
| **40FA4.8SF** | 4.77 | 0.55 | 0.991 | 8.91 | 0.75 | 0.969 |
| **25SL6SF** | 5.59 | 0.43 | 0.993 | 15.04 | 1.48 | 0.962 |
| **40SL4.8SF** | 6.25 | 0.41 | 0.997 | 17.68 | 1.61 | 0.961 |

The fact that the binding relationship is non-linear is important, since it has been shown *(Nilsson et al., 1993; Martin-Perez et al., 2000)* that the choice of the binding relationship has a considerable influence on the results of service-life predictions. This issue is discussed in Chapter 5.

#### 4.1.1.7 Effect of SCM (W/CM = 0.3)

Figure 4-10 shows the chloride binding isotherms of all the cementitious mixtures tested at 0.3 W/CM. These results clearly show that the binding capacity varies considerably with the mixture composition, and is influenced by both the type and replacement level of SCM. It is also obvious that the control mixture, OPC, has a higher binding capacity than the majority of the mixtures tested. This was unexpected since the addition of GGBFS or fly ash (Class F) was expected to increase binding judging by the general trends in the literature *(Dhir et al., 1996, 1997; Wiens & Schiessl, 1997)*. Yet, these results show that GGBFS slightly increased chloride binding at substitution levels of 25% while 25% fly ash reduced binding. Even at a replacement level of 40% the fly ash still reduced binding at the lower concentrations (0.1, 0.3, 0.5 M), but increased binding

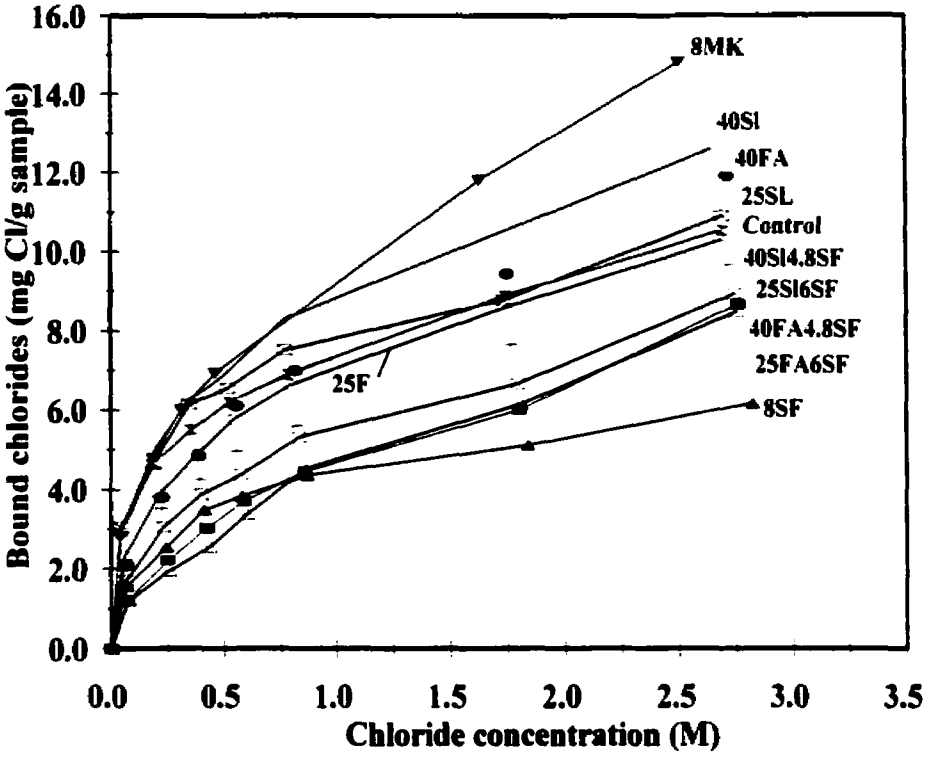


Figure 4-10: Chloride binding isotherms of the cementitious pastes with W/CM of 0.3. T =23°C.

at higher concentrations (2.0, 3.0 M). The 8MK (8% metakaolin) mixture exhibited the highest chloride binding, and the 8SF (8% silica fume) mix exhibited the lowest binding. The ternary blends with GGBFS and silica fume addition, exhibited higher binding capacities than the 8SF mix showing the beneficial effect of the GGBFS addition. The ternary blends with fly ash and silica fume performed better than the 8SF mix only at chloride concentrations higher than 0.7 M. It is of interest to notice that the binding capacity of the control mixture at lower chloride concentration (< 0.3 M) was among the best. This suggests that at low chloride concentrations the OPC substitution with SCMs did not generally benefit the chloride binding capacity.

The performance of the Class F fly ash was not expected. The relatively high aluminate and silicate content in the fly ash should increase the amount of C-S-H and C-A-H phases, and consequently chloride binding would be expected to increase. Furthermore, the substitution with fly ash should reduce the pH of the pore solution, which would result in an increase in chloride binding as suggested from the reported results in the literature *(Tritthart, 1989b)*. On the other hand, only reactive alumina and silica in the glass phase of the fly ash will participate in the reaction, and the

fly ash reaction is very slow. The fly ash pastes were two months old when they were exposed to chloride solutions. Keeping this in mind, one possible reason for the poor performance of the fly ash pastes is that the pozzolanic activity of the fly ash did not develop soon enough for its beneficial effect to be realised, especially at a W/CM ratio of 0.3 in sealed conditions. Another possibility is the use of superplasticiser in the mixes. In this context, it is interesting to mention that *Haque and Kayyali (1995)* found that the addition of a superplasticiser to fly ash concretes reversed the beneficial effect of fly ash on chloride binding. This was attributed to the negative charge imparted by the superplasticizer to the cement particles, resulting in a reduction of chloride adsorption by the hydration products.

#### 4.1.1.8 Effect of Temperature

Before discussing the results from this test, it is important to mention that during the testing, the measures taken to prevent evaporation for exposure at 38°C temperature were unfortunately insufficient and evaporation occured as a result. The evaporation rates were close to 10 % of the initial volumes of the chloride solutions. Taking that into account, corrections had to be applied to the titration results. Two assumptions are made in the correction process: 1) the ratio of the initial and equilibrium volumes of the host solution is equal to the ratio of the initial and equilibrium weight of the host solution, and 2) the evaporation does not affect the equilibrium between bound and free chloride. This means that the amount of chloride in the host solution, at equilibrium, is the same with or without evaporation. The corrected chloride concentrations at equilibrium are obtained as follow:

$$V_{sol} / V_{ee} = W_{sol} / W_{ee}$$

$$C_e * V_{sol} = C_{ee} * V_{ee}$$

$$C_e = C_{ee} * V_{ee} / V_s = C_{ee} * W_{ee} / W_{sol}$$

where $V_{sol}$: initial volume of host solution (without evaporation).

$V_{ee}$: volume of host solution at equilibrium after evaporation occurred.

$W_{sol}$: initial weight of host solution (without evaporation)

$W_{ee}$: weight of host solution at equilibrium after evaporation occured.

$C_e$: chloride concentration at equilibrium (without evaporation).

$C_{ee}$: measured chloride concentration at equilibrium after evaporation occurred.

The assumption that the equilibrium between free and bound chloride remained stable during evaporation is not accurate, and the higher the evaporation, the higher the error in the resulting estimation of the bound chloride.

Figure 4-11 shows a typical result of the effect of temperature on the binding isotherms (the chloride binding isotherm at 38°C was plotted against $C_e$ ). It was expected that an increase in temperature would cause a decrease in binding similar to the general trend from the results reported in the literature. This, however, was not the case, at least for part of the concentration range examined, as shown in Figure 4-11. Starting from the lowest concentration tested, chloride binding decreased with an increase in temperature. This trend was sustained up to a chloride concentration around 0.75 M. However, this trend was reversed at higher chloride concentrations. Because evaporation occured at 38°C , these results were judged inconclusive, and as previously stated, it was decided to repeat this test for mixtures with a W/CM ratio of 0.5.

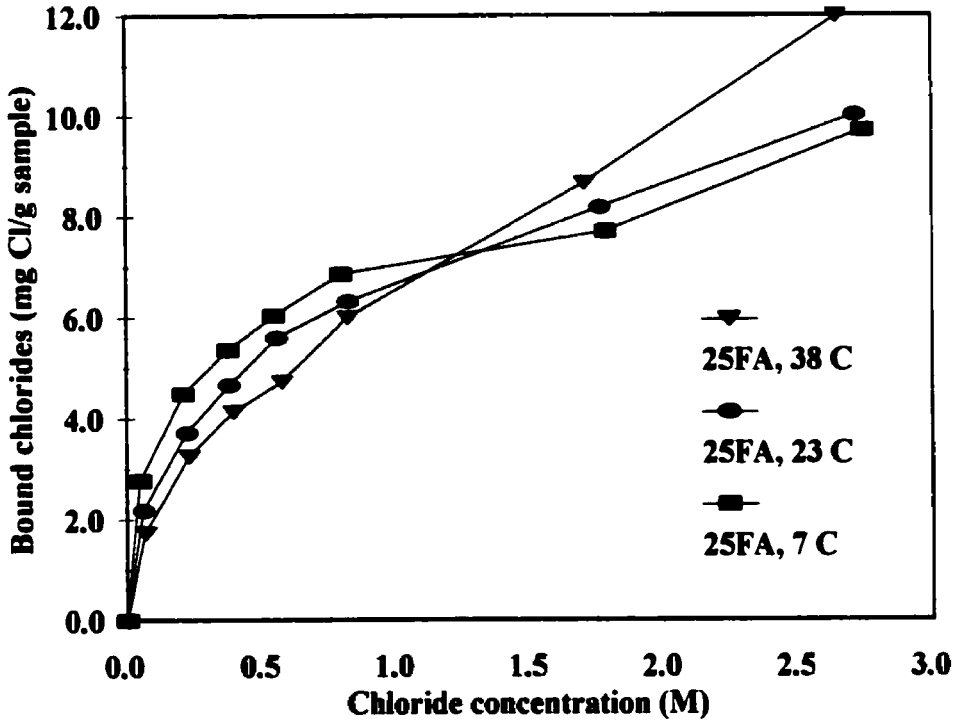


Figure 4-11: Effect of temperature on the chloride binding capacity of the 25FA paste with W/CM of 0.3.

#### 4.1.1.9 Effect of SCM (W/CM = 0.5)

Figure 4-12 shows the effect of SCM replacement of cement on the chloride binding capacity. The results show again the considerable influence of SCM replacement of cement on the binding capacity. This time however, the mixtures containing SCM exhibited higher binding capacities than the ones with a 0.3 W/CM and having the same SCM types and replacement levels. This was not the case for the control mix which exhibited only slightly higher binding at 0.5 W/CM ratio than at 0.3 W/CM ratio. Unlike the case of the 0.3 W/CM, the 25FA mix exhibited a higher binding capacity than the control mix. In fact, all three mixes containing fly ash bound more chlorides than the control mix. The 8MK and 8SF mixes bound the most and least amount of chloride respectively.

Figure 4-13 shows the chloride binding isotherms for mixtures cured for 9 months. Similar trends to those in Figure 4-12 can also be seen in this figure. The ternary mixture containing 25% GGBFS and 8% silica fume exhibited higher binding than the control mixture, while the ternary mixture with 25% fly ash and 8% silica fume only exhibited higher binding at chloride concentrations higher than 1 M.

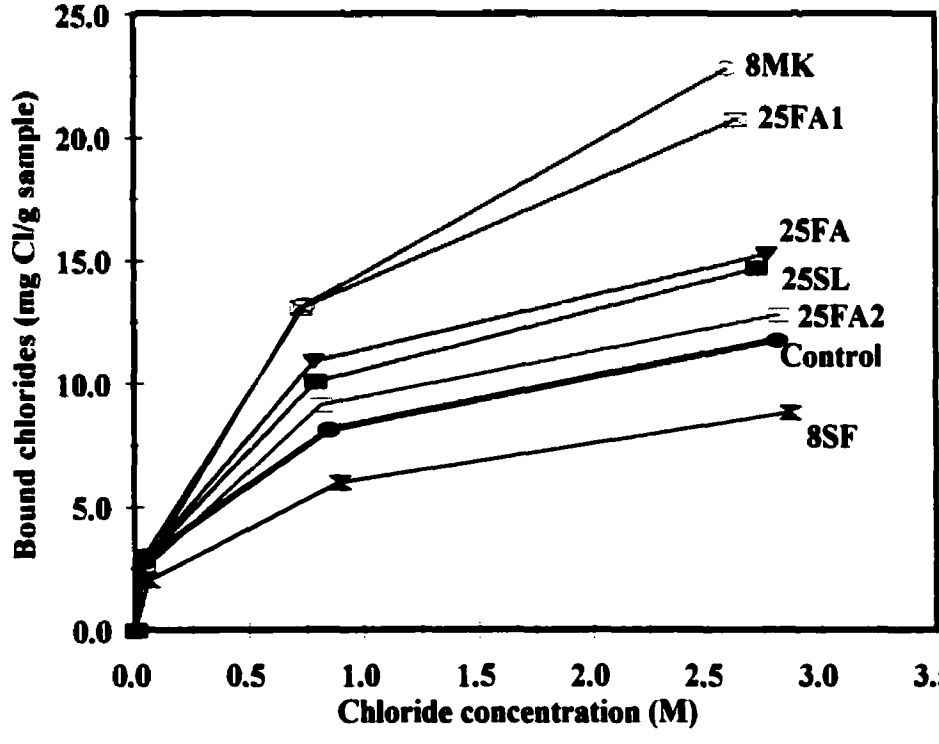


Figure 4-12: Chloride binding isotherms of pastes made of different cementitious systems with W/CM of 0.5 and 2 months age.

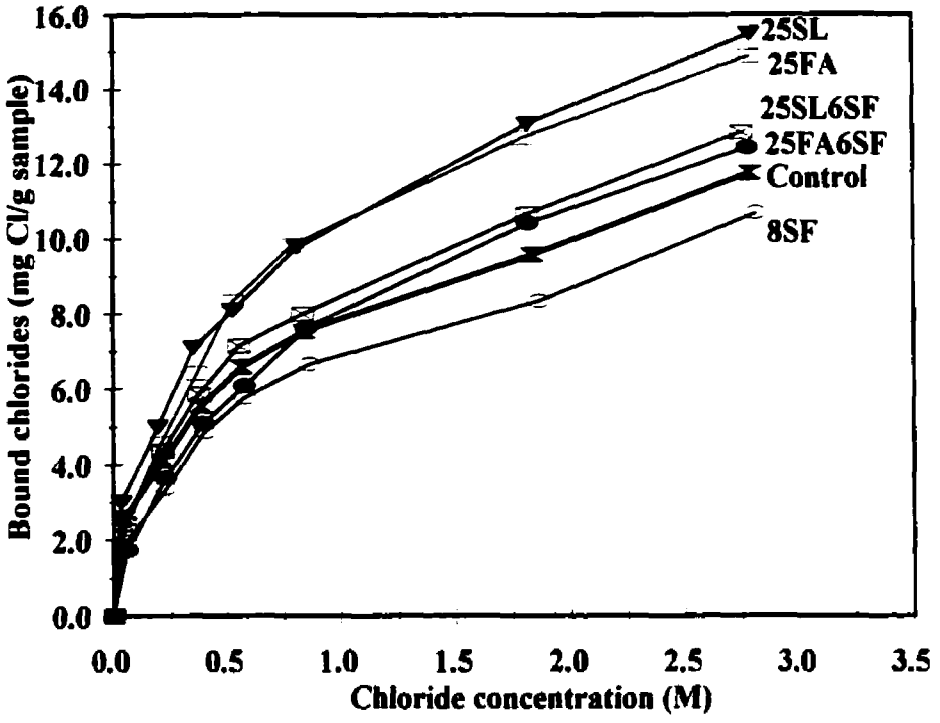


Figure 4-13: Chloride binding isotherms of pastes made of different cementitious systems with a W/CM of 0.5 and 9 months age.

The striking aspect of the results shown in Figures 4-12 and 4-13 is that the binding capacity of the control mixture at 0.5 W/CM ranks among the lowest binding capacities, whereas it ranks among the highest for mixes at W/CM ratio of 0.3. This is due to the fact that mixtures with SCMs addition exhibited a noticeable increase in binding capacity compared to the slight increase exhibited by the control mixture, when the W/CM ratio was increased from 0.3 to 0.5. This is probably due to the higher hydration rates in the mixes with W/CM ratio of 0.5, which also means higher pozzolanic activity of the added SCMs. This higher pozzolanic activity in mixes with metakaolin, fly ash, or GGBFS addition, will result in the formation of more C-A-H, C-A-S-H, and C-S-H phases, and a consequent increase in chemical and physical binding capacity. In the case of silica fume, it is more difficult to explain why the addition of silica fume to cement causes a reduction in binding. The resulting increase in C-S-H and reduction in pH, should supposedly increase binding, and the small dilution of $C_3A$ alone cannot possibly account for the reduction. It has been suggested that the decrease in the C/S ratio of the C-S-H results in a reduction of bound chloride *(Beaudoin et al., 1990; Glasser, 1993)*. This would explain why, despite the increase in C-S-H, the overall effect would be a decrease in binding.

It is interesting to notice that while all three fly ash mixes exhibited higher binding than the control mixes, there was no obvious criteria or factor such as $Al_2O_3$ or CaO content that was decisive in the way they ranked among each other, indicating the possibility that more than one factor influence the performance of the fly ash. It should be mentioned in this context, that the 25FA2 paste which had the highest binding capacity of the three fly ash-cement pastes, contained fly ash having high alumina content and relatively high calcium content. Another possible explanation for the unpredictability of the fly ash performance is that chloride binding properties of fly ash do not depend on the total content of alumina and silica, but on the quantity of reactive alumina and silica, since only the reactive part of the alumina and silica participates in the pozzolanic activity of the fly ash, and consequently the binding reactions. It seems, however, that a higher number of fly ash should be tested to be able to determine the important factors affecting the performance of fly ash in fly ash-cement pastes.

The use of the method described by *Tang and Nilsson (1993)* to examine the effect of SCM on the chloride binding capacity of SCM-cement mixtures was reported by other workers *(Dhir et al., 1994, 1996; Delagrave et al., 1997)*. These workers used crushed samples instead of discs, which were used in this thesis. Although, the cementitious material used will have a marked influence on the binding capacity, it is reasonable to compare the binding capacities of mixtures having close chemical composition. It is generally noticed that the results of other studies are remarkably higher than the results of this study for pastes of close mixture design. The differences seem to increase with chloride exposure. The results of *Dhir et al. (1994, 1996)* represent an extreme case in this respect. These results show binding capacities for GGBFS-cement pastes (33.3%) and fly ash-cement pastes (33%) (see Figures 2-8 and 2-9) that are as much as 70% higher than those of the 25SL (25% GGBFS) and 25FA (25% fly ash) pastes at 1 M exposures, and are 200% higher at 3 M exposures. The results of *Dhir et al. (1994, 1996)* indicates that the binding isotherms are linear. But, the results presented in this thesis, and those of *Delagrave et al., 1997* clearly show non-linear binding isotherms. It should be mentioned that *Dhir et al. (1994, 1996)* used a different method to determine the equilibrium chloride concentrations, which might have contributed to the observed differences. Nevertheless, the differences in sample preparation did contribute to the observed differences between the chloride binding capacities. Preliminary test results at the University of Toronto indicate that crushing the samples have a remarkable effect on the results (see AppendixE).

#### 4.1.1.10 Effect of W/CM

The results of Sections 4.1.6.2 and 4.1.7.4 showed that the blended cement mixtures exhibited apparent differences in their chloride binding capacities when tested at 0.3 and 0.5 W/CM (Figure 4-14). These mixtures contained a superplasticiser at 0.3 W/CM since it was difficult to produce mixtures of reasonable workability at this W/CM without the use of a superplasticiser . The use of superplasticiser could have confounded the effect of W/CM ratio, since it has been reported that some superplasticisers influence the binding capacity *(Byfors, 1986; Glasser, 1991; Haque & Kayyali, 1995a)*. *Delagrave et al. (1997)*, obtained a similar trend when they tested a silica fume-cement paste (6% silica fume) at W/CM of 0.25 and 0.45. Their results showed the degree of hydrations of the two pastes were markedly different (47% and 62% respectively). The authors argued that the low degree of hydration in the paste with W/CM of 0.25 has probably enhanced the influence of silica fume on the mean C/S ratio of the C-S-H, since silica fume is still very reactive material even in low W/CM mixtures. According to the authors, the reduction in the C/S ratio of the C-S-H would reduce the number of adsorption sites. Their results also showed a marked reduction in the Friedel's salt peaks at low W/CM ratio (this was also observed in the present results), which led them to suggest that the formation of Friedel's salt is not only affected by the mix composition but is also affected by the porosity of the paste and the pore solution chemistry. It is suggested here that the observed lower binding capacities, at 0.3 W/CM, of mixtures containing fly ash, slag, or metakaolin is due in part to the lower formation of Friedel's salt, which is governed by the porosity and the degree of hydration of the paste. It could also be due to a possible lower adsorption capacity of the C-S-H at low W/CM ratio.

Figure 4-15 shows the effect of the W/CM on the binding capacity of the control mixture. While the difference in binding between the mixtures with 0.3 and 0.5 W/CM is small but noticeable, the difference between the ones with 0.5 and 0.7 W/CM is negligible. This fact possibly indicates that it is not the W/CM per se that is influencing the binding, but it is rather the degree of hydration, which is influenced by W/CM, that affects the binding capacity. This observation is consistent with observations made by other researchers (*Sandberg & Larsson, 1993; Tang & Nilsson, 1993)*.

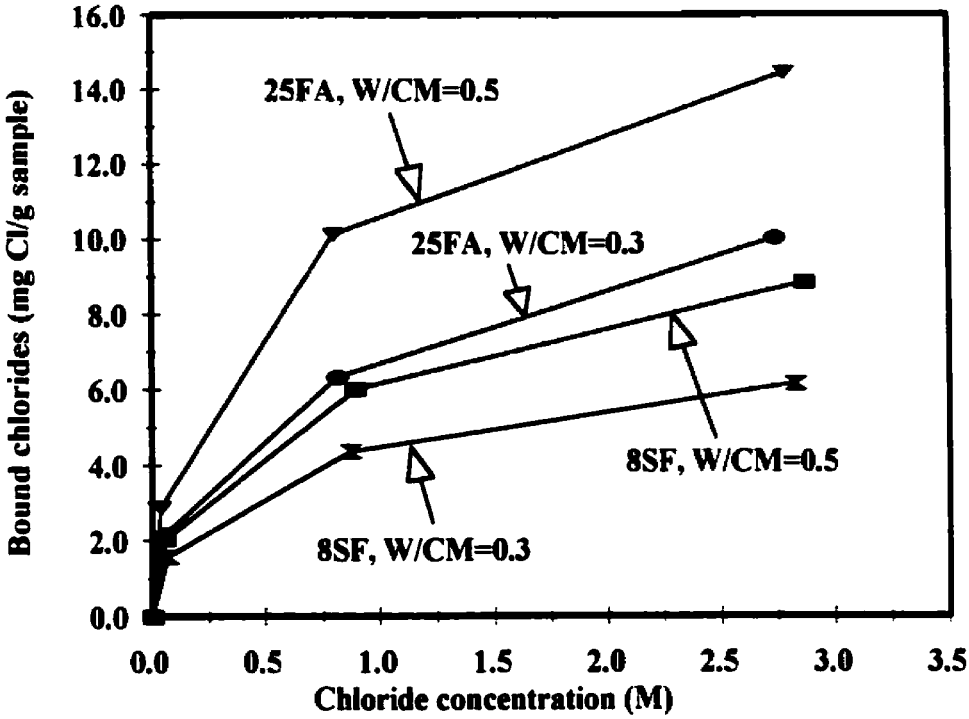


Figure 4-14: Chloride binding isotherms of the 25FA and 8SF pastes at different W/CM ratios.

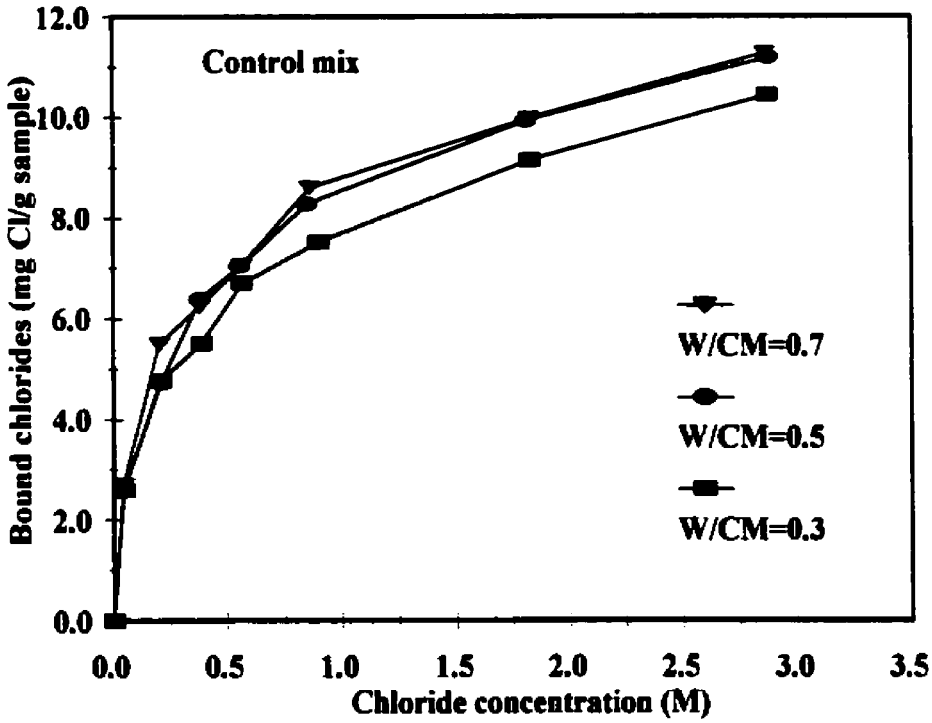


Figure 4-15: Chloride binding isotherms of the control mix at different W/CM ratios.

#### 4.1.1.11 Effect of Age

Five mixtures were tested for the effect of the curing period on the chloride binding capacity. They were tested at the ages of 2 months and 9 months. The results showed that in most cases there was no difference in the binding capacity between the 2 month and the 9 month cured pastes as shown in Figures 4-16 and 4-17. Of the five tested pastes, only the the 8% silica fume mix exhibited an increase in its chloride binding capacity at high chloride concentrations (1 M, and 3 M) with additional curing. This doesn't neccesarily mean that the initial curing period has no influence on the binding capacity. But in this case, it is possible that the differences in the degrees of hydration between the specimens tested at 2 months and those tested at 9 months were not large enough (taking into account that the specimens continued to hydrate while being stored in the chloride solutions for 6 to 8 weeks before being titrated) to cause differences in the chloride binding capacities that are large enough to be detected by the method used.

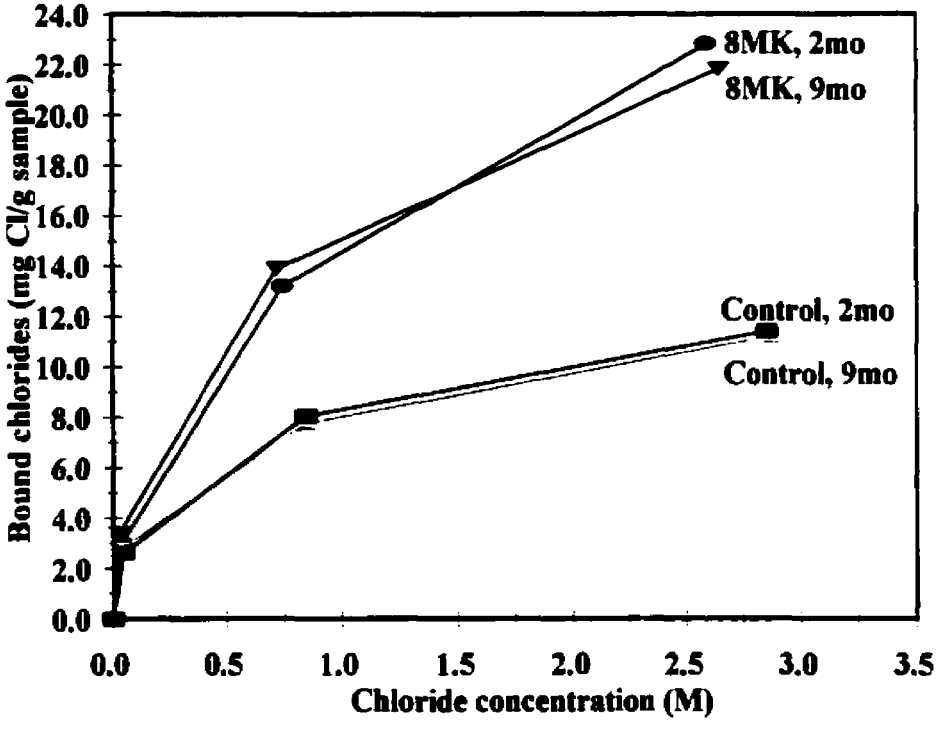


Figure 4-16: Effect of age on the chloride binding capacity of the control mix and the 8MK paste. W/CM = 0.5.

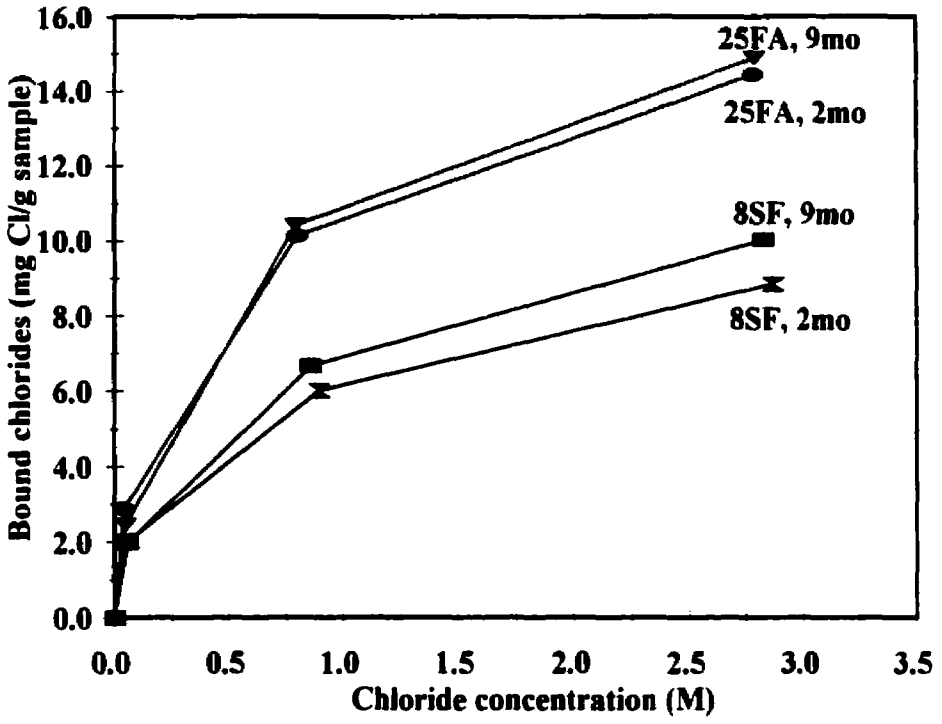


Figure 4-17: Effect of age on the chloride binding capacity of the 25FA and 8SF pastes. W/CM=0.5.

#### 4.1.1.12 X-Ray Diffraction Results

Figure 4-18 shows the XRD patterns of samples of the control paste exposed to different chloride concentrations. The main purpose of the XRD patterns was to investigate the formation of Friedel's salt as a result of exposure to chloride solutions. One of the main problems of identifiying Friedel's salt in XRD patterns is that the maximum intensity peak correponding to Friedel's salt almost coincides with that of the $C_4AH_{13}$ phase. Therefore, it is difficult to distinguish between the two peaks. The XRD pattern of the sample that was not exposed to chloride (0 M) showed the existence of a small peak at the d spacing 7.9Å, which was attributed to the $C_4AH_{13}$ phase in the hydrated paste. However, the XRD patterns in Figure 4-18 also revealed that the peak at d spacing = 7.9Å was increasing with increasing concentrations of chloride in the exposure solutions. This means that the increase was the result of the formation of Friedel's salt, since there is no reason to attribute this increase to the formation of $C_4AH_{13}$ as a result of increasing chloride concentrations. In fact, it would be expected that the $C_4AH_{13}$ would transform into Friedel's salt when exposed to increasing chloride concentrations. Hence, it was concluded that the peaks at 7.9Å are Friedel's salt peaks. In

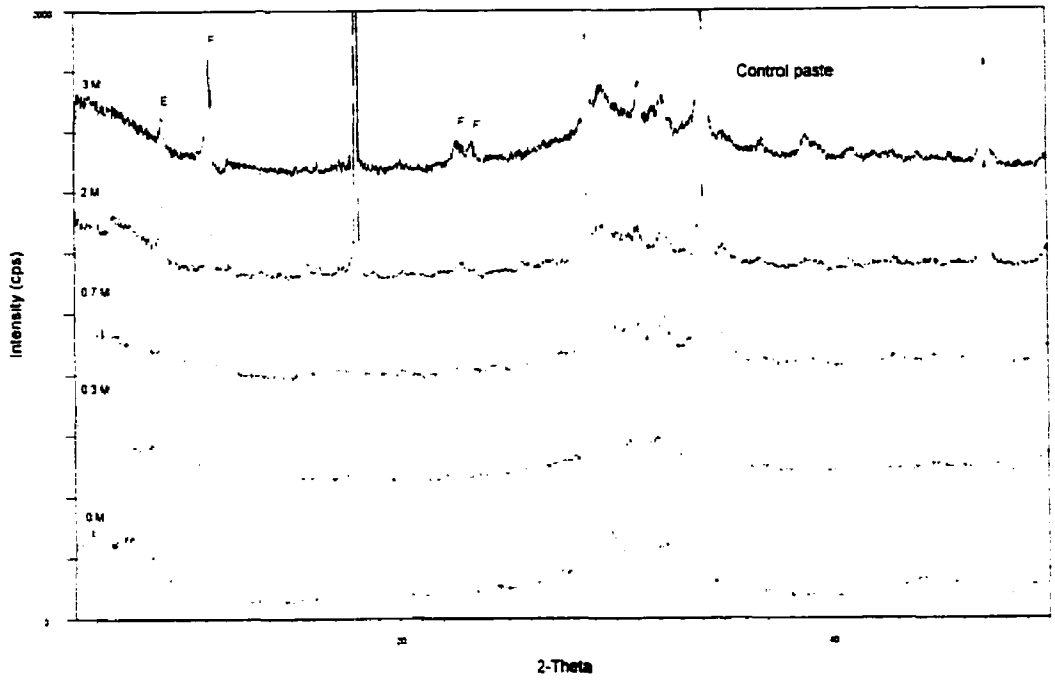


Figure 4-18: XRD patterns of samples of the control paste exposed to different chloride concentrations. E: ettringite, F: Friedel's salt

addition, the increase in these peaks with increasing chloride concentrations indicated an increase in the amount of Friedel's salt. Another important fact revealed in these XRD patterns was the decrease in the ettringite peaks at 3 M exposure, which probably means that the ettringite was partially transformed into Friedel's salt at 3 M exposure. The decrease in ettringite peaks at 3 M exposure was also observed in the XRD patterns of samples of other cements (C1 and C7), as shown later in this chapter

Figure 4-19 shows the XRD patterns of samples of several pastes that were exposed to 3 M chloride solutions. These patterns show the effect of SCM replacements on the intensities of Friedel's salt peaks, and therefore, on the amount of Friedel's salt formed. There was a positive correlation between the maximum intensity peaks of the Friedel's salt phase and the chloride binding capacities of the samples as shown in Figure 4-20. The higher the binding capacity of a sample, the higher the maximum intensity peak of the Friedel's salt phase in the XRD pattern of that sample (the higher the amount of Friedel's salt). This shows that the increase in the binding capacity caused by the partial replacement of cement with metakaolin and fly ash is at least partially due to the increase

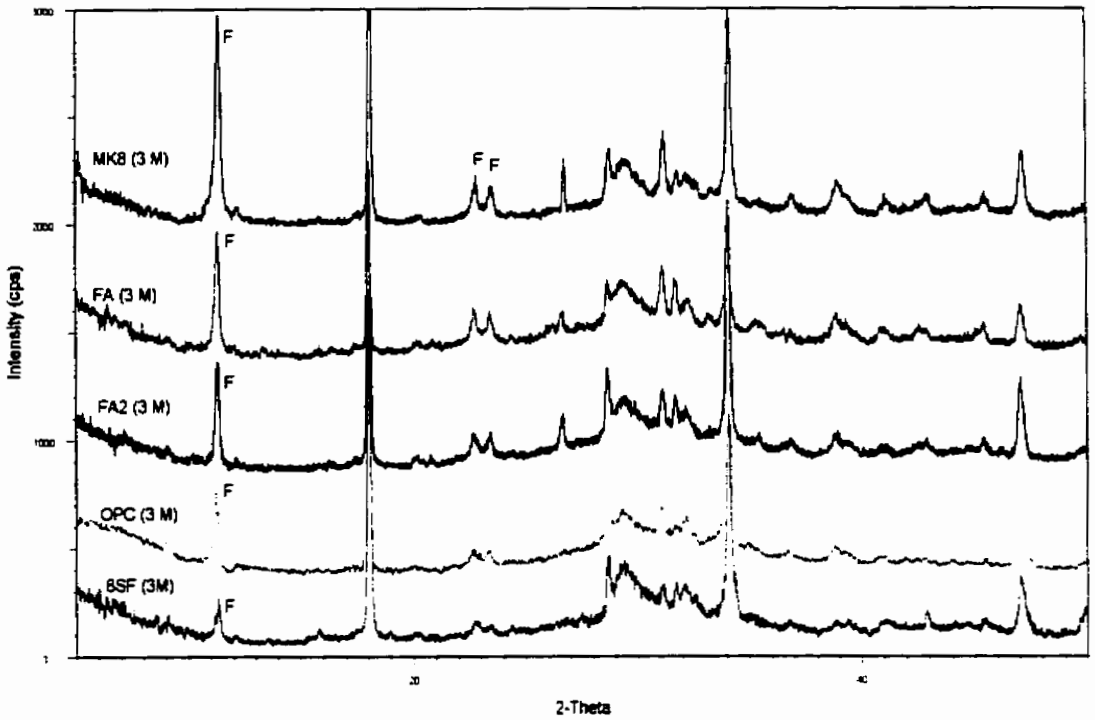


Figure 4-19: Comparison of Friedel's salt peaks in the XRD patterns of specimens of different blended cement pastes, exposed to 3 M chloride solutions. F: Friedel's salt.

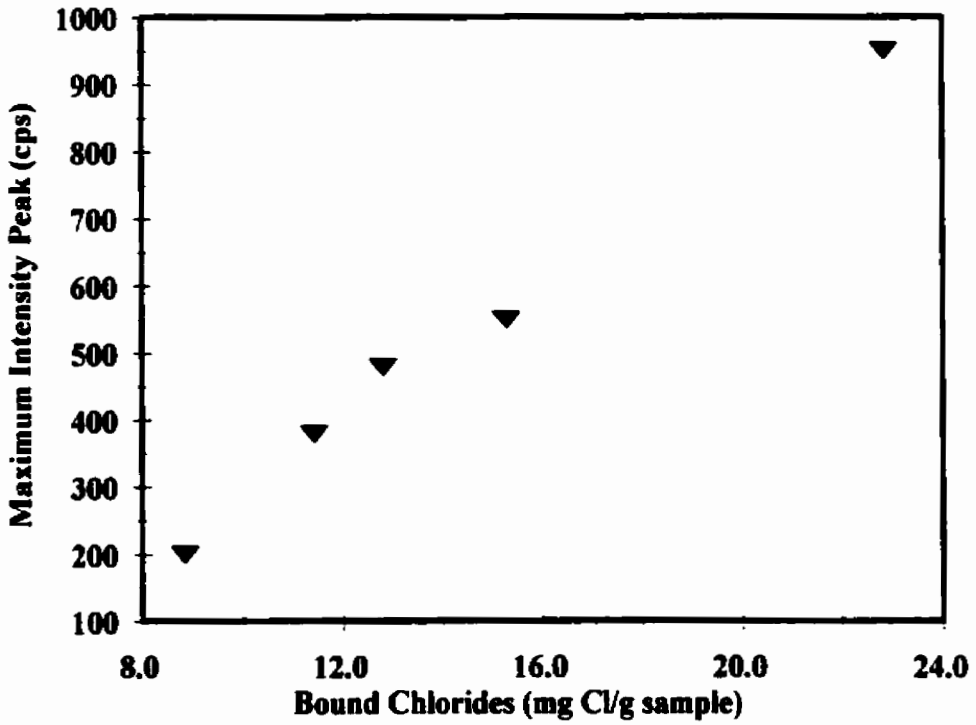


Figure 4-20: Correlation between the maximum intensity peak of Friedel's salt (d=7.9Å) and the chloride binding capacity of samples of blended cement pastes, exposed to 3 M chloride solutions.

in the chemical binding capacity due to the high alumina contents of these SCM's. This fact is further confirmed in Figure 4-21 which shows the XRD patterns of samples of the 8MK paste that were exposed to different chloride concentrations. At high concentrations, the intensities of the Friedel's salt peaks showed large increases in comparison with those of the control samples. At low concentration (0.1 M), the maximum intensity peak of the Friedel's salt phase was very small despite the decrease in the monosulphate peak. It is possible that the monosulphate was partially transformed into the $C_6A_2.C\bar{S}.CaCl_2.24H_2O$ phase, although it is difficult to confirm that from the XRD patterns.

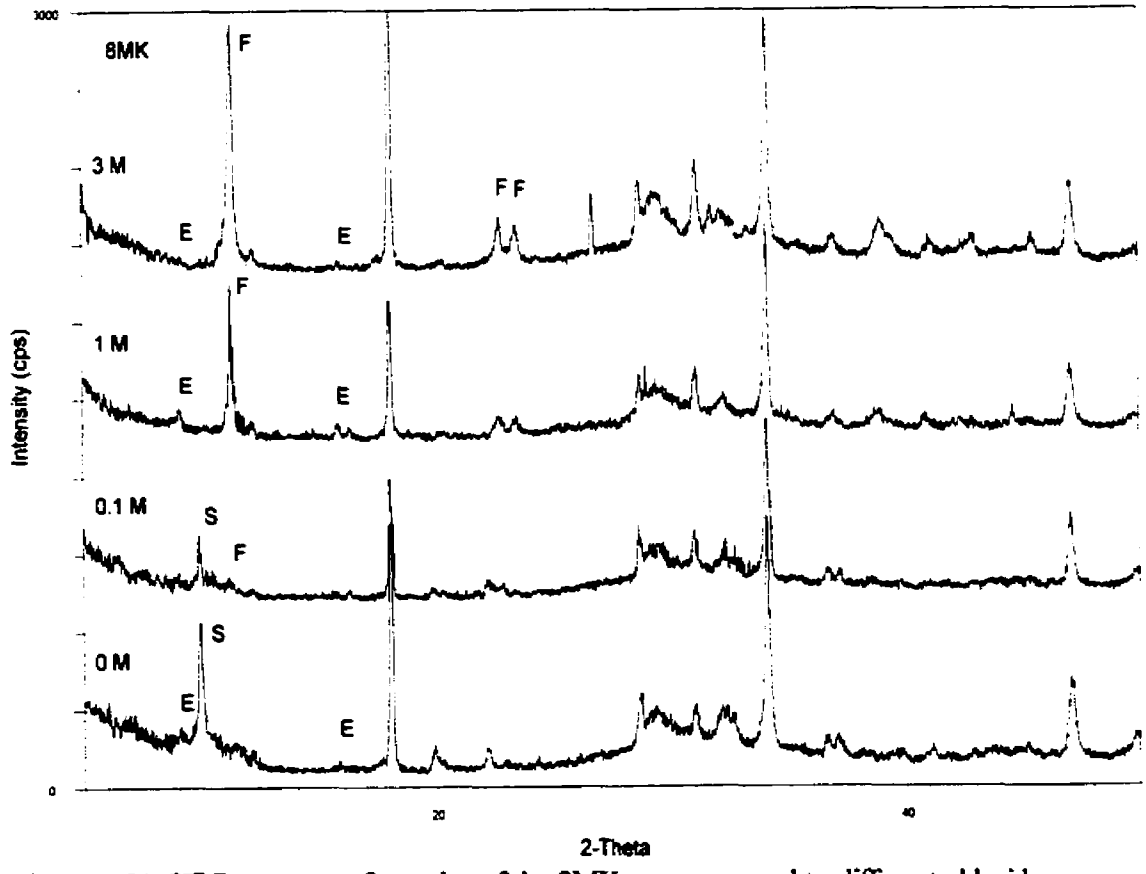


Figure 4-21: XRD patterns of samples of the 8MK paste exposed to different chloride concentrations. E:ettringite, F: Friedel's salt, S: monosulphate.

### 4.1.2 Ponding Method

#### 4.1.2.1 Analysis of Data

The experimental procedures involved in the ponding method were described in detail in section 3.3 of Chapter 3. After titration, data about the total chloride content, free chloride concentration and hydroxyl ion concentration at different depths of the cement paste becomes available. The total chloride profile is presented as total chloride content (% by mass of cement) versus depth. Similarily, the free chloride and hyroxyl ion profiles are plotted as free chloride and hydroxyl ion concentrations (mole/litre) respectively versus depth. The bound chlorides are calculated from the difference between the total and free chlorides at every depth. However, since the total chlorides and free chlorides are obtained in different units, values need to be converted before a calculation of the bound chlorides can be done. In order to do the conversion, a knowledge of the evaporable water content is necessary (assuming that the volume of the pore solution containing the free chlorides is equal to the volume of the evaporable water ):

$$w_e = (W_s - W_d)/ W_d$$

where : $w_e$ : evaporable water content, g water/g sample

$W_s$ : mass of the saturated sample, g

$W_d$ : mass of the dry sample , g

For each of the tested pastes, a cylinder was taken out of the chloride solution at the end of the exposure period, and was sliced across the depth with a dry diamond blade. Four samples (15 to 30 g) were immediately weighed ($W_s$), and then dried to constant mass in an oven at 105°C ($W_d$). The $w_e$ was the average of the four determination from the four samples (Table 4-3).

The bound chlorides are calculated using the following formula:

$$C_b = C_t - 35.453 * w_e * C_f$$

where: $C_b$ : bound chloride, mg Cl/g sample

$C_t$ : total chloride, mg Cl/g sample

$C_f$ : free chloride, mmol/ml,

and 35.453 is the molar mass of the chloride ion, g.

the binding isotherms can be presented either as free versus bound chlorides, or free versus total chlorides.

Table 4-3: Evaporable water content ($w_e$) of the tested pastes. $w_e$ was the average of 4 measurements.

| Mix | $w_e$ of 4 different measurements (4 different samples) | | | | $w_e$ |
|---|---|---|---|---|---|
| | $w_e$ (#1) | $w_e$ (#2) | $w_e$ (#3) | $w_e$ (#4) | average |
| OPC | 0.2890 | 0.2991 | 0.3081 | 0.2979 | 0.299 |
| 8SF | 0.3425 | 0.3417 | 0.3370 | 0.3376 | 0.340 |
| 8MK | 0.3150 | 0.3292 | 0.3245 | 0.3364 | 0.326 |
| 25FA | 0.3409 | 0.3524 | 0.3543 | 0.3509 | 0.350 |

### 4.1.2.2 Hydroxyl Ion Profiles

The hydroxyl ion profiles are shown in Figures 4-22 to 4-25. These results show that the hydroxyl ion concentration in the pore solution decreases with decreasing depth from the exposed surface of the specimens. This is due to the leaching of hydroxide as a result of chloride ingress into the cement. This counter diffusion of hydoxyl ions should be taken into consideration in service life prediction models because of the effect on initiation time. In addition, when accounting for chloride binding in service life modelling, the variation of the pH across the depth of the concrete envelope and its influence on chloride binding should be taken into account as well.

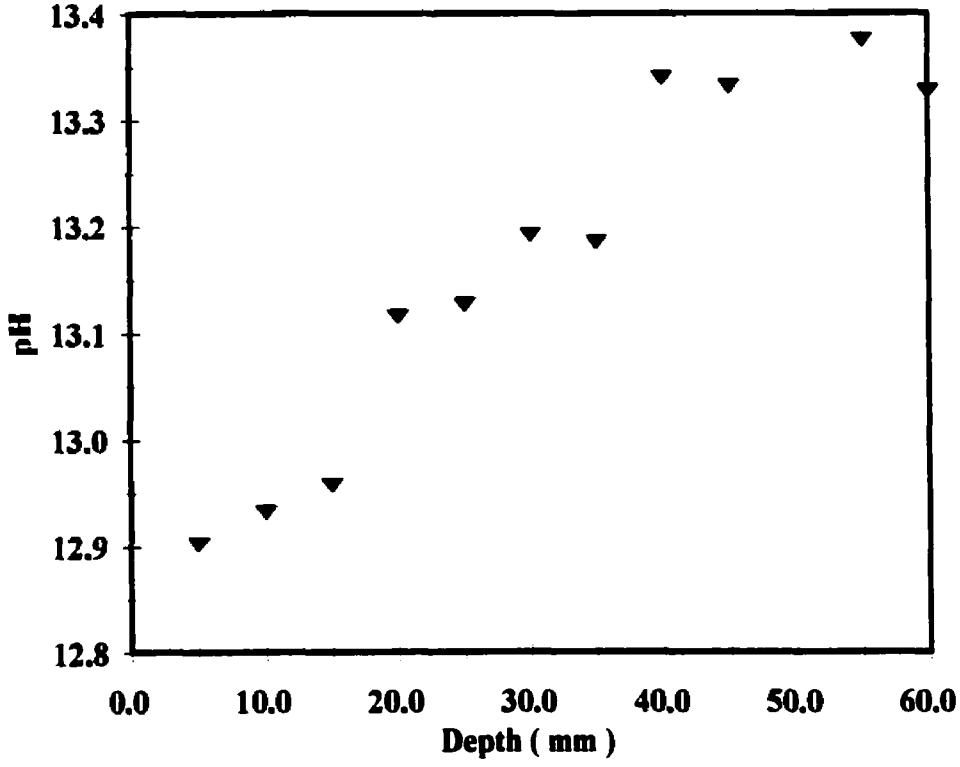


Figure 4-22: Change of pH with depth in the control paste. pH values were calculated from [$OH^-$] measurements.

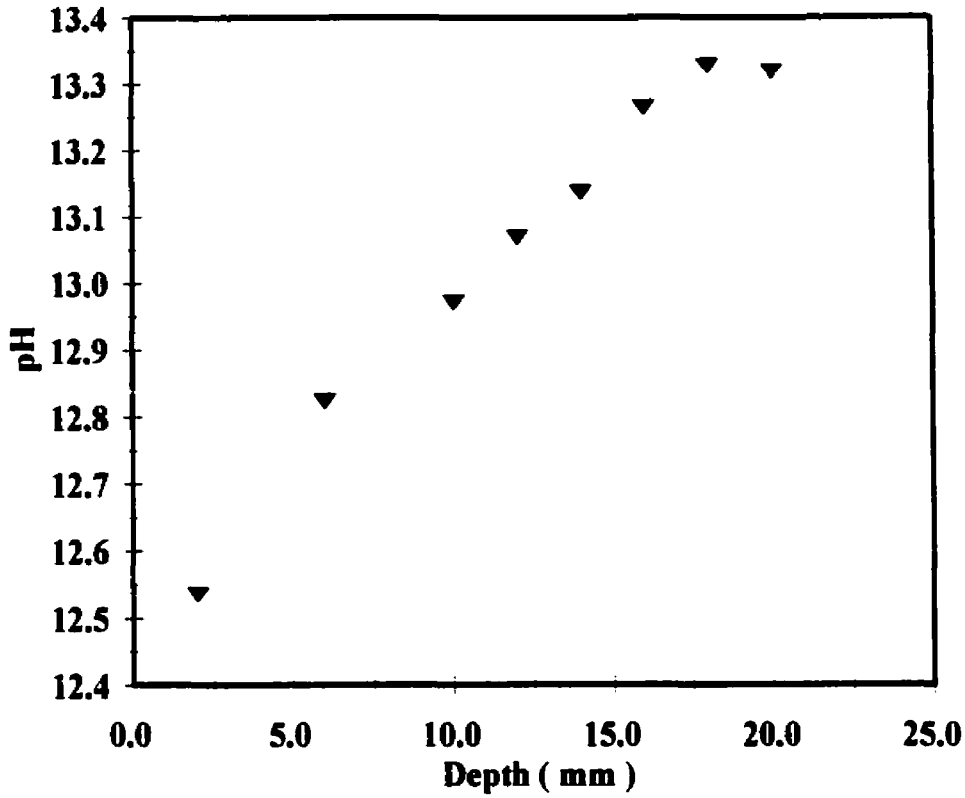


Figure 4-23: Change of pH with depth in the 8SF (8% silica fume) paste. pH values were calculated from [$OH^-$] measurements.

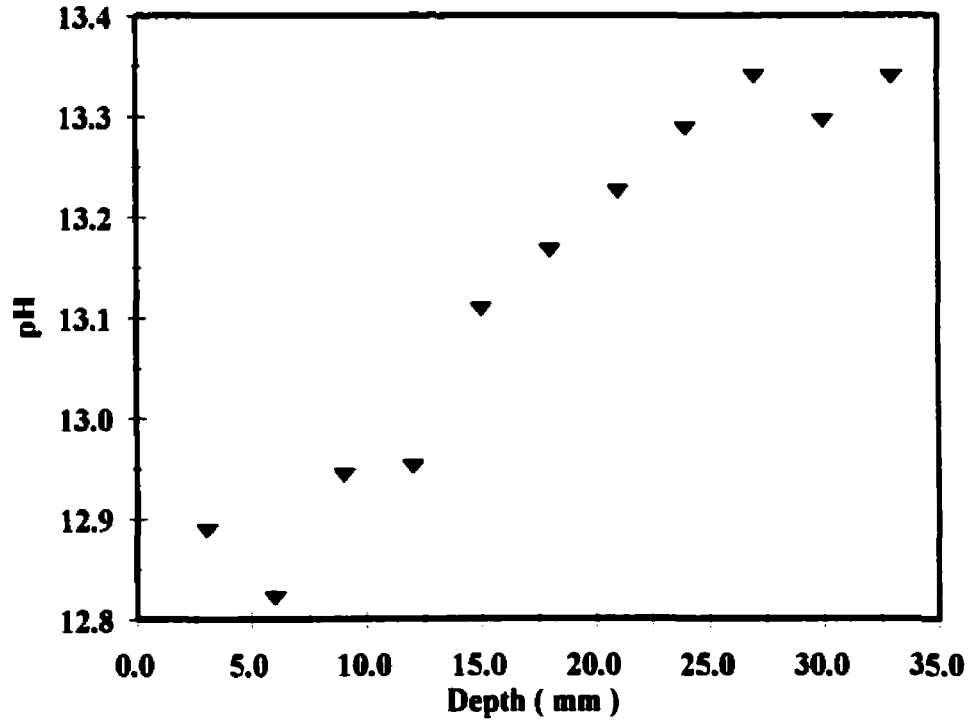


Figure 4-24: Change of pH with depth in the 25FA (25% fly ash) paste. pH values were calculated from [$OH^-$] measurements.

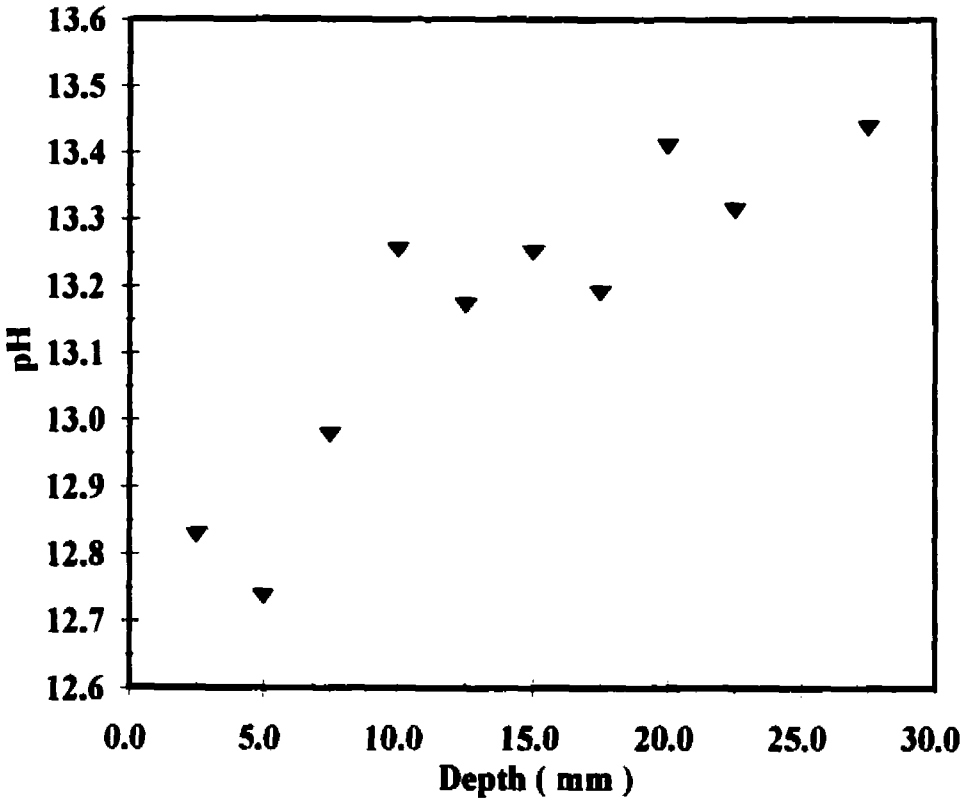


Figure 4-25: Change of pH with depth in the 8MK (8% metakaolin) paste. pH values were calculated from [$OH^-$] measurements.

#### 4.1.2.3 Free Chloride Profiles

Figures 4-26 to 4-29 show the free chloride profiles of the four mixtures. Since in this case, the cement pastes are saturated and submerged in the chloride solution, the chloride ions penetrate the cement pastes by diffusion. This diffusion mechanism is described by Fick's second law. Assuming that the diffusion coefficient is constant with depth, Crank's solution to this equation was fitted to the experimental data using Equation (2-2). Table 4-4 summarizes the results which include the apparent diffusion coefficients, the coefficients of determination ($r^2$), and the surface concentrations. It can be seen from the coefficients of determination that the solution to Fick's second law provides a good fit to the free chloride profiles. It should be mentioned that the use of Crank's solution to Fick's second law as presented in Equation (2-2), assumes that chloride binding is linear, an assumption that is not accurate as shown earlier in this chapter. An account of the non-linearity of chloride binding in Fick's equation should result in even better fits. The four mixtures ranked as follows:

$$D_a\,(OPC) > D_a\,(25FA) > D_a\,(8MK) > D_a\,(8SF)$$

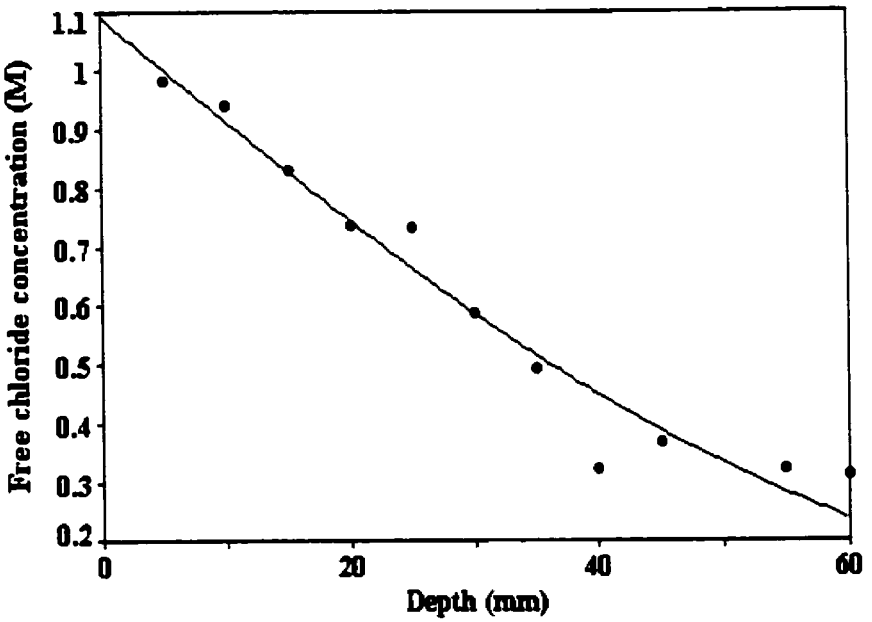


Figure 4-26: Free chloride profile of the control mix. The data was fit with Crank's solution to Fick's second law of diffusion.

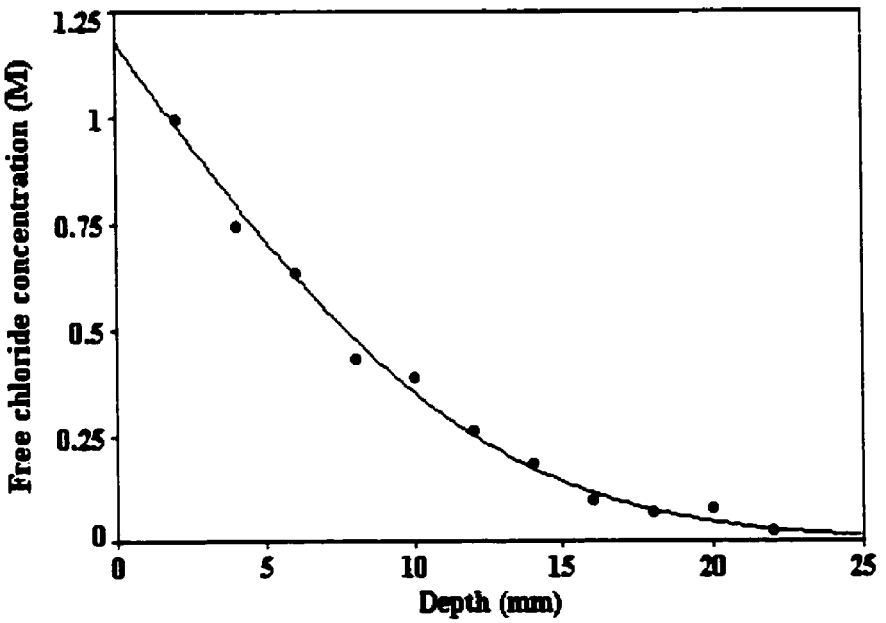


Figure 4-27: Free chloride profile of the 8SF paste. The data was fit with Crank's solution to Fick's second law of diffusion.

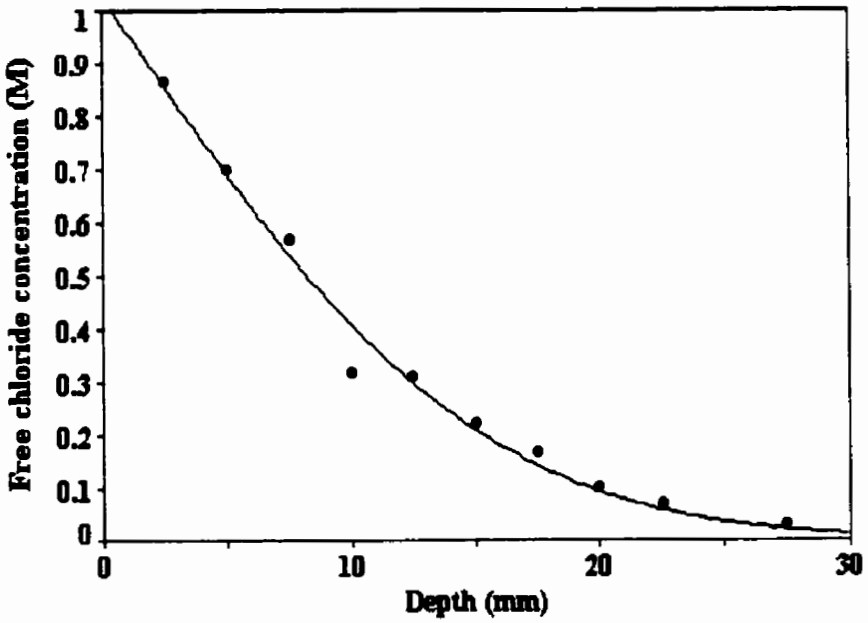


Figure 4-28: Free chloride profile of the 8MK paste. The data was fit with Crank's solution to Fick's second law of diffusion.

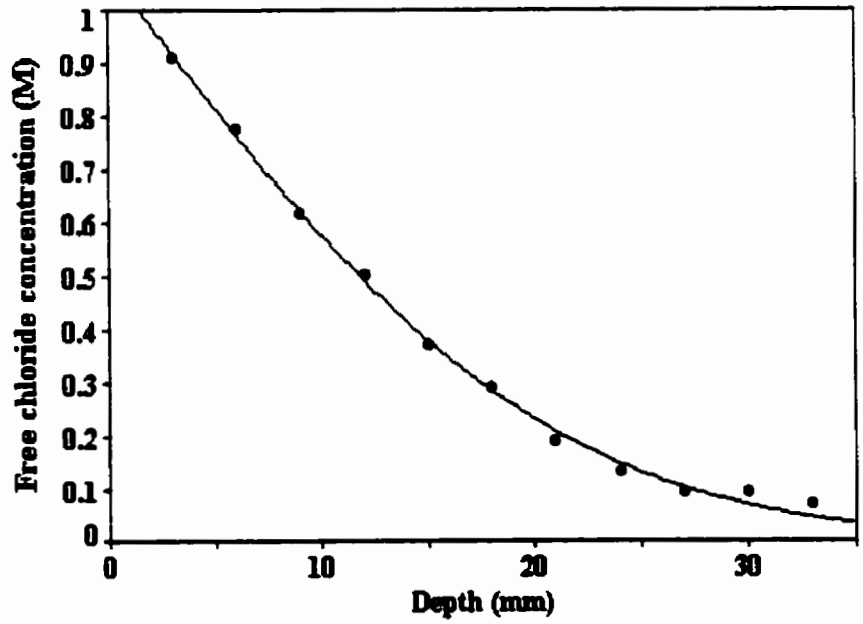


Figure 4-29: Free chloride profile of the 25FA paste. The data was fit with Crank's solution to Fick's second law of diffusion.

Table 4-4: The diffusion coefficient ($D_a$), surface concentration ($C_s$), and the coefficient of det.($r^2$) of the control, 25FA, 8MK, and 8SF pastes, determined by using the free chloride profiles.

| Mixture | $D_a$ ($m^2/s$) | $C_s$ (mol/l) | $r^2$ |
|---|---|---|---|
| **OPC** | $24.85 \times 10^{-12}$ | 1.09 | 0.955 |
| **25FA** | $2.71 \times 10^{-12}$ | 1.08 | 0.997 |
| **8MK** | $1.44 \times 10^{-12}$ | 1.03 | 0.986 |
| **8SF** | $0.99 \times 10^{-12}$ | 1.15 | 0.993 |

#### 4.1.2.4 Total Chloride Profiles

The total chloride profiles of the four mixtures, are shown in Figures 4-30 to 4-33. Similar to the case of free chloride profiles, Equation (2-2) was fitted to the experimental data. The results are summarized in Table 4-5. Equation (2-2) provides a good fit for all profiles as shown by the coefficients of determination ($r^2$). The apparent diffusion coefficients obtained for these profiles were different from those obtained for the free chloride profiles, despite the fact that they are the same according to Equation (2-1). This might be partly due to the assumption in Equation (2-2) that chloride binding is linear. The ranking of the diffusion coefficients was slightly different this time with the 8SF mixture having a higher $D_a$ than the 8MK mixture. The ranking of the OPC, 25FA, and 8SF mixtures, were in agreement with results obtained for concrete mixtures using the same cementitious materials and proportions, but with lower W/CM ratio (0.4) and shorter exposure duration (12 months) *(McGrath, 1995)*.

Table 4-5: The diffusion coefficient ($D_a$), surface concentration ($C_s$), and the coefficient of det.($r^2$) of the control, 25FA, 8MK, and 8SF pastes, determined by using the total chloride profiles

| Mixture | $D_a$ ($m^2/s$) | $C_s$ (mmol Cl/g cement) | $r^2$ |
|---|---|---|---|
| **OPC** | $59.6 \times 10^{-12}$ | 0.62 | 0.989 |
| **25FA** | $3.50 \times 10^{-12}$ | 0.74 | 0.99 |
| **8MK** | $1.27 \times 10^{-12}$ | 0.98 | 0.993 |
| **8SF** | $1.89 \times 10^{-12}$ | 0.66 | 0.998 |

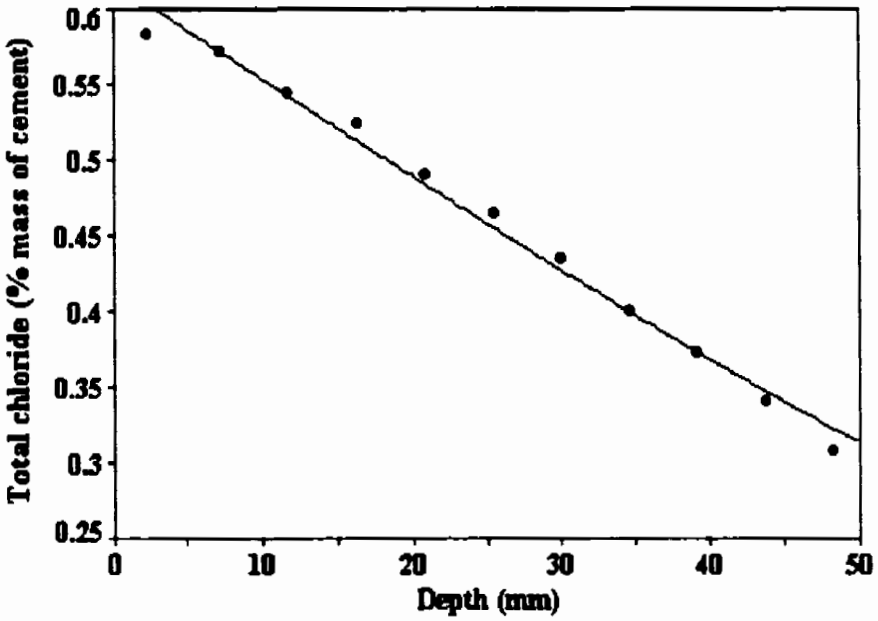


Figure 4-30: Total chloride profile of the control paste. The data was fit with Crank's solution to Fick's second law of diffusion.

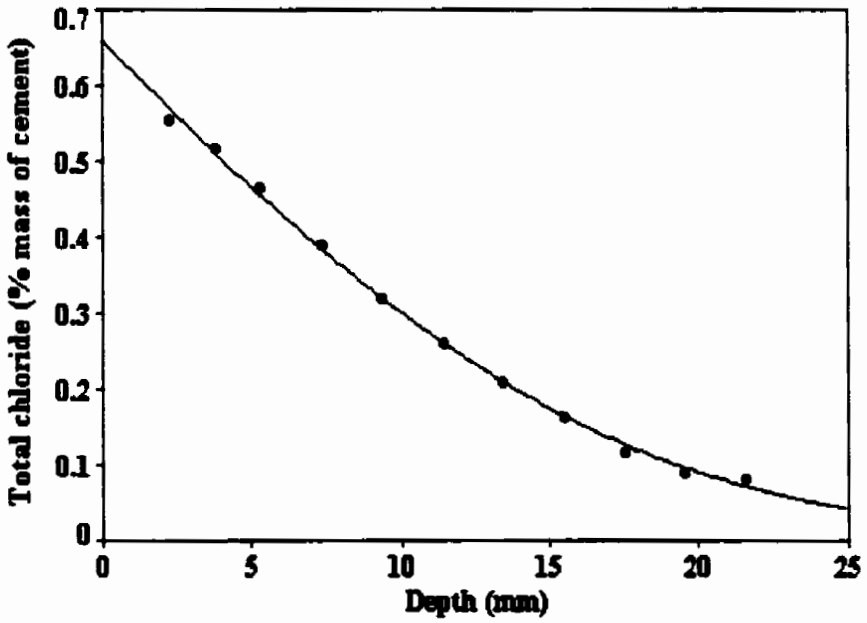


Figure 4-31: Total chloride profile of the 8SF paste. The data was fit with Crank's solution to Fick's second law of diffusion.

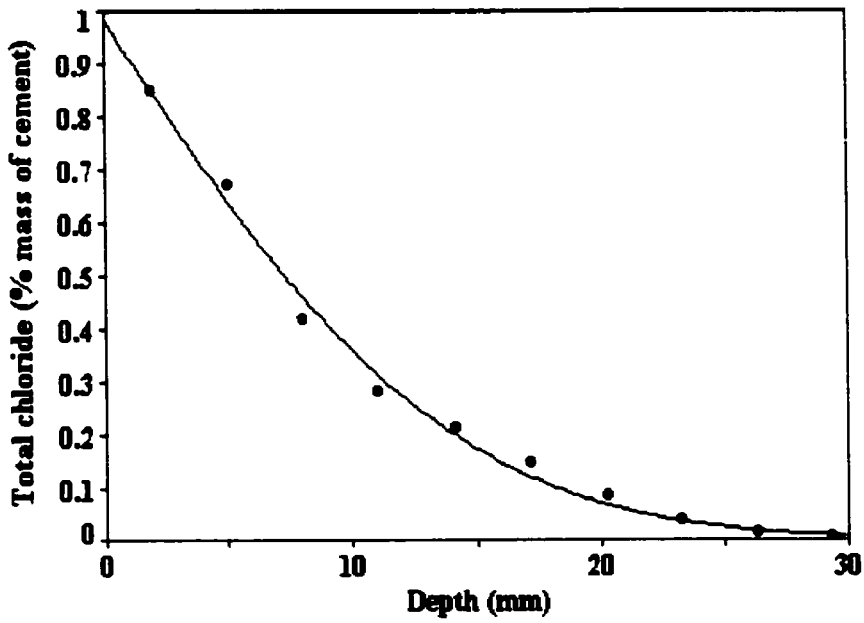


Figure 4-32: Total chloride profile of the 8MK paste. The data was fit with Crank's solution to Fick's second law of diffusion.

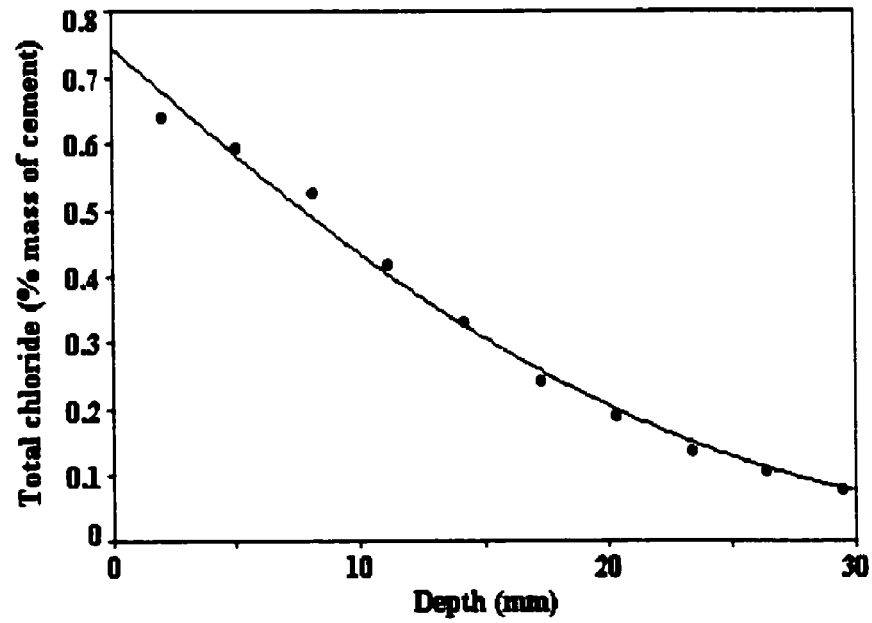


Figure 4-33: Total chloride profile of the 25FA paste. The data was fit with Crank's solution to Fick's second law of diffusion.

#### 4.1.2.5 Chloride Binding Isotherms

Figure 4-34 shows the chloride binding isotherms of all four mixtures tested in this study. With the exception of the 25FA mixture, the ranking of the mixtures according to their chloride binding capacities was the same as the one obtained from the equilibrium test method. The 8MK mixture exhibited the highest binding capacity, and the 8SF mixture exhibited the lowest binding capacity. The 25FA mixture ranked the segond highest at chloride concentrations above 0.5 M , but was the lowest at concentrations below 0.5 M.

The Freundlich and the Langmuir isotherms were fitted to these chloride binding isotherms. Table 4-6 show the results presnted as α and β coefficient for each isotherm, and the coefficient of determination ($r^2$) of each fit. The coefficients of determination indicate that both isotherms provided good fits for all the pastes. This confirms that the chloride binding isotherms are non-linear as previously found in the equilibrium test method. The Freundlich and Langmuir isotherms provided very close fits in terms of the coefficients of determination. Freundlich isotherm fit was slightly better in the case of the 8SF and 8MK mixtures, while the Langmuir isotherm fit was slightly better in the case of the control mixture and the 25FA mixture.

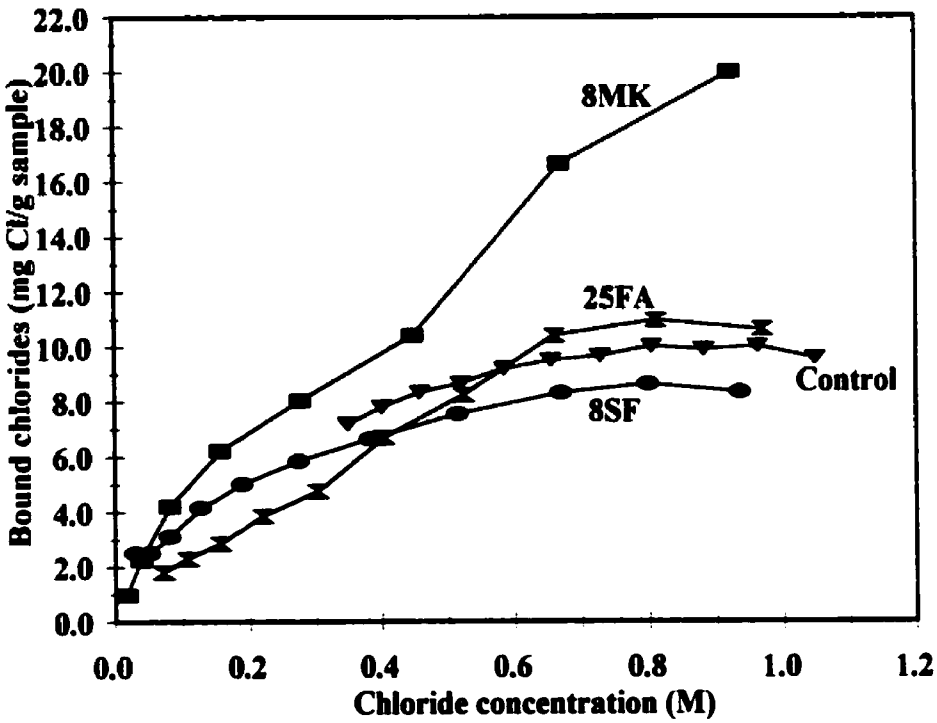


Figure 4-34: Chloride binding isotherms of the control, 8SF, 8MK, and 25FA pastes obtained using the ponding method.

Table 4-6: The coefficients of the Freundlich, and Langmuir isotherms (and coefficients of determination, $r^2$) of the control, 25FA, 8MK, and 8SF pastes. The coefficients correspond to units of chloride binding capacity: mg Cl/g sample.

| | Mix | α | β | $r^2$ |
|---|---|---|---|---|
| Freundlich | control | 10.21 | 0.26 | 0.983 |
| | 25FA | 12.25 | 0.71 | 0.961 |
| | 8MK | 21.09 | 0.71 | 0.99 |
| | 8SF | 9.35 | 0.39 | 0.985 |
| | Mix | a | b | $r^2$ |
| Langmuir | control | 54.94 | 4.42 | 0.99 |
| | 25FA | 23.06 | 0.95 | 0.974 |
| | 8MK | 37.36 | 0.81 | 0.98 |
| | 8SF | 58.12 | 5.75 | 0.981 |

Figures 4-35 to 4-38 compare between the chloride binding isotherms obtained from the ponding and equilibrium testing methods. The results show that the binding capacities obtained from the ponding method are generally higher than the ones obtained from the equilibrium method. While the agreement was good in the case of the 25FA and 8MK mixtures, the differences were generally between 20% to 30% in the case of the control and the 8SF mixtures. Taking into account the inaccuracies and assumptions made in both methods, and especially in the ponding method, the agreement between the results is considered to be good. It is worth mentioning that the binding isotherms obtained from the equilibrium method were obtained at a constant pH, while the binding isotherms from the ponding method were obtained at variable pH. This pH variation across the depth would have affected the binding isotherms obtained fron the ponding method, since it is shown later in section 4.2.2.1 that the pH of the pore solution affects the chloride binding. It might have also partly contributed to the innacuracies in the comparisons between the binding isotherms obtained from both methods.

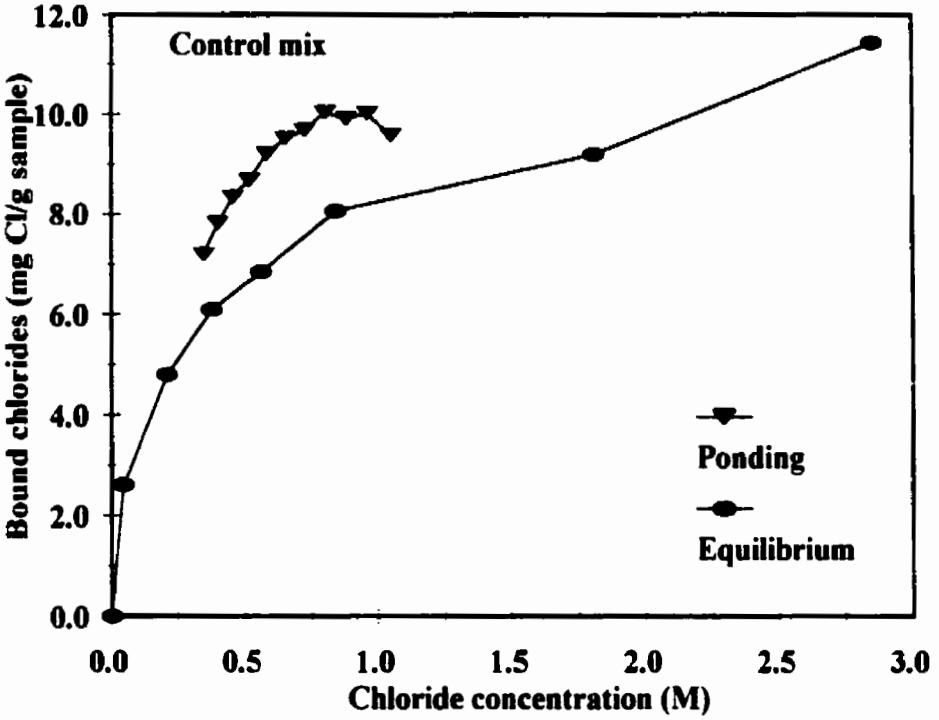


Figure 4-35: Comparison of the chloride binding isotherms of the control mix obtained using the Equilibrium method or the ponding method.

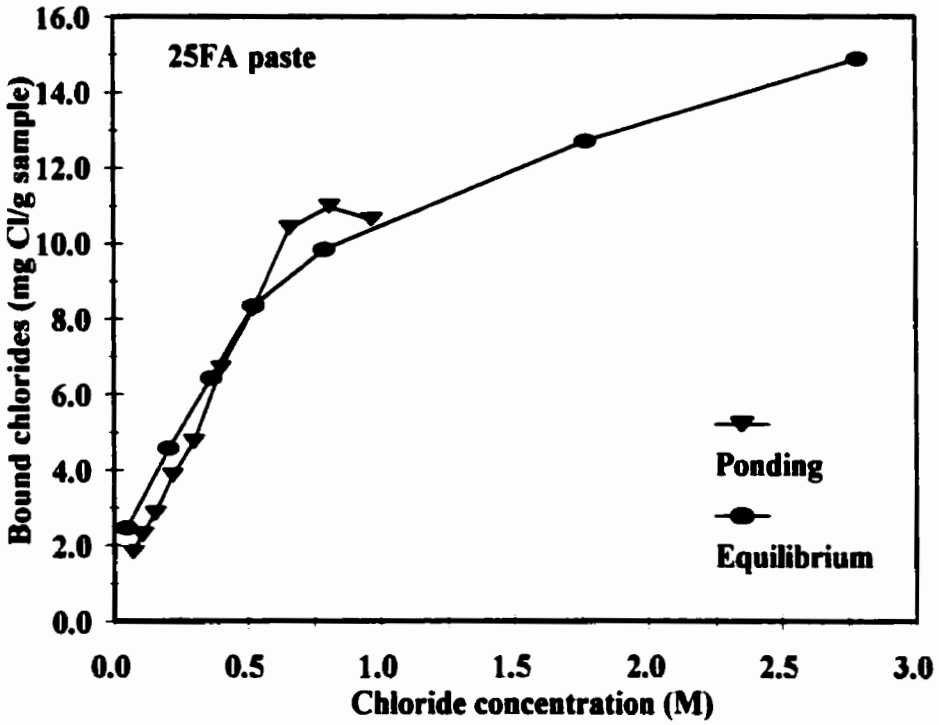


Figure 4-36: Comparison of the chloride binding isotherms of the 25FA paste obtained using the Equilibrium method or the ponding method.

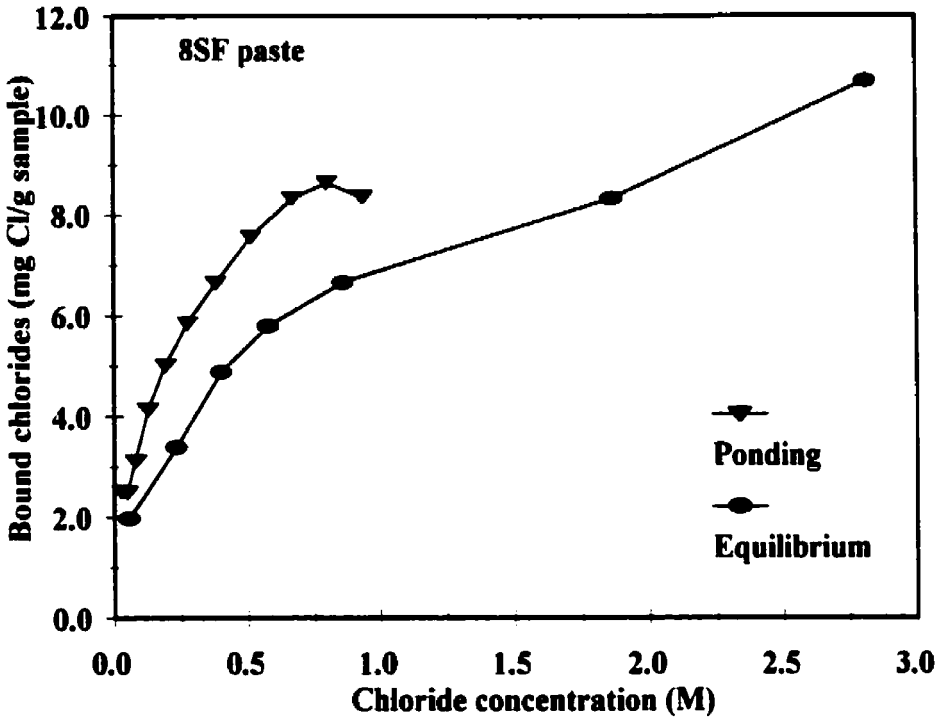


Figure 4-37: Comparison of the chloride binding isotherms of the 8SF paste obtained using the Equilibrium method or the ponding method.

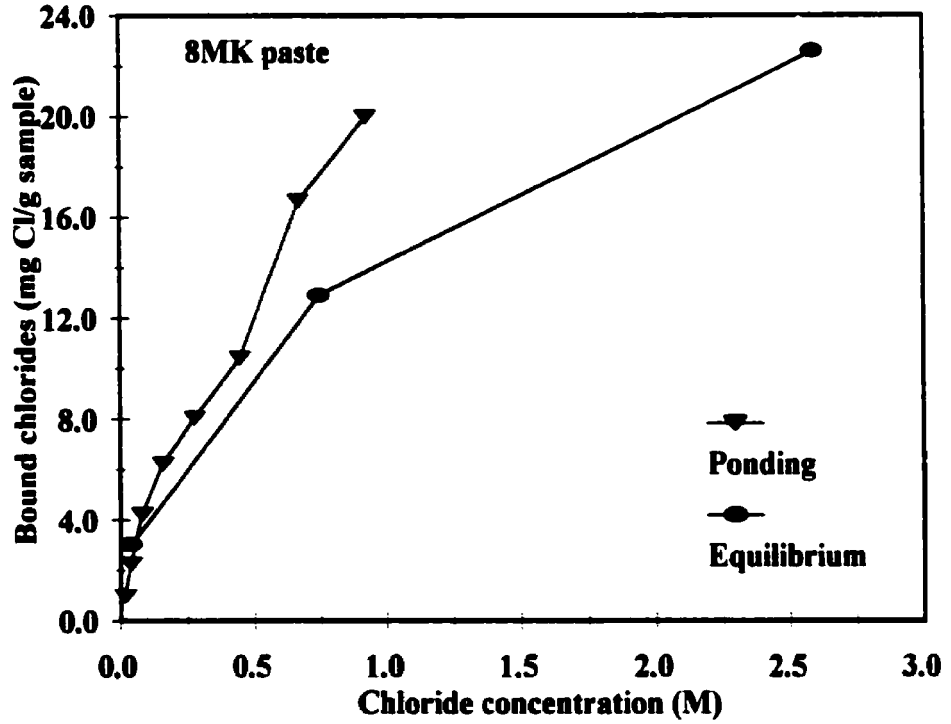


Figure 4-38: Comparison of the chloride binding isotherms of the 8MK paste obtained using the Equilibrium method or the ponding method.

## 4.2 Phase Two

### 4.2.1 Effect of Cement Composition

#### 4.2.1.1 Cement Type

As mentioned in Chapter 3, 9 different Portland cements and clinkers were used for this series of tests. They were chosen to reflect a variety of $C_3A$, $C_4AF$, sulphate, and alkali contents. It was thought that the results would reveal important information about the role of these components in the chloride binding process. Figure 4-39 shows the binding isotherms of the different cements. The results are also presented in Table 4-7. In general, it can be noticed that cements with higher $C_3A$ contents exhibited higher chloride binding capacities than cements with lower $C_3A$ contents. This trend was clear at chloride concentrations of 1.0 M and 3.0 M. A statistical analysis was performed on the data in order to get more information about the effect of cement components on the chloride binding capacity. The analysis was two parts: in part one, a muti-variable linear regression analysis, involving cement components versus the bound chloride, was conducted for each of the tested chloride concentrations.

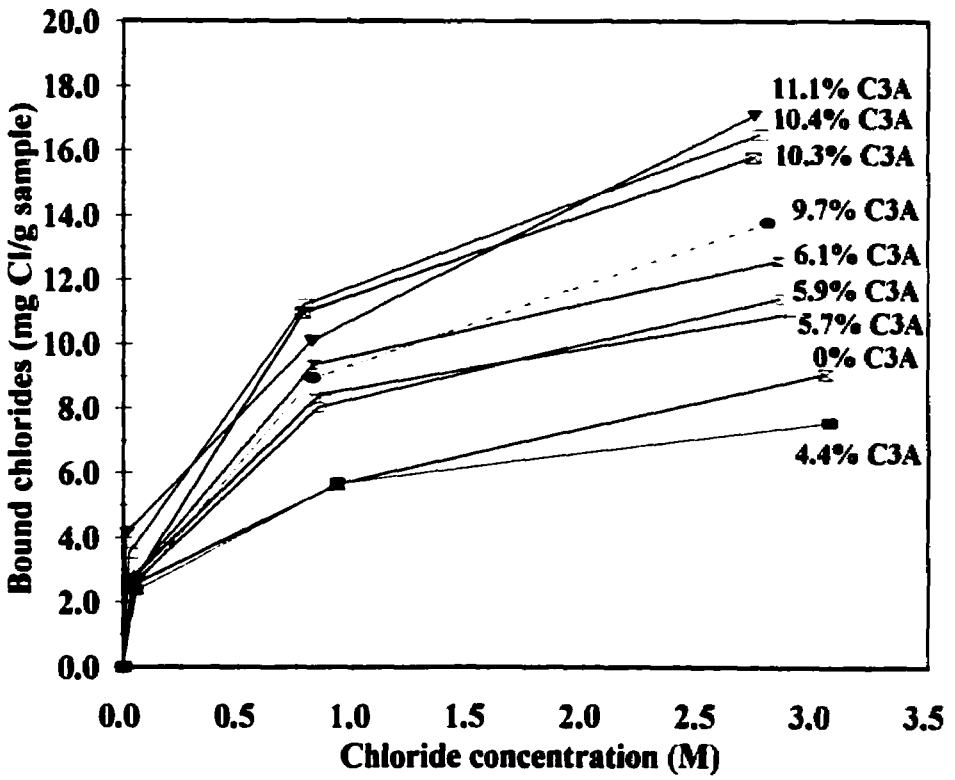


Figure 4-39: Chloride binding isotherms of cement pastes made from several cements with different chemical compositions. W/CM = 0.5, age = 2 months.

Table 4-7: Chloride binding capacities (mg Cl/g sample) of the tested cement pastes, at 0.1 M, 1.0 M, and 3.0 M chloride concentrations. W/CM = 0.5

| Cement | $C_3A$ (%) | Chloride concentration in the host solution | | |
|---|---|---|---|---|
| | | 0.1 M | 1 M | 3 M |
| C1 | 0 | 2.59 | 5.66 | 9.1 |
| C2 | 10.29 | 2.61 | 10.97 | 15.81 |
| C3 | 9.74 | 2.48 | 8.97 | 13.79 |
| C4 | 11.08 | 4.16 | 10.11 | 17.12 |
| C5 | 6.06 | 2.78 | 9.36 | 12.6 |
| C6 | 10.43 | 3.53 | 11.24 | 16.52 |
| C7 | 4.39 | 2.39 | 5.71 | 7.59 |
| C8 | 5.74 | 2.8 | 8.45 | 10.94 |
| Control | 5.95 | 2.61 | 8.06 | 11.4 |

concentrations (0.1M, 1.0M, 3.0M). The independent variables included the $C_3A$ content, $C_4AF$ content, $C_3S+C_2S$ content, and the $SO_3$ content. Table 4-8 shows the values of the different cement components in the cements. The $Na_2O_e$ content was excluded from the analysis after a preliminary

Table 4-8: Contents of cement components that were considered in the correlation study with the chloride binding capacities of the cements

| | Cement components and their contents | | | | |
|---|---|---|---|---|---|
| mix | $C_3A$ (%) | $C_4AF$ (%) | $SO_3$ (%) | $C_3S+C_2S$ (%) | $Na_2Oe$ (%) |
| C1 | 0 | 13.62 | 2.65 | 78.69 | 0.28 |
| C2 | 10.29 | 7.75 | 4.12 | 68.46 | 1.19 |
| C3 | 9.74 | 8.03 | 4.43 | 66.94 | 1.19 |
| C4 | 11.08 | 6.81 | 0.32 | 78.61 | 0.48 |
| C5 | 6.06 | 9.36 | 1.44 | 75.27 | 0.64 |
| C6 | 10.43 | 6.26 | 1.35 | 74.22 | 1.03 |
| C7 | 4.39 | 0.82 | 2.14 | 88.8 | 0.29 |
| C8 | 5.74 | 9.79 | 1 | 75.43 | 0.56 |
| Control | 5.95 | 8.79 | 2.79 | 75.19 | 0.58 |

correlation study revealed the $Na_2O_e$ had good correlation with the $C_3S+C_2S$ content, and some correlation between the $Na_2O_e$ and $C_3A$ content, as shown in Table 4-9. The analysis was done using single-, double-, and multi-variables versus the bound chloride. The aim was to obtain more information on the roles of the individual components, and on the mutual influence of some components (e.g. the influence of $SO_3$ on $C_3A$). In part two, a similar analysis was performed, involving cement components versus the $\alpha$ and $\beta$ coefficients of the Freundlich isotherms. It was hoped that these analyses would provide information on the roles of the different cement components in chloride binding, the relative importance of chemical and physical binding, and whether the binding isotherms could be predicted from the cement components.

Table 4-9: Correlation coefficients ($r^2$) among the cement components.

| | $C_3A$ | $C_4AF$ | $C_3S+C_2S$ | $SO_3$ | $Na_2O_e$ |
|---|---|---|---|---|---|
| $C_3A$ | 1 | 0.13 | 0.26 | 0 | 0.53 |
| $C_4AF$ | 0.13 | 1 | 0.2 | 0.01 | 0 |
| $C_3S+C_2S$ | 0.26 | 0.2 | 1 | 0.27 | 0.73 |
| $SO_3$ | 0 | 0.01 | 0.27 | 1 | 0.29 |
| $Na_2O_e$ | 0.53 | 0 | 0.73 | 0.29 | 1 |

Tables 4-10 and 4-11 present the results of the first part of the statistical analysis. Table 4-10 shows the coefficients of determination, $r^2$, of the different permutations. On a single basis, the results show that the $C_3A$ content is the only factor that correlated well with the binding capacity at high concentrations (1 M, 3 M). This indicates that the $C_3A$ content is the most decisive factor (on an individual basis) in chloride binding at high concentrations. The low correlation of $C_3A$ at low chloride concentration indicates that other factors have decisive roles in chloride binding at low chloride concentrations.

On a pairwise basis, the ($C_3A$, $C_4AF$) pair has the best correlation with the binding capacity at high chloride concentrations (1 M, 3 M). The contribution of $C_4AF$ was notable as shown in Table 4-10. This indicates that the $C_4AF$ content possibly plays a detectable role in binding at high chloride concentrations. This also indicates that chemical binding is a major part of the binding capacity at high chloride concentrations. It is interesting to notice that the pair of $C_3A$ and $SO_3$ contents correlates the best at low chloride concentrations. The results in Table 4-10 indicate that the $SO_3$ content has a negative influence on binding, and its role is more decisive than the $C_3A$ role.

Table 4-10: Coefficients of determination ($r^2$) of various permutations of cement components versus the binding capacity, at different chloride concentrations.

| no. of tested variables | Cement components | $r^2$ coefficients at different chloride concentrations | | |
|---|---|---|---|---|
| | | 0.1 M | 1 M | 3 M |
| 1 | $C_3A$ | 0.3 | 0.78 | 0.79 |
| | $C_4AF$ | 0.01 | 0 | 0 |
| | $C_3S+C_2S$ | 0 | 0.42 | 0.36 |
| | $SO_3$ | 0.48 | 0.01 | 0.01 |
| 2 | $C_3A$, $C_4AF$ | 0.32 | 0.87 | 0.91 |
| | $C_3A$, $C_3S+C_2S$ | 0.44 | 0.83 | 0.82 |
| | $C_3A$, $SO_3$ | 0.78 | 0.79 | 0.8 |
| | $C_4AF$, $C_3S+C_2S$ | 0.01 | 0.56 | 0.46 |
| | $C_4AF$, $SO_3$ | 0.48 | 0.01 | 0.01 |
| | $C_3S+C_2S$, $SO_3$ | 0.62 | 0.65 | 0.58 |
| 3 | $C_3A$, $C_4AF$, $C_3S+C_2S$ | 0.96 | 0.87 | 0.95 |
| | $C_3A$, $C_4AF$, $SO_3$ | 0.82 | 0.89 | 0.93 |
| | $C_3A$, $C_3S+C_2S$, $SO_3$ | 0.78 | 0.91 | 0.88 |
| | $C_4AF$, $C_3S+C_2S$, $SO_3$ | 0.66 | 0.88 | 0.74 |
| 4 | $C_3A$, $C_4AF$, $C_3S+C_2S$, $SO_3$ | 0.96 | 0.91 | 0.95 |

Table 4-11: Coefficients of the cement components in selected multiple linear regression equations that correlate the best with the binding capacity at different chloride concentrations. The equations have the form: $C_b = a+bx_1+cx_2+...$, where a, b, c,... represent the intercept and the slopes of cement components respectively. $x_1$ $x_2$, ... represent the cement components.

| | Variables $x_1, x_2, ...$ | Intercept a | $C_3A$ b | $C_4AF$ c | $C_3S+C_2S$ d | $SO_3$ e |
|---|---|---|---|---|---|---|
| 0.1 M | $C_3A$, $SO_3$ | 2.91 | 0.09 | — | — | -0.29 |
| | $C_3A$, $C_4AF$, $C_3S+C_2S$ | -11.82 | 0.29 | 0.22 | 0.14 | — |
| 1.0 M | $C_3A$, $C_4AF$ | 3.25 | 0.56 | 0.19 | — | — |
| | $C_3A$, $C_4AF$, $C_3S+C_2S$ | 1.71 | 0.58 | 0.21 | 0.02 | — |
| | $C_3A$, $C_4AF$, $SO_3$ | 3.55 | 0.56 | 0.2 | — | -0.17 |
| 3.0 M | $C_3A$, $C_4AF$ | 3.25 | 0.94 | 0.36 | — | — |
| | $C_3A$, $C_4AF$, $C_3S+C_2S$ | -15.18 | 1.2 | 0.62 | 0.19 | — |
| | $C_3A$, $C_4AF$, $SO_3$ | 3.79 | 0.95 | 0.38 | — | -0.31 |

The previous results suggest that the $SO_3$ has a more negative influence on $C_3A$ at low chloride concentrations than at high chloride concentrations.

On a multivariable basis the results show that the group of $C_3A$, $C_4AF$, and $C_3S+C_2S$ contents correlate best with the binding capacity at almost all concentrations. The correlation with the binding capacity is very good. It is very interesting to notice the linear regression equations at low and high concentrations in Table 4-10; the coefficients of the $C_3A$, $C_4AF$, and $C_3S+C_2S$, suggest that the $C_3S+C_2S$ content plays the major in chloride binding at low chloride concentrations, and also plays a major role along with the $C_3A$ and $C_4AF$ at high chloride concentrations. The reason for the poor correlation between the $C_3S+C_2S$ content and the binding capacity is due to the relatively small variation in the $C_3S+C_2S$ content of the different cements. The good correlation of the $C_3A$ content with the binding capacity at high chloride concentrations is due to the relatively large variation in the $C_3A$ content of the different cements. On the other hand, the regression equation of the $C_3A$, $C_4AF$, and $C_3S+C_2S$ at 1M chloride concentration indicates that the role of the $C_3S+C_2S$ is minor in comparison with the combined role of $C_3A$ and $C_4AF$, which does not fit well with the results of the 0.1 M and 3 M concentration.

Before analyzing the results of part two of the statistical analysis, it is convenient to review the influence of the $\alpha$ and $\beta$ parameters of the Freundlich isotherm on the shape of that function which describes the binding capacity at different chloride concentrations. With a Freundlich isotherm, $C_b$ is a linear function of $\alpha$ . This means that for a constant $\beta$, any change in $\alpha$ affects the binding isotherm in a proportional way: if $\alpha$ increases by 100%, then the binding capacity, at any concentration, increases by 100%. Also with a Freundlich isotherm, $C_b$ is a non-linear function of $\beta$:

for $C_f < 1$ if $\beta$ increases, then $C_b$ decreases,

for $C_f > 1$ if $\beta$ increases, then $C_b$ increases.

Within the ranges of values of the $\alpha$ and $\beta$ parameters obtained in this study (Table 4-12), the influence of $\beta$ is minor at chloride concentrations higher than 1 M. The influence of $\beta$ is small but noticeable at low chloride concentrations. Hence, while $\alpha$ has a decisive influence on the binding capacity at all concentrations, $\beta$ has an apparent influence on the binding capacity only at low concentrations. The binding capacity is proportional to $\alpha$, and inversely proportional to $\beta$.

Table 4-12:α and β parameters(Freundlich isotherm) correspondent to the cements used in this study.

| Cement | Freundlich parameters | |
|---|---|---|
| | α | β |
| C1 | 6.17 | 0.35 |
| C2 | 11.11 | 0.37 |
| C3 | 9.34 | 0.39 |
| C4 | 12.05 | 0.31 |
| C5 | 9.20 | 0.33 |
| C6 | 11.95 | 0.32 |
| C7 | 5.67 | 0.29 |
| Control | 8.15 | 0.34 |

Table 4-13 shows the coefficients of determination, $r^2$, of the various permutations of cement components versus the α and β parameters. The $C_3A$ content is the only single variable that correlates well with α (positive correlation), and the $SO_3$ (negative correlation) content as well as the $C_3S+C_2S$ content (negative correlation) have correlation coefficients with β higher than 0.5. On a pairwise basis, the $C_3A$, $C_4AF$ pair correlates best with α, while the $SO_3$, $C_3S+C_2S$ correlates best with β. These results mean that α is mostly influenced by $C_3A$ and $C_4AF$, and β, which affects the lower part of the binding isotherm, is mostly influenced by $SO_3$ and the $C_3S+C_2S$. The mutivariable analysis shows that the $C_3A$, $C_4AF$, $SO_3$ group of variables has very good correlations with both α and β. Also, the $C_3A$, $C_4AF$, $C_3S+C_2S$ group correlated very well with α. These results indicate that the binding isotherm of a cement can be predicted from the contents of some of the cement components. If this finding holds true for other cases, it would be of practical significance, since it would enable the determination of the binding isotherm without the need for binding tests. The linear regression equations show that $C_3A$, $C_4AF$, and $C_3S+C_2S$ have positive influence on the binding capacity, and the $SO_3$ has a negative influence on the binding capacity. The equation correlating $C_3A$, $C_4AF$, and $C_3S+C_2S$ to the value of the α coefficient is

$$\alpha = -12.44 + 0.86*C_3A + 0.44*C_4AF + 0.16*(C_3S+C_2S).$$

This equation shows that α is mostly sensitive to the $C_3A$ content, and least to the $C_3S+C_2S$ content.

Table 4-13: Coefficients of determination ($r^2$) of various permutations of cement components with the α and β parameters.

| nb of tested variables | Cement components | Coefficients of determination ( $r^2$) | |
|---|---|---|---|
| | | α | β |
| 1 | $C_3A$ | 0.8 | 0.04 |
| | $C_4AF$ | 0 | 0.18 |
| | $C_3S+C_2S$ | 0.31 | 0.63 |
| | $SO_3$ | 0.03 | 0.7 |
| 2 | $C_3A$, $C_4AF$ | 0.9 | 0.33 |
| | $C_3A$, $C_3S+C_2S$ | 0.82 | 0.69 |
| | $C_3A$, $SO_3$ | 0.84 | 0.74 |
| | $C_4AF$, $C_3S+C_2S$ | 0.42 | 0.64 |
| | $C_4AF$, $SO_3$ | 0.03 | 0.82 |
| | $C_3S+C_2S$, $SO_3$ | 0.59 | 0.88 |
| 3 | $C_3A$, $C_4AF$, $C_3S+C_2S$ | 0.94 | 0.72 |
| | $C_3A$, $C_4AF$, $SO_3$ | 0.94 | 0.94 |
| | $C_3A$, $C_3S+C_2S$, $SO_3$ | 0.91 | 0.88 |
| | $C_4AF$, $C_3S+C_2S$, $SO_3$ | 0.79 | 0.91 |
| 4 | $C_3A$, $C_4AF$, $C_3S+C_2S$, $SO_3$ | 0.95 | 0.96 |

Table 4-14: Coefficients of the cement components in selected linear regression equations that correlate the best with the α parameter.

| Variables | Intercept | $C_3A$ | $C_4AF$ | $C_3S+C_2S$ | $SO_3$ | $r^2$ |
|---|---|---|---|---|---|---|
| $C_3A$, $C_4AF$ | 2.77 | 0.65 | 0.22 | — | — | 0.9 |
| $C_3A$, $C_4AF$, $C_3S+C_2S$ | -12.44 | 0.86 | 0.44 | 0.16 | — | 0.94 |
| $C_3A$, $C_4AF$, $SO_3$ | 3.38 | 0.65 | 0.24 | — | -0.4 | 0.94 |

Table 4-15: Coefficients of the cement components in selected linear regression equations that correlate the best with the β parameter.

| Variables | Intercept | $C_3A$ | $C_4AF$ | $C_3S+C_2S$ | $SO_3$ | $r^2$ |
|---|---|---|---|---|---|---|
| $C_3S+C_2S$, $SO_3$ | 0.5 | — | — | -0.003 | 0 | 0.88 |
| $C_3A$, $C_4AF$, $SO_3$ | 0.23 | 0.003 | 0.005 | — | 0 | 0.94 |
| $C_4AF$, $C_3S+C_2S$, $SO_3$ | 0.44 | — | 0.002 | -0.002 | 0 | 0.91 |

The results of the statistical analysis showed the following:

1- The $C_3A$ content of cement is a good indicator of the chloride binding capacity at high chloride concentrations (e.g. 1 M, 3 M), but not at low concentrations. While this indicates a decisive role of the $C_3A$ in chloride binding at high chloride concentrations, it does not necessarily mean that the $C_3A$ makes a major contribution to the binding capacity. The results of this analysis pointed to the possibility that the $C_3S$ and $C_2S$ might be responsible for a major part of the binding capacity despite its poor correlation with the binding capacity. The poor correlation might be due to the relatively small variation in the $C_3S+C_2S$ content among the different cements, resulting in small differences in their contribution to the binding capacity. On the other hand, the relatively large variations in the $C_3A$ contents of the different cements result in relatively large differences in their contributions to the binding capacity, which makes the binding capacity more sensitive to the $C_3A$ content. The low correlation between the $C_3A$ and the binding capacity at low chloride concentrations, and the good correlation between the $C_3A$, $SO_3$ and the binding capacity suggest that the negative influence of $SO_3$ on the role of $C_3A$ is more noticeable at low chloride concentrations.

2- The good correlation of the $C_3A$, $C_4AF$ pair with the binding capacity at high chloride concentrations but not at low concentration, suggests that the role of the chemical binding capacity is more pronounced at high chloride concentrations than at low concentrations.

3- More than one cement component affects the chloride binding capacity, including $C_3A$, $C_4AF$, $C_3S+C_2S$, $SO_3$, and probably other factors that were not addressed here

4- The binding isotherms ($\alpha$ and $\beta$ of the Freundlich isotherm) can be reasonably predicted from the cement composition (as the results of the second part of this analysis indicate). The $\alpha$ coefficient can be predicted by either of the following equations, based on Bogue calculated compounds:

$$\alpha = 0.86*C_3A + 0.44*C_4AF + 0.16*(C_3S+C_2S) - 12.44 \quad (r^2 = 0.94) \quad (4\text{-}6)$$

$$\alpha = 0.65*C_3A + 0.24*C_4AF - 0.35*SO_3 + 3.38 \quad (r^2 = 0.94) \quad (4\text{-}7)$$

The $\beta$ coefficient can be predicted by the following equation:

$$\beta = 0.003*C_3A + 0.005*C_4AF + 0.019*SO_3 + 0.23 \quad (r^2 = 0.94) \quad (4\text{-}8)$$

Because of the small size of the sample (number of tested cements) tested in this analysis, it is not known how general these prediction equations are. To check these prediction equations, an attempt was made to predict the chloride binding isotherms of two cements that were used by *Delagrave et al. (1997)*. The two Portland cements were ASTM Type I and Type V. Table 4-16 shows the Bogue composition, $SO_3$ content, and fineness of the two cements, and of the control (OPC) cement used in this thesis. Table 4-17 presents the predicted binding capacities, using equations 4-6 and 4-8, and the experimental binding capacities, obtained from the Freundlich isotherms that were fitted to the experimental data. The chloride binding capacity of the control cement paste is also presented in Table 4-17 for the purpose of the discussion.

Table 4-16: Mineralogical composition, $SO_3$ content, and fineness of the two cements (and the control mix) used to check the equations for predicting the constants of the Freundlinch isotherm.

| | $C_3A$ (%) | $C_4AF$ (%) | $C_3S$ (%) | $C_2S$ (%) | $SO_3$ (%) | Blaine ($m^2/kg$) |
|---|---|---|---|---|---|---|
| **Type I** | 7.4 | 5.1 | 68.7 | 5.8 | 3.5 | 462 |
| **Type V** | 1.8 | 13.3 | 54.9 | 22.5 | 2.2 | 380 |
| **OPC (control)** | 5.9 | 8.8 | 57.6 | 17.6 | 2.8 | 326 |

Table 4-17: Predicted and experimental chloride binding capacities of the two tested cements. The binding capacities of the control mix (OPC) are also included.

| | Predicted | | Experimental Data* | | |
|---|---|---|---|---|---|
| | Type I | Type V | Type I | Type V | control |
| **0.1 M** | 3.7 | 3.4 | 3.4 | 3.6 | 3.7 |
| **0.2 M** | 4.7 | 4.2 | 4.9 | 5.1 | 4.7 |
| **0.5 M** | 6.4 | 5.8 | 7.8 | 7.8 | 6.4 |
| **0.6 M** | 6.8 | 6.2 | 8.6 | 8.5 | 6.8 |
| **1.0 M** | 8.1 | 7.3 | 11.2 | 10.9 | 8.2 |

* Values presented in this table were obtained from the Freundlich isotherms that were fitted to the experimental chloride binding data

While the experimental binding capacities of the two cement pastes were almost the same, the predicted binding capacities of the paste made with the Type I cement was only slightly higher (10%) than those of the paste made with the Type V cement. This slight difference (despite the

considerable difference in the $C_3A$ contents) reflects the fact that the $C_4AF$ content is emphasised in Equation 4-6 (the slope of $C_4AF$ is half that of the $C_3A$). The predicted binding capacities were generally lower than the experimentally obtained ones. The differences increased at higher concentrations ($\geq$0.5 M), and were between 20%-25%. However, these differences were not totally due to the prediction model. The data of *Delagrave et al. (1997)* were obtained from powdered samples, while the data in this research were obtained from broken discs. As mentioned earlier, powdered samples tend to give higher binding capacities than samples made from discs, especially at higher concentrations. Data in Table 4-17 show the higher binding capacities of the Type I cement paste (obtained with powdered samples) compared to those of the control paste (obtained with samples made from discs), despite their close chemical composition. However, the predicted binding capacity of the Type I cement paste is almost the same as the binding capacity of the control paste. Hence, part of the observed differences is possibly due to the differences in the experimental procedures. It seems that the prediction of binding isotherms of cement pastes is possible. But, more work is needed to be able to produce a reliable prediction model. Since the experimental method used to produce binding data will influence the prediction models, it is important to elaborate a method that would produce chloride binding data that are close to what will be obtained under realisitc conditions. Also, the more is the number of cements tested, the more likely it is to cover the different factors that affect the chloride binding capacity. Finally, a very important criterion in the development of a prediction model, is the choice of factors that are considered influencial in the binding capacity. Some factors were omitted in the present attempt and need to be considered in future ones.

#### 4.2.1.2 Effect of Sulphate Content

As mentioned in Chapter 3, cements C1 and C4 were chosen to study the effect of sulphate content on the chloride binding capacity of cement. About 4% and 7 % $SO_3$ were added (as gypsum) to C1 and C4 respectively. It was assumed that the added $SO_3$ would convert the $C_4AF$ of the C1 cement (0% $C_3A$, 14% $C_4AF$) into ettringite (assuming that they totally react together), and the $C_3A$ and $C_4AF$ of the C4 clinker (11% $C_3A$, 7% $C_4AF$) would be mostly converted into ettringite. Thus, it was also assumed that any observed reductions in the chloride binding capacities were the results of decreases in the chemical binding capacities. Figures 4-40 and 4-41 show the effect of sulphate content on the chloride binding capacities of the two cement pastes. These results show large reductions in the binding capacities of the two cements as a result of the $SO_3$ additions. Four observations can me made regarding these results. First, the increase in the $SO_3$ contents of the two cements had an important (negative) impact on their binding capacities. This confirms the finding in the previous section regarding the negative role of sulphate in chloride binding. It should be kept in mind, however, that the sulphate contents in this study were much higher than the normal sulphate

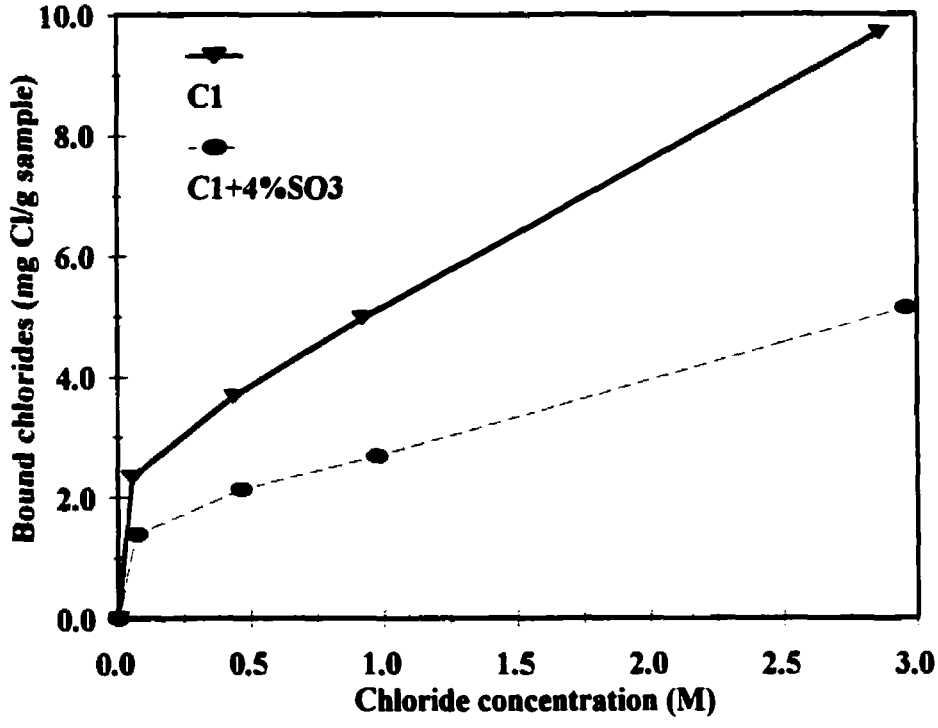


Figure 4-40: Chloride binding isotherms of the C1 paste (0% $C_3A$, 13.6% $C_4AF$) and the C1-4$SO_3$ paste. The increase in the $SO_3$ content of the C1-4$SO_3$ paste caused a large reduction in its binding capacity.

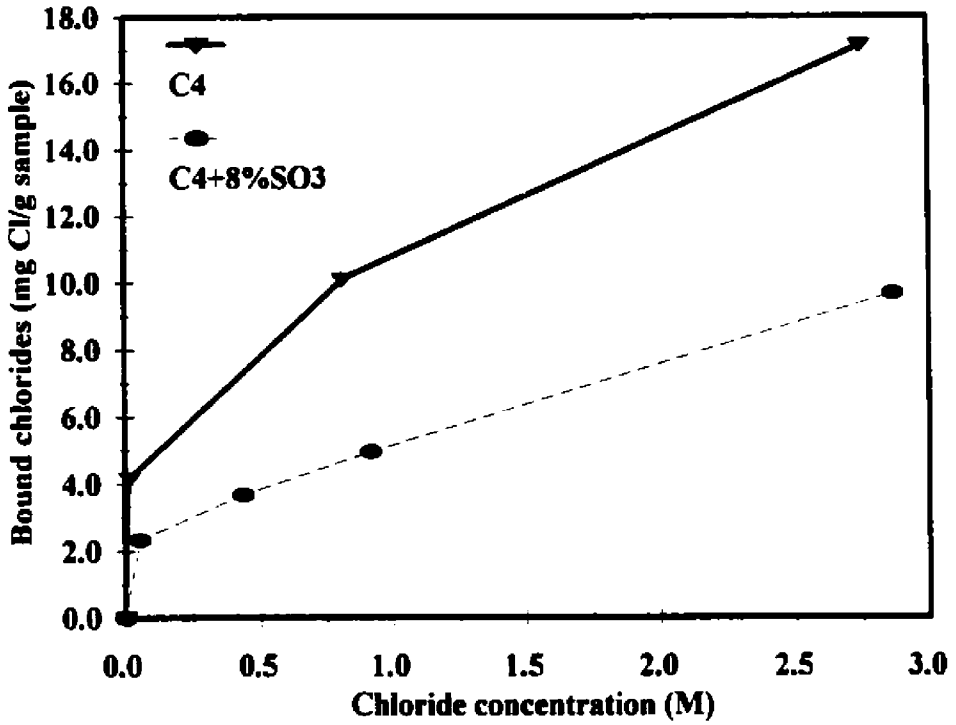


Figure 4-41: Chloride binding isotherms of the C4 paste (11.1% $C_3A$) and the C4-7$SO_3$ paste. The increase in the $SO_3$ content of the C4-7$SO_3$ paste, caused a large decrease in its binding capacity

contents in cements. Hence, the actual effect of the $SO_3$ content on the binding capacity is not as strong as the results of this section show. Second, the large decrease in the binding capacity of the C4 cement is an indirect proof of the importance of the chemical binding capacity of that cement, and consequently the importance of the $C_3A$ in chloride binding. Third, the decrease in the binding capacity of the C1 cement is an indication of the ability of this cement (with 0% $C_3A$) to chemically bind chlorides, and that the $C_4AF$ most likely binds chlorides and plays a noteworthy role in chloride binding as indicated in the previous section. Finally, the fact that these two cement pastes still had considerable capacities to bind chlorides, especially in the case of the C1 cement, is an indication of the existence of other mechanisms of chloride binding (assuming that ettringite does not bind nor is transformed into Friedel's salt), particularly physical binding.

#### 4.2.1.3 Effect of Cement Fineness

Figure 4-42 shows chloride binding isotherms of the C2 and C3 cements. These two cements were from the same source, and had very similar compositions except that they had different fineness. C2 was a CSA Type 10 cement with a surface area of 407 $m^2/kg$ and C3 was a CSA Type 30 cement with a surface area of 523 $m^2/kg$, and with 0.3% more $SO_3$. The results show that C3, which had a higher surface area than C2, had a lower binding capacity. The difference between their binding capacities was small (< 20%). Part of this difference might be attributed to the small differences in the $C_3A$ and $SO_3$ contents. To avoid any other influences than the surface area, another test was conducted where the binding capacity of the paste, made with C4 clinker (320 $m^2/kg$), was compared to that of a paste, made with otherwise the same clinker, except that the clinker was ground for extra two hours (411 $m^2/kg$) before mixing. The results showed that the pastes had similar chloride binding capacities as shown in Figure 4-43. The results of these two tests indicate that the influence of the cement fineness is likely small, but the added gypsum, in the case of C3 cement, to control higher fineness, may have a negative impact on binding.

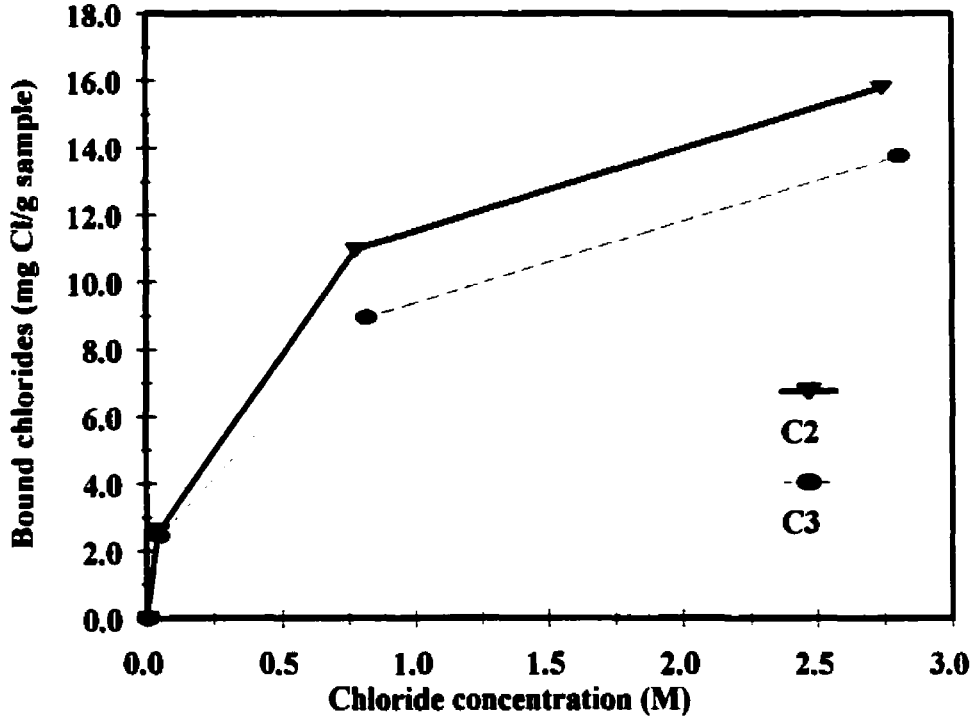


Figure 4-42: Chloride binding isotherms of the C2 paste and the C3 paste. The two cements are from the same source and are otherwise similar except that C2 is CSA Type 10 and C3 is CSA Type 30.

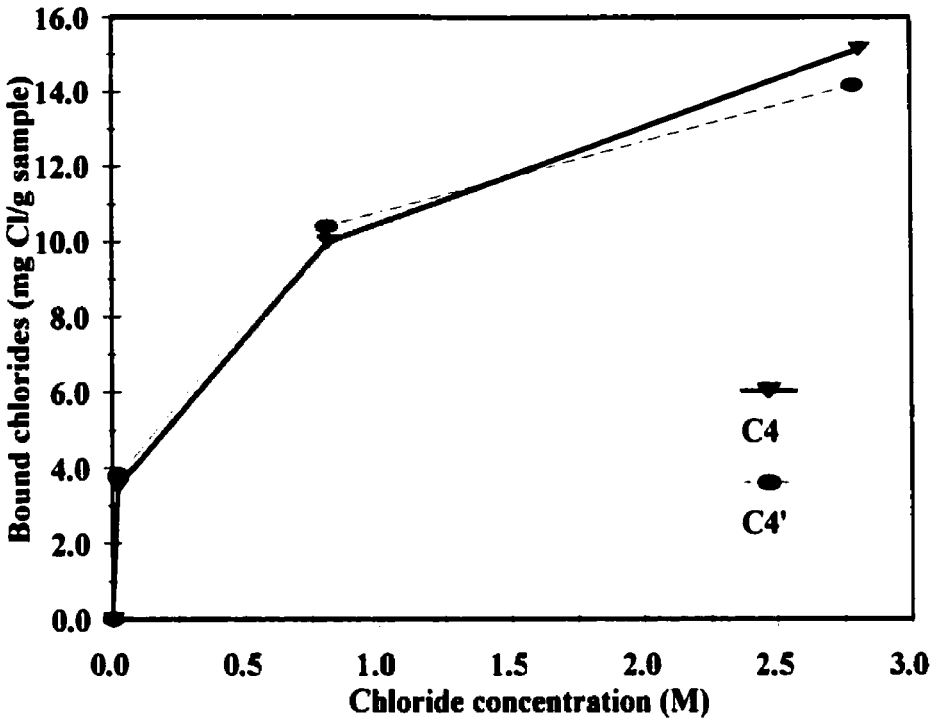


Figure 4-43: Chloride binding isotherms of the C4 paste and the C4' paste. Both pastes were made from the same cement (C4), except that the cement of the C4' paste was ground for an extra two hours before being cast and tested for chloride binding.

### 4.2.2 Influence of Environmental Factors

#### 4.2.2.1 Effect of pH

The results of this study show that an increase in the pH or hydroxyl ion concentration of the host solution will result in a reduction of the chloride binding capacities of the three tested mixtures. These results are in agreement with the literature *(Tritthart, 1989b)*. Figures 4-44 to 4-46 show the effect of pH on the binding capacity of the OPC, 8SF, and the 8MK pastes respectively. In general, the effect of pH is rather negligible between pH=13 and pH=13.4, and the effect is small but significant between pH=13 and pH=13.7. The effect of pH varies with the chloride concentration. While it is significant at low chloride concentration, it is almost insignificant at higher chloride concentrations (especially at 3 M) as shown in Figure 4-47. It is important to mention that the pH values shown in the previous figures represent the initial hydroxyl ion concentrations in the host solutions. These values changed after equilibrium was established between the pore solutions and the host solutions, which resulted in a reduction in the pH of solutions with initial pH=14 and in an increase in the pH of solutions with initial pH=13.

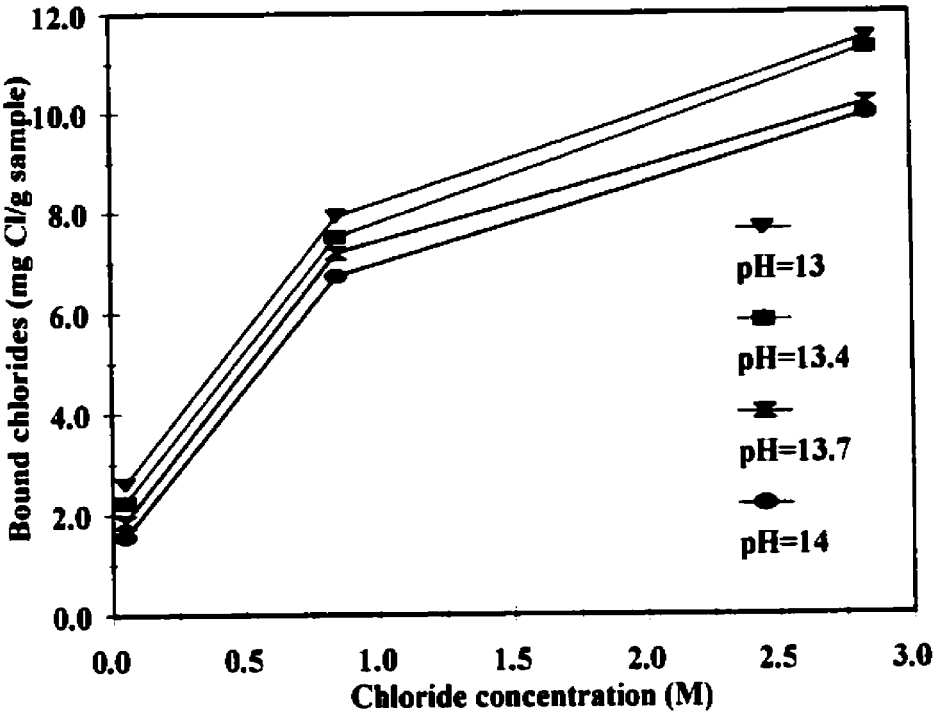


Figure 4-44: Effect of the pH of the solution on the chloride binding capacity of the control mix with W/CM of 0.5.

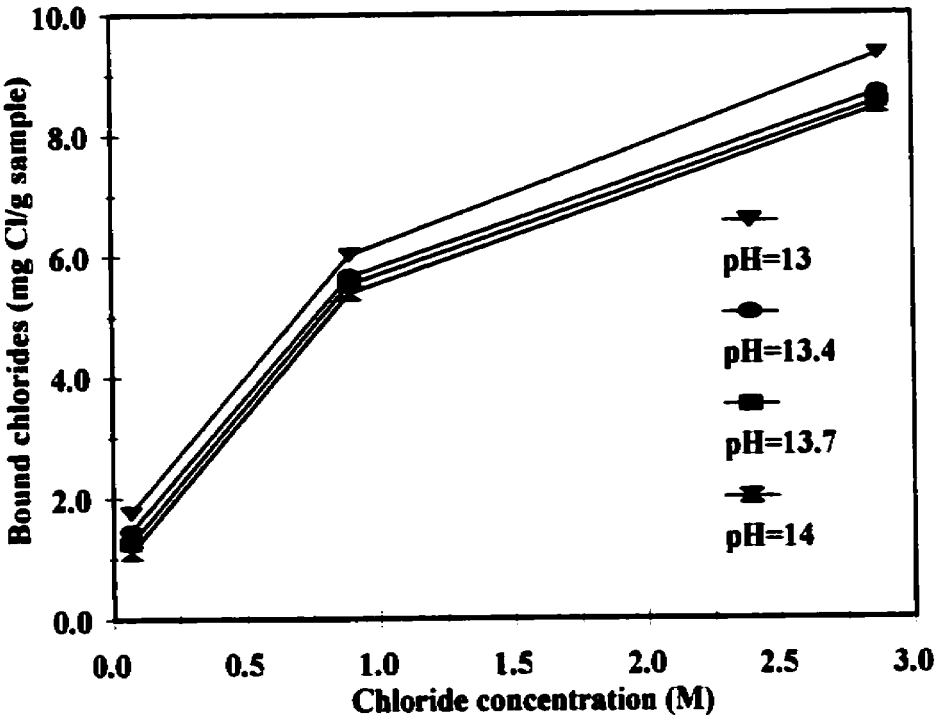


Figure 4-45: Effect of the pH of the solution on the chloride binding capacity of the 8SF paste with W/CM of 0.5.

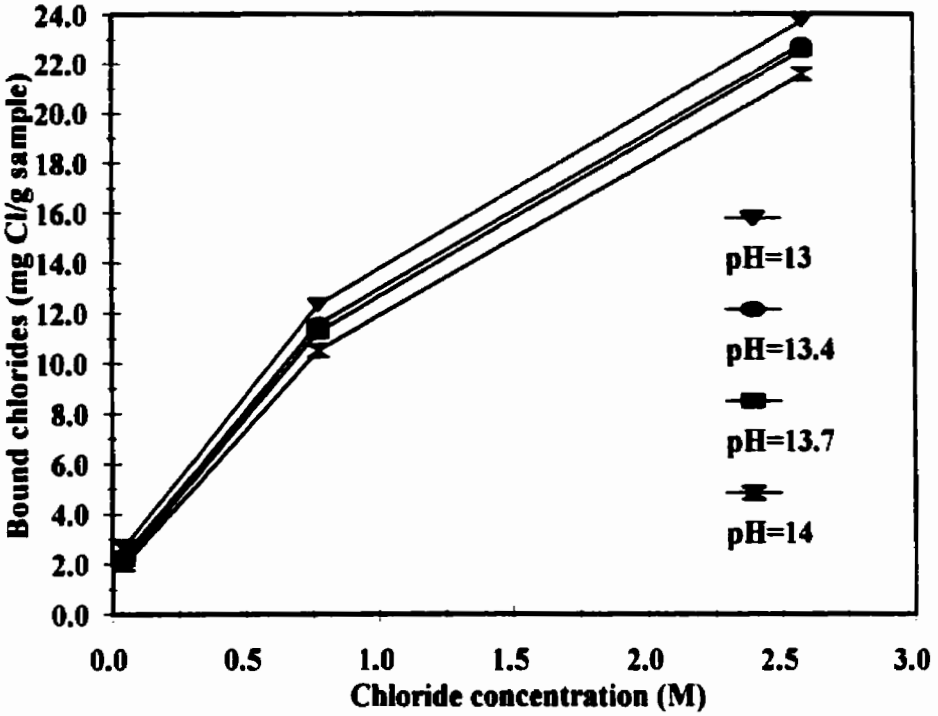


Figure 4-46: Effect of the pH of the solution on the chloride binding capacity of the 8MK paste with W/CM of 0.5.

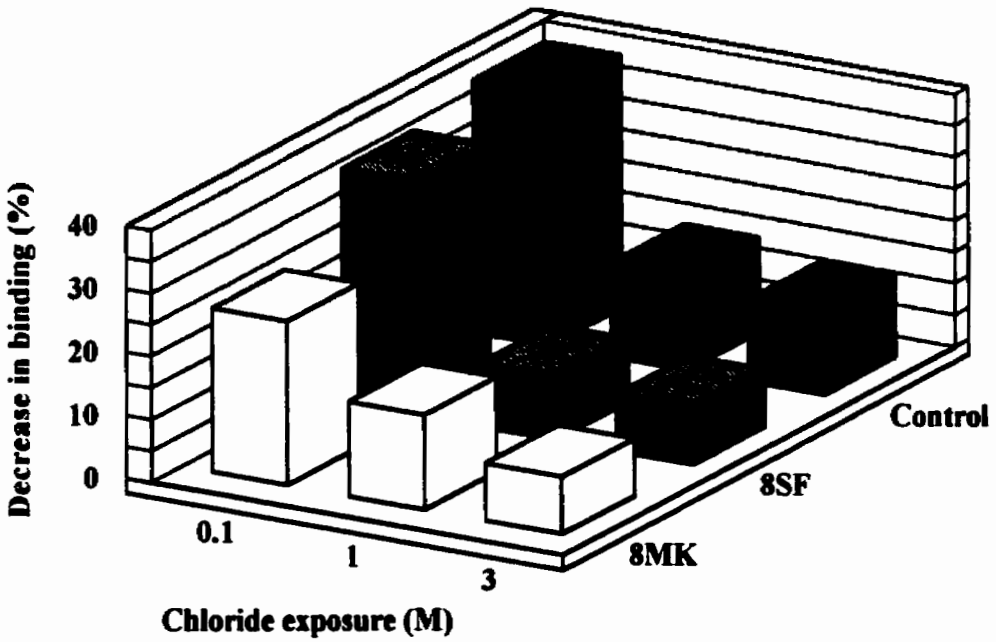


Figure 4-47: Effect of the increase in the pH of the host solutions (from pH=13 to pH=14) on the chloride binding capacities of pastes at different chloride exposures. W/CM = 0.5.

The results reveal a stronger effect of pH on chloride binding when they are presented as a function of equilibrium pH, as shown in Figures 4-48 to 4-50. It is interesting to notice that the effect of pH on the binding capacity of these pastes is linear over the range of pH studied. This fact makes it easier to predict the binding capacity at other pH levels.

It is known that in concrete structures subjected to chloride ingress, a counter diffusion of $OH^-$ results from the diffusion of $Cl^-$. This results in variation of the pH across the depth of the concrete cover. The results of this section show that this variation in pH affects the binding capacity. Hence, the use of chloride binding isotherms, determined in the laboratory at constant pH, will results in errors when used in service life prediction models.

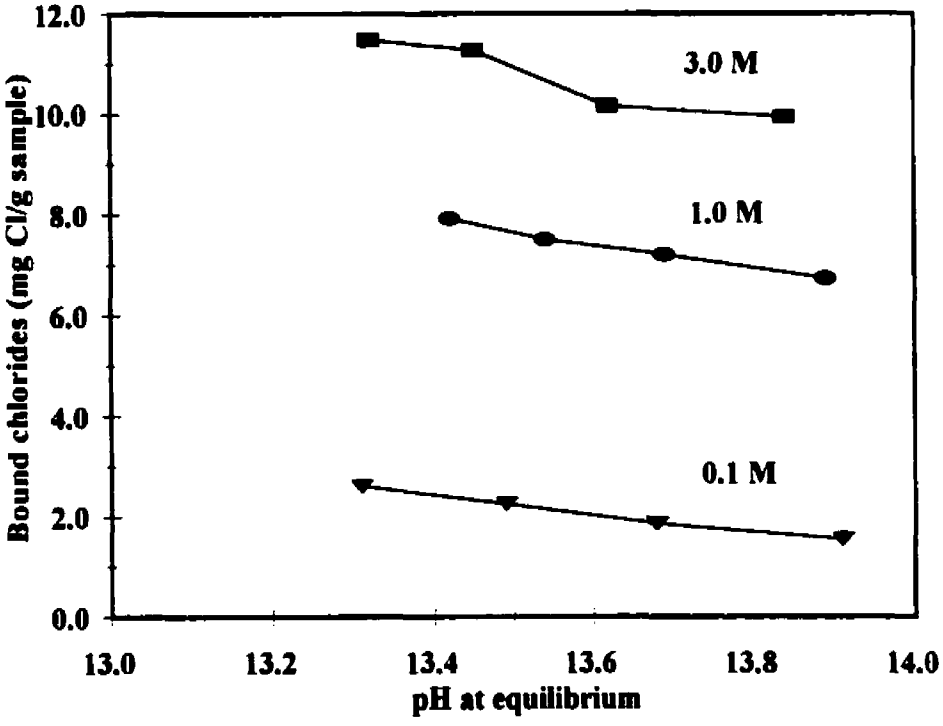


Figure 4-48: Influence of the pH of the host solution (at equilibrium) on the chloride binding capacity of the control mix at different chloride exposures. W/CM = 0.5.

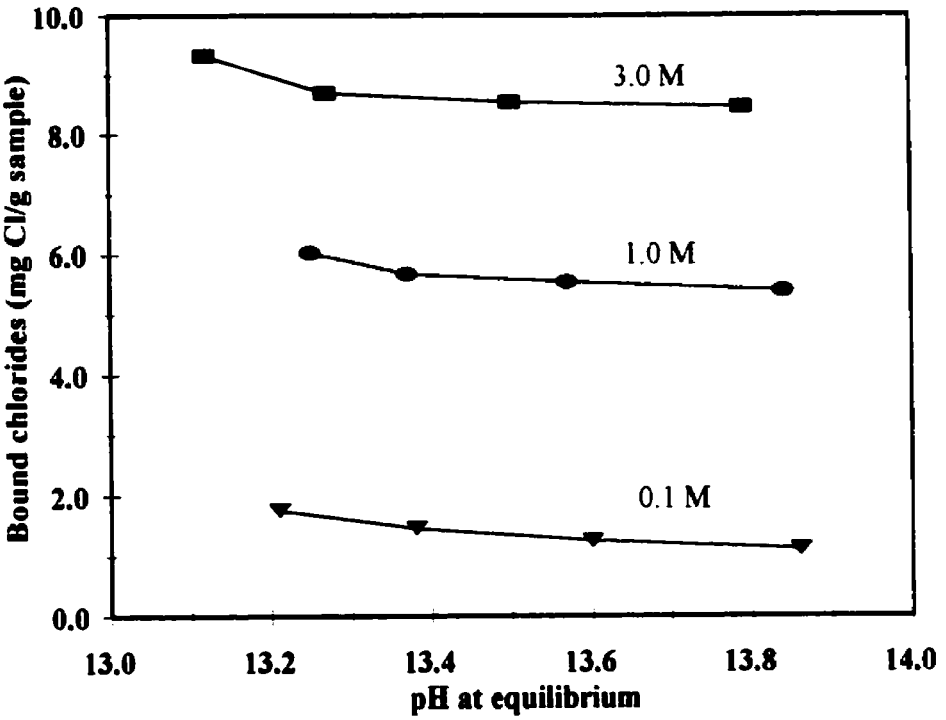


Figure 4-49: Influence of the pH of the host solution (at equilibrium) on the chloride binding capacity of the 8SF paste at different chloride concentrations. W/CM = 0.5.

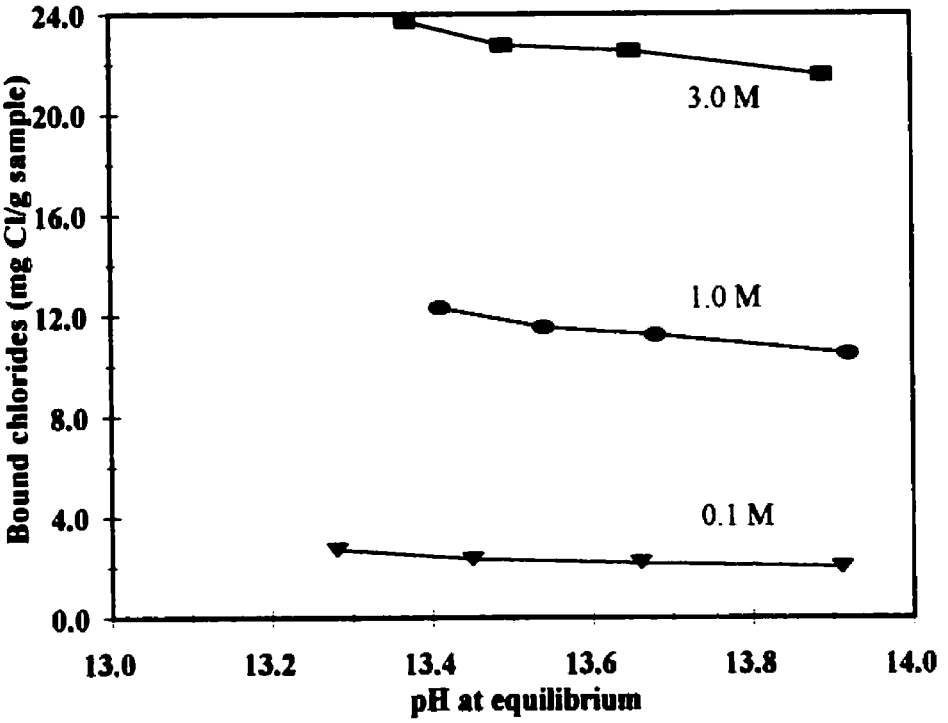


Figure 4-50: Influence of the pH of the host solution (at equilibrium) on the chloride binding capacity of the 8MK paste at different chloride concentrations. W/CM = 0.5.

#### 4.2.2.2 Effect of Sulphate Ion Concentration

An increase in sulphate ion concentration in the host solution led to a reduction in the binding capacities of all three mixes studied. This trend is in agreement with the reported results in the literature *(Byfors, 1986; Sandberg & Larsson, 1993)*. Figures 4-51 to 4-53 show typical results of the influence of sulphate ion on the binding capacity of the OPC, 8SF, and 8MK pastes. At a concentration of 0.01 M, the influence of sulphate ion is negligible and this is true for all three mixes. But, at a 0.1 M concentration the effect is rather strong, as shown in Figure 4-54. The two sulphate concentrations chosen in this study represent moderate and extreme exposure conditions in terms of severity according to the British Standard BS8110. While this classification is related to soils containing sulphates and is addressed to the problem of sulphate attack, this study is more concerned with the presence of sulphates in environments where chloride attack is the main durability issue. This is the case of marine structures exposed to sea water, where the presence of sulphates is another environmental factor that will affect chloride binding. In this case the amount of sulphates in sea water is more pertinent to the problem, and this amount happens to fall in the severe and very severe

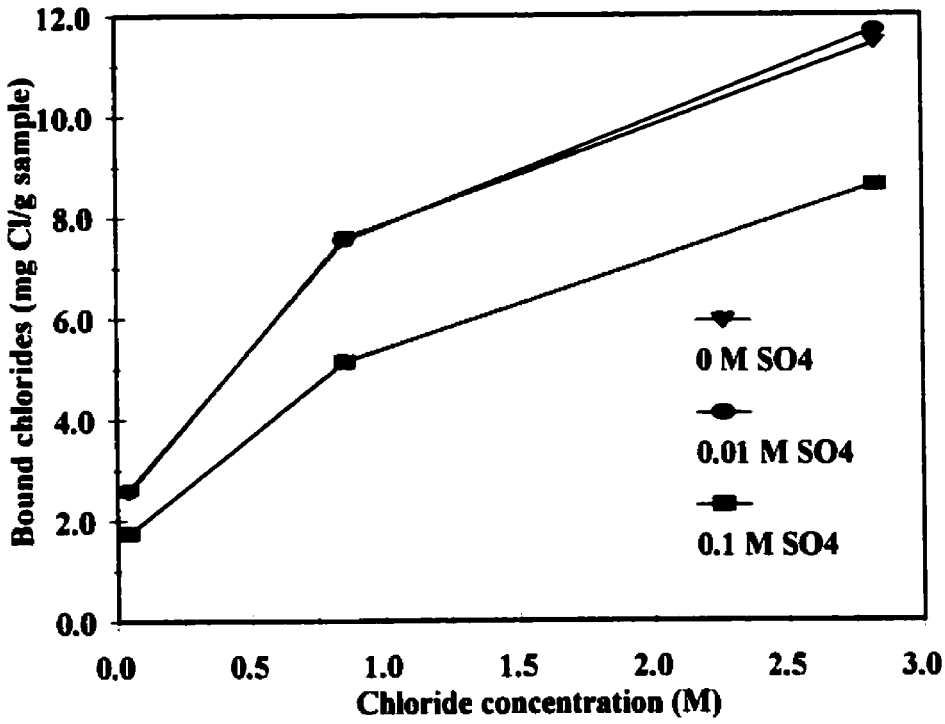


Figure 4-51: Effect of the sulphate ion concentration of the host soluiton on the chloride binding capacity of the control mix. W/CM = 0.5.

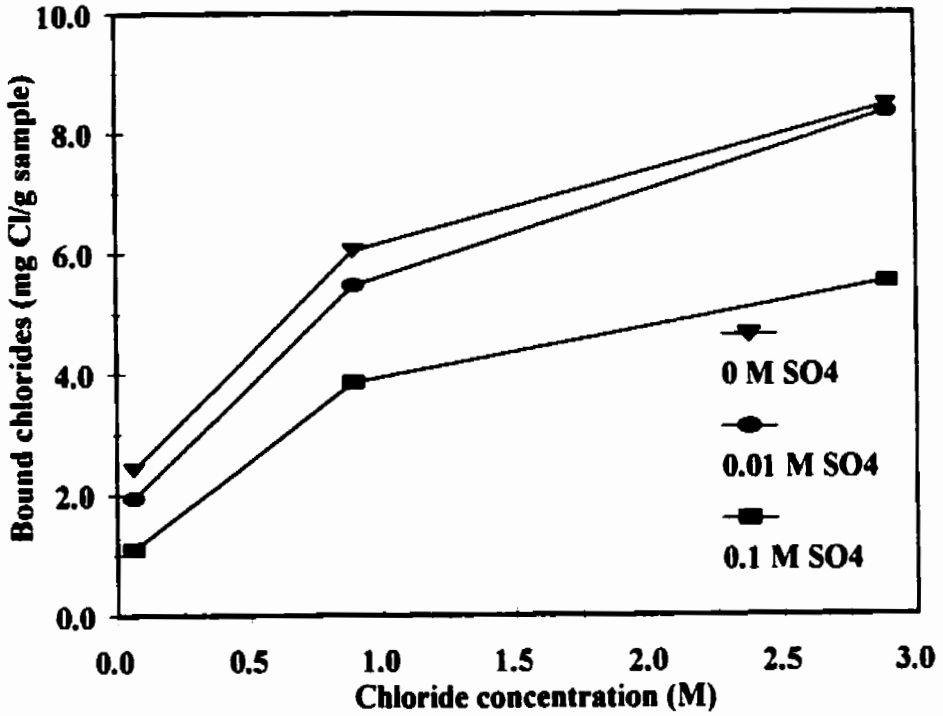


Figure 4-52: influence of sulphate ion concentration of the host solution on the chloride binding capacity of the 8SF paste with a W/CM of 0.5.

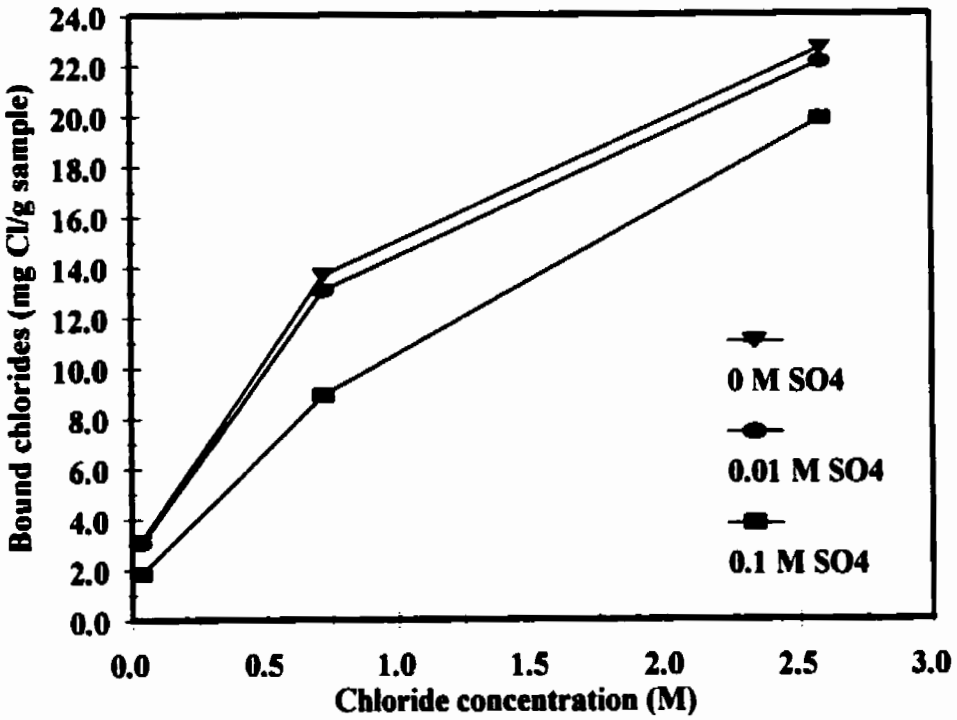


Figure 4-53: influence of the sulphate ion concentration of the host solution on the chloride binding capacity of the 8MK paste with W/CM of 0.5.

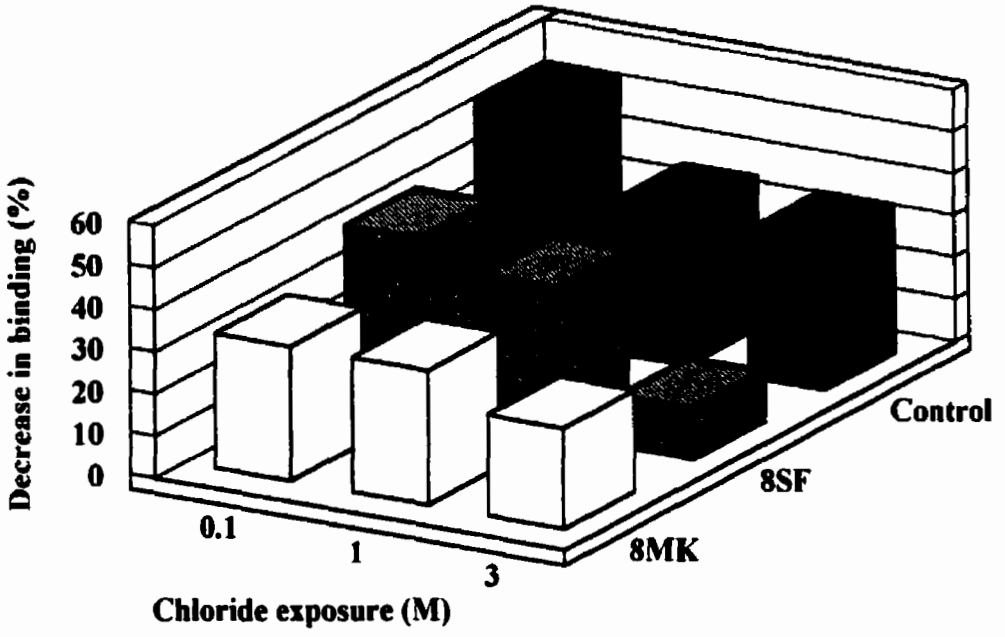


Figure 4-54: Decrease in the chloride binding capacities of pastes as a result of an increase in the sulphate ion concentration of the host solution from 0 M to 0.1 M. W/CM = 0.5.

category according to the above mentioned classification. In other words, it is between the two chosen concentrations, and as an example, the $SO_4$ content of the Mediterranean sea is 3.06 (g/L) or 0.032 M *(Eglinton, 1998)*. Judging from the results of this study, it is appropriate to assume that sulphates in actual exposure conditions have a negative effect on chloride binding. It is , however, worth mentioning that the rate of sulphate penetration into the concrete will be lower than that of the chloride penetration.

#### 4.2.2.3 Effect of Temperature

The results from this study confirm the trend found in the case of the mixes with W/CM of 0.3: the effect of temperature on binding is concentration dependent. Figures 4-55 to 4-57 show the effect of temperature on the binding isotherms of the OPC, 8SF, and 8MK pastes. The binding increases with a decrease in temperature at 0.1 M and 1 M concentrations. But at 3 M concentration, this trend is reversed and the binding capacity increases with an increase in temperature.

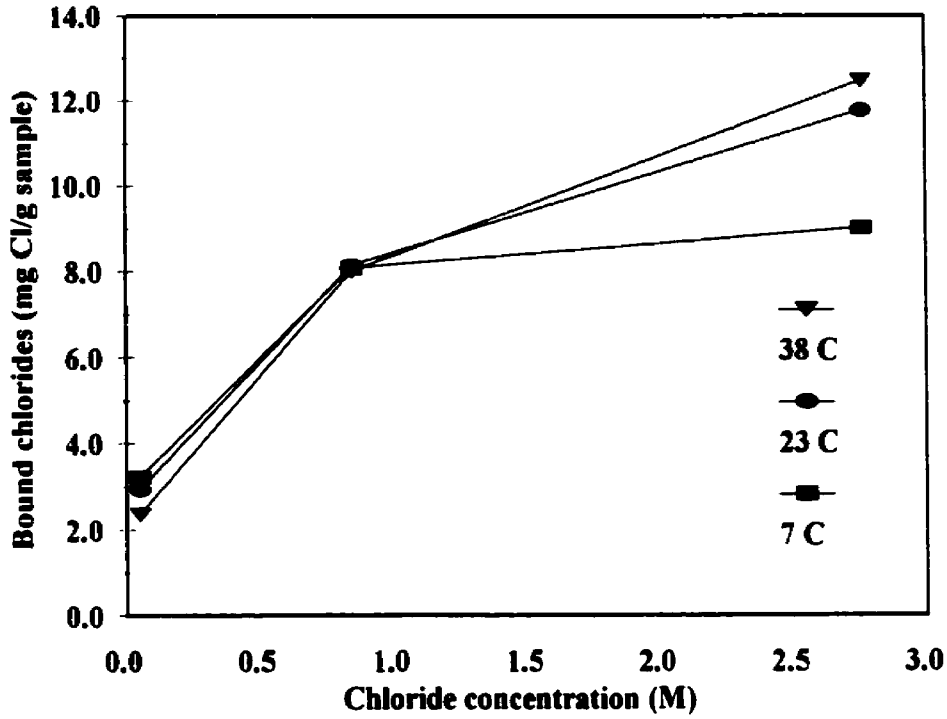


Figure 4-55: Effect of temperature on the chloride binding capacity of the OPC control mix. W/CM = 0.5.

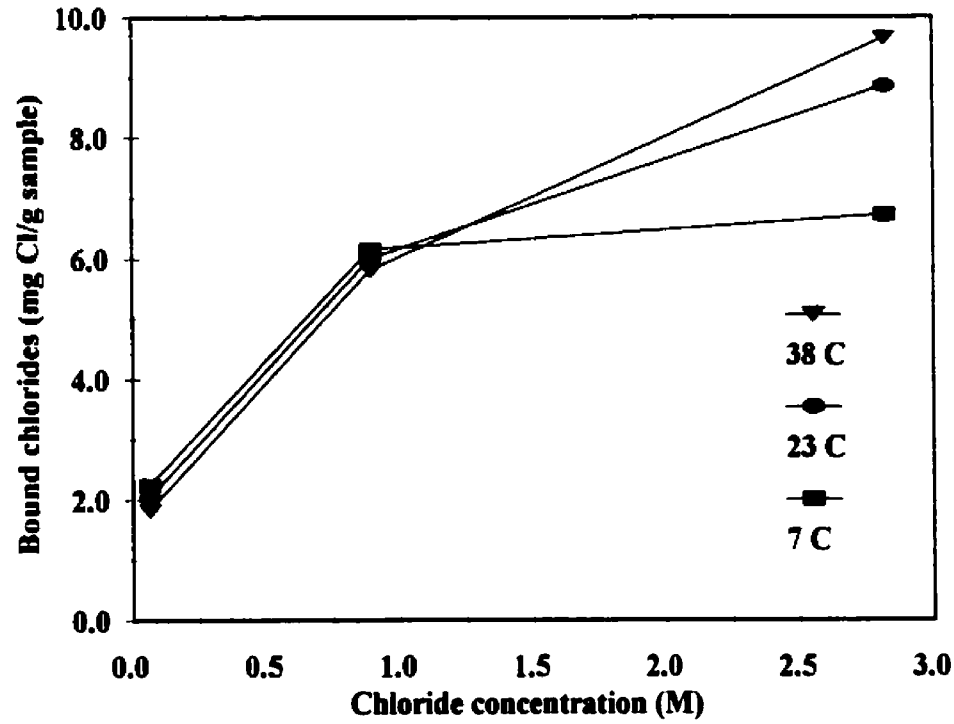


Figure 4-56: Effect of temperature on the chloride binding capacity of the 8SF (8% silica fume) paste. W/CM = 0.5.

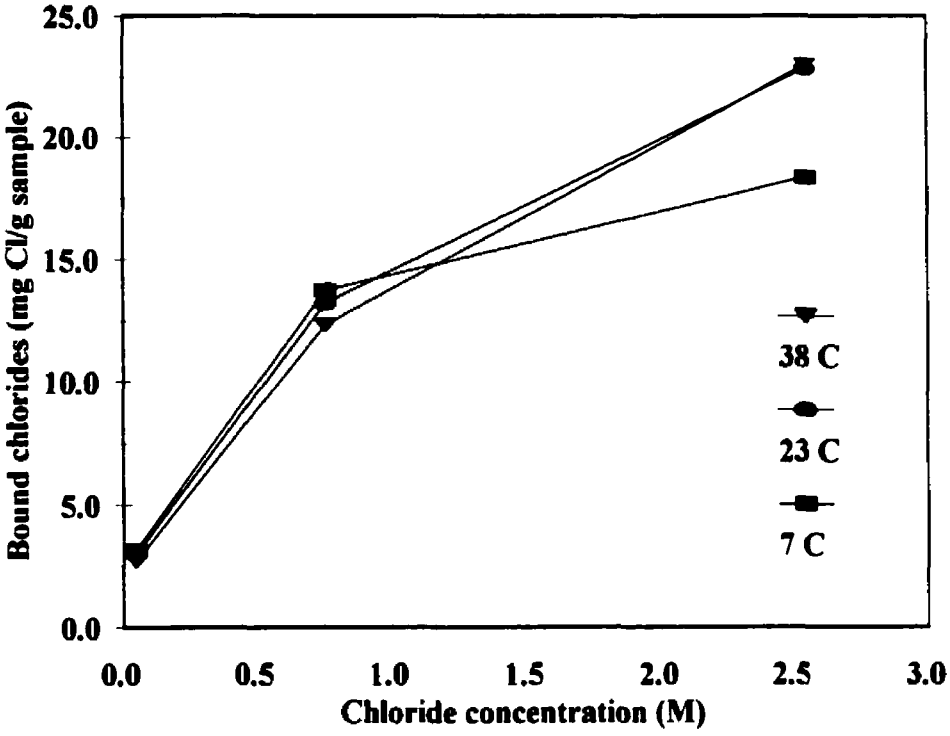


Figure 4-57: Effect of temperature on the chloride binding capacity of the 8MK (8% metakaolin) paste. W/CM = 0.5.

The temperature effect is small at 0.1 M, but it is minor at 1 M. It is interesting to mention that *Roberts (1962)* found no noticable increase in the solubility of pure Friedel's salt, stored in a saturated $Ca(OH)_2$ solution, between 25° C and 55° C. Also, results by *Maslehuddin et al. (1997)* showed a relatively small decrease in the binding capacities of mortar pastes, made with plain and blended cements, when the temperature was raised form 25° C to 40° C.

As mentioned before, most of the published results in the literature show that chloride binding decreases with an increase in temperature (*Roberts, 1962;Hussain & Rasheeduzzafar, 1993; Maslehuddin et al., 1996, 1997; Larsen, 1995).* All reported results however, come from studies using admixed chlorides. A closer look at these results show that the free chloride concentration in the pore solution is at maximum around 1 M. None of these studies involve a case were the free chloride concentration is considerably higher than 1 M. The results of this study agree with the results found in the literature since they show the same trend for chloride concentrations of up to 1 M. At high chloride concentrations (3 M), these results show that chloride binding increases with an increase in temperature. A possible explanation for this behaviour is that the major mechanism

controlling binding at high chloride concentrations is positively affected by an increase in temperature, leading to an increase in the binding capacity.

#### 4.2.2.4 Effect of Carbonation

The experimental results from the study of the effect of carbonation on the chloride binding capacity of cementitious pastes show that pre-carbonation of the cementitious pastes has a negative effect on chloride binding. Figures 4-58 to 4-60 show the effect of carbonation on the binding capacities of the OPC and 8SF and 8MK pastes respectively. These pastes were carbonated before being exposed to chloride solutions. It is obvious that carbonation greatly reduces the binding capacity of all mixtures. The carbonated samples had their binding capacities reduced by more than 90% in almost all cases compared to the non-carbonated samples. This very negative effect of carbonation is probably due to the fact that $CO_2$ reacts with and eventually decomposes all of the cement hydrates, forming calcium carbonate *(Massazza, 1998)*. The binding capacity of the carbonated OPC paste

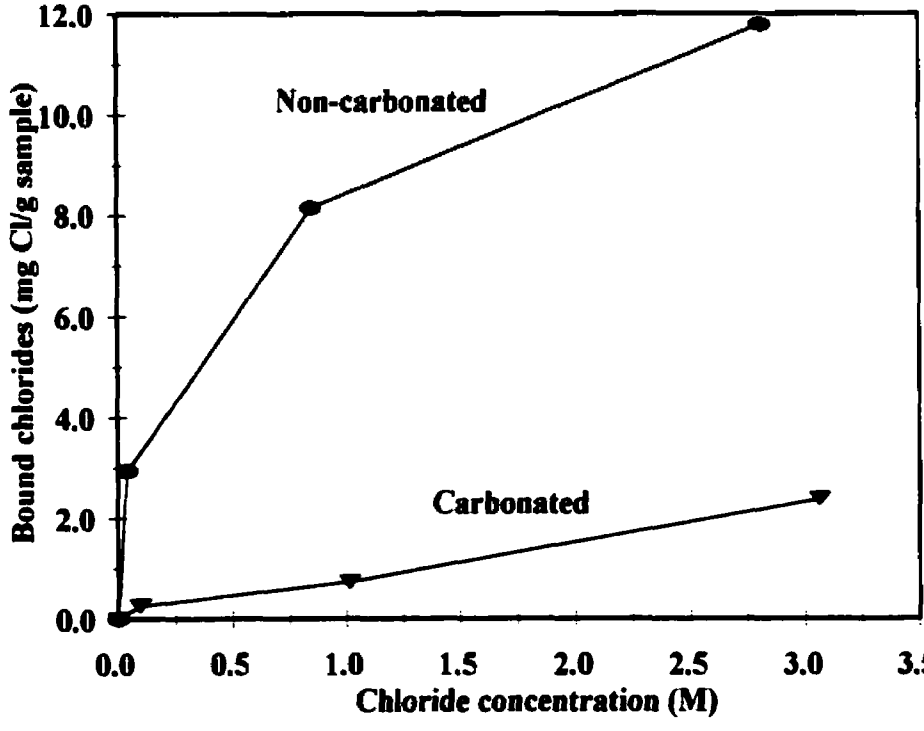


Figure 4-58: Effect of carbonation on the chloride binding capacity of the OPC control paste. W/CM = 0.5.

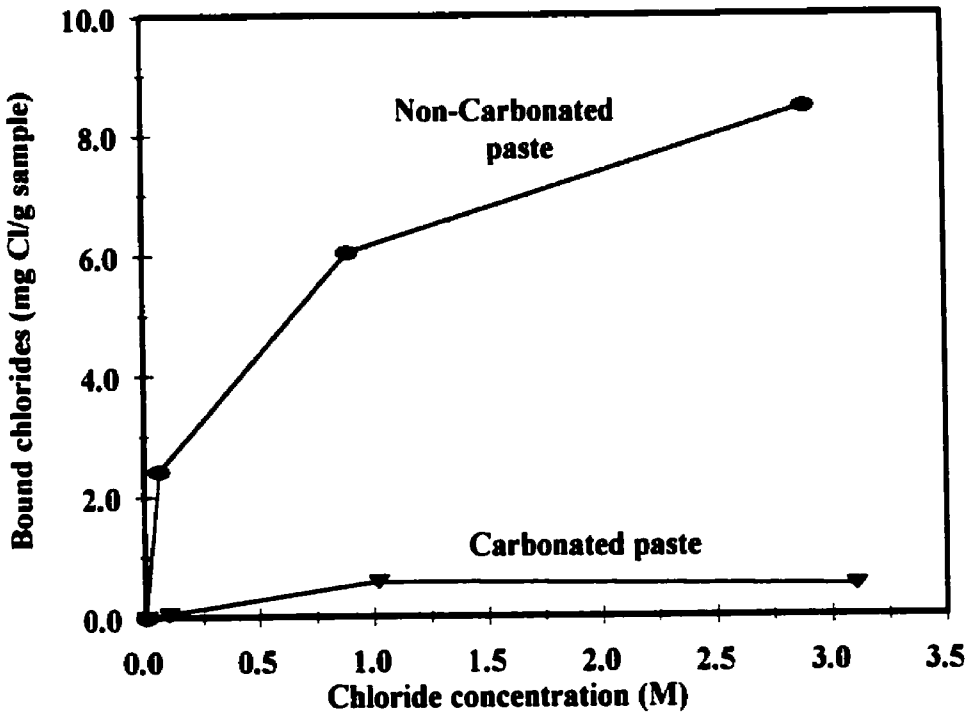


Figure 4-59: Effect of carbonation on the chloride binding capacity of the 8SF (8% silica fume) paste. W/CM = 0.5.

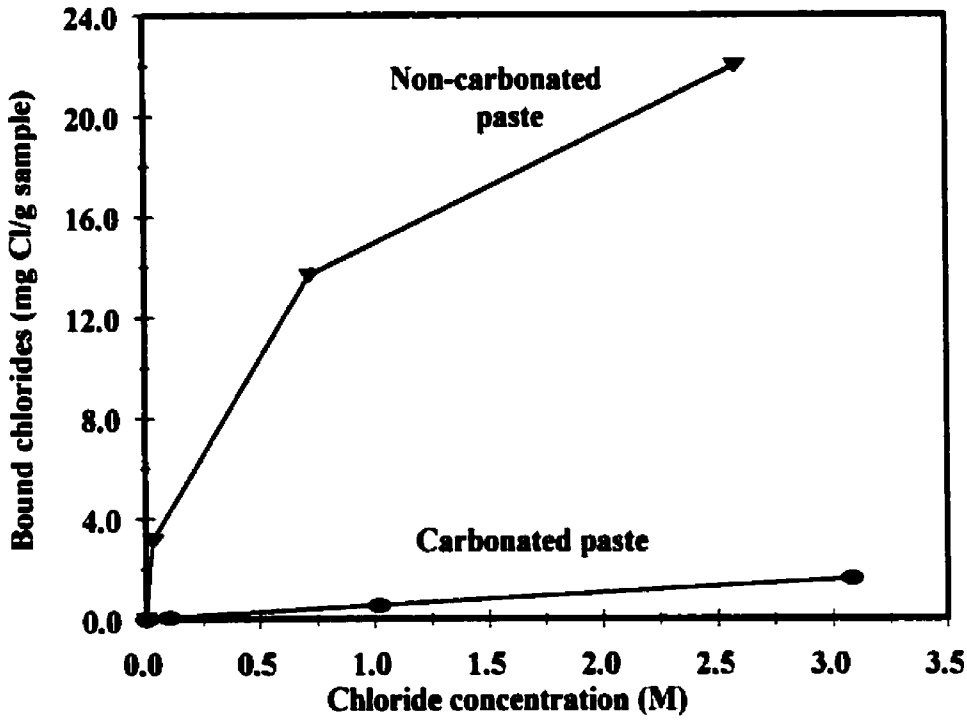


Figure 4-60: Effect of carbonation on the chloride binding capacity of the 8MK (8% metakaolin) paste. W/CM = 0.5.

was higher than those of the carbonated 8SF and 8MK pastes, especially at a concentration of 3M in the host solution. This might be explained by the fact that these mixes were exposed for a longer time to the $CO_2$ gas mixture than was the OPC paste, as explained in Chapter 3. The longer exposure period had probably led to the transformation of more cement hydrates (calcium aluminate hydrates and calcium silicate hydrates), responsible for binding, in the 8SF and 8MK pastes than in the OPC paste. This might have resulted in the lower binding capacities of these pastes .

#### 4.2.2.5 Desorption Isotherms

Five different mixes were tested for desorption. Two samples (25 g) from each mix were exposed to 200 and 1000 ml of distilled water (saturated with $Ca(OH)_2$, pH = 12.5) respectively. The samples were initially exposed to 3 M NaCl solution (at T= 23 °C) for about one year before the start of the desorption tests. Table 4-18 summarizes the results of this test. At 200 ml dilution, all four mixtures retained around 80% of their initially bound chlorides. The chloride concentrations at equilibrium were between 0.1 M and 0.14 M for the four mixtures. This indicates the existence of hysteresis in chloride binding and desorption. It should be mentioned that the higher binding capacity observed during desorption is partly due to the difference in the pH of the solutions during adsorption and desorption. The pH of the solution in the desorption tests was around 12.5 while it was around 13 in the adsorption tests. The lower pH increases the chloride binding capacity as shown in section 4.2.2.1). At 1000 ml dilution, the average amount of retained chloride was around 40 %. The equilibrium chloride concentrations were close to 0 M, and varied between 0.02 M and 0.03 M. An interesting fact to notice about these results is the strong non-linearity of the desorption isotherms at low chloride concentrations indicating the possibility that most of the bound chlorides may be released at 0.0 M chloride concentration. Figures 4-61 to 4-64 show the desorption isotherms of the 4 tested pastes.

Table 4-18: Results of the desorption test on samples of several cementitious pastes.

| mix | Initial Exposure ( M ) | Water Added (ml) | Final [Cl⁻] (pH=12.5) | $C_b$ Before (mg Cl/g sample) | $C_b$ After (mg Cl/g sample) | % remaining bound |
|---|---|---|---|---|---|---|
| Control | 3.0 | 200 | 0.123 | 11.43 | 8.73 | 76 |
| 8MK | 3.0 | 200 | 0.138 | 22.82 | 19.21 | 84 |
| 8SF | 3.0 | 200 | 0.137 | 8.86 | 6.92 | 78 |
| C4 | 3.0 | 200 | 0.104 | 17.12 | 14.42 | 84 |
| Control | 3.0 | 1000 | 0.029 | 11.2 | 4.26 | 38 |
| 8MK | 3.0 | 1000 | 0.035 | 21.8 | 13.08 | 40 |
| 8SF | 3.0 | 1000 | 0.032 | 7.94 | 3.14 | 39 |
| C4 | 3.0 | 1000 | 0.022 | 16.81 | 5.23 | 31 |

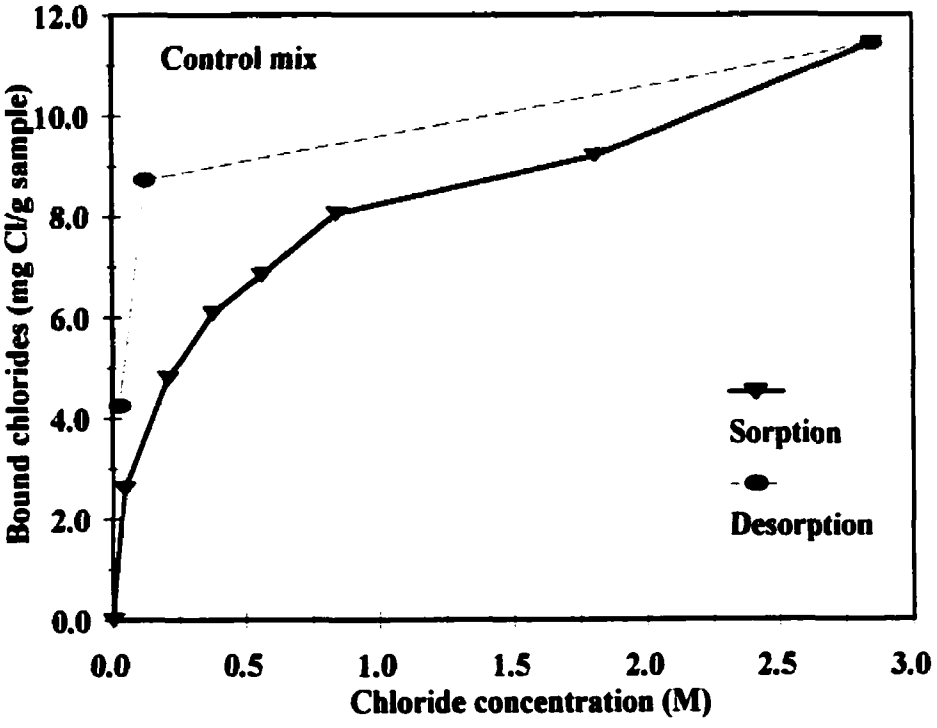


Figure 4-61: Chloride binding and desorption isotherms of the control paste. W/CM = 0.5.

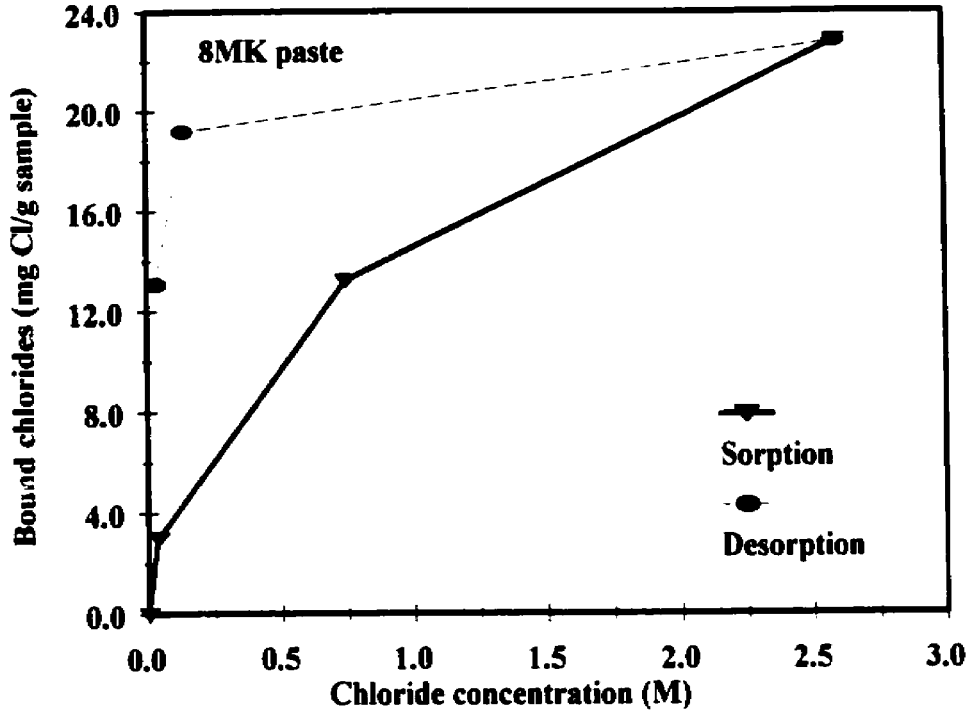


Figure 4-62: Chloride binding and desorption isotherms of the 8MK paste. W/CM = 0.5.

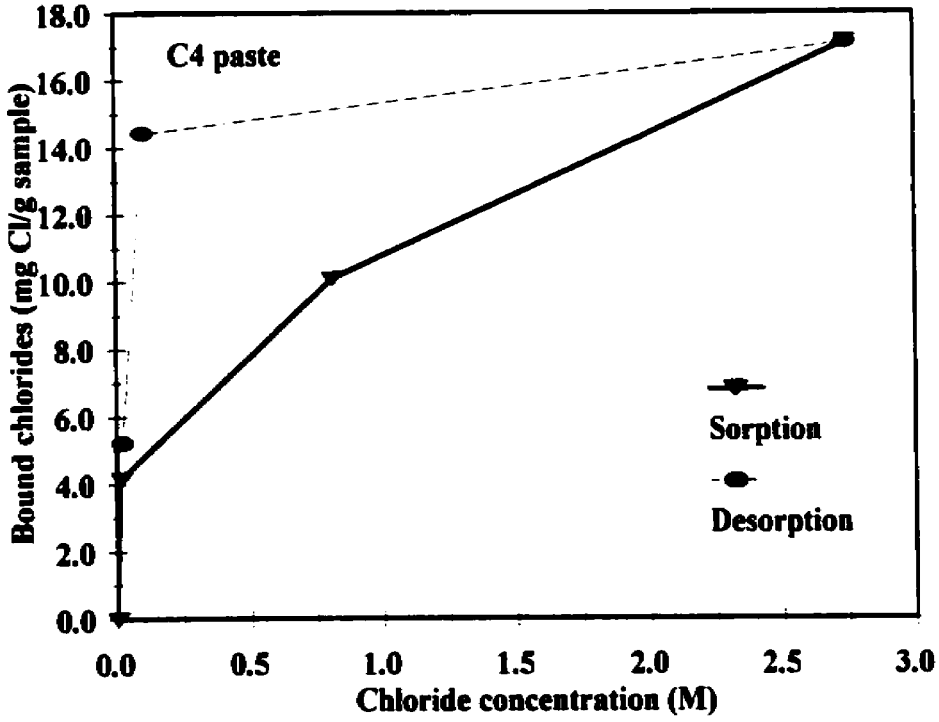


Figure 4-63: Chloride binding and desorption isotherms of the C4 paste. W/CM = 0.5.

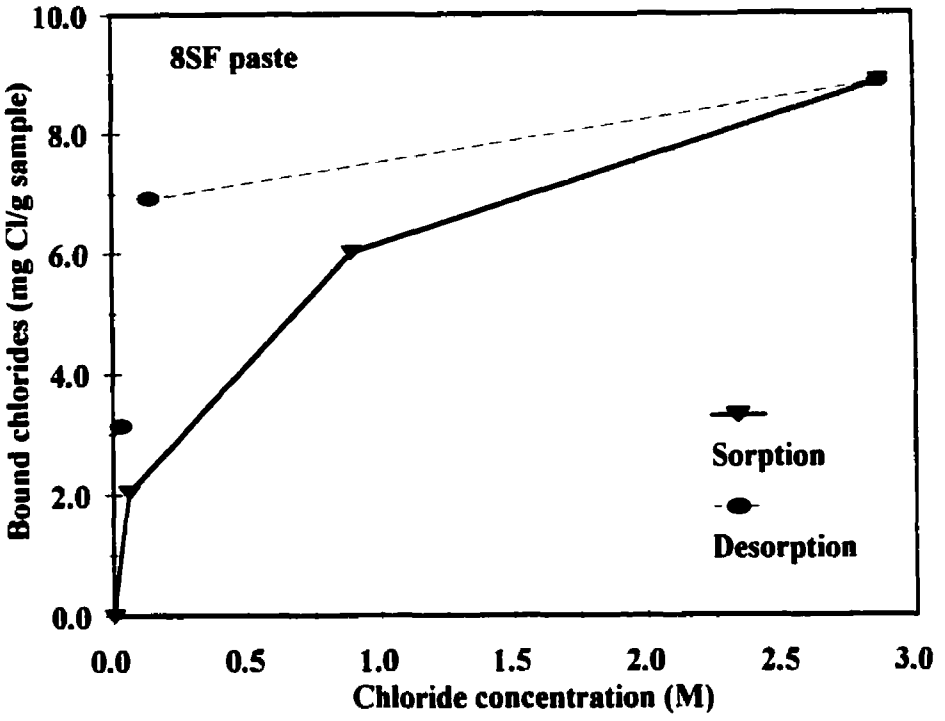


Figure 4-64: Chloride binding and desorption isotherms of the 8SF paste. W/CM = 0.5.

#### 4.2.2.6 X-Ray Diffraction Results

Figures 4-65 and 4-66 show the XRD patterns of samples of the C1 and C7 cements. The reduction in the ettringite peaks at 3 M chloride concentration is also observed in these two pastes indicating more the possibility that ettringite starts to transform into Friedel's salt at 3 M concentration. More interesting observations were also made from the XRD patterns of the C1 paste. The C1 cement did not contain $C_3A$ (according to the Bogue calculation). However, the XRD patterns of samples of this paste, exposed to different chloride concentrations, showed the existence of Friedel's salt peaks. These peaks appeared at 0.1 M chloride exposure, and exhibited an increase in intensity at 3 M chloride exposure. This meant that these peaks were those of the iron equivalent of the Friedel's salt phase, $C_3F.CaCl_2.10H_2O$, since the $C_4AF$ content of the C1 cement was 13.6% by mass of cement. These peaks provide direct proof of the influence of the $C_4AF$ phase in chloride binding.

Figure 4-67 shows the XRD patterns of samples of the C6 paste exposed to different chloride concentrations. At 0 M concentrations, two maximum intensity peaks of interest were identified; the first was that of the monosulphate phase, and the second was that of the monocarboaluminate

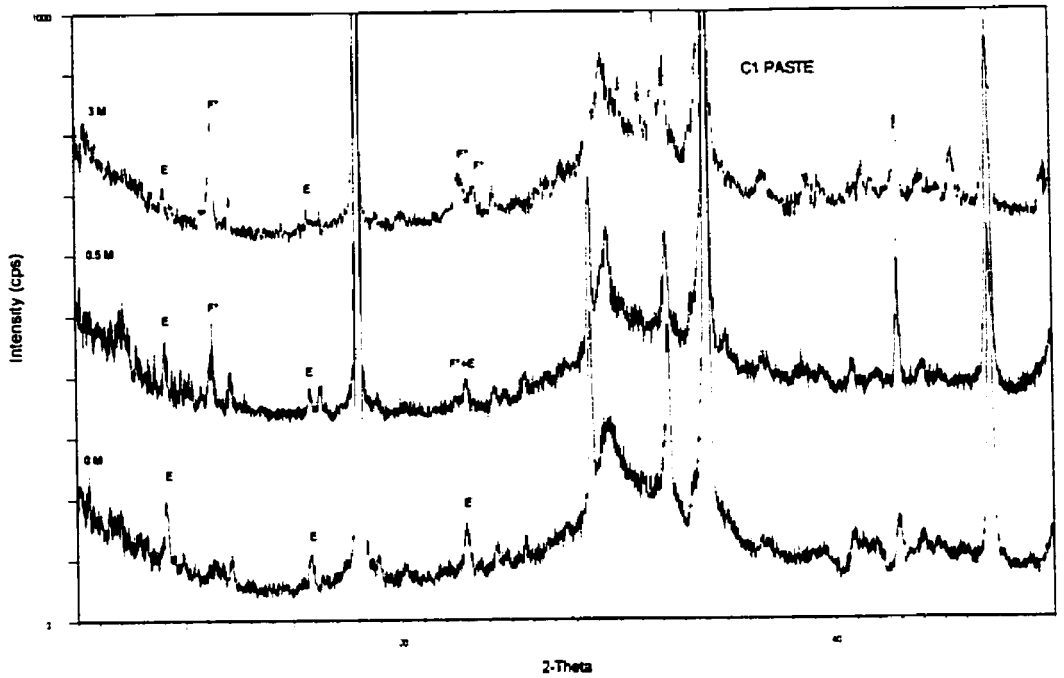


Figure 4-65: XRD patterns of samples of the C1 paste exposed to different chloride concentrations. E:ettringite, F*: iron equivalent of Friedel's salt.

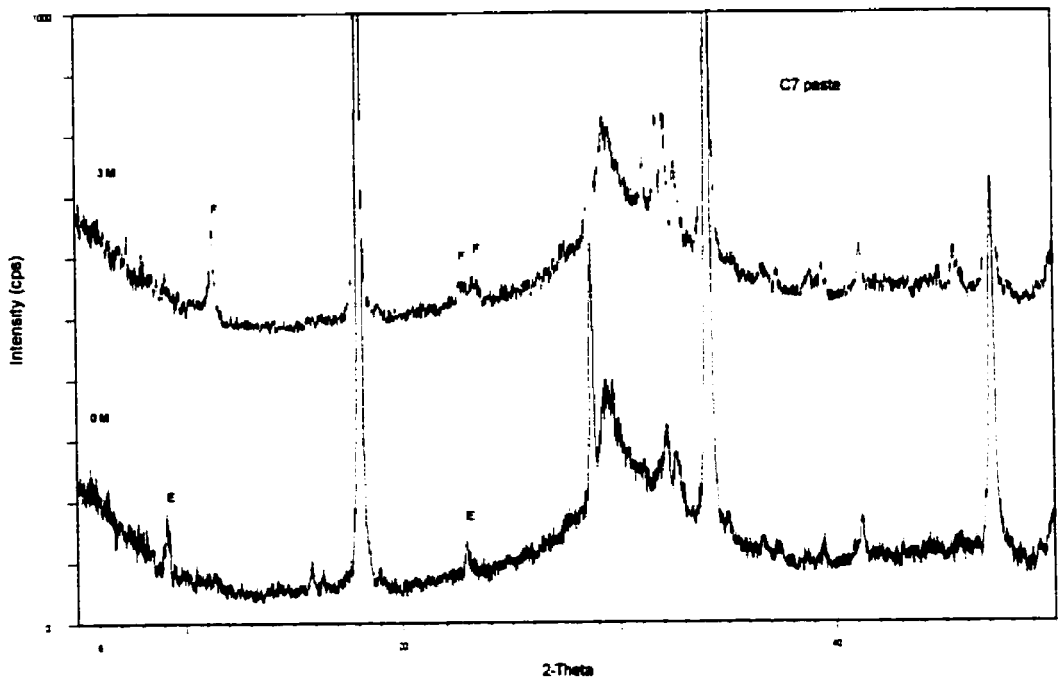


Figure 4-66: XRD patterns of samples of the C7 paste exposed to different chloride concentrations. E:ettringite, F: Friedel's salt.

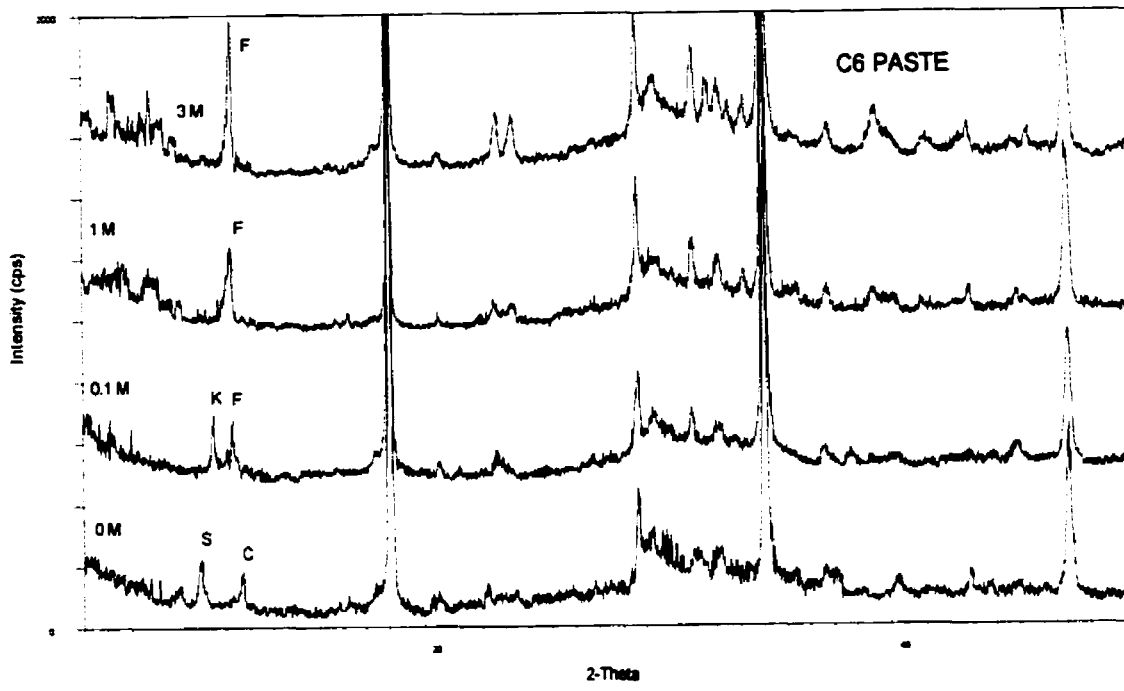


Figure 4-67: XRD patterns of samples of the C6 paste exposed to different chloride concentrations. C: monocaboaluminate, E:ettringite, F: Friedel's salt, K: Kuzel's salt, S: monosulphate

phase, $C_3A.CaCO_3.24H_2O$. The monocarboaluminate phase was probably formed during mixing or hydration (the cement may have contained $CaCO_3$), since carbonation was unlikely to occur during sample preparation because of the steps taken to minimize carbonation. The monocarboaluminate peak and the monosulphate peak dissappeared at 0.1 M chloride exposure. Two new peaks appeared at this exposure; one was identified as a Friedel's salt peak, and the other was identified as that of the $C_6A_2.C\bar{S}.CaCl_2.24H_2O$ phase. In fact, the maximum intensity peak of the $C_6A_2.C\bar{S}.CaCl_2.24H_2O$ phase was the closest match to the second peak, although it was not a perfect match. *Taylor (1992)* mentioned the existence of The $C_6A_2.C\bar{S}.CaCl_2.24H_2O$ phase, and *Glasser (1999)* named it Kuzel's salt after its discoverer. *Glasser (1999)* obtained this phase by reacting monosulphate and Friedel's salt (1/1 molar ratio), and found that its crystal structure was different than those of Friedel's salt and monosulphate. The important thing about the possible formation of this phase is the fact that Friedel's salt was not the only compound responsible for the chemical binding of chloride. An equally important phenomenon revealed in these XRD patterns is the contribution of the monosulphate phase to the binding of chloride through the possible transformation into the

$C_6A_2.C\bar{S}.CaCl_2.24H_2O$ compound at 0.1 M exposure, and into Friedel's salt at 1 M and 3 M exposure. Similarly to the case of the control paste, the Friedel's salt peaks increased with an increase of chloride concentrations in the exposure solutions.

Figure 4-68 shows the XRD patterns of samples of the C2 paste. Unfortunately, there was no background sample unexposed to chloride solution to compare with the exposed samples. Still, the comparison of the XRD patterns of the samples exposed to different chloride concentrations was revealing. The C2 paste had the highest sulphate content of all the cements used in this research, and evidence of this was seen in the sample exposed to 0.1 M chloride solution were the ettringite and monosulphate peaks were still dominant among the calcium aluminate hydrates. It was hard to confirm the existence of Friedel's salt at this concentration without a background sample, espesially since the Friedel's salt maximum intensity peak was very small at this concentration and could have easily been that of the $C_4AH_{13}$ phase. One peak was of particular interest at the 0.1 M exposure, since it had a d-spacing very close to that of the maximum intensity peak of the $C_6A_2.C\bar{S}.CaCl_2.24H_2O$ phase. But once again, it was difficult to confirm whether this peak was in

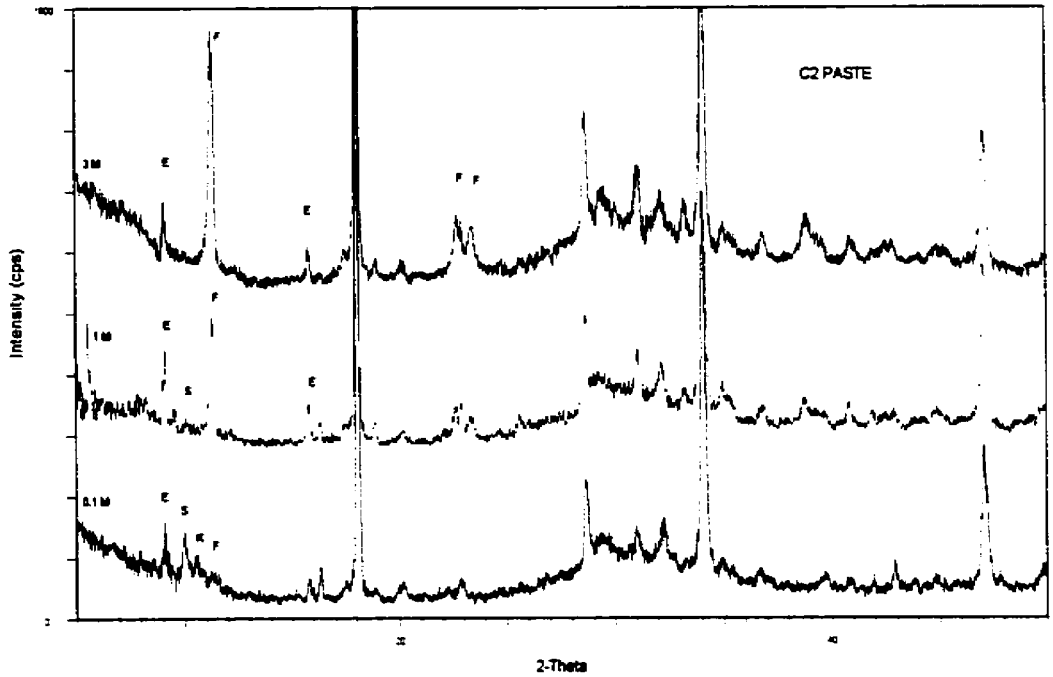


Figure 4-68: XRD patterns of samples of the C2 paste exposed to different chloride concentrations. E:ettringite, F: Friedel's salt, K: Kuzel's salt, S: monosulphate.

fact that of the $C_6A_2.C\bar{S}.CaCl_2.24H_2O$ phase without the XRD of a background sample. The formation of this phase was associated with a decrease in the intensities of the monosulphate peaks. indicating the transformation of a part of the monosulphate into the $C_6A_2.C\bar{S}.CaCl_2.24H_2O$ phase. as was shown in the XRD patterns of the sample of the C6 paste exposed to 0.1 M chloride solution. It was not possible, however, in the case of the C2 paste to confirm that a decrease in the maximum intensity peak of the monosulphate phase took place at 0.1 M exposure, despite the fact that this peak almost dissapeared at 1 M exposure, indicating the contribution of this Afm phase to chloride binding. Figure 4-68 clearly shows the increase in the intensities of the Friedel's salt peaks with the increasing chloride concentrations of the exposure solutions. This trend was also seen in the XRD patterns of samples of the C4 paste, as shown in Figure 4-69. The C4 cement was not interground with gypsum when it was in clinker form, and had the lowest sulphate content of all cements. This is why there was no signs of the maximum intensity peaks of either ettringite or monosulphate in the XRD pattern of the background sample (0 M chloride exposure). In fact. it was the peaks of other calcium aluminate hydrates that were dominant in the XRD pattern of the C4 background sample.

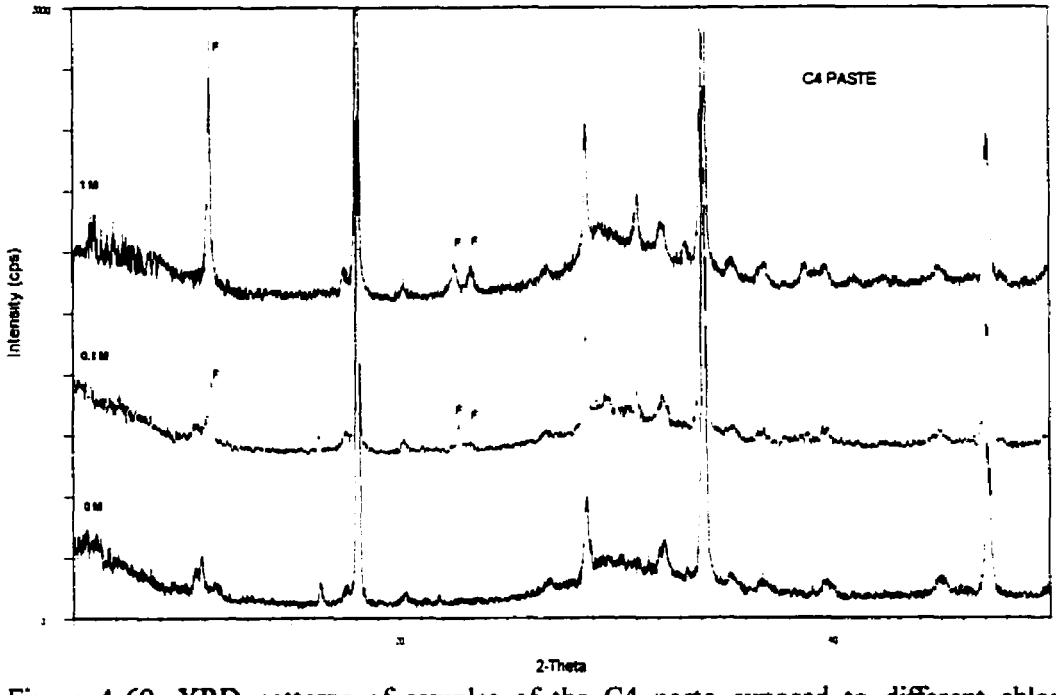


Figure 4-69: XRD patterns of samples of the C4 paste exposed to different chloride concentrations. F: Friedel's salt.

These peaks decreased in the sample exposed to 0.1 M chloride solution, and Friedel's salt peaks appeared, indicating the transformation of these phases into Friedel's salt. It is interesting to notice that the maximum intensity peak of the Friedel's salt phase at 0.1 M exposure had the highest intensity compared to the ones in the rest of the cement pastes at 0.1 M exposure. The XRD results of the C4 paste, together with those of the C6 paste provided clear evidence of the formation of Friedel's salt at the low 0.1 M exposure.

Figure 4-70 shows the XRD patterns of samples of the C4-7$SO_4$ paste that were stored in different chloride concentrations. The first thing to notice in these patterns is the large maximum intensity peak of the ettringite phase which was the result of the sulphate addition to the C4 clinker. This phase was non-existent in the C4 paste before the sulphate addition. This confirms that most of the $C_3A$ and $C_4AF$ was transformed into ettringite, and that the reduction in the binding capacity was mostly due to the reduction in the chemical binding capacity. A comparison between Figures 4-50 and 4-51 shows the large reduction in the intensities of the Friedel's salt peaks of the C4-7$SO_4$ samples compared to those of the C4 samples. Nevertheless, small Friedel's salt peaks were present

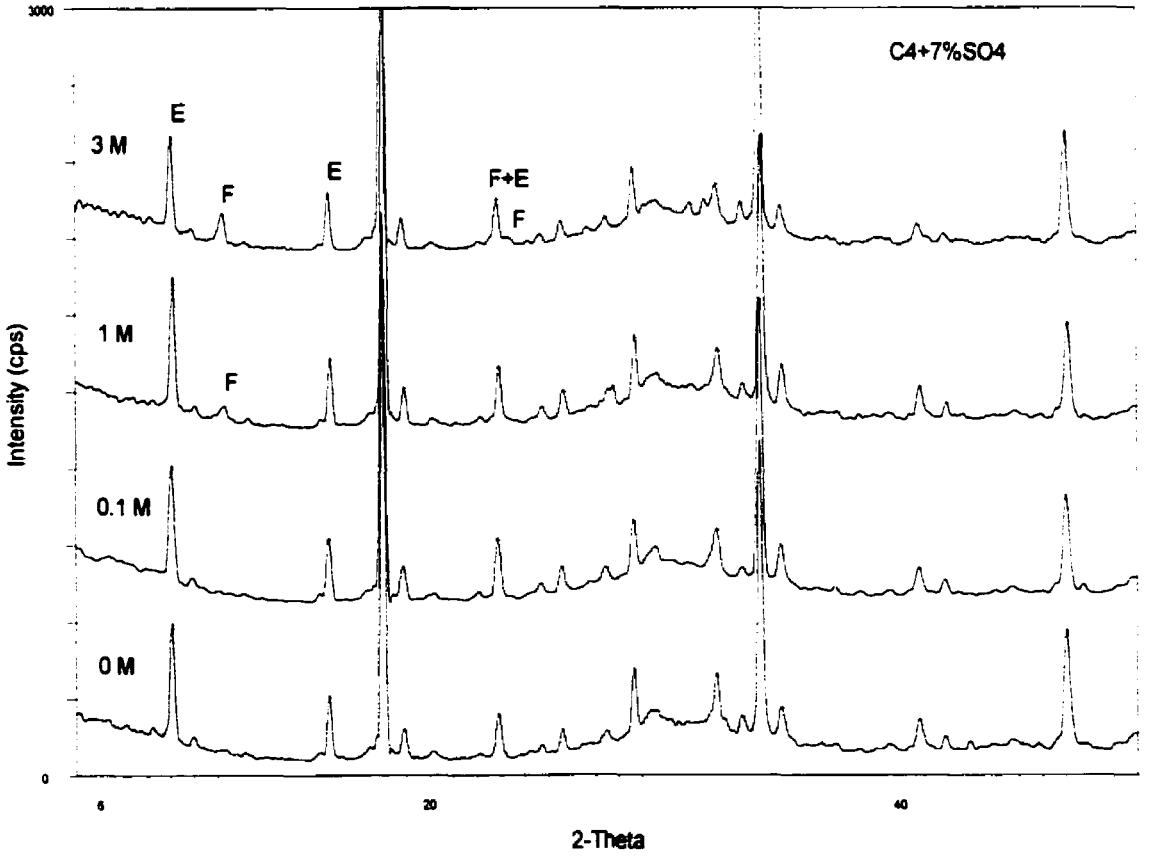


Figure 4-70: XRD patterns of samples of the C4-7$SO_3$ paste exposed to different chloride concentrations. E:ettringite, F: Friedel's salt.

at 1 M and 3 M chloride exposure, and the ettringite peaks exhibited a small reduction at 3 M chloride exposure. This indicates that despite the large decrease in the binding capacity, a part of that binding capacity of the C4-7$SO_3$ paste, at these concentrations, was due to chemical binding. This indirectly prooves that the binding capacity of the C4 paste was largely a chemical binding capacity at high concentrations (1 M , and 3 M). At 0.1 M concentration, there was no trace of Friedel's salt. This reinforces the earlier suggestion that the C-S-H might play a appreciable role, at least at low concentration.

Figure 4-71 shows the XRD patterns of samples of the control paste which were stored in chloride solutions (3 M) having different pH levels (pH=13 and pH=14). These XRD patterns show that the intensities of Friedel's salt peaks are almost the same in both samples. This was not unexpected since the change in the chloride binding capacities of the two samples is small (<20%) which probably makes it difficult to observe any change in the intensity of the Friedel's salt peaks. It is also possible that the observed change in the binding capacity is caused mostly by physical binding, since the higher $OH^-$ concentration at higher pH increases the competition for adsorption sites on the surface of the C-S-H.

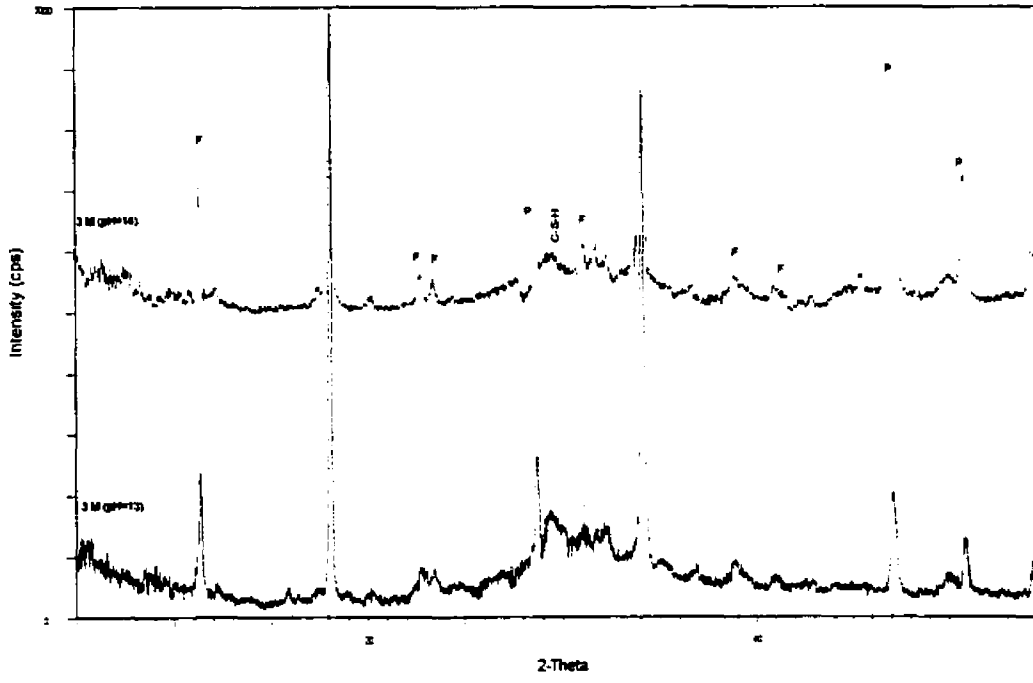


Figure 4-71: XRD patterns of samples of the control paste exposed to chloride solutions (3 M) with different pH values (13, 14). F: Friedel's salt, P: portlandite.

Figure 4-72 shows the XRD patterns of samples of the control paste which were stored in chloride solutions (3 M) with different sulphate ion concentrations (0 M and 0.1 M). These patterns show that there is a reduction in the intensities of the Friedel's salt peaks of the sample exposed to 0.1 M sulphate ion concentration. This result indicates that the presence of sulphate in the host solution had a negative effect on the chemical binding capacity of the control paste.

Figures 4-73 and 4-74 show the XRD patterns of carbonated and non-carbonated samples of the control paste and the 8MK paste. The XRD patterns of the carbonated samples of both pastes show the prevalence of calcite and vaterite in these samples. They also show the absence of Friedel's salt peaks in comparison with the non-carbonated samples. These XRD patterns explain the very low binding capacities of the carbonated pastes. The transformation of the cement hydrates into carbonated products neutralises the ability of the carbonated cement paste to bind chlorides.

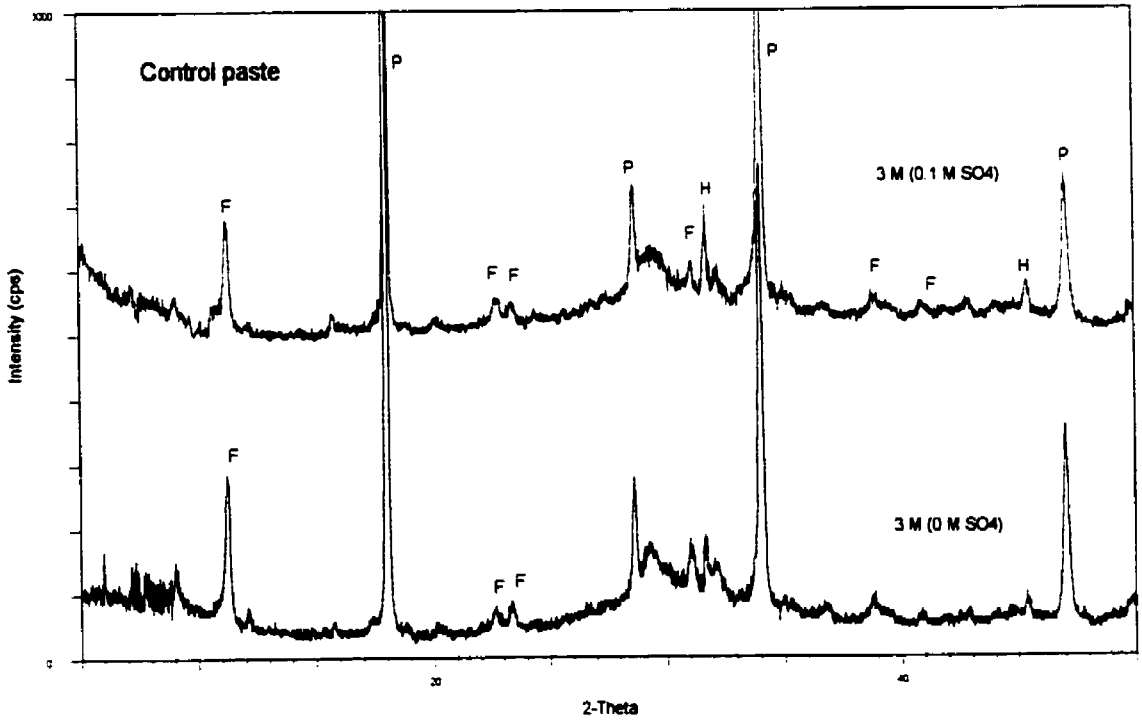


Figure 4-72: XRD patterns of samples of the control paste exposed to 3 M chloride solutions with different sulphate ion concentrations (0.0 M, 0.1 M). F: Friedel's salt, H: Halite (NaCl), P: portlandite ( $Ca(OH)_2$ ).

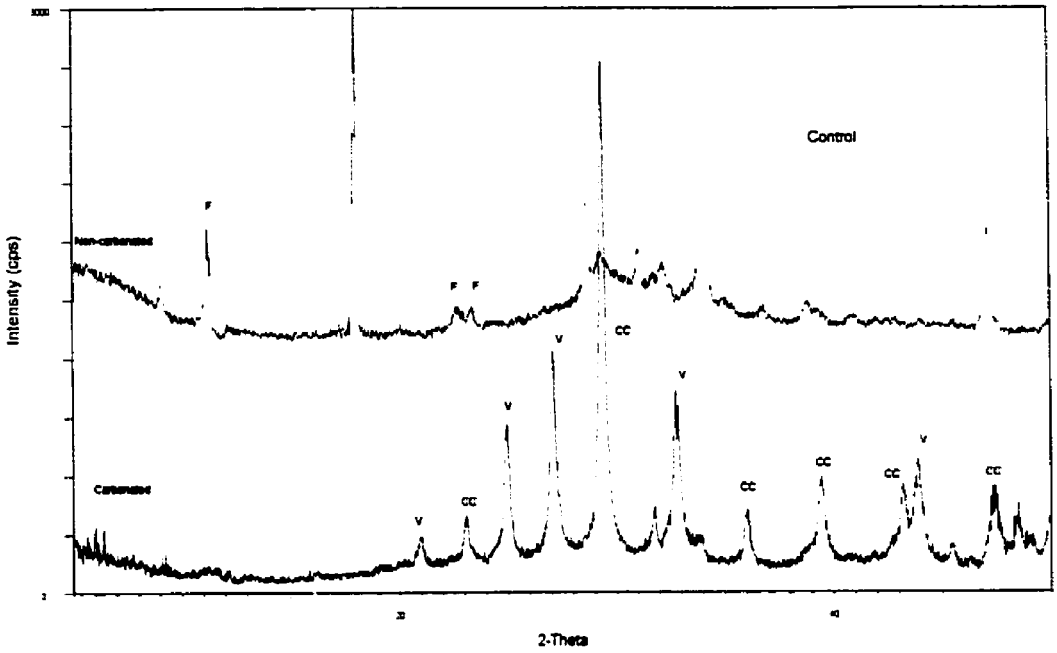


Figure 4-73: XRD patterns of samples of the control paste that were either carbonated or non-carbonated before being exposed to chloride solutions (3 M). CC: calcite, F: Friedel's salt, V: vaterite.

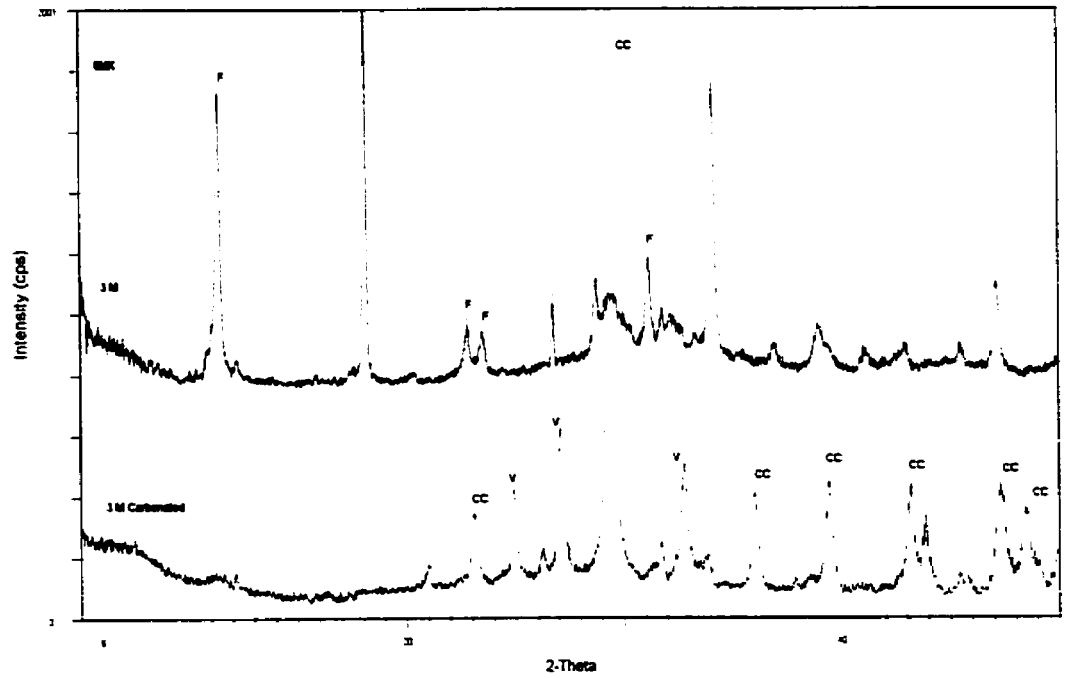


Figure 4-74: XRD patterns of samples of the 8MK paste that were either carbonated or non-carbonated before being exposed to chloride solutions (3 M). CC: calcite, F: Friedel's salt, V: vaterite.

Figures 4-75 and 4-76 show the XRD patterns of samples of the control paste and the 8MK paste that where subjected to leaching desorption, after being stored in 3 M chloride solutions until equilibrium. The XRD patterns show that the peaks of Friedel's salt decrease with a decrease in chloride concentration, indicating that chemical binding decreases with the decrease in chloride concentration. However, these XRD patterns also show that the intensity of the Friedel's salt peaks after the decrease in chloride concentration are still higher than those of samples initially stored in chloride concentrations of comparable levels. This observation applies to both the control paste and the 8MK paste. It is interseting to notice in Figure 4-76 the formation of a new peak in the XRD of the sample of the 8MK paste diluted in 1000 ml distilled water (saturated with lime). This peak was attributed to the Kuzel's salt phase, because of its close proximity to the maximum intensity peak of this phase. If this suggestion is true, it might indicate that the chemical binding process is reversible.

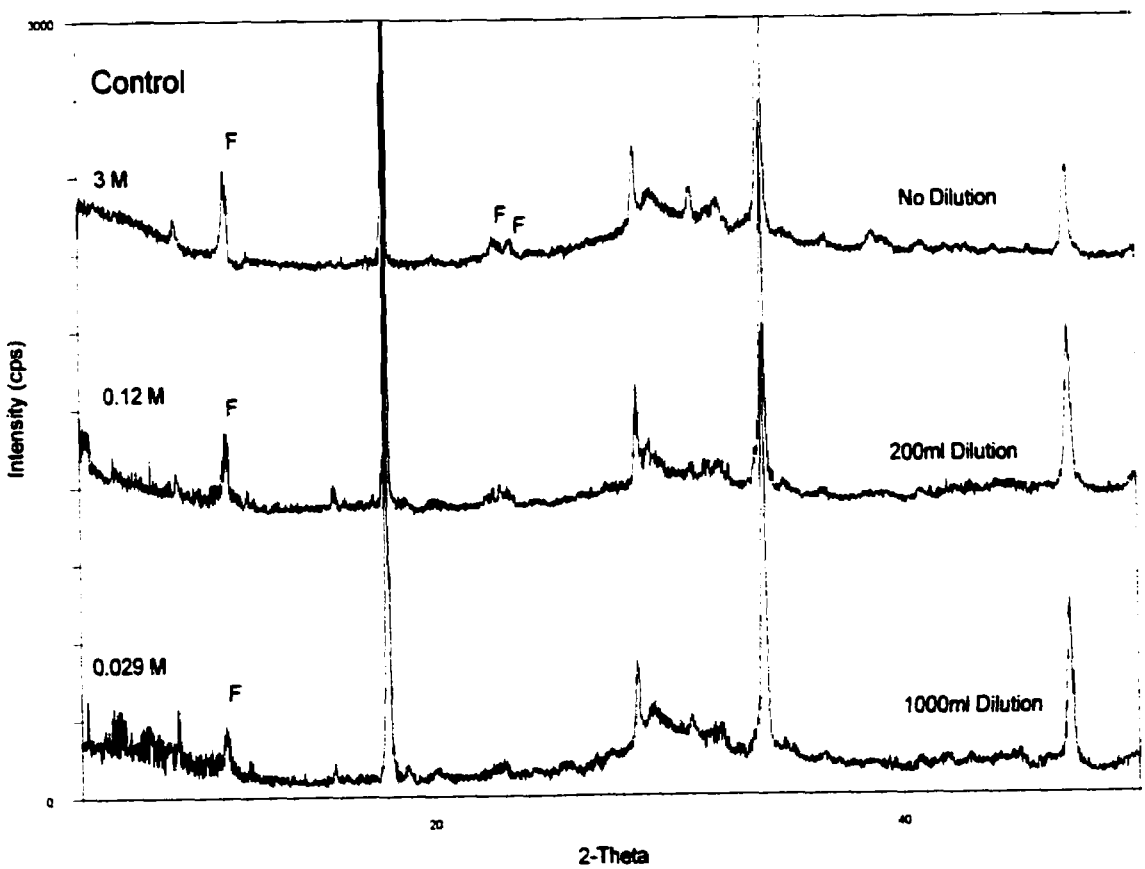


Figure 4-75: XRD patterns of samples of the control paste that have been exposed to different volumes of chloride free solutions (saturated with lime), after being exposed to 3 M chloride solutions. F: Friedel's salt.

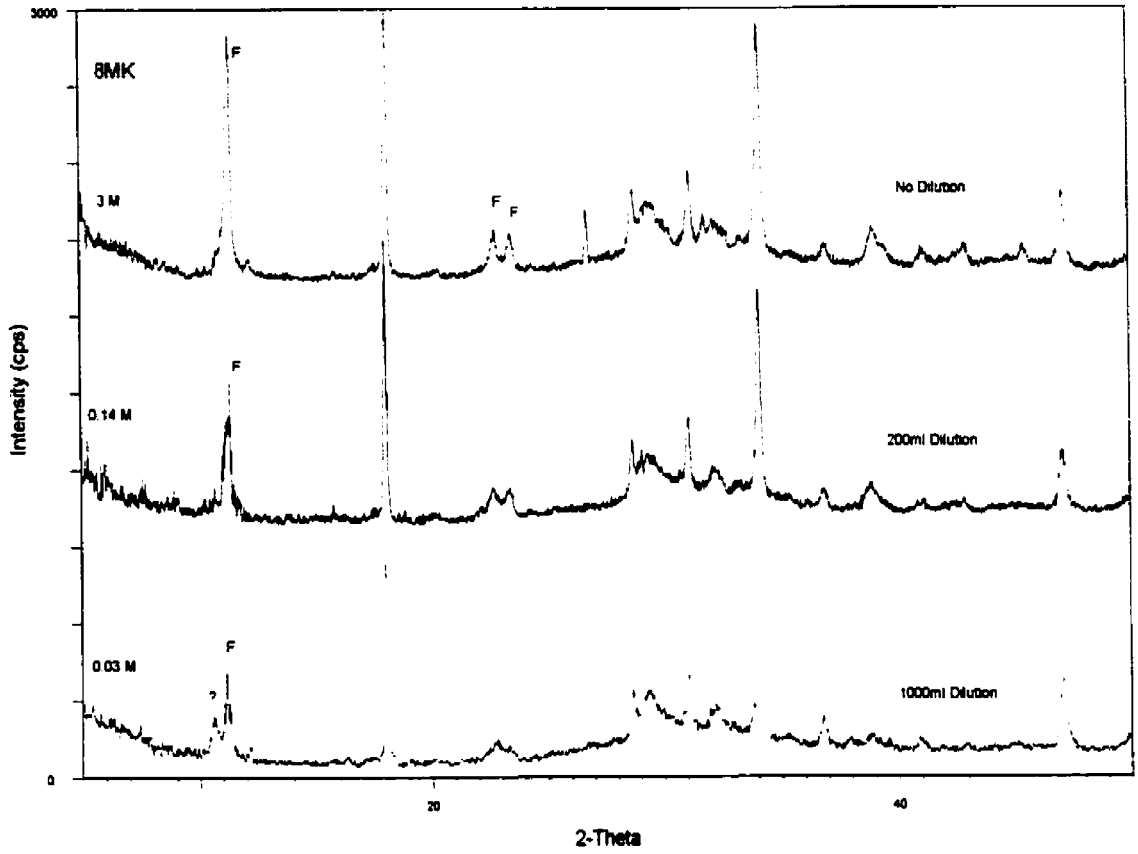


Figure 4-76: XRD patterns of samples of the 8MK paste that have been exposed to different volumes of chloride free solutions (saturated with lime), after being exposed to 3 M chloride solutions. F: Friedel's salt, ? = Kuzel's salt (probably).

## 4.3 PHASE THREE

### 4.3.1 SCM-Lime Mixtures

#### 4.3.1.1 Chloride Binding Isotherms

Before discussing the results of the SF-lime mixes, it is worth mentioning again that the reason for this study was primarily to investigate the binding properties of silica fume, and to try to better understand why the chloride binding capacity decreases when silica fume is added to cement. The results of this study should provide information not only on the binding capacity of the silica fume as a binder, but should also give an idea about the binding capacity of C-S-H in general since, due to the very high $SiO_2$ content of silica fume, the hydrates formed in this case would be C-S-H. The different ratios of SF/lime were chosen to represent regular to extreme replacement levels of silica fume in cement, and also to try to influence the C/S ratio in the C-S-H. The reason for this was to try to check the validity of the argument mentioned before that ascribes the decrease in binding to a reduction in the C/S ratio of the C-S-H.

Figure 4-77 shows the binding isotherms of the three SF-lime mixtures. While the SF12 (silica fume/lime = 1/2) paste exhibited a capacity to bind chloride, the SF11 (silica fume/lime = 1/1) exhibited a very small binding capacity, and the SF21 (silica fume/lime = 2/1) paste had no binding capacity. Since these pastes had a high W/CM and were cured at 38°C for two months, they would have a high degree of hydration and they would be mostly composed of C-S-H. The XRD results (Figure 4-80) showed the formation of C-S-H as the main hydration product in the SF12 and SF21 pastes, which means that C-S-H most probably formed in the SF11 paste as well. The XRD pattern of a sample of the SF21 paste revealed that all $Ca(OH)_2$ was consumed in the reaction with silica fume, as shown in Figure 4-78. A semi-quantitative XRD analysis showed that the SF12 sample contained around 20% $Ca(OH)_2$. This meant that 70% of the original $Ca(OH)_2$ had reacted with silica fume. Assuming that all the silica fume had reacted, then the average C/S ratios in the C-S-H of the SF21 and SF12 pastes would be 0.42 and 1.24 respectively. Also, the amount of C-S-H in the SF21 paste would be higher than those in the SF12 paste. However, the assumption that all the silica fume had reacted, might not be true in the case of the SF21paste, since the resulting C/S ratio (0.42) is too low. Values of C/S ratio as low as 0.65 were reported in low lime C-S-H in silica fume-lime mixtures dispersed in water (water/solid = 200) *(Grutzeck et al., 1989)*. While the C/S ratio in the SF21 paste might not be 0.42, it is most likely lower than the C/S ratio in the SF12 paste.

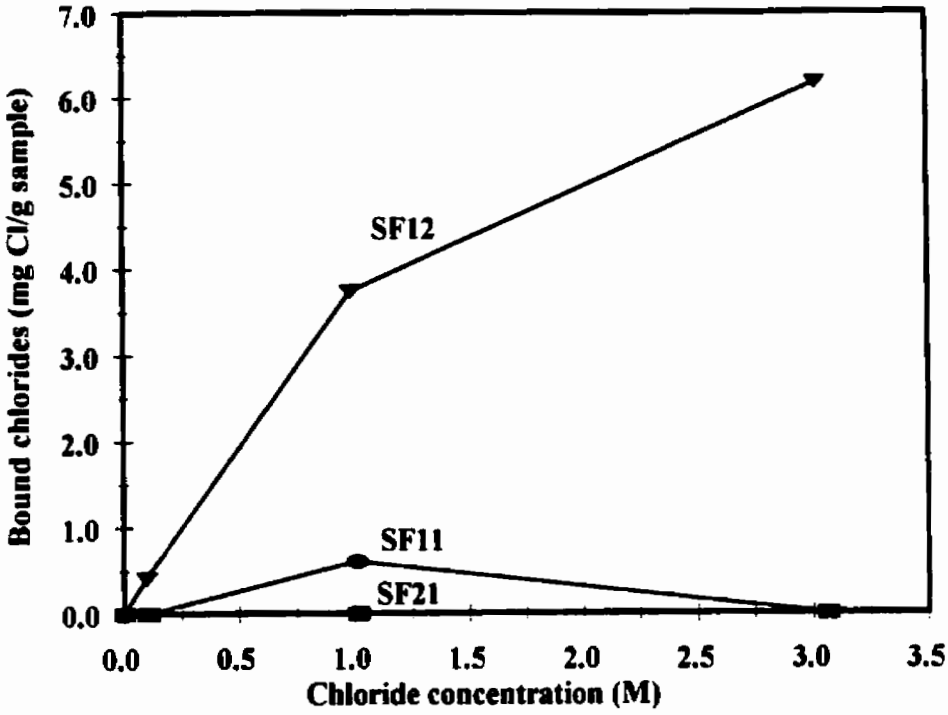


Figure 4-77: Chloride binding isotherms of the SF-lime pastes. The pastes were cured for 2 months at 38°C, and had a W/CM = 2.

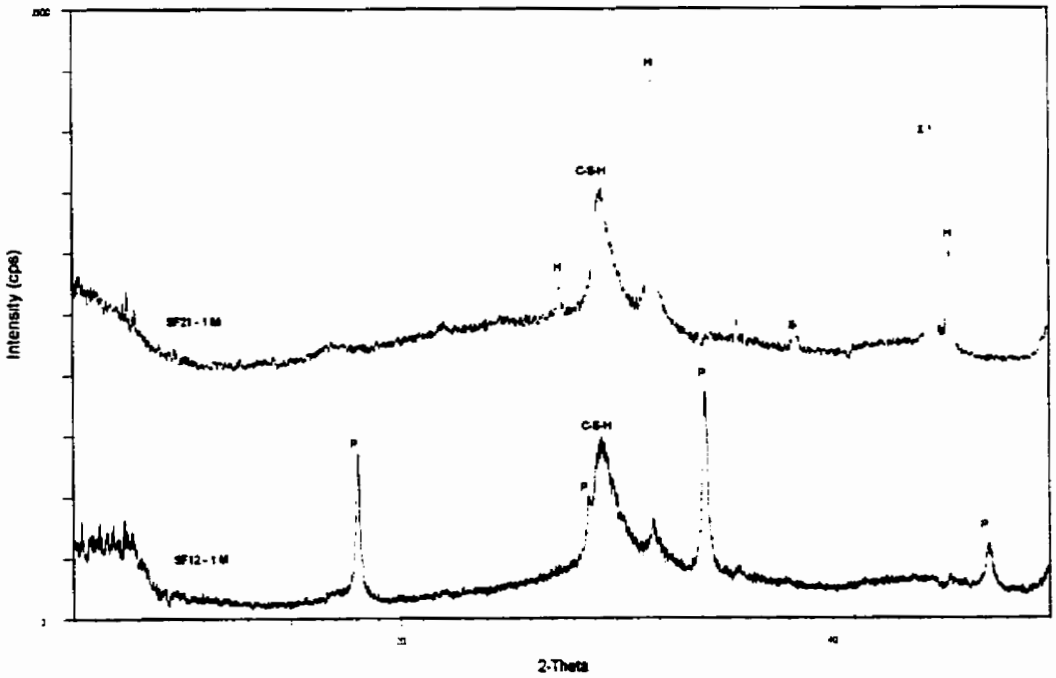


Figure 4-78: XRD patterns of samples of the SF12 paste and the SF21 paste that were exposed to 1 M chloride solution. P:portlandite, H: halite (NaCl), X: container' reflection

The XRD pattern of the SF21 paste indicated that all the $Ca(OH)_2$ reacted with the silica fume, and formed C-S-H. Yet this paste had no binding capacity. This results indicate that the observed differences in the chloride binding capacities of the SF-lime pastes are not due to differences in the amounts of the C-S-H in the different pastes. Instead, they might be attributed to the possible differences in the properties of the C-S-H formed in the different pastes. The differences in the chloride binding capacities of the C-S-H might be related to the differences in their C/S: the higher the C/S ratio of the C-S-H, the higher the binding capacity of the C-S-H. This is in agreement with suggestions in the literature *(Tuthill, 1978; Beaudoin et al., 1990)* as mentioned above.

*Nilsson et al. (1996)* suggested that the partial replacement of cement with silica fume will have 3 main effects that will influence the binding capacity. 1) a reduction in the pH of the pore solution which will increase chloride binding, 2) a dilution of $C_3A$ which will reduce binding, and 3) an increase in the amount of the C-S-H which should increase binding. It is also known that this replacement results in the formation of C-S-H with lower C/S than the C-S-H formed without the presence of silica fume *(Massazza, 1998)*. It is not likely that the dilution of the $C_3A$ can solely explain the observed reduction in the binding capacity as a result of the partial replacement of cement with silica fume. The results of this section show that C-S-H can have different binding capacities, and suggest that a lower C/S (in the C-S-H) will lead to a lower binding capacity. Therefore, it is possible that despite the increase in the amount of the C-S-H as a result of the partial replacement with silica fume, the net effect would be a decrease in the amount of bound chloride by the C-S-H. This effect, in addition to the $C_3A$ dilution, would explain the reduction in chloride binding observed in the 8SF paste.

Figure 4-79 shows the binding isotherms of the three MK-lime pastes. The first thing to notice about these results is the much larger binding capacity of the MK-lime pastes compared to their equivalent SF-lime pastes. The metakaolin chemical composition is about 52% $SiO_2$ and about 45% $Al_2O_3$. The products of hydration of the MK-lime mixtures are C-S-H, C-A-S-H, and C-A-H. It is therefore expected that the calcium aluminate hydrates and the C-S-H would contribute to the binding capacity. From a consideration of the mix proportions and molar ratios of the C/S and C/A in the MK-lime mixtures, it is possible that the C/S ratio of the C-S-H to be higher in the MK-lime mixtures than in the SF-lime mixtures with similar proportions. Hence, the binding capacities of the C-S-H in the MK-lime pastes might possibly be higher than the binding capacities of the C-S-H

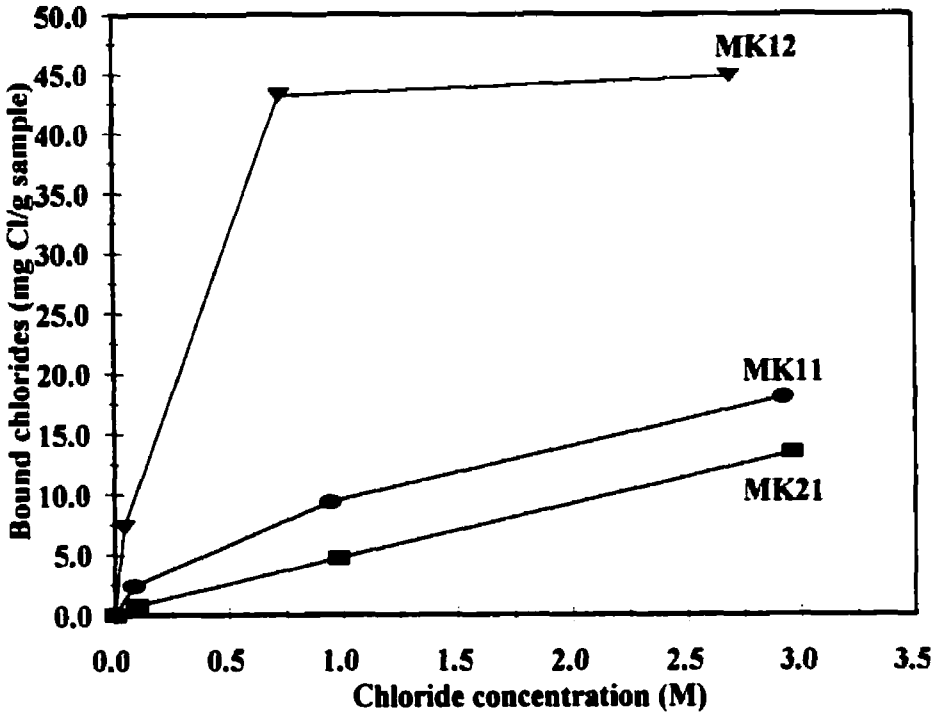


Figure 4-79: Chloride binding isotherms of the MK-lime pastes. The pastes were cured for 2 months at 38°C, and had a W/CM = 2.

in the equivalent SF-lime pastes. This means that the observed differences between the binding capacities of the MK-lime pastes and the SF-lime pastes are not only due to the high alumina content of the metakaolin, but may also be due to the higher binding capacity of the C-S-H in the MK-lime pastes.

There are also large differences in the chloride binding capacities of the MK-lime pastes. The binding capacities were larger, the higher the mass ratio of $Ca(OH)_2$ to metakaolin ($Ca(OH)_2$/MK) of the pastes were. The MK12 (metakaolin/lime = 1/2) paste, which had the highest $Ca(OH)_2$/MK ratio, exhibited the highest chloride binding capacity and the MK21 (metakaolin/lime = 2/1) paste, which had the lowest $Ca(OH)_2$/MK ratio exhibited the lowest binding capacity. The XRD results (Figures 4-80 and 4-81) revealed the differences in the types and amounts of hydration products of these pastes, resulting from the different $Ca(OH)_2$/MK ratios . This seems to have affected the chemical binding capacities (and probably the physical binding capacities) of these pastes. Therefore, it is suggested that the $Ca(OH)_2$/MK ratio did probably influence the binding capacities of the MK-lime pastes through its influence on the type of hydration products of these pastes.

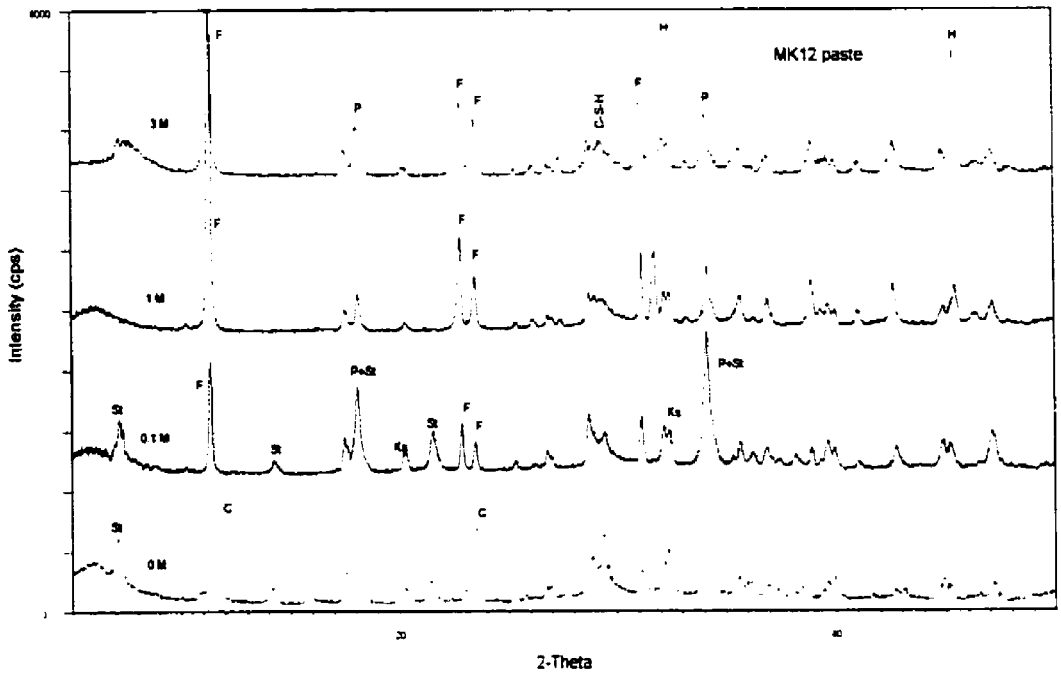


Figure 4-80: XRD patterns of samples of the MK12 paste that were exposed to different chloride concentrations. C: monocarboaluminate, F: Friedel's salt, H: NaCl, Ks: katoite (silication) P: portlandite, St: stratlingite.

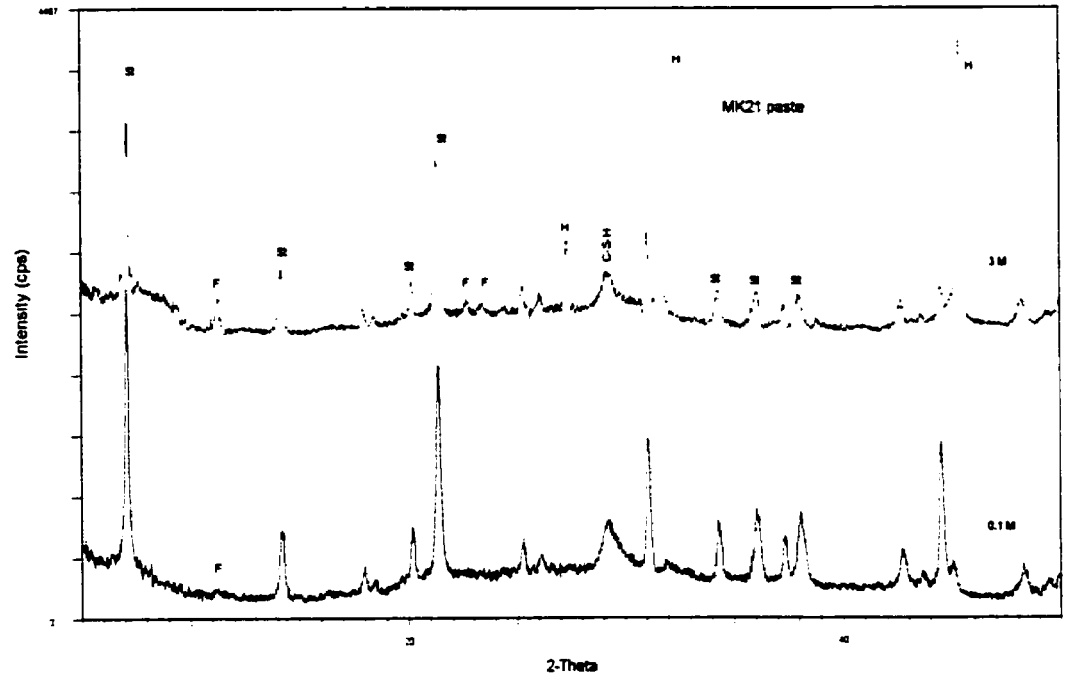


Figure 4-81: XRD patterns of samples of the MK21 paste that were exposed to different chloride concentrations. F: Friedel's salt, H: NaCl, St: stratlingite

The results of the GGBFS-cement mixtures were also interesting. The 50SL (50% GGBFS) paste had a higher binding capacity than the 100SL (100% GGBFS) paste. The 100SL paste (cured for 6 months) had even a lower binding capacity than the control paste as shown in Figure 4-82. This indicates the existence of a critical GGBFS replacement level above which the binding capacity of the resulting mixture would be lower than that of the control paste. These results and those of the MK-lime mixtures suggest that the C/A and C/S are important factors beside the alumina content that determine the binding capacity of SCM-cement mixtures.

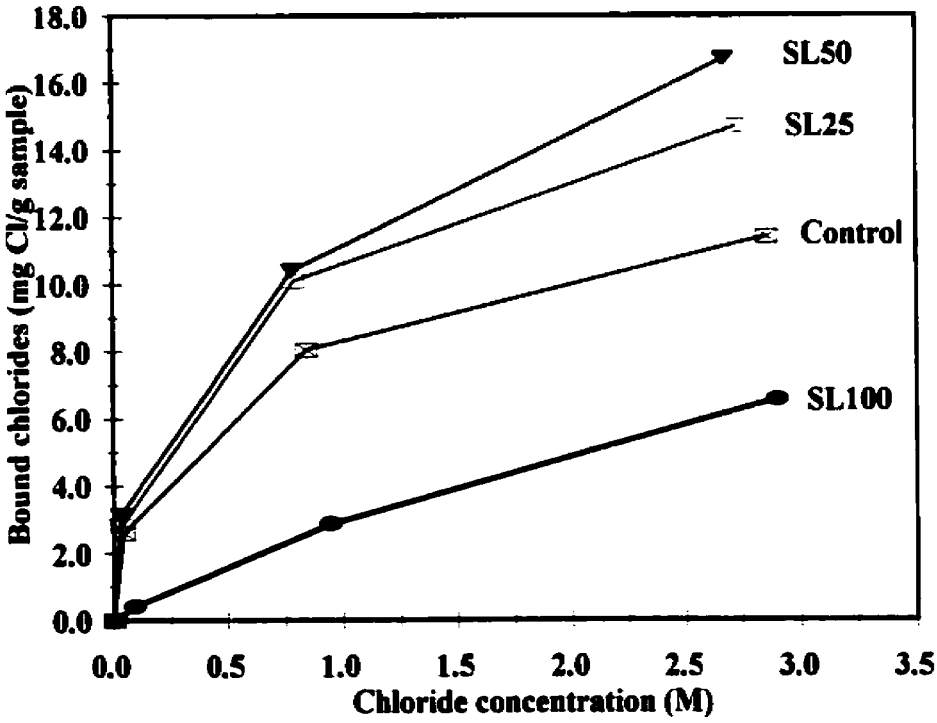


Figure 4-82: Chloride binding isotherms of pastes with various GGBFS replacement levels, and the control paste.

#### 4.3.1.2 X-Ray Diffraction Results

Figure 4-80 shows the XRD patterns of samples of the MK12 paste exposed to 0 M, 0.1 M, 1.0 M, and 3.0 M [NaCl]. At 0 M chloride exposure, several hydration products were identified. They included portlandite, stratlingite, C-S-H, $Ca_3Al_2(SiO_4)(OH)_8$, and $Ca_3AlFe(SiO_4)(OH)_8$. In addition to these compounds, the largest intensity peak was identified as corresponding to the AFm compound, $C_3A.CaCO_3.11H_2O$, known as monocarboaluminate. This phase is known to occur as a hydration product in pozzolana-lime mixtures *(Massazza, 1998)*.

At 0.1 M exposure, there was no major change in the XRD pattern except the disappearance of the peaks of $C_3A.CaCO_3.11H_2O$, and the appearance of peaks which were identified as those of Friedel's salt. This meant that monocarboaluminate transformed into Friedel's salt. It is interesting to notice that this result and that of the C6 cement indicate that the monocarboaluminate phase is transformed to Friedel's salt at low chloride concentrations (< 0.1 M).

At 1 M exposure, the maximum intensity peak corresponding to Friedel's salt increased substantially, indicating the formation of Friedel's salt. The peaks of the stratlingite compound decreased substantially, in addition to those of the $Ca_3Al_2(SiO_4)(OH)_8$ and $Ca_3AlFe(SiO_4)(OH)_8$ compounds which showed a decrease as well. These reductions indicated that these compounds likely did contribute to the formation of Friedel's salt.

The XRD pattern of the sample exposed to 3 M was very similar to that of the sample exposed to 1 M, indicating that no changes occured between the two exposures. The Friedel's salt peaks had similar intensities. This is consistent with the binding capacities of the two samples which were also very similar as shown in Figure 4-79. These results point to the possibility that chemical binding, through the formation of Friedel's salt, is mostly responsible for the binding capacity of the MK12 paste. The large intensities of the Friedel's salt peaks in the samples compared to those in the samples of the cement pastes, reinforce this possibility.

Figure 4-81 shows the XRD patterns of samples of the MK21 paste exposed to 0.1 M, and 3.0 M [NaCl]. The hydration products of the MK21 paste were different than those of the MK12 paste as shown in the XRD pattern of the 0 M sample in Figure 4-80. The main peaks were those of stratlingite in addition to C-S-H. Beside the stratlingite, there were no clear signs of other AFm compounds or calcium aluminate hydrates. There was no signs of portlandite either. This difference in the hydration products between the MK12 and the MK21 pastes is related to the mass ratio of metakaolin to $Ca(OH)_2$.

At 0.1 M exposure, there was no major change in the XRD pattern compared to the one at 0 M. There was a very small peak at 7.8 Å d spacing, which was identified as representing Friedel's salt. This was consistent with the relatively smaller binding capacity of the MK21 paste (compared to that of the MK12 paste ) at 0.1 M concentration. The Friedel's salt peaks became more obvious at 3 M exposure, although, they were still very small compared to those of the MK12 paste. The increase in Friedel's salt peaks was coupled with a small reduction in the stratlingite peaks. The persistence of a large part of the stratlingite peaks at 3 M chloride concentration indicated that most of the stratlingite phase was still present at 3 M chloride concentration. This observation might be significant in relation to the influence of cement replacement with silica fume. on the chloride binding capacity; it is expected that C-A-S-H would form (as product of hydration of the calcium aluminate) in the case of cement replacement with silica fume. Since the previous results indicate that C-A-S-H tend to persist at higher chloride concentrations without fully transforming into Friedel's salt. it is suggested that the expected reduction in the chemical binding capacity is not only due to dilution of the $C_3A$ content (and $C_4AF$ content), but it is also possibly due to the formation of C-A-S-H which would probably cause a further reduction in the binding capacity.

The binding isotherms and the XRD patterns of the MK12 and MK21 pastes showed a correlation between the chloride binding capacity and the Friedel's salt content (as reflected by the highest intensity peaks). The MK12 paste had a much higher binding capacity and a much higher Friedel's salt peaks than the MK21 paste. This indicates a main role of the chemical binding capacity in the overall binding capacity of the MK-lime pastes. However, it does not necessarily mean a minor role of the C-S-H in the overall binding capacity, since it is possible that the binding capacity of the C-S-H to be higher in the MK-lime pastes than in the SF-lime pastes (of similar SCM/lime proportions), owing to the higher C/S ratio in the MK-lime mixture (although, this does not automatically mean that the C/S ratio of the C-S-H that forms is higher than that in the equivalent SF-lime mixture, owing to the competition between the alumina and silica for calcium). It is also possible that the binding capacity of the C-S-H is higher in the MK12 paste than in the MK21 paste, due to the higher C/S ratio in the MK12 mixture. Hence, while the chemical binding capacity certainly contributed to the higher binding capacity of the MK12 paste (compared to that of the MK21 paste), it is possible that the C-S-H also contributed to the higher binding capacity of the MK12 paste. It is very interesting to notice that the MK21 paste, which contained a higher amount of alumina than the MK12 paste, had a lower chemical binding capacity. This result means that the

alumina content (or the metakaolin content) of the mixture is not the only factor that affects the chemical binding capacity, but the $Ca(OH)_2$/metakaolin ratio is also important. The different $Ca(OH)_2$/metakaolin ratios of these two mixtures influenced the calcium aluminate hydrates (types and amounts), and this seems to have influenced their chemical binding capacities.

### 4.3.2 Pure Phases

#### 4.3.2.1 Chloride Binding Isotherms

Figure 4-83 shows the chloride binding isotherms of the pure phases. As mentioned in Chapter 3 (see Table 3-16), the $C_3A$ pastes contained mixtures of pure $C_3A$, gypsum, and $Ca(OH)_2$. Two gypsum to $C_3A$ molar ratios were tested: 0.4 and 0.8. The $C_4AF$ paste was of similar composition with a gypsum to $C_4AF$ ratio of 0.8. As expected, the $C_3A4$ paste had the largest binding capacity, since it had the largest $C_3A$ content. The $C_3S$ and $C_2S$ pastes had much lower binding capacities than the $C_3A$ and $C_4AF$ pastes. Another thing to notice in Figure 4-83 was the binding capacity of $C_4AF$ paste which despite being lower than that of $C_3A8$ paste at 0.5 M and 1 M chloride concentrations was comparable at the other concentrations. This means that $C_4AF$ in pure form at least, has a substantial ability for chloride binding. But this fact may not necessarily hold true for the $C_4AF$ phase in Portland cement since the ferrite hydrates may actually have a range of compositions of which the $C_4AF$ is only an average one. In addition, this phase can contain up to 13% of impurities *(Taylor, 1992)*. Nevertheless, these results favour the possibility of an effective role being played by $C_4AF$.

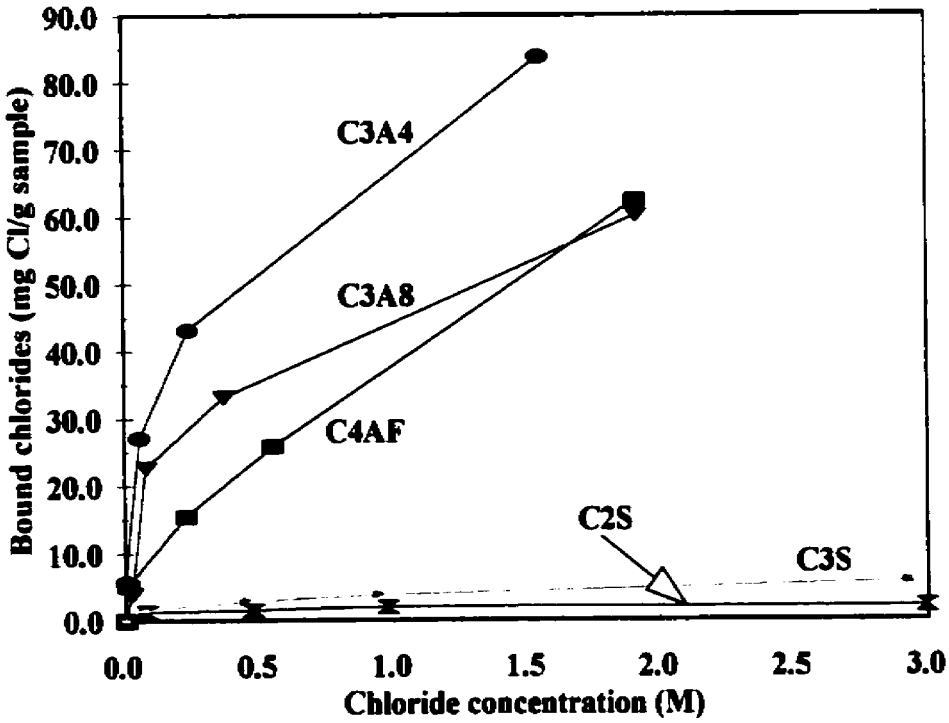


Figure 4-83: Chloride binding isotherms of the $C_3A4$, $C_3A8$, $C_4AF$, $C_3S$, and $C_2S$ pastes. W/CM = 0.5.

The $C_3A4$ paste had a higher binding capacity than the $C_3A8$ paste. This was, of course, partly due to the lower $C_3A$ content in the $C_3A8$ paste. But, the higher gypsum content in the $C_3A8$ paste did most likely contribute to this effect as well. When more sulphate is used, such in the case of $C_3A8$ mixture, more sulfoaluminate products are formed and less calcium aluminate hydrates would be available for reaction with chloride ions. It would have been very interesting to test more gypsum/$C_3A$ ratios to determine the limits of the binding capacity of the $C_3A$ and correlate the results with the binding capacities of different types of Portland cements. Unfortunately, the quantity of pure $C_3A$ was very limited.

Another important fact revealed by these results, was the relatively significant binding capacity of the $C_3S$ paste in comparison with the control cement paste as shown in Figure 4-84. This is in agreement with the results found by *Blunk et al. (1986)* and *Wowra and Setzer (1997, 2000)* who found the $C_3S$ paste had a noticeable binding capacity for external chlorides. It is interesting to note the difference in the binding capacities of $C_3S$ and $C_2S$. From a consideration of the hydration reactions of the $C_3S$ and $C_2S$ paste (Equations 4-1 and 4-2), it would be expected that the $C_2S$ paste would bind more chlorides on a mass basis. The results, however, show that the $C_3S$ paste had a higher binding

$$2C_2S + 4H \rightarrow C_3S_2H_3 + CH \qquad (4\text{-}1)$$

$$2C_3S + 6H \rightarrow C_3S_2H_3 + 3CH \qquad (4\text{-}2)$$

capacity than the $C_2S$ paste. These results might be attributed to the lower degree of hydration of $C_2S$ compared to $C_3S$, after a 2 months hydration period (Figure 4-85). This means lower amounts of C-S-H being formed and consequently lower adsorption sites in the $C_2S$ paste.

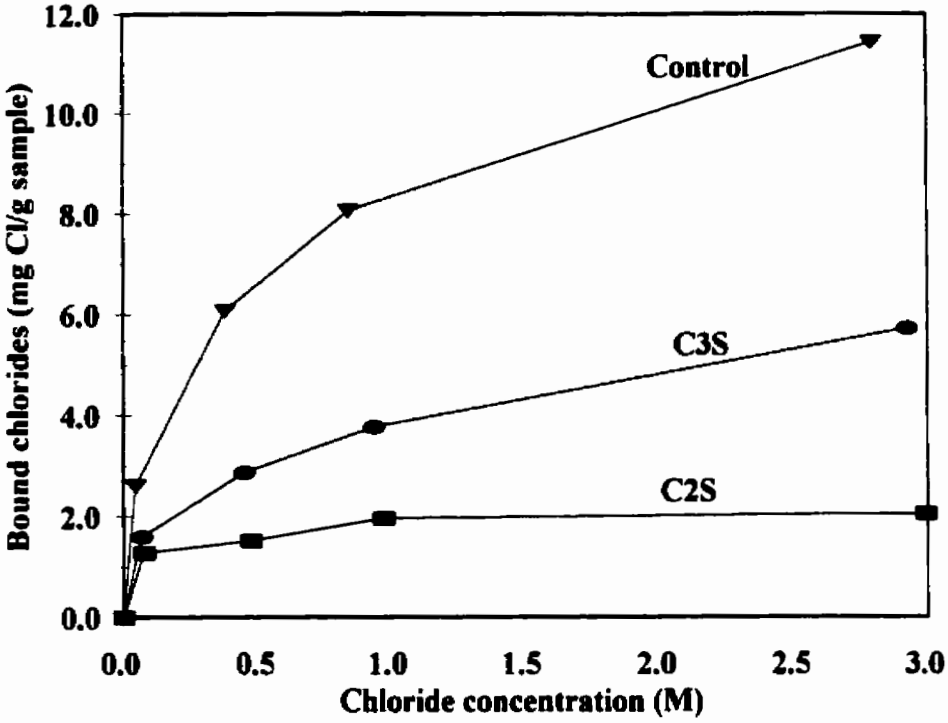


Figure 4-84: Comparison between the chloride binding capacities of the control, $C_3S$, and $C_2S$ pastes. W/CM = 0.5.

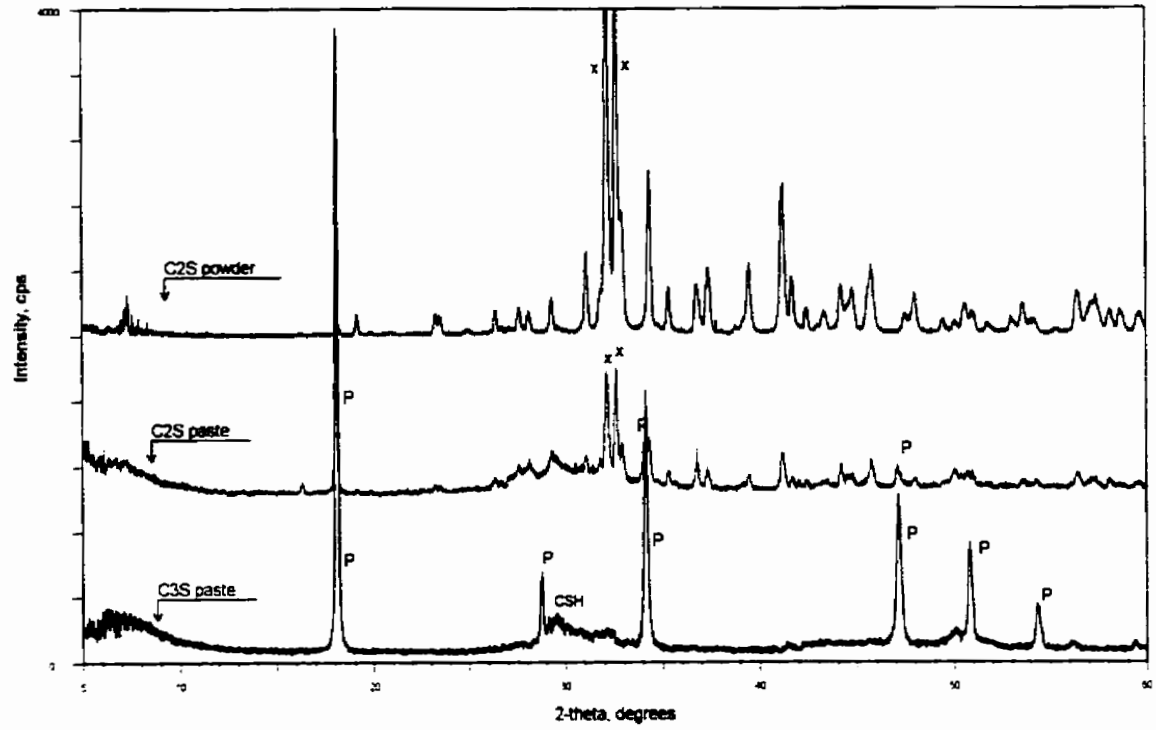


Figure 4-85: Comparison of the XRD pattern of the $C_2S$ paste with those of the $C_3S$ paste and the unhydrated $C_2S$ powder. The XRD pattern shows the existence of unhydrated larnite ($Ca_2SiO_4$) in the $C_2S$ paste. X: larnite.

### 4.3.2.2 Effect of pH and Sulphate Ion

Figures 4-86 and 4-87 show the effect of hydroxyl ion and sulphate ion concentration in the pore solution on the binding capacity of the $C_3A8$ paste. An increase in the concentration of any of these two ions results in a decrease in the binding capacity of the $C_3A8$ paste. In the case of hydroxyl ion, these results agree with those of *Roberts (1962)* who found that a quantity of Friedel's salt was partially decomposed when it was exposed to a solution that had a higher pH than the original solution in which it was stored. One possible reason for this, is that the increase in $OH^-$ concentration will increase the competition between the $OH^-$ and $Cl^-$ ions for chemical reactions with the unhydrated $C_3A$ or for ion exchange sites in the AFm phases, which will result in lower chloride binding than in the case of a lower pH.

The decrease in binding capacity as a result of an increase in sulphate concentration might be due to the competition between sulphate and chloride ions for chemical reaction with the unhydrated $C_3A$ and the calcium aluminate hydrates. So, the more sulphate ions there are, the less Friedel's salt will form.

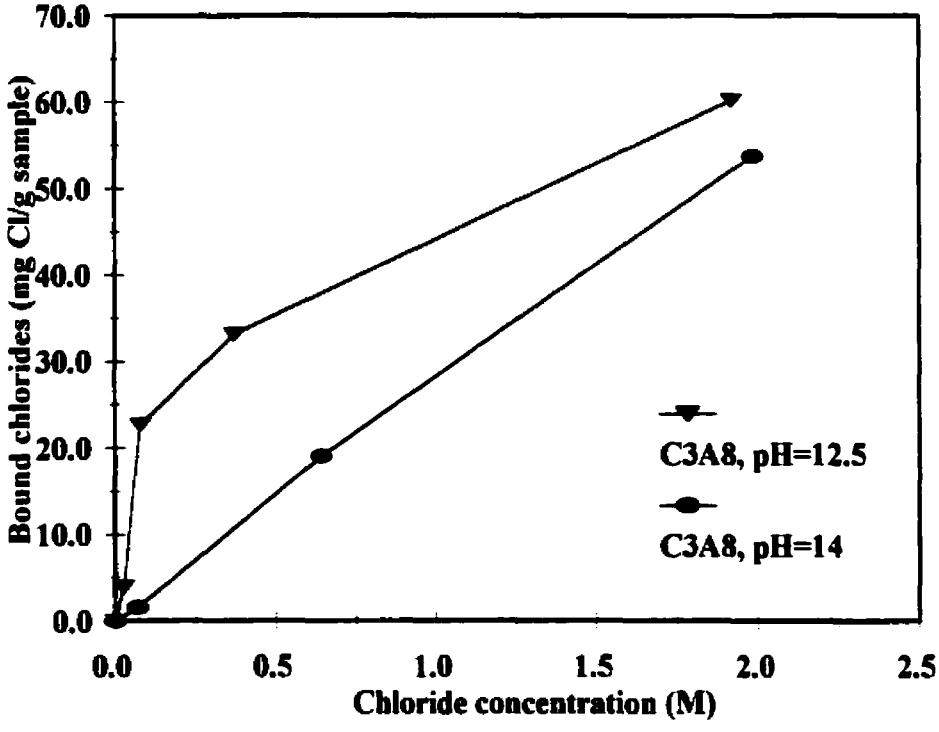


Figure 4-86: Influence of the pH of the host solution on the chloride binding capacity of the $C_3A8$ paste. W/CM = 0.5.

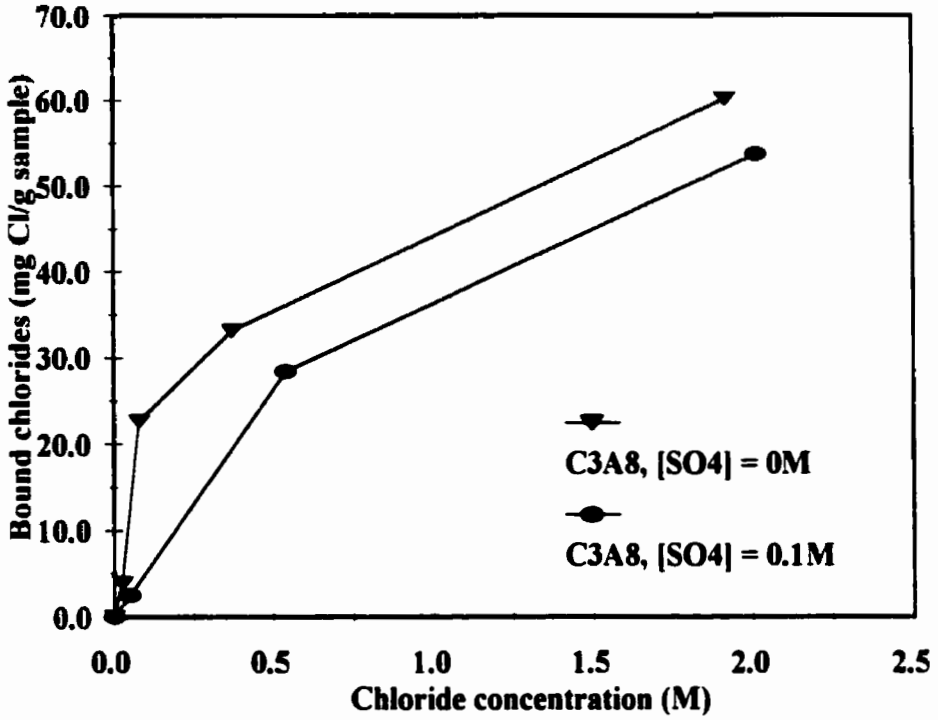


Figure 4-87: Influence of the sulphate ion concentration of the host solution on the chloride binding capacity of the $C_3A8$ paste. W/CM = 0.5.

The effects of hydroxyl and sulphate ion concentration in the external solution on the binding capacity of $C_3S$ are shown in Figures 4-88 and 4-89. Similar to their effect on $C_3A$, an increase in the concentration of these ions reduces the binding capacity of $C_3S$. Since chloride binding by the $C_3S$ occurs through physical adsorption on the surface of the C-S-H, the reduction in both cases is probably due to the increased competition between the hydroxyl or sulphate ions and the chloride ions for adsorption sites on the surface of the C-S-H gel, in the electrical double layer.

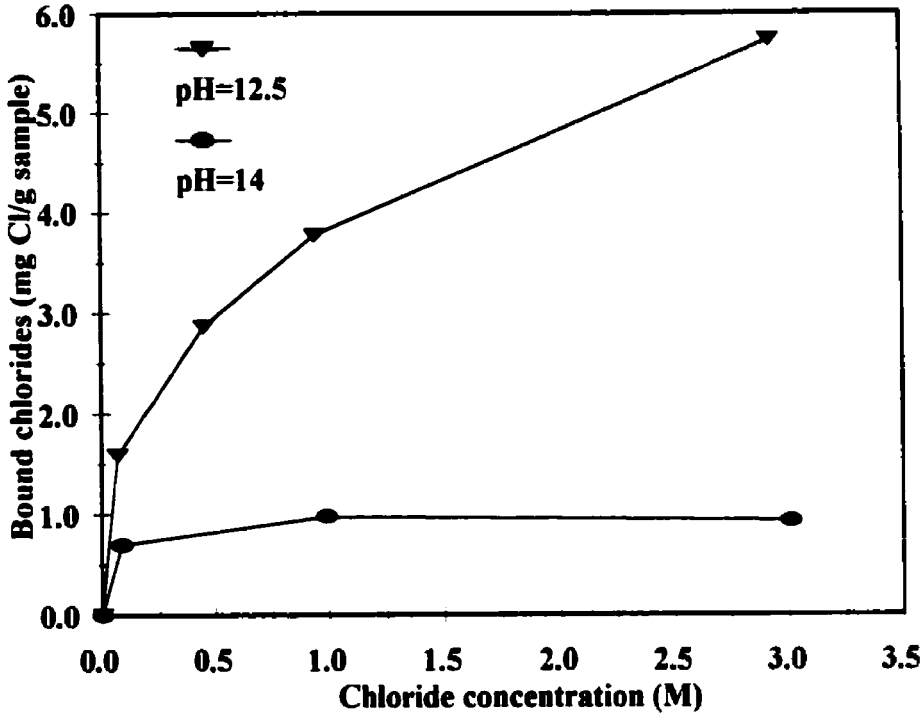


Figure 4-88: Influence of the pH of the host solution on the chloride binding capacity of the $C_3S$ paste. W/CM = 0.5.

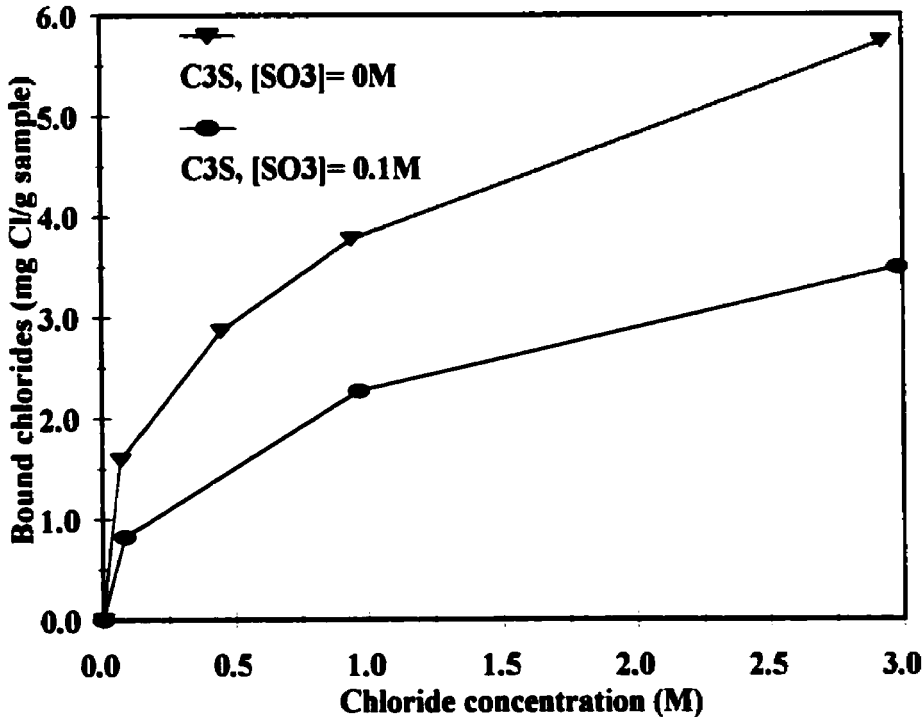


Figure 4-89: Influence of the sulphate ion concentration of the host solution on the chloride binding capacity of the $C_3S$ paste. W/CM = 0.5.

#### 4.3.2.3 Effect of Temperature

Figure 4-90 shows the effect of temperature on the binding capacity of the $C_3S$ paste. For the range of temperatures tested, this effect seems to be small and almost negligible at low chloride concentrations. Nevertheless, it is interesting to note that, unlike the behaviour by cement pastes, when tested at different temperatures, the binding decreased with an increase in temperature for all the concentrations studied; there was no limiting concentration above which this trend was reversed.

In the case of the $C_3A8$ paste, the results in Figure 4-91 show a similar behaviour to that of the cement pastes. However, it is hard to tell with confidence whether this was a real trend or the result of a small error, since the difference in binding between 23°C and 38°C at 3 M chloride concentration is so small. If a third temperature was tested, it would have been easier to judge. But, unfortunately there were not enough samples to test at 7°C.

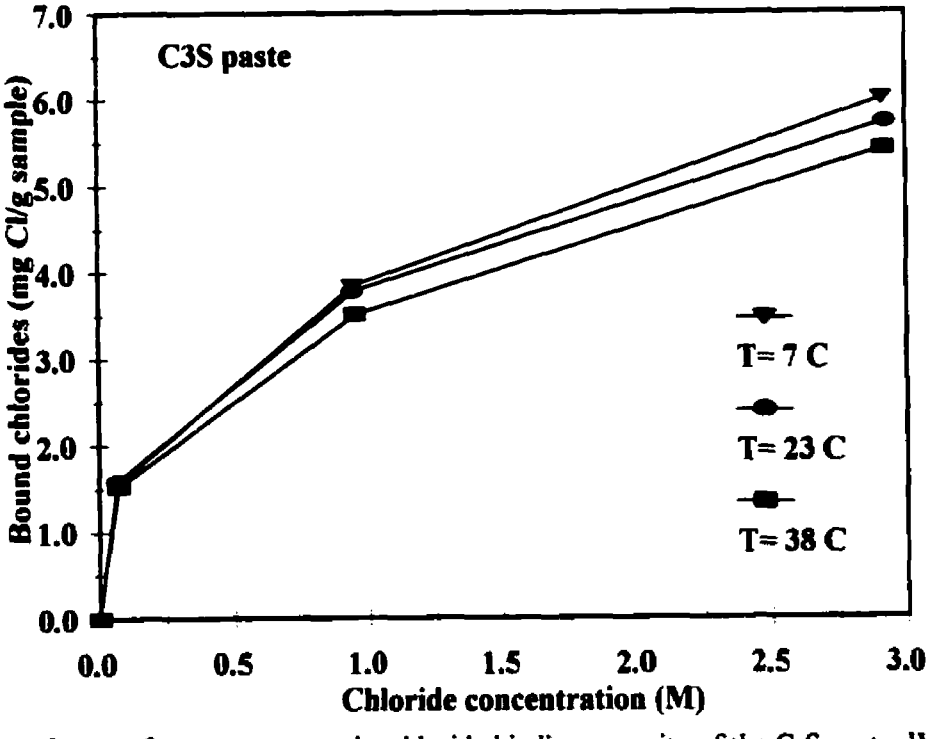


Figure 4-90: Influence of temperature on the chloride binding capacity of the $C_3S$ paste. W/CM=0.5.

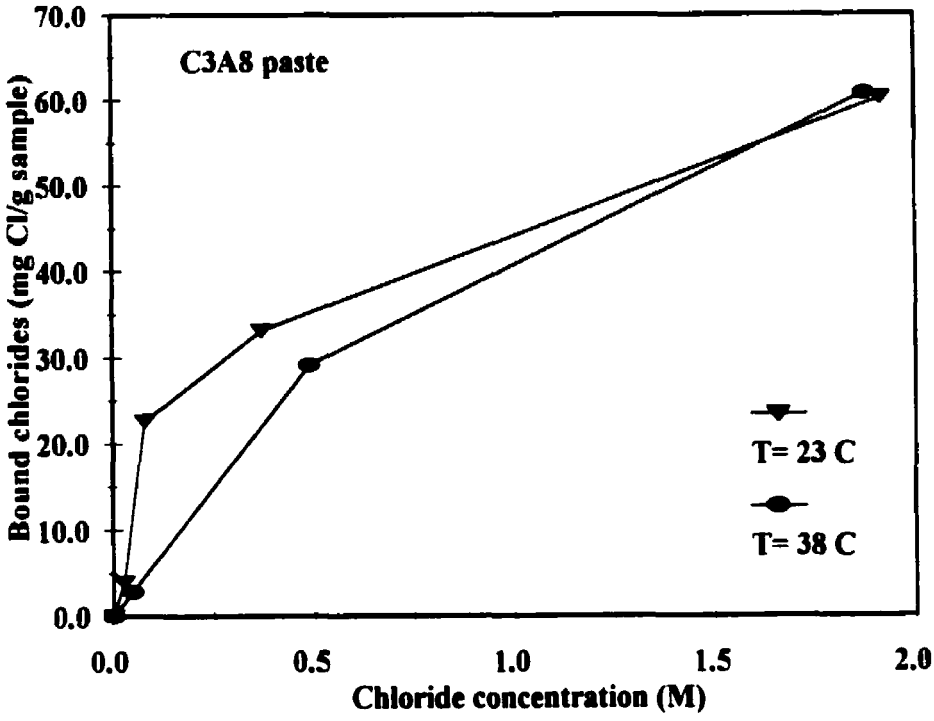


Figure 4-91: Influence of temperature on the chloride binding capacity of the $C_3A$ paste. W/CM=0.5.

#### 4.3.2.4 Effect of Carbonation

Carbonated samples of $C_3A8$ showed no signs of any binding capacity as shown in Figure 4-92. This probably means that all calcium aluminate hydrates able to react with chloride or incorporate chloride ions in their structure were transformed by the reaction with $CO_3^{2-}$ ions to form $CaCO_3$ and other products. The carbonated $C_3S$ samples, bound very small amounts of chloride as shown in Figure 4-93. There was a 90% or more decrease in their binding capacities. These results are consistent with those of the cement pastes, and show that the carbonation of cement paste before exposure to chloride solutions, greatly reduces its chemical and physical binding capacities.

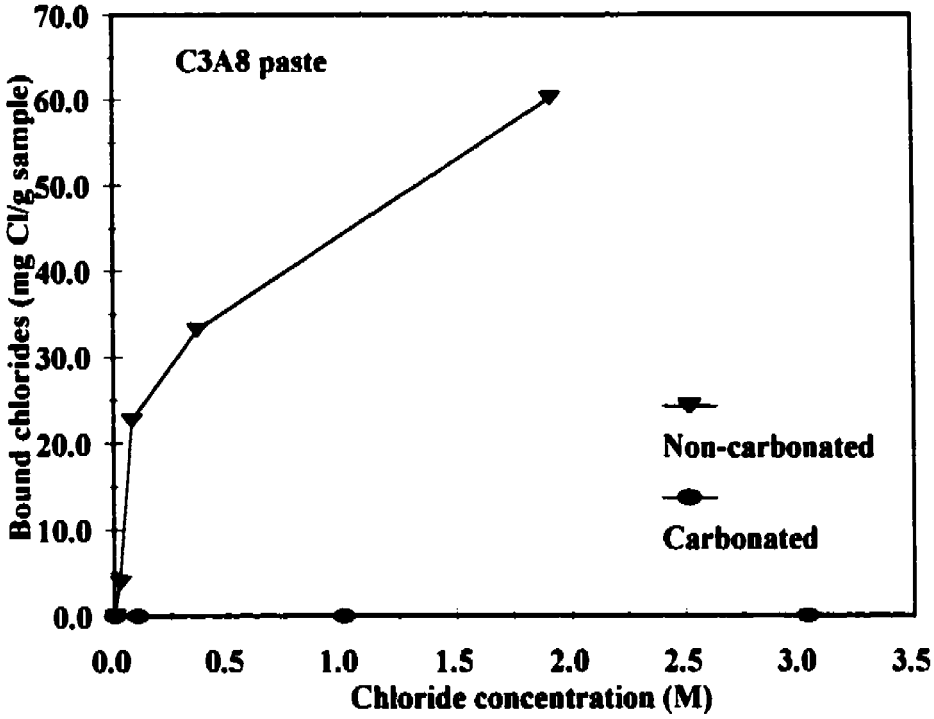


Figure 4-92: Influence of carbonation on the chloride binding capacity of the $C_3A8$ paste. W/CM=0.5

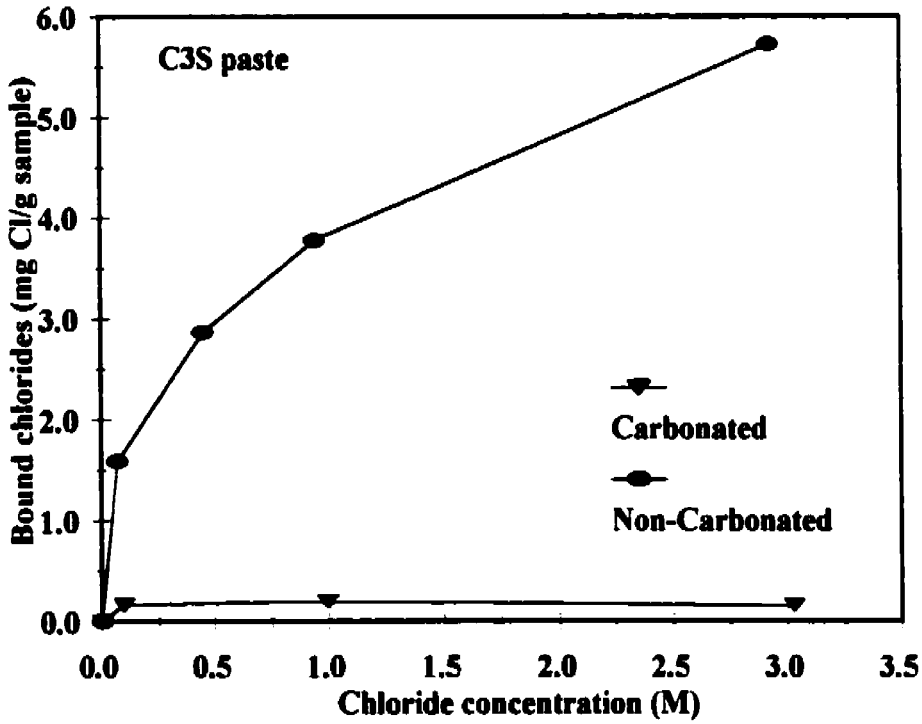


Figure 4-93: Influence of carbonation on the chloride binding capacity of the $C_3S$ paste. W/CM=0.5

#### 4.3.2.5 Desorption Isotherms

Two samples were chosen for the desorption test. The $C_3A8$ sample was originally exposed to a 1 M NaCl solution with a pH of 14, while the $C_3S$ sample was originally exposed to the standard 1M NaCl solution (pH = 12.5). One litre of distilled water saturated with $Ca(OH)_2$ was used for desorption. The $C_3A8$ sample was diluted around 230 times and the $C_3S$ sample was diluted around 160 times. The equilibrium concentrations after dilution were close to zero being 0.0079 M in the case of $C_3S$ sample and 0.01 M in the case of the $C_3A8$ sample (Table 4-19). Figures 4-94 and 4-95 show the results of the desorption test for both samples. While 25% of the originally bound chloride remained bound after desorption in the $C_3A$ sample, almost all of the bound chlorides were desorbed in the $C_3S$ sample. The total desorption of chloride from the $C_3S$ paste, with the reduction in chloride concentration to almost 0 M, is typical of physical adsorption; at equilibrium, the amount of adsorbed chloride is equal to the amount of desorbed chloride, and there is an equilibrium between the adsorbed chloride and the free chloride concentration in the pore solution. When the chloride concentration drops, chloride desorption becomes higher than chloride adsorption, until a new equilibrium is established. These results confirm that chlorides that are physically adsorbed can be desorbed through dilution.

Althought a major part of the bound chloride, in the $C_3A$ paste, was released in the solution, the process of chloride binding by the $C_3A$ paste was not reversible, and the desorption result indicates the existence of hysteresis in this process. The release of bound chloride from the $C_3A$ paste was not unexpected. *Roberts (1962)*, who studied the solubility of Friedel's salt in saturated lime water, found that chloride was always present in the equilibrium solution, and the amount of chloride released into solution was a function of the solution/solid ratio (or the chloride concentration in the solution). The higher the solution/solid ratio (or the lower the concentration) was, the higher the amount of chloride released into solution. He noticed an incongruent solubility of Friedel's salt and that the final solid consisted mostly of a $C_3A.CaCl_2.aq$-$C_4A.aq$ solid solution. In another test, he added $CaCl_2$ to a solution containing $C_4A.19H_2O$, a $C_3A.CaCl_2.aq$-$C_4A.aq$ solid solution was formed, and the molar ratio $CaCl_2/Al_2O_3$ of the solid solution increased with the increase of equilibrium $CaCl_2$ concentration. He suggested that the formation of the solid solution involved the replacement of $OH^-$ ions in the original structure of $C_4A.19H_2O$ with $Cl^-$ ions, and that this replacement was dependent on the chloride concentration of the solution. These results by *Roberts (1962)* might explain the observed behaviour of the $C_3A8$ paste when exposed to 1 litre of

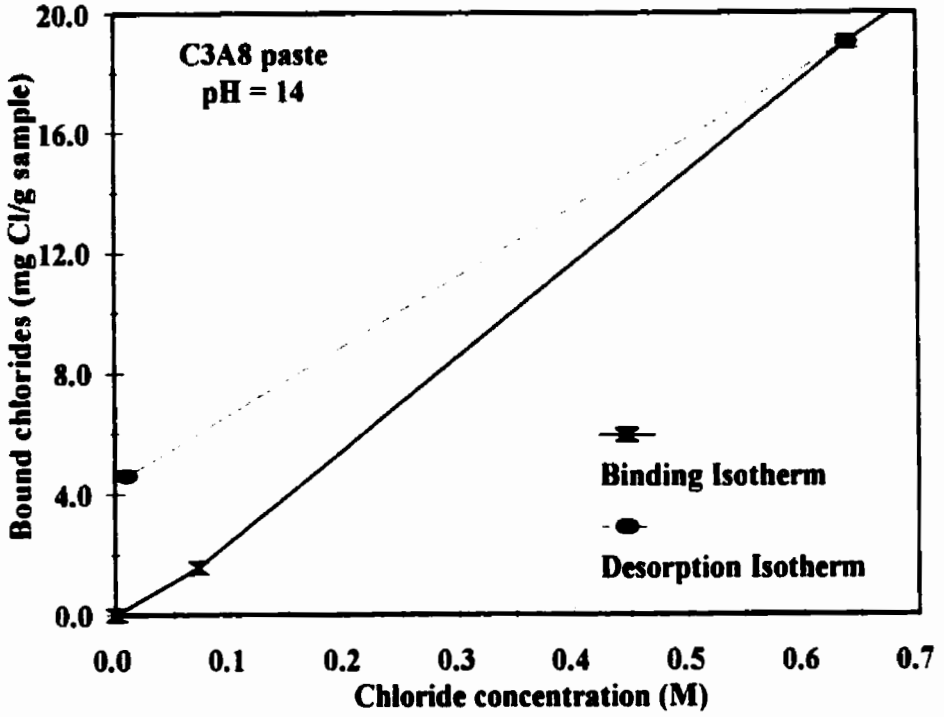


Figure 4-94 Influence of the decrease in the chloride concentration of the host solution (after equilibrium) on the chloride binding capacity of the $C_3A8$ paste (pH=14). W/CM=0.5

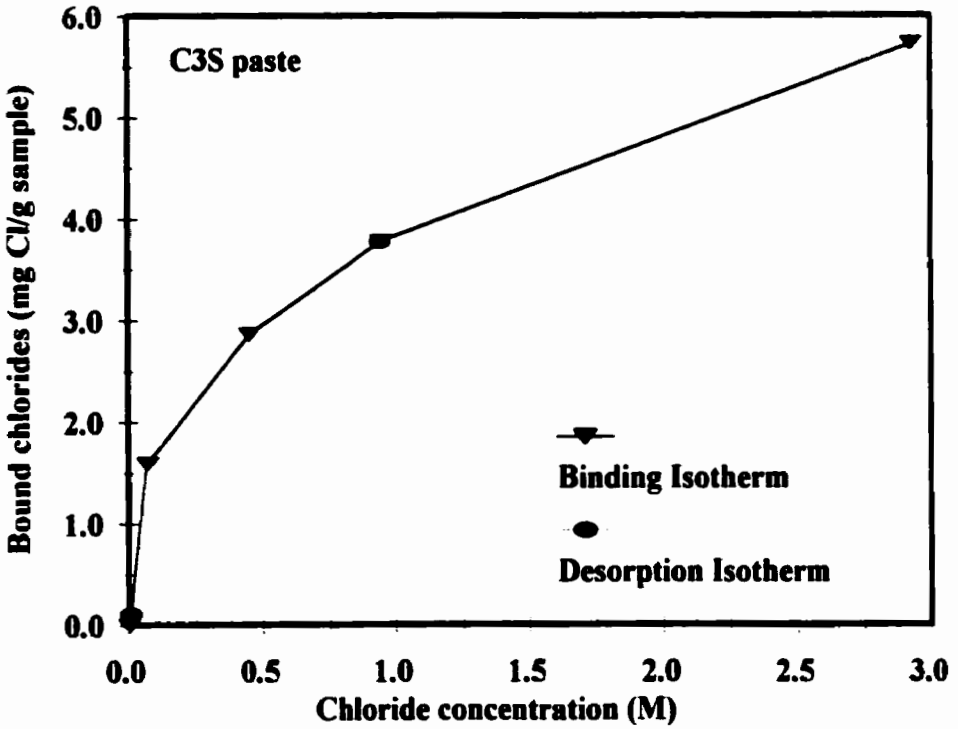


Figure 4-95: Influence of the decrease in the chloride concentration of the host solution (after equilibrium) on the chloride binding capacity of the $C_3S$ paste. W/CM=0.5

saturated lime solution. The large reduction of the chloride concentration of the exposure solution might have resulted in the release of bound chloride so that a new equilibrium was established between the free and bound chloride. It is possible that the released $Cl^-$ ions were replaced by $OH^-$ ions through an ion exchange mechanism. It is interesting to note that the $C_3A8$ sample lost more chlorides than the cement samples. This might be due to the fact that it was diluted more than twice than these samples and this might have caused more dissolution of the Friedel's salt and the chemically adsorbed chlorides.

Table 4-19: Results of the desorption test on samples of the $C_3S$ and $C_3A8$ pastes.

| mix | Initial Exposure (M) | Water Added (ml) | Final [Cl⁻] (M) | $C_b$ Before | $C_b$ After | % chloride remaining |
|---|---|---|---|---|---|---|
| $C_3S$ | 1 | 1000 | 0.008 | 3.78 | 0 | 0 |
| $C_3A8$(pH=14) | 1 | 1000 | 0.01 | 19.02 | 4.61 | 24 |

#### 4.3.2.6 Effect of $C_3A$ Addition to C1 Cement

Figure 4-96 shows the effect of $C_3A$ addition on the binding capacity of the C1 cement. The binding increases substantially with the increase in the level of cement substitution with $C_3A$. The data from this test present a more useful picture of the role of the $C_3A$ in the chloride binding capacity in cement, since they show the behaviour of the pure $C_3A$ in an actual cement environment. The increase in binding at each substitution level might be used as a rough measure of the binding capacity of $C_3A$ in a cement with similar composition to this synthetic cement. These results reinforce the argument that $C_3A$ content is a major factor influencing the binding capacity of cements. As mentioned in Chapter 3, the two levels of substitution (6.3% and 10%) were used to simulate Type 20 and Type 10 Portland cements. The results of this test are, however, higher than those of the Types 20 and 10 cements. This might be partially due to the much higher $C_4AF$ content in the synthetic cements, and/or the lower $SO_3$/ ($C_3A$+$C_4AF$) mass ratios in the synthetic cements.

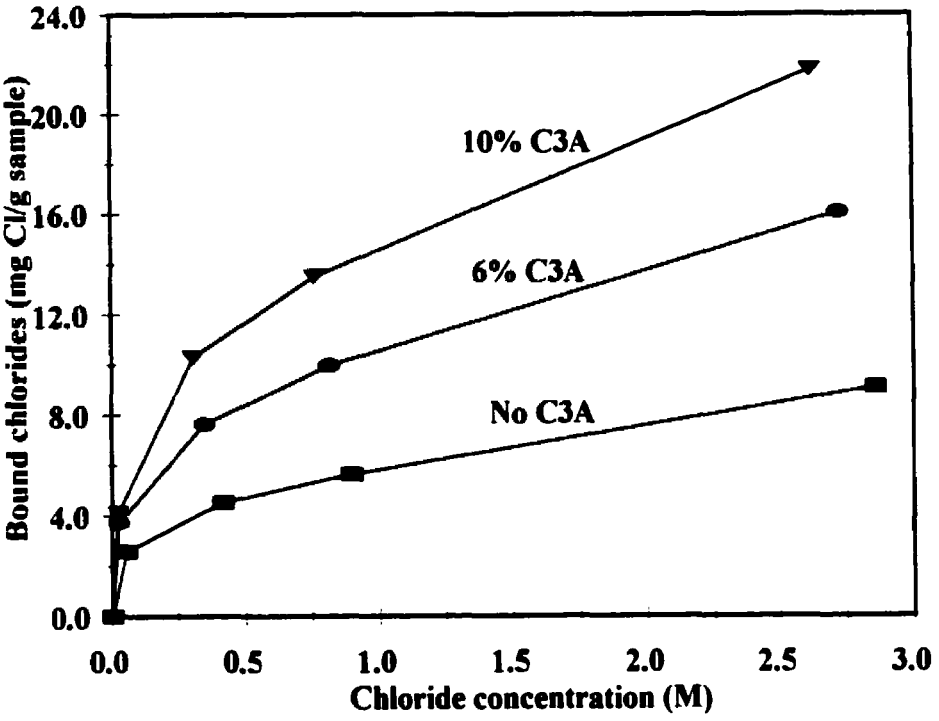


Figure 4-96: Influence of cement replacement with pure $C_3A$ on the chloride binding capacity of the C1cement. W/CM = 0.5.

#### 4.3.2.7 Effect of $C_4AF$ Addition to a Low $C_4AF$ Cement

The addition of $C_4AF$ to the cement low in iron oxide increased the binding capacity as shown in Figure 4-97. The data of this test provide a more useful picture about the role of $C_4AF$ in chloride binding in cement paste, since they show the behaviour of the pure $C_4AF$ phase in an actual cement environment. These results add to the series of findings pointing towards the possibility of a role being played by the $C_4AF$. It is very interesting to note that the increase in binding due to the addition of $C_4AF$ is lower than that due to the addition of an equivalent amount of $C_3A$ to the low $C_3A$ cement. This result confirms that $C_4AF$ binds less chloride than $C_3A$. Consequently, its role is less important than that of $C_3A$.

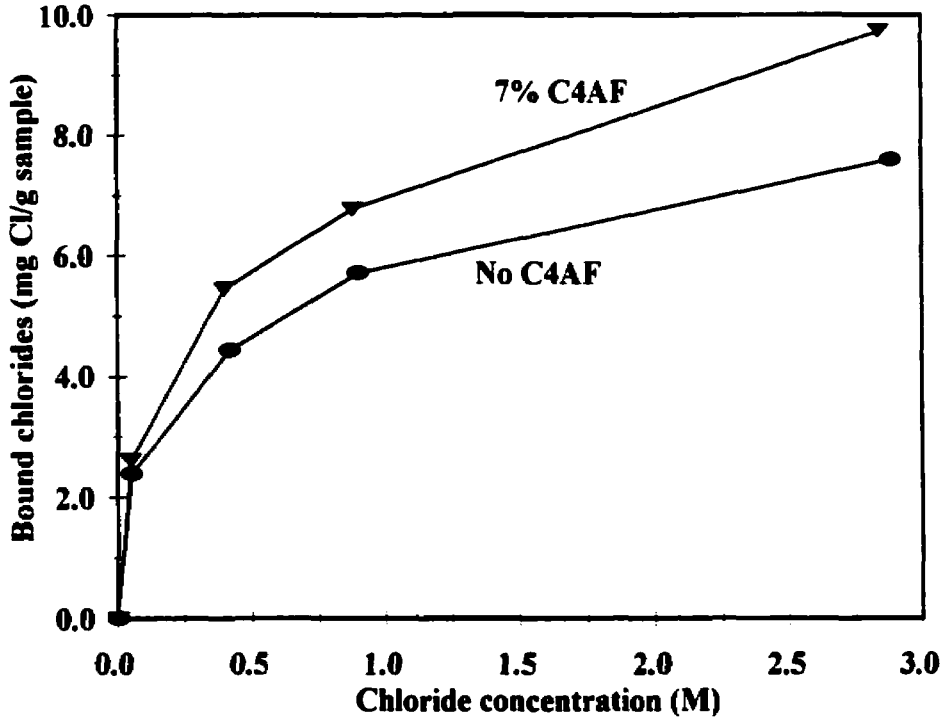


Figure 4-97: Influence of cement replacement with pure $C_4AF$ on the chloride binding capacity of the C7 cement. W/CM = 0.5.

#### 4.3.2.8 X-Ray Diffraction Results

Figures 4-98 and 4-99 show the XRD patterns of samples of the $C_3A4$ paste that were exposed to chloride solutions of different concentrations. At 0 M [NaCl] exposure, the largest peaks were identified as those corresponding to the calcium aluminate sulphate hydroxide hydrate, $Ca_8Al_4O_{12}SO_4(OH)_2.24H_2O$. There is no agreement in the literature on whether this phase is a distinct compound or a solid solution between hydroxy AFm and sulphate AFm, although there is an agreement that $OH^-$ can replace about half of the $SO_4^{2-}$ in sulphate AFm according to *Glasser et al. (1999)*. The second largest peaks were identified with the Katoite phase, $Ca_3Al_2(OH)_{12}$ or $C_3AH_6$. There was also a relatively small peak which was identified with the $C_4AH_{13}$ phase. At 0.1 M [NaCl] exposure, there was a decrease in the intensities of peaks corresponding to the $C_3AH_6$ and a decrease in the intensity of the peaks corresponding to the $Ca_8Al_4O_{12}SO_4(OH)_2.24H_2O$ phase. The reduction in those peaks was accompannied by the appearrance of new peaks which were identified as those of the Friedel's salt and the calcium alumino chloride sulphate hydrate, $Ca_8Al_4O_{12}Cl_2SO_4.24H_2O$. This means that Friedel's salt and the $Ca_8Al_4O_{12}Cl_2SO_4.24H_2O$ phase were

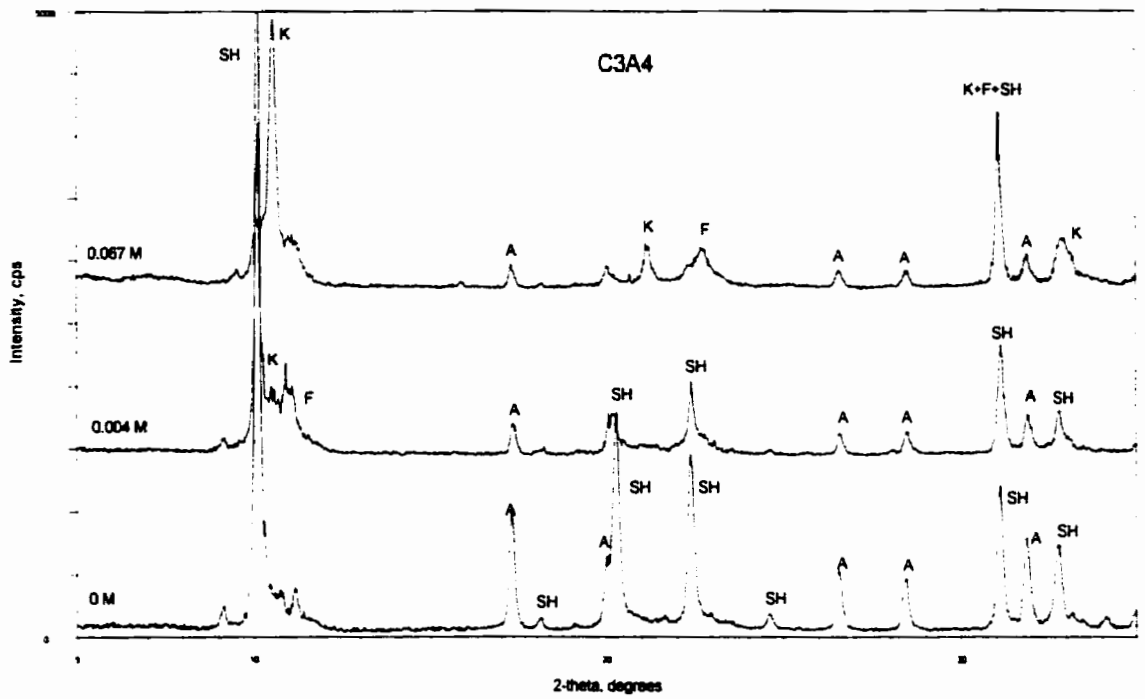


Figure4-98: XRD patterns of samples of the $C_3A4$ paste that were exposed to 0.0, 0.1, and 0.5 M chloride solutions. The patterns are labeled with the equilibrium chloride concentrations of the corresponding samples. A: katoite ($C_3AH_6$), F: Friedel's salt, K: Kuzel's salt, SH: solid solution sulphate-hydoxide Afm

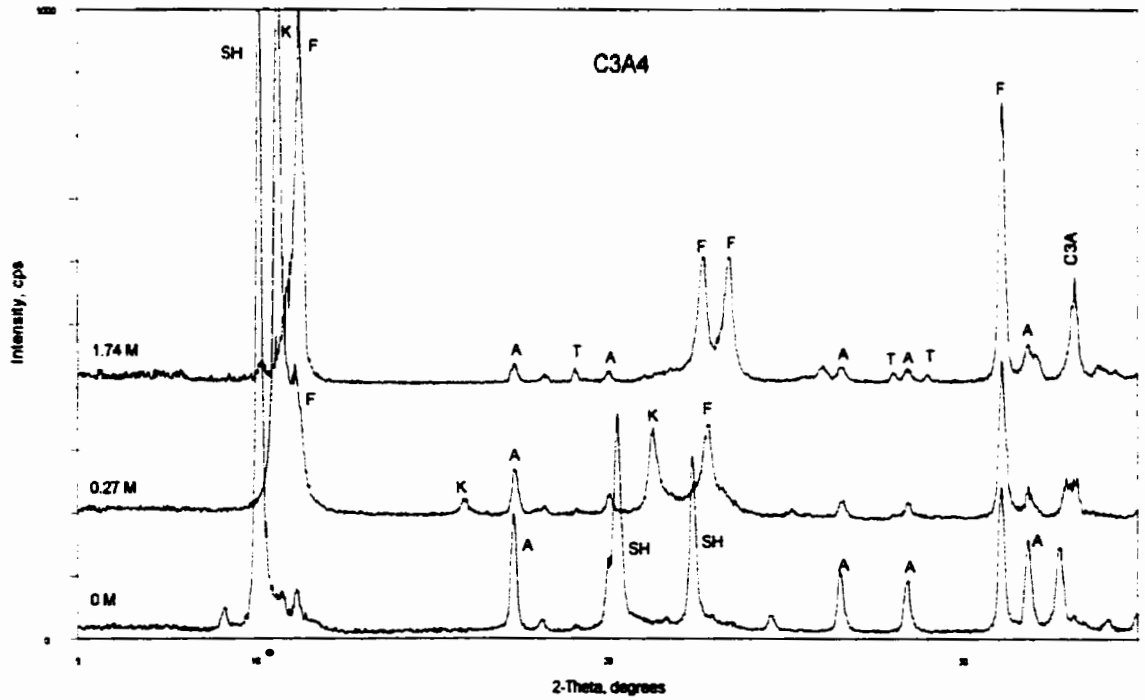


Figure4-99: XRD patterns of samples of the $C_3A4$ paste that were exposed to 0, 1.0, and 3.0 M chloride solutions. The patterns are labeled with the equilibrium chloride concentrations of the corresponding samples. T: thenardite.

formed due to the presence of chloride in the solution. The Friedel's salt is at least partly formed by the conversion of the $C_3AH_6$. There is also a good possibility that the $C_4AH_{13}$ was converted too, although it is not possible to confirm that by XRD test since the peaks of both phases are coincident. The $Ca_8Al_4O_{12}Cl_2SO_4.24H_2O$ phase was formed as a result of a reaction between the $Ca_8Al_4O_{12}SO_4(OH)_2.24H_2O$ phase and chloride.

At 0.5 M [NaCl] exposure, there was a sharp decrease in the maximum peak of the $Ca_8Al_4O_{12}SO_4(OH)_2.24H_2O$ phase and a sharp increase in the maximum peak of the $Ca_8Al_4O_{12}Cl_2SO_4.24H_2O$ phase. The maximum peak corresponding to Friedel's salt increased slightly, and no noticeable change was observed in the peaks of the $C_3AH_6$ phase. These changes mean that the $Ca_8Al_4O_{12}SO_4(OH)_2.24H_2O$ phase has transformed into the $Ca_8Al_4O_{12}Cl_2SO_4.24H_2O$ phase indicating that the $OH^-$ was replaced by the $Cl^-$.

At 1 M [NaCl] exposure, the maximum peak of the $Ca_8Al_4O_{12}SO_4(OH)_2.24H_2O$ phase disappeared, while the peaks of the $Ca_8Al_4O_{12}Cl_2SO_4.24H_2O$ phase and Friedel's salt increased as shown in Figure 4-99. It is interesting to notice that the increase in the peaks of Friedel's salt occured with the disappearence of the $Ca_8Al_4O_{12}SO_4(OH)_2.24H_2O$ peaks. This probably means that the formation of Friedel's salt at 0.1 M and 0.5 M exposures was due to the conversion of the $C_3AH_6$ and the $C_4AH_{13}$ phases and not the $Ca_8Al_4O_{12}SO_4(OH)_2.24H_2O$. The increase in the intensities of the Friedel's salt peaks at 0.1 M exposure was probably due to the conversion of the $Ca_8Al_4O_{12}Cl_2SO_4.24H_2O$ phase into Friedel's salt by replacing the $SO_4^{2-}$ with $Cl^-$.

At 3 M [NaCl] exposure, there was a huge decrease in the maximum intensity peak representing the $Ca_8Al_4O_{12}Cl_2SO_4.24H_2O$ phase. It was difficult to tell whether this peak has completely disappeared or not. There was also a substantial increase in the maximum intensity peak corresponding to Friedel's salt. This indicates the almost total conversion of the $Ca_8Al_4O_{12}Cl_2SO_4.24H_2O$ phase into Friedel's salt at 3 M exposure.

Figures 4-100 and 4-101 show the XRD patterns of samples of the $C_3A8$ paste exposed to several chloride solutions concentrations. The similarity between the XRD patterns of the $C_3A8$ and the $C_3A4$ pastes can easily be noticed. But there are differences as well, that are related to the compositions of the two mixtures. The first difference to notice is the absence of peaks representing the $C_3AH_6$ phase, indicating the absence of this phase in the $C_3A8$ paste. In addition, the main peaks at 0 M [NaCl] exposure correspond to the sulphate AFm, or monosulphate phase, $3CaO.Al_2O_3.CaSO_4.12H_2O$, as opposed to the $Ca_8Al_4O_{12}SO_4(OH)_2.24H_2O$ phase in the $C_3A4$ paste.

The reason for this difference is related to the higher $CaSO_4$ / $C_3A$ molar ratio in the $C_3A8$ paste than in the $C_3A4$ paste.

At 1M exposure, the peaks of the monosulphate phase almost disappeared, and the largest intensity peak was that of the $Ca_8Al_4O_{12}Cl_2SO_4.24H_2O$ phase. This indicates the transformation of the monosulphate phase into the $Ca_8Al_4O_{12}Cl_2SO_4.24H_2O$ phase through the partial replacement of the $SO_4^{2-}$ with $Cl^-$. It is very interesting to notice the almost inexistence of peaks corresponding to Friedel's salt at 1M exposure, so that the chemical binding of chloride is happening almost entirely through the formation of the $Ca_8Al_4O_{12}Cl_2SO_4.24H_2O$ phase and not through the formation of Friedel's salt. Another interesting thing to notice is the increase in the peaks of ettringite. It is not known if the formation of ettringite was the result of the transformation of the monosulphate into the $Ca_8Al_4O_{12}Cl_2SO_4.24H_2O$ phase and the consequent release of $SO_4^{2-}$ into the pore solution. This, however, did not happen in the case of the $C_3A4$ paste where the sulphate content was half of that in the $C_3A8$ paste. It is important to mention in this context that the samples of the $C_3A8$ exposed to chloride concentrations higher than 0.5 M partially disintegrated and turned into powder. This reinforces the possibility of ettringite formation as a result of exposure to chloride solutions.

At 3 M exposure, there was almost no peaks representing the monosulphate phase or the $Ca_8Al_4O_{12}Cl_2SO_4.24H_2O$ phase, and the largest intensity peak was that of Friedel's salt. This indicated the transformation of the monosulphate into Friedel's salt through the full replacement of $SO_4^{2-}$ with $Cl^-$. Peaks corresponding to the ettringite phase were also present, but with lower intensities than those found at 1 M exposure, indicating that the amount of ettringite formed at 3 M exposure was less than that formed at 1 M exposure. In addition, there was also peaks representing the thenardite phase, indicating that the $SO_4^{2-}$ released in the transformation of the monosulphate to Friedel's salt were also incorporated in thenardite ($Na_2SO_4.10H_2O$) in addition to ettringite. Although it is hard to judge from one case, the possible reason for the difference in the amounts of ettringite at 1 M and 3 M exposure, is the same as in the case of the cement pastes; the ettringite becomes less stable at 3 M [NaCl] exposure, and when equlibrium is reached, less ettringite is formed at 3 M exposure than at 1 M exposure.

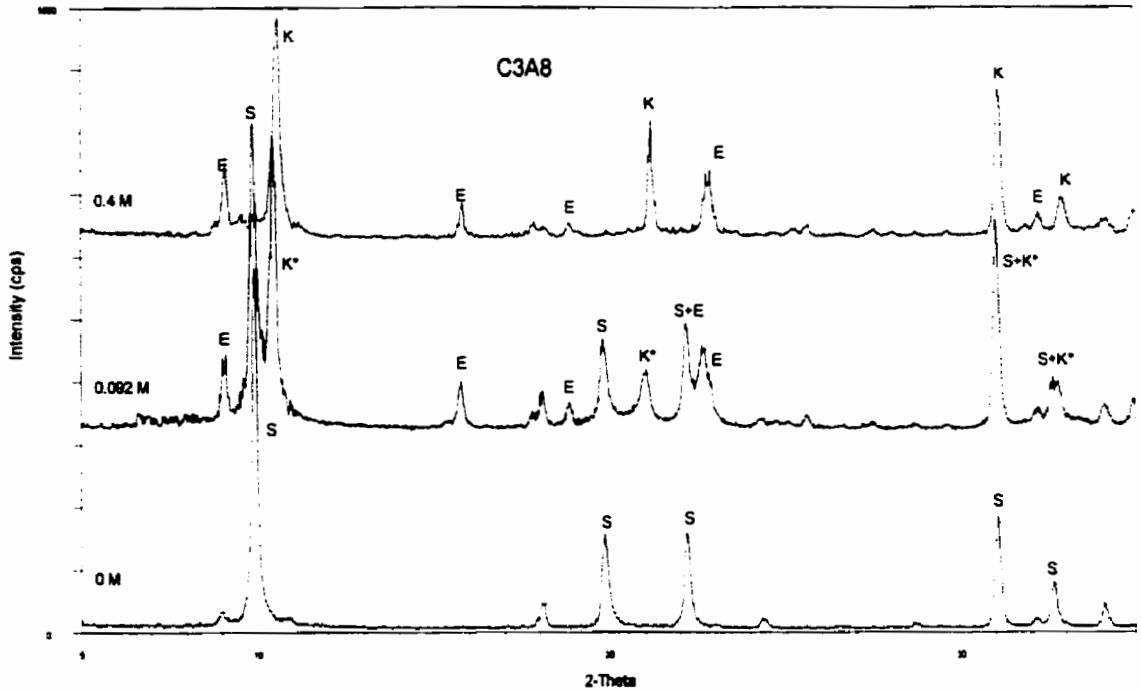


Figure 4-100: XRD patterns of samples of the $C_3A8$ paste that were exposed to 0, 0.5, and 1 M chloride solutions. The patterns are labeled with the equilibrium chloride concentrations of the corresponding samples. E: ettringite, K: Kuzel's salt, K*: Variation of K, S: monosulphate.

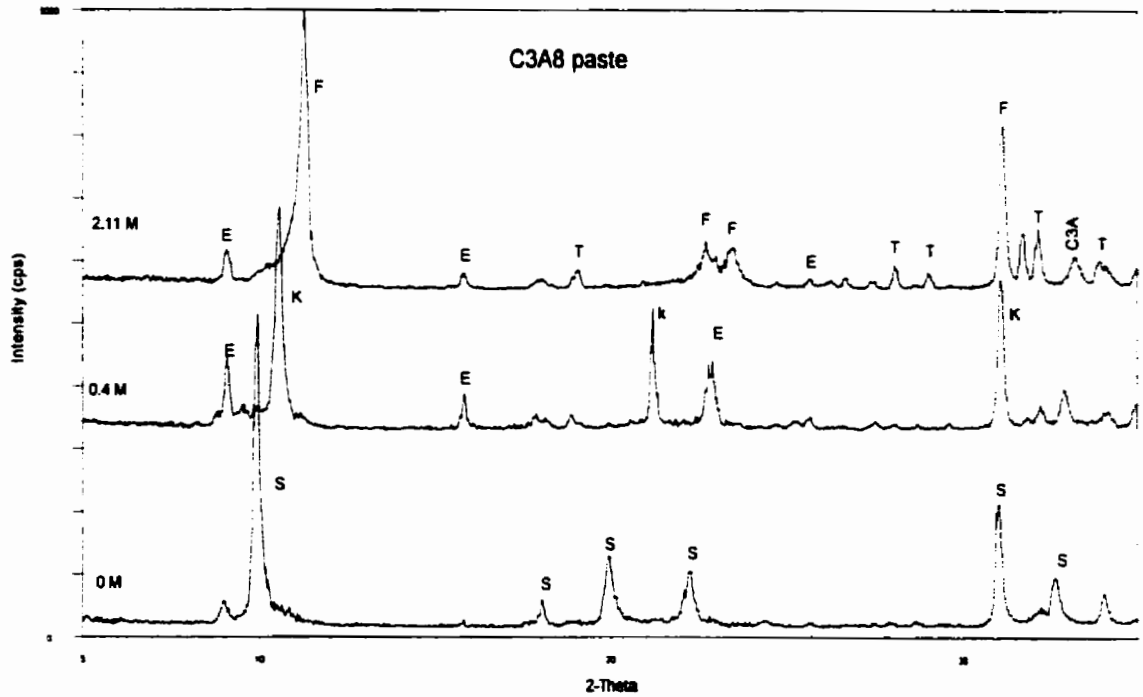


Figure 4-101: XRD patterns of samples of the $C_3A8$ paste that were exposed to 0, 1, and 3 M chloride solutions. The patterns are labeled with the equilibrium chloride concentrations of the corresponding samples. E: ettringite, F: Friedel's salt, K: kuzel's salt, S: monosulphate, T: thenardite.

Figure 4-102 show the XRD patterns of samples of the $C_4AF$ paste exposed to 0 M and 3 M chloride solutions. The dominant peaks at 0 M exposure were those of the ferrite equivalent of the monosulphate phase, $C_3F.CaSO_4.12H_2O$. There was also a presence of peaks corresponding to other calcium alumino-ferrite hydrates including those of the $C_3FH_6$. The monosulphate peaks almost disappear at 3 M exposure, and the most dominant peaks were those of the ferrite equivalent of Friedel's salt, $C_3F.CaCl_2.10H_2O$, indicating the transformation of $C_3F.CaSO_4.12H_2O$ into $C_3F.CaCl_2.10H_2O$.

Figure 4-103 compares the XRD patterns of samples of the $C_3A8$ paste that were exposed to 3 M NaCl solutions with different pH levels. As mentioned before, the composition of the exposure solutions were different. While one solution was saturated with $Ca(OH)_2$ to obtain a pH of 12.5, NaOH was used in the other solution to obtain a pH of 14. The main difference between the two patterns is that the peaks of the $Ca_8Al_4O_{12}Cl_2SO_4.24H_2O$ phase were still present in the XRD pattern of the sample exposed to the solution with the higher pH. This means that this sample was still less saturated with chloride than the one exposed to the lower pH solution. It also explains its

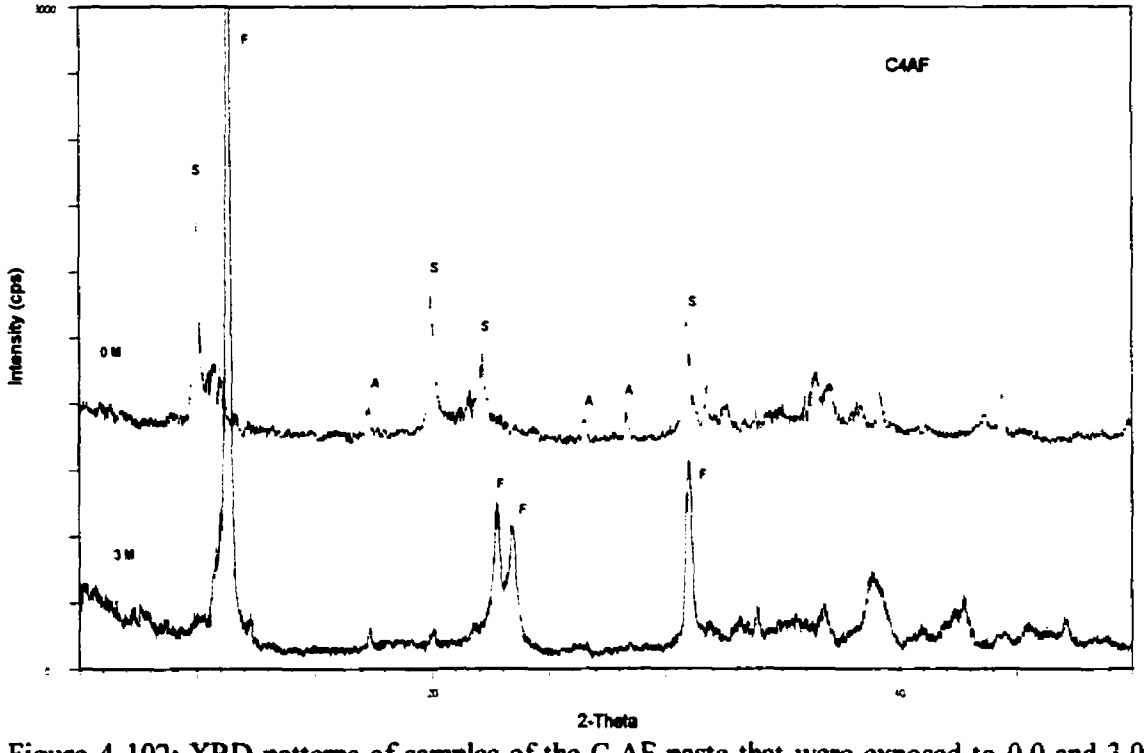


Figure 4-102: XRD patterns of samples of the $C_4AF$ paste that were exposed to 0.0 and 3.0 M chloride solutions. A: katoite ($C_3AH_6$), F: Friedel's salt (iron equivalent), S: monosulphate.

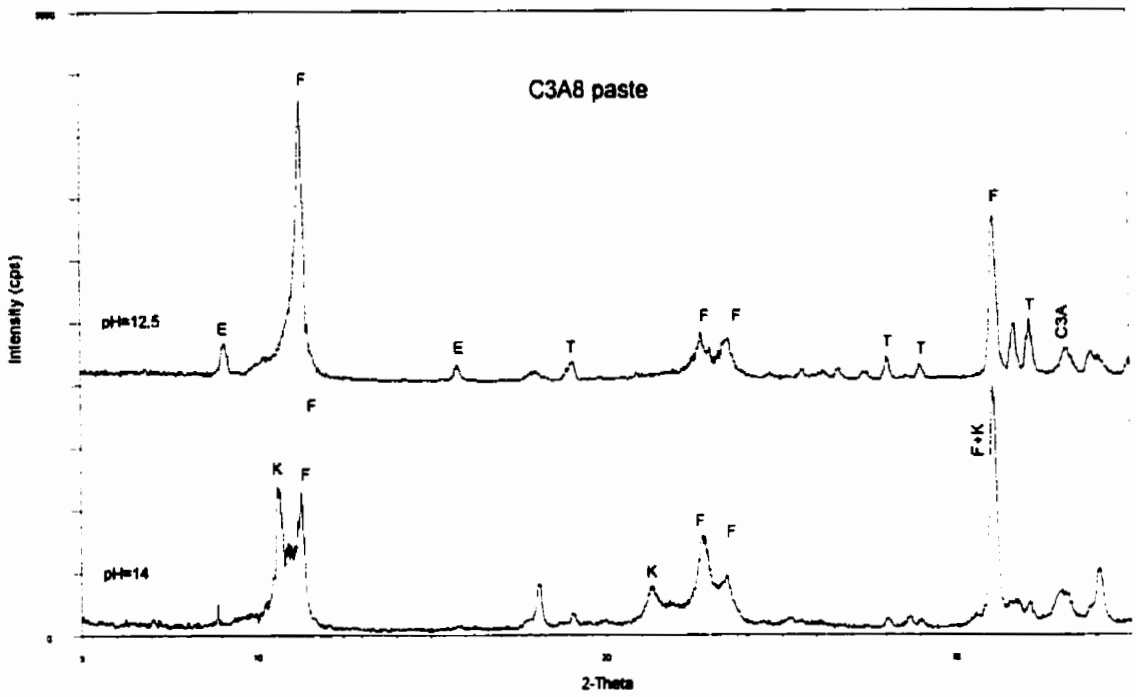


Figure4-103: Comparison between XRD patterns of samples of the $C_3A8$ paste exposed to 3.0 M chloride solutions with different pH values. E: ettringite, F: Friedel's salt, K: Kuzel's salt, T: thenardite.

lower binding capacity compared to that of the sample exposed to the lower pH solution. It is not known, however, why the higher pH of the exposure solution did cause the $Ca_8Al_4O_{12}Cl_2SO_4.24H_2O$ phase to persist more at high chloride concentration, and not transform to Friedel's salt.

Figure 4-104 compares the XRD patterns of samples of the $C_3A8$ paste that were exposed to 3 M NaCl solutions with different sulphate ion concentrations. As mentioned before, the composition of the exposure chloride solutions were different. While the chloride solution with 0.1 M $[SO_4^{2-}]$ had $Na_2SO_4$ to get the desired sulphate concentration, and NaOH to get the desired pH, the chloride solution with 0 M $[SO_4^{2-}]$ was saturated with $Ca(OH)_2$ to get the desired pH. This difference in composition might have had an influence in addition to the influence of sulphate ion concentraion. It is unfortunate that there was not enough materials for an extra sample to be prepared with a chloride solution containing NaOH instead of $Ca(OH)_2$.

The main difference that might explain the lower binding capacity of the sample exposed to 0.1 M $[SO_4^{2-}]$, is the presence of peaks of the $Ca_8Al_4O_{12}Cl_2SO_4.24H_2O$ phase in its XRD patterns. This indicates that it is less saturated with chloride than the one exposed to 0 M $[SO_4^{2-}]$, since the

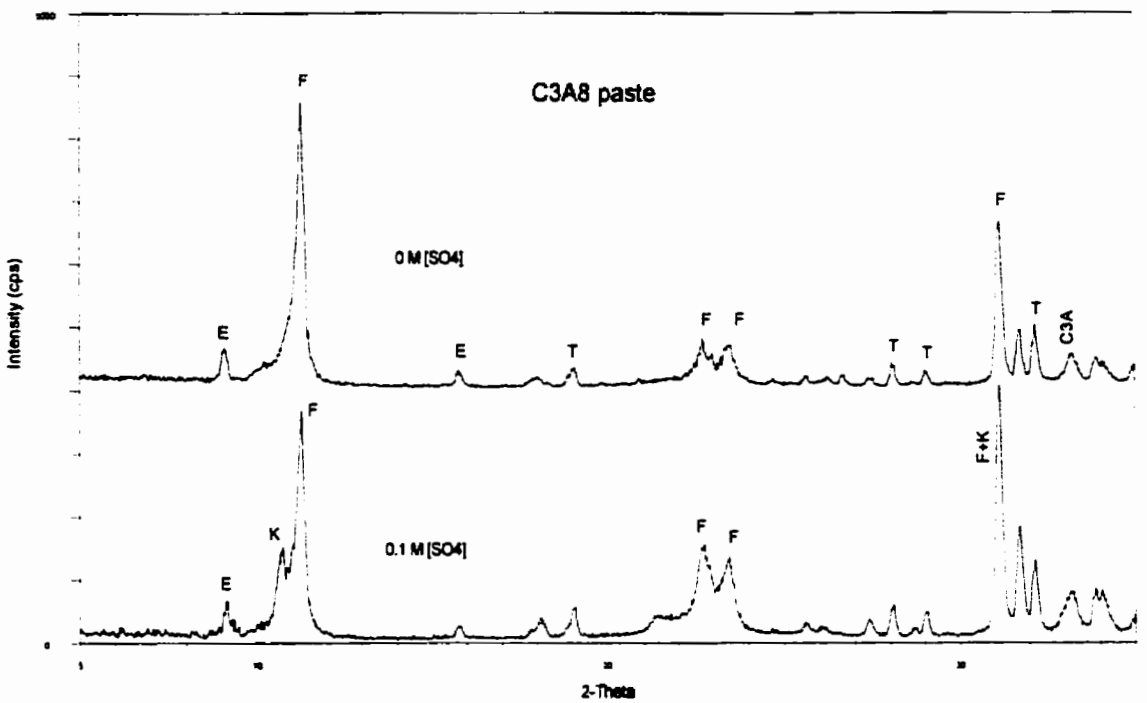


Figure 4-104: Comparison between XRD patterns of samples of the $C_3A8$ paste exposed to 3.0 M chloride solutions containing no sulphate or 0.1 M sulphate ion concentrations. E: ettringite, F: Friedel's salt, K: Kuzel's salt, T: thenardite.

XRD pattern of the latter shows that the monosulphate phase has almost totally converted into Friedel;'s salt. The persistence of the $Ca_8Al_4O_{12}Cl_2SO_4.24H_2O$ phase at 3 M [NaCl] exposure in the case of the sample exposed to 0.1 M [$SO_4^{2-}$] is probably due to the high sulphate ion concentration in the solution, which makes this phase more stable at 3 M NaCl concentration.

Figure 4-105 shows the XRD patterns of samples of the PC1-10$C_3A$ paste exposed to several chloride concentrations. At 0 M exposure, the maximum peak of the monosulphate phase is the most noticeable of the calcium aluminate hydrates. This peak was substantially reduced at 0.1 M exposure, and new peaks appeared. It was hard to confirm the existence of Friedel's salt at 0.1 M exposure since the corresponding peaks did not increase compared to those at 0 M exposure. Therefore, these peaks could have been those of the $C_4AH_{13}$ phase. A group of the newly formed peaks at 0.1 M exposure were very close, in terms of their d spacing, to those of the $Ca_8Al_4O_{12}Cl_2SO_4.24H_2O$ phase, but with a slight shift to the left. Since the monosulphate's maximum intensity peak was reduced following the sample's exposure to chloride solution, the monosulphate phase was most probably transformed into a chloride bearing phase. In addition, the

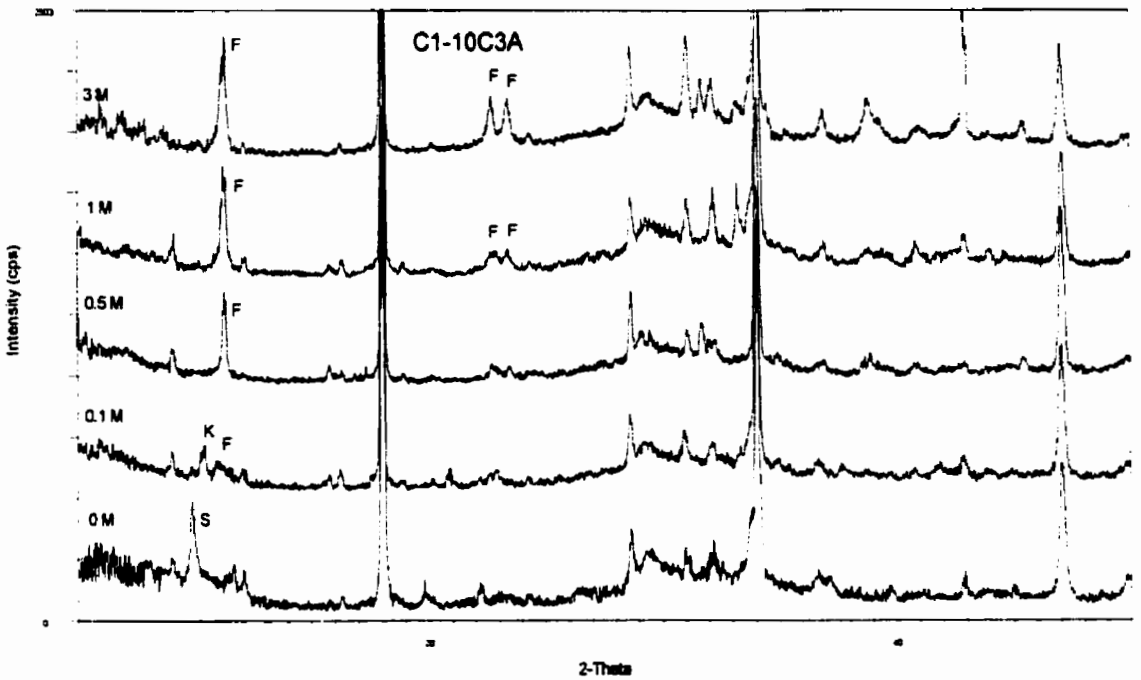


Figure 4-105: XRD patterns of samples of the C1-10$C_3$A paste that were exposed to different chloride concentrations. F: Friedel's salt, K: Kuzel's salt, S: monosulphate.

results of the XRD patterns of the $C_3A$ pastes showed the formation of this phase at lower chloride concentrations before the eventual formation of Friedel's salt. Since there is no known phase containing sulphate and chloride ions other than the $Ca_8Al_4O_{12}Cl_2SO_4.24H_2O$ phase, it is reasonable to assume that those peaks are in fact those of the $Ca_8Al_4O_{12}Cl_2SO_4.24H_2O$ phase, although there is no explanation for the slight shift. The fact that these peaks did not appear at 0.5 M exposure is another indication that they correspond to a phase containing chloride other than Friedel's salt. This phase did not form at 0.5 M exposure, and instead, Friedel's salt was formed. The Friedel's salt peaks were relatively large at 0.5 M exposure, and there were no signs of the monosulphate peaks indicating that the monosulphate phase was transformed into Friedel's salt. Similar observations can be made of the XRD pattern at 1 M exposure, except that the Friedel's salt peaks were larger than those at 0.5 M exposure.

At 3 M exposure, there was a decrease in the ettringite peaks in addition to the substantial decrease in the monosulphate peaks. There was also an increase in the Friedel's salt peaks compared to those at 1 M exposure. The reduction in the ettringite peaks is consistent with earlier observations of this reduction in the XRD patterns of other cement pastes at 3 M exposure.

Figure 4-106 compares between the XRD patterns of samples of the C7 and C7-7$C_4AF$ pastes that were exposed to 3 M chloride solutions. These patterns show that the maximum intensity peak of Friedel's salt was slightly higher in the C7-7$C_4AF$ sample, indicating the effect of the pure $C_4AF$ addition on the binding capacity.

Finally, there were no differences noted between the XRD patterns of samples of the $C_3S$ paste that were exposed to chloride solutions of different compositions, as shown in Figure 4-107.

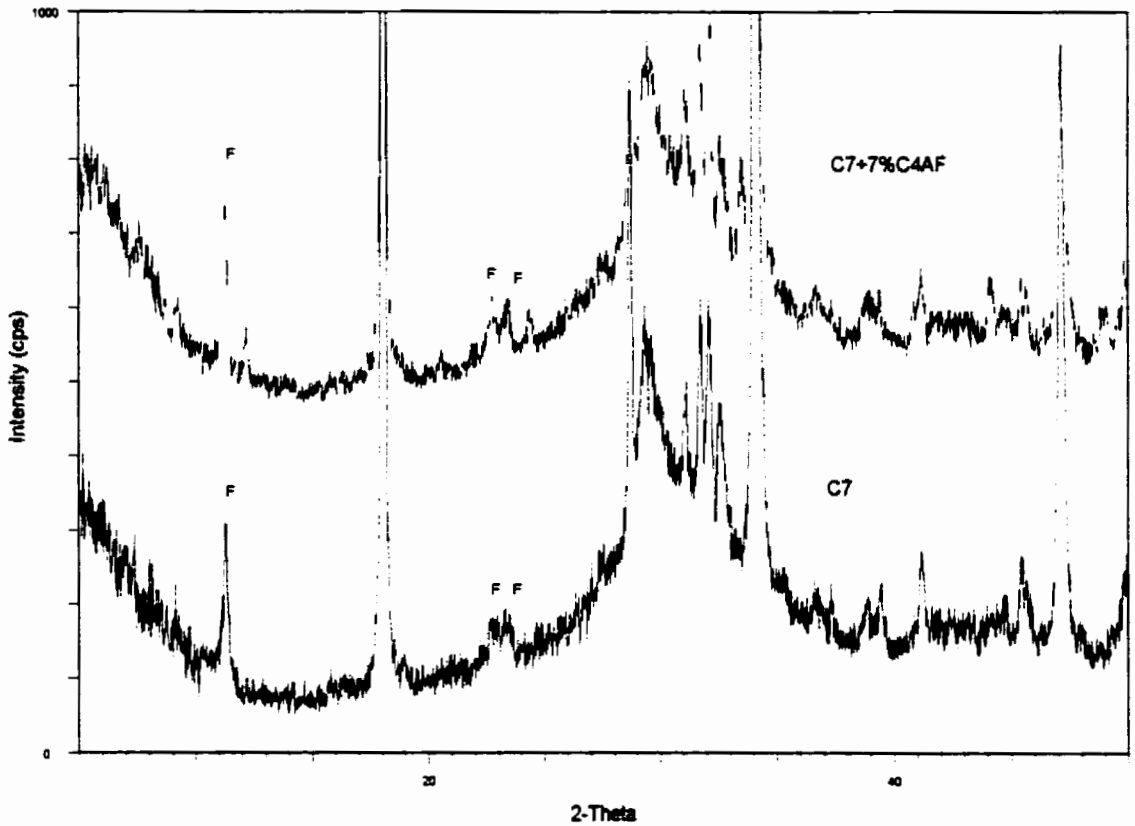


Figure 4-106: Comparison between the XRD patterns of samples of the C7 paste and the C7-7$C_4AF$ paste that were exposed to 3 M chloride solutions. F: Friedel's salt.

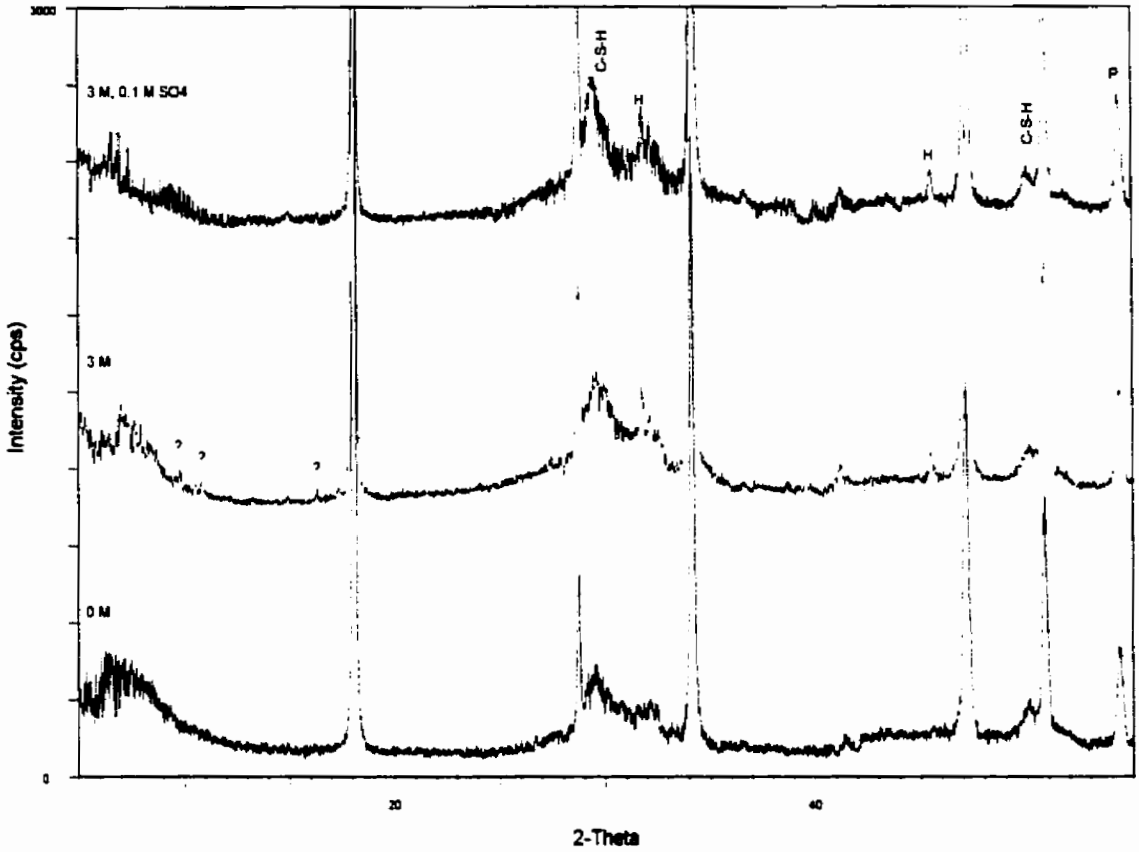


Figure 4-107: Comparison between the XRD of samples of the $C_3S$ paste exposed to chloride solutions of different concentrations or different compositions. P: portlandite, H: Halite.

# CHAPTER 5

# DISCUSSIONS

## 5.1 Mechanisms of Chloride Binding

This discussion focuses on the chloride binding mechanisms through chemical reactions between the cement hydrates and the chlorides. By re-examining the XRD results of the cement pastes and the $C_3A$ pastes, and analyzing the important transformations or phase changes that took place, we reach a better understanding of the mechanisms involved in chemical chloride binding in cement pastes. First, the XRD patterns of the $C_3A4$ and the $C_3A8$ pastes are re-examined. This is followed by highlighting the main observations from the XRD patterns of some of the tested cement pastes. Then, a comparison is done between the findings from both sets. Finally, some observations are made regarding the chloride binding process. It is the author's opinion that the listed observations in this discussion represent one of the most significant contribution of this thesis to the subject of study.

Figures 4-100 to 4-102 of the XRD patterns of the $C_3A4$ and $C_3A8$ pastes showed the gradual changes in peaks that took place with the increase in chloride concentration. These changes reflected the phase transformations that took place, in which the C-A-H converted into chloride bearing phases as the chloride concentration increased. These phase transformations are presented in Figures 5- 1 and 5-2. In these figures, the data points for each phase were obtained using the "maximum intensity peak" corresponding to that phase, and presenting it as a percentage of its highest value in the concentration range tested. Based on the above mentioned figures, the following observations can be made:

a) Many C-A-H phases were involved in binding chlorides. There was clear evidence of the transformation of several phases into Friedel's salt ($C_3A.CaCl_2.10H_2O$), including $C_3AH_6$, $C_4A\bar{S}H_{12}$ (or $C_3A.C\bar{S}.12H_2O$), and $C_4AH_x$. These phases transformed at different rates depending on the chloride concentrations.

b) Contrary to what is commonly believed, the monosulphate phase started to transform in the presence of chlorides. This transformation was gradual and concentration dependent. The transformation started a low chloride concentrations, and the $C_6A_2.C\bar{S}.CaCl_2.24H_2O$ phase (Kuzel's salt) was formed and not Friedel's salt. The formation of the $C_6A_2.C\bar{S}.CaCl_2.24H_2O$

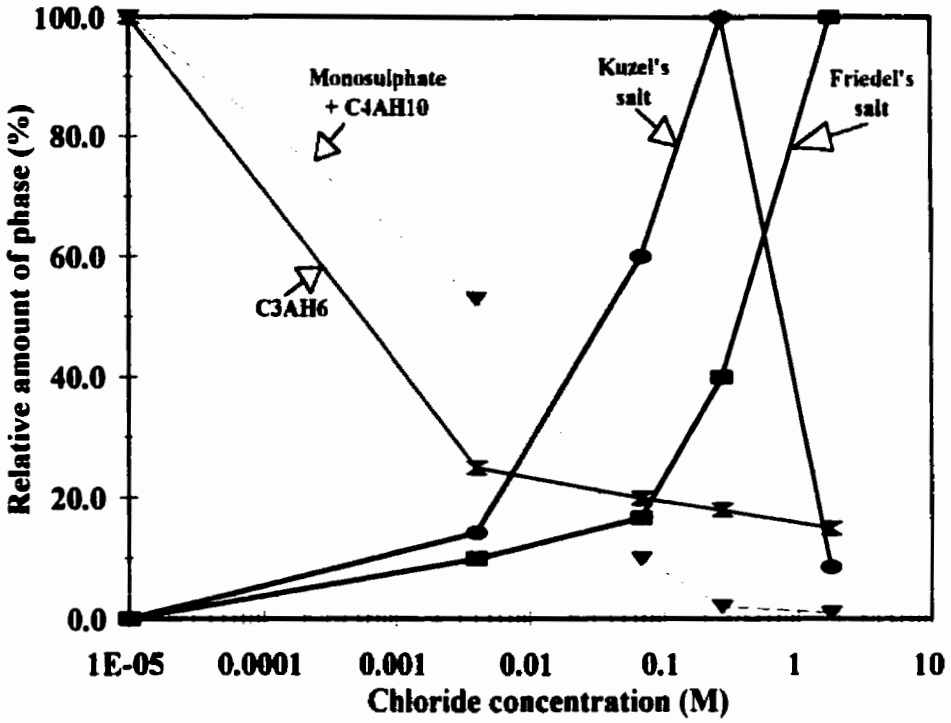


Figure 5-1: Phase transformations in the $C_3A4$ paste with increasing chloride concentration in the host solution.

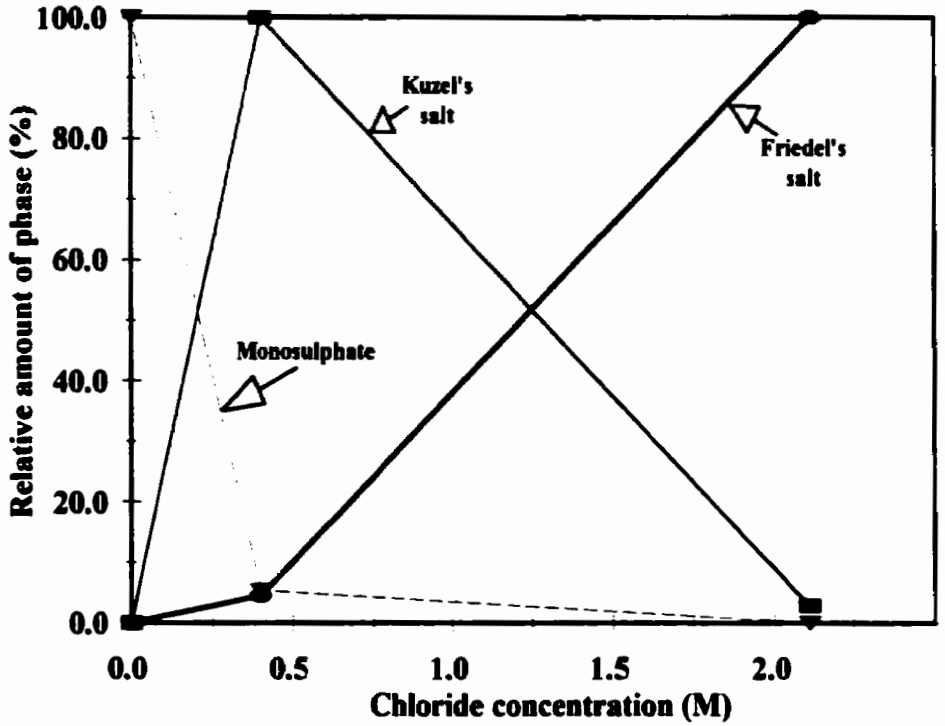


Figure 5-2: Phase transformations in the $C_3A8$ paste with increasing chloride concentration in the host solution.

phase continued at higher chloride concentrations (0.4 M in the $C_3A$ paste), and it seems that the monosulphate fully transforms into the $C_6A_2.C\bar{S}.CaCl_2.24H_2O$ phase before the final transformation into Friedel's salt at high concentration.

c) Friedel's salt formed at very low concentrations in the $C_3A4$ paste, and gradually increased with increasing concentrations. However, the $C_6A_2.C\bar{S}.CaCl_2.24H_2O$ phase had a dominant presence, in both the $C_3A4$ and the $C_3A8$ pastes, in the lower chloride concentration range. In fact, there was almost no presence of Friedel's salt in the $C_3A8$ paste at chloride concentrations as high as 0.4 M. Hence, the $C_6A_2.C\bar{S}.CaCl_2.24H_2O$ phase was a major compound incorporating chlorides at low concentrations.

d) There was evidence from the XRD patterns of the $C_3A8$ pastes to suggest that the ettringite phase might partially transform into Friedel's salt in the presence of chlorides at high concentrations (>2 M).

The results of the $C_3A$ pastes revealed very interesting facts related to chemical binding, but they also indicated the need for more testing to help in better understanding the chemical binding. In particular, it is recommended that two extreme cases should be examined: a pure $C_3A$ paste (100% $C_3A$), and a pure ettringite paste (100% ettringite). The testing of the $C_3A$ paste (100% $C_3A$) would provide information on the binding capacity of C-A-H not containing sulphate ($C_3AH_6$, $C_4AH_{10}$) including their rate of transformation into Friedel's salt as a function of chloride concentration. It could also provide information on whether these phases would be fully converted (maximum binding capacity) below 3M chloride concentrations. Testing of the ettringite paste would provide important information on the binding capacity of ettringite as a function of chloride concentration. It might also provide important information on whether the chemical binding capacity is limited to the formation of chemical compounds bearing chlorides, or also involves other mechanisms such as chemisorption. In addition, a larger number of chloride concentrations should be tested in the 0 M - 3 M concentration range, especially at the higher concentrations, to provide more detailed information about the transformations that occur during chloride binding.

The XRD patterns of several cement pastes, examined in Chapter 4 (Section 4.1.7.10), showed that many of the phenomena that were observed in the $C_3A4$ and $C_3A8$ pastes were also observed in some of those cement pastes. They are summarized in the following:

d) In addition to many C-A-H phases which were involved in chloride binding, the

monosulphate phase started binding chloride at low chloride concentrations as can be seen in the XRD patterns of the C6, 8MK, and C1-10$C_3A$ pastes (and probably the C4 paste) (Figures 4-67, 4-21, 4-96, 4-69). There was also some evidence of formation of the $C_6A_2.C\bar{S}.CaCl_2.24H_2O$ phase at low concentrations in the case of the C6 paste and the C1-10$C_3A$ paste (and probably the C4 paste) (Figures 4-67, 4-96, 4-69).

e) Friedel's salt formed at low chloride concentration (0.1 M exposure). This was clear in the case of the C4 and C6 pastes (Figures 4-69, 4-67) which had low $SO_3$ contents. However, from XRD patterns, it was not possible to know with certainty whether small amounts of Friedel's salt had formed in other pastes. At higher chloride exposures, the formation of Friedel's salt was clear as in the case of the control and the C1 pastes (Figures 4-16, 4-65). Friedel's salt increased with the increase in chloride concentration in all the examined cement pastes. This indicates that the chemical binding capacity was concentration dependent. Also, the chemical binding capacity was still unexhausted at high concentrations (> 1.0 M).

f) There was enough evidence to suggest that the ettringite phase did become unstable at high concentrations (> 2.0 M) and partialy decomposed to give Friedel's salt. This was clearly seen in the case of the control, C1, C7, C1-10$C_3A$, and C4-7$SO_4$ pastes (Figures 4-65, 4-66, 4-96, 4-70).

These results show that despite the differences in composition between the pure $C_3A$ pastes and the cement pastes, there were many similarities in their behaviour regarding the chemical binding of chlorides. The XRD of the $C_3A$ pastes proved to be invaluable to the understanding of some of the processes involved in the chemical binding of chlorides. It clearly revealed some of the transformations, also observed in the cement pastes, that led to the chemical binding of chlorides. These results, along with those of the cement pastes, provide insight into some of the mechanisms of chloride binding. The following observations are made regarding the chloride binding process:

h) The chemical binding capacity (formation of chloride products) was a gradual process that was a function of the chloride concentration. The dependence of the chemical binding capacity on chloride concentration stems from the fact that several C-A-H phases (including monosulphate and ettringite), involved in chloride binding, transformed to Friedel's salt at

different rates and in different chloride concentration ranges. The increase in the peaks of Friedel's salt between 1.0 M and 3.0 M exposures (all examined pastes) indicated that the chemical binding capacity was not exhausted at low concentrations and kept increasing at concentrations above 1.0 M in a similar way to the total binding capacity.

i) The sulphate content of cement played an important role in the chemical binding capacity at low chloride concentrations. Higher contents of sulphates in cements led to the formation of more monosulphate or ettringite or both. This reduced the amount of Friedel's salt. because of the lower chloride binding capacity of these phases at low chloride concentrations (ettringite had seemingly no binding capacity and monosulphate transformed to the $C_6A_2.C\bar{S}.CaCl_2.24H_2O$ phase at low chloride concentration). This might explain the results of the mutivariable analysis in Chapter 4 (Section 4.2.1.1) which revealed a poor correlation between the $C_3A$ content and the binding capacity at low chloride concentrations, while there was a good correlation between a combination of the $SO_3$ and $C_3A$ and the binding capacity of cement. It can also explain why the C2 and C3 pastes (high $SO_3$ contents) had lower binding capacities than the control and C5 pastes at 0.1M despite having higher $C_3A$ contents than those pastes. At higher chloride concentrations (eg 1.0 M, 3.0 M), the influence of sulphate decreased since the monosulphate transformed into Friedel's salt and ettringite started to transform at high concentrations (between 2.0 M and 3.0 M). This might explain the good correlation between the $C_3A$ content and the binding capacity of cement at high concentrations (eg 1.0 M, 3.0 M). Hence, it is suggested that the importance of $C_3A$ in relation to the chloride binding capacity is concentration dependent. While it is generally a decisive factor at high chloride concentrations, its importance at low concentration is related to the $SO_3$ content of cement. When the $SO_3$ content is lower, the $C_3A$ content becomes more influential on the binding capacity, and when the $SO_3$ content is higher, the $C_3A$ content becomes less influential.

## 5.2 Roles of Cement Phases in Chloride Binding:

### 5.2.1 Introduction:

The results of this research, as presented in Chapter 4, provide a good background for the following general discussion about the role of the individual phases in chloride binding. This discussion is two parts. In part one, the roles of the individual cement phases are examined in the light of the results of the various parts of this research, including those of the pure phases and the cement pastes as well as other results that are relevant to the discussion. In part two, an attempt is made to quantify the roles of the different cement phases. This is done by using the binding capacities of the pastes made of the pure phases to predict the contribution of the individual cement phases to the binding capacity.

### 5.2.2 Role of $C_3A$:

Regarding the role of the $C_3A$ phase, there was a lot of evidence indicating that the $C_3A$ content of cement plays an important role in the chloride binding capacity. The pastes produced with "pure" $C_3A$ ($C_3A4$ and $C_3A8$) exhibited substantial binding capacities which were much higher than those produced with "pure" $C_3S$ and $C_2S$ pastes as shown in Figure 5-3. However, while these results showed the substantial binding capacity of the pure $C_3A$ phase, they did not provide a realistic estimate of the contribution of the $C_3A$ phase in cement to the chloride binding capacity. The reasons for this were the high $C_3A$ contents in the $C_3A$ pastes (63% in the $C_3A8$ paste and 75% in the $C_3A4$ paste). That is why the substitution of the C1 cement (0% $C_3A$ content) with 6% and10% pure $C_3A$ was a more realistic test for determining the role of $C_3A$ phase in the binding capacity of cement. The results of this test showed the large increases in the binding capacities of the resulting cements, C1-6$C_3A$ and C1-10$C_3A$, in comparison with the C1 cement (Figure 4-96). Table 5-1 shows the percentage increase in the binding capacities at different chloride concentrations. The contributions of the pure $C_3A$ phase to the binding capacities were estimated by assuming that the increases in the binding capacities of the C1-6$C_3A$ and C1-10$C_3A$ pastes were due to the pure $C_3A$. These results showed an important contribution of the $C_3A$ phase to the binding capacities of these pastes (45% and 60% respectively). The results of Section 4.2.1.1 on the binding capacities of several cement pastes showed the good correlation between the $C_3A$ content of cement and the chloride binding capacity at high chloride concentrations. In fact, the $C_3A$ content was the only single parameter that correlated well with the binding capacity at high concentrations.

Table 5-1: Comparison between the chloride binding capacities of the C1, C1-6$C_3A$, C1-10$C_3A$ pastes at different chloride concentrations.

| NaCl sol. Conc. (M) | Bound Chloride (mg Cl/g sample) | | | Increase in Binding (mg Cl/g sample) | | % Increase in Binding Compared to C1 | | % Contribution of $C_3A$ to Binding* | |
|---|---|---|---|---|---|---|---|---|---|
| | C1 | C1+ 6% $C_3A$ | C1 + 10%$C_3A$ | C1 + 6%$C_3A$ | C1 + 10%$C_3A$ | C1 + 6%$C_3A$ | C1 + 10%$C_3A$ | C1 + 6%$C_3A$ | C1 + 10%$C_3A$ |
| 0.1 | 2.80 | 5.05 | 6.75 | 2.25 | 3.95 | 80.3 | 141.1 | 44.6 | 58.5 |
| 1.0 | 6.20 | 11.18 | 15.34 | 4.98 | 9.14 | 80.3 | 147.4 | 44.5 | 59.6 |
| 3.0 | 9.08 | 16.35 | 22.70 | 7.27 | 13.62 | 80.1 | 150.0 | 44.5 | 60.0 |

* The contribution of the $C_3A$ phase was estimated by assuming that the increase in binding was due to the $C_3A$ substitution.

This, however, was not the case at low concentrations. The $C_3A$ content had a poor correlation with the binding capacity. But, a combination of the $C_3A$ and $SO_3$ contents correlated well with the binding capacity, suggesting an influence of the $SO_3$ content on the effectiveness of the $C_3A$ phase in binding chlorides, especially at low concentrations. The XRD results of the cement pastes and

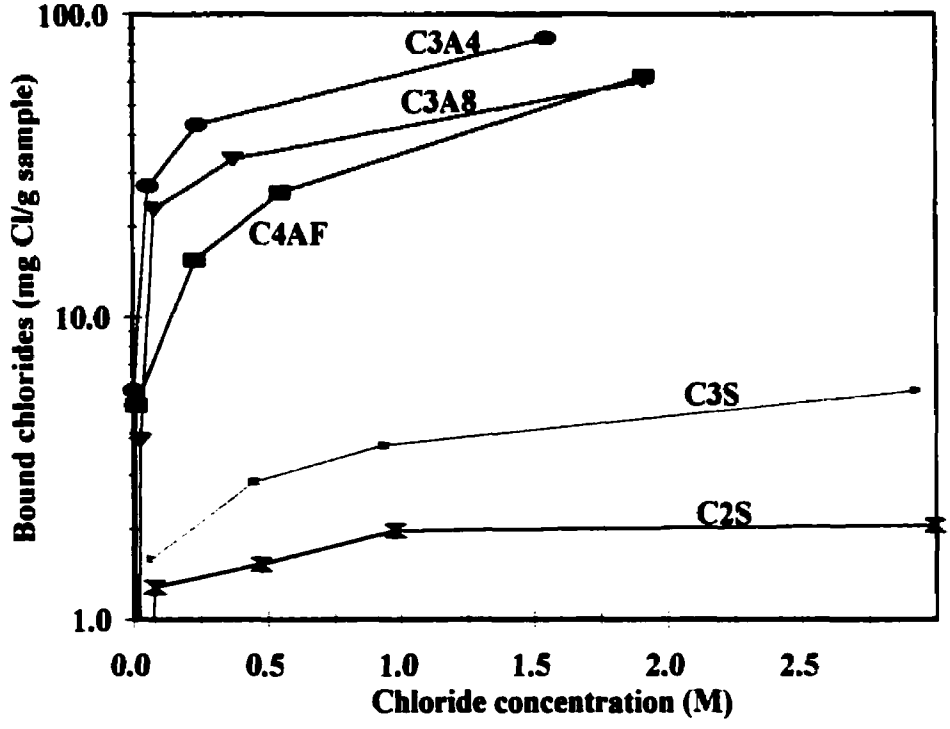


Figure 5-3: Chloride binding isotherms of pastes made from pure cement phases

the $C_3A$ pastes confirmed the effect of the SO on the binding capacity of the C A at low concentrations. The XRD results of the cementitious pastes also showed the correlation between the maximum intensity peaks of the Friedel's salt phase and the chloride binding capacity at high concentrations as shown in Figure 5-4, confirming the results of the statistical study that showed the importance of the $C_3A$ phase at high concentrations. Finally, the results of Section 4.2.1.2, on the effect of the $SO_3$ content on the binding capacity of cement, showed a large reduction in the binding capacity of C4-7$SO_3$ paste, compared to that of the C4 paste, resulting from the substitution of the C4 cement with 7% $SO_3$ (Table 5-2) This reduction was attributed mostly to the chemical binding capacity (mostly caused by the $C_3A$ content), since it was assumed that the sulphate would initially

Table 5-2: Comparison between the binding capacities of the C4 and C4-7$SO_3$ cement pastes.

| NaCl sol. Conc. (M) | Bound Chloride (mg Cl/g sample) | | % Decrease in Binding Compared to C4 |
|---|---|---|---|
| | C4 | C4-7$SO_3$ | |
| 0.1 | 5.93 | 2.16 | 63.6 |
| 1 | 12.24 | 5.95 | 51.4 |
| 3 | 17.30 | 9.65 | 44.2 |

combine with the $C_3A$ and the $C_4AF$ phases to form ettringite and monosulphate prior to chloride exposure. The XRD results of the C4-7$SO_3$ paste (Figure 4-70) showed the formation of a large maximum intensity peak corresponding to the ettringite phase. These XRD results also showed the formation of Friedel's salt peaks at 1.0 M and 3.0 M chloride exposures, indicating a contribution of the chemical binding capacity to the binding capacity of the C4-$SO_3$ paste. This was expected since the added sulphate was not enough to combine with all the $C_3A$ and $C_4AF$ phases to form ettringite. These results showed the major role of the $C_3A$ phase in the binding capacity of the C4 paste.

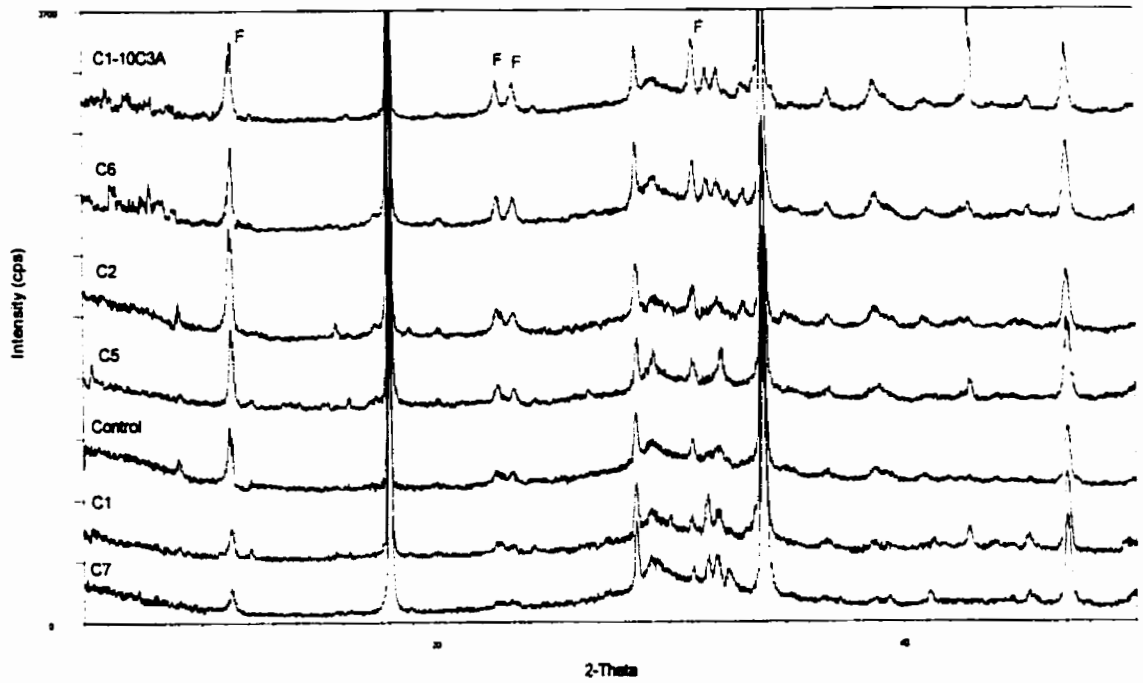


Figure 5-4: XRD patterns of various cement pastes, placed in order of increasing binding capacities (bottom to top), show a correlation between the binding capacity and Friedel's salt peaks (especially peaks different than the maximum intensity peak)

### 5.2.3 Role of $C_4AF$:

In the case of the $C_4AF$ phase, there was evidence indicating that the $C_4AF$ plays a notable role in chloride binding. The pure $C_4AF$ paste had a very high binding capacity as shown in Figure 5-3. The substitution of the C7 cement with 7% pure $C_4AF$ resulted in a small but significant increase in the chloride binding capacity of the resulting paste over that of the C7 paste as shown in Table 5-3. The best evidence, however, of an effective role of the $C_4AF$ phase in chloride binding came from

Table 5-3: Comparison between the binding capacities of the C7 and C7-7$C_4AF$ cement pastes.

| NaCl sol. Conc. (M) | Bound Chloride (mg Cl/g sample) | | Increase in Binding Compared to C7 (mg Cl/g sample) | % Increase in Binding Compared to C7 |
|---|---|---|---|---|
| | C7 | C7-7$C_4AF$ | | |
| 0.1 | 2.97 | 3.43 | 0.46 | 15.5 |
| 0.5 | 5.70 | 7.06 | 1.36 | 23.9 |
| 1 | 7.77 | 9.95 | 2.18 | 28.1 |

tests performed on the C1 cement. The XRD patterns of samples of the C1 paste, exposed to different chloride concentrations (Figure 4-65), showed the formation of Friedel's salt peaks. However, since the $C_3A$ content of the C1 cement was 0% (Bogue calculation), it was suggested that these peaks were those of the iron equivalent of Friedel's salt, $C_3F.CaCl_2.10H_2O$. This was the most direct proof of the role of $C_4AF$ in chloride binding. The results of the test of the effect of the $SO_3$ content on the binding capacity of C1 cement (Section 4.2.1.2) showed that the substitution of the C1 cement with 4% $SO_3$ (added as gypsum) reduced the the binding capacity of the resulting mixture, C1-4$SO_3$, by half compared to that of the C1 cement, as shown in Table 5-4. This reduction is mostly attributed to the reduction in the chemical binding capacity of the C1-4$SO_3$, since it was assumed that the sulphate would combine with all the $C_4AF$ phase to form ettringite prior to chloride

Table 5-4: Comparison between the binding capacities of the C1 and C1-4$SO_3$ cement pastes.

| NaCl sol. Conc. (M) | Bound Chloride (mg Cl/g sample) | | % Decrease in Binding Compared to C1 |
|---|---|---|---|
| | C1 | C1-4$SO_3$ | |
| 0.1 | 2.80 | 1.29 | 53.9 |
| 1.0 | 6.20 | 3.29 | 46.9 |
| 3.0 | 9.08 | 5.15 | 43.3 |

exposure, eliminating the chemical binding capacity. Hence, the reduction noted in Table 5-4 is an indirect measure of the chemical binding capacity of the C1 cement, which in this case, is the binding capacity of the $C_4AF$ phase. This showed the important role of the $C_4AF$ phase in the binding capacity of the C1 cement.

### 5.2.4 Role of $C_3S$,$C_2S$

The role of the silicate phases ($C_3S$, $C_2S$) in chloride binding was more difficult to elucidate since it is very difficult to prove the existence of that role through direct evidence from cement pastes. It is believed that these phases bind chloride mostly by physical adsorption on their surfaces, but there is no experimental procedure to prove that this adsorption is taking place, unlike the case of the

calcium aluminate-ferrite phases where the existence of chemical chloride binding can be proved by the presence of Friedel's salt through XRD and DTA tests. The use of SEM is unreliable since the sample preparation involves drying, and this results in the deposition of any chlorides, that were in the pore solution, on the surfaces of the CSH gel. Thus, the distinction between adsorbed or deposited chloride becomes very difficult. That is why the study of the pure $C_3S$ and $C_2S$ phases was the main source used to examine the role of these phases in chloride binding in cement phases. The results of Section 4.3.2.1 showed that the $C_3S$ and $C_2S$ pastes bind noticeable amounts of chloride, but their binding capacities were much lower than those of the $C_3A$ pastes and the $C_4AF$ paste as shown in Figure 5-3. But, it should be kept in mind that the hydrates of the silicates phases constitute 80% to 90% of the amount of cement hydrates. Therefore, assuming that the $C_3S$ and $C_2S$ phases in cement have the same binding properties as the pure $C_3S$ and $C_2S$ phases, this contribution is relatively meaningful when the actual binding capacities of the different cements are taken into account. The results of Section 4.2.1.2 (Table 5-4) may have possibly provided the best proof of a significant (and maybe a major role in the case considered) role of the $C_3S$ (and $C_2S$) phase in chloride binding. As mentioned in the previous paragraph, it was assumed that the chemical binding capacity of the C1-4$SO_3$ paste was mostly eliminated as a result of the sulphate substitution and formation of ettringite. This meant that, unless the ettringite can bind chloride in forms other than Friedel's salt, the chloride binding capacity of the C1-4$SO_3$ paste was mostly the $C_3S$ (and $C_2S$) binding capacity (at least until 1.0 M concentration). The results in Table 5-4 show that this binding capacity was indeed important, and was about 50% of the binding capacity of the C1 paste.

### 5.2.5 Estimation of the Contribution of $C_3A$, $C_4AF$, and ($C_3S$, $C_2S$):

In the second part of this discussion, an attempt is made to quantify the roles of the cement phases. The contribution of the different cement phases to the chloride binding capacities of 4 cement pastes were estimated. The chosen cement pastes represented a wide range of phase compositions. The following assumptions were made in order to estimate the contribution of each phase:

a) the chloride binding capacity of a cement is the sum of the chloride binding capacities of the different cement phases

b) the behavior of the cement phases is the same as the behavior of the correspondent pure

phases

c) the amounts of hydrates (% by mass) produced by the $C_3S$ and $C_2S$ phases are equal to their respective contents (% by mass) in the cement,

d) the amounts of hydrates produced by the $C_3A$ and $C_4AF$ phases is estimated from their respective contents (% by mass) in the cement and the pure mixtures (see Appendix D)

e) the chloride binding capacity of each phase is estimated from the Freundlich isotherm of the corresponding pure phase.

The results of these estimations are shown in Table 5-5. It is interesting to notice that the predicted binding capacities at 0.1 M chloride concentration were very close to the actual ones, while the predicted binding capacities at 3 M were higher than the actual ones. The estimates of the contribution of the $C_4AF$ phase were considered particulary high at 3 M, when taking into account the results of this research regarding the role $C_4AF$. This was partly responsible for the observed differences between the predicted and the actual binding capacities at high chloride concentration. These inaccuracies were kept in mind when interpreting these results.

It was obvious that these results revealed more interesting information about the cement phases than the simple examination of the binding isotherms of the pure phases. One of the more interesting observations shown in Table 5-5 is that the combined contribution of $C_3A$ and $C_4AF$ to the binding capacity at 0.1 M cannot account for the total binding capacities of the cement pastes. This supports earlier results that indicate a noticeable contribution of the C-S-H to the binding capacity of cement. According to these estimations, the contribution of the calcium silicate phases to the binding capacity was significant in normal Portland cements. In cements with low aluminate and ferrite, the calcium silicate phases had major contribution to the binding capacities. There was, however, no large variation in the amounts of bound chlorides (by the $C_3S$ and $C_2S$ phases) amongst the various cements. This was the result of the relatively small binding capacities of the $C_3S$ and $C_2S$ pastes, and the relatively small variations in the contents of the the calcium silicate phases of cements. This might explain the poor correlation between the silicate phase content and the binding capacity of cement that was seen in Section 4.2.1.1. On the other hand, due to the high binding capacities of the pure $C_3A$ pastes, and the relatively large variations in the $C_3A$ contents of the cements, the estimated amounts of chloride, bound by the $C_3A$ phase, showed large variations amongst the different cement pastes. These variations were decisive in determining the ranking of the overall binding capacities of the cements. This might possibly explain the good correlation

between the $C_3A$ content and the binding capacity at high concentrations as shown in Section 4.2.1.1.

The estimates of the rates of contribution of the silicate phases to the binding capacity varied between 20% to 55%. These rates were higher, the lower were the binding capacities of the cements. It is interesting to notice that the rates of contribution of the silicates to the binding capacity of the

Table 5-5: Estimated contributions of the cement phases to the chloride binding capacities of various cements.

| | | Contribution of Cement Phases to Binding | | | | | | Binding Capacity of Cement | | | |
|---|---|---|---|---|---|---|---|---|---|---|---|
| | | $C_3S + C_2S$ | | $C_3A$ | | $C_4AF$ | | Estimated † | | Actual ‡ | |
| Mix | [$Cl^-$] | 0.1 M | 3.0 M | 0.1 M | 3.0 M | 0.1 M | 3.0 M | 0.1 M | 3.0 M | 0.1 M | 3.0 M |
| C1 | Bound Chloride mg Cl/g sample | 1.4 | 4.0 | 0.0 | 0.0 | 1.4 | 13.2 | 2.8 | 17.2 | 2.79 | 9.08 |
| | %* | 50% | 44% | 0% | 0% | 50% | 145% | 100% | 189% | 100% | 100% |
| C7 | Bound Chloride mg Cl/g sample | 1.5 | 4.4 | 1.2 | 4.6 | 0.1 | 0.8 | 2.8 | 9.8 | 2.98 | 7.77 |
| | %* | 50% | 57% | 40% | 60% | 3% | 10% | 113% | 127% | 100% | 100% |
| C5 | Bound Chloride mg Cl/g sample | 1.2 | 3.4 | 2.2 | 7.3 | 0.8 | 8.2 | 4.2 | 18.9 | 4.38 | 13.31 |
| | %* | 27% | 26% | 50% | 55% | 18% | 62% | 96% | 142% | 100% | 100% |
| OPC | Bound Chloride mg Cl/g sample | 1.3 | 3.5 | 1.4 | 5.4 | 0.8 | 8.2 | 3.5 | 17.1 | 3.82 | 11.54 |
| | %* | 34% | 30% | 37% | 47% | 21% | 71% | 92% | 148% | 100% | 100% |
| C6 | Bound Chloride mg Cl/g sample | 1.3 | 3.6 | 3.7 | 12.0 | 0.6 | 5.4 | 5.6 | 21.0 | 5.82 | 16.59 |
| | %* | 22% | 22% | 64% | 72% | 10% | 33% | 96% | 127% | 100% | 100% |
| C2 | Bound Chloride mg Cl/g sample | 1.2 | 3.4 | 2.5 | 9.6 | 0.8 | 7.2 | 4.5 | 20.2 | 4.73 | 16.93 |
| | %* | 25% | 20% | 53% | 57% | 17% | 43% | 95% | 119% | 100% | 100% |

† The binding capacity is the sum of the estimated contribution of the different phases.

‡The binding capacities are calculated from the binding isotherms (Freundlich isotherms) of the different cements.

*The % contribution of the different phases are calculated with respect to the actual binding capacities of cements

C1 cement were close to those obtained in Table 5-4. suggesting that these numbers might be close to the actual contributions of the silicate phases to the binding capacity of the C1 paste. The contribution of the $C_3A$ phase varied between 0% and 70% with the average between 40% and 55% for the normal cement compositions.

As mentioned earlier. these estimations were made possible as a result of the several assumptions stated in the begining, and hence, these estimations are not accurate. When $C_3S$ hydrates in the presence of alumina or sulphate in cement pastes, and $C_3A$ hydrates in the presence of silica, it would be expected that the resulting hydrates would be influenced by the presence of these components. Also the actual cement phases differ from the pure ones, especially in the case of $C_4AF$, which contains up to 13% impurities (unlike the "pure" $C_4AF$ which is 99% pure). Nevertheless, these estimations provide approximate distributions of chlorides among the different phases in cements. They are also helpful in further analyzing the results of the 'pure" pastes in the light of other results obtained in this research, by revealing information which is difficult to detect by simply looking at the binding isotherms of the "pure" pastes.

To summarize. The results indicate that the contributions of the chemical ($C_3A$, $C_4AF$) and physical binding capacities ($C_3S$, $C_2S$) to the chloride binding capacity of cement are dependent on the chloride concentration and cement type, but are significant in most cases. The $C_3S$ (and $C_2S$) and $C_4AF$ phases bind noticeable amounts of chloride, and all four mineral phases contribute to the chloride binding capacity. The chloride binding capacity of the $C_4AF$ phase is markedly lower than that of the $C_3A$. In general, the $C_3A$ content (and chemical binding capacity) of cement play a decisive role in the chloride binding capacity at high concentrations, but not at low concentrations. The reason for this behaviour at low concentrations is partially linked to the effect of sulphate content of the cement. These findings represent another very significant contribution of this thesis to the subject of chloride binding.

**5.3 Role of Sulphates in Chloride Binding:**

The results of this research show that the presence of sulphates, whether in the chloride host solutions or as part of the cement composition, has a negative effect on the chloride binding capacity of cement. Sulphates in the cement mainly influence the chemical binding capacity of the cement. External sulphates, on the other hand, influence both the chemical and the physical binding capacities. The mechanisms of influence of sulphates that are part of the cement composition differ form those of external sulphates that enter in the pore solution of the hardened cement pastes.

Section 5.1 provided a discussion of how the sulphate content in cement influences the type and quantity of the calcium aluminate hydrates that are produced, and how this in turn influence the chemical binding capacity of cement especially at low chloride concentrations. In the case of external sulphates, the results of this research shows that the effect on chloride binding depends on the concentration of sulphates in the solution; the effect is minor at 0.01 M, but it is appreciable at 0.1 M. The results of the pure $C_3A8$ and pure $C_3S$ pastes show that the binding capacities of these pastes are reduced in the presence of sulphates in the chloride solution (Figures 4-87, 4-89). This indicates that the presence of sulphates probably affects both the chemical and the physical binding capacities of cement pastes. The XRD results in Figure 4-72 showed that less Friedel's salt was formed in the control paste in the presence of sulphates in the chloride solution, thus, indicating the negative effect of sulphates on the chemical binding capacity of cement. As for the effect of sulphates on the physical binding capacity of cement, the results of the $C_3S$ paste are the only indication of the possible negative effect of sulphates on the physical binding capacity. Still, the presence of sulphates in the pore solution will likely lead to a competition between the $SO_4^{2-}$ and $Cl^-$ ions for adsorption sites on the surface of the C-S-H. Consequently, fewer chloride ions are physically bound in the presence of sulphate ions in the solution.

**5.4 Effect of pH on Chloride Binding:**

The results in Section 4.2.2.1 showed that an increase in the pH of the pore solution of cement paste will decrease the chloride binding capacity. This was the case for the three pastes tested including the control, SF8, and the MK8 (Figures 4-44 to 4-46). All three pastes showed similar trends in their response to the increase in the pH of the storage chloride solution. The influence of pH on chloride binding was concentration dependent. The effect was higher at 0.1 M chloride exposure, than it was at 1 M and 3 M chloride exposure (Figure 4-47).

The testing of the $C_3A8$ and $C_3S$ pastes showed that the pH affect the chloride binding of both pastes (Figures 4-86, 4-88). This indicates that both chemical and physical binding capacities of a cement paste are probably affected by a change in the pH. The binding capacities of both pastes were reduced as a result of an increase in the pH of the host solutions.

The XRD patterns of samples of the OPC pastes exposed to chloride solutions of different pH values, did not unfortunately show any evidence of the effect of pH on chemical binding, through their influence on the Friedel's salt peaks, as shown in Figure 4-71. This was somehow expected, since the variation in chloride binding at high concentration was too small to be detected in the peaks. The only evidence of this nature was provided by the XRD patterns of samples of the $C_3A8$ paste exposed to chloride solutions (3 M) with different pH values, as shown in Figure 4-103. The maximum intensity peak of the $C_6A_2.C\bar{S}.CaCl_2.24H_2O$ phase was still present in the sample exposed to the chloride solution with the higher pH, whereas it dissapeared (converted to Friedel's salt) in the sample exposed to the solution with the lower pH. *Roberts (1962)* found that a sample of Friedel's salt had a higher solubility in an alkali solution saturated with lime than in a saturated lime solution, and the solubility increased with increasing alkali concentration. This might explain the lower binding capacity at higher pH.

The reduction in the chloride binding capacity of the $C_3S$ paste, as a result of the increase in the pH of the chloride solution, was probably caused by the increased competition between the chloride and hydroxyl ions for adsorption sites on the surface of the C-S-H.

**5.5 Effect of Temperature on Chloride Binding:**

The results of this research indicated that the effect of temperature on chloride binding is concentration dependent (Section 4.2.2.3). At 0.1 M chloride concentration, an increase in exposure temperature from 7° C to 38° C causes a decrease in chloride binding. At 3 M chloride concentration, an increase in exposure temperature from 7° C to 38° C causes an increase in chloride binding (Figures 4-55 to 4-57). While these results seem to partly disagree with the published results in the literature, a closer look at the published results show that the free chloride concentrations used in these previous studies were equal or lower than 1 M. In this chloride concentration range, the results of this study are consistent with previously published findings. There are no published data showing the effect of temperature on chloride binding at higher chloride concentrations (eg. 3M) that contradict with the results of this study at 3 M chloride concentration.

The results of the pure pastes ($C_3A8$ and $C_3S$) regarding the effect of temperature on chloride binding were interesting. Those of the $C_3S$ paste clearly show that its chloride binding capacity increases with a decrease in temperature from 38° C to 7° C at all tested concentrations (0.1 M, 1 M,3 M), although the effect of temperature was very small (Figure 4-90). Those of the $C_3A8$ paste were ambiguous at high concentrations (3M) (Figure 4-91). This indicates that the observed trend in the cement pastes at 3 M is probably not caused by physical binding, and might be caused by chemical binding. This suggestion makes sense since chemical binding is expected to account for the major part of chloride binding at 3 M, and the effect of temperature on chloride binding at 3 M will reflect the effect on chemical binding more than the effect on physical binding.

In this context, it is interesting to refer to results by *Glasser (2000)*, which showed that ettringite cured in 1.5 M NaCl solution remains stable at 25° C but decomposes and forms Friedel's salt at 55° C as shown in Figure 5-5. The study, however, did not include testing at NaCl concentrations higher than 1.5 M. The results of this research show that ettringite in cement pastes does decompose and forms Friedel's salt at chloride concentrations around 3 M and at 22° C. From the results of both studies it is suggested that at 3 M NaCl concentration and at 40° C, the decomposition of ettringite into Friedel's salt is probably accelerated and chloride binding is increased. This can explain the observed effect of temperature on chloride binding at 3 M NaCl concentration.

At 0.1 M and 1 M NaCl concentrations, both chemical and physical binding were influenced the same way by temperature, as can be seen from the results of the $C_3A8$ and the $C_3S$ pastes (Figures

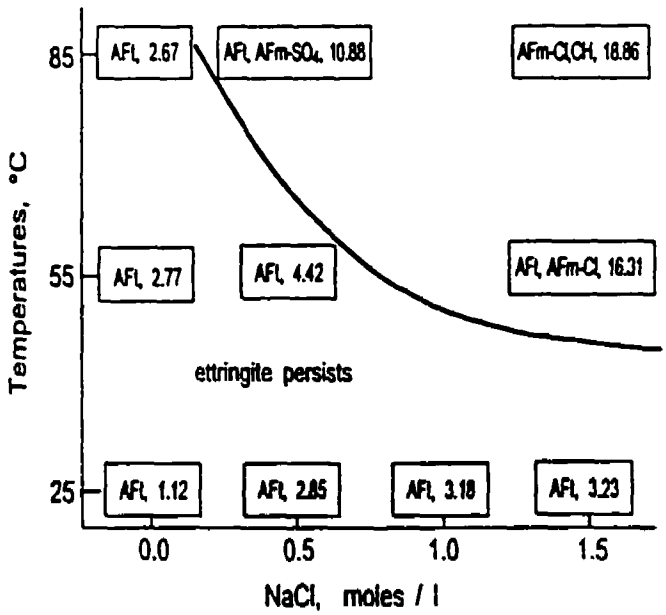


Figure 5-5: Solubility of ettringite in sodium chloride solutions at different temperatures. Values in boxes are $SO4^{2-}$ in mmoles/l. *(Glasser, 2000)*

4-90, 4-91). However, the effect of temperature on the chloride binding capacities of the two pastes is small. The results on the effect of temperature for the cement pastes tend to agree with those of the pure pastes; the influence of temperature is insignificant at 1 M, and generally small at 0.1 M.

**5.6 Effect of Carbonation on Chloride Binding:**

The results of this research indicate that fully carbonated cementitious pastes have no ability to bind chlorides. All three tested pastes, control, MK8, and SF8, exhibited no noticeable capacity to bind chlorides when they were carbonated (Figures 4-58 to 4-60). Similarly, carbonated $C_3A8$ and $C_3S$ pastes hardly had any chloride binding capacities, indicating that carbonation probably destroys the chemical and the physical binding capacities. It is known that the $CO_2$ eventually react with and decompose all the cement hydrates, forming calcium carbonate *(Massazza, 1998)*. Only calcium carbonate, silica hydrates, alumina hydrates, and ferric oxide hydrates, are stable in the cement-water-carbon dioxide system *(Verbeck, 1958))*. This explains the severe effect of carbonation on the binding capacity. The XRD patterns of samples of fully carbonated cement pastes submerged in chloride solutions, clearly showed that the main phase was calcium carbonate (calcite and vaterite) (Figures 4-73, 4-74). They also showed no signs of the formation of Friedel's salt despite the disappearance of the monosulphate and ettringite peaks originally found in the non-carbonated MK8 paste and control paste respectively.

Tests involving the carbonation of samples after being submerged in chloride solutions were not completed. These tests are more practically interesting than those mentioned above, since in real conditions carbonation occurs after the concrete has been exposed to chlorides. Nonetheless, it is expected that the effect of $CO_2$ on the binding capacity will be the same as in the first case, and all phases containing calcium will be eventually transformed into calcium carbonate. This suggestion is supported by the results of a study by *Suryavanshi & Swamy (1996)*, where they investigated the effect of carbonation on the stability of Friedel's salt by exposing reinforced concrete slabs (made with different W/CM ratios and with different cementitious systems) to the laboratory environment for 3 years, after being exposed to multiple cycles of chloride ponding (4% NaCl) and drying. The XRD patterns showed that Friedel's salt was either absent or present in small amounts in the top layers of the slabs, depending on the severity of carbonation. However, the presence of Friedel's salt was clear at the bottom layers which were either slightly carbonated or not carbonated.

**5.7 Chloride Desorption:**

The results of the desorption tests showed that when samples of cementitious pastes previously cured in sodium chloride solutions were submerged in lime saturated distilled water, part of the bound chloride was released into the solution (Section 4.2.2.5). In other words, the reduction in the chloride concentration in the pore solution of a cementitious paste resulted in the partial release of bound chloride. This means that chloride binding is not an irreversible process, and that a portion of the chloride ions that have been bound by the cement hydrates and rendered passive may be released later in the pore solution.

The results of the desorption tests of the $C_3A8$ and $C_3S$ pastes indicated that both chemical and physical binding might be affected by the reduction in chloride concentration in the pore solution of cement pastes (Section 4.3.2.5). It is interesting to notice that while the sample of $C_3S$ paste released all bound chlorides, the specimen of the $C_3A8$ paste still retained around 25% of the originally bound chloride, at a very low concentration storage solution. The amount of chlorides retained by the $C_3A8$ paste is higher than what would be bound at that same concentration, indicating that part of the bound chlorides in the $C_3A8$ paste is irreversibly bound.

The XRD patterns of samples of the control mixture and the MK8 mixture revealed that the intensities of Friedel's salt peaks decreased with the decrease in chloride concentrations. But at the same time, the XRD patterns also showed that Friedel's salt peak remained in both samples at very low concentrations (Figures 4-75, 4-76). This confirms that chemical binding is not irreversible, but a portion of the chemically bound chlorides is irreversibly bound. It is interesting to notice that the XRD pattern of the sample of the MK8 paste clearly revealed the formation of a new peak accompanying the decomposition of Friedel's salt (Figure4-76). This peak was identified as probably that of the $C_6A_2.C\bar{S}.CaCl_2.24H_2O$ phase, since it coincided well with the maximum intensity peak of that phase.

**5.8 Influence of SCM on Chloride Binding:**

The results of this research relating to the influence of cement substitution with SCM on the chloride binding capacity were generally consistent with the main trends found in the literature. Cement replacement with 8% silica fume resulted in the reduction of the binding capacity. Replacement with metakaolin (8%) or GGBFS (25%, 40%, 50%) increased the binding capacity, which also increased with the increase in replacement levels of the GGBFS. Three types of fly ash (Type F, Type CH, and Type CI) (25%, W/CM=0.5) increased the binding capacity at high chloride concentrations (1 M, 3 M), but their effects were generally minor at low concentration (0.1 M). The effect of SCM substitution on the chloride binding capacity was apparently influenced by the W/CM. The metakaolin, GGBFS, and fly ash had less positive influence on the binding capacity at a W/CM of 0.3 than at a W/CM of 0.5. The cement substitution with 25% fly ash (Type F) has even resulted in a small reduction of the binding capacity. The influence of the W/CM is possibly due to the lower degree of hydration and to the denser microstructure of the SCM-cement pastes with W/CM of 0.3. This would result in a lower number of reactive sites for chloride binding.

The XRD of samples of the MK8, FA1, and FA2 pastes showed an increase in the peaks of Friedel's salt (Figure 4-19), clearly indicating that the positive influence of those SCM on the binding capacity is at least partly due to their high alumina contents.

The results of the SCM-lime mixtures (Section 4.3.1) revealed interesting facts which helped in the interpretation of the results of the SCM-cement mixtures, and in better understanding of the possible mechanisms of influence associated with the SCM substitution. The results of the SF-lime pastes indicated that the differences in the binding capacities of those pastes were mainly caused by the type of C-S-H in those pastes. The C-S-H of the different SF-lime mixtures had different C/S ratios, as suggested by the results of XRD and binding capacity tests. The SF12 paste, which contained C-S-H with the highest C/S, had the highest binding capacity, and SF21, which contained C-S-H with the lowest C/S, had no binding capacity. This indicated that the binding capacity of C-S-H is function of the C/S, decreasing with the decrease in the C/S. This supports the suggestions by some workers *(e.g. Glass et al., 1997)* that the observed reduction in the binding capacity, brought about by the cement substitution with silica fume, is due to the lowering of the C/S of the C-S-H. The XRD patterns of the MK21 paste, which showed that straetlingite was still present at 3 M chloride exposure, point to the possibility that the influence of cement substitution with silica fume on the binding capacity of $C_3A$ is more than a simple dilution effect, and the formation of C-A-S-H

might further reduce the binding capacity of the $C_3A$.

The results of the MK-lime pastes were very interesting. The three pastes (MK12, MK11, MK21), which contained different proportions of metakaolin and lime, had considerably different chloride binding capacities (Figure 4-79 ). The XRD results of the MK12 paste and the MK21 paste revealed differences in the type and proportions of the C-A-H between the two pastes (Figures 4-80, 4-81). Furthermore, the intensities of peaks of Friedel's salt were much larger in samples of the MK12 paste than in those of the MK21 paste, despite the fact that the metakaolin (and alumina) content of the MK21 mixture was twice as much as that of the MK12 mixture. These results indicated that the binding capacity of these pastes was not only dependent on the alumina (and probably the silica) content of the mixture, but also on the C/A (and probably the C/S) of the mixture which influenced the type and proportions of the hydrates, and consequently the binding capacity of the mixture. The XRD results suggested that Stratlingite (which has lower C/A ratio) has lower binding capacity than $C_4AH_x$, or $C_3AH_6$. The results of the SF-lime pastes suggested that the C-S-H, with lower C/S ratio, have a lower binding capacity than C-S-H with higher C/S ratio. It is, therefore, suggested that when the C/A and C/S of an SCM-cement mixture decrease, calcium silicate hydrates (C-S-H), and calcium aluminate silicate hydrates (C-A-S-H) (such as straetlingite ($C_2ASH_8$)) with lower C/A and C/S ratios, forms in higher proportions. These hydrates seem to have lower binding capacities than C-A-H and C-S-H with higher C/A (such as $C_4AH_{13}$, and $C_3AH_6$) and C/S ratios respectively, which tend to form more when the C/A and C/S of an SCM-cement mixture increase. This suggestion can explain why the binding capacity of the SL100 (100% GGBFS) paste (which has high alumina but low calcium content) was smaller than that of the control paste as shown in Figure 4-101. It can also explains why the 25FA2 paste, made with FA2 fly ash (which have high alumina and high calcium contents), has a higher binding capacity than the other fly ash-cement pastes. This finding is considered another valuable contribution of this thesis to the knowledge of chloride binding in cement paste. The practical implications of this finding is that the continuous increase in the replacement level of an SCM does not necessarily result in an automatic increase in the chloride binding capacity of the SCM-cement mixture. Instead, it is suggested that every SCM-cement mixture has an optimum replacement level at which the binding capacity reached a maximum, and a critical replacement level above which the binding capacity is lower than that of the control paste. Results by *Dhir et al. (1997)* showed the existence of an optimum fly ash replacement level (50%) in a fly ash-cement mixture.

To summarize, The net effect of SCM on the binding capacity of the SCM-cement mixture seems to mainly depend on the resulting types and amounts of C-A-H, C-S-H, and C-A-S-H in the SCM-cement paste. These hydrates are influenced by the C/A and C/S ratios (of the SCM-cement mixture), which, in turn, are influenced by the chemical composition of the cementitious materials and the SCM replacement level. The results of this research showed that the substitution of cement with SCM, having high alumina content, generally increase the binding capacity of the resulting mixture. There was evidence of an increase in Friedel's salt in the SCM-cement pastes, indicating that the high alumina content of the SCM is partly responsible for the the increase in the binding capacity. There were, however, some doubts concerning the alleged positive effect of SCM replacement on the binding capacity of the C-S-H, at least in the case of silica fume substitution; Tests of silica fume-lime mixtures revealed that the binding capacity of C-S-H is function of C/S, and a lower C/S results in a lower binding capacity. Also, the reduction in the binding capacity of $C_3A$, as a result of the silica fume substitution, might be more than a simple dilution, since the formation of C-A-S-H might cause a further reduction in the binding capacity of the $C_3A$.

**5.9 Ponding Method Vs Equilibrium Method:**

The results of the binding capacities of four mixtures, determined by using the ponding method and the equilibrium method, were generally close. Taking into account the differences in the assumptions in both methods, in the conditions of exposure, and in the experimental procedures for determining bound chloride, it was expected to see differences in the results of the two methods. It is interesting to notice that the binding capacities obtained by the ponding method were generally higher than those obtained by the equilibrium method. This was unexpected, since some published results showed that the pore solution expression generally overestimate the free chloride concentration in the pore solution *(Tritthart, 1989a; Larsson, 1993)*. Also, the use of evaporable water content as representing the pore solution, in which chloride ions are dissolved, is doubtful. The results by *Mangat & Molloy (1995)* suggest that only a part of the evaporable water is free pore water. *Nilsson et al. (1996)* suggest the use of empty porosity at 11% or 45% RH as a better alternative for the amount of pore solution than the evaporable water. This means that the binding capacities determined using the ponding method could be underestimated. Despite this, the results showed that the binding capacities obtained by the ponding method were generally higher than those obtained by the equilibrium method, especially at high chloride concentrations. While it is not unlikely that this might be due to experimental error, it is possible that the reason or reasons for these results might be due to some of the underlying assumptions in these two methods.

In the case of the ponding method, one of the assumption is related to the determination of free chloride concentration at different depths. When slicing the cylinders with a dry saw, evaporation occurs, and the chloride concentration increases. It was assumed that by slicing the samples, for measuring evaporable water, in a similar manner, the effect of evaporation on the chloride concentration would be cancelled. But, it is not necessary true that evaporation would result in an equivalent increase in the chloride concentration of the expressed pore solution, since only a small fraction of the pore solution is extracted. Hence , using the evaporable water, determined from sliced samples, might be underestimating the free chloride content. However, even if the values of the evaporable water, determined from crushed samples, are used, the binding capacities of the ponding method are still higher

In the case of the equilbrium method, it is unlikely that an experimental error is responsible for the observed results, since the binding capacities were reproduced more than once and at different times. One tacit assumption is that the chloride solution absorbed by the sample acts as a solvent. If it is

suggested that not all the evaporable water content is free pore water (11% to 45% is adsorbed), it might be possible that part of the host solution that is absorbed into the sample becomes adsorbed to the pore walls and cease being a part of the bulk pore solution. If this suggestion is true, this will lead to a rise in the equilibrium chloride concentration, and the binding capacity will be underestimated.

In any case, more investigation is required to determine whether the observed behaviour was simply the result of experimental error or is related to some underlying assumptions in these methods. One beneficial suggestion is to also compare the Tang and Nilsson method to another equilibrium method, where a sample is stored in a chloride solution of fixed concentration and the total chloride content of the sample is determined (at equilibrium), giving one binding point at the exposure concentration. From the knowledge of the evaporable water, the binding capacity can be determined. This way, the determination of the binding capacity will be limited to the measurement of the total chloride content and evaporable water, and potential experimental errors will be reduced in comparison with the ponding method. The free chloride concentration can also be determined by pore squeezing the sample. This would enable the comparison between the concentration from pore squeezing to the concentration of the exposure solution. Moreover, this method allows for more similar exposure conditions to the Tang and Nilsson method (duration, static binding capacity) to minimize the factors that might affect the results. The comparison between these two methods would help in identifying the sources of differences in the results, and determine whether some assumptions affect the accuracy of the results.

**5.10 Chloride Binding and Service Life Prediction:**

The significance of chloride binding in the chloride penetration process was mentioned in the introduction. This significance stems from the fact that the binding of chlorides along the penetration path retards the penetration process and increases the time for corrosion initiation. Therefore, it is essential to account for chloride binding in models that describe the penetration process, in order to obtain more accurate service life predictions. This section discusses the impact of the considered chloride binding relationship on the predicted time-dependent chloride profiles and service lives. Although many transport mechanisms may be involved in the chloride penetration process, this discussion focuses on the case where diffusion is the sole chloride transport mechanism, assuming the concrete cover is fully saturated. In this case, chloride ions penetrate the concrete by diffusion due to the concentration gradient between the exposed concrete surface and the pore solution of the cement matrix (diffusion driving force). This process is described by Fick's first law of diffusion, in which the chlorides flux is proportional to the concentration gradient $\partial C_f/\partial x$ *(Crank, 1975)*, and is given by:

$$J_c = -D_e w_e \frac{\partial C_f}{\partial x} \qquad [\text{kg/(m}^2\text{.s)}] \qquad (5\text{-}1)$$

where $J_c$ is the flux of chloride ions (kg/m$^2$.s), $D_e$ is the effective diffusion coefficient (m$^2$/s), $w_e$ is the evaporable water content (m$^3$ evaporable water/m$^3$ concrete), and $C_f$ is the free chloride concentration (kg/m$^3$ of pore solution) at a depth $x$ (m). The negative sign in equation 5-1 indicates that the diffusion occurs in the opposite direction to that of increasing chloride concentration. It is assumed here that the evaporable water content, $w_e$, is the water in which chloride diffusion occurs. By applying the law of mass conservation to diffusing chlorides, the following equation is obtained:

$$\frac{\partial C_t}{\partial t} = -\frac{\partial J_c}{\partial x} \qquad [\text{kg/(m}^3\text{.s)}] \qquad (5\text{-}2)$$

where $C_t$ is the total chloride concentration (kg/m$^3$ of concrete), and t is the time (s). By substituting Equation 5-1 in Equation 5-2, we obtain the equation governing the mechanism of chloride diffusion in concrete (Fick's second law), which is given by:

$$\frac{\partial C_t}{\partial t} = \frac{\partial}{\partial x}(D_e w_e \frac{\partial C_f}{\partial x}) \qquad [kg/(m^3.s)] \qquad (5\text{-}3)$$

By taking into account chloride binding, expressed by the following equation:

$$C_t = C_b + w_e C_f \qquad (kg/m^3 \text{ of concrete}) \qquad (5\text{-}4)$$

and by substituting equation 5-4 into equation 5-3, the following modified Fick's second law results

$$\frac{\partial C_t}{\partial t} = \frac{\partial}{\partial x}(D_a \frac{\partial C_f}{\partial x}) \qquad [kg/(m^3.s)] \qquad (5\text{-}5)$$

with

$$D_a = \frac{D_e}{1 + \frac{1}{w_e}\frac{\partial C_b}{\partial C_f}} \qquad (m^2/s) \qquad (5\text{-}6)$$

where $D_a$ is the apparent diffusion coefficient ($m^2/s$), and $\partial C_b/\partial C_f$ is the slope of the chloride binding isotherm.

This equation cannot be solved without using numerical methods, because of the dependency of $D_a$ on $C_f$ in the case of non-linear chloride binding isotherms. It was solved numerically in space as a boundary-value problem and in time as an initial-value problem using one-dimensional finite-difference (Crank-Nicolson scheme). The set of simultaneous equations resulting from applying the finite-difference scheme to Equation 5-1 was solved in time steps until a specified chloride threshold was attained at the level of rebars. The initial and boundary conditions used for the numerical analyses were the following:

for $t = 0$ $\quad C_f = C_0 \quad$ at $x > 0$

for $t > 0$ $\quad C_f = C_s \quad$ at $x = 0$

$\quad C_f = C_0 \quad$ at $x = L$

where $t$ is the time, $C_0$ is the background chloride concentration in the concrete pore solution before the penetration of chlorides , $C_s$ is the chloride concentration of the solution in contact with the concrete surface, and $L$ is the thickness of the reinforced concrete member. The thickness was assumed to be much larger than the penetration depth. A value of $L$ = 0.2 m was used in the numerical analyses.

The analyses were performed with a computer model. Three cases were considered: one in which chloride binding was neglected, a second one where a linear chloride binding isotherm was assumed, and a third case in which a Freundlich binding isotherm (non-linear binding) was considered. The three studied cases and their influence on the apparent diffusion coefficient and on the diffusion equation (5-5) are presented in the following:

No binding:

$$C_b = 0 \qquad \frac{\partial C_b}{\partial C_f} = 0 \qquad D_a = D_e \tag{5-7}$$

Linear chloride binding isotherm:

$$C_b = k\,C_f \qquad \frac{\partial C_b}{\partial C_f} = k \qquad D_a = \frac{D_e}{1 + \frac{k}{w_e}} \tag{5-8}$$

Freundlich chloride binding isotherm:

$$C_b = \alpha\,C_f^{\beta} \qquad \frac{\partial C_b}{\partial C_f} = \alpha\,\beta\,C_f^{\beta-1} \qquad D_a = \frac{D_e}{1 + \frac{1}{w_e}\alpha\,\beta\,C_f^{\beta-1}} \tag{5-9}$$

Note that in the case of the non-linear Freundlich isotherm, $D_a$ is dependent on the free chloride concentration, but it is constant in the case of no binding or linear binding isotherm. The chloride binding data of the 40SL (40% GGBFS, W/CM = 0.3) paste (Figure 5-6) was used to calculate the chloride binding parameters required for performing the analyses. Other parameters were also

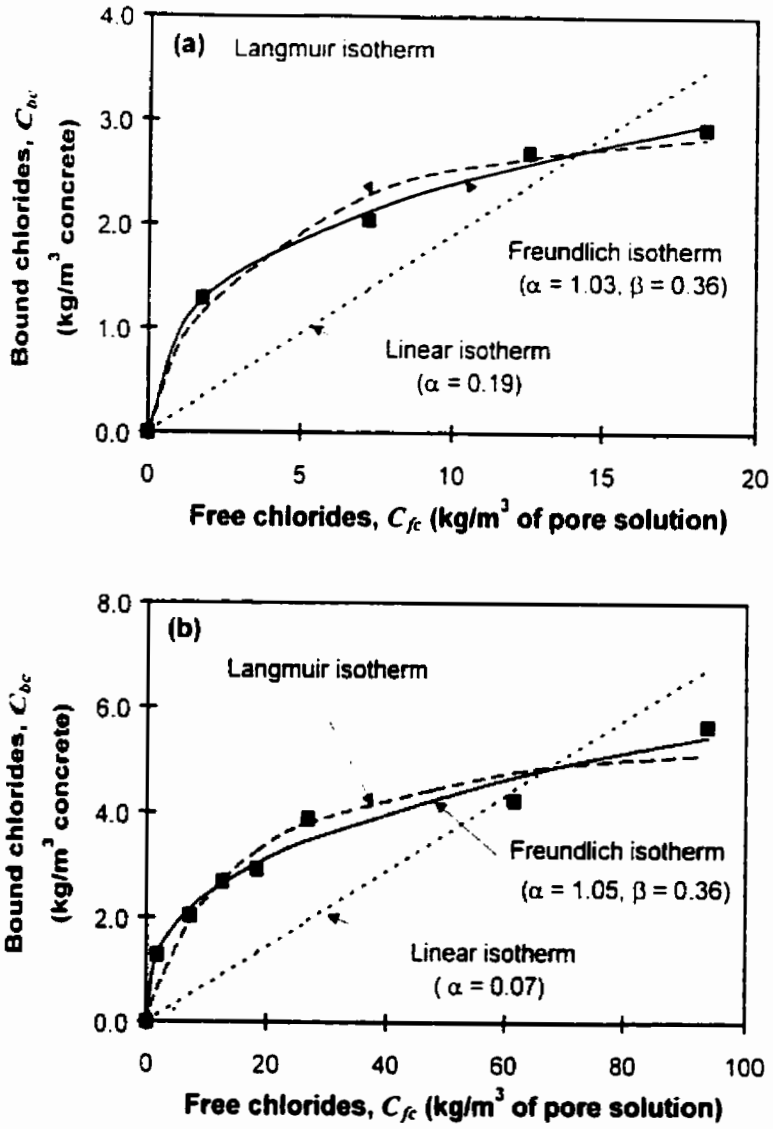


Figure 5-6: Chloride binding data of the 40SL (40% GGBFS) paste, fitted with a Freundlich, Langmuir, and Linear isotherm for two different exposure conditions: (a) $C_s$ = 0.5 M and (b) $C_s$ = 2.5 M.

assumed in order to translate the binding data from cement paste to concrete. It was assumed that the concrete evaporable water content $w_e$ was 8 %, the binder content was 450 kg/m$^3$ of concrete, and the effective diffusion coefficient $D_e$ was $1.0 \times 10^{-12}$ m$^2$/s. Two surface chloride concentrations were chosen: 0.5 M and 2.5 M . The first simulates submersion in sea water, and the second simulates conditions of marine structures in the splash zone or bridge decks exposed to de-icing salts.

Figures 5-7 and 5-8 show the predicted free chloride profiles and total chloride profiles after 5 years and 50 years exposure periods for the 0.5 M exposure. When non-linear binding is considered the predicted free chloride concentration at a given depth is lower than when linear binding or no binding is assumed (Figure 5-7). The difference becomes more pronounced at greater depths as the time of exposure increases. This indicates that the nature of the chloride binding relationship is more significant at low chloride concentrations, where the reduction in the apparent diffusion coefficient becomes more pronounced for the Freundlich isotherm. The total chloride profiles in Figure 5-8 show that when chloride binding (linear or non-linear) is accounted for in the diffusion equation, the predicted total chloride concentrations are higher than when no binding is assumed, and this is true for most of the penetration depth except at low concentrations (due to the retardation effect of binding). The higher chloride concentrations, when binding is taken into account, simply mean that more chlorides being bound along the diffusion path. The differences between the free chloride profiles and the total chloride profiles emphasize the importance of defining the nature of the chloride threshold, i.e., in terms of free or total chlorides. The choice of the threshold results in noticeable differences in service life predictions. It seems more appropriate to define the threshold value in terms of free chlorides, since free chlorides are the ones that penetrate and initiate corrosion. Of course, some of the bound chlorides could become free if conditions change, and present a risk for corrosion. But, defining chloride threshold in terms of total chloride is not the better solution. Attempting to account for factors that would affect chloride binding (adsorption and desorption) during the penetration process (pH, temperature, wetting and drying...) would be more appropriate.

Figure 5-9 shows the predicted service lives for the three chloride binding cases considered in this discussion, and for the two surface exposures. Two different concrete covers were considered (40 and 60 mm), and a free chloride threshold of 0.09% by mass of cementitious materials (5.0 kg/m$^3$ of pore solution). The results clearly show the considerable effect of chloride binding on the predicted times to steel depassivation. In the case of the 0.5 M chloride exposure, the predicted times to steel depassivation, when no binding is considered, are 3 times lower than the times predicted when a freundlich binding isotherm is considered. Even the nature of the binding isotherm has a considerable effect on the predicted values. It is worth mentioning again that the results of this research clearly showed the non-linear nature of the chloride binding isotherms. Therefore, it is important not only to account for chloride binding in service-life prediction models, but to also

account for the accurate representation of the chloride binding relationship. It should be noted that the case of no binding considered in this example does not really represent service-life models which do not explicitly account for chloride binding in the diffusion equation; the diffusion coefficient used in these models is the apparent diffusion coefficient $D_a$ and not the effective diffusion coefficient $D_e$. Chloride binding is implicitly included in the apparent diffusion coefficient considered in these models. This is equivalent to the case where a linear binding isotherm is considered in the diffusion equation.

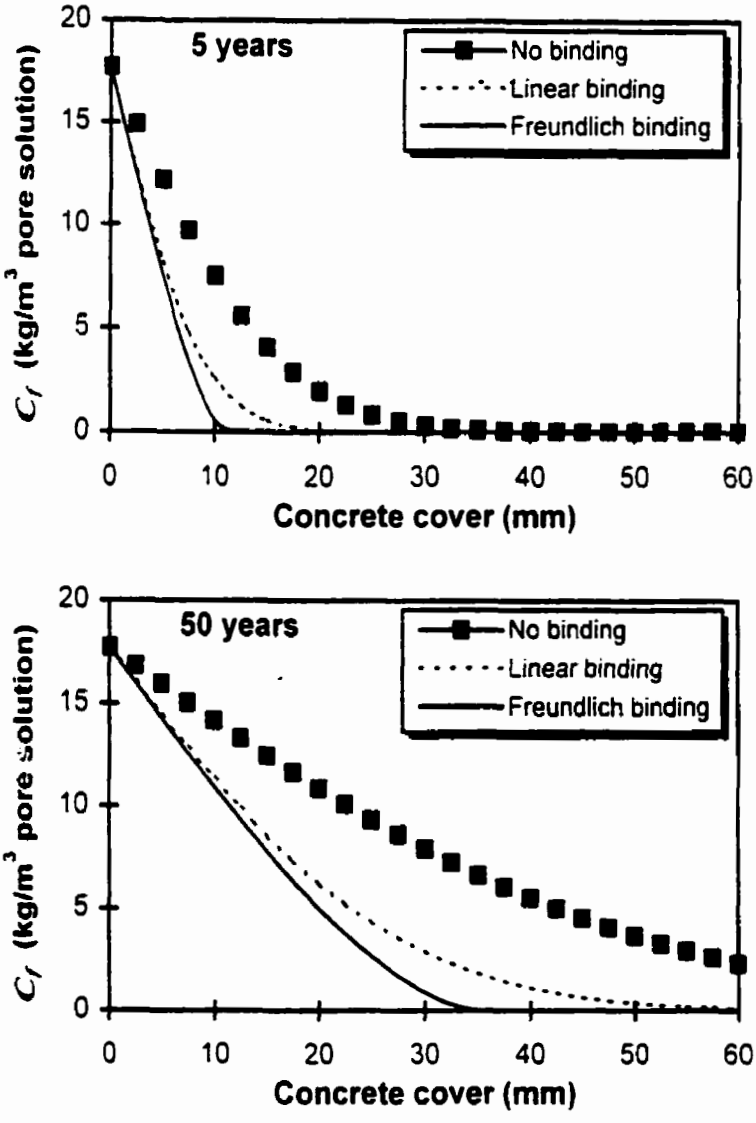


Figure 5-7: Predicted free chloride concentration profiles at (a) 5 years and (b) 50 years for 0.5 M exposure conditions.

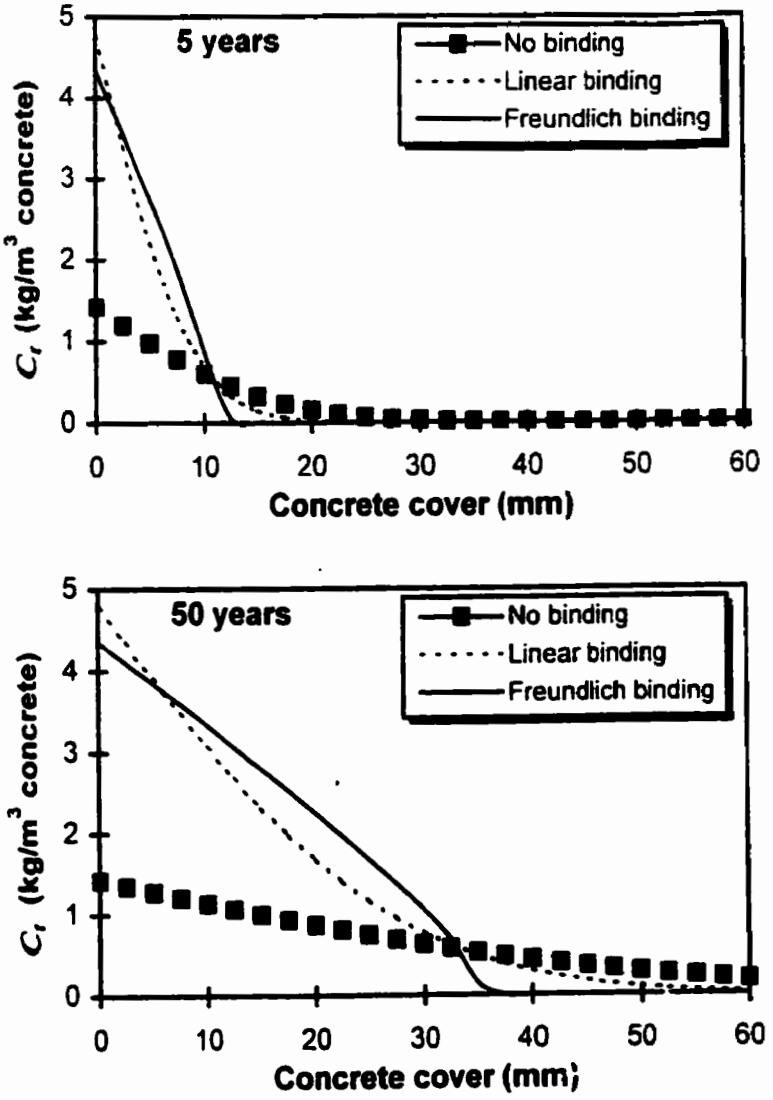


Figure 5-8: Predicted total chloride concentration profiles at (a) 5 years and (b) 50 years for 0.5 M exposure conditions.

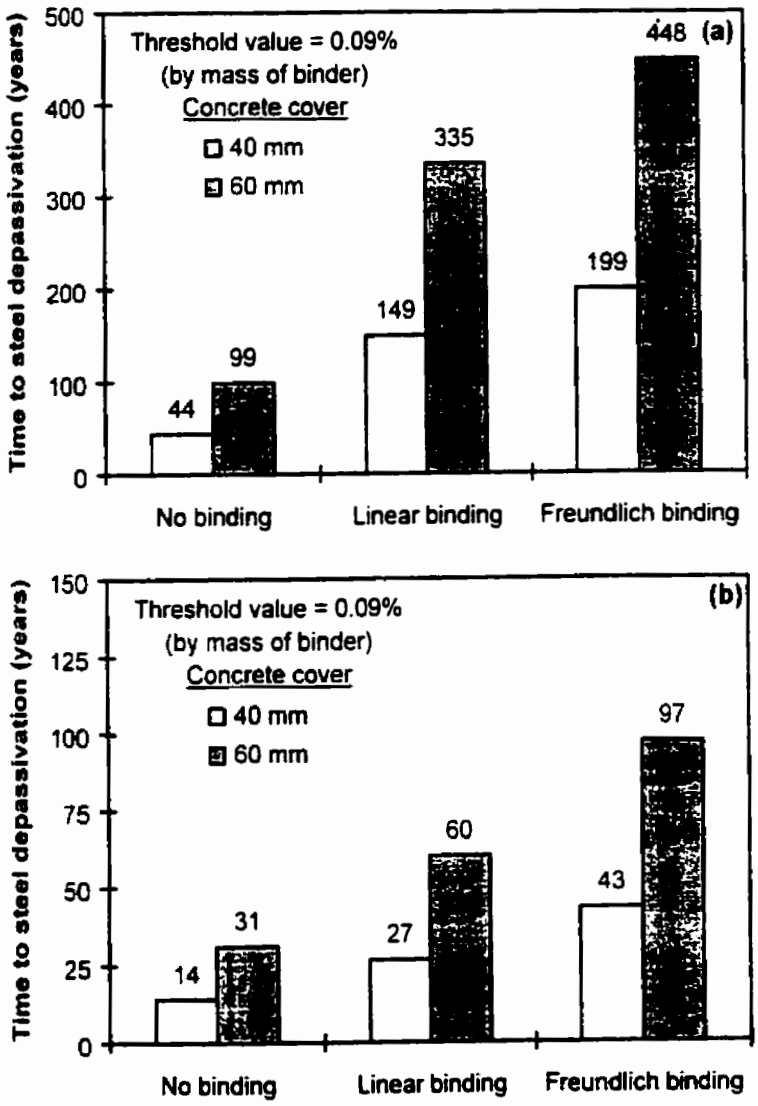


Figure 5-9: Predicted service-lives for three cases considered, and for different concrete covers assuming a chloride threshold value of 0.09% by mass of binder (5.0 kg/m$^3$ of pore solution) and for two different exposure conditions: (a) $C_s$ = 0.5 M and (b) $C_s$ = 2.5 M.

# CHAPTER 6

# CONCLUSIONS AND RECOMMENDATIONS

## 6.1 Conclusions

The previous two chapters presented the results and analyses of the various studies performed in this research. These studies provided much needed data about the binding of chlorides in hardened cement pastes. While all the obtained results are considered useful to the field of studies, some are more important because of the insight they provide in some areas and/or because of the new questions they arouse, prompting research to move into new directions.

The most significant findings of this thesis were related to the chemical binding in cement pastes, the influence of SCM, the roles of cement mineral phases, and to service life predictions. These findings were reached from the analyses of the results of different studies, although, the results of the XRD tests were crucial. These findings are listed in the following section in relation to the different aspects of the chloride binding problem.

### 6.1.1 Important Findings

1. Chemical binding
   - A. The monosulphate phase does react with chlorides. The reaction starts at chloride concentrations below 0.1 M. The reaction products are concentration dependent. At low chloride concentrations, Kuzel's salt forms (previously unknown to form as a reaction products containing chlorides) and persist for a noticeable chloride concentration range ($0\ M < C_f < 1\ M$). At high chloride concentrations, Friedel's salt forms. The monosulphate seems to fully transform into Friedel's salt at chloride concentrations below 1 M.
   - B. Evidence from several cement pastes suggest that even ettringite starts to transform into Friedel's salt at high chloride concentrations ($2\ M < C_f < 3\ M$).
   - C. Several other C-A-H react with chlorides, including $C_4AH_x$, $C_3AH_6$, monocarboaluminate, and stratlingite. The transformation and stability of all the above mentioned C-A-H phases in the presence of chlorides are concentration dependent, explaining the dependence of the chemical binding capacity on chloride

concentration. Some phases seem to fully transform to Friedel's salt at low concentrations ($C_4AH_x$), while others partially transform and persist at chloride exposure of 3 M (i.e. stratlingite).

D. Friedel's salt peaks increase with increasing chloride concentrations, even at concentrations above 1 M. indicating that the chemical binding capacity is not exhausted at low concentrations.

E. Friedel's salt starts to decompose when chloride concentration is reduced (desorption tests). There is evidence suggesting that Kuzel's salt might re-form following the reduction of chloride concentration and decomposition of Friedel's salt

2. Influence of SCM

The effect of an SCM on the chloride binding capacity of the SCM-cement mixture depends not only on the alumina content of the SCM, but also depends on the overall C/A and C/S ratios of the SCM-cement mixture, which seem to influence the type of the C-A-H and C-S-H products, which in turn influence the chloride binding capacity. There are indications that when the C/A and C/S ratios of a mixture become lower, more stratlingite ($C_2ASH_8$) and C-S-H (with lower C/S ratio) form. Stratlingite seem to have lower binding capacities than $C_4AH_x$, or $C_3AH_6$, and C-S-H, with lower C/S ratio, seem to have a lower binding capacity than C-S-H with higher C/S ratio.

3. Roles of cement phases

The results indicate that the contributions of the chemical ($C_3A$, $C_4AF$) and physical binding capacities ($C_3S$, $C_2S$) to the chloride binding capacity of cement are dependent on the chloride concentration and cement type, but are significant in most cases. The $C_3S$ (and $C_2S$) and $C_4AF$ phases bind noticeable amounts of chloride, and all four mineral phases contribute to the chloride binding capacity. The chloride binding capacity of the $C_4AF$ phase is markedly lower than that of the $C_3A$. In general, the $C_3A$ content (and chemical binding capacity) of cement play a decisive role in the chloride binding capacity at high concentrations, but not at low concentrations. The reason for this behaviour at low concentrations is partially linked to the effect of sulphate content of the cement.

4. Service life modelling

Taking chloride binding into account in mathematical models, aiming at predicting chloride penetration and service life, will have a significant effect on the predicted durability. Even the type of the relationship considered (linear or non-linear) will have a significant effect on the predictions. The use of non-linear binding isotherms results in significantly longer service-lives than when linear binding isotherms are used. The results in this thesis clearly show the the chloride binding isotherms are non-linear and best fit a Freundlich isotherm of the form $C_b = \alpha C_f^{\beta}$. Finally, the criteria for defining the chloride threshold (i.e., free or total chloride concentration) will result in totally different predictions of service life.

The following subsections present more detailed conclusions related to the different aspects of the chloride binding process.

### 6.1.2 Effect of Cement Composition on the Chloride Binding Capacity

#### 6.1.2.1 $C_3A$

The $C_3A$ plays an important role in the chloride binding capacity of cement, as indicated by the results from different studies in this research. The pure $C_3A$ paste had the highest chloride binding capacities, the partial substitution of cement C1 with pure $C_3A$ lead to large increase in the binding capacity, the addition of sulphate to the C4 cement and the resulting reduction in the chloride binding capacity indicated the importance of the chemical binding capacity (mostly due to $C_3A$) to the binding capacity of the C4 cement, and the $C_3A$ content was the only single variable that correlated well with the binding capacity of cement at high concentrations.

Because of the high binding capacity of $C_3A$ and the relatively large variation in the $C_3A$ content in cement, The $C_3A$ content, is a good indicator of the binding capacity of cement in the high chloride concentration range (1.0 M - 3.0 M). but at low concentrations (0.1 M), the $C_3A$ content is not a good indicator of the chloride binding capacity. It is suggested that its effect on the binding capacity is related to the sulphate content. The higher the sulphate content is, the lower the effect of $C_3A$.

#### 6.1.2.2 $C_4AF$

The $C_4AF$ plays a significant role in the chloride binding capacity of cement. Strong evidence found

in this research support this conclusion. The $C_4AF$ phase, in pure form, had a high chloride binding capacity, and the partial substitution of the C7 cement with pure $C_4AF$ resulted in a significant increase in the chloride binding capacity. XRD patterns of samples of the C1 cement paste (0% $C_3A$) showed the formation of the iron equivalent of Friedel's salt, $C_3F.CaCl_2.10H_2O$. The partial substitution of the C1 cement with sulphate (to convert all the $C_4AF$ into ettringite during hydration) resulted in a decrease in the binding capacity, a decrease that was considered as the approximate contribution of the $C_4AF$ phase to the binding capacity of the C1 cement paste. The binding capacity of the $C_4AF$ phase is lower than that of the $C_3A$ phase. Results from this research suggest that the binding capacity of $C_4AF$ is probably about one third of the binding capacity of $C_3A$

#### 6.1.2.3 $C_3S$, $C_2S$

The $C_3S$ (and $C_2S$) generally play a significant role in the chloride binding capacity of cement. This conclusion is based on the results of different tests. The pure $C_3S$ paste bound significant amount of chloride in comparison with the control paste. The partial substitution of the C1 cement with sulphate (to make the chemical binding capacity inert) and the resulting binding capacity indicated that the physical binding capacity was significant, if not important, since it was assumed that the binding capacity of the resulting cement represented mainly the physical binding capacity of the original C1 cement. From the results in this research, it is estimated that the contribution of $C_3S$ to the binding capacity could possibly range from 25% to over 50%.

#### 6.1.2.4 $SO_3$

The sulphate content of cement has a negative influence on the binding capacity. It significantly affects the chemical binding capacity especially at low chloride concentration (0.1 M). Sulphates react with $C_3A$ and $C_4AF$ to form monosulphate and ettringite. This reduces the chemical binding capacity. As the chloride concentration increases, the monosulphate slowly transforms into Kuzel's salt first, and then into Friedel's salt at higher concentrations. The ettringite starts to transform at higher concentrations (3 M). These transformations explain why the sulphate content is more influential at low chloride concentrations.

### 6.1.2.5 Supplementary Cementing Materials

**Silica Fume**

The partial substitution of OPC with 8% silica fume caused a significant reduction in the chloride binding capacity. This reduction was observed at different W/CM (0.3, 0.5), different exposures, and different chloride concentrations. This reduction cannot be explained by the dilution of the $C_3A$ alone. Testing of silica fume-lime mixtures showed that the C-S-H produced by the different mixtures had different chloride binding capacities, and this was attributed to the difference in the average C/S ratios of the C-S-H . The lower the average C/S ratio was, the lower the binding capacity of the C-S-H. It is suggested that this finding might explain the reduction in the chloride binding capacity resulting from the partial substitution with silica fume.

**Fly ash**

Blended OPC-fly ash pastes (25% fly ash, W/CM = 0.5), containing a Type F, a Type CH, and a Type CI fly ash respectively, generally had higher chloride binding capacities than the OPC paste. XRD results of samples exposed to high chloride concentrations (3.0 M) provided evidence that the high alumina contents of the fly ashes were partly responsible for the observed increases in the chloride binding capacities of their corresponding pastes. There was no clear correlation between the chloride binding capacity and the calcium or alumina content of the fly ash.

At a W/CM ratio of 0.3, the Type F fly ash did not perform as well as it did at a W/CM ratio of 0.5. At 25% replacement level it reduced the chloride binding capacity, and at 40% replacement level it increased the binding capacity only at high chloride concentrations (above 1.0 M). It was suggested that this behaviour might be related to the degree of hydration and/or the microstructure of the OPC-fly ash paste.

**GGBFS**

The partial replacement of OPC with GGBFS (25%, 40%, at W/CM = 0.3; 25%, 50% at W/CM = 0.5) lead to an increase in the chloride binding capacity. This increase was observed at different W/CM ratios, and at several chloride concentrations. Also, the chloride binding capacity increased with an increase in the replacemnt levels of GGBFS. However, the binding capacity of a 100%

GGBFS paste was significantly lower than that of the OPC paste. This result indicates the existence of an optimum GGBFS replacement level where the binding capacity reaches a maximum, and a higher GGBFS replacement level, above which the chloride binding capacity will be lower than that of the OPC paste.

**Metakaolin**

The partial substitution of OPC with metakaolin (8%) increased the binding capacity. The increase was observed at different W/CM ratios (0.3, 0.5), different exposures, and different chloride concentrations. The increase in the binding capacity was higher at the higher W/CM ratio. XRD tests provided evidence of an increase in the amount of Friedel's salt at high chloride concentrations (1.0 M, 3.0 M) in the presence of metakaolin. This showed that the high alumina content of the metakaolin was partly responsible for the increase in the binding capacity. The testing of the metakolin-lime mixtures showed that the binding capacity decreased with an increase in the metakaolin to lime ratio (by mass). The XRD results revealed that the hydrated metakaolin-lime pastes had significant differences in the types and amounts of C-A-H (and probably the C/S of the C-S-H), which significantly affected the chemical binding capacity (and probably the physical binding capacity). It is therefore suggested that in cement-metakaolin mixtures, an increase in the metakaolin replacement level does not necessarily mean an automatic increase in the binding capacity. The lime to metakaolin ratio of the mixture is a significant factor to take into account in addition to the metakaolin content.

### 6.1.3 Pore Solution

#### 6.1.3.1 Hydroxyl Ion Concentration

An increase in the hydroxyl ion concentration of the host solution (13.0, 13.4, 13.7, 14.0) reduced the binding capacities of the three tested cement pastes. The effect was more pronounced at low chloride concentration (0.1 M) than at high chloride concentrations (1.0 M, 3.0 M). The effect was insignificant for small variations in the pH, but it was significant for relatively large variations in the pH. The binding capacities of the pure $C_3A$ and $C_3S$ pastes were reduced as a result of an increase of the pH of the host solutions, suggesting that the chemical and physical binding capacities are

negatively affected by an increase in the hydroxyl ion concentration of the host solutions.

#### 6.1.3.2 Sulphate Ion Concentration

The presence of sulphate ions in the host solution had a negative effect on the chloride binding capacities of the three tested cement pastes. The effect was insignificant at 0.01 M [$SO_4^{2-}$], but it was significant at 0.1 M [$SO_4^{2-}$]. The results from the study of the pure $C_3A$ and $C_3S$ pastes suggest that the presence of sulphate in the pore solution negatively affects both the chemical and the physical binding capacities.

### 6.1.4 Environment

#### 6.1.4.1 Temperature

An increase in the exposure temperature from 0°C to 23°C to 38°C reduced the chloride binding capacities of all three tested mixtures at 0.1 M and 1.0 M chloride concentrations. The reductions in the chloride binding capacities of the different mixtures were, however, small, especially at 1.0 M chloride exposure. A similar trend was observed in the pure $C_3S$ and $C_3A$ pastes.

At 3.0 M chloride concentrations, an increase in the exposure temperature from 0°C to 23°C to 38°C resulted in an increase in the binding capacities of all three tested pastes. This trend was not observed in the case of the pure $C_3S$ paste, and the results of the $C_3A$ paste were not conclusive. It is suggested that the ettringite phase transforms into Friedel's salt at a faster rate at 3.0 M chloride exposure, which might explain the observed behaviour of the three pastes at high chloride concentrations.

#### 6.1.4.2 Carbonation

Carbonation has a very severe negative effect on the chloride binding capacity of cement pastes. Three different precarbonated pastes that were exposed to chloride solutions of different concentrations had almost no chloride binding capacity. The precarbonation of these pastes resulted in the transformation of C-S-H and C-A-H into $CaCO_3$, which led to the loss of their chloride binding capacities compared to the equivalent non-carbonated pastes. Since carbonation is

accompanied with a sharp reduction in the pH of the pore solution, the simultaneous occurrence of carbonation and chloride attack create the most favourable conditions for corrosion initiation.

### 6.1.5 Chloride Binding and Desorption Isotherms

The chloride binding isotherms are nonlinear. The Freundlich isotherm ($C_b = \alpha C_f^{\beta}$) is the best fit for the chloride binding isotherms. Desorption isotherms show the existence of hysteresis in the chloride binding process. Chloride binding is largely reversible. Desorption tests of pure pastes ($C_3S$, $C_3A8$) indicates that physical binding is fully reversible, and chemical binding is largely reversible.

## 6.2 Recommendations

1. The chloride binding properties of the hydrated $C_3A$ phase should be further investigated. While the study of the $C_3A$ paste provided important information on the chloride binding process, some questions were left unanswered. The binding properties of a $C_3A$ (100%) paste should be investigated. Several concentrations (from low to high) should be tested to check the dependence of the chloride binding capacity on the chloride concentrations, and to know when the binding capacity is exhausted. Also, the binding properties of an ettringite paste (100%) should be investigated, to check if this paste can bind chloride, at low concentrations, without the formation of Friedel's salt, and to confirm the transformation of the ettringite paste into Friedel's salt at high chloride concentration. The results of this investigation would show whether the addition of sulphate to Portland cement, to transform the $C_3A$ and $C_4AF$ into ettringite, is an appropriate method to investigate the approximate distribution of chloride between the C-S-H and the C-A-H.

2. The result of the statistical analysis, showing that the chloride binding capacity can be predicted from cement composition are promising. More investigation should be done to check the validity of the predictions. This could be done by testing new cements from different sources and comparing the results of the tests and the predictions from the relationships obtained in this research. Ultimately, the binding capacity of blended cement should be able to be predicted from the composition of the mixture. More testing of blended cements is needed before this is possible.

3. The influence of SCM substitution on the chloride binding capacity of cement should be investigated more, to better understand the mechanisms of influence of SCM on the binding capacity. The effect of $C_2ASH_8$ formation (when cement is partially substituted with silica fume) on the chloride binding capacity of $C_3A$, in the silica fume- cement system, should be investigated by testing silica fume-$C_3A$ mixtures. The exact role of the C-S-H (formed from the pozzolanic reactions) as a function of chloride concentrations and SCM replacement

levels should be investigated in the cases of fly ash, GGBFS, and metakaolin substitutions. Similarly, the role of the C-A-H at high SCM replacement levels should also be investigated. To be able to model the chloride binding capacity of cement-SCM system, an attempt should be made to correlate the chloride binding capacity of the cement-SCM system with variables related to the basic mixture components such as the overall C/S ratio, C/A ratio, and alumina content of the cement-SCM mixture. The tests should include several fly ashes (including Class F, Class CI, and Class CH), more than one GGBFS and silica fume. Several replacement levels (especially in the case of fly ash and GGBFS) and several chloride concentrations should be tested too.

4. The effect of temperature should be further investigated, especially at high chloride concentrations (2.0 M, 3.0 M). The validity of the explanation, provided for the behaviour of the tested pastes at high chloride concentrations (3.0 M), could be checked by testing a cement like C4 (ground clinker without the addition of gypsum). More temperatures should be tested, including temperatures below zero and as high as 70°C. Also, different types of cement should be tested (e.g. CSA Type 10 and Type 50 with large differences in the $C_3A$ contents).

5. The results of this research indicate that carbonated pastes (prior to chloride exposure) have no capacity to bind chloride, irrespective of their compositions. A more practical situation, however, is when pastes are carbonated after chloride exposure. A study of carbonation after chloride binding would provide information about the kinetics of deterioration of the binding capacity, particularly the chemical binding capacity.

# REFERENCES

Al-Hussaini. M.J., Sangha, C.M., Plunkett, B.A., Walden. P.J. 1990, "The Effect of Chloride Ion Source on the Free Chloride Ion Percentages in OPC Mortars," *Cement and Concrete Research*. V. 20. No. 5, pp. 739-745.

Andrade. C., Page C. L. 1986, "Pore solution chemistry and corrosion in hydrated cement systems containing chloride salts: a study of cation specific effects". *British Corrosion Journal*, V. 21, No. 1. pp. 49-53.

Arsenault, J., Bigas, J.P., Ollivier, J.P., 1995, "Determination of Chloride Diffusion Coefficient using Two Different Steady-State Methods: Influence of Concentration Gradient". Chloride Penetration into Concrete, *Proceedings of the International RILEM Workshop*, Ed. L.O. Nilsson and J.P. Ollivier, pp. 150-160.

Arya. C., Buenfeld, N.R., Newman. J.B. 1987, "Assessment of simple methods of determining the free chloride content of cement paste," *Cement and Concrete Research*. V. 17, No. 6, pp. 907-918.

Arya. C., Buenfeld, N.R., Newman, J.B. 1990, "Factors influencing chloride binding in concrete," *Cement and Concrete Research*. V. 20, No. 2, pp. 291-300.

Arya, C., Newman. J.B.1990, "An Assessment of Four Methods of Determining the Free Chloride Content of Conrete," *Materials and Structures*. V. 23, pp.319-330.

Arya. C., Xu, Y. 1995, "Effect of Cement Type on Chloride Binding and Corrosion of Steel in Concrete," *Cement and Concrete Research*. V. 25, No. 4, pp. 893-902.

Barneyback, R.S., Diamond, S. 1981, "Expression and Analysis of Pore Fluids from Hardened Cement Pastes and Mortars," *Cement and Concrete Research*, V. 11, No. 2, pp. 279-285.

Ben-Yair. M. 1974, *Cement and Concrete Research*, V. 4, No. 408.

Beaudoin, J.J., Ramachandran, V.S., Feldman, R.F.v 1990, "Interaction of Chloride and C-S-H," *Cement and Concrete Research*, V. 20, No. 6, pp. 875-883.

Bickley, J.A. 2000, "High-performance concrete: state-of-the-art"

Bigas, J.P., Lambert, F., Ollivier, J.P. 1995, "An Original Method to Determine The Non-Linear Chloride Binding Isotherm from Bulk Specimens of Mortar", Chloride Penetration into Concrete, *Proceedings of the International RILEM Workshop*, Ed. L.O. Nilsson and J.P. Ollivier, pp. 43-50.

Birnin-Yauri, U.A. and Glasser, F.P. 1998, "Friedel's salt, $Ca_2Al(OH)_6(Cl,OH)_2H_2O$: its solid solutions and their role in chloride binding", *Cement and Concrete Research*, V. 28, No. 12, pp. 1713-1723.

Blunk, G., Gunkel, P., Smolczyk, H.-G. 1986, "On the Distribution of Chloride Between the Hardening Cement paste and Its Pore Solution." *8th International Congress on the Chemistry of Cement*, pp. 85-90.

Boddy, A., Bentz, E., Thomas, M.D.A., Hooton, R.D. 1999, "An overview and sensitivity study of a multimechanistic chloride transport model", *Cement and Concrete Research*, Vol. 29, pp. 827-837

Byfors, K. 1986, "Chloride binding in cement paste," *Nordic Concrete Research*, No. 5, pp. 27-38.

Byfors, K., Hansson, C.M., Tritthart, J. 1986, "Pore Solution Expression as a Method to Determine the Influence of Mineral Additives on Chloriode Binding," *Cement and Concrete Research*, V. 16, No. 5, pp.760-770.

Byfors, K. 1990, *Chloride-Initiated Reinforcement Corrosion. Chloride binding*, CBI Report 1:90, 121 p..

Castellote, M., Andrade, C., Alonso, C. 1999, "Chloride-binding isotherms in concrete submitted to non-steady-state migration experiments," *Cement and Concrete Research*, V. 29, pp. 1799-1806.

Chatterji, S., Kawarmura, M. 1992, "Electrical double layer, ion transport and reactions in hardened cement paste," *Cement and Concrete Research*, V. 22, No. 5, pp. 774-782.

Crank, J. 1975, "The Mathematics of diffusion", 2nd edition Clarendon Oxford.

Damidot, D., Birnin-Yauri, U.A., Glasser, F.P. 1994, "Thermodynamic investigation of the CaO-$Al_2O_3$- $CaCl_2$-H2O system at 25 °C and the influence of $Na_2O$", Il Cemento, V. 4, pp. 243-254.

Delagrave, A., Pigeon, M., Revertégat, É. 1994, "Influence of Chloride Ions and pH Level on the Durability of High Performance Cement Pastes," *Cement and Concrete Research*, V. 24, No. 8, pp. 1433-1443.

Delagrave, A., Pigeon, M., Marchand, J., Revertegat, E. 1996, "Influence of Chloride Ions and pH Level on the Durability of High Performance Cement Pastes (Part II)," *Cement and Concrete Research*, V. 26, No. 5, pp. 749-760.

Delagrave, A., Marchand, J., Ollivier, J.P., Julien, S., Hazrati, K. 1997, "Chloride Binding Capacity of Various Hydrated Cement Paste Systems," *Advanced Cement Based Materials*, 6, pp. 28-35.

Dhir, R.K., Jones, M.R., McCarthy, M.J. 1994, "PFA concrete: chloride-induced reinforcement corrosion," *Magazine of Concrete Research*, V. 46, No. 169, pp. 269-277.

Dhir, R.K., El-Mohr, M.A.K., Dyer, T.D. 1996, "Chloride Binding in GGBS Concrete," *Cement and Concrete Research*, V. 26, No. 12, pp. 1767-1773.

Dhir, R.K., El-Mohr, M.A.K., Dyer, T.D. 1997, "Developing Chloride Resisting Concrete Using PFA," *Cement and Concrete Research*, V. 27, No. 11, pp. 1633-1639.

Diamond, S., Dolch, W.L. 1964, "Studies on Tobermorite-Like Calcium Silicate Hydrates," *HRB Record* no. 62, pp. 62-79.

Diamond, S. 1986, "Chloride Concentrations in Concrete Pore Solutions Resulting from Calcium and Sodium Chloride Admixtures," *Cement, Concrete and Aggregates*, V. 8, No. 2, pp. 97-102.

Ehtesham Hussain, S., Rasheeduzzafar 1993, "Influence of Microsilica on Protection From Chloride-Induced Corrosion of Reinforcing Steel," *Journal of Materials in Civil Engineering*, V. 5, No. 2, pp. 155-169.

Enevoldsen, J.N., Hansson, C.M., Hope, B.B. 1994, "Binding of Chloride in Mortar Containing Admixed or Penentrated Chlorides," *Cement and Concrete Research*, Vol. 24, No. 8, pp.1525-1533.

Geiseler, J., Kollo, H., Lang, E. 1995, "Influence of Blast Furnace Cements on Durability of Concrete Structures," *ACI Materials Journal*, V. 92, No. 3, pp. 252-257.

Gerwick, B.C. 1994, "The Economic Aspects of Durability-How much added expense can be justified?", *P H Mehta Symposium on Durability of Concrete*, ACI CANMET, Nice, pp. 1-19.

Glass, G.K., Buenfeld, N.R. 1995, "The Determination of Chloride Binding Relationships", Chloride Penetration into Concrete, *Proceedings of the International RILEM Workshop*, Ed. L.O. Nilsson and J.P. Ollivier, pp. 36-42.

Glass, G.K., Wang, Y., Buenfeld, N.R. 1996, "An Investigation of Experimental Methods Used to Determine Free and Total Chloride Contents," *Cement and Concrete Research*, V. 26, No. 9, pp. 1443-1449.

Glass, G.K., Hassanein, N.M., Buenfeld, N.R. 1997, "Neural network modelling of chloride binding," *Magazine of Concrete Research*, V. 49, No. 181, pp. 323-335.

Glass, G.K., Stevenson, G.M., Buenfeld, N.R. 1998, "Chloride-Binding Isotherms From the Diffusion Cell Test," *Cement and Concrete Research*, V. 28, No. 7, pp. 939-945.

Glasser, F.P. 1991, "Coexisting solids and aqueous phase in Portland Cement," Chapter 8 in *Hydration and Setting of Cements*, Edited by A. Nonat and J.C. Mutin, RILEM Workshop, Dijon.

Glasser, F.P. 1999, "Role of Chemical Binding in Diffusion and Mass Transport," *International Conference on Ion and Mass Transport in Cement-Based Materials*, Toronto, Canada.

Glasser, F.P., Kindness, A., Stronach, S.A. 1999, "Stability and solubility relationships in AFm phases Part I. Chloride, sulfate and hydroxide", Cement and Concrete Research, V. 29, pp. 861-866.

Glasser, F.P. 2000, Private Communication.

Grutzeck, M., Benesi, A., Fanning, B. 1989, Silicon-29 "Magic Angle Spinnig Nuclear Magnetic Resonance Study of Calcium Silicate Hydrates", *Journal of the American Ceramic Society*, V.6, No. 72, pp. 665-668.

Haque, M.N., Kayyali, O.A. 1995a, "Free and Water Soluble Chloride in Concrete," *Cement and Concrete Research*, V. 25, No. 3 pp. 531-542.

Haque, M.N., Kayyali, O.A. 1995b, "Aspects of chloride ion determination in concrete," *ACI Materials Journal*, V. 92, No. 5, pp. 532-541.

Holden, W.R., Page, C.L., Short, N.R. 1983, "The influence of chlorides and sulphates on durability," Chapter 9 in *Corrosion of Reinforcement in Concrete Construction*, Edited by A.P. Crane, Ellis Horwood Ltd. Chickester, pp. 143-150.

Hooton, R.D., McGrath, P.F. 1995, "Issues related to recent developments in service life specifications for concrete structures", Chloride Penetration into Concrete, *Proceedings of the International RILEM Workshop*, Ed. L.O. Nilsson and J.P. Ollivier, pp. 389-397.

Hussain, S.E., Rasheeduzzafar 1993, "Effect of Temperature on Pore Solution Composition in Plain Cements," *Cement and Concrete Research*, V. 26, No. 6, pp. 1357-1368.

Hussain, S.E., Rasheeduzzafar, Al-Musalam, A., Al-Gahtani, A.S. 1995, "Factors Affecting Threshold Chloride for Reinforcement Corrosion in Concrete," *Cement and Concrete Research*, V. 25, No. 7, pp. 1543-1555.

Hussain, S.E., Rasheeduzzafar 1994a, "Influence of Sulfates on Chloride Binding in Cements,"*Cement and Concrete Research*, V. 24, No. 1, pp. 8-24.

Hussain, S.E., Rasheeduzzafar 1994b, "Corrosion Resistance Performance of Fly Ash Blended Cement Concrete," *ACI Materials Journal*, V. 91, No. 3, pp. 264-272.

Jawed, I., Skalny, J., Young, J.F. 1983, Chapter 6 of *Structure and Performance of Cements*, Edited by P. Barnes, 563p., Applied Science Publishers Ltd., Esses.

Kayyali, O.A., Haque, M.N. 1988, "Effect of Carbonation on the Chloride Concentration in Pore Solution of Mortars with and without Fly Ash," *Cement and Concrete Research*, V. 18, No. 4, pp. 636-648.

Kayyali, O.A., Qasrawi, M.Sh. 1992, "Chloride Binding Capacity in Cement-Fly-Ash Pastes," *Journal of Materials in Civil Engineering*, V. 4, No. 1, pp. 16-25.

Kayyali, O.A., Haque, M.N. 1995, "The Cl-/OH- Ratio in Chloride-Contaminated Concrete - a Most Important Criterion," *Magazine of Concrete Research*, V. 47, No. 172, pp. 235-242.

Kouloumbi, N., Batis, G., Malami, Ch. 1994, "The Anticorrosive Effect of Fly Ash, Slag and a Greek Pozzolan in Reinforced Concrete," *Cement and Concrete Composites*, V. 16, pp. 253-260.

Lambert, p., Page, C.L., Short, N.R. 1985, "Pore solution chemistry of the hydrated system tricalcium silicate/sodium chloride/water," *Cement and Concrete Research*, V.15, No. 4, pp.675-680.

Laidler, K.J., Meiser, J.H. 1982, *Physical Chemistry*, The Benjamin Cummings Publishing

Company, California.

Larsen, C.K. 1995, "Effect of type of Aggregate, Temperature and Drying/Rewetting on Chloride Binding and Pore Solution Composition", Chloride Penetration into Concrete, *Proceedings of the International RILEM Workshop*, Edited by L.O. Nilsson and J.P. Ollivier.

Larsen, C.K. 1998, "Chloride binding in concrete-Effect of surrounding environment and concrete composition", *Ph.D. Thesis*, The Norwegian University of Science and Technology, Norway.

Larsson, J. 1995, "The Enrichement of Chlorides in Expressed Concrete Pore Solution Submerged in Saline Solution", Corrosion of Reinforcement, *Proceedings of the Nordic Seminar in Lund*, Edited by K. Tuutti.

Maage, M., Helland, S., Poulsen, E., Vennesland, O., Carlsen, J.E. 1995, "Service life prediction of existing concrete structures exposed to marine environment", ACI Materials Journal, pp. 1-7.

Mangat, P.S., Molloy, B.T. 1995, "Chloride binding in concrete containing PFA, gbs or silica fume under sea water exposure," *Magazine of Concrete Research*, V. 47, No. 171, pp. 129-141.

Martin-Perez, B., Zibara, H., Hooton, R.D., Thomas, M.D.A. 2000, "A Study of the Effect of Chloride Binding on Service Life Predictions", *Cement and Concrete Research*, V. 30, pp. 1215-1223.

Maslehuddin, M., Page, C.L., Rasheeduzzafar 1996, "Temperature effect on the pore solution chemistry in contaminated cements," *Magazine of Concrete Research*, V. 49, No. 5, pp. 1767-1773.

Maslehuddin, M., Page, C.L., Rasheeduzzafar, Al-Mana, A.I. 1996, "Effect of Temperature on Pore Solution Chemistry and Reinforcement Corrosion in Contaminated Concrete," Proc. of 4th Int. Symposium on *Corrosion of Reinforcement in Concrete Construction*, Cambridge, pp. 67-75.

Massazza, F. 1998, "Pozzolana and Pozzolanic Cements", *Lea's Chemistry of Cement and Concrete*, 4th edition, Arnold publishers, London, pp. 546.

McGrath, P. 1996, "Development of Test Methods for Predicting Chloride Penetration into High Performance Concrete", *Ph.D. Thesis*, University of Toronto.

Mehta, P.K. 1977, "Effect of Cement Composition on Corrosion of Reinforcing Steel in Concrete," *Chloride Corrosion of Steel in Concrete*, ASTM STP 629, Edited by D.E. Tonini and S.W. Dean Jr., pp. 12-19.

Midgley, H.G., Illston, J.M. 1984, "The penetration of Chlorides into hardened cement pastes," *Cement and Concrete Research*, V. 14, No. 4, pp. 546-558.

Monfore, G.E., Verbeck, G.J. 1960, "Influence of the Cement on Corrosion Behaviour of Steel in Concrete," *Journal of American Concrete Institute*, pp. 491-515, November issue.

Nagataki, S., Otsuki, N., Wee, T.H., Nakashita, K. 1993, "Condensation of Chloride Ion in Hardened

Cement Matrix Materials and on Embedded Steel Bars," *ACI Materials Journal*, V. 90, No. 4, pp. 323-332.

Neville, A.M. 1990, *Properties of Concrete*, 3rd Edition, Pitman Publishing, London.

Neville, A. 1995, "Chloride attack of reinforced concrete: an overview," *Materials and Structures*, V. 28, pp. 63-70.

Nilsson, L.-O., Poulson, E., Sandberg, P., Sorensen, H.E., Klinghoffer, O. 1996, *"HETEK, Chloride penetration into concrete, State-of-the-Art, Transport processes, corrosion initiation, test methods and prediction models,"* Report no. 53, Edited by J.M. Fredriksen, The Road Directorate, Denmark, 151 p..

Page, C.L., Vennesland, O. 1983, "Pore Solution Composition and Chloride Binding Capacity of Silica Fume Cement Pastes," *Material and Construction*, V.16, No. 19, pp. 19-25.

Pereira, C.J., Hegedus, L.L. 1984, "Diffusion and reaction of chloride ions in porous concrete", *Proceedings of the 8th International Symposium on Chemical Reaction Engineering*, Edinburgh, Scotland, pp. 427-438.

Ramachandran, V.S. 1971, "Possible states of chloride in the hydration of tricalcium silicate in the presence of calcium chloride," Materiaux et Constructions, V. 4, No. 19, pp. 3-12.

Ramachandran, V.S., Seeley, R.C., Polomark, G.M. 1984, "Free and combined chloride in hydrating cement and cement components," *Materiaux et Constructions*, V. 17, No. 100, pp.285-289.

Ramachandran, V.S., Feldman, R.F., Beaudoin, J.J., 1981, *"Concrete Science"*, Heyden & Son Ltd., London, p. 19.

Rasheeduzzafar, Ehtesham Hussain, S., Al-Gahtani, A.S. 1991a, "Pore Solution Compostion and Reinforcement Corrosion Characteristics of Microsilica Blended Cement Concrete," *Cement and Concrete Research*, V. 21, No. 6, pp. 1035-1047.

Rasheeduzzafar, Ehtesham Hussain, S., Al-Saadoun, S.S. 1991b, "Effect of Cement Composition on Chloride Binding and Corrosion of Reinforcing Steel in Concrete," *Cement and Concrete Research*, V. 21, No. 5, pp. 777-794.

Rasheeduzzafar 1992, "Influence of Cement Composition on Concrete Durability," *ACI Materials Journal*, V. 89, No. 6, pp.574-585.

Rasheeduzzafar, Ehtesham Hussain, S., Al-Saadoun, S.S. 1992, "Effect of Tricalcium Aluminate Content of Cement on Chloride Binding and Corrosion of Reinforcing Steel in Concrete," *ACI Materials Journal*, V. 89, No. 1, pp.3-12.

Richartz, W. 1969, "Die Bindung von Chlorid bei der Zementerhärtung," *Zement-Kalk-Gips*, V. 22, No. 10, pp. 447-456.

Roberts, M.H. 1962, "Effect of calcium chloride on the durability of pre-tensioned wire in prestressed concrete." *Magazine of Concrete Research*, V. 14, No. 42, pp. 143-154.

Saito, M., Kawamura, M. 1992, "Effects of Sodium Chloride on the Hydration Products in the Interfacial Zone Between Cement Paste and Alkali-Reactive Aggregate," *Interfaces in Cementitious Composites*, RILEM, Edited by J.C. Maso, E. & FN Spon, London, pp. 33-41.

Sandberg, P., Larsson, J. 1993, "Chloride Binding in Cement Pastes in Equilibrium with Synthetic Pore Solutions", *Chloride Penetration into Concrete Structures*, Nordic Miniseminar. Ed. L.O. Nilsson, pp. 98-107.

Sandberg, P. 1999, "Studies of chloride binding in concrete exposed in a marine environment". Cement and Concrete Research, V. 29, pp. 472-477.

Scrivener, K.L., Capmas, A. 1998, "Calcium Aluminate Cements". *Lea's Chemistry of Cement and Concrete*, 4th edition, Arnold publishers, London, pp. 756.

Schweite, H.E., Ludwig, U., Albeck, J. 1969, "Combination of Calcium Chloride and Calcium Sulfate in Hydration of Aluminate-Ferritic Clinker Constituents", *Zement Kalk-Gips*, No. 5, pp. 225-234.

Sergi, G., Yu, S.W., Page, C.L. 1992, "Diffusion of chloride and hydroxyl ions in cementitious materials exposed to a saline environment," *Magazine of Concrete Research*, V. 44, No. 158, pp. 63-69.

Suryavanshi, A.K., Scantlebury, J.D., Lyon, S.B.1995, "The Binding of Chloride Ions by Sulphate Resistant Portland Cement," *Cement and Concrete Research*, V. 25, No. 3, pp. 581-592.

Suryavanshi, A.K., Scantlebury, J.D., Lyon, S.B. 1996, "Mechanisms of Friedel's Salt Formation in Cements Rich in Tri-calcium Aluminate," *Cement and Concrete Research*, V. 26, No. 5, pp. 717-727.

Suryavanshi, A.K., Swamy, R.N. 1996, "Stability of Friedel's Salt in Carbonated Concrete Structural Elements," *Cement and Concrete Research*, V. 26, No. 5, pp. 729-741.

Talib, A.Y., Rasheeduzzafar, Al-Gahtani, A.S. 1994, "Effect of Temperature on the Chloride Binding Capacity of Silica Fume Blended Cement," *Proc. of Int. Conference on Corrosion and Corrosion Protection of Steel in Concrete*, Sheffield, pp. 806-816.

Tang, L., Nilsson, L-O. 1993, "Chloride Binding Capacity and Binding Isotherms of OPC Pastes and Mortars," *Cement and Concrete Research*, V. 23, No. 2, pp. 247-253.

Tang, L., Nilsson, L.-O. 1995, "Chloride binding isotherms- "An approach by applying the modified BET equation", Chloride Penetration into Concrete, *Proceedings of the International RILEM Workshop*, Ed. L.O. Nilsson and J.P. Ollivier, pp. 36-42.

Tang, L. 1996, *Chloride Transport in Concrete - Measurement and Prediction*, PhD Thesis,

Chalmers University of Technology, Dept. Of Building Materials.

Taylor, H.F.W. 1992, *Cement Chemistry*, 2nd edition, 475 p., Academic Press Ltd., London.

Thomas, M.D.A., Pantazopoulou, S.J., Martin Perez, B. 1995, "Serivice life modelling of reinforced concrete structures exposed to chloride - a literature review" University of Toronto.

Tritthart, J. 1989, "Chloride Binding in Cement. I. Investigations to Determine the Composition of Porewater in Hardened Cement," *Cement and Concrete Research*, V. 19, No. 4, pp. 586-594.

Tritthart, J. 1989, "Chloride Binding in Cement II. The influence of the hydroxide concentration in the pore solution of hardened cement paste on chloride binding," *Cement and Concrete Research*, V. 19, No. 5, pp. 683-691, 1989.

Tuutti, K. 1982, "Analysis of pore solution squeezed out of cement paste and mortar," *Nordic Concrete Research*, V. 1, pp. 25.1-25.16.

Verbeck, G.J. 1968, *Performance of Concrete*, E.G.Swenson, Ed., University of Toronto Press, Toronto, pp. 113-124.

Verbeck, S. 1958, "Carbonation of Hydrated Portland Cement", Cement and Concrete, Los Angeles, *1956, American Society for Testing Materials Special Technical Publication 205*, pp. 17-36.

Wiens, U., Schiessl, P. 1997, "Chloride Binding of Cement Paste Containing Fly Ash," *Proc. 10th ICCC*, Edited by H. Justnes, V. 4, paper 4iv016, 10 p., Gothenburg, Sweden.

Wood, J.G.M., Crerar, J. 1995, "Analysis of chloride ingress variability and prediction of long term deterioration - a review of data from the Tay Road Bridge", *Structural Faults and Repair*, London

Wowra, O., Setzer, M.J. 1997, "Sorption of chlorides on hydrated cements and C3S pastes," *Frost Resistance of Concrete*, edited by M.J. Setzer and R. Auberg, E & FN Spon, London, pp. 147-153.

Wowra, O., Setzer, M.J. 2000, "About the Interaction of Chloride and Hardened Cement Paste", *2nd International RILEM Workshop on Testing and Modelling the Chloride Ingress into Concrete*, Paris, France.

Xu, Y. 1997, "The influence of sulphates on chloride binding and pore solution chemistry," *Cement and Concrete Research*, V. 27, No. 12, pp. 1841-1850.

Yonezawa, T., Ashworth, V., Procter, R.P.M. 1989, "The Mechanism of Fixing $Cl^-$ by Cement Hydrates Resulting in the Transformation of NaCl to NaOH," *8th International Conference on Alkali-Aggregate Reaction*, pp. 153-160.

Yu, S.W., Sergi, G., Page, C.L. 1993, "Ionic Diffusion Across an Interface Between Chloride-Free and Chloride Containing Cementitious Materials," *Magazine of Concrete Research*, V. 45, No. 165, pp. 257-261.

# Appendix A

## Results of Phase One

### A.1 Introduction

The results presented in this appendix are referred to in Section 4-1. Table A-1 shows the chemical compositions of the SCM used in this research. and Table A-2 presents the proportioning of the cementitious mixtures used in Phase 1.

Table A-1: Chemical Composition of the Supplementary Cementing Materials

| Amount (%) | Silica Fume SKW | Metakaolin | GGBFS Lafarge Slag | Fly Ash Ft. Martin Alegheney Type F FA | Fly Ash Coal Creek Type CH FA2 | Fly Ash Colombia Type CI FA1 |
|---|---|---|---|---|---|---|
| $SiO_2$ | 94.48 | 52.01 | 36.18 | 53.89 | 40.82 | 43.07 |
| $Al_2O_3$ | 0.24 | 44.72 | 10.02 | 24.65 | 11.09 | 20.78 |
| $TiO_2$ | 0.01 | 1.6 | 0.67 | 1.14 | 0.47 | 1.10 |
| $P_2O_5$ | 0.14 | 0.09 | 0.01 | 0.71 | 0.10 | 0.67 |
| $Fe_2O_3$ | 0.63 | 0.58 | 0.50 | 8.63 | 6.21 | 5.41 |
| CaO | 0.44 | 0.00 | 35.49 | 4.37 | 29.89 | 17.72 |
| SrO | 0.02 | 0.02 | 0.04 | 0.16 | 0.30 | 0.54 |
| MgO | 0.38 | 0.00 | 0.66 | 0.83 | 4.41 | 4.18 |
| $Mn_2O_3$ | 0.03 | 0.01 | 13.58 | 0.05 | 0.06 | 0.17 |
| $Na_2O_3$ | 0.16 | 0.32 | 0.43 | 0.6 | 1.14 | 1.46 |
| $K_2O$ | 1.01 | 0.19 | 0.50 | 2.14 | 1.71 | 0.75 |
| $Na_2O_e$ | 0.82 | 0.45 | 0.77 | 2.07 | 2.26 | 1.95 |
| $SO_3$* | 0.36 | 0.12 | 1.51 | 0.61 | 2.17 | 2.17 |
| LOI@1000 | 2.87 | 0.9 | 1.72 | 1.53 | 1.30 | 2.57 |

* $SO_3$ based on sulphur determined by LECO

Table A-2: Proportioning of Mixtures Used in Phase 1

| Mix | W/CM | OPC (%) | SF (%) | MK (%) | FA (%) | BFS (%) |
|---|---|---|---|---|---|---|
| OPC | 0.3, 0.5, 0.7 | 100 | | | | |
| 8SF | 0.3, 0.5 | 92 | 8 | | | |
| 8MK | 0.3, 0.5 | 92 | | 8 | | |
| 25FA | 0.3, 0.5 | 75 | | | 25 | |
| 25FA1 | 0.5 | 75 | | | 25 | |
| 25FA2 | 0.5 | 75 | | | 25 | |
| 40FA | 0.3 | 60 | | | 40 | |
| 25SL | 0.3, 0.5 | 75 | | | | 25 |
| 40SL | 0.3 | 60 | | | | 40 |
| 25FA6SF | 0.3, 0.5 | 69 | 6 | | 25 | |
| 40FA5SF | 0.3 | 55.2 | 4.8 | | 40 | |
| 25SL6SF | 0.3, 0.5 | 69 | 6 | | | 25 |
| 40SL5SF | 0.3 | 55.2 | 4.8 | | | 40 |

**A.2 Results of mixtures with W/CM = 0.3**

Tables A-3 to A25 present the results of mixtures with W/CM ratio of 0.3. The chloride binding capacities of pastes, tested at 38 °C, are corrected to take into account the effect of evaporation. The correction factors are calculated from the initial and final weights of the host solution. Two assumptions are made in the correction process: 1) the ratio of the initial and equilibrium volumes of the host solution is equal to the ratio of the initial and equilibrium weight of the host solution, and 2) the evaporation does not affect the equilibrium between bound and free chloride. This means that the amount of chloride in the host solution, at equilibrium, is the same with or without evaporation. The corrected chloride concentrations at equilibrium are obtained as follow:

$$V_s / V_{ee} = W_s / W_{ee} \qquad \text{(A-1)}$$

$$C_e * V_s = C_{ee} * V_{ee} \qquad \text{(A-2)}$$

$$C_e = C_{ee} * V_{ee} / V_s = C_{ee} * W_{ee} / W_s \qquad \text{(A-3)}$$

where $V_s$ initial volume of host solution (without evaporation).

$V_{ee}$: volume of host solution at equilibrium after evaporation occurred.

$W_s$: initial weight of host solution (without evaporation)

$W_{ee}$: weight of host solution at equilibrium after evaporation occured.

$C_e$: chloride concentration at equilibrium (without evaporation).

$C_{ee}$: measured chloride concentration at equilibrium after evaporation occurred.

The correction factors in Tables A-6, A-10, A-14, and A-19, are equal to the $W_{ee} / W_s$ ratios of the different samples. The corrected equilibrium chloride concentrations ($C_e$) presented in these tables are the obtained using equation A-3.

The accuracy of the corrected chloride binding capacities obviously depends on the accuracy of the 2 previously mentioned assumptions. In fact, both assumptions results in errors. While the first assumption does not have significant effect on the results, The second assumption significantly oversetimates the chloride binding capacity at low concentrations (eg 0.1 M, 0.3 M). Nevertheless, the observed effects of temperature at high chloride concentrations are true effect.

## Control, W/CM = 0.3, curing: 2 months

Table A-3: Chloride binding capacity of the control paste.

| Solution Volume | Dry sample mass | Initial Conc. | Equilibrium Conc. | Bound Chloride |
|---|---|---|---|---|
| $V_s$ (ml) | $W_d$ (g) | $C_i$ (mol/l) | $C_e$ (mol/l) | $C_b$ mg Cl/g Sple |
| 33.745 | 21.882 | 0.101 | 0.047 | 2.93 |
| 27.399 | 21.901 | 0.304 | 0.198 | 4.69 |
| 25.407 | 23.682 | 0.508 | 0.363 | 5.51 |
| 23.826 | 23.516 | 0.709 | 0.536 | 6.22 |
| 21.428 | 23.378 | 1.006 | 0.791 | 6.98 |
| 20.216 | 22.658 | 2.015 | 1.755 | 8.21 |
| 20.017 | 22.298 | 3.030 | 2.694 | 10.69 |

## Control (replica), W/CM = 0.3, curing: 2 months

Table A-4: Chloride binding capacity of a replica of the control paste.

| Solution Volume | Dry sample mass | Initial Conc. | Equilibrium Conc. | Bound Chloride |
|---|---|---|---|---|
| $V_s$ (ml) | $W_d$ (g) | $C_i$ (mol/l) | $C_e$ (mol/l) | $C_b$ mg Cl/g Sple |
| 37.702 | 22.787 | 0.101 | 0.047 | 3.17 |
| 27.438 | 23.239 | 0.508 | 0.364 | 6.02 |
| 24.274 | 22.750 | 0.709 | 0.539 | 6.45 |
| 20.224 | 23.008 | 1.006 | 0.777 | 7.14 |
| 20.875 | 22.621 | 2.015 | 1.737 | 9.08 |
| 21.310 | 22.224 | 3.030 | 2.677 | 12.00 |

## Control, W/CM = 0.3, curing: 2 months, T = 7°C (storage temperature)

Table A-5: Chloride binding capacity of the control paste, stored at 7°C.

| Solution Volume | Dry sample mass | Initial Conc. | Equilibrium Conc. | Bound Chloride |
|---|---|---|---|---|
| $V_s$ (ml) | $W_d$ (g) | $C_i$ (mol/l) | $C_e$ (mol/l) | $C_b$ mg Cl/g Sple |
| 35.968 | 22.732 | 0.101 | 0.047 | 3.04 |
| 29.287 | 22.233 | 0.304 | 0.212 | 4.29 |
| 22.317 | 19.400 | 0.508 | 0.382 | 5.13 |
| 23.261 | 22.842 | 0.709 | 0.559 | 5.40 |
| 20.349 | 22.298 | 1.006 | 0.815 | 6.19 |
| 20.523 | 21.910 | 2.015 | 1.763 | 8.38 |
| 20.466 | 22.538 | 3.030 | 2.726 | 9.80 |

## Control, W/CM = 0.3, curing: 2 months, T = 38°C

Table A-6: Chloride binding capacity of the control paste, stored at 38°C.

| Solution Volume | Dry sample mass | Initial Conc. | Equilibrium Conc. | Bound Chloride |
|---|---|---|---|---|
| $V_s$ (ml) | $W_d$ (g) | $C_i$ (mol/l) | $C_e$ (mol/l) | $C_b$ mg Cl/g Sple |
| 34.831 | 22.436 | 0.101 | 0.056 (0.969)* | 2.48 |
| 29.119 | 22.187 | 0.304 | 0.219 (0.966)* | 3.97 |
| 25.456 | 22.778 | 0.508 | 0.398 (0.963)* | 4.35 |
| 21.245 | 20.876 | 0.709 | 0.566 (0.954)* | 5.18 |
| 20.503 | 22.861 | 1.006 | 0.808 (0.955)* | 6.29 |
| 18.749 | 20.553 | 2.015 | 1.720 (0.953)* | 9.55 |
| 20.286 | 22.132 | 3.030 | 2.695 (0.962)* | 10.90 |

*The equilibrium chloride concentrations, shown in Table A-6, are the adjusted concentrations, using the measured chloride concentrations and the correction factors shown between parantheses.

## 8SF, W/CM = 0.3, curing: 2 months

Table A-7: Chloride binding capacity of the 8SF paste.

| Solution Volume | Dry sample mass | Initial Conc. | Equilibrium Conc. | Bound Chloride |
|---|---|---|---|---|
| $V_s$ (ml) | $W_d$ (g) | $C_i$ (mol/l) | $C_e$ (mol/l) | $C_b$ mg Cl/g Sple |
| 35.778 | 22.719 | 0.101 | 0.073 | 1.58 |
| 30.375 | 23.273 | 0.304 | 0.249 | 2.55 |
| 25.936 | 22.581 | 0.508 | 0.422 | 3.50 |
| 20.806 | 22.489 | 0.709 | 0.592 | 3.85 |
| 20.474 | 21.621 | 1.006 | 0.876 | 4.36 |
| 20.569 | 22.655 | 2.015 | 1.856 | 5.12 |
| 19.093 | 22.387 | 3.030 | 2.826 | 6.17 |

## 8SF(replica), W/CM = 0.3, curing: 2 months

Table A-8: Chloride binding capacity of a replica of the 8SF paste.

| Solution Volume | Dry sample mass | Initial Conc. | Equilibrium Conc. | Bound Chloride |
|---|---|---|---|---|
| $V_s$ (ml) | $W_d$ (g) | $C_i$ (mol/l) | $C_e$ (mol/l) | $C_b$ mg Cl/g Sple |
| 34.881 | 21.503 | 0.101 | 0.071 | 1.70 |
| 29.861 | 22.870 | 0.304 | 0.246 | 2.68 |
| 25.259 | 22.787 | 0.508 | 0.421 | 3.41 |
| 23.027 | 21.833 | 0.709 | 0.602 | 4.00 |
| 20.388 | 22.641 | 1.006 | 0.873 | 4.24 |
| 21.117 | 22.081 | 2.015 | 1.870 | 4.93 |
| 21.103 | 22.787 | 3.030 | 2.823 | 6.81 |

## 8SF, W/CM = 0.3, curing: 2 months, T = 7°C

Table A-9: Chloride binding capacity of the 8SF paste, stored at 7°C.

| Solution Volume | Dry sample mass | Initial Conc. | Equilibrium Conc. | Bound Chloride |
|---|---|---|---|---|
| $V_s$ (ml) | $W_d$ (g) | $C_i$ (mol/l) | $C_e$ (mol/l) | $C_b$ mg Cl/g Sple |
| 36.825 | 21.889 | 0.101 | 0.073 | 1.66 |
| 31.136 | 22.876 | 0.304 | 0.248 | 2.68 |
| 25.515 | 22.286 | 0.508 | 0.428 | 3.24 |
| 23.553 | 19.978 | 0.709 | 0.625 | 3.52 |
| 19.627 | 22.258 | 1.006 | 0.883 | 3.84 |
| 20.792 | 22.138 | 2.015 | 1.884 | 4.35 |
| 20.601 | 21.058 | 3.030 | 2.880 | 5.20 |

## 8SF, W/CM = 0.3, curing: 2 months, T = 38°C

Table A-10: Chloride binding capacity of the 8SF paste, stored at 38°C.

| Solution Volume | Dry sample mass | Initial Conc. | Equilibrium Conc. | Bound Chloride |
|---|---|---|---|---|
| $V_s$ (ml) | $W_d$ (g) | $C_i$ (mol/l) | $C_e$ (mol/l) | $C_b$ mg Cl/g Sple |
| 35.081 | 22.793 | 0.101 | 0.070 (0.936)* | 1.69 |
| 29.782 | 23.255 | 0.304 | 0.241 (0.926)* | 2.85 |
| 26.790 | 21.778 | 0.508 | 0.421 (0.920)* | 3.78 |
| 23.378 | 23.033 | 0.709 | 0.588 (0.915)* | 4.35 |
| 20.243 | 22.701 | 1.006 | 0.853 (0.901)* | 4.84 |
| 20.569 | 22.119 | 2.015 | 1.841 (0.910)* | 5.72 |
| 20.313 | 21.898 | 3.030 | 2.788 (0.913)* | 7.97 |

*The equilibrium chloride concentrations, shown in Table A-6, are the adjusted concentrations, using the measured chloride concentrations and the correction factors shown between parantheses.

## 25SL, W/CM = 0.3, curing: 2 months

Table A11: Chloride binding capacity of the 25SL paste.

| Solution Volume | Dry sample mass | Initial Conc. | Equilibrium Conc. | Bound Chloride |
|---|---|---|---|---|
| $V_s$ (ml) | $W_d$ (g) | $C_i$ (mol/l) | $C_e$ (mol/l) | $C_b$ mg Cl/g Sple |
| 37.114 | 23.375 | 0.101 | 0.047 | 3.07 |
| 30.415 | 23.544 | 0.304 | 0.203 | 4.64 |
| 26.976 | 23.695 | 0.508 | 0.356 | 6.15 |
| 23.719 | 23.535 | 0.709 | 0.526 | 6.55 |
| 21.851 | 23.563 | 1.006 | 0.777 | 7.52 |
| 21.971 | 23.620 | 2.015 | 1.749 | 8.78 |
| 21.570 | 23.864 | 3.030 | 2.690 | 10.90 |

## 25SL (replica), W/CM = 0.3, curing: 2 months

Table A-12: Chloride binding capacity of a replica of the 25SL paste.

| Solution Volume | Dry sample mass | Initial Conc. | Equilibrium Conc. | Bound Chloride |
|---|---|---|---|---|
| $V_s$ (ml) | $W_d$ (g) | $C_i$ (mol/l) | $C_e$ (mol/l) | $C_b$ mg Cl/g Sple |
| 37.324 | 23.145 | 0.101 | 0.047 | 3.11 |
| 24.986 | 22.303 | 0.304 | 0.191 | 4.48 |
| 25.691 | 23.033 | 0.508 | 0.358 | 5.94 |
| 23.923 | 23.257 | 0.709 | 0.524 | 6.76 |
| 20.320 | 22.930 | 1.006 | 0.769 | 7.43 |
| 20.393 | 23.098 | 2.015 | 1.733 | 8.82 |
| 20.744 | 22.022 | 3.030 | 2.705 | 10.86 |

## 25SL, W/CM = 0.3, curing: 2 months, T = 7°C

Table A-13: Chloride binding capacity of the 25SL paste, stored at 7°C.

| Solution Volume | Dry sample mass | Initial Conc. | Equilibrium Conc. | Bound Chloride |
|---|---|---|---|---|
| $V_s$ (ml) | $W_d$ (g) | $C_i$ (mol/l) | $C_e$ (mol/l) | $C_b$ mg Cl/g Sple |
| 34.762 | 23.196 | 0.101 | 0.044 | 3.01 |
| 30.751 | 23.497 | 0.304 | 0.194 | 5.12 |
| 25.927 | 23.328 | 0.508 | 0.351 | 6.19 |
| 23.495 | 23.686 | 0.709 | 0.522 | 6.56 |
| 21.948 | 23.497 | 1.006 | 0.791 | 7.11 |
| 20.272 | 23.460 | 2.015 | 1.778 | 7.26 |
| 20.663 | 23.639 | 3.030 | 2.740 | 8.99 |

## 25SL, W/CM = 0.3, curing: 2 months, T = 38°C

Table A-14: Chloride binding capacity of the 25SL paste. stored at 38°C.

| Solution Volume | Dry sample mass | Initial Conc. | Equilibrium Conc. | Bound Chloride |
|---|---|---|---|---|
| $V_s$ (ml) | $W_d$ (g) | $C_i$ (mol/l) | $C_e$ (mol/l) | $C_b$ mg Cl/g Sple |
| 37.932 | 23.902 | 0.101 | 0.049 (0.973)* | 2.92 |
| 29.188 | 22.660 | 0.304 | 0.199 (0.966)* | 4.79 |
| 25.230 | 23.403 | 0.508 | 0.351 (0.959)* | 6.01 |
| 23.242 | 23.554 | 0.709 | 0.520 (0.958)* | 6.63 |
| 21.004 | 22.736 | 1.006 | 0.756 (0.951)* | 8.19 |
| 20.086 | 21.428 | 2.015 | 1.696 (0.957)* | 10.60 |
| 20.556 | 23.450 | 3.030 | 2.604 (0.959)* | 13.23 |

*The equilibrium chloride concentrations, shown in Table A-6, are the adjusted concentrations, using the measured chloride concentrations and the correction factors shown between parantheses.

## 40SL, W/CM = 0.3, curing: 2 months

Table A-15: Chloride binding capacity of the 40SL paste.

| Solution Volume | Dry sample mass | Initial Conc. | Equilibrium Conc. | Bound Chloride |
|---|---|---|---|---|
| $V_s$ (ml) | $W_d$ (g) | $C_i$ (mol/l) | $C_e$ (mol/l) | $C_b$ mg Cl/g Sple |
| 35.878 | 22.918 | 0.101 | 0.047 | 3.01 |
| 28.902 | 22.463 | 0.304 | 0.194 | 5.00 |
| 25.985 | 23.271 | 0.508 | 0.350 | 6.25 |
| 20.748 | 21.368 | 0.709 | 0.508 | 6.91 |
| 21.322 | 21.897 | 1.006 | 0.765 | 8.31 |
| 19.696 | 22.138 | 2.015 | 1.726 | 9.11 |
| 20.574 | 22.445 | 3.030 | 2.642 | 12.60 |

## 25FA, W/CM = 0.3, curing: 2 months

Table A-16: Chloride binding capacity of the 25FA paste.

| Solution Volume | Dry sample mass | Initial Conc. | Equilibrium Conc. | Bound Chloride |
|---|---|---|---|---|
| $V_s$ (ml) | $W_d$ (g) | $C_i$ (mol/l) | $C_e$ (mol/l) | $C_b$ mg Cl/g Sple |
| 33.366 | 21.297 | 0.101 | 0.062 | 2.18 |
| 28.635 | 22.012 | 0.304 | 0.223 | 3.72 |
| 23.003 | 21.955 | 0.508 | 0.382 | 4.68 |
| 21.001 | 20.555 | 0.709 | 0.554 | 5.61 |
| 24.846 | 26.006 | 1.006 | 0.819 | 6.33 |
| 18.554 | 20.066 | 2.015 | 1.765 | 8.21 |
| 18.563 | 20.809 | 3.030 | 2.713 | 10.03 |

## 25FA (replica), W/CM = 0.3, curing: 2 months

Table A-17: Chloride binding capacity of a replica of the 25FA paste.

| Solution Volume | Dry sample mass | Initial Conc. | Equilibrium Conc. | Bound Chloride |
|---|---|---|---|---|
| $V_s$ (ml) | $W_d$ (g) | $C_i$ (mol/l) | $C_e$ (mol/l) | $C_b$ mg Cl/g Sple |
| 37.792 | 23.364 | 0.101 | 0.060 | 2.34 |
| 29.040 | 21.959 | 0.304 | 0.221 | 3.89 |
| 25.240 | 22.887 | 0.508 | 0.383 | 4.88 |
| 24.089 | 23.243 | 0.709 | 0.552 | 5.77 |
| 20.744 | 22.830 | 1.006 | 0.800 | 6.63 |
| 20.987 | 23.158 | 2.015 | 1.748 | 8.58 |
| 21.238 | 22.755 | 3.030 | 2.689 | 11.27 |

## 25FA, W/CM = 0.3, curing: 2 months, T = 7°C

Table A-18: Chloride binding capacity of the 25FA paste, stored at 7°C.

| Solution Volume | Dry sample mass | Initial Conc. | Equilibrium Conc. | Bound Chloride |
|---|---|---|---|---|
| $V_s$ (ml) | $W_d$ (g) | $C_i$ (mol/l) | $C_e$ (mol/l) | $C_b$ mg Cl/g Sple |
| 34.831 | 21.485 | 0.101 | 0.053 | 2.78 |
| 29.386 | 21.673 | 0.304 | 0.210 | 4.50 |
| 24.926 | 21.476 | 0.508 | 0.378 | 5.37 |
| 21.878 | 20.884 | 0.709 | 0.546 | 6.06 |
| 19.685 | 21.523 | 1.006 | 0.794 | 6.88 |
| 18.610 | 19.653 | 2.015 | 1.785 | 7.72 |
| 19.137 | 20.104 | 3.030 | 2.742 | 9.72 |

## 25FA, W/CM = 0.3, curing: 2 months, T = 38°C

Table A-19: Chloride binding capacity of the 25FA paste, stored at 38°C.

| Solution Volume | Dry sample mass | Initial Conc. | Equilibrium Conc. | Bound Chloride |
|---|---|---|---|---|
| $V_s$ (ml) | $W_d$ (g) | $C_i$ (mol/l) | $C_e$ (mol/l) | $C_b$ mg Cl/g Sple |
| 33.097 | 21.081 | 0.101 | 0.070 (0.969)* | 1.73 |
| 27.953 | 21.767 | 0.304 | 0.232 (0.962)* | 3.26 |
| 23.494 | 22.491 | 0.508 | 0.396 (0.955)* | 4.15 |
| 22.423 | 22.529 | 0.709 | 0.575 (0.955)* | 4.73 |
| 16.420 | 18.252 | 1.006 | 0.817 (0.939)* | 6.02 |
| 17.365 | 21.937 | 2.015 | 1.706 (0.948)* | 8.68 |
| 19.371 | 22.106 | 3.030 | 2.644 (0.958)* | 11.98 |

*The equilibrium chloride concentrations, shown in Table A-6, are the adjusted concentrations, using the measured chloride concentrations and the correction factors shown between parantheses.

## 40FA, W/CM = 0.3, curing: 2 months

Table A-20: Chloride binding capacity of the 40FA paste.

| Solution Volume | Dry sample mass | Initial Conc. | Equilibrium Conc. | Bound Chloride |
|---|---|---|---|---|
| $V_s$ (ml) | $W_d$ (g) | $C_i$ (mol/l) | $C_e$ (mol/l) | $C_b$ mg Cl/g Sple |
| 31.741 | 19.376 | 0.101 | 0.065 | 2.12 |
| 27.646 | 19.488 | 0.304 | 0.228 | 3.81 |
| 26.034 | 20.560 | 0.508 | 0.399 | 4.88 |
| 21.897 | 19.031 | 0.709 | 0.568 | 5.76 |
| 20.195 | 18.760 | 1.006 | 0.823 | 7.00 |
| 20.718 | 19.189 | 2.015 | 1.767 | 9.49 |
| 21.400 | 20.196 | 3.030 | 2.713 | 11.90 |

## 8MK, W/CM = 0.3, curing: 2 months

Table A-21: Chloride binding capacity of the 8MK paste.

| Solution Volume | Dry sample mass | Initial Conc. | Equilibrium Conc. | Bound Chloride |
|---|---|---|---|---|
| $V_s$ (ml) | $W_d$ (g) | $C_i$ (mol/l) | $C_e$ (mol/l) | $C_b$ mg Cl/g Sple |
| 27.624 | 19.812 | 0.101 | 0.044 | 2.84 |
| 25.085 | 20.875 | 0.304 | 0.190 | 4.85 |
| 19.747 | 21.800 | 0.508 | 0.319 | 6.08 |
| 17.923 | 21.893 | 0.709 | 0.468 | 7.00 |
| 20.040 | 23.077 | 2.015 | 1.631 | 11.82 |
| 18.401 | 23.187 | 3.030 | 2.503 | 14.82 |

## 25SL6SF, W/CM = 0.3, curing: 2 months

Table A-22: Chloride binding capacity of the 25SL6SF paste.

| Solution Volume | Dry sample mass | Initial Conc. | Equilibrium Conc. | Bound Chloride |
|---|---|---|---|---|
| $V_s$ (ml) | $W_d$ (g) | $C_i$ (mol/l) | $C_e$ (mol/l) | $C_b$ mg Cl/g Sple |
| 35.699 | 22.982 | 0.101 | 0.070 | 1.72 |
| 31.008 | 23.103 | 0.304 | 0.240 | 3.06 |
| 25.358 | 23.010 | 0.508 | 0.408 | 3.89 |
| 22.852 | 22.655 | 0.709 | 0.586 | 4.38 |
| 20.648 | 23.355 | 1.006 | 0.836 | 5.32 |
| 20.708 | 22.469 | 2.015 | 1.811 | 6.67 |
| 20.233 | 23.057 | 3.030 | 2.743 | 8.93 |

## 40SL5SF, W/CM = 0.3, curing: 2 months

Table A-23: Chloride binding capacity of the 40SL5SF paste.

| Solution Volume | Dry sample mass | Initial Conc. | Equilibrium Conc. | Bound Chloride |
|---|---|---|---|---|
| $V_s$ (ml) | $W_d$ (g) | $C_i$ (mol/l) | $C_e$ (mol/l) | $C_b$ mg Cl/g Sple |
| 35.390 | 22.883 | 0.101 | 0.065 | 2.00 |
| 31.413 | 23.229 | 0.304 | 0.230 | 3.53 |
| 26.240 | 23.257 | 0.508 | 0.402 | 4.26 |
| 23.105 | 23.473 | 0.709 | 0.566 | 4.98 |
| 20.571 | 23.201 | 1.006 | 0.827 | 5.62 |
| 20.894 | 22.509 | 2.015 | 1.783 | 7.65 |
| 20.592 | 23.342 | 3.030 | 2.721 | 9.67 |

## 25FA6SF, W/CM = 0.3, curing: 2 months

Table A-24: Chloride binding capacity of the 25FA6SF paste.

| Solution Volume | Dry sample mass | Initial Conc. | Equilibrium Conc. | Bound Chloride |
|---|---|---|---|---|
| $V_s$ (ml) | $W_d$ (g) | $C_i$ (mol/l) | $C_e$ (mol/l) | $C_b$ mg Cl/g Sple |
| 35.679 | 23.230 | 0.101 | 0.079 | 1.21 |
| 31.908 | 23.053 | 0.304 | 0.264 | 1.96 |
| 25.927 | 22.922 | 0.508 | 0.444 | 2.57 |
| 23.573 | 23.090 | 0.709 | 0.615 | 3.39 |
| 20.686 | 22.196 | 1.006 | 0.869 | 4.53 |
| 20.820 | 22.689 | 2.015 | 1.826 | 6.16 |
| 19.954 | 22.857 | 3.030 | 2.756 | 8.47 |

## 40FA5SF, W/CM = 0.3, curing: 2 months

Table A-25: Chloride binding capacity of the 40FA5SF paste.

| Solution Volume | Dry sample mass | Initial Conc. | Equilibrium Conc. | Bound Chloride |
|---|---|---|---|---|
| $V_s$ (ml) | $W_d$ (g) | $C_i$ (mol/l) | $C_e$ (mol/l) | $C_b$ mg Cl/g Sple |
| 34.941 | 23.419 | 0.101 | 0.078 | 1.23 |
| 30.474 | 23.005 | 0.304 | 0.257 | 2.22 |
| 25.789 | 22.827 | 0.508 | 0.432 | 3.04 |
| 23.105 | 23.381 | 0.709 | 0.603 | 3.73 |
| 20.686 | 23.118 | 1.006 | 0.865 | 4.46 |
| 20.745 | 23.419 | 2.015 | 1.823 | 6.02 |
| 20.879 | 23.165 | 3.030 | 2.759 | 8.66 |

### A.3 Results of mixtures with W/CM = 0.5

Tables A-26 to A-39 show the chloride binding isotherms of pastes with W/CM ratio of 0.5. Some of the pastes were cured for 2 months ( Tables A-26 to A-31) before being exposed to chloride solutions, while the other pastes were cured for 9 months (Tables A-32 to A-39) before being exposed to chloride solutions.

## Control, W/CM = 0.5, curing = 2 months

Table A-26: Chloride binding capacity of the control paste.

| Solution Mass | Solution Density | Solution Volume | Sample Mass | Dry Sample Mass | Initial Conc. | Equilibrium Conc. | Bound Chloride |
|---|---|---|---|---|---|---|---|
| $W_{sol}$ (g) | $d_s$ (g/ml) | $V_{sol}$ (ml) | $W_{ss}$ (g) | $W_d$ (g) | $C_i$ (mol/l) | $C_e$ (mol/l) | $C_b$ mg Cl/g Sple |
| 32.05 | 1.003 | 31.95 | 24.50 | 22.98 | 0.101 | 0.041 | 2.94 |
| 33.43 | 1.040 | 32.15 | 24.93 | 23.38 | 1.009 | 0.841 | 8.15 |
| 35.80 | 1.115 | 32.12 | 24.82 | 23.28 | 3.015 | 2.774 | 11.79 |

## 8SF, W/CM = 0.5, curing = 2 months

Table A-27: Chloride binding capacity of the 8SF paste.

| Solution Mass | Solution Density | Solution Volume | Sample Mass | Dry Sample Mass | Initial Conc. | Equilibrium Conc. | Bound Chloride |
|---|---|---|---|---|---|---|---|
| $W_{sol}$ (g) | $d_s$ (g/ml) | $V_{sol}$ (ml) | $W_{ss}$ (g) | $W_d$ (g) | $C_i$ (mol/l) | $C_e$ (mol/l) | $C_b$ mg Cl/g Sple |
| 32.31 | 1.003 | 32.21 | 24.81 | 23.27 | 0.101 | 0.059 | 2.04 |
| 33.10 | 1.040 | 31.83 | 24.24 | 22.74 | 1.009 | 0.887 | 6.01 |
| 35.47 | 1.115 | 31.83 | 24.85 | 23.31 | 3.015 | 2.832 | 8.86 |
| 35.94 | 1.115 | 32.25 | 24.64 | 23.11 | 3.015 | 2.855 | 7.94 |

## 8MK, W/CM = 0.5, curing = 2 months

Table A-28: Chloride binding capacity of the 8MK paste.

| Solution Mass | Solution Density | Solution Volume | Sample Mass | Dry Sample Mass | Initial Conc. | Equilibrium Conc. | Bound Chloride |
|---|---|---|---|---|---|---|---|
| $W_{sol}$ (g) | $d_s$ (g/ml) | $V_{sol}$ (ml) | $W_{11}$ (g) | $W_d$ (g) | $C_i$ (mol/l) | $C_e$ (mol/l) | $C_b$ mg Cl/g Sple |
| 32.17 | 1.003 | 32.07 | 24.86 | 23.32 | 0.101 | 0.039 | 3.01 |
| 33.54 | 1.040 | 32.26 | 24.76 | 23.23 | 1.009 | 0.740 | 13.23 |
| 35.71 | 1.115 | 32.04 | 24.45 | 22.93 | 3.015 | 2.554 | 22.82 |
| 35.57 | 1.115 | 31.92 | 24.53 | 23.01 | 3.015 | 2.584 | 21.18 |

## 25FA, W/CM = 0.5, curing: 2 months

Table A-29: Chloride binding capacity of the 25FA paste.

| Sample Mass | Solution Mass | Solution Density | Solution Volume | Dry Sample Mass | Initial Conc. | Equilibrium Conc. | Bound Chloride |
|---|---|---|---|---|---|---|---|
| $W_{11}$ (g) | $W_{sol}$ (g) | $d_s$ (g/ml) | $V_{sol}$ (ml) | $W_d$ (g) | $C_i$ (mol/l) | $C_e$ (mol/l) | $C_b$ mg Cl/g Sple |
| 24.47 | 29.45 | 1.003 | 29.36 | 22.85 | 0.101 | 0.038 | 2.88 |
| 24.77 | 30.61 | 1.040 | 29.44 | 23.13 | 1.008 | 0.765 | 10.93 |
| 24.74 | 32.75 | 1.115 | 29.39 | 23.10 | 3.021 | 2.682 | 15.27 |

## 25FA2, W/CM = 0.5, curing: 2 months

Table A-30: Chloride binding capacity of the 25FA1 paste.

| Sample Mass | Solution Mass | Solution Density | Solution Volume | Dry Sample Mass | Initial Conc. | Equilibrium Conc. | Bound Chlori |
|---|---|---|---|---|---|---|---|
| $W_{11}$ (g) | $W_{sol}$ (g) | $d_s$ (g/ml) | $V_{sol}$ (ml) | $W_d$ (g) | $C_i$ (mol/l) | $C_e$ (mol/l) | $C_b$ mg Cl/g Sple |
| 24.88 | 29.19 | 1.003 | 29.10 | 23.32 | 0.101 | 0.043 | 2.57 |
| 24.89 | 29.83 | 1.040 | 28.69 | 23.32 | 1.008 | 0.798 | 9.16 |
| 24.62 | 32.69 | 1.115 | 29.33 | 23.07 | 3.021 | 2.736 | 12.81 |

## 25FA1, W/CM = 0.5, curing: 2 months

Table A-31: Chloride binding capacity of the 25FA2 paste.

| Sample Mass | Solution Mass | Solution Density | Solution Volume | Dry Sample Mass | Initial Conc. | Equilibrium Conc. | Bound Chloride |
|---|---|---|---|---|---|---|---|
| $W_{11}$ (g) | $W_{sol}$ (g) | $d_s$ (g/ml) | $V_{sol}$ (ml) | $W_d$ (g) | $C_i$ (mol/l) | $C_e$ (mol/l) | $C_b$ mg Cl/g Sple |
| 24.86 | 29.56 | 1.003 | 29.47 | 23.44 | 0.101 | 0.042 | 2.63 |
| 24.93 | 30.43 | 1.040 | 29.27 | 23.51 | 1.008 | 0.710 | 13.12 |
| 24.91 | 32.58 | 1.115 | 29.23 | 23.49 | 3.021 | 2.551 | 20.73 |

## Control, W/CM = 0.5, 9 months curing

Table A-32: Chloride binding capacity of the control paste.

| Solution Volume | Dry Sample Mass | Initial Conc. | Equilibrium Conc. | Bound Chloride |
|---|---|---|---|---|
| $V_{sol}$ (ml) | $W_d$ (g) | $C_i$ (mol/l) | $C_e$ (mol/l) | $C_b$ mg Cl/g Sple |
| 29.28 | 22.98 | 0.101 | 0.044 | 2.60 |
| 29.28 | 23.09 | 0.308 | 0.217 | 4.12 |
| 29.25 | 23.08 | 0.510 | 0.386 | 5.58 |
| 28.99 | 23.18 | 0.709 | 0.561 | 6.60 |
| 29.01 | 23.11 | 1.007 | 0.838 | 7.55 |
| 29.31 | 23.06 | 2.044 | 1.831 | 9.58 |
| 29.45 | 23.04 | 3.045 | 2.786 | 11.77 |

## 25FA, W/CM = 0.5, 9 months curing

Table A-33: Chloride binding capacity of the 25FA paste.

| Solution Volume | Dry Sample Mass | Initial Conc. | Equilibrium Conc. | Bound Chloride |
|---|---|---|---|---|
| $V_{sol}$ (ml) | $W_d$ (g) | $C_i$ (mol/l) | $C_e$ (mol/l) | $C_b$ mg Cl/g Sple |
| 29.68 | 22.99 | 0.101 | 0.047 | 2.47 |
| 28.89 | 22.98 | 0.308 | 0.206 | 4.57 |
| 28.98 | 22.98 | 0.510 | 0.366 | 6.44 |
| 29.03 | 22.99 | 0.709 | 0.523 | 8.34 |
| 29.18 | 23.01 | 1.007 | 0.788 | 9.84 |
| 29.34 | 23.02 | 2.044 | 1.762 | 12.70 |
| 29.56 | 18.42 | 3.045 | 2.784 | 14.89 |

## 25SL, W/CM = 0.5, 9 months curing

Table A-34: Chloride binding capacity of the 25SL paste.

| Solution Volume | Dry Sample Mass | Initial Conc. | Equilibrium Conc. | Bound Chloride |
|---|---|---|---|---|
| $V_{sol}$ (ml) | $W_d$ (g) | $C_i$ (mol/l) | $C_e$ (mol/l) | $C_b$ mg Cl/g Sple |
| 29.51 | 22.82 | 0.101 | 0.035 | 3.03 |
| 28.10 | 22.84 | 0.308 | 0.193 | 5.01 |
| 28.40 | 22.81 | 0.510 | 0.349 | 7.10 |
| 28.54 | 22.86 | 0.709 | 0.526 | 8.11 |
| 28.47 | 22.53 | 1.007 | 0.789 | 9.79 |
| 28.57 | 22.74 | 2.044 | 1.750 | 13.08 |
| 28.83 | 22.78 | 3.045 | 2.700 | 15.49 |

## 25FA6SF, W/CM = 0.5, 9 months curing

Table A-35: Chloride binding capacity of the 25FA6SF paste.

| Solution Volume | Dry Sample Mass | Initial Conc. | Equilibrium Conc. | Bound Chloride |
|---|---|---|---|---|
| $V_{sol}$ (ml) | $W_d$ (g) | $C_i$ (mol/l) | $C_e$ (mol/l) | $C_b$ mg Cl/g Sple |
| 28.19 | 22.80 | 0.101 | 0.061 | 1.76 |
| 29.69 | 22.99 | 0.308 | 0.228 | 3.67 |
| 28.80 | 23.11 | 0.510 | 0.395 | 5.09 |
| 29.04 | 22.97 | 0.709 | 0.574 | 6.09 |
| 29.46 | 22.77 | 1.007 | 0.841 | 7.64 |
| 28.96 | 22.79 | 2.044 | 1.812 | 10.42 |
| 29.60 | 22.96 | 3.045 | 2.773 | 12.44 |

## 25SL6SF, W/CM = 0.5, 9 months curing

Table A-36: Chloride binding capacity of the 25SL6SF paste.

| Solution Volume | Dry Sample Mass | Initial Conc. | Equilibrium Conc. | Bound Chloride |
|---|---|---|---|---|
| $V_{sol}$ (ml) | $W_d$ (g) | $C_i$ (mol/l) | $C_e$ (mol/l) | $C_b$ mg Cl/g Sple |
| 29.53 | 22.68 | 0.101 | 0.048 | 2.44 |
| 29.60 | 22.71 | 0.308 | 0.214 | 4.38 |
| 27.89 | 22.69 | 0.510 | 0.375 | 5.86 |
| 28.86 | 22.67 | 0.709 | 0.551 | 7.16 |
| 28.89 | 22.72 | 1.007 | 0.830 | 8.00 |
| 28.16 | 22.81 | 2.044 | 1.800 | 10.67 |
| 28.89 | 22.67 | 3.045 | 2.761 | 12.84 |

## 8SF, W/CM = 0.5, 9 months curing

Table A-37: Chloride binding capacity of the 8SF paste.

| Solution Volume | Dry Sample Mass | Initial Conc. | Equilibrium Conc. | Bound Chloride |
|---|---|---|---|---|
| $V_{sol}$ (ml) | $W_d$ (g) | $C_i$ (mol/l) | $C_e$ (mol/l) | $C_b$ mg Cl/g Sple |
| 27.99 | 22.96 | 0.101 | 0.055 | 1.98 |
| 28.47 | 22.82 | 0.308 | 0.232 | 3.39 |
| 28.64 | 22.89 | 0.510 | 0.400 | 4.88 |
| 28.73 | 22.96 | 0.709 | 0.579 | 5.80 |
| 28.98 | 22.81 | 1.007 | 0.859 | 6.66 |
| 29.11 | 22.80 | 2.044 | 1.859 | 8.34 |
| 29.22 | 22.82 | 3.045 | 2.825 | 10.02 |

## Control, W/CM = 0.5, 9 months curing

Table A-38: Chloride binding capacity of the control paste.

| Solution Volume | Dry Sample Mass | Initial Conc. | Equilibrium Conc. | Bound Chloride |
|---|---|---|---|---|
| $V_{sol}$ (ml) | $W_d$ (g) | $C_i$ (mol/l) | $C_e$ (mol/l) | $C_b$ mg Cl/g Sple |
| 29.14 | 23.56 | 0.101 | 0.037 | 2.80 |
| 29.18 | 23.74 | 1.008 | 0.829 | 7.79 |
| 29.30 | 23.01 | 3.021 | 2.777 | 11.00 |

## 8MK, W/CM = 0.5, 9 months curing

Table A-39: Chloride binding capacity of the 8MK paste.

| Solution Volume | Dry Sample Mass | Initial Conc. | Equilibrium Conc. | Bound Chloride |
|---|---|---|---|---|
| $V_{sol}$ (ml) | $W_d$ (g) | $C_i$ (mol/l) | $C_e$ (mol/l) | $C_b$ mg Cl/g Sple |
| 28.92 | 22.85 | 0.101 | 0.026 | 3.38 |
| 29.70 | 23.06 | 1.008 | 0.703 | 13.91 |
| 29.03 | 22.58 | 3.021 | 2.547 | 21.57 |

### A.4 Reproducibility (control paste)

Tables A-40 to A-43 show the chloride binding isotherms of four replicas of the control paste.

## Control (replica 1), W/CM = 0.5, curing: 2 months

Table A-40: Chloride binding capacity of the control paste (replica 1).

| Solution Mass | Solution Density | Solution Volume | Sample Mass | Dry Sample Mass | Initial Conc. | Equilibrium Conc. | Bound Chloride |
|---|---|---|---|---|---|---|---|
| $W_{sol}$ (g) | $d_s$ (g/ml) | $V_{sol}$ (ml) | $W_{11}$ (g) | $W_d$ (g) | $C_i$ (mol/l) | $C_e$ (mol/l) | $C_b$ mg Cl/g Sple |
| 30.29 | 1.003 | 30.20 | 24.92 | 22.74 | 0.101 | 0.046 | 2.61 |
| 30.37 | 1.012 | 30.00 | 24.94 | 22.76 | 0.312 | 0.209 | 4.80 |
| 30.51 | 1.020 | 29.91 | 25.02 | 22.83 | 0.510 | 0.379 | 6.08 |
| 30.49 | 1.028 | 29.65 | 24.92 | 22.74 | 0.711 | 0.562 | 6.85 |
| 31.42 | 1.040 | 30.22 | 24.68 | 22.52 | 1.013 | 0.843 | 8.06 |
| 32.37 | 1.078 | 30.04 | 25.10 | 22.90 | 2.004 | 1.806 | 9.21 |
| 33.58 | 1.115 | 30.13 | 25.03 | 22.84 | 3.096 | 2.852 | 11.43 |

## Control (replica 2), W/CM = 0.5, curing: 2 months

Table A-41: Chloride binding capacity of the control paste (replica 2).

| Solution Mass | Solution Density | Solution Volume | Sample Mass | Dry Sample Mass | Initial Conc. | Equilibrium Conc. | Bound Chloride |
|---|---|---|---|---|---|---|---|
| $W_{sol}$ (g) | $d_s$ (g/ml) | $V_{sol}$ (ml) | $W_{11}$ (g) | $W_d$ (g) | $C_i$ (mol/l) | $C_e$ (mol/l) | $C_b$ mg Cl/g Sple |
| 31.19 | 1.003 | 31.09 | 25.11 | 22.95 | 0.101 | 0.046 | 2.66 |
| 30.39 | 1.012 | 30.02 | 25.01 | 22.86 | 0.312 | 0.204 | 5.02 |
| 30.65 | 1.020 | 30.05 | 25.11 | 22.95 | 0.510 | 0.379 | 6.09 |
| 30.60 | 1.028 | 29.76 | 24.78 | 22.65 | 0.711 | 0.561 | 6.96 |
| 31.23 | 1.040 | 30.03 | 24.73 | 22.60 | 1.013 | 0.848 | 7.78 |
| 32.27 | 1.078 | 29.94 | 24.88 | 22.74 | 2.004 | 1.800 | 9.54 |
| 36.69 | 1.115 | 32.92 | 24.85 | 22.71 | 3.096 | 2.890 | 10.60 |

## Control (replica 3), W/CM = 0.5, curing: 2 months

Table A-42: Chloride binding capacity of the control paste (replica 3).

| Solution Mass | Solution Density | Solution Volume | Sample Mass | Dry Sample Mass | Initial Conc. | Equilibrium Conc. | Bound Chloride |
|---|---|---|---|---|---|---|---|
| $W_{sol}$ (g) | $d_s$ (g/ml) | $V_{sol}$ (ml) | $W_{11}$ (g) | $W_d$ (g) | $C_i$ (mol/l) | $C_e$ (mol/l) | $C_b$ mg Cl/g Sple |
| 30.26 | 1.003 | 30.17 | 25.27 | 23.07 | 0.101 | 0.045 | 2.62 |
| 30.52 | 1.012 | 30.15 | 25.24 | 23.05 | 0.312 | 0.206 | 4.92 |
| 30.32 | 1.020 | 29.72 | 25.23 | 23.04 | 0.510 | 0.379 | 6.01 |
| 32.87 | 1.028 | 31.97 | 25.04 | 22.86 | 0.711 | 0.568 | 7.08 |
| 31.79 | 1.040 | 30.57 | 24.94 | 22.77 | 1.013 | 0.840 | 8.22 |
| 33.93 | 1.078 | 31.48 | 25.14 | 22.96 | 2.004 | 1.810 | 9.41 |
| 32.54 | 1.115 | 29.20 | 25.15 | 22.96 | 3.013 | 2.752 | 11.79 |

## Control (replica 4), W/CM = 0.5, curing: 2 months

Table A-43: Chloride binding capacity of the control paste (replica 4).

| Solution Mass | Solution Density | Solution Volume | Sample Mass | Dry Sample Mass | Initial Conc. | Equilibrium Conc. | Bound Chloride |
|---|---|---|---|---|---|---|---|
| $W_{sol}$ (g) | $d_s$ (g/ml) | $V_{sol}$ (ml) | $W_{11}$ (g) | $W_d$ (g) | $C_i$ (mol/l) | $C_e$ (mol/l) | $C_b$ mg Cl/g Sple |
| 30.29 | 1.003 | 30.20 | 25.15 | 23.01 | 0.101 | 0.046 | 2.58 |
| 30.70 | 1.012 | 30.33 | 24.38 | 22.31 | 0.312 | 0.212 | 4.79 |
| 32.65 | 1.020 | 32.01 | 24.70 | 22.60 | 0.510 | 0.386 | 6.23 |
| 30.79 | 1.028 | 29.95 | 24.90 | 22.78 | 0.711 | 0.558 | 7.11 |
| 31.52 | 1.040 | 30.31 | 25.06 | 22.93 | 1.013 | 0.848 | 7.70 |
| 32.46 | 1.078 | 30.12 | 25.03 | 22.90 | 2.004 | 1.799 | 9.55 |
| 36.59 | 1.115 | 32.83 | 25.04 | 22.91 | 3.096 | 2.862 | 11.88 |

### A.5 Influence of sample size

Tables A-44 to A-46 show the results of the influence of sample size on the chloride binding capacities of the control, 8SF, and 8MK pastes.

## Control, W/CM = 0.5, curing: 2 months

Table A-44: Influence of sample size on the chloride binding capacity of the control paste.

| Sample Mass | Solution Mass | Solution Density | Solution Volume | Dry Sample Mass | Initial Conc. | Equilibrium Conc. | Bound Chloride |
|---|---|---|---|---|---|---|---|
| $W_{11}$ (g) | $W_{sol}$ (g) | $d_s$ (g/ml) | $V_{sol}$ (ml) | $W_d$ (g) | $C_i$ (mol/l) | $C_e$ (mol/l) | $C_b$ mg Cl/g Sple |
| 12.38 | 15.20 | 1.115 | 13.64 | 11.34 | 3.021 | 2.772 | 10.60 |
| 24.73 | 32.49 | 1.115 | 29.15 | 22.65 | 3.021 | 2.775 | 11.18 |
| 49.53 | 67.32 | 1.115 | 60.40 | 45.37 | 3.021 | 2.790 | 10.90 |

## 8SF, W/CM = 0.5, curing: 2 months

Table A-45: Influence of sample size on the chloride binding capacity of the 8SF paste.

| Sample Mass | Solution Mass | Solution Density | Solution Volume | Dry Sample Mass | Initial Conc. | Equilibrium Conc. | Bound Chloride |
|---|---|---|---|---|---|---|---|
| $W_{11}$ (g) | $W_{sol}$ (g) | $d_s$ (g/ml) | $V_{sol}$ (ml) | $W_d$ (g) | $C_i$ (mol/l) | $C_e$ (mol/l) | $C_b$ mg Cl/g Sple |
| 12.48 | 17.14 | 1.115 | 15.38 | 11.41 | 3.021 | 2.843 | 8.48 |
| 24.06 | 32.79 | 1.115 | 29.42 | 21.99 | 3.021 | 2.842 | 8.45 |
| 49.79 | 66.44 | 1.115 | 59.61 | 45.51 | 3.021 | 2.840 | 8.37 |

## 8MK, W/CM = 0.5, curing: 2 months

Table A-46: Influence of sample size on the chloride binding capacity of the 8MK paste.

| Sample Mass | Solution Mass | Solution Density | Solution Volume | Dry Sample Mass | Initial Conc. | Equilibrium Conc. | Bound Chloride |
|---|---|---|---|---|---|---|---|
| $W_{11}$ (g) | $W_{sol}$ (g) | $d_s$ (g/ml) | $V_{sol}$ (ml) | $W_d$ (g) | $C_i$ (mol/l) | $C_e$ (mol/l) | $C_b$ mg Cl/g Sple |
| 12.49 | 16.89 | 1.115 | 15.15 | 11.58 | 3.021 | 2.580 | 20.44 |
| 24.69 | 32.30 | 1.115 | 28.98 | 22.88 | 3.021 | 2.544 | 21.38 |
| 50.33 | 67.55 | 1.115 | 60.61 | 46.65 | 3.021 | 2.573 | 20.62 |

### A.6 Influence of solution volume

Tables A-47 to A-49 show the results of the influence of host solution volume on the chloride binding capacities of the control, 8SF, and 8MK pastes.

## Control, W/CM = 0.5, curing: 2 months

Table A-47: Influence of the host solution volume on the chloride binding capacity of the control paste.

| Sample Mass | Solution Mass | Solution Density | Solution Volume | Dry Sample Mass | Initial Conc. | Equilibrium Conc. | Bound Chloride |
|---|---|---|---|---|---|---|---|
| $W_{11}$ (g) | $W_{sol}$ (g) | $d_s$ (g/ml) | $V_{sol}$ (ml) | $W_d$ (g) | $C_i$ (mol/l) | $C_e$ (mol/l) | $C_b$ mg Cl/g Sple |
| 24.87 | 30.64 | 1.115 | 27.49 | 22.78 | 3.021 | 2.753 | 11.43 |
| 25.04 | 42.48 | 1.115 | 38.12 | 22.94 | 3.021 | 2.843 | 10.45 |
| 24.89 | 71.40 | 1.115 | 64.06 | 22.80 | 3.021 | 2.911 | 10.88 |

## 8SF, W/CM = 0.5, curing: 2 months

Table A-48: Influence of the host solution volume on the chloride binding capacity of the 8SF paste.

| Sample Mass | Solution Mass | Solution Density | Solution Volume | Dry Sample Mass | Initial Conc. | Equilibrium Conc. | Bound Chloride |
|---|---|---|---|---|---|---|---|
| $W_{11}$ (g) | $W_{sol}$ (g) | $d_s$ (g/ml) | $V_{sol}$ (ml) | $W_d$ (g) | $C_i$ (mol/l) | $C_e$ (mol/l) | $C_b$ mg Cl/g Sple |
| 25.02 | 32.36 | 1.115 | 29.04 | 22.87 | 3.021 | 2.846 | 7.87 |
| 24.88 | 39.99 | 1.115 | 35.88 | 22.74 | 3.021 | 2.877 | 8.03 |
| 24.75 | 61.27 | 1.115 | 54.97 | 22.62 | 3.021 | 2.920 | 8.65 |

## 8MK, W/CM = 0.5, curing: 2 months

Table A-49: Influence of the host solution volume on the chloride binding capacity of the 8MK paste.

| Sample Mass | Solution Mass | Solution Density | Solution Volume | Dry Sample Mass | Initial Conc. | Equilibrium Conc. | Bound Chloride |
|---|---|---|---|---|---|---|---|
| $W_{11}$ (g) | $W_{sol}$ (g) | $d_s$ (g/ml) | $V_{sol}$ (ml) | $W_d$ (g) | $C_i$ (mol/l) | $C_e$ (mol/l) | $C_b$ mg Cl/g Sple |
| 25.43 | 29.76 | 1.115 | 26.70 | 23.57 | 3.021 | 2.512 | 20.43 |
| 24.44 | 40.26 | 1.115 | 36.12 | 22.65 | 3.021 | 2.622 | 22.55 |
| 25.14 | 61.38 | 1.115 | 55.07 | 23.30 | 3.021 | 2.767 | 21.24 |

## A.7 Results of the ponding tests

### A.7.1 Hydroxyl ion profiles

Tables A-50 to A-53 show the hydroxyl ion concentrations, or the pH values, across the depth of the specimen of the 4 tested pastes.

### Control, W/CM = 0.5, curing: 2 months, ponding: 16 months

Table A-50: pH values and $OH^-$ ion concentrations across the depth of the control paste.

| Depth from the Surface (mm) | Hydroxyl Ion Concentration (mol/l) | pH |
|---|---|---|
| 5 | 0.080 | 12.90 |
| 15 | 0.091 | 12.96 |
| 10 | 0.086 | 12.93 |
| 20 | 0.131 | 13.12 |
| 25 | 0.134 | 13.13 |
| 30 | 0.156 | 13.19 |
| 35 | 0.154 | 13.19 |
| 40 | 0.219 | 13.34 |
| 45 | 0.215 | 13.33 |
| 55 | 0.237 | 13.38 |
| 60 | 0.213 | 13.33 |

### 8SF, W/CM = 0.5, curing: 2 months, ponding: 16 months

Table A-51: pH values and $OH^-$ ion concentrations across the depth of the 8SF paste.

| Depth from the Surface (mm) | Hydroxyl Ion Concentration (mol/l) | pH |
|---|---|---|
| 2 | 0.034 | 12.54 |
| 6 | 0.067 | 12.82 |
| 10 | 0.094 | 12.97 |
| 12 | 0.117 | 13.07 |
| 14 | 0.137 | 13.14 |
| 16 | 0.184 | 13.26 |
| 18 | 0.213 | 13.33 |
| 20 | 0.208 | 13.32 |
| 22 | 0.260 | 13.42 |

## 8MK, W/CM = 0.5, curing: 2 months, ponding: 16 months

Table A-52: pH values and $OH^-$ ion concentrations across the depth of the 8MK paste.

| Depth from the Surface (mm) | Hydroxyl Ion Concentration (mol/l) | pH |
|---|---|---|
| 2.5 | 0.067 | 12.83 |
| 5 | 0.055 | 12.74 |
| 7.5 | 0.095 | 12.98 |
| 10 | 0.180 | 13.25 |
| 12.5 | 0.148 | 13.17 |
| 15 | 0.178 | 13.25 |
| 17.5 | 0.155 | 13.19 |
| 20 | 0.257 | 13.41 |
| 22.5 | 0.206 | 13.31 |
| 27.5 | 0.274 | 13.44 |

## 25FA, W/CM = 0.5, curing: 2 months, ponding: 16 months

Table A-53: pH values and $OH^-$ ion concentrations across the depth of the 25FA paste.

| Depth from the Surface (mm) | Hydroxyl Ion Concentration (mol/l) | pH |
|---|---|---|
| 3 | 0.077 | 12.89 |
| 6 | 0.066 | 12.82 |
| 9 | 0.088 | 12.94 |
| 12 | 0.090 | 12.95 |
| 15 | 0.128 | 13.11 |
| 18 | 0.147 | 13.17 |
| 21 | 0.168 | 13.23 |
| 24 | 0.194 | 13.29 |
| 27 | 0.218 | 13.34 |
| 30 | 0.197 | 13.29 |
| 33 | 0.218 | 13.34 |

### A.7.2 Free chloride profiles

Tables A-54 to A-57 present the free chloride concentrations across the depth of specimen of the tested pastes.

## Control, W/CM = 0.5, curing: 2 months, ponding: 16 months

Table A-54: Free chloride concentrations across the depth of the control paste.

| Depth from the Surface (mm) | Free Chloride Concentration (ppm) | Free Chloride Concentration (mol/l) |
|---|---|---|
| 5.0 | 34697.0 | 0.979 |
| 10.0 | 33249.0 | 0.938 |
| 15.0 | 29369.0 | 0.828 |
| 20.0 | 26011.0 | 0.734 |
| 25.0 | 25824.3 | 0.728 |
| 30.0 | 20686.0 | 0.583 |
| 35.0 | 17324.0 | 0.489 |
| 40.0 | 11357.0 | 0.320 |
| 45.0 | 12974.3 | 0.366 |
| 55.0 | 11304.3 | 0.319 |
| 60.0 | 10924.8 | 0.308 |

## 8SF, W/CM = 0.5, curing: 2 months, ponding: 16 months

Table A-55: Free chloride concentrations across the depth of the 8SF paste.

| Depth from the Surface (mm) | Free Chloride Concentration (ppm) | Free Chloride Concentration (mol/l) |
|---|---|---|
| 2.0 | 35160.0 | 0.992 |
| 4.0 | 26348.0 | 0.743 |
| 6.0 | 22260.0 | 0.628 |
| 8.0 | 15095.0 | 0.426 |
| 10.0 | 13528.0 | 0.382 |
| 12.0 | 9187.0 | 0.259 |
| 14.0 | 6479.0 | 0.183 |
| 16.0 | 3345.0 | 0.094 |
| 18.0 | 2316.0 | 0.065 |
| 20.0 | 2639.9 | 0.074 |
| 22.0 | 732.0 | 0.021 |

## 8MK, W/CM = 0.5, curing: 2 months, ponding: 16 months

Table A-56: Free chloride concentrations across the depth of the 8MK paste.

| Depth from the Surface (mm) | Free Chloride Concentration (ppm) | Free Chloride Concentration (mol/l) |
|---|---|---|
| 2.5 | 30574.0 | 0.862 |
| 5.0 | 24658.0 | 0.696 |
| 7.5 | 20006.0 | 0.564 |
| 10.0 | 11093.0 | 0.313 |
| 12.5 | 10888.0 | 0.307 |
| 15.0 | 7799.2 | 0.220 |
| 17.5 | 5759.0 | 0.162 |
| 20.0 | 3507.6 | 0.099 |
| 22.5 | 2343.0 | 0.066 |
| 27.5 | 959.4 | 0.027 |

## 25FA, W/CM = 0.5, curing: 2 months, ponding: 16 months

Table A-57: Free chloride concentrations across the depth of the 25FA paste.

| Depth from the Surface (mm) | Free Chloride Concentration (ppm) | Free Chloride Concentration (mol/l) |
|---|---|---|
| 3.0 | 32196.0 | 0.908 |
| 6.0 | 27475.0 | 0.775 |
| 9.0 | 21854.0 | 0.616 |
| 12.0 | 17764.0 | 0.501 |
| 15.0 | 13018.0 | 0.367 |
| 18.0 | 10137.0 | 0.286 |
| 21.0 | 6609.0 | 0.186 |
| 24.0 | 4649.9 | 0.126 |
| 27.0 | 3197.0 | 0.086 |
| 30.0 | 3166.6 | 0.086 |
| 33.0 | 2419.0 | 0.065 |

### A.7.3 Total chloride profiles

Tables A-58 to A-64 show the total chloride content across the depth of specimen of the 4 tested pastes. Except for the 8SF paste, 2 specimen of each of the other pastes (control, 8MK, 25FA) were analysed for their total chloride contents. Originally, 3 specimen of each paste were selected to be analysed for their total chloride profiles. However, difficulties were encountered in setting up the specimen for grinding, and some of the specimen broke under pressure during the grinding process.

## Control, W/CM = 0.5, curing: 2 months, ponding: 16 months, specimen 1

Table A-58: Total chloride contents across the depth of the control paste (specimen 1).

| Depth from the Surface (mm) | Total Chloride Content (% mass cement paste) | Total Chloride Content (mmol/g cement paste) |
|---|---|---|
| 2.79 | 2.245 | 0.633 |
| 7.87 | 2.099 | 0.592 |
| 12.95 | 1.981 | 0.559 |
| 18.03 | 1.820 | 0.513 |
| 23.11 | 1.609 | 0.454 |
| 28.19 | 1.585 | 0.447 |
| 33.27 | 1.413 | 0.399 |
| 38.35 | 1.333 | 0.376 |
| 43.43 | 1.180 | 0.333 |
| 48.51 | 1.116 | 0.315 |
| 53.59 | 0.965 | 0.272 |

## Control, W/CM = 0.5, curing: 2 months, ponding: 16 months, specimen 2

Table A-59: Total chloride contents across the depth of the control paste (specimen 2).

| Depth from the Surface (mm) | Total Chloride Content (% mass cement paste) | Total Chloride Content (mmol/g cement paste) |
|---|---|---|
| 2.29 | 2.069 | 0.584 |
| 7.11 | 2.022 | 0.570 |
| 11.68 | 1.926 | 0.543 |
| 16.26 | 1.855 | 0.523 |
| 20.83 | 1.739 | 0.490 |
| 25.40 | 1.644 | 0.464 |
| 29.97 | 1.541 | 0.435 |
| 34.54 | 1.418 | 0.400 |
| 39.12 | 1.319 | 0.372 |
| 43.69 | 1.206 | 0.340 |
| 48.26 | 1.088 | 0.307 |

## 8SF, W/CM = 0.5, curing: 2 months, ponding: 16 months

Table A-60: Total chloride contents across the depth of the 8SF paste.

| Depth from the Surface (mm) | Total Chloride Content (% mass cement paste) | Total Chloride Content (mmol/g cement paste) |
|---|---|---|
| 2.29 | 1.964 | 0.554 |
| 3.81 | 1.828 | 0.516 |
| 5.33 | 1.640 | 0.463 |
| 7.37 | 1.377 | 0.388 |
| 9.40 | 1.127 | 0.318 |
| 11.43 | 0.915 | 0.258 |
| 13.46 | 0.730 | 0.206 |
| 15.49 | 0.566 | 0.160 |
| 17.53 | 0.409 | 0.115 |
| 19.56 | 0.310 | 0.088 |
| 21.59 | 0.287 | 0.081 |

## 8MK, W/CM = 0.5, curing: 2 months, ponding: 16 months, specimen 1

Table A-61: Total chloride contents across the depth of the 8MK paste (specimen 1).

| Depth from the Surface (mm) | Total Chloride Content (% mass cement paste) | Total Chloride Content (mmol/g cement paste) |
|---|---|---|
| 1.52 | 3.068 | 0.865 |
| 5.33 | 2.438 | 0.688 |
| 9.14 | 1.559 | 0.440 |
| 12.95 | 1.125 | 0.317 |
| 16.76 | 0.803 | 0.227 |
| 20.57 | 0.515 | 0.145 |
| 24.38 | 0.269 | 0.076 |
| 28.19 | 0.117 | 0.033 |
| 32.00 | 0.070 | 0.020 |
| 35.81 | 0.069 | 0.019 |
| 39.62 | 0.066 | 0.019 |

## 8MK, W/CM = 0.5, curing: 2 months, ponding: 16 months, specimen 2

Table A-62: Total chloride contents across the depth of the 8MK paste (specimen 2).

| Depth from the Surface (mm) | Total Chloride Content (% mass cement paste) | Total Chloride Content (mmol/g cement paste) |
|---|---|---|
| 1.91 | 3.002 | 0.847 |
| 4.95 | 2.380 | 0.671 |
| 8.00 | 1.473 | 0.416 |
| 11.05 | 0.996 | 0.281 |
| 14.10 | 0.739 | 0.209 |
| 17.15 | 0.511 | 0.144 |
| 20.19 | 0.298 | 0.084 |
| 23.24 | 0.134 | 0.038 |
| 26.29 | 0.042 | 0.012 |
| 29.34 | 0.023 | 0.006 |

## 25FA, W/CM = 0.5, curing: 2 months, ponding: 16 months, specimen 1

Table A-63: Total chloride contents across the depth of the 25FA paste (specimen 1).

| Depth from the Surface (mm) | Total Chloride Content (% mass cement paste) | Total Chloride Content (mmol/g cement paste) |
|---|---|---|
| 2.03 | 2.266 | 0.639 |
| 5.08 | 2.102 | 0.593 |
| 8.13 | 1.859 | 0.524 |
| 11.18 | 1.476 | 0.416 |
| 14.22 | 1.171 | 0.330 |
| 17.27 | 0.852 | 0.240 |
| 20.32 | 0.659 | 0.186 |
| 23.37 | 0.479 | 0.135 |
| 26.42 | 0.362 | 0.102 |

## 25FA, W/CM = 0.5, curing: 2 months, ponding: 16 months, specimen 2

Table A-64: Total chloride contents across the depth of the 25FA paste (specimen 1).

| Depth from the Surface (mm) | Total Chloride Content (% mass cement paste) | Total Chloride Content (mmol/g cement paste) |
|---|---|---|
| 1.91 | 2.321 | 0.655 |
| 6.48 | 1.993 | 0.562 |
| 11.05 | 1.450 | 0.409 |
| 15.62 | 0.892 | 0.252 |
| 20.19 | 0.543 | 0.153 |
| 24.77 | 0.328 | 0.093 |
| 29.34 | 0.181 | 0.051 |
| 33.91 | 0.125 | 0.035 |
| 38.48 | 0.096 | 0.027 |

### A.7.4 Chloride binding isotherms

Tables A-65 to A-71 show the chloride binding isotherms of the four tested pastes, using the ponding method. Except for the 8SF paste, the binding isotherms of the three other pastes were determined from the two total chloride profiles.

## Control, W/CM = 0.5, curing: 2 months, ponding: 16 months

Table A-65: Chloride binding capacity of the control paste, from the ponding method.

| Depth (mm) | Total Chloride Content* (mg Cl/g cement paste) | Free Chloride Concentration (mol/l) | Bound Chloride (mg Cl/g cement paste) |
|---|---|---|---|
| 2.79 | 22.448 | 1.039 | 11.44 |
| 7.87 | 20.987 | 0.948 | 10.93 |
| 12.95 | 19.811 | 0.859 | 10.70 |
| 18.03 | 18.198 | 0.773 | 10.00 |
| 23.11 | 16.087 | 0.690 | 8.77 |
| 28.19 | 15.846 | 0.611 | 9.37 |
| 33.27 | 14.134 | 0.536 | 8.45 |
| 38.35 | 13.333 | 0.467 | 8.38 |
| 43.43 | 11.804 | 0.403 | 7.53 |
| 48.51 | 11.160 | 0.345 | 7.50 |
| 53.59 | 9.650 | 0.293 | 6.54 |

* Resuts from specimen 1

## Control, W/CM = 0.5, curing: 2 months, ponding: 16 months

Table A-66: Chloride binding capacity of the control paste, from the ponding method.

| Depth (mm) | Total Chloride Content* (mg Cl/g cement paste) | Free Chloride Concentration (mol/l) | Bound Chloride (mg Cl/g cement paste) |
|---|---|---|---|
| 2.29 | 20.692 | 1.048 | 9.58 |
| 7.11 | 20.224 | 0.962 | 10.03 |
| 11.68 | 19.261 | 0.882 | 9.92 |
| 16.26 | 18.552 | 0.803 | 10.04 |
| 20.83 | 17.387 | 0.727 | 9.68 |
| 25.40 | 16.443 | 0.654 | 9.51 |
| 29.97 | 15.408 | 0.584 | 9.21 |
| 34.54 | 14.180 | 0.519 | 8.68 |
| 39.12 | 13.193 | 0.457 | 8.35 |
| 43.69 | 12.062 | 0.400 | 7.82 |
| 48.26 | 10.881 | 0.348 | 7.19 |

* Results from specimen 2

## 8SF, W/CM = 0.5, curing: 2 months, ponding: 16 months

Table A-67: Chloride binding capacity of the 8SF paste, from the ponding method.

| Depth (mm) | Total Chloride Content (mg Cl/g cement paste) | Free Chloride Concentration (mol/l) | Bound Chloride (mg Cl/g cement paste) |
|---|---|---|---|
| 2.29 | 19.638 | 0.935 | 8.36 |
| 3.81 | 18.277 | 0.798 | 8.66 |
| 5.33 | 16.404 | 0.669 | 8.34 |
| 7.37 | 13.772 | 0.514 | 7.57 |
| 9.40 | 11.270 | 0.382 | 6.67 |
| 11.43 | 9.149 | 0.274 | 5.85 |
| 13.46 | 7.303 | 0.190 | 5.02 |
| 15.49 | 5.663 | 0.126 | 4.14 |
| 17.53 | 4.095 | 0.081 | 3.12 |
| 19.56 | 3.105 | 0.050 | 2.50 |
| 21.59 | 2.868 | 0.030 | 2.51 |

## 8MK, W/CM = 0.5, curing: 2 months, ponding: 16 months

Table A-68: Chloride binding capacity of the 8MK paste, from the ponding method.

| Depth (mm) | Total Chloride Content* (mg Cl/g cement paste) | Free Chloride Concentration (mol/l) | Bound Chloride (mg Cl/g cement paste) |
|---|---|---|---|
| 1.91 | 30.023 | 0.897 | 19.66 |
| 4.95 | 23.801 | 0.692 | 15.80 |
| 8.00 | 14.732 | 0.509 | 8.85 |
| 11.05 | 9.959 | 0.355 | 5.86 |
| 14.10 | 7.394 | 0.235 | 4.68 |
| 17.15 | 5.111 | 0.147 | 3.41 |
| 20.19 | 2.983 | 0.087 | 1.98 |
| 23.24 | 1.341 | 0.048 | 0.78 |
| 26.29 | 0.420 | 0.025 | 0.13 |

* Results from specimen 2

## 8MK, W/CM = 0.5, curing: 2 months, ponding: 16 months

Table A-69: Chloride binding capacity of the 8MK paste, from the ponding method.

| Depth (mm) | Total Chloride Content (mg Cl/g cement paste) | Free Chloride Concentration (mol/l) | Bound Chloride (mg Cl/g cement paste) |
|---|---|---|---|
| 1.52 | 30.679 | 0.923 | 20.01 |
| 5.33 | 24.379 | 0.668 | 16.66 |
| 9.14 | 15.585 | 0.447 | 10.42 |
| 12.95 | 11.254 | 0.276 | 8.07 |
| 16.76 | 8.033 | 0.156 | 6.23 |
| 20.57 | 5.149 | 0.081 | 4.22 |
| 24.38 | 2.688 | 0.038 | 2.25 |
| 28.19 | 1.168 | 0.016 | 0.98 |

* Results from specimen 1

## 25FA, W/CM = 0.5, curing: 2 months, ponding: 16 months

Table A-70: Chloride binding capacity of the 25FA paste, from the ponding method.

| Depth (mm) | Total Chloride Content (mg Cl/g cement paste) | Free Chloride Concentration (mol/l) | Bound Chloride (mg Cl/g cement paste) |
|---|---|---|---|
| 1.91 | 23.206 | 0.975 | 11.11 |
| 6.48 | 19.930 | 0.739 | 10.76 |
| 11.05 | 14.498 | 0.528 | 7.94 |
| 15.62 | 8.917 | 0.355 | 4.51 |
| 20.19 | 5.433 | 0.223 | 2.66 |
| 24.77 | 3.280 | 0.131 | 1.65 |
| 29.34 | 1.809 | 0.072 | 0.91 |
| 33.91 | 1.249 | 0.037 | 0.79 |
| 38.48 | 0.957 | 0.018 | 0.74 |

* Results from specimen 2

## 25FA, W/CM = 0.5, curing: 2 months, ponding: 16 months

Table A-71: Chloride binding capacity of the 2 paste, from the ponding method.

| Depth (mm) | Total Chloride Content (mg Cl/g cement paste) | Free Chloride Concentration (mol/l) | Bound Chloride (mg Cl/g cement paste) |
|---|---|---|---|
| 2.03 | 22.655 | 0.968 | 10.64 |
| 5.08 | 21.018 | 0.809 | 10.98 |
| 8.13 | 18.592 | 0.659 | 10.41 |
| 11.18 | 14.758 | 0.523 | 8.27 |
| 14.22 | 11.707 | 0.403 | 6.70 |
| 17.27 | 8.521 | 0.303 | 4.77 |
| 20.32 | 6.589 | 0.220 | 3.85 |
| 23.37 | 4.793 | 0.156 | 2.86 |
| 26.42 | 3.619 | 0.107 | 2.29 |
| 29.46 | 2.695 | 0.071 | 1.82 |

* Results from specimen 1

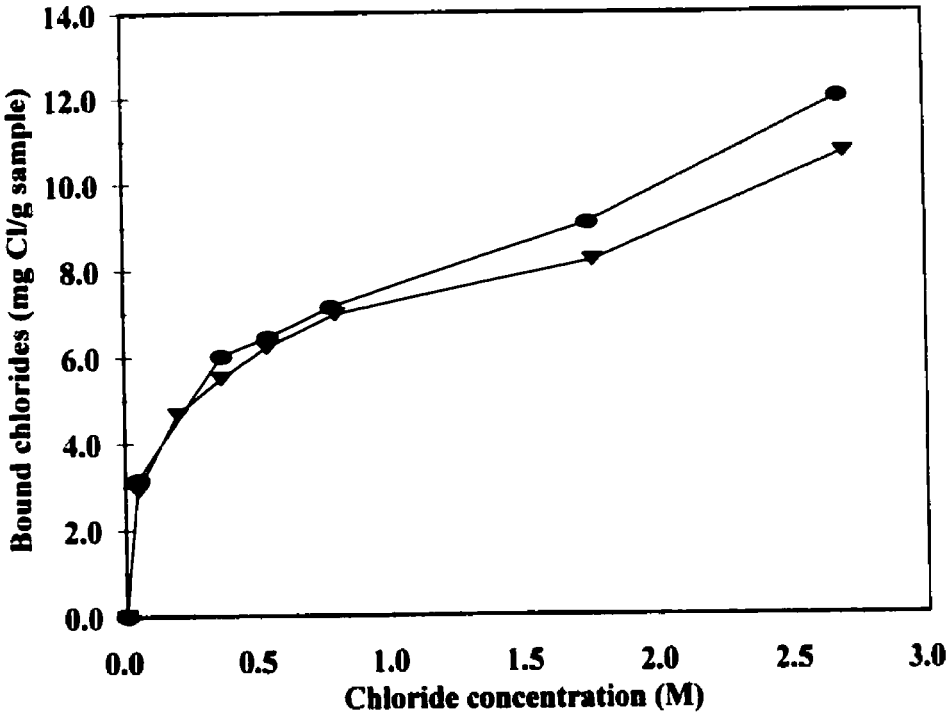


Figure A-1: Chloride binding isotherms of 2 replicas of the control paste. W/CM = 0.3.

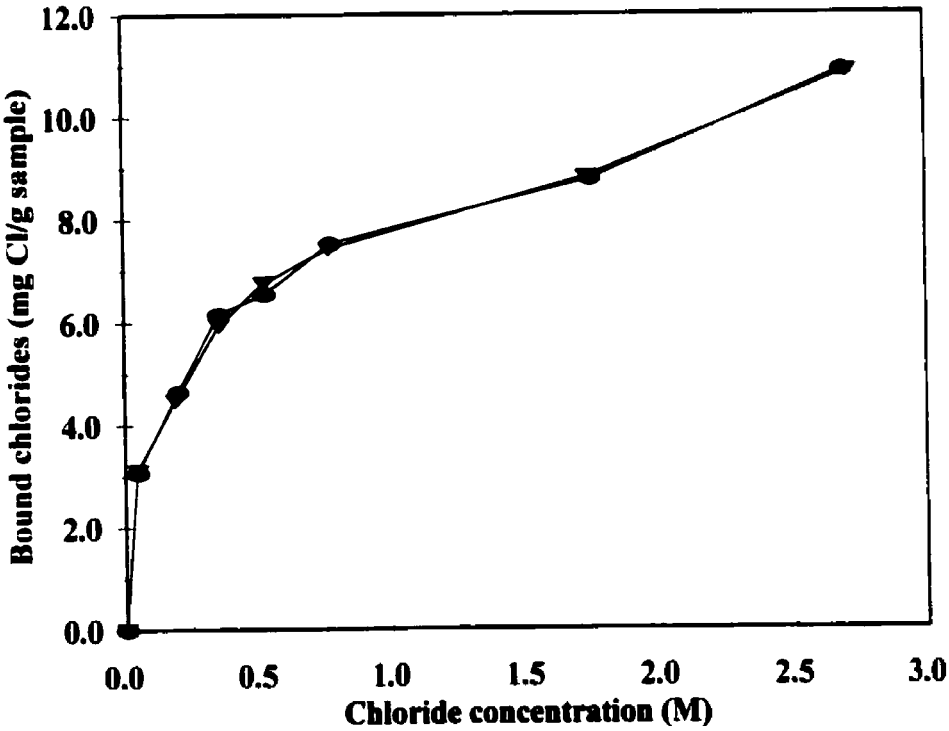


Figure A-2: Chloride binding isotherms of 2 replicas of the 25SL paste. W/CM = 0.3.

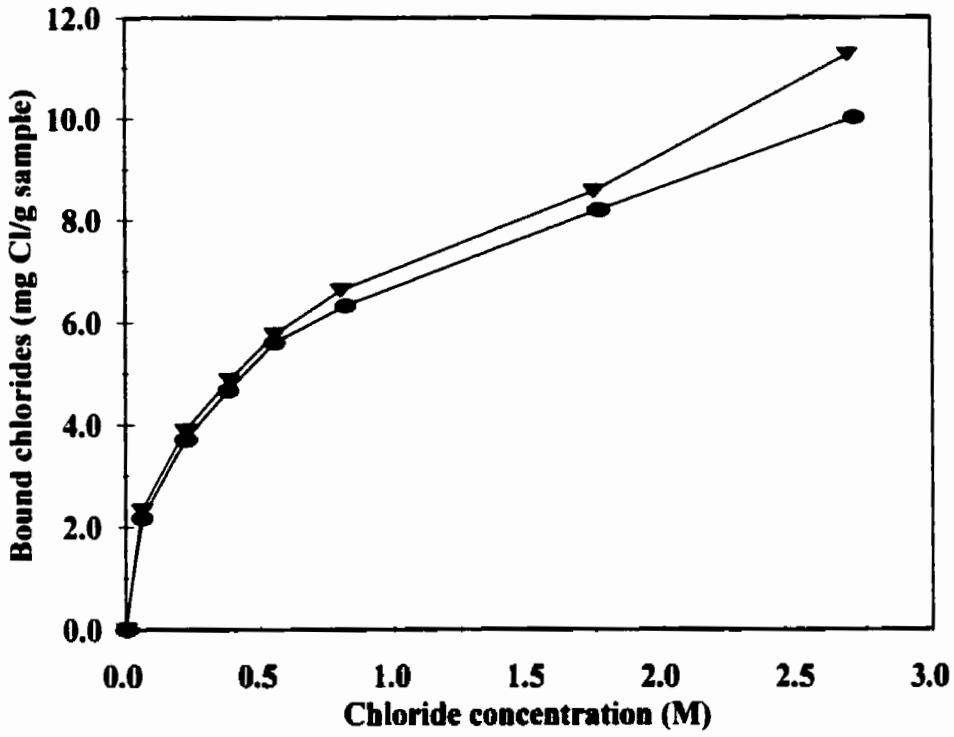


Figure A-3: Chloride binding isotherms of 2 replicas of the 25FA paste. W/CM = 0.3.

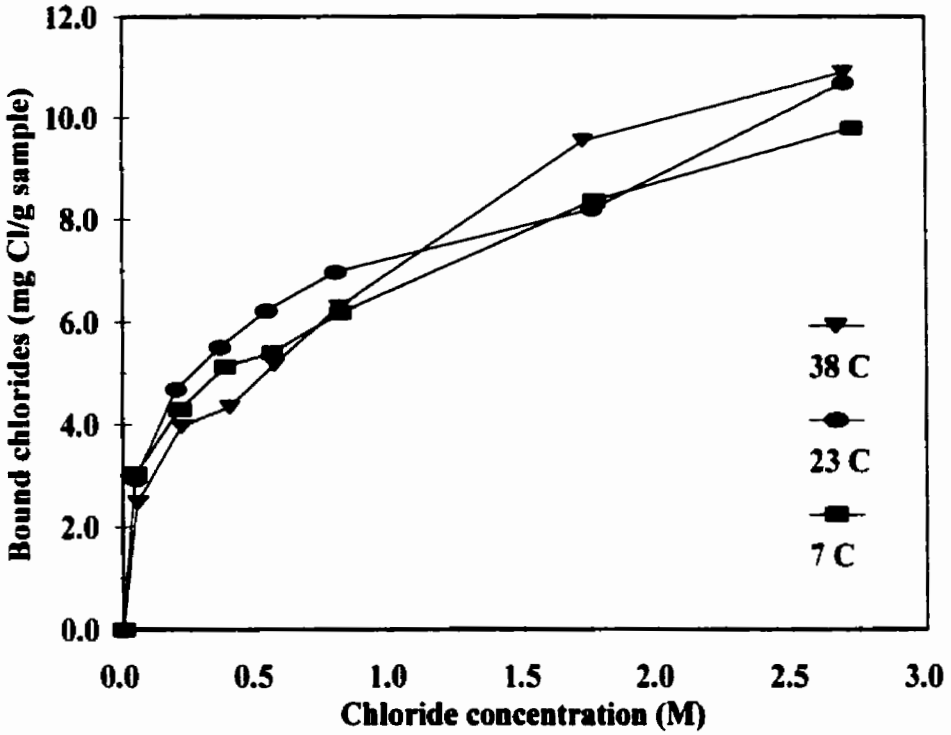


Figure A-4: Chloride binding isotherms of the control paste at temperatures: 7°C, 23°C, and 38°C. W/CM = 0.3.

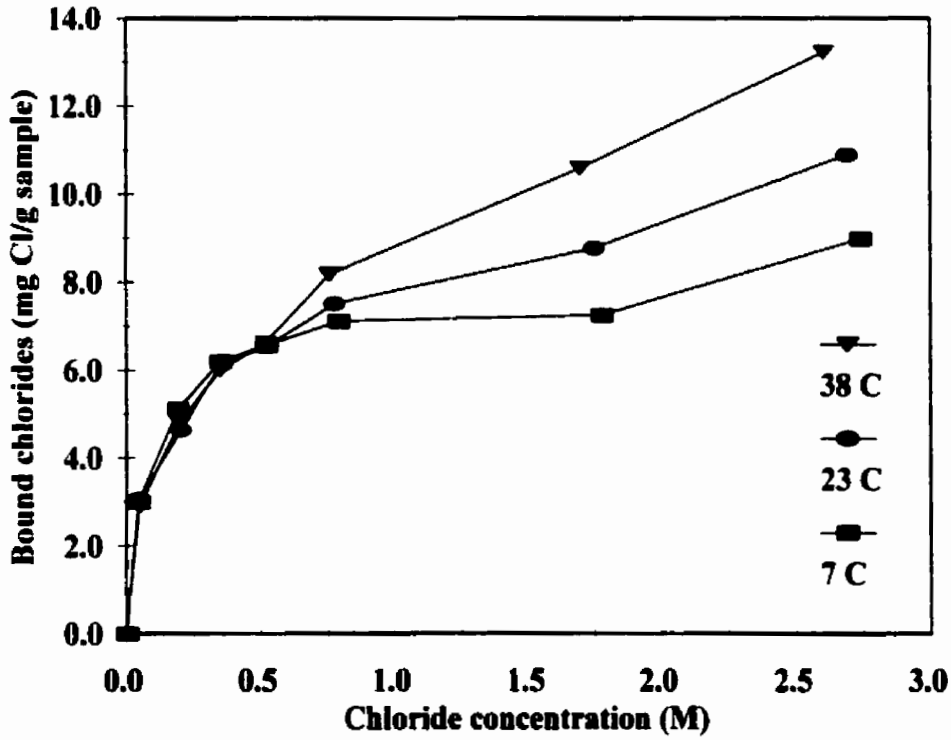


Figure A-5: Chloride binding isotherms of the 25SL paste at temperatures: 7°C, 23°C, and 38°C. W/CM = 0.3.

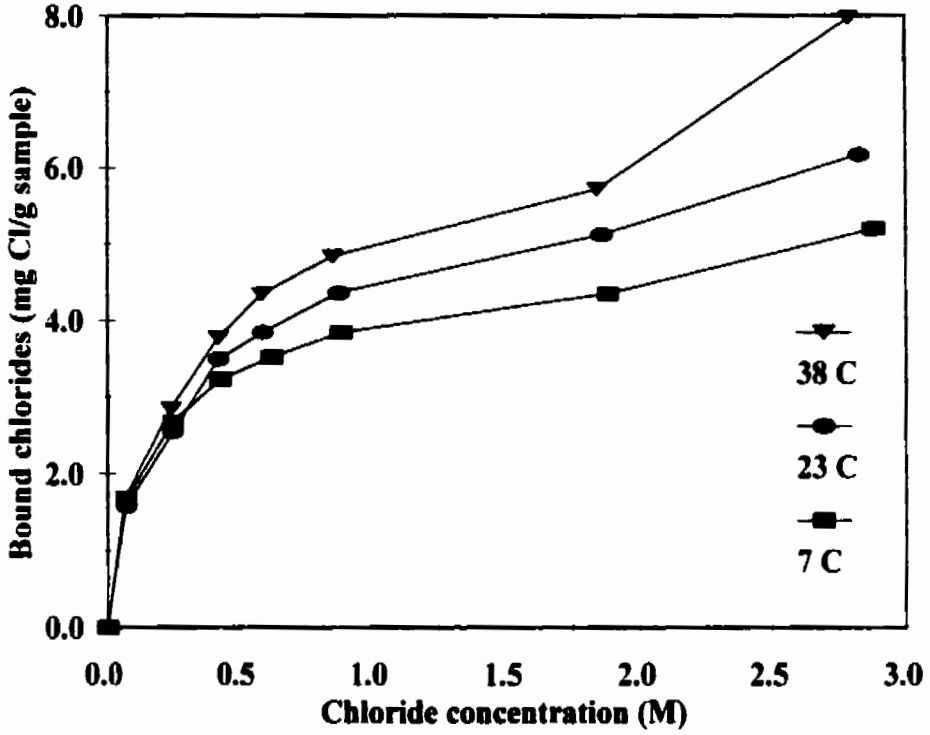


Figure A-6: Chloride binding isotherms of the 25SF paste at temperatures: 7°C, 23°C, and 38°C. W/CM = 0.3.

# Appendix B

## Results of Phase Two

### B.1 Introduction

The results presented in this appendix are referred to in section 4-2. Table B-1 shows the chemical composition of the different cements used in Phase 2. The chemical compostions of the metakaolin and silica fume, used in Phase 2, are shown in Table A-1 of Appendix A. The mix proportions of the 8SF and 8MK are presented in Table A-2 of Appendix A.

Table B-1: Chemical Composition of Portland Cements

| Amount (%) | C1 | C2 | C3 | C4 | C5 | C6 | C7 | OPC Control |
|---|---|---|---|---|---|---|---|---|
| $SiO_2$ | 21.41 | 18.89 | 18.42 | 21.25 | 21.59 | 20.61 | 24.49 | 21.26 |
| $Al_2O_3$ | 2.81 | 5.51 | 5.36 | 5.61 | 4.25 | 5.25 | 1.83 | 4.09 |
| $TiO_2$ | 0.14 | 0.25 | 0.24 | 0.34 | 0.28 | 0.27 | 0.09 | 0.2 |
| $P_2O_5$ | 0.27 | 0.3 | 0.28 | 0.18 | 0.07 | 0.13 | 0.13 | 0.07 |
| $Fe_2O_3$ | 4.48 | 2.55 | 2.64 | 2.24 | 3.08 | 2.06 | 0.27 | 2.89 |
| CaO | 65.27 | 62.38 | 61.33 | 67.56 | 62.71 | 63.87 | 68.84 | 63.58 |
| SrO | 0.11 | 0.3 | 0.28 | 0.15 | 0.08 | 0.09 | 0.12 | 0.12 |
| MgO | 0.98 | 2.75 | 2.61 | 1.26 | 3.27 | 2.73 | 0.6 | 2.47 |
| $Mn_2O_3$ | 0.12 | 0.11 | 0.1 | 0.07 | 0.08 | 0.06 | 0.03 | 0.06 |
| $Na_2O_3$ | 0.12 | 0.51 | 0.49 | 0.28 | 0.21 | 0.31 | 0.24 | 0.17 |
| $K_2O$ | 0.24 | 1.04 | 1.06 | 0.3 | 0.66 | 1.09 | 0.07 | 0.62 |
| $Na_2O_e$ | 0.28 | 1.19 | 1.19 | 0.48 | 0.64 | 1.03 | 0.29 | 0.58 |
| $SO_3$* | 2.65 | 4.12 | 4.43 | 0.32 | 1.44 | 1.35 | 2.14 | 2.79 |
| LOI@1000 | 1.46 | 1.02 | 2.44 | 0.24 | 1.5 | 1.94 | 1.2 | 0.99 |
| (%) | BOGUE COMPOSITION | | | | | | | |
| $C_3S$ | 70 | 57.9 | 57.2 | 71.6 | 54.1 | 61.2 | 75.3 | 57.6 |
| $C_2S$ | 8.6 | 10.5 | 9.7 | 7 | 21.2 | 13 | 13.5 | 17.6 |
| $C_3A$ | 0 | 10.3 | 9.7 | 11.1 | 6.1 | 10.4 | 4.4 | 5.9 |
| $C_4AF$ | 13.6 | 7.7 | 8 | 6.8 | 9.4 | 6.3 | 0.8 | 8.8 |

*$SO_3$ based on sulphur determined by LECO

### B.2 Results of the cements test

Tables B-2 to B-8 present the results of the chloride binding capacities of different cement pastes.

## C2, W/CM = 0.5, 2 months curing

Table B-2: Chloride binding capacity of the C2 paste.

| Sample Mass | Solution Mass | Solution Density | Solution Volume | Dry Sample Mass | Initial Conc. | Equilibrium Conc. | Bound Chloride |
|---|---|---|---|---|---|---|---|
| $W_{11}$ (g) | $W_{sol}$ (g) | $d_s$ (g/ml) | $V_{sol}$ (ml) | $W_d$ (g) | $C_i$ (mol/l) | $C_e$ (mol/l) | $C_b$ mg Cl/g Sple |
| 25.35 | 29.47 | 1.003 | 29.38 | 23.98 | 0.101 | 0.041 | 2.62 |
| 24.84 | 30.60 | 1.040 | 29.43 | 23.50 | 1.008 | 0.761 | 10.97 |
| 24.92 | 32.43 | 1.115 | 29.10 | 23.57 | 3.021 | 2.659 | 15.81 |

## C3, W/CM = 0.5, 2 months curing

Table B-3: Chloride binding capacity of the C3 paste.

| Sample Mass | Solution Mass | Solution Density | Solution Volume | Dry Sample Mass | Initial Conc. | Equilibrium Conc. | Bound Chloride |
|---|---|---|---|---|---|---|---|
| $W_{11}$ (g) | $W_{sol}$ (g) | $d_s$ (g/ml) | $V_{sol}$ (ml) | $W_d$ (g) | $C_i$ (mol/l) | $C_e$ (mol/l) | $C_b$ mg Cl/g Sple |
| 25.06 | 29.13 | 1.003 | 29.04 | 23.64 | 0.101 | 0.044 | 2.48 |
| 24.97 | 30.32 | 1.040 | 29.16 | 23.55 | 1.008 | 0.803 | 8.97 |
| 25.17 | 33.30 | 1.115 | 29.88 | 23.74 | 3.021 | 2.711 | 13.79 |

## C8, W/CM = 0.5, 2 months curing

Table B-4: Chloride binding capacity of the C8 paste.

| Sample Mass | Solution Mass | Solution Density | Solution Volume | Dry Sample Mass | Initial Conc. | Equilibrium Conc. | Bound Chloride |
|---|---|---|---|---|---|---|---|
| $W_{11}$ (g) | $W_{sol}$ (g) | $d_s$ (g/ml) | $V_{sol}$ (ml) | $W_d$ (g) | $C_i$ (mol/l) | $C_e$ (mol/l) | $C_b$ mg Cl/g Sple |
| 25.06 | 32.22 | 1.003 | 32.12 | 23.52 | 0.101 | 0.043 | 2.80 |
| 24.99 | 32.06 | 1.040 | 30.83 | 23.45 | 1.008 | 0.826 | 8.45 |
| 25.03 | 34.15 | 1.115 | 30.64 | 23.49 | 3.021 | 2.784 | 10.94 |
| 24.98 | 34.20 | 1.115 | 30.69 | 23.44 | 3.021 | 2.789 | 10.75 |

## C5, W/CM = 0.5, 2 months curing

Table B-5: Chloride binding capacity of the C5 paste.

| Sample Mass | Solution Mass | Solution Density | Solution Volume | Dry Sample Mass | Initial Conc. | Equilibrium Conc. | Bound Chloride |
|---|---|---|---|---|---|---|---|
| $W_{11}$ (g) | $W_{sol}$ (g) | $d_s$ (g/ml) | $V_{sol}$ (ml) | $W_d$ (g) | $C_i$ (mol/l) | $C_e$ (mol/l) | $C_b$ mg Cl/g Sple |
| 24.01 | 30.64 | 1.003 | 30.54 | 22.74 | 0.101 | 0.043 | 2.78 |
| 25.05 | 31.77 | 1.040 | 30.55 | 23.73 | 1.008 | 0.803 | 9.36 |
| 24.50 | 34.18 | 1.115 | 30.67 | 23.21 | 3.021 | 2.752 | 12.60 |

## C6, W/CM = 0.5, 2 months curing

Table B-6: Chloride binding capacity of the C6 paste.

| Sample Mass | Solution Mass | Solution Density | Solution Volume | Dry Sample Mass | Initial Conc. | Equilibrium Conc. | Bound Chloride |
|---|---|---|---|---|---|---|---|
| $W_{11}$ (g) | $W_{sol}$ (g) | $d_s$ (g/ml) | $V_{sol}$ (ml) | $W_d$ (g) | $C_i$ (mol/l) | $C_e$ (mol/l) | $C_b$ mg Cl/g Sple |
| 24.94 | 30.68 | 1.003 | 30.58 | 23.45 | 0.101 | 0.025 | 3.53 |
| 24.98 | 31.68 | 1.040 | 30.47 | 23.48 | 1.008 | 0.763 | 11.24 |
| 25.02 | 33.89 | 1.115 | 30.41 | 23.52 | 3.021 | 2.686 | 15.35 |
| 24.02 | 33.85 | 1.115 | 30.37 | 22.58 | 3.021 | 2.674 | 16.52 |

## C4, W/CM = 0.5, 2 months curing

Table B-7: Chloride binding capacity of the C4 paste.

| Sample Mass | Solution Mass | Solution Density | Solution Volume | Dry Sample Mass | Initial Conc. | Equilibrium Conc. | Bound Chloride |
|---|---|---|---|---|---|---|---|
| $W_{11}$ (g) | $W_{sol}$ (g) | $d_s$ (g/ml) | $V_{sol}$ (ml) | $W_d$ (g) | $C_i$ (mol/l) | $C_e$ (mol/l) | $C_b$ mg Cl/g Sple |
| 24.35 | 30.61 | 1.003 | 30.51 | 22.93 | 0.101 | 0.013 | 4.16 |
| 24.78 | 31.82 | 1.040 | 30.60 | 23.33 | 1.008 | 0.790 | 10.11 |
| 24.88 | 34.03 | 1.115 | 30.53 | 23.43 | 3.021 | 2.650 | 17.12 |
| 24.68 | 32.87 | 1.115 | 29.49 | 23.24 | 3.021 | 2.647 | 16.81 |

## C1, W/CM = 0.5, 2 months curing

Table B-8: Chloride binding capacity of the C1 paste.

| Sample Mass | Solution Mass | Solution Density | Solution Volume | Dry Sample Mass | Initial Conc. | Equilibrium Conc. | Bound Chloride |
|---|---|---|---|---|---|---|---|
| $W_{11}$ (g) | $W_{sol}$ (g) | $d_s$ (g/ml) | $V_{sol}$ (ml) | $W_d$ (g) | $C_i$ (mol/l) | $C_e$ (mol/l) | $C_b$ mg Cl/g Sple |
| 20.00 | 29.59 | 1.003 | 29.50 | 18.44 | 0.101 | 0.056 | 2.59 |
| 20.29 | 28.01 | 1.020 | 27.46 | 18.71 | 0.506 | 0.419 | 4.53 |
| 19.88 | 27.60 | 1.040 | 26.54 | 18.33 | 1.010 | 0.900 | 5.66 |
| 19.96 | 31.17 | 1.115 | 27.97 | 18.41 | 3.030 | 2.861 | 9.10 |

## C7, W/CM = 0.5, 2 months curing

Table B-9: Chloride binding capacity of the C7 paste.

| Sample Mass | Solution Mass | Solution Density | Solution Volume | Dry Sample Mass | Initial Conc. | Equilibrium Conc. | Bound Chloride |
|---|---|---|---|---|---|---|---|
| $W_{11}$ (g) | $W_{sol}$ (g) | $d_s$ (g/ml) | $V_{sol}$ (ml) | $W_d$ (g) | $C_i$ (mol/l) | $C_e$ (mol/l) | $C_b$ mg Cl/g Sple |
| 20.04 | 26.56 | 1.003 | 26.48 | 18.62 | 0.101 | 0.054 | 2.39 |
| 20.08 | 27.13 | 1.020 | 26.59 | 18.66 | 0.506 | 0.418 | 4.44 |
| 19.98 | 27.91 | 1.040 | 26.84 | 18.57 | 1.010 | 0.899 | 5.71 |
| 20.08 | 30.62 | 1.115 | 27.47 | 18.66 | 3.030 | 2.884 | 7.59 |

**B.3 Results of tests on the effect of cement fineness**

Tables B-10 and B-11 show the results of the effect of cement fineness on the chloride binding capacity of pastes. Cement C4 was ground for an extra 2 hours, and the binding capacity of the resulting cement was compared to that of cement C4 without the extra grinding. Also, cements C2 and C3 are produced from the same plant and are of similar composition except for their fineness. Their binding capacities are shown in Tables B-2 and B-3.

## C4, W/CM = 0.5, 2 months curing

Table B-10: Chloride binding capacity of the C4 paste.

| Sample Mass | Solution Mass | Solution Density | Solution Volume | Dry Sample Mass | Initial Conc. | Equilibrium Conc. | Bound Chloride |
|---|---|---|---|---|---|---|---|
| $W_{11}$ (g) | $W_{sol}$ (g) | $d_s$ (g/ml) | $V_{sol}$ (ml) | $W_d$ (g) | $C_i$ (mol/l) | $C_e$ (mol/l) | $C_b$ mg Cl/g Sple |
| 25.35 | 30.51 | 1.003 | 30.41 | 23.87 | 0.101 | 0.022 | 3.54 |
| 25.14 | 32.73 | 1.040 | 31.48 | 23.67 | 1.006 | 0.794 | 10.01 |
| 24.87 | 42.59 | 1.115 | 38.21 | 23.42 | 3.032 | 2.770 | 15.15 |

## C4 (2 extra hours grinding), W/CM = 0.5, 2 months curing

Table B-11: Chloride binding capacity of the C4 paste, made with C4 cement ground for an extra 2 hours.

| Sample Mass | Solution Mass | Solution Density | Solution Volume | Dry Sample Mass | Initial Conc. | Equilibrium Conc. | Bound Chloride |
|---|---|---|---|---|---|---|---|
| $W_{11}$ (g) | $W_{sol}$ (g) | $d_s$ (g/ml) | $V_{sol}$ (ml) | $W_d$ (g) | $C_i$ (mol/l) | $C_e$ (mol/l) | $C_b$ mg Cl/g Sple |
| 23.59 | 30.55 | 1.003 | 30.45 | 22.21 | 0.101 | 0.022 | 3.81 |
| 24.31 | 32.15 | 1.040 | 30.92 | 22.89 | 1.006 | 0.788 | 10.41 |
| 24.25 | 35.49 | 1.115 | 31.84 | 22.83 | 3.032 | 2.745 | 14.19 |

### B.4 Results of tests on the effect of $SO_3$ content of cements

Tables B-12 and B-13 present the results of the effect of $SO_3$ content of cements on the chloride binding capacity.

## C4-7SO3, W/CM = 0.5, 2 months curing

Table B-12: Chloride binding capacity of the C4-7SO3 paste.

| Sample Mass | Solution Mass | Solution Density | Solution Volume | Dry Sample Mass | Initial Conc. | Equilibrium Conc. | Bound Chloride |
|---|---|---|---|---|---|---|---|
| $W_{11}$ (g) | $W_{sol}$ (g) | $d_s$ (g/ml) | $V_{sol}$ (ml) | $W_d$ (g) | $C_i$ (mol/l) | $C_e$ (mol/l) | $C_b$ mg Cl/g Sple |
| 24.16 | 32.24 | 1.003 | 32.14 | 22.45 | 0.101 | 0.054 | 2.35 |
| 25.12 | 31.43 | 1.020 | 30.81 | 23.34 | 0.505 | 0.426 | 3.68 |
| 25.08 | 32.12 | 1.040 | 30.89 | 23.31 | 1.008 | 0.902 | 4.98 |
| 25.52 | 34.70 | 1.115 | 31.13 | 23.72 | 3.027 | 2.819 | 9.70 |

## C1-4SO3, W/CM = 0.5, 2 months curing

Table B-13: Chloride binding capacity of the C1-4SO3 paste.

| Sample Mass | Solution Mass | Solution Density | Solution Volume | Dry Sample Mass | Initial Conc. | Equilibrium Conc. | Bound Chloride |
|---|---|---|---|---|---|---|---|
| $W_{11}$ (g) | $W_{sol}$ (g) | $d_s$ (g/ml) | $V_{sol}$ (ml) | $W_d$ (g) | $C_i$ (mol/l) | $C_e$ (mol/l) | $C_b$ mg Cl/g Sple |
| 24.16 | 30.31 | 1.003 | 30.22 | 22.75 | 0.101 | 0.071 | 1.39 |
| 25.36 | 30.94 | 1.020 | 30.33 | 23.88 | 0.505 | 0.457 | 2.14 |
| 23.88 | 33.02 | 1.040 | 31.76 | 22.49 | 1.008 | 0.954 | 2.69 |
| 25.25 | 34.50 | 1.115 | 30.96 | 23.78 | 3.027 | 2.915 | 5.15 |

### B.5 Results of tests on the effect of pH

Tables B-14 to B-25 show the results of the effect of pH of the host solution on the chloride binding capacity of pastes. The pH of the host solutions at equilibrium are also shown in these tables.

## Control, W/CM = 0.5, curing: 2 months, pH = 13.0 (host solution)

Table B-14: Chloride binding capacity of the Control paste. The host solution pH=13.

| Solution Mass | Solution Density | Solution Volume | Sample Mass | Dry Sample Mass | Initial Conc. | Equilibrium Conc. | Bound Chloride | Equilibrium pH |
|---|---|---|---|---|---|---|---|---|
| $W_{sol}$ (g) | $d_s$ (g/ml) | $V_{sol}$ (ml) | $W_{11}$ (g) | $W_d$ (g) | $C_i$ (mol/l) | $C_e$ (mol/l) | $C_b$ mg Cl/g Sple | pH |
| 31.78 | 1.009 | 31.51 | 24.80 | 23.26 | 0.101 | 0.047 | 2.61 | 13.31 |
| 32.93 | 1.044 | 31.53 | 24.76 | 23.23 | 1.007 | 0.842 | 7.93 | 13.42 |
| 35.85 | 1.119 | 32.05 | 24.23 | 22.73 | 3.028 | 2.798 | 11.48 | 13.37 |

## Control, W/CM = 0.5, curing: 2 months, pH = 13.4 (host solution)

Table B-15: Chloride binding capacity of the Control paste. The host solution pH=13.4.

| Solution Mass | Solution Density | Solution Volume | Sample Mass | Dry Sample Mass | Initial Conc. | Equilibrium Conc. | Bound Chloride | Equilibrium pH |
|---|---|---|---|---|---|---|---|---|
| $W_{sol}$ (g) | $d_s$ (g/ml) | $V_{sol}$ (ml) | $W_{11}$ (g) | $W_d$ (g) | $C_i$ (mol/l) | $C_e$ (mol/l) | $C_b$ mg Cl/g Sple | pH |
| 32.38 | 1.013 | 31.96 | 24.83 | 23.29 | 0.101 | 0.054 | 2.25 | 13.49 |
| 32.38 | 1.050 | 30.83 | 24.77 | 23.23 | 1.008 | 0.848 | 7.52 | 13.54 |
| 35.92 | 1.124 | 31.96 | 24.79 | 23.25 | 3.019 | 2.788 | 11.28 | 13.49 |

## Control, W/CM = 0.5, curing: 2 months, pH = 13.7 (host solution)

Table B-16: Chloride binding capacity of the Control paste. The host solution pH=13.7.

| Solution Mass | Solution Density | Solution Volume | Sample Mass | Dry Sample Mass | Initial Conc. | Equilibrium Conc. | Bound Chloride | Equilibrium pH |
|---|---|---|---|---|---|---|---|---|
| $W_{sol}$ (g) | $d_s$ (g/ml) | $V_{sol}$ (ml) | $W_{11}$ (g) | $W_d$ (g) | $C_i$ (mol/l) | $C_e$ (mol/l) | $C_b$ mg Cl/g Sple | pH |
| 32.20 | 1.023 | 31.49 | 24.86 | 23.32 | 0.101 | 0.062 | 1.86 | 13.68 |
| 33.35 | 1.057 | 31.56 | 24.77 | 23.23 | 1.012 | 0.863 | 7.21 | 13.69 |
| 35.62 | 1.134 | 31.42 | 25.07 | 23.52 | 3.025 | 2.810 | 10.16 | 13.65 |

## Control, W/CM = 0.5, curing: 2 months, pH = 14.0 (host solution)

Table B-17: Chloride binding capacity of the Control paste. The host solution pH=14.

| Solution Mass | Solution Density | Solution Volume | Sample Mass | Dry Sample Mass | Initial Conc. | Equilibrium Conc. | Bound Chloride | Equilibrium pH |
|---|---|---|---|---|---|---|---|---|
| $W_{sol}$ (g) | $d_s$ (g/ml) | $V_{sol}$ (ml) | $W_{11}$ (g) | $W_d$ (g) | $C_i$ (mol/l) | $C_e$ (mol/l) | $C_b$ mg Cl/g Sple | pH |
| 32.94 | 1.044 | 31.54 | 24.62 | 23.09 | 0.101 | 0.069 | 1.56 | 13.91 |
| 34.08 | 1.078 | 31.62 | 24.93 | 23.38 | 1.011 | 0.870 | 6.74 | 13.89 |
| 38.39 | 1.151 | 33.35 | 25.00 | 23.45 | 3.027 | 2.829 | 9.95 | 13.89 |

## 8SF, W/CM = 0.5, curing: 2 months, pH = 13.0 (host solution)

Table B-18: Chloride binding capacity of the 8SF paste. The host solution pH=13.

| Solution Mass | Solution Density | Solution Volume | Sample Mass | Dry Sample Mass | Initial Conc. | Equilibrium Conc. | Bound Chloride | Equilibrium pH |
|---|---|---|---|---|---|---|---|---|
| $W_{sol}$ (g) | $d_s$ (g/ml) | $V_{sol}$ (ml) | $W_{11}$ (g) | $W_d$ (g) | $C_i$ (mol/l) | $C_e$ (mol/l) | $C_b$ mg Cl/g Sple | pH |
| 33.65 | 1.009 | 33.36 | 24.80 | 22.96 | 0.101 | 0.067 | 1.77 | 13.21 |
| 34.20 | 1.044 | 32.75 | 25.03 | 23.17 | 1.007 | 0.886 | 6.03 | 13.25 |
| 35.60 | 1.119 | 31.83 | 24.97 | 23.12 | 3.028 | 2.837 | 9.32 | 13.12 |

## 8SF, W/CM = 0.5, curing: 2 months, pH = 13.4 (host solution)

Table B-19: Chloride binding capacity of the 8SF paste. The host solution pH=13.4.

| Solution Mass | Solution Density | Solution Volume | Sample Mass | Dry Sample Mass | Initial Conc. | Equilibrium Conc. | Bound Chloride | Equilibrium pH |
|---|---|---|---|---|---|---|---|---|
| $W_{sol}$ (g) | $d_s$ (g/ml) | $V_{sol}$ (ml) | $W_{11}$ (g) | $W_d$ (g) | $C_i$ (mol/l) | $C_e$ (mol/l) | $C_b$ mg Cl/g Sple | pH |
| 32.27 | 1.013 | 31.85 | 24.13 | 22.34 | 0.101 | 0.072 | 1.46 | 13.38 |
| 33.22 | 1.050 | 31.63 | 24.91 | 23.06 | 1.008 | 0.891 | 5.67 | 13.37 |
| 35.60 | 1.124 | 31.67 | 24.61 | 22.78 | 3.019 | 2.843 | 8.69 | 13.27 |

## 8SF, W/CM = 0.5, curing: 2 months, pH = 13.7 (host solution)

Table B-20: Chloride binding capacity of the 8SF paste. The host solution pH=13.7.

| Solution Mass | Solution Density | Solution Volume | Sample Mass | Dry Sample Mass | Initial Conc. | Equilibrium Conc. | Bound Chloride | Equilibrium pH |
|---|---|---|---|---|---|---|---|---|
| $W_{sol}$ (g) | $d_s$ (g/ml) | $V_{sol}$ (ml) | $W_{11}$ (g) | $W_d$ (g) | $C_i$ (mol/l) | $C_e$ (mol/l) | $C_b$ mg Cl/g Sple | pH |
| 32.51 | 1.023 | 31.79 | 24.96 | 23.11 | 0.101 | 0.075 | 1.26 | 13.60 |
| 33.81 | 1.057 | 32.00 | 24.26 | 22.46 | 1.012 | 0.903 | 5.55 | 13.57 |
| 35.87 | 1.134 | 31.64 | 24.73 | 22.89 | 3.025 | 2.850 | 8.55 | 13.50 |

## 8SF, W/CM = 0.5, curing: 2 months, pH = 14.0 (host solution)

Table B-21: Chloride binding capacity of the 8SF paste. The host solution pH=14.

| Solution Mass | Solution Density | Solution Volume | Sample Mass | Dry Sample Mass | Initial Conc. | Equilibrium Conc. | Bound Chloride | Equilibrium pH |
|---|---|---|---|---|---|---|---|---|
| $W_{sol}$ (g) | $d_s$ (g/ml) | $V_{sol}$ (ml) | $W_{11}$ (g) | $W_d$ (g) | $C_i$ (mol/l) | $C_e$ (mol/l) | $C_b$ mg Cl/g Sple | pH |
| 33.26 | 1.044 | 31.85 | 24.89 | 23.04 | 0.101 | 0.079 | 1.11 | 13.86 |
| 34.39 | 1.078 | 31.91 | 24.26 | 22.46 | 1.011 | 0.904 | 5.40 | 13.84 |
| 36.96 | 1.151 | 32.11 | 24.87 | 23.02 | 3.027 | 2.856 | 8.46 | 13.79 |

## 8MK, W/CM = 0.5, curing: 2 months, pH = 13.0 (host solution)

Table B-22: Chloride binding capacity of the 8MK paste. The host solution pH=13.

| Solution Mass | Solution Density | Solution Volume | Sample Mass | Dry Sample Mass | Initial Conc. | Equilibrium Conc. | Bound Chloride | Equilibrium pH |
|---|---|---|---|---|---|---|---|---|
| $W_{sol}$ (g) | $d_s$ (g/ml) | $V_{sol}$ (ml) | $W_{11}$ (g) | $W_d$ (g) | $C_i$ (mol/l) | $C_e$ (mol/l) | $C_b$ mg Cl/g Sple | pH |
| 32.09 | 1.009 | 31.81 | 24.70 | 23.10 | 0.101 | 0.045 | 2.72 | 13.28 |
| 33.22 | 1.044 | 31.81 | 23.72 | 22.19 | 1.007 | 0.764 | 12.33 | 13.41 |
| 35.73 | 1.119 | 31.94 | 24.72 | 23.12 | 3.028 | 2.544 | 23.71 | 13.32 |

## 8MK, W/CM = 0.5, curing: 2 months, pH = 13.4 (host solution)

Table B-23: Chloride binding capacity of the 8MK paste. The host solution pH=13.4.

| Solution Mass | Solution Density | Solution Volume | Sample Mass | Dry Sample Mass | Initial Conc. | Equilibrium Conc. | Bound Chloride | Equilibrium pH |
|---|---|---|---|---|---|---|---|---|
| $W_{sol}$ (g) | $d_s$ (g/ml) | $V_{sol}$ (ml) | $W_{11}$ (g) | $W_d$ (g) | $C_i$ (mol/l) | $C_e$ (mol/l) | $C_b$ mg Cl/g Sple | pH |
| 32.31 | 1.013 | 31.89 | 24.24 | 22.67 | 0.101 | 0.054 | 2.33 | 13.45 |
| 33.39 | 1.050 | 31.79 | 24.37 | 22.79 | 1.008 | 0.774 | 11.56 | 13.54 |
| 35.43 | 1.124 | 31.52 | 24.96 | 23.35 | 3.019 | 2.544 | 22.75 | 13.45 |

## 8MK, W/CM = 0.5, curing: 2 months, pH = 13.7 (host solution)

Table B-24: Chloride binding capacity of the 8MK paste. The host solution pH=13.7.

| Solution Mass | Solution Density | Solution Volume | Sample Mass | Dry Sample Mass | Initial Conc. | Equilibrium Conc. | Bound Chloride | Equilibrium pH |
|---|---|---|---|---|---|---|---|---|
| $W_{sol}$ (g) | $d_s$ (g/ml) | $V_{sol}$ (ml) | $W_{11}$ (g) | $W_d$ (g) | $C_i$ (mol/l) | $C_e$ (mol/l) | $C_b$ mg Cl/g Sple | pH |
| 32.58 | 1.023 | 31.86 | 24.35 | 22.78 | 0.101 | 0.057 | 2.18 | 13.66 |
| 34.07 | 1.057 | 32.24 | 23.33 | 21.82 | 1.012 | 0.798 | 11.24 | 13.68 |
| 37.60 | 1.134 | 33.16 | 22.85 | 21.37 | 3.025 | 2.615 | 22.55 | 13.62 |

## 8MK, W/CM = 0.5, curing: 2 months, pH = 14.0 (host solution)

Table B-25: Chloride binding capacity of the 8MK paste. The host solution pH=14.

| Solution Mass | Solution Density | Solution Volume | Sample Mass | Dry Sample Mass | Initial Conc. | Equilibrium Conc. | Bound Chloride | Equilibrium pH |
|---|---|---|---|---|---|---|---|---|
| $W_{sol}$ (g) | $d_s$ (g/ml) | $V_{sol}$ (ml) | $W_{11}$ (g) | $W_d$ (g) | $C_i$ (mol/l) | $C_e$ (mol/l) | $C_b$ mg Cl/g Sple | pH |
| 33.21 | 1.044 | 31.80 | 24.69 | 23.09 | 0.101 | 0.060 | 2.01 | 13.91 |
| 34.15 | 1.078 | 31.68 | 24.68 | 23.08 | 1.011 | 0.795 | 10.52 | 13.92 |
| 36.54 | 1.151 | 31.75 | 25.02 | 23.40 | 3.027 | 2.578 | 21.58 | 13.84 |

### B.6 Results of the effect of sulphate ion concentration

Tables B-26 to B-34 show the results of the effect of sulphate ion concentration, in the host solution, on the chloride binding capacity of pastes.

## Control, W/CM = 0.5, curing: 2 months, $[SO_4^{2-}]$ = 0 M (host solution)

Table B-26: Chloride binding capacity of the Control paste. $[SO_4^{2-}]$ = 0 M in the host solution.

| Solution Mass | Solution Density | Solution Volume | Sample Mass | Dry Sample Mass | Initial Conc. | Equilibrium Conc. | Bound Chloride |
|---|---|---|---|---|---|---|---|
| $W_{sol}$ (g) | $d_s$ (g/ml) | $V_{sol}$ (ml) | $W_{11}$ (g) | $W_d$ (g) | $C_i$ (mol/l) | $C_e$ (mol/l) | $C_b$ mg Cl/g Sple |
| 28.56 | 1.004 | 28.45 | 25.06 | 23.51 | 0.100 | 0.041 | 2.56 |
| 32.15 | 1.039 | 30.96 | 24.84 | 23.30 | 1.007 | 0.846 | 7.58 |
| 34.91 | 1.114 | 31.33 | 24.98 | 23.43 | 3.019 | 2.778 | 11.43 |

## Control, W/CM = 0.5, curing: 2 months, $[SO_4^{2-}]$ = 0.01 M (host solution)

Table B-27: Chloride binding capacity of the Control paste. $[SO_4^{2-}]$= 0.01 M in the host solution.

| Solution Mass | Solution Density | Solution Volume | Sample Mass | Dry Sample Mass | Initial Conc. | Equilibrium Conc. | Bound Chloride |
|---|---|---|---|---|---|---|---|
| $W_{sol}$ (g) | $d_s$ (g/ml) | $V_{sol}$ (ml) | $W_{11}$ (g) | $W_d$ (g) | $C_i$ (mol/l) | $C_e$ (mol/l) | $C_b$ mg Cl/g Sple |
| 31.26 | 1.004 | 31.14 | 25.16 | 23.60 | 0.101 | 0.045 | 2.60 |
| 32.41 | 1.039 | 31.19 | 24.90 | 23.36 | 1.007 | 0.847 | 7.55 |
| 34.53 | 1.114 | 30.99 | 24.92 | 23.38 | 3.023 | 2.774 | 11.69 |

## Control, W/CM = 0.5, curing: 2 months, $[SO_4^{2-}]$ = 0.1 M (host solution)

Table B-28: Chloride binding capacity of the Control paste. $[SO_4^{2-}]$ = 0.1 M in the host solution.

| Solution Mass | Solution Density | Solution Volume | Sample Mass | Dry Sample Mass | Initial Conc. | Equilibrium Conc. | Bound Chloride |
|---|---|---|---|---|---|---|---|
| $W_{sol}$ (g) | $d_s$ (g/ml) | $V_{sol}$ (ml) | $W_{11}$ (g) | $W_d$ (g) | $C_i$ (mol/l) | $C_e$ (mol/l) | $C_b$ mg Cl/g Sple |
| 31.67 | 1.015 | 31.19 | 24.73 | 23.20 | 0.101 | 0.065 | 1.74 |
| 32.57 | 1.050 | 31.02 | 24.97 | 23.42 | 1.010 | 0.901 | 5.15 |
| 34.97 | 1.125 | 31.10 | 24.91 | 23.37 | 3.013 | 2.830 | 8.64 |

## 8SF, W/CM = 0.5, curing: 2 months, $[SO_4^{2-}]$ = 0 M (host solution)

Table B-29: Chloride binding capacity of the 8SF paste. $[SO_4^{2-}]$ = 0 M in the host solution.

| Solution Mass | Solution Density | Solution Volume | Sample Mass | Dry Sample Mass | Initial Conc. | Equilibrium Conc. | Bound Chloride |
|---|---|---|---|---|---|---|---|
| $W_{sol}$ (g) | $d_s$ (g/ml) | $V_{sol}$ (ml) | $W_{11}$ (g) | $W_d$ (g) | $C_i$ (mol/l) | $C_e$ (mol/l) | $C_b$ mg Cl/g Sple |
| 42.13 | 1.004 | 41.97 | 24.51 | 22.69 | 0.100 | 0.063 | 2.42 |
| 32.89 | 1.039 | 31.67 | 24.82 | 22.98 | 1.007 | 0.883 | 6.04 |
| 34.66 | 1.114 | 31.11 | 25.02 | 23.16 | 3.019 | 2.842 | 8.45 |

## 8SF, W/CM = 0.5, curing: 2 months, $[SO_4^{2-}]$ = 0.01 M (host solution)

Table B-30: Chloride binding capacity of the 8SF paste. $[SO_4^{2-}]$ = 0.01 M in the host solution.

| Solution Mass | Solution Density | Solution Volume | Sample Mass | Dry Sample Mass | Initial Conc. | Equilibrium Conc. | Bound Chloride |
|---|---|---|---|---|---|---|---|
| $W_{sol}$ (g) | $d_s$ (g/ml) | $V_{sol}$ (ml) | $W_{11}$ (g) | $W_d$ (g) | $C_i$ (mol/l) | $C_e$ (mol/l) | $C_b$ mg Cl/g Sple |
| 31.15 | 1.004 | 31.03 | 24.99 | 23.13 | 0.101 | 0.060 | 1.95 |
| 32.22 | 1.039 | 31.01 | 25.03 | 23.17 | 1.007 | 0.891 | 5.47 |
| 35.61 | 1.114 | 31.96 | 25.00 | 23.14 | 3.023 | 2.853 | 8.34 |

## 8SF, W/CM = 0.5, curing: 2 months, $[SO_4^{2-}]$ = 0.1 M (host solution)

Table B-31: Chloride binding capacity of the 8SF paste. $[SO_4^{2-}]$ = 0.1 M in the host solution.

| Solution Mass | Solution Density | Solution Volume | Sample Mass | Dry Sample Mass | Initial Conc. | Equilibrium Conc. | Bound Chloride |
|---|---|---|---|---|---|---|---|
| $W_{sol}$ (g) | $d_s$ (g/ml) | $V_{sol}$ (ml) | $W_{11}$ (g) | $W_d$ (g) | $C_i$ (mol/l) | $C_e$ (mol/l) | $C_b$ mg Cl/g Sple |
| 31.15 | 1.015 | 30.68 | 24.99 | 23.13 | 0.101 | 0.078 | 1.11 |
| 32.33 | 1.050 | 30.79 | 24.92 | 23.07 | 1.010 | 0.929 | 3.86 |
| 34.75 | 1.125 | 30.90 | 25.07 | 23.21 | 3.013 | 2.896 | 5.53 |

## 8MK, W/CM = 0.5, curing: 2 months, $[SO_4^{2-}]$ = 0 M (host solution)

Table B-32: Chloride binding capacity of the 8MK paste. $[SO_4^{2-}]$ = 0 M in the host solution.

| Solution Mass | Solution Density | Solution Volume | Sample Mass | Dry Sample Mass | Initial Conc. | Equilibrium Conc. | Bound Chloride |
|---|---|---|---|---|---|---|---|
| $W_{sol}$ (g) | $d_s$ (g/ml) | $V_{sol}$ (ml) | $W_{11}$ (g) | $W_d$ (g) | $C_i$ (mol/l) | $C_e$ (mol/l) | $C_b$ mg Cl/g Sple |
| 30.87 | 1.004 | 30.75 | 25.04 | 23.42 | 0.100 | 0.033 | 3.14 |
| 31.88 | 1.039 | 30.70 | 25.04 | 23.42 | 1.007 | 0.712 | 13.69 |
| 34.13 | 1.114 | 30.63 | 24.99 | 23.37 | 3.019 | 2.531 | 22.66 |

## 8MK, W/CM = 0.5, curing: 2 months, $[SO_4^{2-}]$ = 0.01 M (host solution)

Table B-33: Chloride binding capacity of the 8MK paste. $[SO_4^{2-}]$ = 0.01 M in the host solution.

| Solution Mass | Solution Density | Solution Volume | Sample Mass | Dry Sample Mass | Initial Conc. | Equilibrium Conc. | Bound Chloride |
|---|---|---|---|---|---|---|---|
| $W_{sol}$ (g) | $d_s$ (g/ml) | $V_{sol}$ (ml) | $W_{11}$ (g) | $W_d$ (g) | $C_i$ (mol/l) | $C_e$ (mol/l) | $C_b$ mg Cl/g Sple |
| 31.01 | 1.004 | 30.89 | 25.03 | 23.41 | 0.101 | 0.035 | 3.06 |
| 31.93 | 1.039 | 30.73 | 25.03 | 23.41 | 1.007 | 0.725 | 13.09 |
| 35.19 | 1.114 | 31.59 | 24.75 | 23.15 | 3.023 | 2.565 | 22.14 |

## 8MK, W/CM = 0.5, curing: 2 months, $[SO_4^{2-}]$ = 0.1 M (host solution)

Table B-34: Chloride binding capacity of the 8MK paste. $[SO_4^{2-}]$ = 0.1 M in the host solution.

| Solution Mass | Solution Density | Solution Volume | Sample Mass | Dry Sample Mass | Initial Conc. | Equilibrium Conc. | Bound Chloride |
|---|---|---|---|---|---|---|---|
| $W_{sol}$ (g) | $d_s$ (g/ml) | $V_{sol}$ (ml) | $W_{11}$ (g) | $W_d$ (g) | $C_i$ (mol/l) | $C_e$ (mol/l) | $C_b$ mg Cl/g Sple |
| 31.38 | 1.015 | 30.91 | 25.03 | 23.41 | 0.101 | 0.062 | 1.85 |
| 32.69 | 1.050 | 31.13 | 23.55 | 22.03 | 1.010 | 0.832 | 8.93 |
| 34.50 | 1.125 | 30.68 | 25.02 | 23.40 | 3.013 | 2.585 | 19.88 |

### B.7 Results of the effect of temperature

Tables B-35 to B-43 show the results of the effect of temperature on the chloride binding capacity. The specimen were stored at 3 different temperatures: 7°C, 23°C, and 38°C.

## Control, W/CM = 0.5, curing = 2 months, T = 7°C

Table B-35: Chloride binding capacity of the 8MK paste. The storage temperature is 7°C.

| Solution Mass | Solution Density | Solution Volume | Sample Mass | Dry Sample Mass | Initial Conc. | Equilibrium Conc. | Bound Chloride |
|---|---|---|---|---|---|---|---|
| $W_{sol}$ (g) | $d_s$ (g/ml) | $V_{sol}$ (ml) | $W_{11}$ (g) | $W_d$ (g) | $C_i$ (mol/l) | $C_e$ (mol/l) | $C_b$ mg Cl/g Sple |
| 32.02 | 1.003 | 31.92 | 25.02 | 23.47 | 0.101 | 0.034 | 3.22 |
| 33.44 | 1.040 | 32.16 | 24.90 | 23.36 | 1.009 | 0.843 | 8.09 |
| 34.87 | 1.115 | 31.29 | 24.97 | 23.42 | 3.015 | 2.825 | 9.02 |

## Control, W/CM = 0.5, curing = 2 months, T = 23°C (storage temperature)

Table B-36: Chloride binding capacity of the control paste. The storage temperature is 23°C.

| Solution Mass | Solution Density | Solution Volume | Sample Mass | Dry Sample Mass | Initial Conc. | Equilibrium Conc. | Bound Chloride |
|---|---|---|---|---|---|---|---|
| $W_{sol}$ (g) | $d_s$ (g/ml) | $V_{sol}$ (ml) | $W_{11}$ (g) | $W_d$ (g) | $C_i$ (mol/l) | $C_e$ (mol/l) | $C_b$ mg Cl/g Sple |
| 32.05 | 1.003 | 31.95 | 24.50 | 22.98 | 0.101 | 0.041 | 2.94 |
| 33.43 | 1.040 | 32.15 | 24.93 | 23.38 | 1.009 | 0.841 | 8.15 |
| 35.80 | 1.115 | 32.12 | 24.82 | 23.28 | 3.015 | 2.774 | 11.79 |

## Control, W/CM = 0.5, curing = 2 months, T = 38°C

Table B-37: Chloride binding capacity of the control paste. The storage temperature is 38°C.

| Solution Mass | Solution Density | Solution Volume | Sample Mass | Dry Sample Mass | Initial Conc. | Equilibrium Conc. | Bound Chloride |
|---|---|---|---|---|---|---|---|
| $W_{sol}$ (g) | $d_s$ (g/ml) | $V_{sol}$ (ml) | $W_{11}$ (g) | $W_d$ (g) | $C_i$ (mol/l) | $C_e$ (mol/l) | $C_b$ mg Cl/g Sple |
| 32.09 | 1.003 | 31.99 | 24.68 | 23.15 | 0.101 | 0.053 | 2.36 |
| 33.34 | 1.040 | 32.06 | 24.46 | 22.94 | 1.009 | 0.847 | 8.03 |
| 35.68 | 1.115 | 32.01 | 24.70 | 23.17 | 3.015 | 2.760 | 12.48 |

## 8SF, W/CM = 0.5, curing = 2 months, T = 7°C

Table B-38: Chloride binding capacity of the control paste. The storage temperature is 7°C.

| Solution Mass | Solution Density | Solution Volume | Sample Mass | Dry Sample Mass | Initial Conc. | Equilibrium Conc. | Bound Chloride |
|---|---|---|---|---|---|---|---|
| $W_{sol}$ (g) | $d_s$ (g/ml) | $V_{sol}$ (ml) | $W_{11}$ (g) | $W_d$ (g) | $C_i$ (mol/l) | $C_e$ (mol/l) | $C_b$ mg Cl/g Sple |
| 32.00 | 1.003 | 31.90 | 24.79 | 23.25 | 0.101 | 0.055 | 2.24 |
| 33.58 | 1.040 | 32.29 | 23.90 | 22.42 | 1.009 | 0.888 | 6.16 |
| 34.53 | 1.115 | 30.98 | 24.81 | 23.27 | 3.015 | 2.873 | 6.73 |

## 8SF, W/CM = 0.5, curing = 2 months, T = 23°C

Table B-39: Chloride binding capacity of the 8SF paste. The storage temperature is 23°C.

| Solution Mass | Solution Density | Solution Volume | Sample Mass | Dry Sample Mass | Initial Conc. | Equilibrium Conc. | Bound Chloride |
|---|---|---|---|---|---|---|---|
| $W_{sol}$ (g) | $d_s$ (g/ml) | $V_{sol}$ (ml) | $W_{11}$ (g) | $W_d$ (g) | $C_i$ (mol/l) | $C_e$ (mol/l) | $C_b$ mg Cl/g Sple |
| 32.31 | 1.003 | 32.21 | 24.81 | 23.27 | 0.101 | 0.059 | 2.04 |
| 33.10 | 1.040 | 31.83 | 24.24 | 22.74 | 1.009 | 0.887 | 6.01 |
| 35.47 | 1.115 | 31.83 | 24.85 | 23.31 | 3.015 | 2.832 | 8.86 |
| 35.94 | 1.115 | 32.25 | 24.64 | 23.11 | 3.015 | 2.855 | 7.94 |

## 8SF, W/CM = 0.5, curing = 2 months, T = 38°C

Table B-40: Chloride binding capacity of the 8SF paste. The storage temperature is 38°C.

| Solution Mass | Solution Density | Solution Volume | Sample Mass | Dry Sample Mass | Initial Conc. | Equilibrium Conc. | Bound Chloride |
|---|---|---|---|---|---|---|---|
| $W_{sol}$ (g) | $d_s$ (g/ml) | $V_{sol}$ (ml) | $W_{11}$ (g) | $W_d$ (g) | $C_i$ (mol/l) | $C_e$ (mol/l) | $C_b$ mg Cl/g Sple |
| 33.46 | 1.003 | 33.36 | 24.80 | 23.26 | 0.101 | 0.065 | 1.83 |
| 33.35 | 1.040 | 32.07 | 24.72 | 23.19 | 1.009 | 0.890 | 5.82 |
| 35.64 | 1.115 | 31.98 | 24.68 | 23.15 | 3.015 | 2.818 | 9.65 |

## 8MK, W/CM = 0.5, curing = 2 months, T = 7°C

Table B-41: Chloride binding capacity of the 8SF paste. The storage temperature is 7°C.

| Solution Mass | Solution Density | Solution Volume | Sample Mass | Dry Sample Mass | Initial Conc. | Equilibrium Conc. | Bound Chloride |
|---|---|---|---|---|---|---|---|
| $W_{sol}$ (g) | $d_s$ (g/ml) | $V_{sol}$ (ml) | $W_{11}$ (g) | $W_d$ (g) | $C_i$ (mol/l) | $C_e$ (mol/l) | $C_b$ mg Cl/g Sple |
| 32.21 | 1.003 | 32.11 | 24.86 | 23.32 | 0.101 | 0.036 | 3.16 |
| 34.92 | 1.040 | 33.58 | 24.84 | 23.30 | 1.009 | 0.740 | 13.74 |
| 37.52 | 1.115 | 33.67 | 24.90 | 23.36 | 3.015 | 2.656 | 18.35 |

## 8MK, W/CM = 0.5, curing = 2 months, T = 23°C

Table B-42: Chloride binding capacity of the 8MK paste. The storage temperature is 23°C.

| Solution Mass | Solution Density | Solution Volume | Sample Mass | Dry Sample Mass | Initial Conc. | Equilibrium Conc. | Bound Chloride |
|---|---|---|---|---|---|---|---|
| $W_{sol}$ (g) | $d_s$ (g/ml) | $V_{sol}$ (ml) | $W_{11}$ (g) | $W_d$ (g) | $C_i$ (mol/l) | $C_e$ (mol/l) | $C_b$ mg Cl/g Sple |
| 32.17 | 1.003 | 32.07 | 24.86 | 23.32 | 0.101 | 0.039 | 3.01 |
| 33.54 | 1.040 | 32.26 | 24.76 | 23.23 | 1.009 | 0.740 | 13.23 |
| 35.71 | 1.115 | 32.04 | 24.45 | 22.93 | 3.015 | 2.554 | 22.82 |
| 35.57 | 1.115 | 31.92 | 24.53 | 23.01 | 3.015 | 2.584 | 21.18 |

## 8MK, W/CM = 0.5, curing = 2 months, T = 38°C

Table B-43: Chloride binding capacity of the 8MK paste. The storage temperature is 38°C.

| Solution Mass | Solution Density | Solution Volume | Sample Mass | Dry Sample Mass | Initial Conc. | Equilibrium Conc. | Bound Chloride |
|---|---|---|---|---|---|---|---|
| $W_{sol}$ (g) | $d_s$ (g/ml) | $V_{sol}$ (ml) | $W_{11}$ (g) | $W_d$ (g) | $C_i$ (mol/l) | $C_e$ (mol/l) | $C_b$ mg Cl/g Sple |
| 32.26 | 1.003 | 32.16 | 24.99 | 23.44 | 0.101 | 0.044 | 2.74 |
| 33.35 | 1.040 | 32.07 | 25.02 | 23.47 | 1.009 | 0.754 | 12.34 |
| 35.78 | 1.115 | 32.10 | 24.82 | 23.28 | 3.015 | 2.545 | 22.98 |

## B.8 Results of the effect of carbonation

Tables B-44 to B-46 present the results of the effect of pre-carbonation of pastes on the chloride binding capacity of pastes.

### Control, W/CM = 0.5, curing = 2 months, pre-carbonated

Table B-44: Chloride binding capacity of the pre-carbonated control paste.

| Solution Mass | Solution Density | Solution Volume | Sample Mass | Dry Sample Mass | Initial Conc. | Equilibrium Conc. | Bound Chloride |
|---|---|---|---|---|---|---|---|
| $W_{sol}$ (g) | $d_s$ (g/ml) | $V_{sol}$ (ml) | $W_{11}$ (g) | $W_d$ (g) | $C_i$ (mol/l) | $C_e$ (mol/l) | $C_b$ mg Cl/g Sple |
| 24.86 | 29.18 | 1.003 | 29.09 | 23.80 | 0.101 | 0.095 | 0.26 |
| 24.69 | 31.81 | 1.040 | 30.59 | 23.64 | 1.008 | 0.992 | 0.74 |
| 24.78 | 32.01 | 1.115 | 28.72 | 23.72 | 3.015 | 2.960 | 2.37 |
| 24.85 | 32.26 | 1.115 | 28.95 | 23.79 | 3.021 | 2.982 | 1.70 |

### 8SF, W/CM = 0.5, curing = 2 months, precarbonated

Table B-45: Chloride binding capacity of the pre-carbonated 8SF paste.

| Solution Mass | Solution Density | Solution Volume | Sample Mass | Dry Sample Mass | Initial Conc. | Equilibrium Conc. | Bound Chloride |
|---|---|---|---|---|---|---|---|
| $W_{sol}$ (g) | $d_s$ (g/ml) | $V_{sol}$ (ml) | $W_{11}$ (g) | $W_d$ (g) | $C_i$ (mol/l) | $C_e$ (mol/l) | $C_b$ mg Cl/g Sple |
| 24.99 | 31.65 | 1.003 | 31.55 | 23.73 | 0.101 | 0.100 | 0.06 |
| 22.99 | 32.81 | 1.040 | 31.55 | 21.83 | 1.008 | 0.996 | 0.58 |
| 24.41 | 35.09 | 1.115 | 31.48 | 23.18 | 3.015 | 3.004 | 0.52 |
| 24.38 | 34.99 | 1.115 | 31.39 | 23.15 | 3.021 | 3.021 | 0.00 |

### 8MK, W/CM = 0.5, curing = 2 months, precarbonated

Table B-46: Chloride binding capacity of the pre-carbonated 8MK paste.

| Solution Mass | Solution Density | Solution Volume | Sample Mass | Dry Sample Mass | Initial Conc. | Equilibrium Conc. | Bound Chloride |
|---|---|---|---|---|---|---|---|
| $W_{sol}$ (g) | $d_s$ (g/ml) | $V_{sol}$ (ml) | $W_{11}$ (g) | $W_d$ (g) | $C_i$ (mol/l) | $C_e$ (mol/l) | $C_b$ mg Cl/g Sple |
| 24.78 | 31.26 | 1.003 | 31.16 | 23.36 | 0.101 | 0.099 | 0.09 |
| 24.62 | 32.63 | 1.040 | 31.38 | 23.21 | 1.008 | 0.996 | 0.57 |
| 23.90 | 34.80 | 1.115 | 31.22 | 22.53 | 3.015 | 2.982 | 1.62 |
| 24.93 | 34.79 | 1.115 | 31.22 | 23.50 | 3.021 | 2.979 | 1.95 |

# Appendix C

## Results of Phase Three

### C.1 Introduction:

The results presented in this appendix are referred to in section 4-3. The chemical compositions of the pure phases are presented in Table C-1, and the mixtures design of the pastes made with pure phases, are presented in Table C-2. The mixtures design of the SCM-lime pastes are presented in Table C-3.

Table C-1: Chemical Composition of the Pure Phases

| Amount (%) | Pure $C_2S$ | Pure $C_3S$ | Pure $C_3A$ | Pure $C_4AF$ |
|---|---|---|---|---|
| $SiO_2$ | 33.79 | 24.05 | 0.04 | 0.33 |
| $Al_2O_3$ | 0.07 | 0.22 | 36.37 | 18.76 |
| $TiO_2$ | 0.02 | 0.02 | 0.02 | 0.01 |
| $P_2O_5$ | 0.05 | 0.00 | 0.00 | 0.00 |
| $Fe_2O_3$ | 0.08 | 0.03 | 0.01 | 30.82 |
| CaO | 63.48 | 69.48 | 62.48 | 47.67 |
| SrO | 0.02 | 0.01 | 0.01 | 0.01 |
| MgO | 0.30 | 0.26 | 0.12 | 0.20 |
| $Mn_2O_3$ | 0.02 | 0.01 | 0.01 | 0.04 |
| $Na_2O_3$ | 0.06 | 0.07 | 0.08 | 0.05 |
| $K_2O$ | 0.00 | 0.00 | 0.00 | 0.00 |
| $SO_3$* | 0.07 | 0.08 | 0.08 | 0.19 |
| LOI@1000 | 1.39 | 5.45 | 0.46 | 0.54 |

*$SO_3$ based on sulphur determined by LECO

Table C-2: Proportioning of Mixtures Used in Part 3A

| Mix | W/CM | Composition ( % ) | | | | | |
|---|---|---|---|---|---|---|---|
| | | $C_3S$ | $C_2S$ | $C_3A$ | $C_4AF$ | Gypsum | $Ca(OH)_2$ |
| $C_3S$ | 0.5 | 100 | | | | | |
| $C_2S$ | 0.5 | | 100 | | | | |
| $C_3A8$ | 0.5 | | | 63.23 | | 31.57 | 5.2 |
| $C_3A4$ | 0.5 | | | 75.08 | | 18.74 | 6.18 |
| $C_4AF$ | 0.5 | | | | 75.57 | 20.98 | 3.46 |

Table C-3: Proportioning of Mixtures Used in Phase 3B

| Mix | W/CM | Composition (% mass) | | | | |
|---|---|---|---|---|---|---|
| | | OPC | SF | MK | GGBFS | $Ca(OH)_2$ |
| SF12† | 2 | | 33.33 | | | 66.66 |
| SF11† | 2 | | 50 | | | 50 |
| SF21† | 2 | | 66.66 | | | 33.33 |
| MK12† | 2 | | | 33.33 | | 66.66 |
| MK11† | 2 | | | 50 | | 50 |
| MK21† | 2 | | | 66.66 | | 33.33 |
| 50SL | 0.5 | 50 | | | 50 | |
| 100SL | 0.5 | | | | 100 | |

† The mixing water in the SCM-lime mixtures contained NaOH and KOH in concentrations similar to those of the OPC paste.

**C.2 Results of the SCM-lime pastes:**

The following results in Tables C-4 to C-9 are referred to in subsection 4.3.1, and represent the binding capacities of the SCM-lime pastes. Tables C-10 and C-11 show the binding capacities of the 50SL and 100SL pastes.

## MK11, W/CM = 2, curing: 2 months at 38°C

Table C-4: Chloride binding capacity of the MK11 paste.

| Solution Mass | Solution Density | Solution Volume | Sample Mass | Dry Sample Mass | Initial Conc. | Equilibrium Conc. | Bound Chloride |
|---|---|---|---|---|---|---|---|
| $W_{sol}$ (g) | $d_s$ (g/ml) | $V_{sol}$ (ml) | $W_{11}$ (g) | $W_d$ (g) | $C_i$ (mol/l) | $C_e$ (mol/l) | $C_b$ mg Cl/g Sple |
| 122.73 | 79.14 | 1.003 | 78.89 | 20.71 | 0.102 | 0.084 | 2.46 |
| 129.53 | 84.09 | 1.040 | 80.87 | 22.38 | 1.014 | 0.941 | 9.35 |
| 130.02 | 85.56 | 1.115 | 76.77 | 21.67 | 3.032 | 2.888 | 18.04 |

## MK21, W/CM = 2, curing: 2 months at 38°C

Table C-5: Chloride binding capacity of the MK21 paste.

| Solution Mass | Solution Density | Solution Volume | Sample Mass | Dry Sample Mass | Initial Conc. | Equilibrium Conc. | Bound Chloride |
|---|---|---|---|---|---|---|---|
| $W_{sol}$ (g) | $d_s$ (g/ml) | $V_{sol}$ (ml) | $W_{11}$ (g) | $W_d$ (g) | $C_i$ (mol/l) | $C_e$ (mol/l) | $C_b$ mg Cl/g Sple |
| 135.04 | 90.55 | 1.003 | 90.27 | 22.44 | 0.102 | 0.097 | 0.82 |
| 133.81 | 89.15 | 1.040 | 85.74 | 22.47 | 1.014 | 0.979 | 4.73 |
| 138.17 | 93.62 | 1.115 | 84.00 | 22.38 | 3.032 | 2.931 | 13.48 |

## MK12, W/CM = 2, curing: 2 months at 38°C

Table C-6: Chloride binding capacity of the MK12 paste.

| Solution Mass | Solution Density | Solution Volume | Sample Mass | Dry Sample Mass | Initial Conc. | Equilibrium Conc. | Bound Chloride |
|---|---|---|---|---|---|---|---|
| $W_{sol}$ (g) | $d_s$ (g/ml) | $V_{sol}$ (ml) | $W_{11}$ (g) | $W_d$ (g) | $C_i$ (mol/l) | $C_e$ (mol/l) | $C_b$ mg Cl/g Sple |
| 125.59 | 80.96 | 1.003 | 80.71 | 23.18 | 0.102 | 0.043 | 7.35 |
| 116.19 | 77.63 | 1.040 | 74.66 | 17.56 | 1.014 | 0.727 | 43.20 |
| 131.73 | 87.81 | 1.115 | 78.79 | 22.76 | 3.032 | 2.667 | 44.77 |

## SF11, W/CM = 2, curing: 2 months at 38°C

Table C-7: Chloride binding capacity of the SF11 paste.

| Solution Mass | Solution Density | Solution Volume | Sample Mass | Dry Sample Mass | Initial Conc. | Equilibrium Conc. | Bound Chloride |
|---|---|---|---|---|---|---|---|
| $W_{sol}$ (g) | $d_s$ (g/ml) | $V_{sol}$ (ml) | $W_{11}$ (g) | $W_d$ (g) | $C_i$ (mol/l) | $C_e$ (mol/l) | $C_b$ mg Cl/g Sple |
| 115.70 | 71.10 | 1.003 | 70.88 | 22.56 | 0.102 | 0.105 | -0.35 |
| 125.37 | 80.43 | 1.040 | 77.35 | 22.45 | 1.014 | 1.009 | 0.61 |
| 123.63 | 82.84 | 1.115 | 74.33 | 21.95 | 3.032 | 3.032 | 0.00 |

## SF21, W/CM = 2, curing: 2 months at 38°C

Table C-8: Chloride binding capacity of the SF21 paste.

| Solution Mass | Solution Density | Solution Volume | Sample Mass | Dry Sample Mass | Initial Conc. | Equilibrium Conc. | Bound Chloride |
|---|---|---|---|---|---|---|---|
| $W_{sol}$ (g) | $d_s$ (g/ml) | $V_{sol}$ (ml) | $W_{11}$ (g) | $W_d$ (g) | $C_i$ (mol/l) | $C_e$ (mol/l) | $C_b$ mg Cl/g Sple |
| 133.24 | 89.44 | 1.003 | 89.16 | 21.83 | 0.102 | 0.106 | -0.48 |
| 137.22 | 93.73 | 1.040 | 90.14 | 21.50 | 1.014 | 1.014 | 0.00 |
| 142.85 | 100.14 | 1.115 | 89.85 | 20.71 | 3.032 | 3.032 | 0.00 |

## SF12, W/CM = 2, curing: 2 months at 38°C

Table C-9: Chloride binding capacity of the SF12 paste.

| Solution Mass | Solution Density | Solution Volume | Sample Mass | Dry Sample Mass | Initial Conc. | Equilibrium Conc. | Bound Chloride |
|---|---|---|---|---|---|---|---|
| $W_{sol}$ (g) | $d_s$ (g/ml) | $V_{sol}$ (ml) | $W_{11}$ (g) | $W_d$ (g) | $C_i$ (mol/l) | $C_e$ (mol/l) | $C_b$ mg Cl/g Sple |
| 121.37 | 77.06 | 1.003 | 76.82 | 22.34 | 0.102 | 0.099 | 0.42 |
| 125.00 | 80.87 | 1.040 | 77.77 | 22.39 | 1.014 | 0.983 | 3.75 |
| 133.15 | 88.90 | 1.115 | 79.77 | 22.19 | 3.032 | 2.984 | 6.18 |

## 50SL, W/CM = 0.5, curing: 2 months

Table C-10: Chloride binding capacity of the 50SL paste.

| Sample Mass | Solution Mass | Solution Density | Solution Volume | Dry Sample Mass | Initial Conc. | Equilibrium Conc. | Bound Chloride |
|---|---|---|---|---|---|---|---|
| $W_{11}$ (g) | $W_{sol}$ (g) | $d_s$ (g/ml) | $V_{sol}$ (ml) | $W_d$ (g) | $C_i$ (mol/l) | $C_e$ (mol/l) | $C_b$ mg Cl/g Sple |
| 24.76 | 30.66 | 1.003 | 30.56 | 23.31 | 0.101 | 0.033 | 3.15 |
| 25.09 | 32.12 | 1.040 | 30.89 | 23.62 | 1.006 | 0.781 | 10.42 |
| 25.38 | 34.46 | 1.115 | 30.92 | 23.90 | 3.032 | 2.668 | 16.71 |

## 100SL, W/CM = 0.5, curing: 6 months

Table C-11: Chloride binding capacity of the 100SL paste.

| Sample Mass | Solution Mass | Solution Density | Solution Volume | Dry Sample Mass | Initial Conc. | Equilibrium Conc. | Bound Chloride |
|---|---|---|---|---|---|---|---|
| $W_{11}$ (g) | $W_{sol}$ (g) | $d_s$ (g/ml) | $V_{sol}$ (ml) | $W_d$ (g) | $C_i$ (mol/l) | $C_e$ (mol/l) | $C_b$ mg Cl/g Sple |
| 25.23 | 32.34 | 1.003 | 32.24 | 23.76 | 0.101 | 0.092 | 0.42 |
| 24.91 | 33.97 | 1.040 | 32.67 | 23.46 | 1.006 | 0.947 | 2.88 |
| 23.59 | 34.93 | 1.115 | 31.34 | 22.21 | 3.032 | 2.900 | 6.58 |

### C.3 Results of the pure phases:

The results presented in the following tables (Tables C-12 to C-28) are those of pastes made with pure phases, and are referred to in subsection 4.3.2.

## $C_3A8$, W/CM = 0.5, curing: 2 months

Table C-12: Chloride binding capacity of the $C_3A8$ paste.

| Sample Mass | Solution Mass | Solution Density | Solution Volume | Dry Sample Mass | Initial Conc. | Equilibrium Conc. | Bound Chloride |
|---|---|---|---|---|---|---|---|
| $W_{11}$ (g) | $W_{sol}$ (g) | $d_s$ (g/ml) | $V_{sol}$ (ml) | $W_d$ (g) | $C_i$ (mol/l) | $C_e$ (mol/l) | $C_b$ mg Cl/g Sple |
| 19.86 | 27.33 | 1.003 | 27.24 | 18.20 | 0.101 | 0.027 | 3.94 |
| 19.89 | 27.89 | 1.020 | 27.34 | 18.23 | 0.506 | 0.080 | 22.66 |
| 19.92 | 27.83 | 1.040 | 26.76 | 18.25 | 1.010 | 0.372 | 33.21 |
| 19.71 | 30.57 | 1.115 | 27.43 | 18.06 | 3.034 | 1.916 | 60.18 |
| 19.98 | 31.21 | 1.115 | 28.00 | 18.31 | 3.034 | 1.931 | 59.80 |

## $C_3A4$, W/CM = 0.5, curing: 2 months

Table C-13: Chloride binding capacity of the $C_3A4$ paste.

| Sample Mass | Solution Mass | Solution Density | Solution Volume | Dry Sample Mass | Initial Conc. | Equilibrium Conc. | Bound Chloride |
|---|---|---|---|---|---|---|---|
| $W_{11}$ (g) | $W_{sol}$ (g) | $d_s$ (g/ml) | $V_{sol}$ (ml) | $W_d$ (g) | $C_i$ (mol/l) | $C_e$ (mol/l) | $C_b$ mg Cl/g Sple |
| 19.93 | 27.73 | 1.003 | 27.64 | 17.13 | 0.101 | 0.001 | 5.71 |
| 19.78 | 29.43 | 1.020 | 28.85 | 17.01 | 0.506 | 0.056 | 27.09 |
| 19.84 | 28.02 | 1.040 | 26.95 | 17.05 | 1.010 | 0.238 | 43.24 |
| 19.91 | 30.37 | 1.115 | 27.25 | 17.11 | 3.034 | 1.549 | 83.81 |

## $C_4AF$, W/CM = 0.5, curing: 2 months

Table C-14: Chloride binding capacity of the $C_3AF$ paste.

| Sample Mass | Solution Mass | Solution Density | Solution Volume | Dry Sample Mass | Initial Conc. | Equilibrium Conc. | Bound Chloride |
|---|---|---|---|---|---|---|---|
| $W_{11}$ (g) | $W_{sol}$ (g) | $d_s$ (g/ml) | $V_{sol}$ (ml) | $W_d$ (g) | $C_i$ (mol/l) | $C_e$ (mol/l) | $C_b$ mg Cl/g Sple |
| 20.00 | 27.93 | 1.003 | 27.84 | 18.00 | 0.101 | 0.011 | 4.96 |
| 20.14 | 28.33 | 1.020 | 27.77 | 18.13 | 0.506 | 0.230 | 14.99 |
| 19.85 | 28.62 | 1.040 | 27.52 | 17.87 | 1.010 | 0.552 | 25.05 |
| 20.24 | 30.95 | 1.115 | 27.77 | 18.22 | 3.034 | 1.914 | 60.55 |

## $C_3A8$, W/CM = 0.5, T = 38°C, curing: 2 months

Table C-15: Chloride binding capacity of the $C_3A8$ paste, stored in the host solution at 38 C.

| Sample Mass | Solution Mass | Solution Density | Solution Volume | Dry Sample Mass | Initial Conc. | Equilibrium Conc. | Bound Chloride |
|---|---|---|---|---|---|---|---|
| $W_{11}$ (g) | $W_{sol}$ (g) | $d_s$ (g/ml) | $V_{sol}$ (ml) | $W_d$ (g) | $C_i$ (mol/l) | $C_e$ (mol/l) | $C_b$ mg Cl/g Sple |
| 19.90 | 29.22 | 1.065 | 27.44 | 18.24 | 0.101 | 0.071 | 1.58 |
| 19.95 | 29.29 | 1.100 | 26.63 | 18.28 | 1.008 | 0.640 | 19.02 |
| 19.90 | 31.07 | 1.173 | 26.49 | 18.24 | 3.027 | 1.983 | 53.76 |

## $C_3A8$, W/CM = 0.5, $[SO_4^{2-}]$ = 0.1 M (host solution), curing: 2 months

Table C-16: Chloride binding capacity of the $C_3A8$ paste, $[SO_4^{2-}]$ = 0.1 M (host solution).

| Sample Mass | Solution Mass | Solution Density | Solution Volume | Dry Sample Mass | Initial Conc. | Equilibrium Conc. | Bound Chloride |
|---|---|---|---|---|---|---|---|
| $W_{11}$ (g) | $W_{sol}$ (g) | $d_s$ (g/ml) | $V_{sol}$ (ml) | $W_d$ (g) | $C_i$ (mol/l) | $C_e$ (mol/l) | $C_b$ mg Cl/g Sple |
| 19.92 | 27.02 | 1.049 | 25.77 | 18.25 | 0.101 | 0.051 | 2.53 |
| 16.53 | 27.99 | 1.083 | 25.85 | 15.15 | 1.010 | 0.540 | 28.46 |
| 19.87 | 31.03 | 1.158 | 26.79 | 18.21 | 3.044 | 2.014 | 53.73 |

## $C_3A8$, W/CM = 0.5, pH = 14 (host solution), curing: 2 months

Table C-17: Chloride binding capacity of the $C_3A8$ paste, pH=14 (host solution).

| Sample Mass | Solution Mass | Solution Density | Solution Volume | Dry Sample Mass | Initial Conc. | Equilibrium Conc. | Bound Chloride |
|---|---|---|---|---|---|---|---|
| $W_{11}$ (g) | $W_{sol}$ (g) | $d_s$ (g/ml) | $V_{sol}$ (ml) | $W_d$ (g) | $C_i$ (mol/l) | $C_e$ (mol/l) | $C_b$ mg Cl/g Sple |
| 19.77 | 27.87 | 1.003 | 27.78 | 18.12 | 0.101 | 0.049 | 2.87 |
| 19.83 | 29.85 | 1.040 | 28.71 | 18.17 | 1.010 | 0.489 | 29.18 |
| 19.97 | 30.17 | 1.115 | 27.07 | 18.30 | 3.034 | 1.876 | 60.73 |

## $C_3A8$, W/CM = 0.5, curing: 2 months, Pre-carbonated

Table C-18: Chloride binding capacity of the pre-carbonated $C_3A8$ paste.

| Sample Mass | Solution Mass | Solution Density | Solution Volume | Dry Sample Mass | Initial Conc. | Equilibrium Conc. | Bound Chloride |
|---|---|---|---|---|---|---|---|
| $W_{11}$ (g) | $W_{sol}$ (g) | $d_s$ (g/ml) | $V_{sol}$ (ml) | $W_d$ (g) | $C_i$ (mol/l) | $C_e$ (mol/l) | $C_b$ mg Cl/g Sple |
| 19.97 | 27.50 | 1.003 | 27.41 | 18.30 | 0.100 | 0.100 | 0.00 |
| 19.98 | 97.07 | 1.040 | 93.35 | 18.31 | 1.008 | 1.008 | 0.00 |
| 19.94 | 86.75 | 1.115 | 77.84 | 18.27 | 3.034 | 3.034 | 0.00 |

## C1-6$C_3A$, W/CM = 0.5, curing: 2 months

Table C-19: Chloride binding capacity of the C1-6$C_3A$ paste.

| Sample Mass | Solution Mass | Solution Density | Solution Volume | Dry Sample Mass | Initial Conc. | Equilibrium Conc. | Bound Chloride |
|---|---|---|---|---|---|---|---|
| $W_{11}$ (g) | $W_{sol}$ (g) | $d_s$ (g/ml) | $V_{sol}$ (ml) | $W_d$ (g) | $C_i$ (mol/l) | $C_e$ (mol/l) | $C_b$ mg Cl/g Sple |
| 20.07 | 27.12 | 1.003 | 27.04 | 18.92 | 0.101 | 0.027 | 3.74 |
| 20.05 | 26.82 | 1.020 | 26.29 | 18.90 | 0.506 | 0.351 | 7.65 |
| 19.89 | 28.39 | 1.040 | 27.30 | 18.75 | 1.010 | 0.817 | 9.98 |
| 20.02 | 31.05 | 1.115 | 27.86 | 18.87 | 3.030 | 2.723 | 16.07 |

## C1-10$C_3A$, W/CM = 0.5, curing: 2 months

Table C-20: Chloride binding capacity of the C1-10 $C_3A$ paste.

| Sample Mass | Solution Mass | Solution Density | Solution Volume | Dry Sample Mass | Initial Conc. | Equilibrium Conc. | Bound Chloride |
|---|---|---|---|---|---|---|---|
| $W_{11}$ (g) | $W_{sol}$ (g) | $d_s$ (g/ml) | $V_{sol}$ (ml) | $W_d$ (g) | $C_i$ (mol/l) | $C_e$ (mol/l) | $C_b$ mg Cl/g Sple |
| 20.32 | 27.81 | 1.003 | 27.72 | 18.74 | 0.101 | 0.023 | 4.12 |
| 20.08 | 27.97 | 1.020 | 27.42 | 18.52 | 0.506 | 0.309 | 10.31 |
| 20.16 | 29.93 | 1.040 | 28.78 | 18.59 | 1.010 | 0.764 | 13.52 |
| 19.91 | 30.86 | 1.115 | 27.69 | 18.36 | 3.030 | 2.622 | 21.78 |

## C7-7$C_4AF$, W/CM = 0.5, curing: 2 months

Table C-21: Chloride binding capacity of the C7-7$C_4AF$ paste.

| Sample Mass | Solution Mass | Solution Density | Solution Volume | Dry Sample Mass | Initial Conc. | Equilibrium Conc. | Bound Chloride |
|---|---|---|---|---|---|---|---|
| $W_{11}$ (g) | $W_{sol}$ (g) | $d_s$ (g/ml) | $V_{sol}$ (ml) | $W_d$ (g) | $C_i$ (mol/l) | $C_e$ (mol/l) | $C_b$ mg Cl/g Sple |
| 20.06 | 26.84 | 1.003 | 26.76 | 18.68 | 0.101 | 0.050 | 2.62 |
| 20.08 | 27.23 | 1.020 | 26.69 | 18.70 | 0.506 | 0.398 | 5.45 |
| 19.95 | 27.80 | 1.040 | 26.74 | 18.58 | 1.010 | 0.878 | 6.77 |
| 20.41 | 30.37 | 1.115 | 27.25 | 19.00 | 3.030 | 2.838 | 9.74 |

## $C_2S$, W/CM = 0.5, curing: 2 months

Table C-22: Chloride binding capacity of the $C_2S$ paste.

| Sample Mass | Solution Mass | Solution Density | Solution Volume | Dry Sample Mass | Initial Conc. | Equilibrium Conc. | Bound Chloride |
|---|---|---|---|---|---|---|---|
| $W_{11}$ (g) | $W_{sol}$ (g) | $d_s$ (g/ml) | $V_{sol}$ (ml) | $W_d$ (g) | $C_i$ (mol/l) | $C_e$ (mol/l) | $C_b$ mg Cl/g Sple |
| 20.12 | 29.20 | 1.003 | 29.11 | 19.37 | 0.101 | 0.077 | 1.28 |
| 19.99 | 28.21 | 1.020 | 27.65 | 19.24 | 0.506 | 0.476 | 1.52 |
| 19.93 | 30.34 | 1.040 | 29.18 | 19.18 | 1.010 | 0.974 | 1.97 |
| 20.33 | 30.72 | 1.115 | 27.56 | 19.57 | 3.034 | 2.993 | 2.05 |

## $C_3S$, W/CM = 0.5, curing: 2 months

Table C-23: Chloride binding capacity of the $C_3S$ paste.

| Sample Mass | Solution Mass | Solution Density | Solution Volume | Dry Sample Mass | Initial Conc. | Equilibrium Conc. | Bound Chloride |
|---|---|---|---|---|---|---|---|
| $W_{11}$ (g) | $W_{sol}$ (g) | $d_s$ (g/ml) | $V_{sol}$ (ml) | $W_d$ (g) | $C_i$ (mol/l) | $C_e$ (mol/l) | $C_b$ mg Cl/g Sple |
| 20.03 | 26.82 | 1.003 | 26.74 | 18.52 | 0.101 | 0.070 | 1.59 |
| 19.88 | 27.24 | 1.020 | 26.70 | 18.38 | 0.506 | 0.450 | 2.87 |
| 19.59 | 27.69 | 1.040 | 26.63 | 18.11 | 1.010 | 0.938 | 3.78 |
| 19.74 | 30.21 | 1.115 | 27.11 | 18.25 | 3.034 | 2.925 | 5.73 |
| 20.05 | 30.52 | 1.115 | 27.38 | 18.54 | 3.034 | 2.935 | 5.20 |

## $C_3S$, W/CM = 0.5, curing: 2 months, T = 38°C (storage temperature)

Table C-24: Chloride binding capacity of the $C_3S$ paste, stored at 38°C in host solution.

| Sample Mass | Solution Mass | Solution Density | Solution Volume | Dry Sample Mass | Initial Conc. | Equilibrium Conc. | Bound Chloride |
|---|---|---|---|---|---|---|---|
| $W_{11}$ (g) | $W_{sol}$ (g) | $d_s$ (g/ml) | $V_{sol}$ (ml) | $W_d$ (g) | $C_i$ (mol/l) | $C_e$ (mol/l) | $C_b$ mg Cl/g Sple |
| 19.70 | 27.77 | 1.003 | 27.68 | 18.21 | 0.101 | 0.073 | 1.53 |
| 20.00 | 29.80 | 1.040 | 28.66 | 18.49 | 1.012 | 0.948 | 3.51 |
| 19.93 | 29.71 | 1.115 | 26.66 | 18.43 | 3.024 | 2.918 | 5.42 |

## $C_3S$, W/CM = 0.5, curing: 2 months, T = 7°C (storage temperature)

Table C-25: Chloride binding capacity of the $C_3S$ paste, stored at 7°C in host solution.

| Sample Mass | Solution Mass | Solution Density | Solution Volume | Dry Sample Mass | Initial Conc. | Equilibrium Conc. | Bound Chloride |
|---|---|---|---|---|---|---|---|
| $W_{11}$ (g) | $W_{sol}$ (g) | $d_s$ (g/ml) | $V_{sol}$ (ml) | $W_d$ (g) | $C_i$ (mol/l) | $C_e$ (mol/l) | $C_b$ mg Cl/g Sple |
| 19.91 | 27.67 | 1.003 | 27.58 | 18.41 | 0.101 | 0.072 | 1.56 |
| 20.11 | 27.57 | 1.040 | 26.51 | 18.59 | 1.012 | 0.936 | 3.84 |
| 19.74 | 29.62 | 1.115 | 26.58 | 18.25 | 3.024 | 2.908 | 5.99 |

## $C_3S$, W/CM = 0.5, curing: 2 months, pH = 14 (host solution)

Table C-26: Chloride binding capacity of the $C_3S$ paste, pH=14 (host solution).

| Sample Mass | Solution Mass | Solution Density | Solution Volume | Dry Sample Mass | Initial Conc. | Equilibrium Conc. | Bound Chloride |
|---|---|---|---|---|---|---|---|
| $W_{11}$ (g) | $W_{sol}$ (g) | $d_s$ (g/ml) | $V_{sol}$ (ml) | $W_d$ (g) | $C_i$ (mol/l) | $C_e$ (mol/l) | $C_b$ mg Cl/g Sple |
| 19.89 | 28.45 | 1.065 | 26.72 | 18.39 | 0.101 | 0.087 | 0.70 |
| 19.90 | 29.14 | 1.100 | 26.50 | 18.40 | 1.008 | 0.989 | 0.98 |
| 19.84 | 31.34 | 1.173 | 26.72 | 18.34 | 3.027 | 3.009 | 0.93 |

## $C_3S$, W/CM = 0.5, curing: 2 months, $[SO_4^{2-}]$ = 0.1 M (host solution)

Table C-27: Chloride binding capacity of the $C_3S$ paste, $[SO_4^{2-}]$ = 0.1 M (host solution).

| Sample Mass | Solution Mass | Solution Density | Solution Volume | Dry Sample Mass | Initial Conc. | Equilibrium Conc. | Bound Chloride |
|---|---|---|---|---|---|---|---|
| $W_{11}$ (g) | $W_{sol}$ (g) | $d_s$ (g/ml) | $V_{sol}$ (ml) | $W_d$ (g) | $C_i$ (mol/l) | $C_e$ (mol/l) | $C_b$ mg Cl/g Sple |
| 20.16 | 27.62 | 1.049 | 26.34 | 18.64 | 0.101 | 0.085 | 0.83 |
| 19.97 | 28.47 | 1.083 | 26.29 | 18.46 | 1.010 | 0.965 | 2.27 |
| 19.93 | 32.00 | 1.158 | 27.63 | 18.43 | 3.044 | 2.978 | 3.49 |

## $C_3S$, W/CM = 0.5, curing: 2 months, pre-carbonated

Table C-28: Chloride binding capacity of the pre-carbonated $C_3S$ paste.

| Sample Mass | Solution Mass | Solution Density | Solution Volume | Dry Sample Mass | Initial Conc. | Equilibrium Conc. | Bound Chloride |
|---|---|---|---|---|---|---|---|
| $W_{11}$ (g) | $W_{sol}$ (g) | $d_s$ (g/ml) | $V_{sol}$ (ml) | $W_d$ (g) | $C_i$ (mol/l) | $C_e$ (mol/l) | $C_b$ mg Cl/g Sple |
| 20.05 | 27.52 | 1.003 | 27.43 | 18.54 | 0.100 | 0.097 | 0.17 |
| 19.97 | 28.95 | 1.040 | 27.84 | 18.46 | 1.008 | 0.993 | 0.80 |
| 20.07 | 30.85 | 1.115 | 27.68 | 18.55 | 3.034 | 3.031 | 0.16 |

## C.4 XRD results of "pure" phases:

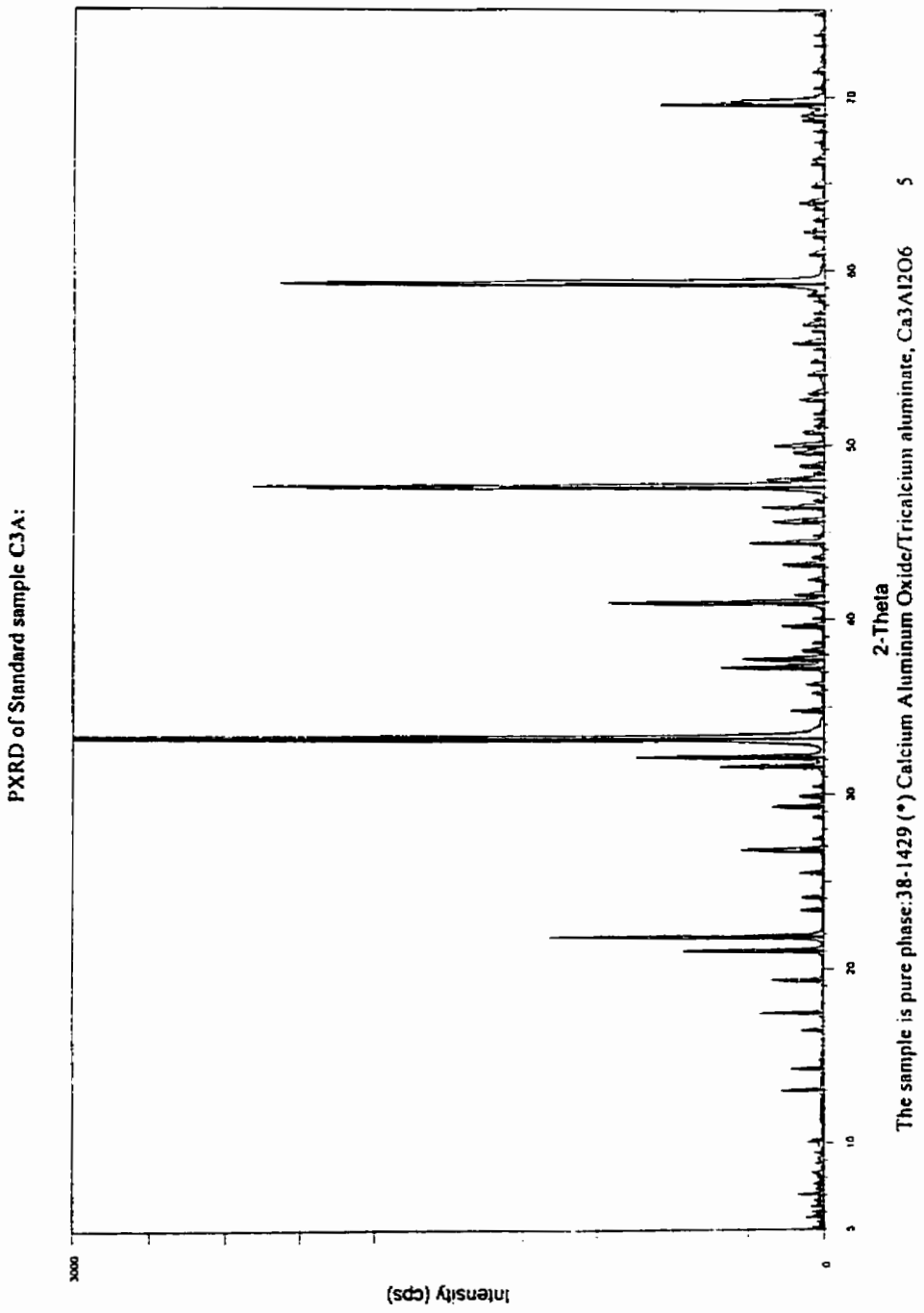

PXRD of Standard sample: C3S (Alite):

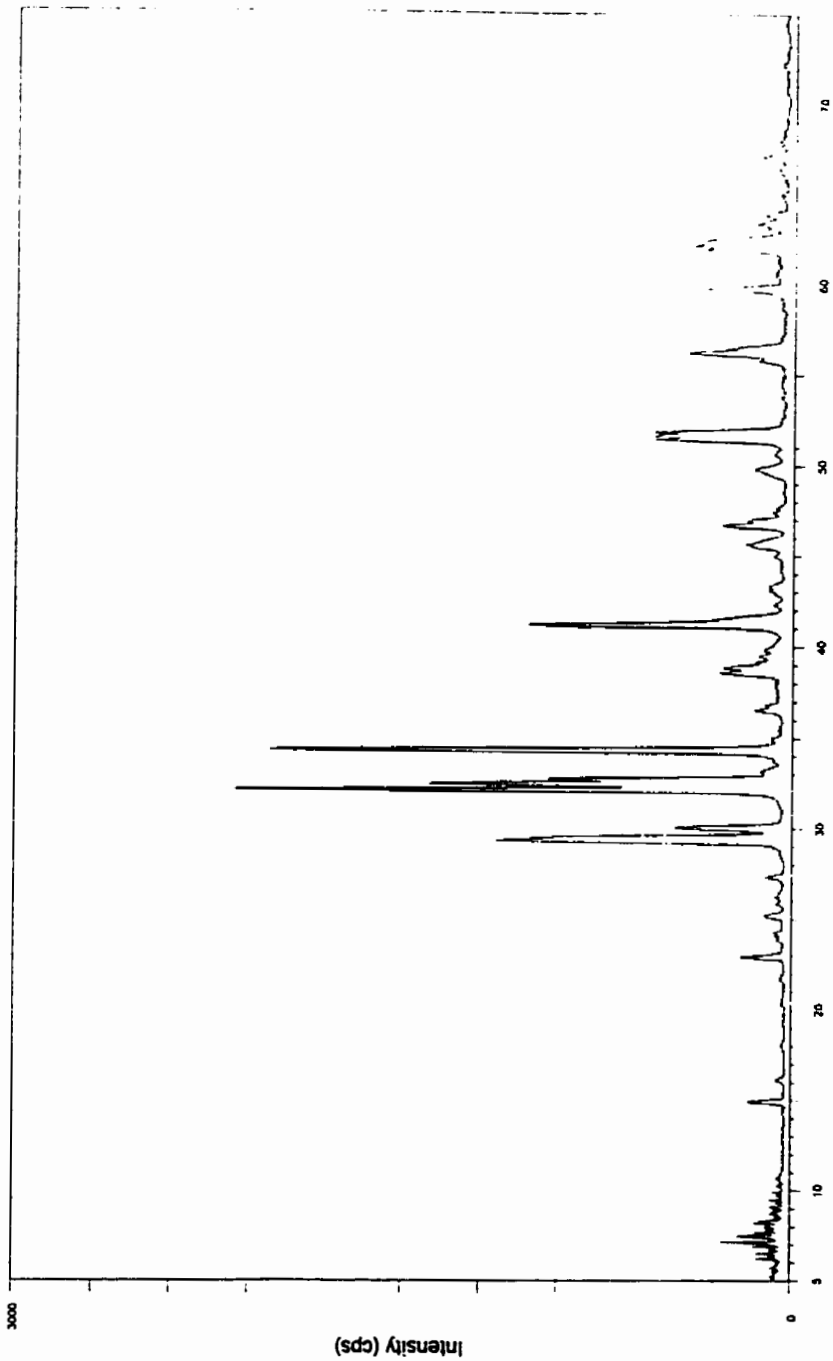


The sample looks pure C3S, probably a mixture of 2-3 polymorphous. There is no any other (extra) peaks of some related cement phases.

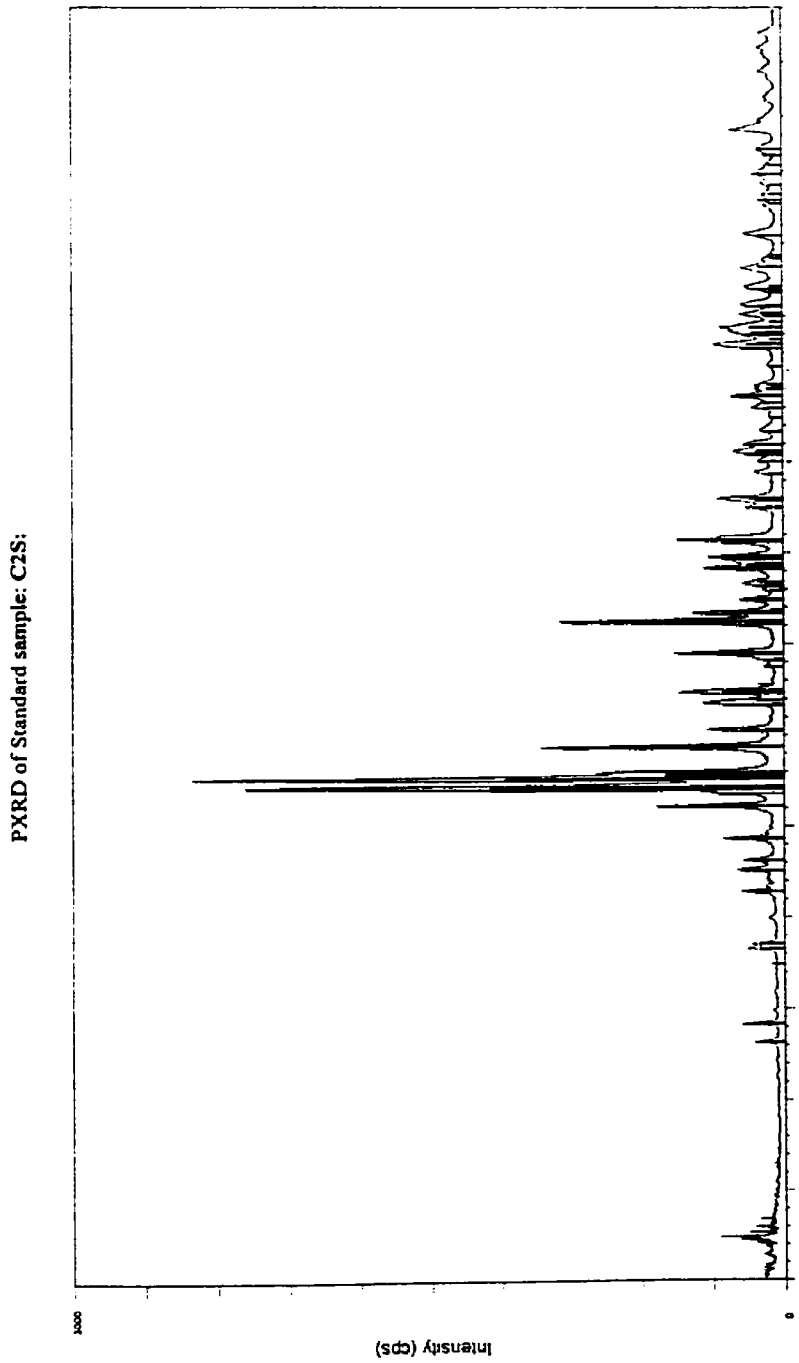
PXRD of Standard sample: C2S:
Intensity (cps)
2-Theta
The sample is a mixture of polymorphous.
33-0302 (*) Larnite, syn Ca2SiO4
09-0351 (D) Larnite, syn Ca2SiO4

PXRD of Standard sample C3A:

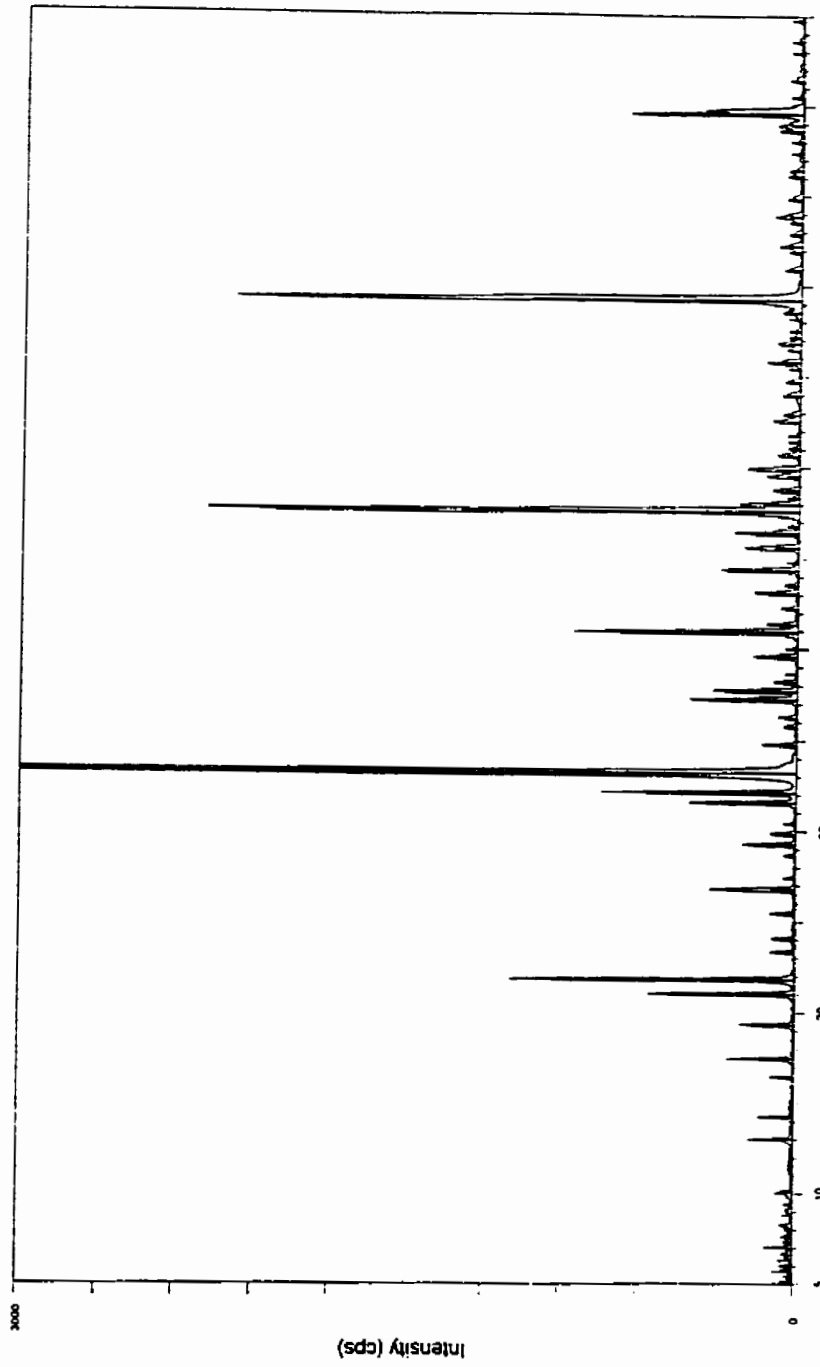


The sample is pure phase:38-1429 (*) Calcium Aluminum Oxide/Tricalcium aluminate, Ca3Al2O6 5

# Appendix D

## Contribution of Cement Phases

### D.1 Example of estimation of contributions of the cement mineral phases to the chloride binding capacity:

The contributions of the mineral phases of the C7 cement to its chloride binding capacity are estimated in this example. The following assumptions are made in order to estimate these contributions:

1. The chloride binding capacities of these phases are assumed to be equal to the chloride binding capacities of the corresponding "pure" pastes.

2. The distribution of hydrates in 1 g of cement paste is assumed to be similar to the distribution of their corresponding mineral phases, determined according to Bogue composition. In the case of the hydrates produced by $C_3A$ and $C_4AF$, the $SO_3$ content of the cement is also added to the $C_3A$ and $C_4AF$ contents according to their respective molar content.

3. The chloride binding capacity of the cement is assumed to be the sum of the binding capacities of the different mineral phases.

Table D-1 shows the chloride binding capacities of the pure pastes and C1 cement at equilibrium chloride concentrations of 0.1 M and 3.0 M. These binding capacities were calculated from the chloride binding isotherms (obtained by fitting Freundlich isotherms to the experimental data) of the pure pastes. The $\alpha$ and $\beta$ coefficients of the Freundlich isotherms are also presented in Table D-1.

Table D-1: Coefficients of Freundlich isotherms and binding capacities of the pure pastes.

| Pure Paste | Coefficients of Freundlich Isotherm | | Chloride Binding Capacity | |
|---|---|---|---|---|
| | α | β | 0.1 M | 3.0 M |
| $C_3S$ | 3.818 | 0.334 | 1.77 | 5.51 |
| $C_2S$ | 1.811 | 0.136 | 1.32 | 2.10 |
| $C_3A4$ | 71.938 | 0.349 | 32.21 | 105.55 |
| $C_3A8$ | 47.172 | 0.395 | 19.00 | 72.80 |
| $C_4AF$ | 39.051 | 0.666 | 8.43 | 81.17 |
| WC | 5.698 | 0.282 | 2.98 | 7.77 |

Table D-2 shows the mineral composition of the C7 cement along with the $SO_3$ content.

Table D-2: Mineral composition of cement C7.

| Cement | $C_3S$ | $C_2S$ | $C_3A$ | $C_4AF$ | $SO_3$ |
|---|---|---|---|---|---|
| C7 | 75.0% | 13.5% | 4.4% | 0.8% | 2.14% |

The distribution of the $SO_3$ between the $C_3A$ and $C_4AF$ phases is determined as follow:

Molar content of $C_3A$ = 4.4 / 270.2 = 0.0163 mole/100 g cement

Molar content of $C_4AF$ = 0.8 / 486.0 = 0.0016 mole/100 g cement

The amount of $SO_3$ that combines with $C_3A$ = 2.14 * 0.0163 / (0.0163+0.0016) = 1.95 %≈ 1.9 %

The amount of $SO_3$ that combines with $C_4AF$ = 2.14-1.95 = 0.19 % ≈ 0.2 %

The amount of hydrates produced by $C_3A$ = 4.4% + 1.9% = 6.3%

The amount of hydrates produced by $C_4AF$ = 0.8% + 0.2% = 1.0%

The amount of hydrates produced by $C_3S$ = 75.0%

The amount of hydrates produced by $C_2S$ = 13.5%

To decide whether the binding capacity of the $C_3A8$ or that of the $C_3A4$ paste represents the binding capacity of $C_3A$ in the C7 cement, the molar ratio of $SO_3$ to $C_3A$ is calculated:

Molar ratio ($SO_3/C_3A$) = (1.9 / 80) / 0.0163 = 1.46

Since the molar ratio is closer to that of the $C_3A8$ paste, the binding capacity of the $C_3A8$ paste is used to estimate the contribution of the $C_3A$ phase. The binding capacities of the different phases at 0.1 M chloride concentration (equilibrium) is calculated as follow:

binding capacity of $C_3S + C_2S$ = (75.0 * 1.77 + 13.5 * 1.32) / 100 = 1.5 mg Cl/g paste

binding capacity of $C_3A$ = 6.3 * 19.00 / 100 = 1.2 mg Cl/g paste

binding capacity of $C_4AF$ = 1.0 * 8.43 / 100 = 0.1 mg Cl/g paste.

The estimated chloride binding capacity of the C7 paste = 1.5 + 1.2 + 0.1 = 2.8 mg Cl/g paste.

The contributions of the various phases (calculated with respect to the actual binding capacity of the C7 cement) are as follow:

contribution of $C_3S + C_2S$ = 1.5 / 2.98 * 100 = 50%

contribution of $C_3A$ = 1.2 / 2.98 * 100 = 40%

contribution of $C_4AF$ = 0.1 / 2.98 * 100 = 3%

# Appendix E

## Effect of Particle Size in the Equilibrium Method

### E.1 Introduction

The results presented in this appendix were obtained from chloride binding tests performed on the OPC control (CSA Type 20) cement and the C1 cement (CSA Type 50). The equilibrium method was used to determine the chloride binding capacity. The purpose of these tests was to investigate the influence of the particle size of the paste samples (stored in chloride solution) on the chloride binding capacity.

### E.2 Experimental Procedures

The cements were mixed at a W/CM of 0.5, and the pastes were cured for 2 months at a temperature of 23 °C. For each of the cement pastes, 2 sets of samples were prepared. The first set of samples were prepared following the procedure described in Chapter 3 (Section 3.3.1). The second set of samples were prepared in a similar way except that the paste samples were wet crushed and water sieved to 0.25-1.5 mm particle size instead of being sliced into discs (50 mm diameter by 1-3mm thick). Three chloride concentrations were tested : 0.1, 1.0, and 3.0 M.

### E.3 Results

Figures E-1 and E-2 show the results for the OPC and the C1 pastes respectively. The results are also presented in Tables E-1 to E-4. These results indicate that powdered samples have between 15% to 25% higher chloride binding capacities than samples made from discs.

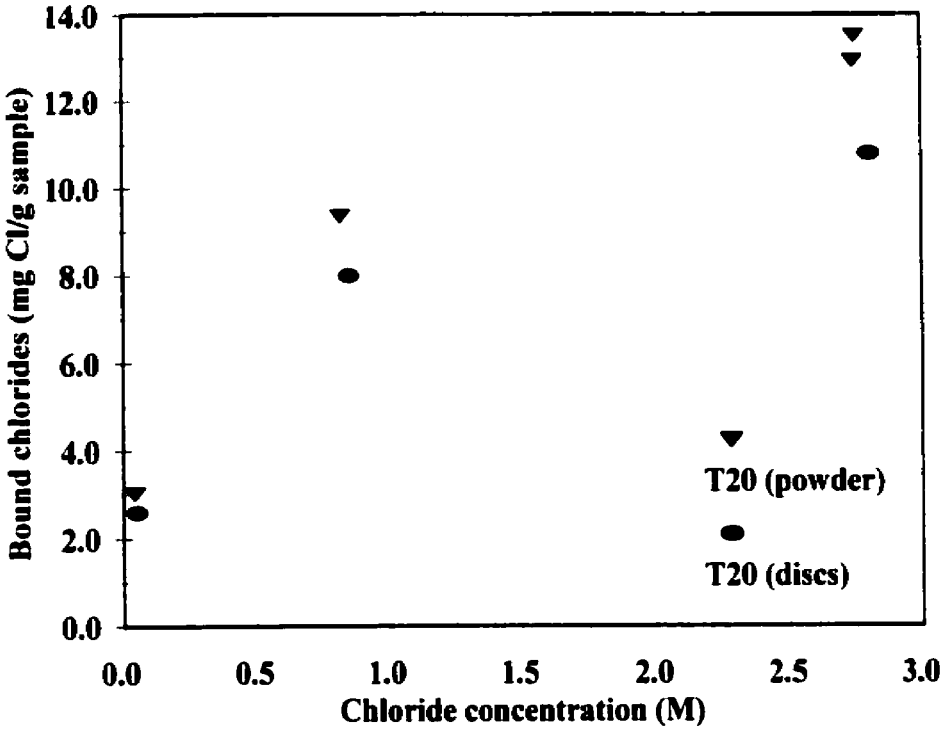


Figure E-1: Chloride binding isotherms of the OPC control paste, obtained from powdered samples and from samples made from discs.

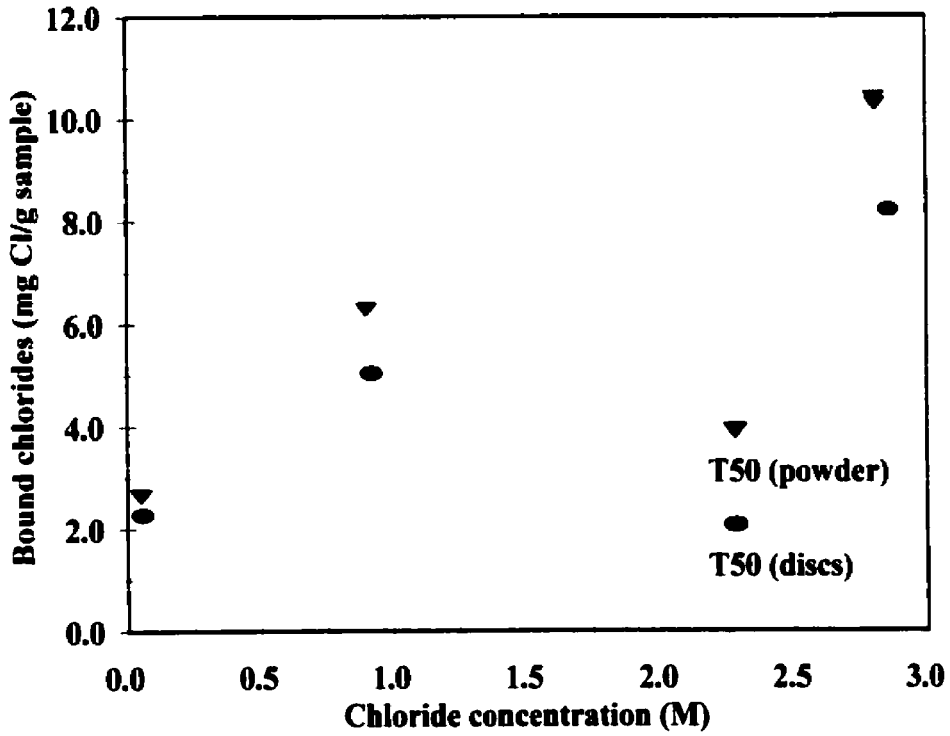


Figure E-2: Chloride binding isotherms of the C1 cement paste, obtained from powdered samples and from samples made from discs.

## OPC (Control), W/CM = 0.5, 2 months curing (samples made from discs)

Table E-1: Chloride binding capacity of the OPC control paste.

| Solution Volume | Dry Sample Mass | Initial Conc. | Equilibrium Conc. | Bound Chloride |
|---|---|---|---|---|
| $V_{sol}$ (ml) | $W_d$ (g) | $C_i$ (mol/l) | $C_e$ (mol/l) | $C_b$ mg Cl/g Sple |
| 28.63 | 23.04 | 0.108 | 0.049 | 2.60 |
| 28.45 | 23.27 | 1.035 | 0.851 | 8.00 |
| 28.54 | 23.18 | 3.045 | 2.798 | 10.79 |

## C1 Cement, W/CM = 0.5, 2 months curing (samples made from discs)

Table E-2: Chloride binding capacity of the C1 cement paste.

| Solution Volume | Dry Sample Mass | Initial Conc. | Equilibrium Conc. | Bound Chloride |
|---|---|---|---|---|
| $V_{sol}$ (ml) | $W_d$ (g) | $C_i$ (mol/l) | $C_e$ (mol/l) | $C_b$ mg Cl/g Sple |
| 28.57 | 23.10 | 0.108 | 0.056 | 2.28 |
| 28.65 | 23.61 | 1.035 | 0.918 | 5.04 |
| 28.88 | 23.60 | 3.045 | 2.856 | 8.21 |

## OPC (Control), W/CM = 0.5, 2 months curing (crushed samples)

Table E-3: Chloride binding capacity of the OPC control paste.

| Solution Volume | Dry Sample Mass | Initial Conc. | Equilibrium Conc. | Bound Chloride |
|---|---|---|---|---|
| $V_{sol}$ (ml) | $W_d$ (g) | $C_i$ (mol/l) | $C_e$ (mol/l) | $C_b$ mg Cl/g Sple |
| 29.48 | 23.08 | 0.108 | 0.041 | 3.03 |
| 27.99 | 23.09 | 1.035 | 0.817 | 9.36 |
| 27.67 | 23.10 | 3.045 | 2.741 | 12.92 |
| 29.63 | 23.13 | 3.045 | 2.748 | 13.50 |

## C1 Cement, W/CM = 0.5, 2 months curing, (crushed samples)

Table E-4: Chloride binding capacity of the C1 cement paste.

| Solution Volume | Dry Sample Mass | Initial Conc. | Equilibrium Conc. | Bound Chloride |
|---|---|---|---|---|
| $V_{sol}$ (ml) | $W_d$ (g) | $C_i$ (mol/l) | $C_e$ (mol/l) | $C_b$ mg Cl/g Sple |
| 29.18 | 22.62 | 0.108 | 0.050 | 2.65 |
| 29.56 | 22.68 | 1.035 | 0.899 | 6.29 |
| 27.62 | 22.70 | 3.045 | 2.807 | 10.28 |
| 27.55 | 22.67 | 3.045 | 2.804 | 10.40 |